DISCRETE SEMICONDUCTORS

Semiconductor Sensors

Data Handbook SC17
2001

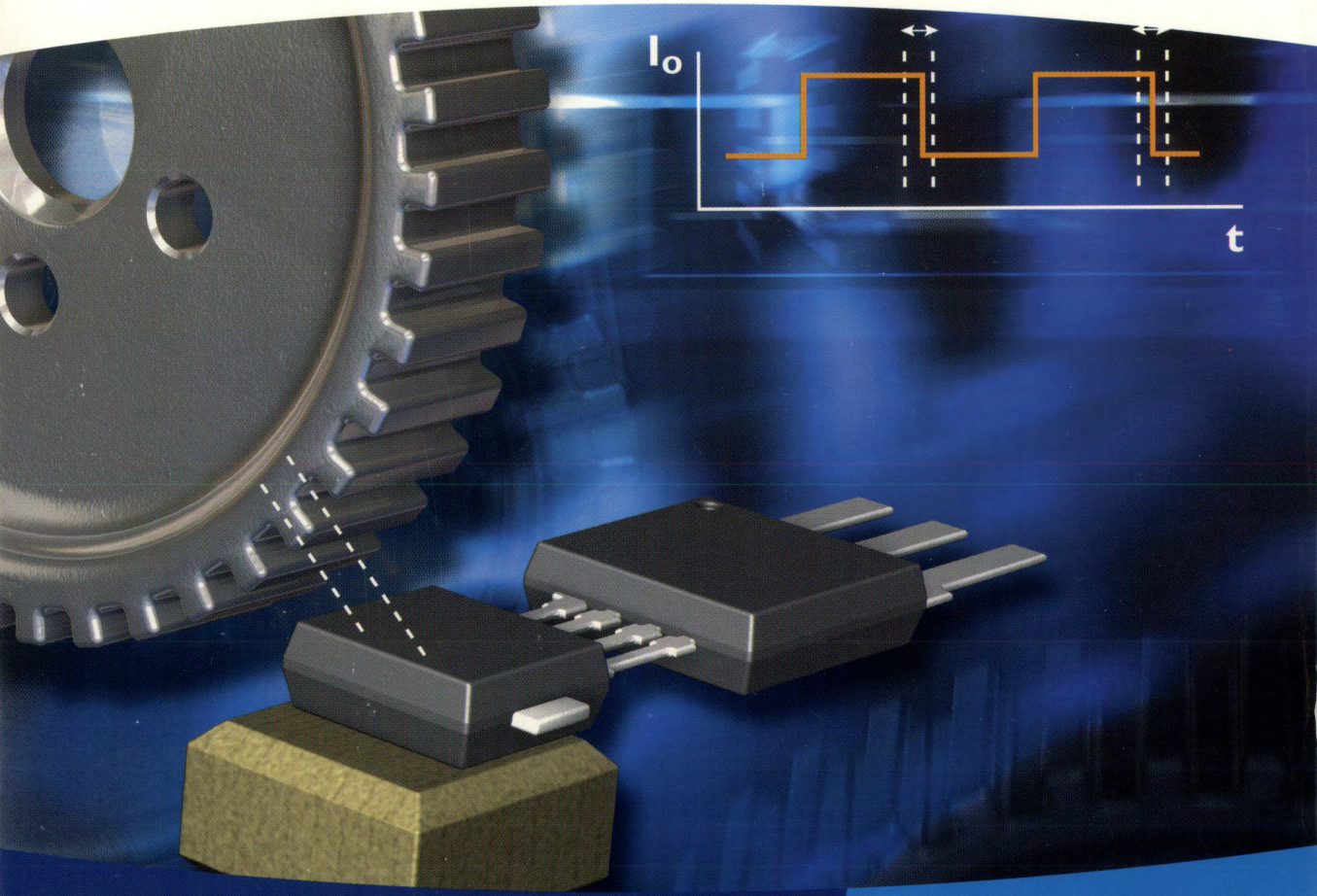

http://www.semiconductors.philips.com

PHILIPS

Let's make things better.

QUALITY ASSURED

Our quality system focuses on the continuing high quality of our components and the best possible service for our customers. We have a three-sided quality strategy: we apply a system of total quality control and assurance; we operate customer-oriented dynamic improvement programmes; and we promote a partnering relationship with our customers and suppliers.

PRODUCT SAFETY

In striving for state-of-the-art perfection, we continuously improve components and processes with respect to environmental demands. Our components offer no hazard to the environment in normal use when operated or stored within the limits specified in the data sheet.

Some components unavoidably contain substances that, if exposed by accident or misuse, are potentially hazardous to health. Users of these components are informed of the danger by warning notices in the data sheets supporting the components. Where necessary the warning notices also indicate safety precautions to be taken and disposal instructions to be followed. Obviously users of these components, in general the set-making industry, assume responsibility towards the consumer with respect to safety matters and environmental demands.

All used or obsolete components should be disposed of according to the regulations applying at the disposal location. Depending on the location, electronic components are considered to be 'chemical', 'special' or sometimes 'industrial' waste. Disposal as domestic waste is usually not permitted.

Semiconductor Sensors

CONTENTS

DATA SHEET STATUS

DATA SHEET STATUS	PRODUCT STATUS	DEFINITIONS [1]
Objective specification	Development	This data sheet contains the design target or goal specifications for product development. Specification may change in any manner without notice.
Preliminary specification	Qualification	This data sheet contains preliminary data, and supplementary data will be published at a later date. Philips Semiconductors reserves the right to make changes at any time without notice in order to improve design and supply the best possible product.
Product specification	Production	This data sheet contains final specifications. Philips Semiconductors reserves the right to make changes at any time without notice in order to improve design and supply the best possible product.

Note

1. Please consult the most recently issued data sheet before initiating or completing a design.

DEFINITIONS

Short-form specification — The data in a short-form specification is extracted from a full data sheet with the same type number and title. For detailed information see the relevant data sheet or data handbook.

Limiting values definition — Limiting values given are in accordance with the Absolute Maximum Rating System (IEC 60134). Stress above one or more of the limiting values may cause permanent damage to the device. These are stress ratings only and operation of the device at these or at any other conditions above those given in the Characteristics sections of the specification is not implied. Exposure to limiting values for extended periods may affect device reliability.

Application information — Applications that are described herein for any of these products are for illustrative purposes only. Philips Semiconductors make no representation or warranty that such applications will be suitable for the specified use without further testing or modification.

DISCLAIMERS

Life support applications — These products are not designed for use in life support appliances, devices, or systems where malfunction of these products can reasonably be expected to result in personal injury. Philips Semiconductors customers using or selling these products for use in such applications do so at their own risk and agree to fully indemnify Philips Semiconductors for any damages resulting from such application.

Right to make changes — Philips Semiconductors reserves the right to make changes, without notice, in the products, including circuits, standard cells, and/or software, described or contained herein in order to improve design and/or performance. Philips Semiconductors assumes no responsibility or liability for the use of any of these products, conveys no licence or title under any patent, copyright, or mask work right to these products, and makes no representations or warranties that these products are free from patent, copyright, or mask work right infringement, unless otherwise specified.

INDEX

Semiconductor Sensors — Index

Replacement/withdrawal types

Typenumber	Reason for deletion	Typenumber	Reason for deletion
KMZ50	Deleted from Roadmap	KM110BH/2470	Discontinued
KM110BH/2130	Discontinued	KTY82-152	Discontinued
KM110BH/2190	Discontinued	KTY83-152	Discontinued
KM110BH/2270	Discontinued	KTY84-150	Discontinued
KM110BH/2430	Discontinued	KTY85-1 series	Discontinued

SELECTION GUIDE

MAGNETORESISTIVE SENSORS FOR MAGNETIC FIELD MEASUREMENT

TYPE[1]	FIELD RANGE (kA/m)	SENSITIVITY $\frac{mV/V}{kA/m}$	BRIDGE RESISTANCE (kΩ)	PACKAGE	PAGE
KMZ10A	−0.5 to +0.5	16	1.2	SOT195	98
KMZ10A1; note 2	−0.05 to +0.05	22	1.3	SOT195	103
KMZ10B	−2.0 to +2.0	4	2.1	SOT195	109
KMZ10C	−7.5 to +7.5	1.5	1.4	SOT195	114
KMZ41	H = 100; note 3	2.8	2.5	SOT96 (SO8)	365
KMZ51	−0.2 to +0.2	16	2	SOT96 (SO8)	119
KMZ52	−0.2 to +0.2	16	2	SOT109 (SO16)	123

Notes

1. In air, 1 kA/m corresponds to 1.25 mT.
2. Field range and sensitivity with switched H_x-field for detection of low magnetic fields.
3. Recommended field strength.

MAGNETORESISTIVE SENSORS FOR ROTATIONAL SPEED MEASUREMENT AND REFERENCE-/MARK DETECTION

TYPE	SENSING DISTANCE (mm)	FREQUENCY RANGE (Hz)	TARGET	PACKAGE	PAGE
KMI15/1	2.5	0 to 25000	note 1	SOT453B	160
KMI15/2	0.4	0 to 25000	note 2	SOT453A	170
KMI15/4	2.0	0 to 25000	note 1	SOT453C	176
KMI16/1	2.4	0 to 25000	note 2	SOT477B	186
KMI18/2	0.1[3]	0 to 25000	note 2	SOT477A	194
KMI18/4	2.2	0 to 25000	note 1	SOT477C	202
KMI20/1	4.0	0 to 2500	note 1	SOT453B	211
KMI20/2	0.2[3]	0 to 2500	note 2	SOT453A	219
KMI20/4	3.6	0 to 2500	note 1	SOT453C	226
KMI22/1	4.0	0 to 2500	note 1	SOT477B	234

Notes

1. Ferromagnetic target wheel.
2. Magnetized target wheel.
3. kA/m.

MAGNETORESISTIVE SENSORS FOR ANGLE MEASUREMENT

Signal conditioning IC

TYPE	ANGLE RANGE (DEG)	DIGITAL OUTPUT	ANALOG OUTPUT	PACKAGE	PAGE
UZZ9000	180	no	linear ratiometric voltage	SO24	376
UZZ9001	180	serial digital (SPI)	no	SO24	386
KMA200	180	serial digital (SPI)	linear ratiometric voltage	SOT637	358

Sensor

TYPE	FIELD RANGE (kA/m)	SENSITIVITY $\frac{mV/V}{kA/m}$	BRIDGE RESISTANCE (kΩ)	PACKAGE	PAGE
KMZ41	H = 100; note 1	2.8	2.5	SOT96 (SO8)	365
KMZ43	H = 25; note 1	2.3	3.7	SOT96 (SO8)	371

Note

1. Recommended field strength.

SILICON SENSORS FOR TEMPERATURE MEASUREMENT

TYPE	TEMPERATURE RANGE (°C)	RESISTANCE		SENSOR ACCURACY		PACKAGE	PAGE
		R (Ω)	at T_{amb} (°C)	°C	at T_{amb} (°C)		
KTY81-110	−55 to +150	990 to 1010	25	±1.3	25	SOD70	418
KTY81-120	−55 to +150	980 to 1020	25	±2.5	25	SOD70	418
KTY81-121	−55 to +150	980 to 1000	25	±1.3	25	SOD70	418
KTY81-122	−55 to +150	1000 to 1020	25	±1.3	25	SOD70	418
KTY81-150	−55 to +150	950 to 1050	25	±6.3	25	SOD70	418
KTY81-151	−55 to +150	950 to 1000	25	±3.2	25	SOD70	418
KTY81-152	−55 to +150	1000 to 1050	25	±3.2	25	SOD70	418
KTY81-210	−55 to +150	1980 to 2020	25	±1.3	25	SOD70	430
KTY81-220	−55 to +150	1960 to 2040	25	±2.5	25	SOD70	430
KTY81-221	−55 to +150	1960 to 2000	25	±1.3	25	SOD70	430
KTY81-222	−55 to +150	2000 to 2040	25	±1.3	25	SOD70	430
KTY81-250	−55 to +150	1900 to 2100	25	±6.3	25	SOD70	430
KTY81-251	−55 to +150	1900 to 2000	25	±3.2	25	SOD70	430
KTY81-252	−55 to +150	2000 to 2100	25	±3.2	25	SOD70	430
KTY82-110	−55 to +150	990 to 1010	25	±1.3	25	SOT23	442
KTY82-120	−55 to +150	980 to 1020	25	±2.5	25	SOT23	442
KTY82-121	−55 to +150	980 to 1000	25	±1.3	25	SOT23	442
KTY82-122	−55 to +150	1000 to 1020	25	±1.3	25	SOT23	442
KTY82-150	−55 to +150	950 to 1050	25	±6.3	25	SOT23	442
KTY82-151	−55 to +150	950 to 1000	25	±3.2	25	SOT23	442

TYPE	TEMPERATURE RANGE (°C)	RESISTANCE		SENSOR ACCURACY		PACKAGE	PAGE
		R (Ω)	at T_{amb} (°C)	°C	at T_{amb} (°C)		
KTY82-210	–55 to +150	1980 to 2020	25	±1.3	25	SOT23	442
KTY82-220	–55 to +150	1960 to 2040	25	±2.5	25	SOT23	442
KTY82-221	–55 to +150	1960 to 2000	25	±1.3	25	SOT23	442
KTY82-222	–55 to +150	2000 to 2040	25	±1.3	25	SOT23	442
KTY82-250	–55 to +150	1900 to 2100	25	±6.3	25	SOT23	442
KTY82-251	–55 to +150	1900 to 2000	25	±3.2	25	SOT23	442
KTY82-252	–55 to +150	2000 to 2100	25	±3.2	25	SOT23	442
KTY83-110	–55 to +175	990 to 1010	25	±1.3	25	SOD68	462
KTY83-120	–55 to +175	980 to 1020	25	±2.5	25	SOD68	462
KTY83-121	–55 to +175	980 to 1000	25	±1.3	25	SOD68	462
KTY83-122	–55 to +175	1000 to 1020	25	±1.3	25	SOD68	462
KTY83-150	–55 to +175	950 to 1050	25	±6.6	25	SOD68	462
KTY83-151	–55 to +175	950 to 1000	25	±3.3	25	SOD68	462
KTY84-130	–40 to +300	970 to 1030	100	±4.8	100	SOD68	471
KTY84-151	–40 to +300	950 to 1000	100	±4.0	100	SOD68	471
KTY84-152	–40 to +300	1000 to 1050	25	±4.0	100	SOD68	471

GENERAL

1 QUALITY

1.1 Total Quality Management

Philips Semiconductors is a Quality Company, aiming towards one ultimate standard, that of Business Excellence. The tool we use in striving towards this goal is our Total Quality Management (TQM) system. The TQM is described in our Quality manuals, and is summarized in the following paragraphs. The Philips Business Excellence Programme as part of TQM follows the European Foundation for Quality Management (EFQM) model. The EFQM award is on the level of the Malcolm Baldridge award.

1.1.1 QUALITY ASSURANCE

Quality Assurance (QA) is based on ISO 9000 standards and customer standards such as QS-9000. Our factories are certified to ISO 9000 and QS-9000 by external inspectorates. Sales organizations and headquarters are also certified to ISO 9000. The products of Philips Semiconductors are in conformance with the requirements of international standards.

1.1.2 PARTNERSHIPS WITH CUSTOMERS

Partnerships with customers include Process Quality measurement co-operation (using PPM), design-in agreements, ship-to-stock, just-in-time, sharing technology roadmaps, a change notification programme, self-qualification programmes and application support.

1.1.3 PARTNERSHIPS WITH SUPPLIERS

Our suppliers are certified to ISO 9000 and participate in ship-to-stock programmes. Key-suppliers receive support and feedback through our Supplier Quality System (SQS) audits.

1.1.4 CONTINUOUS IMPROVEMENT PROGRAMME

The continuous improvement programme incorporates continuous process and system improvement, design improvement, complete use of statistical process control, and logistics improvement, driven by key performance indicators. To encourage improvement in teamwork a very popular Quality Improvement Competition is held yearly. With a large number of improvement teams participating, opportunities arise for the sharing of successful improvement ideas.

1.2 Advanced quality planning

During the design and development of new products and processes, quality is built-in by advanced quality planning. By means of failure-mode-and-effect analysis the critical parameters of a process are identified. Procedures are then laid down to ensure the highest level of performance for these parameters. The capability of process steps is also planned in this phase in preparation for production under statistical process control.

1.3 Quality network

Product quality is the responsibility of the Business Lines, with their Quality and Reliability (Q&R) departments operating in a supportive and controlling manner. The sales organization has Quality Managers who respond to any quality matters raised by customers. Customer complaints are then handled by direct contact between Sales Quality and the relevant Q&R department. General quality requirements are covered by a divisional Quality department.

1.4 Product conformance

The assurance of product conformance is an integral part of our Quality Assurance practice. This is achieved by:

- In-line Quality Assurance to monitor process reproducibility during manufacture. Equipment performance and process steps are under statistical process control.
- Acceptance tests on finished products to verify conformance with the device specification. The test results are used for Quality feedback and corrective actions. Periodic sample inspections to monitor and measure the conformance of products are increasingly being replaced by continuous in-line monitoring.
- Qualification tests.

The inspection and test requirements are detailed in the General Quality Specifications in the SNW-FQ-611 series.

1.5 Product reliability

Highly accelerated tests are implemented to evaluate and monitor product reliability. Rejects from reliability tests are subjected to failure analysis, so that improvements may be made. This analysis also extends to product related customer complaints.

1.6 Customer response

Our quality improvement depends on working together with our customer. We need our customer's input, and we therefore invite constructive comments on all aspects of our performance. For all such matters, please contact your local Philips Semiconductors sales representative.

1 RATING SYSTEMS

The rating systems described are those recommended by the IEC in its publication number 60134.

Remark: It is common practice to use the Absolute Maximum Rating System in published semiconductor data sheets.

1.1 Definitions of terms used

1.1.1 ELECTRONIC DEVICE

An electronic tube or valve, transistor or other semiconductor device.

Remark: This definition excludes inductors, capacitors, resistors and similar components.

1.1.2 CHARACTERISTIC

A characteristic is an inherent and measurable property of a device. Such a property may be electrical, mechanical, thermal, hydraulic, electro-magnetic or nuclear, and can be expressed as a value for stated or recognized conditions. A characteristic may also be a set of related values, usually shown in graphical form.

1.1.3 BOGEY ELECTRONIC DEVICE

An electronic device whose characteristics have the published nominal values for the type. A bogey electronic device for any particular application can be obtained by considering only those characteristics that are directly related to the application.

1.1.4 RATING

A value that establishes either a limiting capability or a limiting condition for an electronic device. It is determined for specified values of environment and operation, and may be stated in any suitable terms.

Remark: Limiting conditions may be either maxima or minima.

1.1.5 RATING SYSTEM

The set of principles upon which ratings are established and which determine their interpretation.

Remark: The rating system indicates the division of responsibility between the device manufacturer and the circuit designer, with the object of ensuring that the working conditions do not exceed the ratings.

1.2 Absolute maximum rating system

Absolute maximum ratings are limiting values of operating and environmental conditions applicable to any electronic device of a specified type, as defined by its published data, which should not be exceeded under the worst probable conditions.

These values are chosen by the device manufacturer to provide acceptable serviceability of the device, taking no responsibility for equipment variations, environmental variations, and the effects of changes in operating conditions due to variations in the characteristics of the device under consideration and of all other electronic devices in the equipment.

The equipment manufacturer should design so that, initially and throughout the life of the device, no absolute maximum value for the intended service is exceeded with any device, under the worst probable operating conditions with respect to supply voltage variation, equipment component variation, equipment control adjustment, load variations, signal variation, environmental conditions, and variations in characteristics of the device under consideration and of all other electronic devices in the equipment.

1.3 Design maximum rating system

Design maximum ratings are limiting values of operating and environmental conditions applicable to a bogey electronic device of a specified type as defined by its published data, and should not be exceeded under the worst probable conditions.

These values are chosen by the device manufacturer to provide acceptable serviceability of the device, taking responsibility for the effects of changes in operating conditions due to variations in the characteristics of the electronic device under consideration.

The equipment manufacturer should design so that, initially and throughout the life of the device, no design-maximum value for the intended service is exceeded with a bogey electronic device, under the worst probable operating conditions with respect to supply voltage variation, equipment component variation, variation in characteristics of all other devices in the equipment, equipment control adjustment, load variation, signal variation and environmental conditions.

1.4 Design centre rating system

Design centre ratings are limiting values of operating and environmental conditions applicable to a bogey electronic device of a specified type as defined by its published data, and should not be exceeded under normal conditions.

These values are chosen by the device manufacturer to provide acceptable serviceability of the device in average applications, taking responsibility for normal changes in operating conditions due to rated supply voltage variation, equipment component variation, equipment control adjustment, load variation, signal variation, environmental conditions, and variations in the characteristics of all electronic devices.

The equipment manufacturer should design so that, initially, no design centre value for the intended service is exceeded with a bogey electronic device in equipment operating at the stated normal supply voltage.

1 LETTER SYMBOLS

1.1 Introduction

The general standards given in *IEC Publication 60027, Letter Symbols to be Used in Electrical Technology,* are applicable, except where this Chapter 1, "Letter Symbols" (1), based on *IEC publications 60747 and 60748,* gives different standards, in which case the latter should be followed.

1.2 Letter symbols for currents, voltages and powers

1.2.1 BASIC LETTERS

Table 1 Recommended basic letters

SYMBOL	DESCRIPTION
I, i	current
V, v	voltage
P, p	power

1.2.1.1 Use of upper-case basic letters

Upper-case basic letters are used for the indication of a constant value of the quantity or of values that are derived from the periodic waveform of a quantity:

- Direct (DC) values
- Maximum (peak) values
- Average (mean) values
- Root-mean-square values
- Peak-to-peak (swing) values.

1.2.1.2 Use of lower-case basic letters

Lower-case basic letters are used for the indication of instantaneous values of the periodic waveform of the quantity.

1.3 Subscripts

Table 2 Recommended general subscripts

SYMBOL	DESCRIPTION
First subscript	
F, f	forward
n	noise
R, r	reverse
Additional subscripts	
(AV)	average value
(BR)	breakdown
(cr), cr	critical
(D)	direct
F, f	forward
M, m	maximum (peak) value with respect to time
MIN, min	minimum (peak) value with respect to time
O, o	open circuit
(OV)	overload
(P-P), (p-p)	peak-to-peak (swing)
R, r	repetitive; recovery; reverse
(RMS), (rms)	root-mean-square value
S, s	short-circuit; surge
(tot), tot	total value

1.3.1 CHOICE BETWEEN UPPER-CASE AND LOWER-CASE SUBSCRIPTS

Where Section 1.7.3.1 lists both upper-case and lower-case letters, the choice between these two styles shall be made according to Section 1.7.3.3 hereafter. If more than one subscript is used, subscripts for which both styles exist shall either be **all** upper-case or **all** lower case.

Examples: h_{FE}, y_{RE}, h_{fe}, but C_{Te} (T has no lower-case variant)

(1) See for detailed information: IEC 60747-1, Chapter V, Letter symbols, general.

1.3.2 USE OF UPPER-CASE SUBSCRIPTS

Upper-case subscripts are used for the indication of values that refer to the total value of the quantity:

- Direct (DC) values (without signal), e.g. I_B
- Instantaneous total values, e.g. i_B
- Average total values, e.g. $I_{B(AV)}$
- Maximum (peak) total values, e.g. I_{BM}
- Root-mean-square total values, e.g. $I_{B(RMS)}$
- Peak-to-peak total values, e.g. $V_{O(P-P)}$

1.3.3 USE OF LOWER-CASE SUBSCRIPTS

Lower-case subscripts are used for the indication of values that refer to the alternating component of the quantity, including small-signal modulations:

- Instantaneous alternating values, e.g. i_b
- maximum (peak) alternating values, e.g. I_{bm}
- Root-mean-square alternating values, e.g. $I_{b(rms)}$ (or I_b, the use of $I_{b(rms)}$ is recommended)
- Peak-to-peak alternating values, e.g. $V_{o(p-p)}$.

Lower-case subscripts are also used in combination with upper-case subscripts to save otherwise necessary parentheses, e.g. V_{CEsat}.

1.3.4 ADDITIONAL RULES FOR SUBSCRIPTS

1.3.4.1 Subscripts for currents

If it is necessary to indicate the terminal carrying the current and after which the current is named, this shall be done by the first subscript with only the exceptions indicated below. The other terminal through which this is flowing may be indicated in the subscript immediately following the first terminal-designation subscript.

Examples of usual indication:

base current of a transistor: I_B, i_B, i_b, I_b

collector current of a transistor for $V_{BE} = 0$: I_{CES}

forward gate current of a field-effect transistor: I_{GF}

Exceptions: In letter symbols for forward or reverse gate currents of thyristors, the letter 'F' or 'R', respectively, precedes the terminal-designation subscript, which then becomes the second subscript, that is:

forward gate current of a thyristor: I_{FG}

reverse gate current of a thyristor: I_{RG}

1.3.4.2 Subscripts for voltages

If it is necessary to indicate the terminals between which a voltage exists, this shall be done by the first two subscripts with only the exceptions indicated below. The first subscript indicates one terminal and the second subscript indicates the reference terminal or circuit node. Where no ambiguity is likely to occur, the letter indicating the reference terminal may be omitted.

Examples of usual indication:

base-emitter voltage of a transistor:
V_{BE}, v_{BE}, v_{be}, V_{be} or V_B

collector-emitter voltage of a transistor for $V_{BE} = 0$: V_{CES}

forward gate-source voltage of a field-effect transistor:
V_{GSF}

Exceptions:

1. Forward gate-cathode voltage of a p-type thyristor:
   V_{FGK}

   Reverse gate-cathode voltage of a p-type thyristor:
   V_{RGK}

   Forward gate-anode voltage of an n-type thyristor:
   V_{FGA}

   Reverse gate-anode voltage of an n-type thyristor:
   V_{RGA}
2. In letter symbols for breakdown voltage, the subscript (BR) is placed before the terminal subscripts:

   collector-emitter breakdown voltage for $I_B = 0$:
   $V_{(BR)CEO}$

1.3.4.3 Subscripts for supply voltages or currents

Supply voltages or supply currents are indicated by repeating the appropriate terminal subscript.

Examples: V_{CC}, I_{EE}.

If it is necessary to indicate a reference terminal, this should be done by a third subscript.

Example: V_{CCE}.

1.3.4.4 Subscripts for devices with more than one terminal of the same kind

If a device has more than one terminal of the same kind, the subscript is formed by the appropriate letter for the terminal, followed by a number. In the case of multiple subscripts, hyphens may be necessary to avoid confusion.

Examples:

I_{B2} (continuous (DC) current flowing into the second base terminal)

V_{B2-E} (continuous (DC) voltage between the terminals of second base and emitter terminals).

1.3.4.5 Subscripts for multiple devices

For multiple unit devices, the subscripts are modified by a number preceding the letter subscript. In the case of multiple subscripts, hyphens may be necessary to avoid confusion.

Examples:

I_{2C} (continuous (DC) current flowing into the collector terminal of the second unit)

$V_{1C\text{-}2C}$ (continuous (DC) voltage between the collector terminals of the first and second units).

1.4 Summary chart for current, voltage and power letter symbols

Table 3 demonstrates the applications of the rules given in Sections 1.2 and 1.3 and can be used to identify letter symbols that are composed in accordance with these rules.

Table 3 Basic letter chart

BASIC LETTERS	
LOWER CASE (i, v, p)	**UPPER CASE (I, V, P)**
Lower case electrode or terminal subscript(s)	
With terminal subscript(s) only: • Instantaneous values of the varying component	With terminal subscript(s) only: • Root-mean-square value of alternating component (use of additional subscript (rms) is recommended
	With terminal subscript(s) and one of the following additional subscripts: • m: maximum instantaneous value of alternating component • min: minimum instantaneous value of alternating component • (rms): root-mean-square value of alternating component • (p-p): peak-to-peak value of alternating component
Upper case electrode or terminal subscript(s)	
With terminal subscript(s) only: • Instantaneous total value	With terminal subscript(s) only: • Value of a direct current or voltage (use of additional subscript (D) is recommended)
	With terminal subscript(s) and one of the following additional subscripts: • D: value of direct current or voltage • (AV): average total value • M: maximum instantaneous total value • MIN: minimum instantaneous total value • (RMS): root-mean-square total value • (P-P): peak-to-peak value of total value

1.5 Application of the rules

Figure 1 represents a transistor collector current as a function of time. It comprises a direct (DC) component (the average value) and an alternating component.

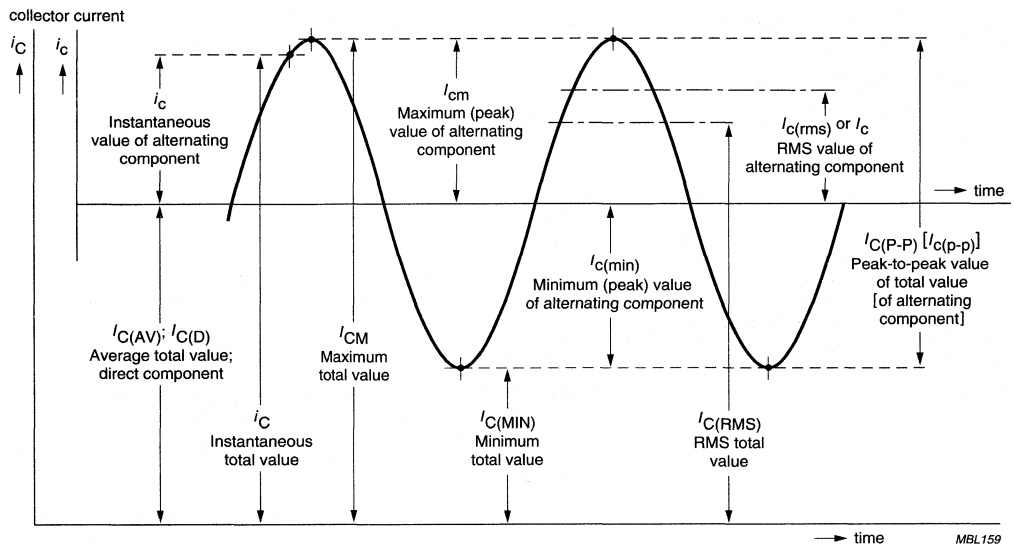

Fig.1 Example of the application of the rules to a periodic quantity

1.6 Indication of the polarity of currents and voltages

1.6.1 CURRENTS (THROUGH A TERMINAL)

1.6.1.1 Basic letter symbol

The basic letter symbol, when composed as detailed as in this document (Section 1.3.4.1), e.g. I_X denotes a conventional current that is considered to have a positive value if it flows from the external circuit into terminal X, or a negative value if it flows out of terminal X into the external circuit.

1.6.1.2 Negated letter symbol

The negated letter symbol, e.g. $-I_X$, denotes a conventional current that is considered to have a positive value if it flows out of terminal X into the external circuit, or a negative value if it flows from the external circuit into terminal X.

Remark: It follows by the application of algebraic rules that: $-I_X = 5$ A can be expressed as $I_X = -5$ A.

1.6.2 VOLTAGES (ACROSS TWO TERMINALS)

1.6.2.1 Basic letter symbol

The basic letter symbol, when composed as detailed in this document (Section 1.3.4.2), e.g. V_{XY} denotes a voltage that is considered to have a positive value if terminal X is at a positive potential with respect to terminal Y, or a negative value if terminal X is at a negative potential with respect to terminal Y.

1.6.2.2 Negated letter symbol

The negated letter symbol, e.g. $-V_{XY}$ denotes a voltage that is considered to have a positive value if terminal X is at a negative potential with respect to terminal Y, or a negative value if terminal X is at a positive potential with respect to terminal Y.

Remark: It follows by the application of algebraic rules that: $-V_{XY} = 5$ V can be expressed as $V_{XY} = -5$ V.

1.7 Letter symbols for electrical parameters

1.7.1 DEFINITION

For the purpose of this publication, the term 'electrical parameter' applies to four-pole matrix parameters, elements of electrical equivalent circuits, electrical impedances and admittances, inductances and capacitances.

1.7.2 BASIC LETTERS

Table 4 comprises the most important basic letters used for electrical parameters of semiconductor devices.

Table 4 Recommended basic letters

SYMBOL	DESCRIPTION
B, b	susceptance; imaginary part of an admittance (y) four-pole matrix parameter
C	capacitance
G, g	conductance; real part of an admittance (y) four-pole matrix parameter
H, h	hybrid (h) four-pole matrix parameter
L	inductance
R, r	resistance; real part of an impedance (z) four-pole matrix parameter
X, x	reactance; imaginary part of an impedance (z) four-pole matrix parameter
Y, y	admittance; admittance (y) four-pole matrix parameter
Z, z	impedance; impedance (z) four-pole matrix parameter

1.7.2.1 Use of upper and lower-case letters

Upper-case letters are used for the representation of:

- Electrical parameters of external circuits and of circuits in which the device forms only a part
- All inductances and capacitances.

Lower-case letters are used for the representation of electrical parameters inherent in the device, with the exception of inductances and capacitances.

1.7.3 SUBSCRIPTS

1.7.3.1 General subscripts

Table 5 comprises the most important general subscripts used for electrical parameters of semiconductor devices.

Table 5 Recommended general subscripts

SUBSCRIPT	DESCRIPTION
F, f	forward; forward transfer
I, i	input
O, o	output
R, r	reverse; reverse transfer; rise; reference point
T	depletion layer
11	input (1)
22	output (1)
12	reverse transfer (1)
21	forward transfer (1)
1	input (2)
2	output (2)

Notes

1. Applicable to four-pole matrix parameters only.
2. Applicable to all electrical parameters except four-pole matrix parameters.

Examples: Z_i, h_f, h_F.

1.7.3.2 Choice between upper-case and lower-case subscripts

Where Section 1.7.3.1 lists both upper-case and lower-case letters, the choice between these two styles shall be made according to Section 1.7.3.3 hereafter. If more than one subscript is used, subscripts for which both styles exist shall either be **all** upper-case or **all** lower case.

Examples: h_{FE}, y_{RE}, h_{fe}, but C_{Te} (T has no lower-case variant).

1.7.3.3 Use of upper and lower-case subscripts

The upper-case variant of a subscript is used for the designation of static (DC) values.

Examples:

h_{FE} (static value of forward current transfer ratio in common-emitter configuration; DC current gain)

R_E (DC value of the external emitter resistance)

The lower-case variant of a subscript is used for the designation of small-signal values.

Examples:

h_{fe} (small-signal value of the short-circuit forward current transfer ratio in common-emitter configuration)

$Z_e = R_e + jX_e$ (small-signal value of the external impedance).

1.7.3.4 Subscripts for four-pole matrix parameters

The first letter subscript (or double numeric subscript) indicates input, output, forward transfer or reverse transfer.

Examples: h_i (or h_{11}), h_o (or h_{22}), h_f (or h_{21}), h_r (or h_{12}).

A further subscript is used for the identification of the circuit configuration. When no confusion is possible, this further subscript may be omitted.

Examples: h_{fe} (or h_{21e}), h_{FE} (or h_{21E}).

If only h_f is written, the circuit configuration must be understood. If only h_{21} is written, the circuit configuration must be understood as well as the kind of parameter (small-signal or static value).

1.7.3.5 Distinction between real and imaginary parts

If it is necessary to distinguish between real and imaginary parts of electrical parameters, no additional subscripts should be used. If basic symbols for the real and imaginary parts exist, these may be used.

Examples: $Z_i = R_i + jX_i$, $y_{fe} = g_{fe} + jb_{fe}$.

If such symbols do not exist, or if they are not suitable, the following notation is used:

Re (h_{ib}) etc. for the real part of h_{ib}

Im (h_{ib}) etc. for the imaginary part of h_{ib}.

1.8 Letter symbols for other quantities

1.8.1 General

Where the following Sections do not give recommendations for a letter symbol, the general recommendations (see IEC Publication 60027) should be followed. If there are no IEC recommendations, the appropriate ISO recommendations should be followed.

1.8.2 Times, durations

The basic letter symbol is:

t

example: t_r (rise time)

1.8.3 Thermal characteristics and related temperatures

1.8.3.1 Basic letter symbol for temperature

The basic letter symbol is:

T , indicating either Celsius or Kelvin temperature.

example: T_{amb} = 25 °C, T_{op} = 295 K.

Remark: The use of the lower-case letter '**t**' is strongly deprecated.

1.8.3.2 General subscripts

Table 6 Recommended general subscripts

SUBSCRIPT	DESCRIPTION
a, A	ambient (1)
c, C	case (1)
f, F	cooling fluid, other than air
j, J	junction (2)
op	operating (3)
r, R	reference point (1)
h	heatsink
mb	mounting base
sb	substrate
sld	soldering
stg	storage
tp	tie-point
th	thermal

Notes

1. The use of longer subscripts as '**case**', '**ref**' and '**amb** is deprecated. If they are used for thermal resistances or impedances, the subscripts shall be separated by hyphens and put in brackets (parenthesis) as shown in the following example: $R_{th(j-a)}$.
2. In data sheets, specifications **always** refer to the **virtual** junction (channel) temperature. Therefore, the letter '**v**' in the subscript may be **omitted**.
3. In letter symbols for operating temperatures, e.g. as in $T_{amb(op)}$ for 'operating ambient temperature', the subscript '(op)' is usually omitted in data sheets if no ambiguity is likely to occur.

1.8.3.3 Composed letter symbols for thermal resistances and impedances

In the letter symbols below, the letters x, y, or X, Y stand for the subscripts that denote the points or regions between which the terminal resistance or impedance extends. These subscripts should be taken from Table 6.

Thermal resistance basic forms:

$R_{th(x-y)}$ or $R_{th(X-Y)}$

examples: $R_{th(j-a)}$, $R_{th(j-mb)}$, $R_{th(h-a)}$

Transient thermal impedance basic forms:

$Z_{th(x-y)}$ or $Z_{th(X-Y)}$

example: $Z_{th(j-mb)}$, $Z_{th(j-a)}$

Transient thermal impedance under pulsed conditions basic forms:

$Z_{thp(x-y)}$ or $Z_{thp(X-Y)}$

example: $Z_{thp(j-mb)}$, $Z_{thp(j-a)}$

1.8.4 FREQUENCIES

The basic letter symbol is:

f

example: f_{osc} (oscillator frequency)

1.8.5 SUNDRY QUANTITIES

Table 7 Recommended quantities and their letter symbols

DESCRIPTION	SYMBOL
Thermal derating factor	K_t
Average noise figure, average noise factor	$\overline{F}$, $F_{(AV)}$
Spot noise figure, spot noise factor	F
Output noise ratio	N_r
Equivalent input noise voltage (of a two-port)	V_n
Equivalent input noise current (of a two-port)	I_n
Noise temperature	T_n
Reference noise temperature	T_o/T_{no}

1.9 Letter symbols for logarithmic scale units for signal ratios expressed in dB

1.9.1 POWER RATIO

The letter symbol (unit) 'dB' is used for the logarithmic scale unit when the logarithm to the base of ten of the ratio of two amounts of power is expressed in decibels using the expression:

$n = 10 \log (P_1/P_2)$ dB

Remark: In principle, the unit 'dB' shall only be used for a ratio of powers, but see also the remark in Section 1.9.2.

1.9.2 VOLTAGE RATIO (OR CURRENT RATIO)

The letter symbol 'dB(V)' (or 'dB(I)') is used for the logarithmic scale unit when the logarithm to the base of ten of the ratio of two amounts of voltage (or current) is expressed in decibels using the expressions:

$n = 20 \log (V_1/V_2)$ dB(V)

or $n = 20 \log (I_1/I_2)$ dB(I)

Remark: When, and only when, the resistances appertaining to V_1 and V_2 (or I_1 and I_2) are equal or negligible difference, the numerical value calculated from the expressions may be labelled with dB because application of the power ratio expression in Section 1.9.1 to the corresponding powers results in the same value of 'n'.

MAGNETORESISTIVE SENSORS FOR MAGNETIC FIELD MEASUREMENT

Magnetoresistive sensors for magnetic field measurement

General

CONTENTS

General field measurement

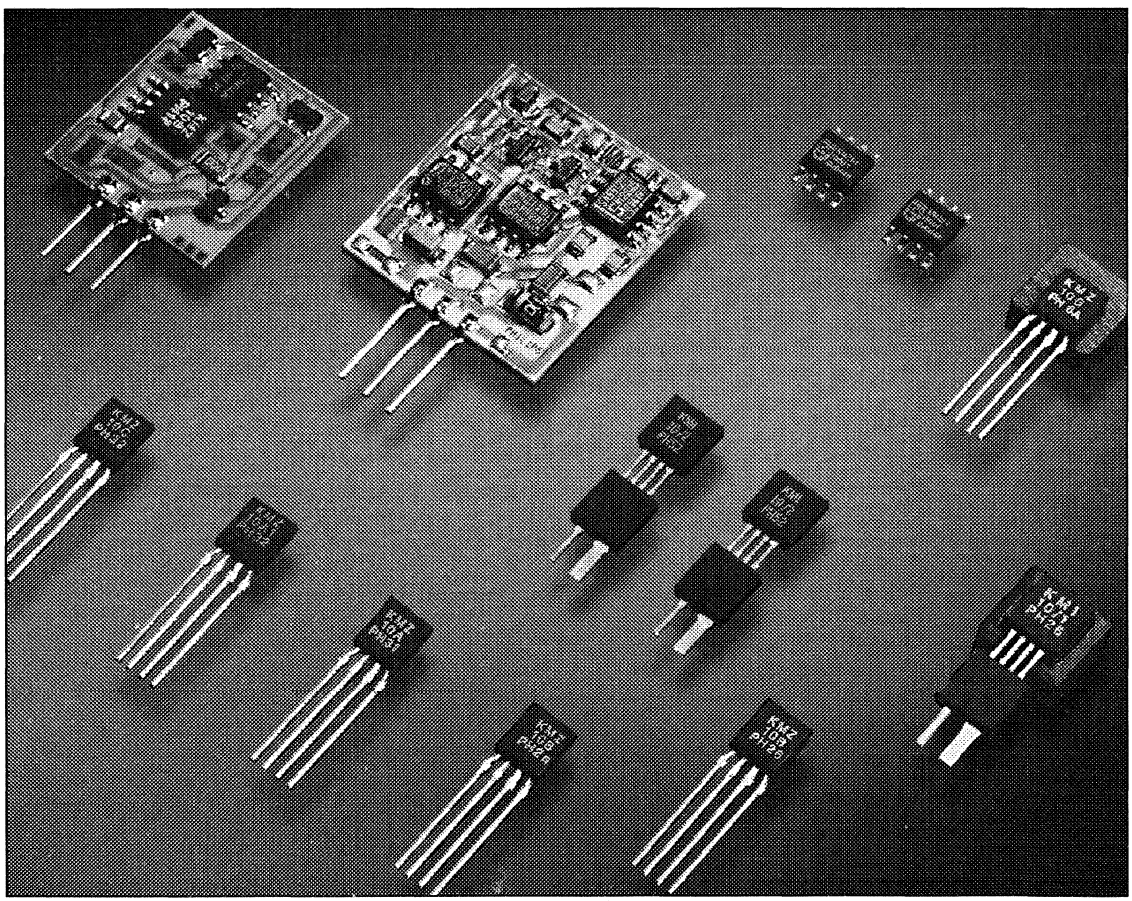

Magnetoresistive sensors for magnetic field measurement

The KMZ range of magnetoresistive sensors is characterized by high sensitivity in the detection of magnetic fields, a wide operating temperature range, a low and stable offset and low sensitivity to mechanical stress. They therefore provide an excellent means of measuring both linear and angular displacement under extreme environmental conditions, because their very high sensitivity means that a fairly small movement of actuating components in, for example, cars or machinery (gear wheels, metal rods, cogs, cams, etc.) can create measurable changes in magnetic field. Other applications for magnetoresistive sensors include rotational speed measurement and current measurement.

Examples where their properties can be put to good effect can be found in automotive applications, such as wheel speed sensors for ABS and motor management systems and position sensors for chassis position, throttle and pedal position measurement. Other examples include instrumentation and control equipment, which often require position sensors capable of detecting displacements in the region of tenths of a millimetre (or even less), and in electronic ignition systems, which must be able to determine the angular position of an internal combustion engine with great accuracy.

Finally, because of their high sensitivity, magnetoresistive sensors can measure very weak magnetic fields and are thus ideal for application in electronic compasses, earth field correction and traffic detection.

If the KMZ sensors are to be used to maximum advantage, however, it is important to have a clear understanding of their operating principles and characteristics, and how their behaviour may be affected by external influences and by their magnetic history.

Operating principles

Magnetoresistive (MR) sensors make use of the magnetoresistive effect, the property of a current-carrying magnetic material to change its resistivity in the presence of an external magnetic field (the common units used for magnetic fields are given in Table 1).

Table 1 Common magnetic units

1 kA/m = 1.25 mTesla (in air)
1 mT = 10 Gauss

The basic operating principle of an MR sensor is shown in Fig.2.

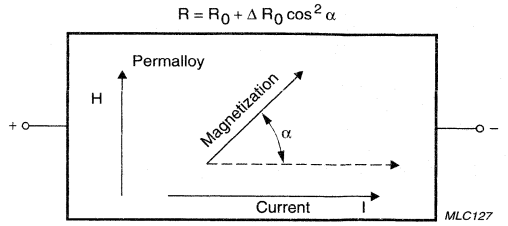

Fig.2 The magnetoresistive effect in permalloy.

Figure 2 shows a strip of ferromagnetic material, called permalloy (20% Fe, 80% Ni). Assume that, when no external magnetic field is present, the permalloy has an internal magnetization vector parallel to the current flow (shown to flow through the permalloy from left to right). If an external magnetic field H is applied, parallel to the plane of the permalloy but perpendicular to the current flow, the internal magnetization vector of the permalloy will rotate around an angle α. As a result, the resistance of R of the permalloy will change as a function of the rotation angle α, as given by:

$$R = R_O + \Delta R_O \cos^2 \alpha \qquad (1)$$

R_0 and ΔR_0 are material parameters and to achieve optimum sensor characteristics Philips use Ni19Fe81, which has a high R_0 value and low magnetostriction. With this material, ΔR_0 is of the order of 3%. For more information on materials, see Appendix 1.

It is obvious from this quadratic equation, that the resistance/magnetic field characteristic is non-linear and in addition, each value of R is not necessarily associated with a unique value of H (see Fig.3). For more details on the essentials of the magnetoresistive effect, please refer to the Section "Further information for advanced users" later in this chapter or Appendix 1, which examines the MR effect in detail.

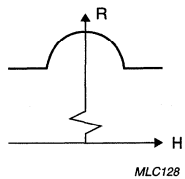

Fig.3 The resistance of the permalloy as a function of the external field.

In this basic form, the MR effect can be used effectively for angular measurement and some rotational speed measurements, which do not require linearization of the sensor characteristic.

In the KMZ series of sensors, four permalloy strips are arranged in a meander fashion on the silicon (Fig.4 shows one example, of the pattern on a KMZ10). They are connected in a Wheatstone bridge configuration, which has a number of advantages:

- Reduction of temperature drift
- Doubling of the signal output
- The sensor can be aligned at the factory.

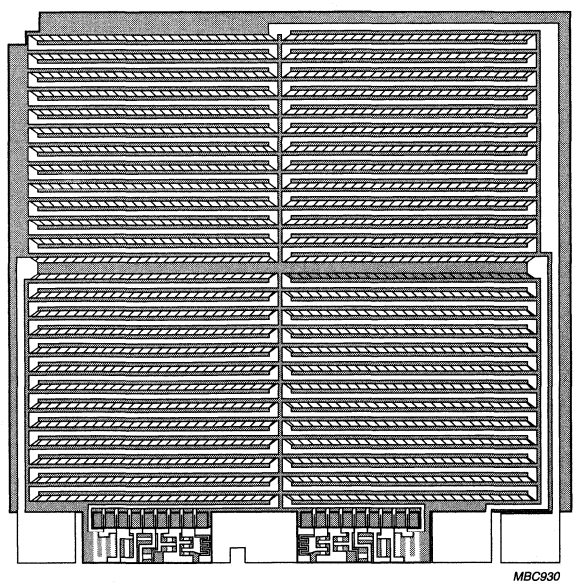

Fig.4 KMZ10 chip structure.

Two further resistors, R_T, are included, as shown in Fig.5. These are for trimming sensor offset down to (almost) zero during the production process.

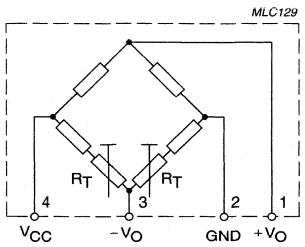

Fig.5 Bridge configuration with offset trimmed to zero, by resistors R_T.

For some applications however, the MR effect can be used to its best advantage when the sensor output characteristic has been linearized. These applications include:

- Weak field measurements, such as compass applications and traffic detection;
- Current measurement; and
- Rotational speed measurement.

For an explanation of how the characteristic is linearized, please refer to the Section "Further information for advanced users" later in this chapter.

Philips magnetoresistive sensors

Based on the principles described, Philips has a family of basic magnetoresistive sensors. The main characteristics of the KMZ sensors are given in Table 2.

Table 2 Main characteristics of Philips sensors

SENSOR TYPE	PACKAGE	FIELD RANGE (kA/m)(1)	V_{CC} (V)	SENSITIVITY $\frac{(mV/V)}{(kA/m)}$	R_{bridge} (kΩ)	LINEARIZE MR EFFECT	APPLICATION EXAMPLES
KMZ10A	SOT195	−0.5 to +0.5	≤9	16.0	1.2	Yes	compass, navigation, metal detection, traffic control
KMZ10A1(2)	SOT195	−0.05 to +0.05	≤9	22.0	1.3	Yes	
KMZ10B	SOT195	−2.0 to +2.0	≤12	4.0	2.1	Yes	current measurement, angular and linear position, reference mark detection, wheel speed
KMZ10C	SOT195	−7.5 to +7.5	≤10	1.5	1.4	Yes	
KMZ51	SO8	−0.2 to +0.2	≤8	16.0	2.0	Yes	compass, navigation, metal detection, traffic control
KMZ52	SO16	−0.2 to +0.2	≤8	16.0	2.0	Yes	

Notes

1. In air, 1 kA/m corresponds to 1.25 mT.
2. Data given for operation with switched auxiliary field.

Flipping

The internal magnetization of the sensor strips has two stable positions. So, if for any reason the sensor is influenced by a powerful magnetic field opposing the internal aligning field, the magnetization may flip from one position to the other, and the strips become magnetized in the opposite direction (from, for example, the '+x' to the '–x' direction). As demonstrated in Fig.6, this can lead to drastic changes in sensor characteristics.

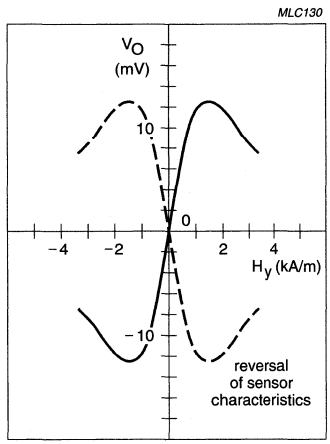

Fig.6 Sensor characteristics.

The field (e.g. '$-H_x$') needed to flip the sensor magnetization, and hence the characteristic, depends on the magnitude of the transverse field 'H_y': the greater the field 'H_y', the smaller the field '$-H_x$'. This follows naturally, since the greater the field 'H_y', the closer the magnetization's rotation approaches 90°, and hence the easier it will be to flip it into a corresponding stable position in the '–x' direction.

Looking at the curve in Fig.7 where H_y = 0.5 kA/m, for such a low transverse field the sensor characteristic is stable for all positive values of H_x and a reverse field of ≈1 kA/m is required before flipping occurs. At H_y = 2 kA/m however, the sensor will flip even at smaller values of 'H_x' (at approximately 0.5 kA/m).

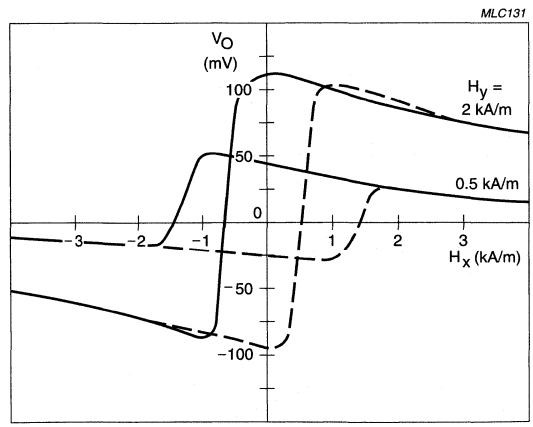

Fig.7 Sensor output 'V_o' as a function of the auxiliary field 'H_x' for several values of transverse field 'H_y'.

Figure 7 also shows that the flipping itself is not instantaneous, because not all the permalloy strips flip at the same rate. In addition, it illustrates the hysteresis effect exhibited by the sensor. For more information on sensor flipping, see Appendix 2 of this chapter.

Effect of temperature on behaviour

Figure 8 shows that the bridge resistance increases linearly with temperature, due to the bridge resistors' temperature dependency (i.e. the permalloy) for a typical KMZ10B sensor. The data sheets show also the spread in this variation due to manufacturing tolerances and this should be taken into account when incorporating the sensors into practical circuits.

In addition to the bridge resistance, the sensitivity also varies with temperature. This can be seen from Fig.9, which plots output voltage against transverse field 'H_y' for various temperatures. Figure 9 shows that sensitivity falls with increasing temperature (actual values for given for every sensor in the datasheets). The reason for this is rather complex and is related to the energy-band structure of the permalloy strips.

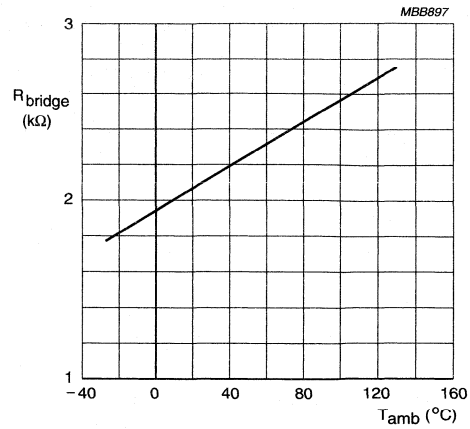

Fig.8 Bridge resistance of a KMZ10B sensor as a function of ambient temperature.

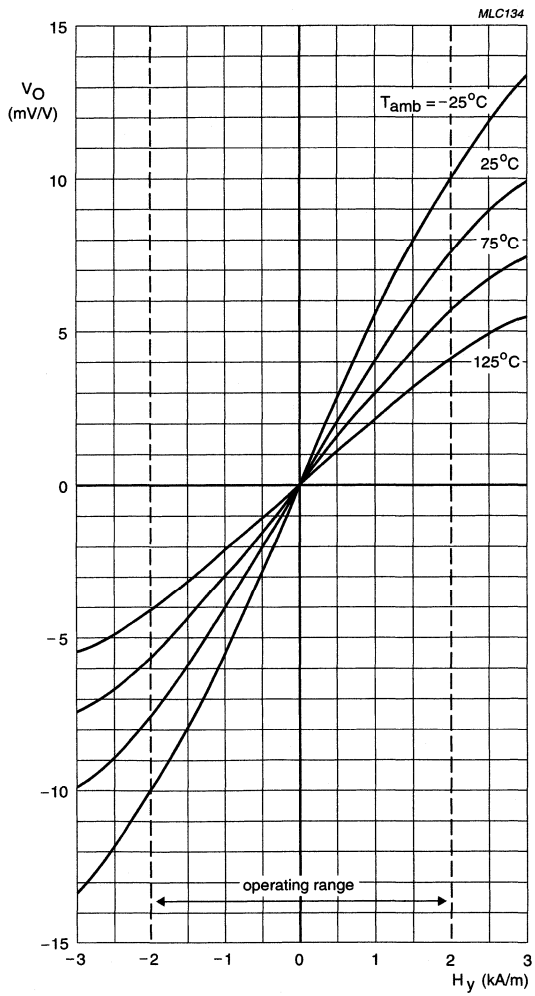

Fig.9 Output voltage 'V_o' as a fraction of the supply voltage of a KMZ10B sensor as a function of transverse field 'H_y' for several temperatures.

Figure 10 is similar to Fig.9, but with the sensor powered by a constant current supply. Figure 10 shows that, in this case, the temperature dependency of sensitivity is significantly reduced. This is a direct result of the increase in bridge resistance with temperature (see Fig.8), which partly compensates the fall in sensitivity by increasing the voltage across the bridge and hence the output voltage. Figure 8 demonstrates therefore the advantage of operating with constant current.

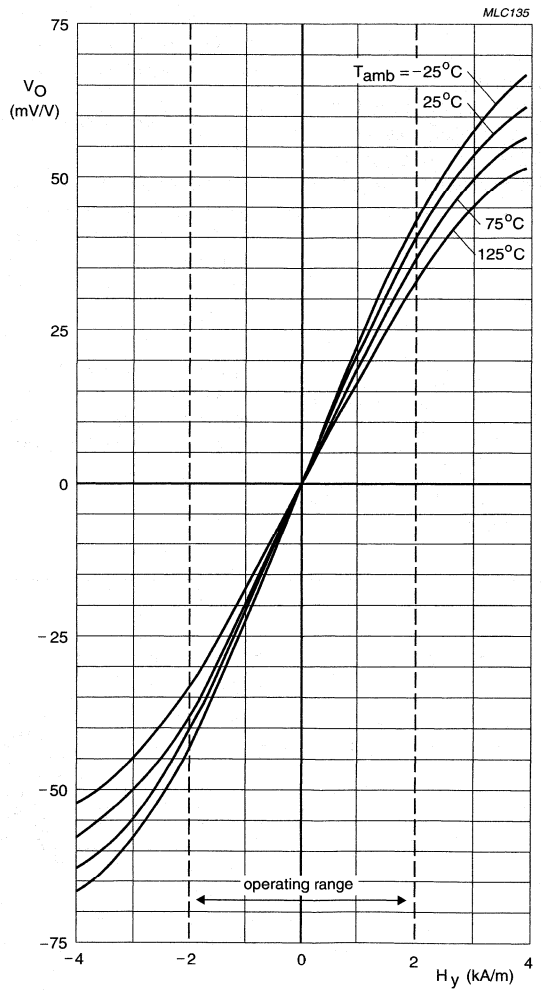

Fig.10 Output voltage 'V_o' of a KMZ10B sensor as a function of transverse field 'H_y' for several temperatures.

Using magnetoresistive sensors

The excellent properties of the KMZ magnetoresistive sensors, including their high sensitivity, low and stable offset, wide operating temperature and frequency ranges and ruggedness, make them highly suitable for use in a wide range of automotive, industrial and other applications. These are looked at in more detail in other chapters in this book; some general practical points about using MR sensors are briefly described below.

Analog application circuitry

In many magnetoresistive sensor applications where analog signals are measured (in measuring angular position, linear position or current measurement, for example), a good application circuit should allow for sensor offset and sensitivity adjustment. Also, as the sensitivity of many magnetic field sensors has a drift with temperature, this also needs compensation. A basic circuit is shown in Fig.11.

In the first stage, the sensor signal is pre-amplified and offset is adjusted. After temperature effects are compensated, final amplification and sensitivity adjustment takes place in the last stage. This basic circuit can be extended with additional components to meet specific EMC requirements or can be modified to obtain customized output characteristics (e.g. a different output voltage range or a current output signal).

Philips magnetoresistive sensors have a linear sensitivity drift with temperature and so a temperature sensor with linear characteristics is required for compensation. Philips KTY series are well suited for this purpose, as their positive Temperature Coefficient (TC) matches well with the negative TC of the MR sensor. The degree of compensation can be controlled with the two resistors R7 and R8 and special op-amps, with very low offset and temperature drift, should be used to ensure compensation is constant over large temperature ranges.

Please refer to part 2 of this book for more information on the KTY temperature sensors; see also the Section "Further information for advanced users" later in this chapter for a more detailed description of temperature compensation using these sensors.

Using magnetoresistive sensors with a compensation coil

For general magnetic field or current measurements it is useful to apply the 'null-field' method, in which a magnetic field (generated by a current carrying coil), equal in magnitude but opposite in direction, is applied to the sensor. Using this 'feedback' method, the current through the coil is a direct measure of the unknown magnetic field amplitude and it has the advantage that the sensor is being operated at its zero point, where inaccuracies as result of tolerances, temperature drift and slight non-linearities in the sensor characteristics are insignificant. A detailed discussion of this method is covered in Chapter "Weak field measurement".

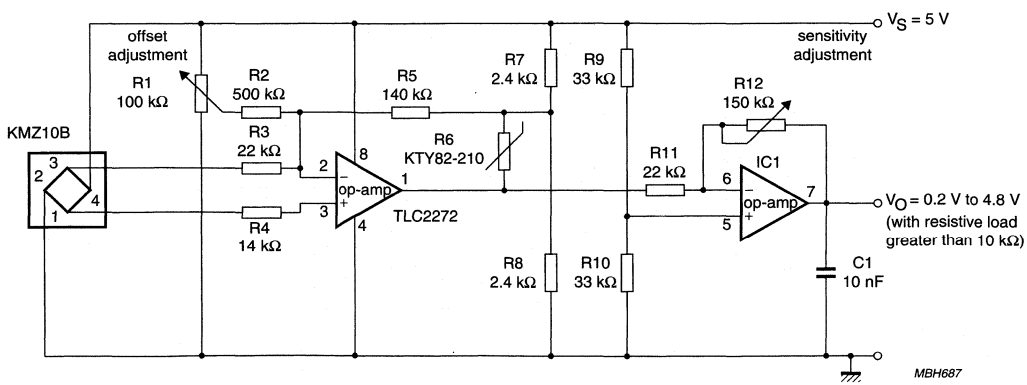

Fig.11 Basic application circuit with temperature compensation and offset adjustment.

Further information for advanced users

THE MR EFFECT

In sensors employing the MR effect, the resistance of the sensor under the influence of a magnetic field changes as it is moved through an angle α as given by:

$$R = R_O + \Delta R_O \cos^2\alpha \quad (2)$$

It can be shown that

$$\sin^2\alpha = \frac{H^2}{H_O^2} \text{ for } H \leq H_O \quad (3)$$

and

$$\sin^2\alpha = 1 \text{ for } H > H_O \quad (4)$$

where H_o can be regarded as a material constant comprising the so called demagnetizing and anisotropic fields.

Applying equations (3) and (4) to equation (2) leads to:

$$R = R_O + \Delta R_O\left(1 - \frac{H^2}{H_O^2}\right) \text{ for } H \leq H_0 \quad (5)$$

$$R = R_O \text{ for } H > H_O \quad (6)$$

which clearly shows the non-linear nature of the MR effect.

More detailed information on the derivation of the formulae for the MR effect can be found in Appendix 1.

LINEARIZATION

The magnetoresistive effect can be linearized by depositing aluminium stripes (Barber poles), on top of the permalloy strip at an angle of 45° to the strip axis (see Fig.12). As aluminium has a much higher conductivity than permalloy, the effect of the Barber poles is to rotate the current direction through 45° (the current flow assumes a 'saw-tooth' shape), effectively changing the rotation angle of the magnetization relative to the current from α to $\alpha - 45°$.

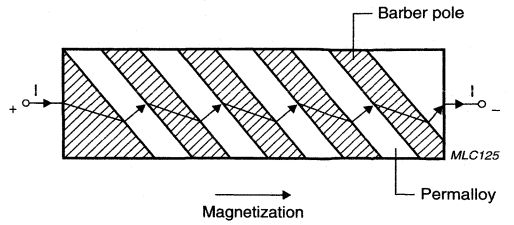

Fig.12 Linearization of the magnetoresistive effect.

A Wheatstone bridge configuration is also used for linearized applications. In one pair of diagonally opposed elements, the Barber poles are at +45° to the strip axis, while in another pair they are at –45°. A resistance increase in one pair of elements due to an external magnetic field is thus 'matched' by a decrease in resistance of equal magnitude in the other pair.
The resulting bridge imbalance is then a linear function of the amplitude of the external magnetic field in the plane of the permalloy strips, normal to the strip axis.

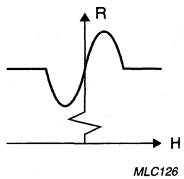

Fig.13 The resistance of the permalloy as a function of the external field H after linearization (compare with Fig.6).

For sensors using Barber poles arranged at an angle of +45° to the strip axis, the following expression for the sensor characteristic can be derived (see Appendix 1 on the MR effect):

$$R = R_O + \frac{\Delta R_O}{2} + \Delta R_O\left(\frac{H}{H_O}\right)\sqrt{1 - \frac{H^2}{H_O^2}} \quad (7)$$

The equation is linear where $H/H_o = 0$, as shown in Fig.7. Likewise, for sensors using Barber poles arranged at an angle of –45°, the equation derives to:

$$R = R_O + \frac{\Delta R_O}{2} - \Delta R_O\left(\frac{H}{H_O}\right)\sqrt{1 - \frac{H^2}{H_0^2}} \quad (8)$$

This is the mirror image of the characteristic in Fig.7. Hence using a Wheatstone bridge configuration ensures the any bridge imbalance is a linear function of the amplitude of the external magnetic field.

FLIPPING

As described in the body of the chapter, Fig.7 shows that flipping is not instantaneous and it also illustrates the hysteresis effect exhibited by the sensor. This figure and Fig.14 also shows that the sensitivity of the sensor falls with increasing 'H_x'. Again, this is to be expected since the moment imposed on the magnetization by 'H_x' directly opposes that imposed by 'H_y', thereby reducing the degree of bridge imbalance and hence the output signal for a given value of 'H_y'.

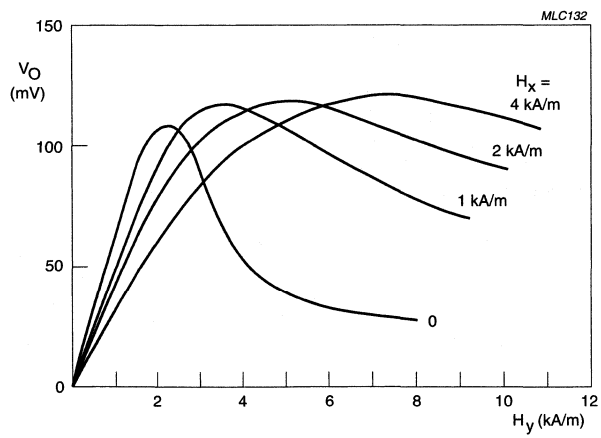

Fig.14 Sensor output 'V_o' as a function of the transverse field 'H_y' for several values of auxiliary field 'H_x'.

The following general recommendations for operating the KMZ10 can be applied:

- To ensure stable operation, avoid operating the sensor in an environment where it is likely to be subjected to negative external fields ('$-H_x$'). Preferably, apply a positive auxiliary field ('H_x') of sufficient magnitude to prevent any likelihood of flipping within he intended operating range (i.e. the range of 'H_y').
- Before using the sensor for the first time, apply a positive auxiliary field of at least 3 kA/m; this will effectively erase the sensor's magnetic 'history' and will ensure that no residual hysteresis remains (refer to Fig.6).
- Use the minimum auxiliary field that will ensure stable operation, because the larger the auxiliary field, the lower the sensitivity, but the actual value will depend on the value of H_d. For the KMZ10B sensor, a minimum auxiliary field of approximately 1 kA/m is recommended; to guarantee stable operation for all values of H_d, the sensor should be operated in an auxiliary field of 3 kA/m.

These recommendations (particularly the first one) define a kind of Safe Operating ARea (SOAR) for the sensors. This is illustrated in Fig.15, which is an example (for the KMZ10B sensor) of the SOAR graphs to be found in our data sheets.

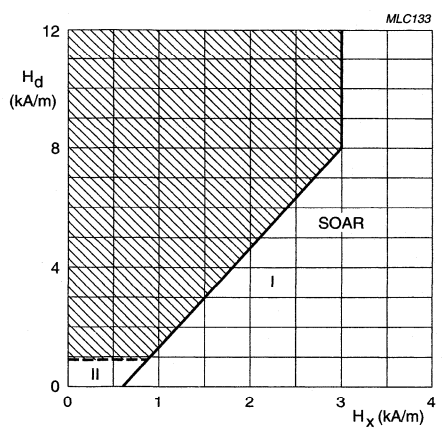

Fig.15 SOAR of a KMZ10B sensor as a function of auxiliary field 'H_x' and disturbing field 'H_d' opposing 'H_x' (area I).

The greater the auxiliary field, the greater the disturbing field that can be tolerated before flipping occurs.
For auxiliary fields above 3 kA/m, the SOAR graph shows that the sensor is completely stable, regardless of the magnitude of the disturbing field. It can also be seen from this graph that the SOAR can be extended for low values of 'H_y'. In Fig.15, (for the KMZ10B sensor), the extension for $H_y < 1$ kA/m is shown.

Temperature compensation

With magnetoresistive sensors, temperature drift is negative. Two circuits manufactured in SMD-technology which include temperature compensation are briefly described below.

The first circuit is the basic application circuit already given (see Fig.11). It provides average (sensor-to-sensor) compensation of sensitivity drift with temperature using the KTY82-210 silicon temperature sensor. It also includes offset adjustment (via R1); gain adjustment is performed with a second op-amp stage. The temperature sensor is part of the amplifier's feedback loop and thus increases the amplification with increasing temperature.

The temperature dependant amplification A and the temperature coefficient TC_A of the first op-amp stage are approximately:

$$A = \frac{R_5}{R_3}\left(1 + \frac{2R_T}{R_7}\right) \text{ for } R_8 = R_7$$

$$TC_A = \frac{TC_{KTY}}{1 + \frac{R_7}{2R_T}} \text{ for } R_8 = R_7$$

R_T is the temperature dependent resistance of the KTY82. The values are taken for a certain reference temperature. This is usually 25 °C, but in other applications a different reference temperature may be more suitable.

Figure 16 shows an example with a commonly-used instrumentation amplifier. The circuit can be divided into two stages: a differential amplifier stage that produces a symmetrical output signal derived from the magnetoresistive sensor, and an output stage that also provides a reference to ground for the amplification stage.

To compensate for the negative sensor drift, as with the above circuit the amplification is again given an equal but positive temperature coefficient, by means of a KTY81-110 silicon temperature sensor in the feedback loop of the differential amplifier.

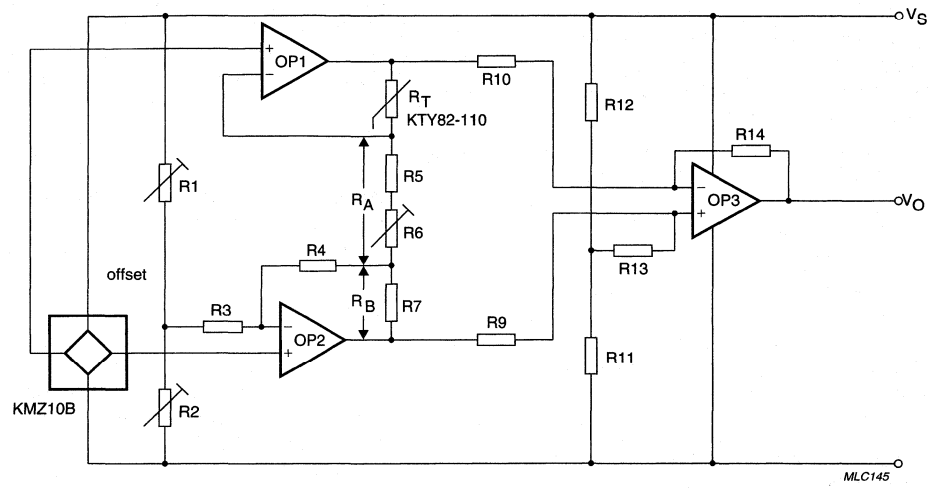

Fig.16 KMZ10B application circuit with instrumentation amplifier.

The amplification of the input stage ('OP1' and 'OP2') is given by:

$$A1 = 1 + \frac{R_T + R_B}{R_A} \quad (9)$$

where R_T is the temperature dependent resistance of the KTY82 sensor and R_B is the bridge resistance of the magnetoresistive sensor.

The amplification of the complete amplifier can be calculated by:

$$A = A1 \times \frac{R_{14}}{R_{10}} \quad (10)$$

The positive temperature coefficient (TC) of the amplification is:

$$TC_A = \frac{R_T \times TC_{KTY}}{R_A + R_B + R_T} \quad (11)$$

For the given negative 'TC' of the magnetoresistive sensor and the required amplification of the input stage 'A1', the resistance 'R_A' and 'R_B' can be calculated by:

$$R_B = R_T \times \left(\frac{TC_{KTY}}{TC_A} \times \left(1 - \frac{1}{A1} \right) - 1 \right) \quad (12)$$

$$R_A = \frac{R_T + R_B}{A1 - 1} \quad (13)$$

where TC_{KTY} is the temperature coefficient of the KTY sensor and TC_A is the temperature coefficient of the amplifier. This circuit also provides for adjustment of gain and offset voltage of the magnetic-field sensor.

APPENDIX 1: THE MAGNETORESISTIVE EFFECT

Magnetoresistive sensors make use of the fact that the electrical resistance ρ of certain ferromagnetic alloys is influenced by external fields. This solid-state magnetoresistive effect, or anisotropic magnetoresistance, can be easily realized using thin film technology, so lends itself to sensor applications.

Resistance- field relation

The specific resistance ρ of anisotropic ferromagnetic metals depends on the angle Θ between the internal magnetization M and the current I, according to:

$$\rho(\Theta) = \rho_{\perp} + (\rho_{\perp} - \rho_{\parallel}) \cos^2 \Theta \quad (1)$$

where $\rho_{\perp}$ and $\rho_{\parallel}$ are the resistivities perpendicular and parallel to M. The quotient $(\rho_{\perp} - \rho_{\parallel})/\rho_{\perp} = \Delta\rho/\rho$ is called the magnetoresistive effect and may amount to several percent.

Sensors are always made from ferromagnetic thin films as this has two major advantages over bulk material: the resistance is high and the anisotropy can be made uniaxial. The ferromagnetic layer behaves like a single domain and has one distinguished direction of magnetization in its plane called the easy axis (e.a.), which is the direction of magnetization without external field influence.

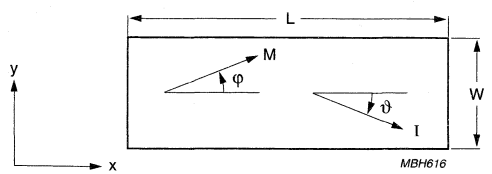

Fig.17 Geometry of a simple sensor.

Figure 17 shows the geometry of a simple sensor where the thickness (t) is much smaller than the width (w) which is in turn, less than the length (l) (i.e. t « w ‹ l). With the current (I) flowing in the x-direction (i.e. q = 0 or Q = f) then the following equation can be obtained from equation 1:

$$R = R_0 + DR \cos^2 f(2)$$

and with a constant current I, the voltage drop in the x-direction U_x becomes:

$$U_x = \rho_{\perp} I \left(\frac{L}{wt}\right)\left(1 + \left(\frac{\Delta\rho}{\rho}\right)\cos^2\phi\right) \quad (3)$$

Besides this voltage, which is directly allied to the resistance variation, there is a voltage in the y-direction, U_y, given by:

$$U_y = \rho_{\perp} I \left(\frac{1}{t}\right)\left(\frac{\Delta\rho}{\rho}\right)\sin\phi\cos\phi \quad (4)$$

This is called the planar or pseudo Hall effect; it resembles the normal or transverse Hall effect but has a physically different origin.
All sensor signals are determined by the angle ϕ between the magnetization M and the 'length' axis and, as M rotates under the influence of external fields, these external fields thus directly determine sensor signals. We can assume that the sensor is manufactured such that the e.a. is in the x-direction so that without the influence of external fields, M only has an x-component ($\phi = 0^{\circ}$ or 180°).

Two energies have to be introduced when M is rotated by external magnetic fields: the anisotropy energy and the demagnetizing energy. The anisotropy energy E_k, is given by the crystal anisotropy field H_k, which depends on the material and processes used in manufacture. The demagnetizing energy E_d or form anisotropy depends on the geometry and this is generally a rather complex relationship, apart from ellipsoids where a uniform demagnetizing field H_d may be introduced. In this case, for the sensor set-up in Fig.17.

$$H_d \approx \frac{t}{w}\left(\frac{M_s}{\mu_0}\right) \quad (5)$$

where the demagnetizing factor N – t/w, the saturation magnetization $M_s \approx 1$ T and the induction constant $\mu 0 = 4\pi^{-7}$ Vs/Am.

The field $H_0 - H_k + t/w(M_0/m_0)$ determines the measuring range of a magnetoresistive sensor, as f is given by:

$$\sin\phi = \frac{H_y}{H_o + \frac{H_x}{\cos\phi}} \quad (6)$$

where $|H_y| \leq |H_0 + H_x|$ and H_x and H_y are the components of the external field. In the simplest case $H_x = 0$, the voltages U_x and U_y become:

$$U_x = \rho_\perp I \left(\frac{L}{wt}\right)\left(1 + \left(\frac{\Delta\rho}{\rho}\right)\left(1 - \left(\frac{H_y}{H_0}\right)^2\right)\right) \quad (7)$$

$$U_y = \rho_\perp I \left(\frac{1}{t}\right)\left(\frac{\Delta\rho}{\rho}\right)\left(\frac{H_y}{H_0}\right)\sqrt{1 - (H_y/H_0)^2} \quad (8)$$

(Note: if $H_x = 0$, then H_0 must be replaced by $H_0 + H_x/\cos\phi$).

Neglecting the constant part in U_x, there are two main differences between U_x and U_y:

1. The magnetoresistive signal U_x depends on the square of H_y/H_0, whereas the Hall voltage U_y is linear for $H_y \ll H_0$.
2. The ratio of their maximum values is L/w; the Hall voltage is much smaller as in most cases L » w.

Magnetization of the thin layer

The magnetic field is in reality slightly more complicated than given in equation (6). There are two solutions for angle ϕ:
$\phi 1 < 90°$ and $\phi 2 > 90°$ (with $\phi 1 + \phi 2 = 180°$ for $H_x = 0$).

Replacing ϕ by $180° - \phi$ has no influence on U_x except to change the sign of the Hall voltage and also that of most linearized magnetoresistive sensors.
Therefore, to avoid ambiguity either a short pulse of a proper field in the x-axis ($|H_x| > H_k$) with the correct sign must be applied, which will switch the magnetization into the desired state, or a stabilizing field Hst in the x-direction can be used. With the exception of $H_y \ll H_0$, it is advisable to use a stabilizing field as in this case, H_x values are not affected by the non-ideal behaviour of the layer or restricted by the so-called 'blocking curve'.

The minimum value of H_{st} depends on the structure of the sensitive layer and has to be of the order of H_k, as an insufficient value will produce an open characteristic (hysteresis) of the sensor. An easy axis in the y-direction leads to a sensor of higher sensitivity, as then $H_o = H_k - H_d$.

Linearization

As shown, the basic magnetoresistor has a square resistance-field (R-H) dependence, so a simple magnetoresistive element cannot be used directly for linear field measurements. A magnetic biasing field can be used to solve this problem, but a better solution is linearization using barber-poles (described later). Nevertheless plain elements are useful for applications using strong magnetic fields which saturate the sensor, where the actual value of the field is not being measured, such as for angle measurement. In this case, the direction of the magnetization is parallel to the field and the sensor signal can be described by a $\cos^2\alpha$ function.

Sensors with inclined elements

Sensors can also be linearized by rotating the current path, by using resistive elements inclined at an angle θ, as shown in Fig.18. An actual device uses four inclined resistive elements, two pairs each with opposite inclinations, in a bridge.

The magnetic behaviour of such is pattern is more complicated as M_0 is determined by the angle of inclination θ, anisotropy, demagnetization and bias field (if present). Linearity is at its maximum for $\phi + \theta \approx 45°$, which can be achieved through proper selection of θ.
A stabilization field (H_{st}) in the x-direction may be necessary for some applications, as this arrangement only works properly in one magnetization state.

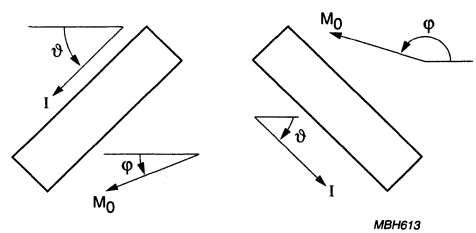

Fig.18 Current rotation by inclined elements (current and magnetization shown in quiescent state).

BARBER-POLE SENSORS

A number of Philips' magnetoresistive sensors use a 'barber-pole' construction to linearize the R-H relationship, incorporating slanted strips of a good conductor to rotate the current. This type of sensor has the widest range of linearity, smaller resistance and the least associated distortion than any other form of linearization, and is well suited to medium and high fields.

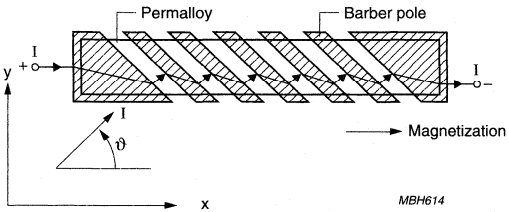

Fig.19 Linearization of the magnetoresistive effect with barber-poles (current and magnetization shown in quiescent state).

The current takes the shortest route in the high-resistivity gaps which, as shown in Fig 19, is perpendicular to the barber-poles. Barber-poles inclined in the opposite direction will result in the opposite sign for the R-H characteristic, making it extremely simple to realize a Wheatstone bridge set-up.

The signal voltage of a Barber-pole sensor may be calculated from the basic equation (1) with $\Theta = \phi + 45^\circ$ ($\theta = +45^\circ$):

$$U_{BP} = \rho_\perp I \left(\frac{L}{wt}\right)\alpha\left(1 + \frac{1}{2}\left(\frac{\Delta\rho}{\rho}\right) \pm \frac{\Delta\rho}{\rho}\frac{H_y}{H_0}\sqrt{1 - \left(\frac{H_y}{H_0}\right)^2}\right) \qquad (9)$$

where a is a constant arising from the partial shorting of the resistor, amounting to 0.25 if barber-poles and gaps have equal widths. The characteristic is plotted in Fig 20 and it can be seen that for small values of H_y relative to H_0, the R-H dependence is linear. In fact this equation gives the same linear R-H dependence as the planar Hall-effect sensor, but it has the magnitude of the magnetoresistive sensor.

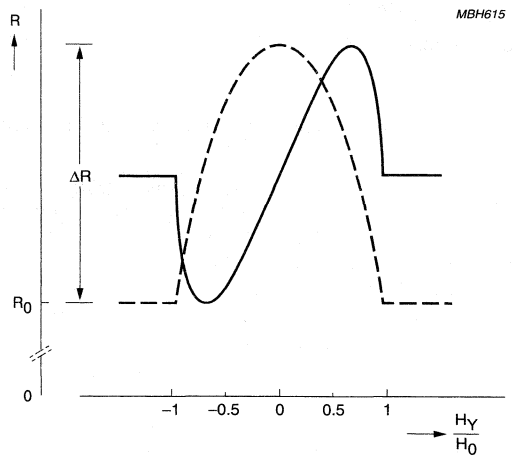

Fig.20 Calculated R-H characteristic of a barber-pole sensor.

Barber-pole sensors require a certain magnetization state. A bias field of several hundred A/m can be generated by the sensing current alone, but this is not sufficient for sensor stabilization, so can be neglected. In most applications, an external field is applied for this purpose.

Sensitivity

Due to the high demagnetization, in most applications field components in the z-direction (perpendicular to the layer plane) can be ignored. Nearly all sensors are most sensitive to fields in the y-direction, with H_x only having a limited or even negligible influence.

Definition of the sensitivity S contains the signal and field variations (DU and DH), as well as the operating voltage U_0 (as D_U is proportional to U_0):

$$S_o = \frac{\Delta U}{\Delta H}\left(\frac{1}{U_0}\right) = \left(\frac{\Delta U}{U_0 \Delta H}\right) \qquad (10)$$

This definition relates DU to a unit operating voltage. The highest (H_G) and lowest (H_{min}) fields detectable by the sensor are also of significance. The measuring range H_G is restricted by non-linearity - if this is assumed at 5%, an approximate value for barber-pole sensors is given by:

$$H_G \approx 0.5(H_0 + H_x) \quad (11)$$

From this and equation (9) for signal voltage (U_{BP}) for a barber-pole sensor, the following simple relationship can be obtained:

$$H_G S_0 \approx 0.5\left(\frac{\Delta\rho}{\rho}\right) \quad (12)$$

Other sensor types have a narrower range of linearity and therefore a smaller useful signal.

The lowest detectable field H_{min} is limited by offset, drift and noise. The offset is nearly cancelled in a bridge circuit and the remaining imbalance is minimized by symmetrical design and offset trimming, with thermal noise negligible in most applications (see section on sensor layout). Proper film deposition and, if necessary, the introduction of a stabilization field will eliminate magnetization switching due to domain splitting and the introduction of 'Barkhausen noise'.

Sensitivity S_0 is essentially determined by the sum of the anisotropy (H_k), demagnetization (H_d) and bias (H_x) fields. The highest sensitivity is achievable with $H_x = 0$ and $H_d \ll H_k$, although in this case S_0 depends purely on H_k which is less stable than H_d. For a permalloy with a thickness greater than or equal to 20 μm, a width in excess of 60 μm is required which, although possible, has the drawback of producing a very low resistance per unit area.

The maximum theoretical S_0 with this permalloy (at H_k = 250 A/m and $\Delta\rho/\rho$ = 2.5%) is approximately:

$$S_0(\max) = 10^{-4}\left(\frac{A}{m}\right)^1 = 100\frac{\left(\frac{mV}{V}\right)}{\left(\frac{kA}{m}\right)} \quad (13)$$

For the same reasons, sensors with reduced sensitivity should be realized with increased H_d, which can be estimated at a maximum for a barber-pole sensor at 40 kA/m. A further reduction in sensitivity and a corresponding growth in the linearity range is attained using a biasing field. A magnetic shunt parallel to the magnetoresistor or only having a small field component in the sensitive direction can also be employed with very high field strengths.

A high signal voltage U_x can only be produced with a sensor that can tolerate a high supply voltage U_o. This requires a high sensor resistance R with a large area A, since there are limits for power dissipation and current density. The current density in permalloy may be very high ($j > 10^6$ A/cm^2 in passivation layers), but there are weak points at the current reversal in the meander (see section on sensor layout) and in the barber-pole material, with five-fold increased current density.

A high resistance sensor with U_0 = 25 V and a maximum S_0 results in a value of 2.5 x 10^{-3} (A/m)$^{-1}$ for Su or, converted to flux density, S_T = 2000 V/T. This value is several orders of magnitude higher than for a normal Hall effect sensor, but is valid only for a much narrower measuring range.

Materials

There are five major criteria for a magnetoresistive material:

- Large magnetoresistive effect Dr/r (resulting in a high signal to operating voltage ratio)
- Large specific resistance r (to achieve high resistance value over a small area)
- Low anisotropy
- Zero magnetostriction (to avoid influence of mechanical stress)
- Long-term stability.

Appropriate materials are binary and ternary alloys of Ni, Fe and Co, of which NiFe (81/19) is probably the most common.

Table 1 gives a comparison between some of the more common materials, although the majority of the figures are only approximations as the exact values depend on a number of variables such as thickness, deposition and post-processing.

Table 3 Comparison of magnetoresistive sensor materials

Materials	ρ (10^{-8}Ωm)	Δρ/ρ(%)	H_k(A/m)
NiFe 81:19	22	2.2	250
NiFe 86:14	15	3	200
NiCo 50:50	24	2.2	2500
NiCo 70:30	26	3.7	2500
CoFeB 72:8:20	86	0.07	2000

Δρ is nearly independent of these factors, but r itself increases with thickness (t ≤ 40 nm) and will decrease during annealing. Permalloys have a low H_k and zero magnetostriction; the addition of C_o will increase Δρ/ρ, but

this also considerably enlarges H_k. If a small temperature coefficient of $\Delta\rho$ is required, NiCo alloys are preferable. The amorphous alloy CoFeB has a low $\Delta\rho/\rho$, high H_k and slightly worse thermal stability but due to the absence of grain boundaries within the amorphous structure, exhibits excellent magnetic behaviour.

APPENDIX 2: SENSOR FLIPPING

During deposition of the permalloy strip, a strong external magnetic field is applied parallel to the strip axis. This accentuates the inherent magnetic anisotropy of the strip and gives them a preferred magnetization direction, so that even in the absence of an external magnetic field, the magnetization will always tend to align with the strips.

Providing a high level of premagnetization within the crystal structure of the permalloy allows for two stable premagnetization directions. When the sensor is placed in a controlled external magnetic field opposing the internal aligning field, the polarity of the premagnetization of the strips can be switched or 'flipped' between positive and negative magnetization directions, resulting in two stable output characteristics.

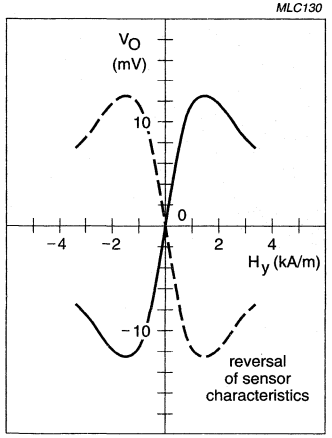

Fig.21 Sensor characteristics.

The field required to flip the sensor magnetization (and hence the output characteristic) depends on the magnitude of the transverse field H_y. The greater this field, the more the magnetization rotates towards 90° and therefore it becomes easier to flip the sensor into the corresponding stable position in the '-x' direction. This means that a smaller $-H_x$ field is sufficient to cause the flipping action

As can be seen in Fig 22, for low transverse field strengths (0.5 kA/m) the sensor characteristic is stable for all positive values of H_x, and a reverse field of approximately 1 kA/m is required to flip the sensor. However at higher values of H_y (2 kA/m), the sensor will also flip for smaller values of H_x (at 0.5 kA/m). Also illustrated in this figure is a noticeable hysteresis effect; it also shows that as the permalloy strips do not flip at the same rate, the flipping action is not instantaneous.

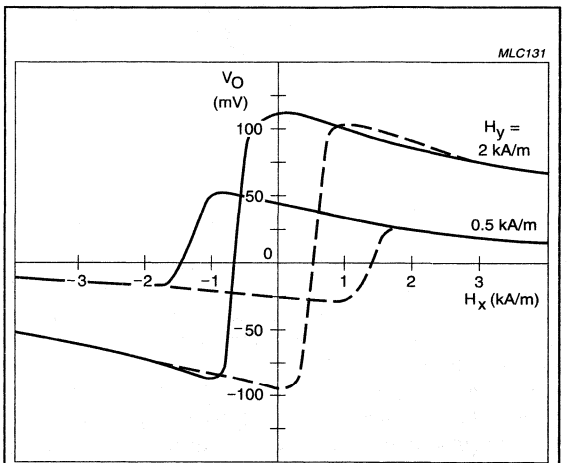

Fig.22 Sensor output 'V_o' as a function of the auxiliary field H_x.

The sensitivity of the sensor reduces as the auxiliary field H_x increases, which can be seen in Fig 22 and more clearly in Fig 23. This is because the moment imposed on the magnetization by H_x directly opposes that of H_y, resulting in a reduction in the degree of bridge imbalance and hence the output signal for a given value of H_y.

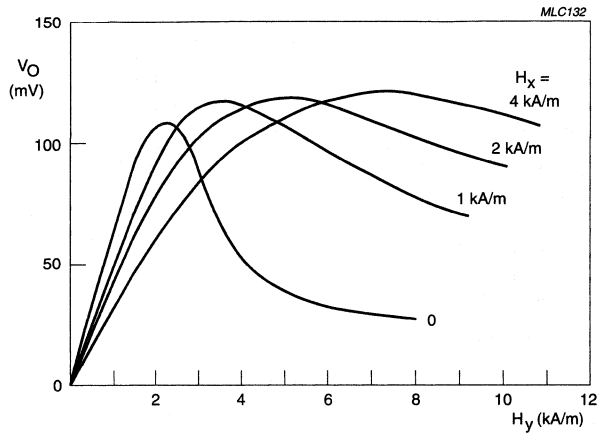

Fig.23 Sensor output 'V_o' as a function of the transverse field H_y.

A Safe Operating ARea (SOAR) can be determined for magnetoresistive sensors, within which the sensor will not flip, depending on a number of factors. The higher the auxiliary field, the more tolerant the sensor becomes to external disturbing fields (H_d) and with an H_x of 3 kA/m or greater, the sensor is stabilized for all disturbing fields as long as it does not irreversibly demagnetize the sensor. If Hd is negative and much larger than the stabilising field H_x, the sensor will flip. This effect is reversible, with the sensor returning to the normal operating mode if H_d again becomes negligible (see Fig 24). However the higher H_x, the greater the reduction in sensor sensitivity and so it is generally recommended to have a minimum auxiliary field that ensures stable operation, generally around 1 kA/m. The SOAR can also be extended for low values of H_x as long as the transverse field is less than 1 kA/m. It is also recommended to apply a large positive auxiliary field before first using the sensor, which erases any residual hysteresis

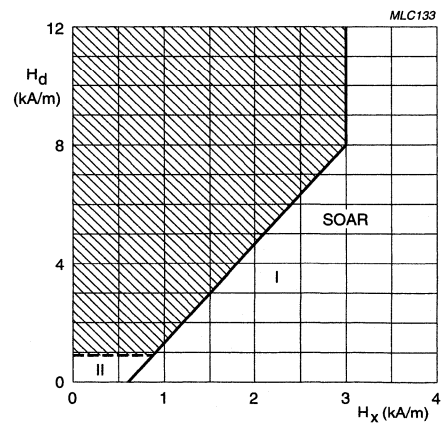

Fig.24 SOAR of a KMZ10B sensor as a function of auxiliary field 'H_x' (MLC133).

APPENDIX 3: SENSOR LAYOUT

In Philips' magnetoresistive sensors, the permalloy strips are formed into a meander pattern on the silicon substrate. With the KMZ10 (see Fig 25) and KMZ51 series, four barber-pole permalloy strips are used while the KMZ41 series has simple elements. The patterns used are different for these three families of sensors in every case, the elements are linked in the same fashion to form the four arms of a Wheatstone bridge. The meander pattern used in the KMZ51 is more sophisticated and also includes integrated compensation and flipping coils (see chapter on weak fields); the KMZ41 is described in more detail in the chapter on angle measurement.

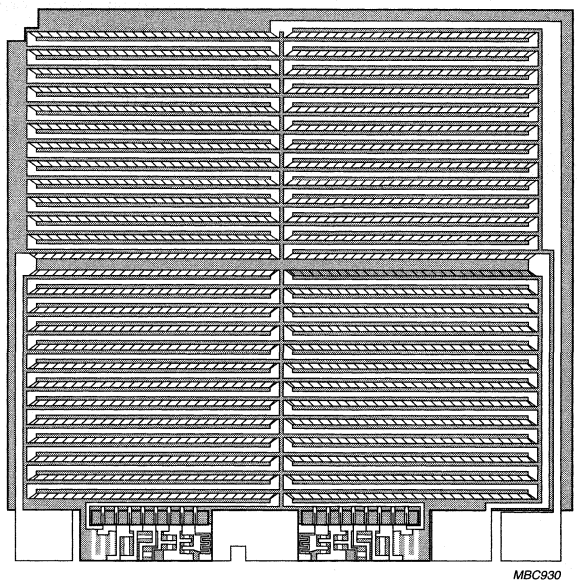

Fig.25 KMZ10 chip structure.

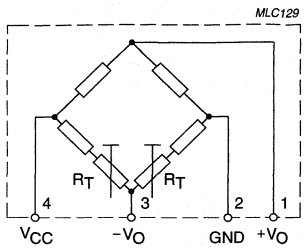

Fig.26 KMZ10 and KMZ11 bridge configuration.

In one pair of diagonally opposed elements the barber-poles are at +45° to the strip axis, with the second pair at −45°. A resistance increase in one pair of elements due to an external magnetic field is matched by an equal decrease in resistance of the second pair. The resulting bridge imbalance is then a linear function of the amplitude of the external magnetic field in the plane of the permalloy strips normal to the strip axis.

This layout largely eliminates the effects of ambient variations (e.g. temperature) on the individual elements and also magnifies the degree of bridge imbalance, increasing sensitivity.

Fig 26 indicates two further trimming resistors (R_T) which allow the sensors electrical offset to be trimmed down to zero during the production process.

WEAK FIELD MEASUREMENT

Contents

- Fundamental measurement techniques
- Application note AN00022: Electronic compass design using KMZ51 and KMZ52
- Application circuit: signal conditioning unit for compass
- Example 1: Earth geomagnetic field compensation in CRT's
- Example 2: Traffic detection
- Example 3: Measurement of current.

Fundamental measurement techniques

Measurement of weak magnetic fields such as the earth's geomagnetic field (which has a typical strength of between approximately 30 A/m and 50 A/m), or fields resulting from very small currents, requires a sensor with very high sensitivity. With their inherent high sensitivity, magnetoresistive sensors are extremely well suited to sensing very small fields.

Philips' magnetoresistive sensors are by nature bi-stable (refer to Appendix 2). 'Standard' techniques used to stabilize such sensors, including the application of a strong field in the x-direction (H_x) from a permanent stabilization magnet, are unsuitable as they reduce the sensor's sensitivity to fields in the measurement, or y-direction (H_y). (Refer to Appendix 2, Fig. A2.2).

To avoid this loss in sensitivity, magnetoresistive sensors can instead be stabilized by applying brief, strong non-permanent field pulses of very short duration (a few μs). This magnetic field, which can be easily generated by simply winding a coil around the sensor, has the same stabilizing effect as a permanent magnet, but as it is only present for a very short duration, after the pulse there is no loss of sensitivity. Modern magnetoresistive sensors specifically designed for weak field applications incorporate this coil on the silicon.

However, when measuring weak fields, second order effects such as sensor offset and temperature effects can greatly reduce both the sensitivity and accuracy of MR sensors. Compensation techniques are required to suppress these effects.

OFFSET COMPENSATION BY 'FLIPPING'

Despite electrical trimming, MR sensors may have a maximum offset voltage of ±1.5 mV/V. In addition to this static offset, an offset drift due to temperature variations of about 6 $(\mu V/V)K^{-1}$ can be expected and assuming an ambient temperature up to 100 °C, the resulting offset can be of the order of 2 mV/V.
Taking these factors into account, with no external field a sensor with a typical sensitivity of 15 mV/V $(kA/m)^{-1}$ can have an offset equivalent to a field of 130 A/m, which is itself about four times the strength of a typical weak field such as the earth's geomagnetic field. Clearly, measures to compensate for the sensor offset value have to be implemented in weak field applications.

A technique called 'flipping' (patented by Philips) can be used to control the sensor. Comparable to the 'chopping' technique used in the amplification of small electrical signals, it not only stabilizes the sensor but also eliminates the described offset effects.

When the bi-stable sensor is placed in a controlled, reversible external magnetic field, the polarity of the premagnetization (M_x) of the sensor strips can be switched or flipped between the two output characteristics (see Fig.27).

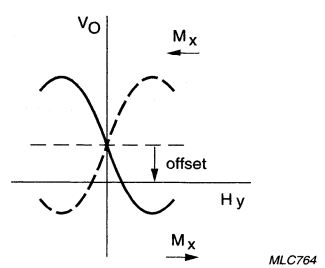

Fig.27 Butterfly curve including offset.

This reversible external magnetic field can be easily achieved with a coil wound around the sensor, consisting of current carrying wires, as described above. Depending on the direction of current pulses through this coil, positive and negative flipping fields in the x-direction ($+H_x$ and $-H_x$) are generated (see Fig.28).

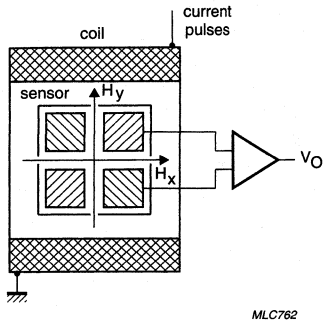

Fig.28 Flipping coil.

Flipping causes a change in the polarity of the sensor output signal and this can be used to separate the offset signal from the measured signal. Essentially, the unknown field in the 'normal' positive direction (plus the offset) is measured in one half of the cycle, while the unknown field in the 'inverted' negative direction (plus the offset) is measured in the second half. This results in two different outputs symmetrically positioned around the offset value. After high pass filtering and rectification a single, continuous value free of offset is output, smoothed by low pass filtering. See Figs 29 and 30.

Offset compensation using flipping requires additional external circuitry to recover the measured signal.

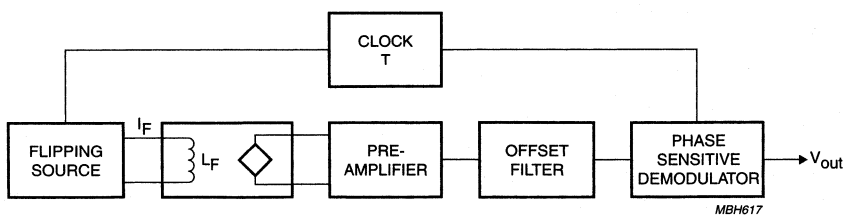

Fig.29 Block diagram of flipping circuit.

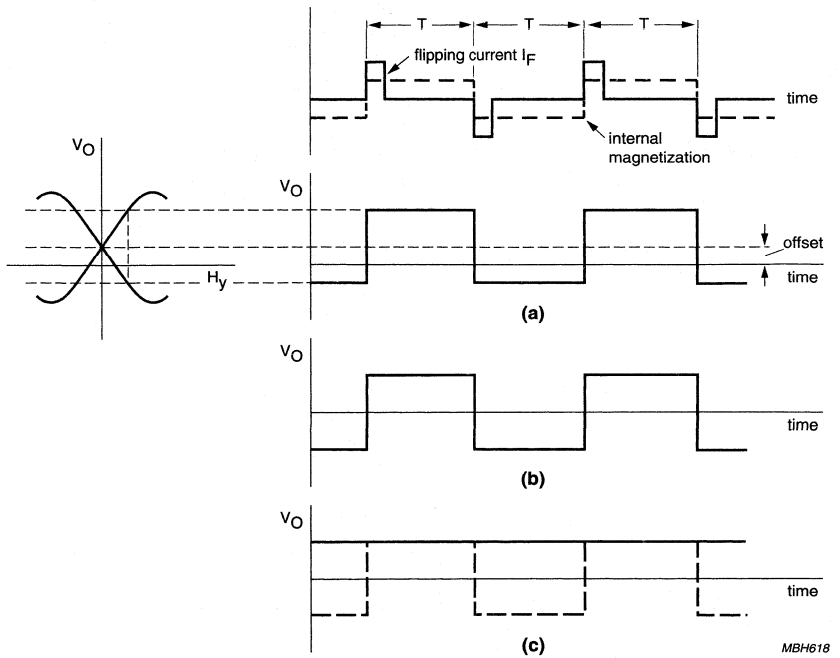

Fig.30 Timing diagram for flipping circuit (a) output voltage; (b) filtered output voltage; (c) output voltage filtered and demodulated.

SENSOR TEMPERATURE DRIFT

The sensitivity of MR sensors is also temperature dependent, with sensitivity decreasing as temperature increases (Fig.31).The effect on sensor output is certainly not negligible, as it can produce a difference of a factor of three within a –25 °C to +125 °C temperature range, for fields up to 0.5 kA/m. This effect is not compensated for by the flipping action described in the last section.

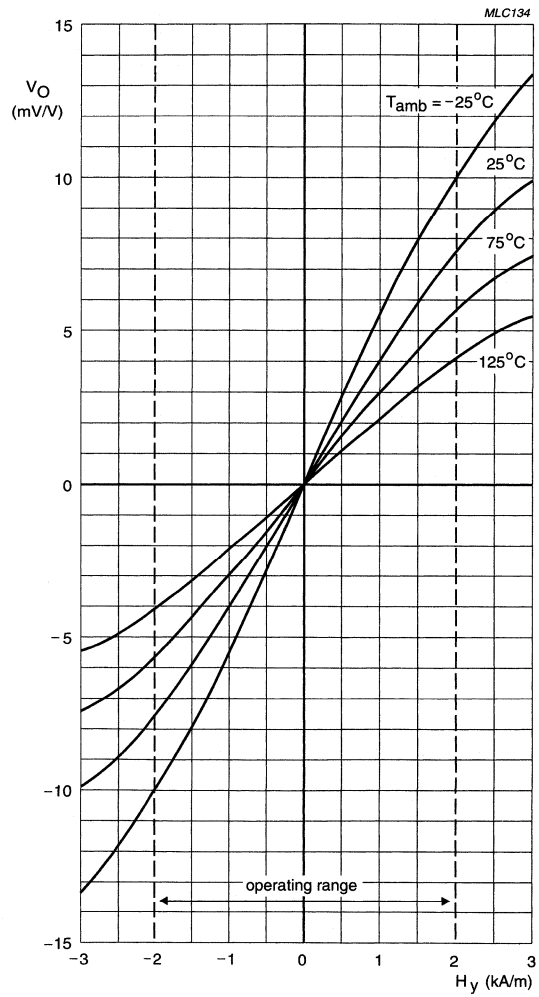

Fig.31 Output voltage 'V_o' as a fraction of the supply voltage for a KMZ10B sensor, as a function of transverse field 'H_y', at several temperatures.

The simplest form of temperature compensation is to use a current source to supply to the sensor instead of a voltage source. In this case, the resulting reduction in sensitivity due to temperature is partially compensated by a corresponding increase in bridge resistance.
Thus a current source not only improves the stability of the output voltage 'V_o', and reduces the variation in sensitivity to a factor of approximately 1.5 (compared to a factor of three using the voltage source). However, this method requires a higher supply voltage, due to the voltage drop of the current source.

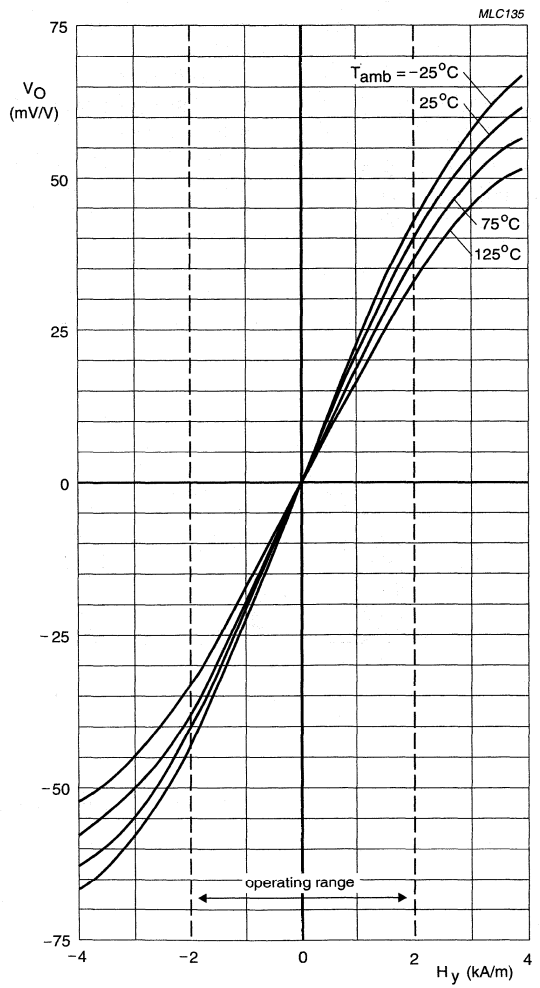

Fig.32 Output voltage 'V_o' of a KMZ10B sensor as a function of transverse field 'H_y' using a current source, for several temperatures.

The optimal method of compensating for temperature dependent sensitivity differences in MR measurements of weak fields uses electro-magnetic feedback. As can be seen from the sensor characteristics in Figs 31 and 32, sensor output is completely independent of temperature changes at the point where no external field is applied (the null-point). By using an electro-magnetic feedback set-up, it is possible to ensure the sensor is always operated at this point.

To achieve this, a second compensation coil is wrapped around the sensor perpendicular to the flipping coil, so that the magnetic field produced by this coil is in the same plane as the field being measured.

Should the measured magnetic field vary, the sensor's output voltage will change, but the change will be different at different ambient temperatures. This voltage change is converted into a current by an integral controller and supplied to the compensation coil, which then itself produces a magnetic field proportional to the output voltage change caused by the change in measured field.

The magnetic field produced by the compensation coil is in the opposite direction to the measured field, so when it is added to the measured field, it compensates exactly for the change in the output signal, regardless of its actual, temperature-dependent value. This principle is called current compensation and because the sensor is always used at its 'zero' point, compensation current is independent of the actual sensitivity of the sensor or sensitivity drift with temperature.

Information on the measured magnetic signal is effectively given by the current fed to the compensating coil. If the field factor of the compensation coil is known, this simplifies calculation of the compensating field from the compensating current and therefore the calculation of the measured magnetic field. If this field factor is not precisely known, then the resistor performing the current/voltage conversion must be trimmed. Figure 34 shows a block diagram of a compensated sensor set-up including the flipping circuit.

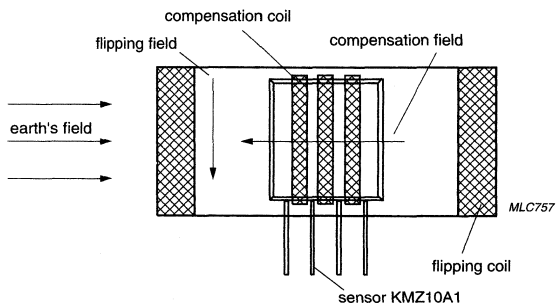

Fig.33 Magnetic field directions and the flipping and compensation coils.

The influence of other disturbing fields can also be eliminated provided they are well known, by adding a second current source to the compensating coil. Such fields might be those arising from the set-up housing, ferromagnetic components placed close to the sensor or magnetic fields from electrical motors.

The brief summary in Table 3 compares the types of compensation and their effects, so they can be assessed for their suitability in a given application. Because these options encompass a range of costs, the individual requirements of an application should be carefully analysed in terms of the performance gains versus relative costs.

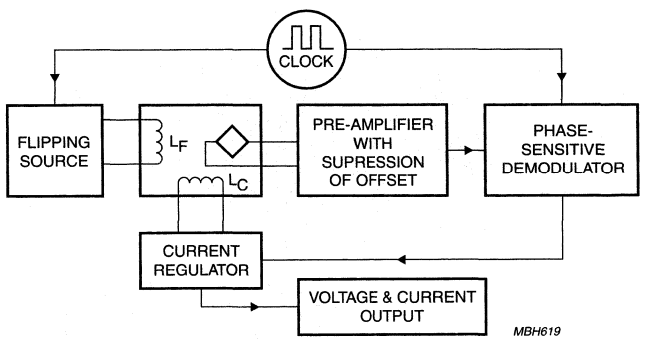

Fig.34 Block diagram of compensation circuit.

Table 4 Summery of compensation techniques

TECHNIQUE	EFFECT
Setting	avoids reduction in sensitivity due to constant stabilization field
Flipping	avoids reduction in sensitivity due to constant stabilization field, as well as compensating for sensor offset and offset drift due to temperature
Current supply	reduction of sensitivity drift with temperature by a factor of two
Electro-magnetic feedback	accurate compensation of sensitivity drift with temperature

PHILIPS SENSORS FOR WEAK FIELD MEASUREMENT

Philips Semiconductors has at present four different sensors suitable for weak field applications, with the primary device being the KMZ51, an extremely sensitive sensor with integrated compensation and set/reset coils.(see Fig.35)

This sensor is ideal for many weak field detection applications such as compasses, navigation, current measurement, earth magnetic field compensation, traffic detection and so on. The integrated set/reset coils provide for both the flipping required in weak field sensors and also allow setting/resetting the orientation of the sensitivity after proximity to large disturbing magnetic fields. Philips also has the KMZ10A and KMZ10A1, similar sensors which do not have integrated coils and therefore require external coils. Table 5 provides a summary of the main single sensors in Philips' portfolio for weak field measurement.

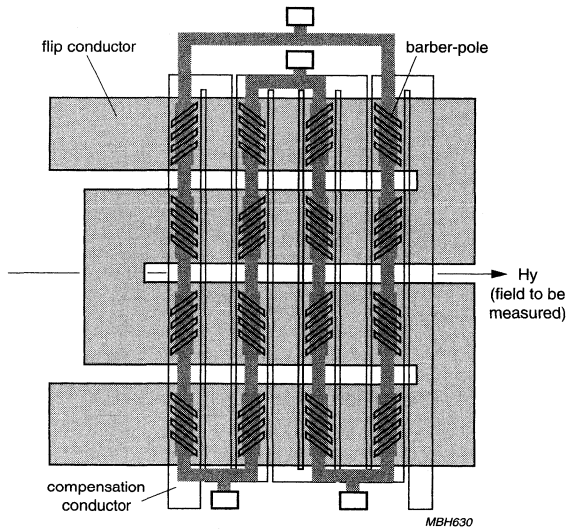

Fig.35 Layout of Philips' KMZ51 magnetoresistive sensor.

Table 5 Properties of Philips Semiconductors single sensors for a weak field applications

	KMZ10A	KMZ10A1	KMZ51	KMZ52	UNIT
Package	SOT195	SOT195	SO8	SO16	–
Supply voltage	5	5	5	5	V
Sensitivity	16(1)	22	16	16	(mV/V)/ (kA/m)
Offset voltage	±1.5	±1.5	±1	±1.5	mV/V
Offset voltage temperature drift	±6	±6	±3	±3	μV/V/K
Applicable field range (y-direction)	±0.5	±0.5	±0.2	±0.2	kA/m
Set/reset coil on-board	no	no	yes	yes	–
Compensation coil on-board	no	no	yes	yes	–

Note

1. H_x = 0.5 kA/m.

APPLICATION NOTE

Electronic Compass Design using KMZ51 and KMZ52

AN00022

Author:

Thomas Stork
Philips Semiconductors
Systems Laboratory Hamburg,
Germany

Keywords

Earth´s magnetic field
Magnetoresistive sensors
8-segment compass
High resolution compass

Number of pages: 38

Date: 00-03-30

Electronic Compass Design using KMZ51 and KMZ52

Application Note AN00022

SUMMARY

This paper describes how to realize electronic compass systems using the magnetoresistive sensors KMZ51 and KMZ52 from Philips Semiconductors. Therefore, firstly an introduction to the characteristics of the earth's magnetic field is given. In the following, the main building blocks of an electronic compass are shown, which are two sensor elements for measuring the x- and y-components of the earth field in the horizontal plane, a signal conditioning unit and a direction determination unit.

To provide an understanding of the sensor elements, the magnetoresistive effect and the optimization of the sensor characteristic by using barber pole structures are described briefly. Also the special features of the KMZ5x products, such as set/reset and compensation coils are pointed out. The signal conditioning unit's basic function is to amplify the sensor output voltages, in order to provide reasonable input signals for the following direction determination unit. Beyond that, offset elimination is an essential task. For high precision systems, also sensitivity shifts due to temperature variations should be compensated. Practical methods to fulfill all these tasks either in hardware or software are given. The direction determination unit is the building block for deriving the azimuth as the desired compass output quantity. The azimuth is the angle between magnetic north and the heading direction. For high resolution compass systems, this has to be done mathematically by applying the arcus tangens function to the ratio of the two sensor signals. It is shown, how to implement this function as software. Without this calculation, a more simple 8-segment compass can be realized, which only indicates the nearest cardinal or intermediate point (N, NE, ...).

Besides realization of the basic compass functions, this paper also covers the calibration of electronic compasses against external error sources like magnetic interference fields, deviation between true and magnetic north and tilt. Finally, determination of system accuracy and examples for complete compass systems are given.

Electronic Compass Design using KMZ51 and KMZ52

Application Note AN00022

CONTENT

LIST OF FIGURES

Electronic Compass Design using KMZ51 and KMZ52

Application Note AN00022

1. INTRODUCTION

The magnetic compass is a crucial navigation tool in many areas, even in times of the global positioning system (GPS). Replacing the "old" magnetic needle compass or the gyrocompass by an electronic solution offers advantages like having a solid-state component without moving parts and the ease of interfacing with other electronic systems.

For the magnetic field sensors within a compass system, the magnetoresistive (MR) technology is the preferable solution. Compared to flux-gate sensors, which could be found in most electronic compasses until now, the MR technology offers a much more cost effective solution, as it requires no coils to be wound and can be fabricated in an IC-like process. Due to their higher sensitivity, MR sensors are also superior to Hall elements in this application field.

The intention of this paper is to give a general introduction of electronic compass design with MR sensors and also to give detailed realization hints. Therefore, the basic characteristics of the earth´s magnetic field are explained and an overview of the building blocks of an electronic compass is given. Following a description of Philips´ magnetoresistive sensors for compass applications, the design of each building block is covered in detail. Here, both hardware and software realisations are shown. Further sections are dedicated to special items like interference field calibration, true north calibration, tilt compensation and system accuracy. Finally, examples for complete compass systems are given, consisting of previously described building blocks.

2. EARTH´S MAGNETIC FIELD

The magnetic field of the earth is the physical quantity to be evaluated by a compass. Thus, an understanding of its basic properties is required, when designing a compass. Figure 1 gives an illustration of the field shape.

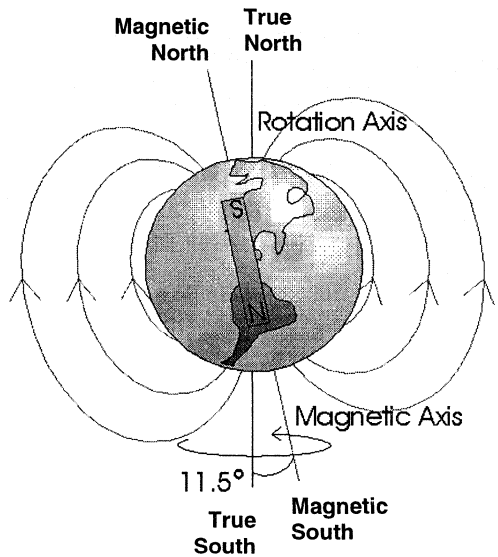

Figure 1 Earth´s magnetic field

The magnetic field strength on the earth varies with location and covers the range from about 20 to 50 A/m. An understanding of the earth´s field shape can be gained, if it is assumed to be generated by a bar magnet within the earth, as pointed out in Figure 1. The magnetic field lines point from the earth´s south pole to its north pole. Fig. 1 indicates, that this is opposite to the physical convention for the poles of a bar magnet (the background is a historical one, in that a bar magnet´s north pole has been defined as that pole, that points towards north in the earth´s magnetic field). The field lines are perpendicular to the earth surface at the poles and parallel at the equator. Thus, the earth field points downwards in the northern hemisphere and upwards in the southern hemisphere. An important fact is, that the magnetic poles do not coincide with the geographical poles, which are defined by the earth´s axis of rotation. The angle between the magnetic and the rotation axis is about 11.5°. As a consequence, the magnetic field lines do not exactly point to geographic or "true" north.

Figure 2 gives a 3-D representation of the earth field vector **He** at some point on the earth. This illustration allows to define the quantities, which are of importance for a compass. Here, the x- and y-coordinates are parallel to the earth´s surface, whereas the z-coordinate points vertically downwards.

- **Azimuth** α
  The angle between magnetic north and the heading direction. Magnetic north is the direction of Heh, the earth´s field component perpendicular to gravity. Throughout this paper, Heh will be referred to as "horizontal" component of the earth´s field. Figure 2 shows, that:

$$\alpha = \arctan\frac{Hey}{Hex} \qquad (1)$$

The azimuth is the reading quantity of a compass. Throughout this paper, α is counted clockwise from magnetic north, i.e. north is 360° or 0°, east is 90°, south is 180°, west is 270°.

- **Inclination or dip** δ
  The angle between the earth´s field vector and the horizontal plane. As already pointed out, the inclination varies with the actual location on earth, being zero at the equator and approaching ±90° near the poles. If a compass is tilt, then inclination has to be considered, as explained in section 9.
- **Declination** λ
  The angle between geographic or true north and magnetic north. Declination is dependent on the actual position on earth. It also has a long term drift. Declination can be to the east or to the west and can reach values of about ±25°. The azimuth measured by a compass has to be corrected by the declination in order to find the heading direction with respect to geographic north. This is pointed out in section 8.

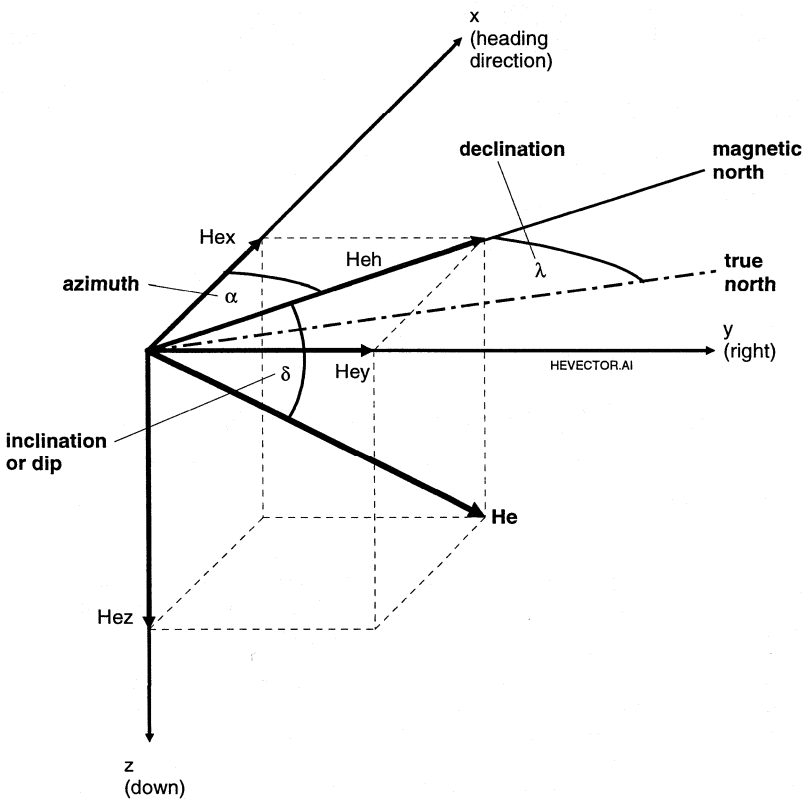

Figure 2 Earth field vector

3. BUILDING BLOCKS OF AN ELECTRONIC COMPASS

Figure 3 shows a functional block diagram of an electronic compass. This is a minimum set-up, i.e. these elements are principally required for any electronic compass. The functional blocks – except the field sensor – can be realized either as hardware or as software. In the following, the functions of each block are summarized. A detailed description of each block together with examples for realization are given in the following sections.

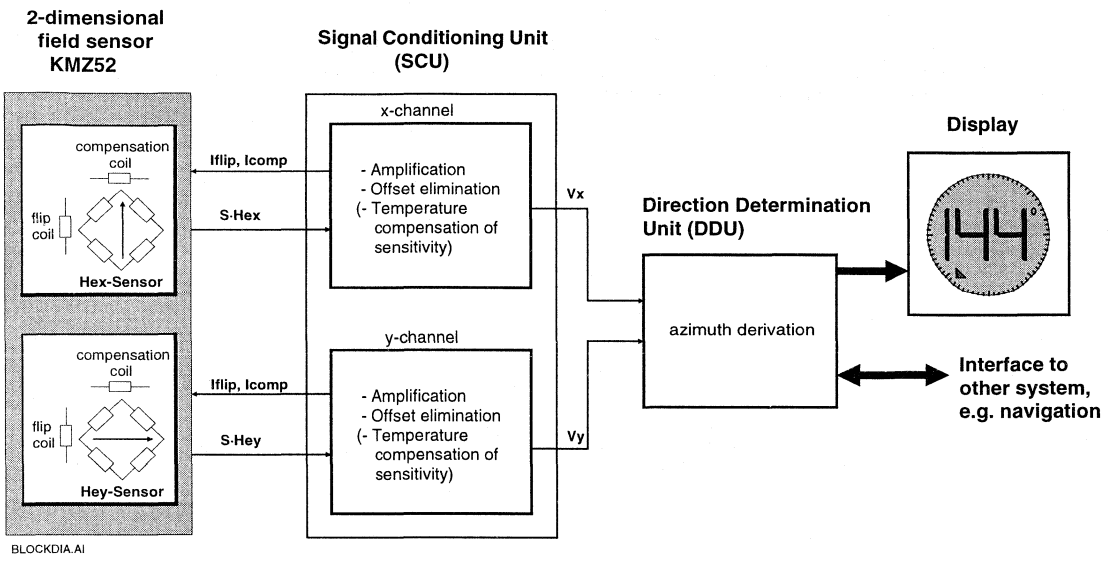

Figure 3 Functional block diagram of an electronic compass

- **Magnetic field sensors**

As already pointed out, the task of a compass is to measure the azimuth α, i.e. the angle between north and heading direction, as defined by equation (1). Therefore, the strengths of two horizontal earth field components have to be measured: one in heading direction (Hex) and one sidewards (Hey). This requires two magnetic field sensors, both aligned parallel to the earth´s surface, but rotated by 90 degrees with respect to each other.

Philips´ magnetoresistive sensor technology is an optimum choice for measuring weak magnetic fields like the earth´s field. The KMZ52 is a sensor device, which is perfectly matched to this application, as it comprises two extremely sensitive field sensors in the required configuration in one SO16 package. Furthermore, the KMZ52 comprises for each of its sensors a set/reset coil needed for offset elimination and a coil for the compensation of sensitivity temperature drift. Thus, the KMZ52 makes any external coils obsolete, which are required when using other sensor products. Section 4 describes Philips´ magnetoresistive sensor technology and introduces those products, which are dedicated to compass applications.

- **Signal conditioning unit (SCU)**

The purpose of this block is to deliver output voltages proportional to the field strengths Hex and Hey respectively. Therefore, the signals delivered by the magnetic field sensors have to be amplified. Also offsets have to be eliminated. Beyond that, the amplification of one SCU channel should be trimable in order to allow

the compensation of sensitivity differences between the x- and the y- field sensor. Optional features for high performance systems are temperature compensation of sensitivity and compensation of the error due to non-orthogonality between the sensors. To fulfill these tasks, the signal conditioning unit has to influence the sensors by controlling their set/reset and compensation coils. The SCU is the most crucial part concerning system accuracy. Section 5 gives a detailed description of the required functions within the signal conditioning unit as well as solutions in hardware and software.

- **Direction determination unit (DDU)**

The function of this block is to derive the desired azimuth information from the measured field strengths Hey and Hex. For high resolution compasses, this can be done by evaluating the arctan function of equation (1) with a microcontroller. With less effort, a simple 8-segment compass can be built up, which only provides major direction indication (N, NE, E, etc.). Section 6 gives some more hints on this.

- **Display / Interface**

Finally, the measured azimuth has to be indicated to the user by a display and/or has to be delivered to another electronic system. The latter could be the navigation system of a car, which uses the compass information for "dead reckoning", i.e. for determination of the relative position during time intervals, where GPS signals cannot be received (e.g. when driving between high buildings). Section 11 shows complete application examples, which give some hints on display driving and interfacing.

- **Further features**

Figure 3 shows those elements, which are required for any electronic compass. However, depending on the actual application, further features may be demanded. The most important of these are:

- Interference field calibration
  In most practical cases, the earth field to be measured is superimposed by other magnetic fields, which would cause a significant measurement error, if not compensated. Section 7 gives an introduction on this topic.
- True north calibration
  As pointed out in section 2, there is a deviation between the magnetic north direction (measured by the compass) and true or geographic north. Section 8 gives more information on this item.
- Tilt compensation
  Equation (1) only yields the correct azimuth, if Hex and Hey are the earth field components in the horizontal plane. Thus, the basic compass sketched in Figure 3 must be held exactly horizontal to work properly. Section 9 discusses the error that occurs, when a compass is tilt and shows how to compensate this error electronically.

4. MAGNETORESISTIVE (MR) SENSORS FOR COMPASS APPLICATIONS

The intention of this section is to describe the basic principles of magnetoresistive sensors, which a compass designer should know. A more detailed description of the magnetoresistive effect can be found in [3].

4.1 The Magnetoresistive Sensor Element

4.1.1 The Magnetoresistive Effect

Magnetoresistive (MR) sensors make use of the magnetoresistive effect, the property of a current carrying magnetic material to change its resistivity in the presence of an external magnetic field. Figure 4 shows a strip of ferromagnetic material, called permalloy (19% Fe, 81% Ni).

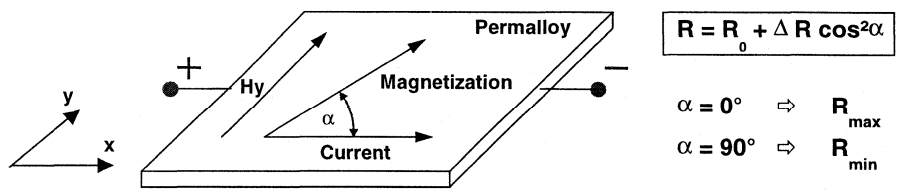

Figure 4 The magnetoresistive effect in permalloy

During deposition of the permalloy strip, a strong external magnetic field is applied parallel to the strip axis. By doing this, a preferred magnetization direction is defined within the strip. In absence of any external magnetic field, the magnetization always points into this direction. In Figure 4, this is assumed to be the x-direction, which is also the direction of current flow. An MR sensor now relies on two basic effects:

- The strip resistance R depends on the angle α between the direction of the current and the direction of the magnetization.
- The direction of magnetization and therefore α can be influenced by an external magnetic field Hy, where Hy is parallel to the strip plane and perpendicular to the preferred direction.

When no external magnetic field is present, the permalloy has an internal magnetization vector parallel to the preferred direction, i.e. $\alpha = 0$. In this case, the strip resistance R has its maximum value Rmax. If now an external magnetic field Hy is applied, the internal magnetization vector of the permalloy will rotate around an angle α. At high field strengths, the magnetization tends to align itself parallel to Hy and the rotation angle α approaches 90°. In this case, the resistance reaches its minimum value Rmin. The equation next to Figure 4 gives the functional dependence between R and α, where Ro = Rmin and ΔR = (Rmax-Rmin). Finally, the function of R versus Hy is as follows:

$$R = R_0 + \Delta R \cdot \left(1 - \left(\frac{H_y}{H_o} \right)^2 \right) \qquad (2)$$

Figure 5a shows a diagram for equation (2). Ho is a parameter, which depends on material and geometry of the strip. Equation (2) is defined for field strength magnitudes of Hy ≤ Ho. For Hy > Ho, R equals Ro. R_0 and ΔR are also material parameters. For permalloy, ΔR is in the range of 2 to 3% of R_0.

4.1.2 Optimization of Sensor Characteristic using Barber Pole Structures

Figure 5a illustrates the sensor characteristic according to (2). For small magnitudes of Hy, the sensitivity is very low and non-linear. Furthermore, this characteristic does not allow to detect, whether Hy is positive or negative. Therefore, the basic sensor structure of Figure 4 has to be improved for compass applications.

The desired sensor improvements can be achieved by depositing aluminium stripes (called barber poles) on top of the permalloy strip at an angle of 45° to the strip axis. Figure 6 shows the principle. As aluminium has a much higher conductivity than permalloy, the effect of the barber pole is to rotate the current direction by 45°, effectively changing the angle between the magnetisation and the electrical current from α to (α - 45°). Graph b) in Figure 5 shows the impact on the sensor characteristic due to the barber pole structure. For weak fields like the earth's field, the sensitivity now is significantly higher, the characteristic is linearized and allows to detect the sign of Hy.

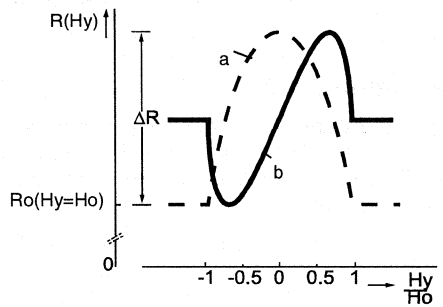

Figure 5 a) R-H characteristic of a standard sensor, b) R-H characteristic of barber pole sensors

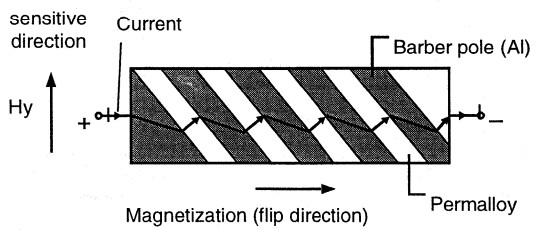

Figure 6 Barber pole sensor

4.1.3 Bridge Configuration

Practically, it is advantageous to build up a sensor element as a Wheatstone bridge, consisting of four magnetoresistive strips, as shown in Figure 7. For compass sensors, barber pole structures are used, where one diagonal pair is orientated at +45° to the strip axis, while the other pair is orientated at -45°. Thus, the resistance variation ΔR due to a magnetic field is converted linearly into a variation of the differential output

voltage $\Delta V = +Vo - (-Vo)$. Moreover, the inherent temperature coefficients of the four bridge resistances are mutually compensated.

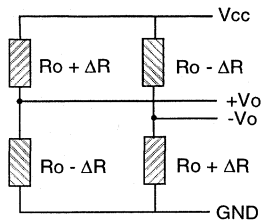

Figure 7 Bridge configuration of barber pole sensors

4.2 Set/Reset and Compensation Coils

MR sensors are by nature bi-stable, i.e. the direction of their internal magnetization can be inverted or "flipped". This can be achieved by a magnetic field of sufficient strength, if that field is applied parallel to the magnetization, but having opposite direction (refer to Figure 8). Flipping causes an inversion of the sensor characteristic, such that the sensor output voltage changes polarity.

MR sensors can be stabilized against unwanted flipping by applying an auxiliary magnetic field parallel to the flipping axis. This field should be pulsed, as a permanent field would decrease the sensitivity. When measuring weak fields, it is even desired to invert or "flip" the sensor characteristic repetitively. This allows to compensate the sensor´s offset in a way comparable to the chopping technique used in the amplification of small electrical signals. A "set/reset" coil near the sensor element is a means to apply the auxiliary field for the flipping.

In high precision compass systems, the sensor must also allow to compensate sensitivity drift with temperature and to compensate interference fields. Both can be done by means of an auxiliary field in the sensitive direction. This can be generated by a "compensation" coil near the sensor element.

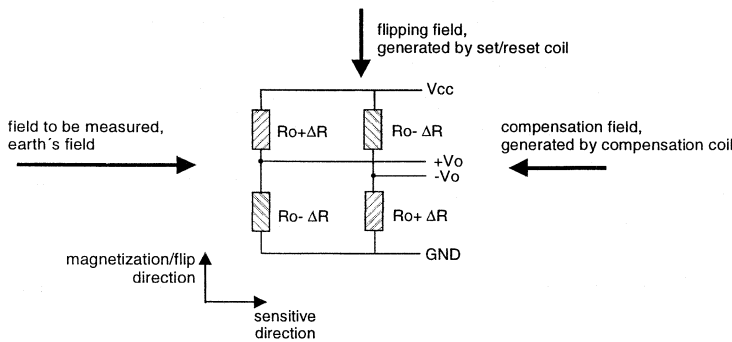

Figure 8 Fields generated by set/reset and compensation coil

Philips MR sensors dedicated for compass applications are available with integrated set/reset and compensation coils, saving the additional cost and effort to provide external coils. Furthermore, as integrated

coils can be arranged much closer to the sensor element, they require significantly less current to generate the required field strengths. This reduces expenditure and thus cost at the signal conditioning unit side.

In the signal conditioning section, the techniques of flipping and compensation are described in detail.

4.3 Philips MR Sensors for Compass Systems

Philips Semiconductors offers at present two sensor products, dedicated to this application field. Both products employ the previously described barber pole structure with its inherent linearity and high sensitivity.

The primary device is the KMZ52, which comprises all elements of a compass sensor system within one package, i.e. two weak field sensors with 90° displacement, each having a set/reset and a compensation coil (ref. to figure 3). The KMZ51 is a single sensor with set/reset and compensation coils. This can be employed together with a KMZ52 to form a three-dimensional sensor, in order to compensate for tilt, as will be described in section 9. Figure 9 shows a simplified circuit diagram of the KMZ51, showing the MR resistor bridge as well as the set/reset and compensation coils. Table 1 provides an overview on Philips' compass sensor portfolio.

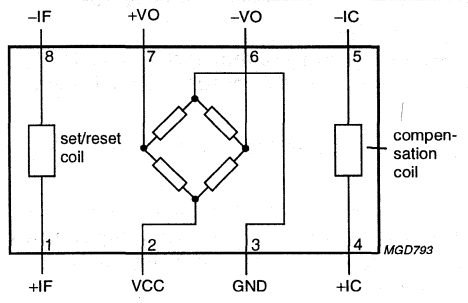

Figure 9 Simplified circuit diagram of KMZ 51

Table 1 Philips MR sensors for compass applications

	KMZ51	KMZ52	UNIT
1- or 2-dimensional sensor	1-dim.	2-dim.	-
Package	SO 8	SO 16	-
recommended supply voltage	5	5	V
typ. sensitivity	16	16	(mV/V) / (kA/m) [1]
offset voltage	-1.5 ... 1.5	-1.5 ... 1.5	mV/V [2]
Applicable field range	-0.2 ... 0.2	-0.2 ... 0.2	kA/m
Integrated set/reset coils for flipping	yes	yes	-
Integrated compensation coils	yes	yes	-

1 Thus, the sensor delivers 16mV per V supply voltage and per kA/m field strength.

2 Thus, the maximum offset voltage is ± 1.5mV per V supply voltage.

5. SIGNAL CONDITIONING UNIT (SCU)

5.1 Requirements

The SCU consists of two separate "channels" fulfilling the basic task of amplifying the x- and y-field sensor output voltages (refer to Figure 3). Considering a minimum earth field strength in the sensor plane of approximately 15 A/m and a sensor sensitivity of typically 80 mV/(kA/m) (at Vcc = 5V, refer to Table 1), an MR sensor will deliver an amplitude of approximately 1.2 mV, when rotated in that field. Therefore, significant amplification is required in order to provide reasonable voltages for the following direction determination stage.

Depending on the desired system accuracy, the SCU has to fulfil up to three further requirements. These are the elimination of the following error sources:

- **Offset voltages Vox, Voy at the SCU output:**
  These are caused by the offsets of the sensor elements and the connected amplifier. Offset of a sensor element arises due to the tolerances and temperature drift of the four magnetoresistive elements, which are arranged as a Wheatstone bridge. Thus, the sensor output voltage deviates from zero, if no magnetic field is applied.
- **Sensitivity difference ΔS between x- and y- channel of the SCU:**
  This is due to tolerance and temperature drift of sensor sensitivities and the following amplification.
- **Non-orthogonality β of sensors:**
  Due to mounting tolerances, the real angular displacement between the sensors deviates from the desired 90° by an angle β.

Equation (3) indicates the effect of these error sources on the azimuth reading. Here it is assumed that the direction determination unit carries out equation (1) by replacing Hey and Hex with the respective SCU output voltages Vy and Vx. As each output voltage equals the measured earth's field component times channel sensitivity plus offset, the azimuth reading is:

$$\alpha = \arctan\frac{Vy}{Vx} = \arctan\frac{He\cdot(S+\Delta S)\cdot\sin(\alpha+\beta)+Voy}{He\cdot S\cdot\cos\alpha+Vox} \qquad (3)$$

Equation (3) becomes identical to equation (1), i.e. the real azimuth is derived, if Vox, Voy, ΔS and β are eliminated. The azimuth errors caused by offsets, ΔS and β are periodic functions of α. The amplitudes of these functions, i.e. the maximum azimuth errors, can be assumed as proportional to the magnitude of the respective error source. Table 2 in section 10 states the equations for these azimuth errors together with an indication of their maximum value depending on the respective error source:

- Offset error: $E_{offset} \approx 0.8$ °/%,
  i.e. an offset to amplitude ratio of 1% causes a max. azimuth error of 0.8 °.
- Sensitivity difference error: $E_{\Delta S} \approx 0.3$ °/%,
  i.e. a ΔS/S ratio of 1% causes an error of 0.3 °.
- Non-orthogonality error: $E_{\beta} \approx 1$ °/°,
  i.e. a 1° deviation from orthogonality between the sensors causes a max. azimuth error of 1°.

The KMZ52 is specified to have an offset voltage of max. ±1.5mV/V and an offset drift of max. ±3μV/(V/K) (refer to Table 1). Thus, at the recommended supply of 5V, the max. offset voltage at 25°C is ±7.5mV and the max. offset drift, e.g. over a temperature range of 100°C, is 1.5mV. Comparing these values with the sensor voltage amplitude of 1.2mV as derived above, it becomes evident, that offset level and even offset temperature drift can be significantly higher than the desired signal. As a consequence, an efficient in-circuit offset compensation is crucial for every compass system, even for "low end" products. Section 5.2 shows techniques to realize this.

To compensate for sensitivity differences ΔS, the SCU should allow to trim its output voltages for equal amplitudes when rotated in the earth field. If high accuracy is desired over a wide temperature range, also an automatic compensation of sensitivity temperature drift should be implemented. Section 5.3 shows the realization.

The maximum non-orthogonality specified for the KMZ52 is 2°, causing a maximum azimuth error of 2°. For applications, where this is not sufficient, section 5.4 shows a principle, to correct this error mathematically.

5.2 Offset Compensation

A technique called "flipping" can be used here, which allows to eliminate the offset similar to the "chopping" technique used for the amplification of small electrical signals: When the bi-stable sensor is subjected to a reversible magnetic field in its flipping direction, its internal magnetization Mx and thus its characteristic Vo vs. Hy is reversed or "flipped" as shown in Figure 10 (refer also to section 4.2). If the flipping is done repetitively, the desired output voltage will change polarity, thus appearing as amplitude of an ac signal. However the offset voltage does not change polarity, thus appearing as a dc offset of that signal. This allows to compensate the sensor´s offset by filtering the dc component from its flipped output signal. A subsequent rectification then allows to convert the ac signal back to the desired dc sensor signal.

Figure 11 shows the block diagram of a flipping circuit. The flipping is generated by applying alternately positive and negative current pulses to the set/reset coil of the sensor. To avoid loss in sensitivity, the current pulses should be short (only a few µs). Although the frequency is not critical, some design hints are given later on when coming to practical solutions. After pre-amplification, a high pass filter removes the sensor offset from the flipped output signal. A synchronous rectifier converts the flipped signal to a dc signal, that is now free of offset. A clock signal is required for controlling the flipping source and the rectifier, which must be synchronized with the flipping. Figure 12 shows a timing diagram with the signals of the flipping circuit.

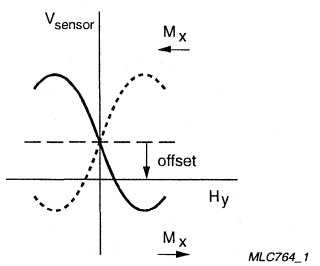

Figure 10 Effect of flipping on sensor characteristic

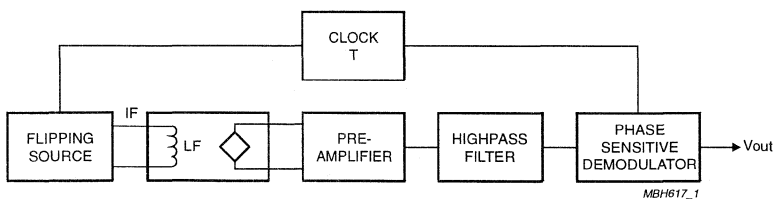

Figure 11 Block diagram of flipping circuit

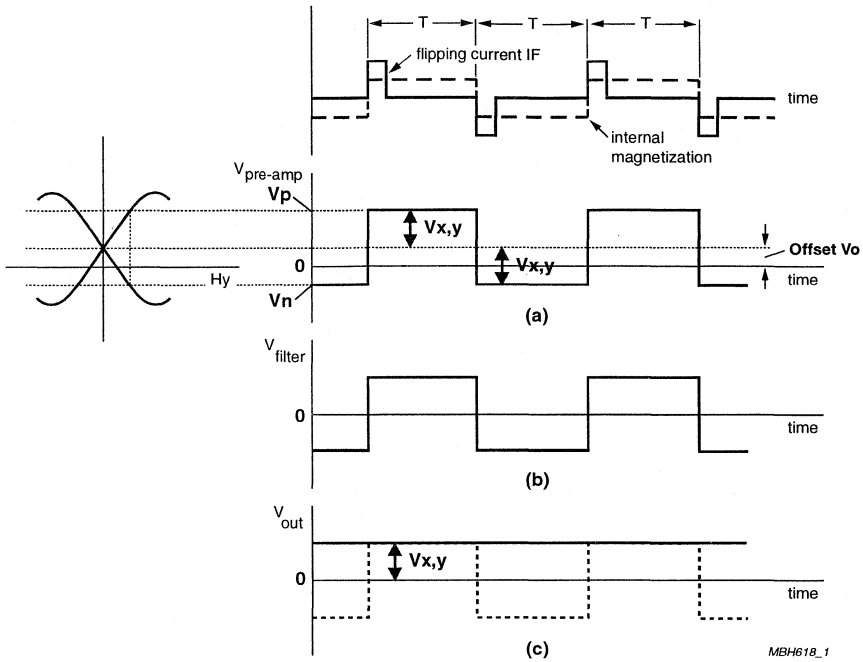

Figure 12 Timing diagram for flipping circuit
(a) voltage at preamp output; (b) voltage at filter output;
(c) voltage at rectifier output

The filter and the synchronous rectifier in Figure 11 can be saved, if a microcontroller with A/D converter is available. In that case, the desired output voltages Vx,y can be calculated from the high-level voltage Vp and the low-level voltage Vn of the flipped and amplified sensor signal (refer to Figure 12a) as:

$$Vx,y = \frac{1}{2} \cdot (Vp - Vn) \qquad (4)$$

Assuming that the offset does not vary rapidly with time, the microcontroller load can be reduced by reading Vp and Vn only after longer time intervals, e.g. minutes, to calculate and store the actual offset voltage Vo:

$$Vo = \frac{1}{2} \cdot (Vp + Vn) \qquad (5)$$

For azimuth calculation, then only one level of the flipped sensor signal has to be read by the microcontroller, e.g. Vp:

$$Vx,y = Vp - Vo \qquad (6)$$

Section 5.4 gives practical circuit examples and design hints for the flipping circuit. A pure hardware solution as well as a realisation using a microcontroller are considered.

5.3 Sensitivity Difference (ΔS) Compensation

At a given temperature, ΔS can be compensated by adjusting the SCU for equal output voltage swings Vy,pp and Vx,pp during compass rotation. The output voltage swings can be equalized by adjusting the amplification of one SCU channel. An alternative software solution would be to correct one output voltage mathematically: As the ratio Vy,pp/Vx,pp equals the ratio of sensitivities Sy/Sx=(S+ΔS)/S, Vy can be corrected as follows:

$$V_{y,corrected} = V_{y,measured} \cdot \frac{V_{x,pp}}{V_{y,pp}} \qquad (7)$$

When determining ΔS by measuring SCU output voltage swings, soft iron interference effects have to be avoided carefully, as these would also appear as difference in output voltage swings (refer to section 7).

To maintain high accuracy over temperature, the temperature drift of sensor sensitivity should be compensated during operation. Figure 13 shows the output characteristic Vo vs. H of a typical MR sensor element at different temperatures. All these curves indicate, that the sensor output is significantly dependent on temperature except at its zero point: a field strength of zero always causes an output voltage of exactly zero, independent of temperature. Of course this is only true disregarding sensor offset. However, offset can be eliminated perfectly by means of the flipping technique, as described above.

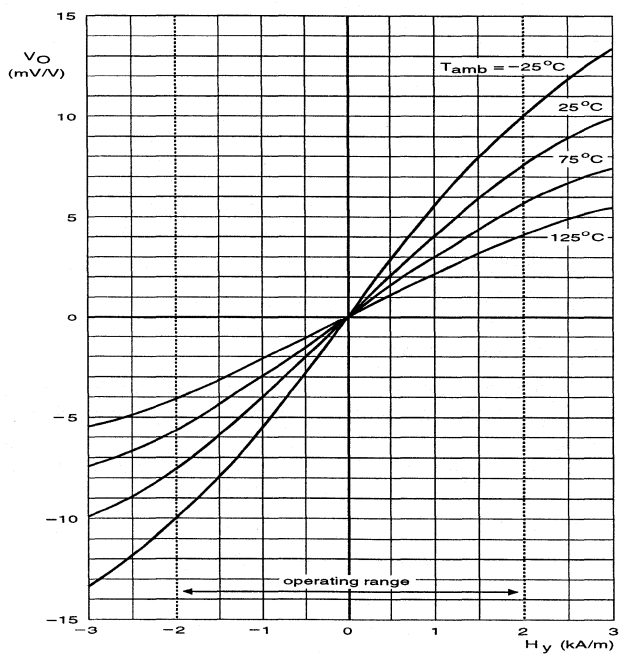

Figure 13 Typical MR sensor output characteristic (KMZ10)

Thus, temperature drift can be compensated by operating the sensors at their zero point. Therefore, the earth field component at each sensor has to be compensated by an opposing field of equal strength. If now magnitude and polarity of this compensation field are known, the measurement task is fulfilled, even though the sensor delivers zero output signal. This method is referred to as "electro-magnetic feedback".

Practically, the compensation field can be generated by supplying a current through an appropriate coil near the sensor. As already pointed out, Philips MR sensors for compass applications come with an integrated compensation coil, allowing to apply the electro-magnetic feedback method without the need for any external coils. Due to the well defined field factor of these integrated compensation coils, there is a well defined proportionality between field strength to be measured and compensation current.

Figure 14 shows a block diagram for an SCU channel employing both flipping and electro-magnetic feedback. The electro-magnetic feedback circuit is a closed-loop controller, in which a current regulator feeds the compensation coil in order to keep the sensor output voltage at zero. In order to achieve a sensor output voltage of exactly zero, a current regulator with integral characteristic is required. The measured field strength can be represented as voltage, proportional to the compensation current.

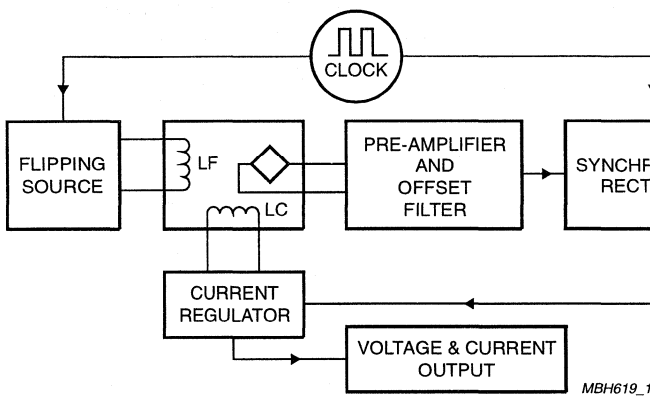

Figure 14 Block diagram of flipping and electro-magnetic compensation circuit

5.4 Non-orthogonality compensation

Up to this point it has been assumed, that the two magnetic field sensors are displaced at an angle of exactly 90°. However, in practice the displacement will deviate by an angle β from the desired orthogonality due to mounting tolerances. This deviation causes an error in compass reading, which is a periodic function of the azimuth (see Table 2 in section 10). The maximum error is approximately equal to the non-orthogonality β. Thus, for the KMZ52 with a specified max. non-orthogonality of 2°, the max. azimuth error is also 2°.

If a higher accuracy is desired, β should be compensated. If the compass is rotated with respect to the earth´s field, then the phase shift between Vx and Vy is 90°±β. Having determined β, the error can be eliminated mathematically:

Assuming, that the SCU delivers the signals $V_y = V_{max} \cdot sin(\alpha + \beta); Vx = V_{max} \cdot cos\alpha$, where α is the azimuth, that a corrected signal $V_{y,corrected} = V_{max} \cdot sin\alpha$ is desired,

and using the trigonometric relationship $\sin(\alpha+\beta) = \sin\alpha\cos\beta + \cos\alpha\sin\beta$,

the corrected Vy is:

$$V_{y,corrected} = \frac{V_y}{cos\,\beta} - V_x \cdot tan\,\beta \qquad (8)$$

5.5 Circuit Design

Figure 15 shows a circuit for one SCU channel (i.e. one field direction Hx or Hy), including pre-amplification, offset compensation by flipping and temperature compensation of sensitivity by electro-magnetic feedback.

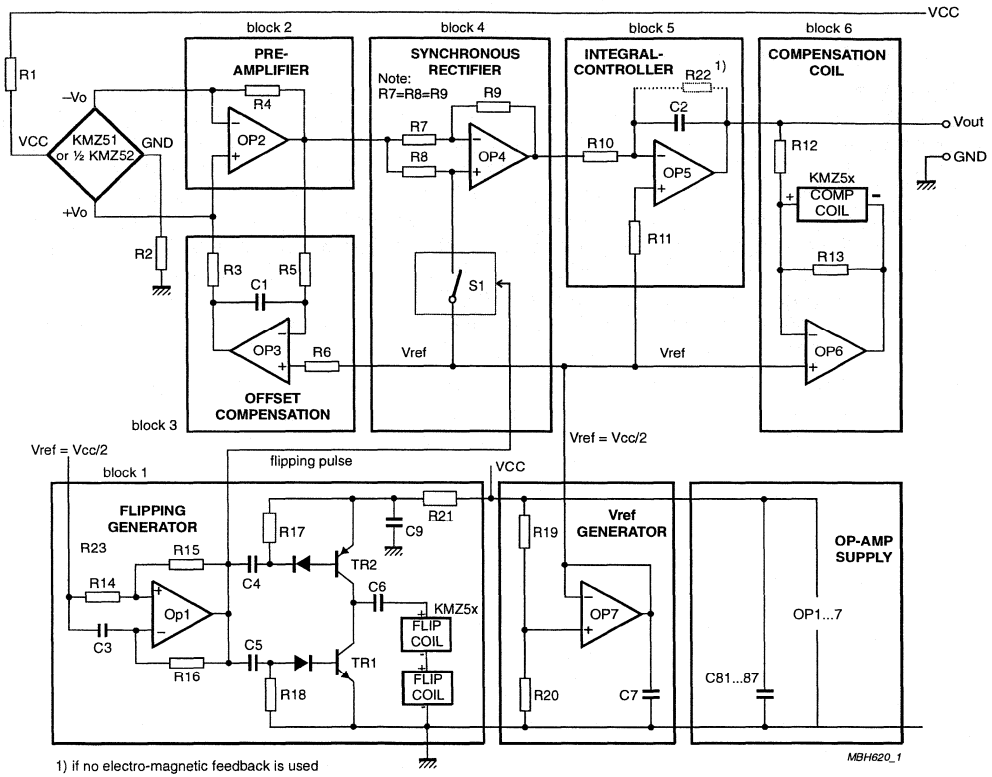

Figure 15 Signal conditioning circuit for one sensor

In the following, a design guideline for the circuit blocks is given. A complete, dimensioned SCU circuit based on Figure 15 are given in [3] and [4]. It should be noted, that this is an application example, which is not optimized. For product development, the design hints given here should be considered carefully.

5.5.1 Supply voltage considerations

The recommended supply voltage for the KMZ52 is 5V. As the sensor output voltages are ratiometric, both sensor elements should be connected to the same supply. For the flip coil driver, a supply of 10V is recommended to drive the required current of typ. 1A through the series connection of both set/reset coils, which may have a total resistance of up to 6Ω. The supply lines of flipping generator and signal circuitry should be carefully decoupled from each other in order to suppress flipping noise at the signal outputs.

The circuit of Figure 15 only requires a single external supply of Vcc = 10V. The flipping generator is supplied from here via decoupling network R21-C9. C9 should deliver the positive flipping current pulses, thus a

capacitor of some µF with low series resistance (e.g. Ta Elco) is recommended here. The time constant R21·C9 must allow C9 to charge up to approximately Vcc between the positive pulses, i.e. during the period of the clock generator. The 5V sensor supply is derived from Vcc by series resistors R1 and R2. A symmetrical OP-Amp supply is provided by connecting the OP-Amp supply pins to Vcc and GND respectively and connecting their reference inputs to Vcc/2, generated by the Vref generator.

5.5.2 Flipping generator (block1)

This block generates the flipping current pulses at a repetition frequency, determined by R16 and C3. The frequency is not critical, considering the flipping function itself. The choice of frequency is a trade-off between average current consumption on the one hand and response time and output ripple on the other hand. A frequency of approximately 1 kHz has proved to be a reasonable compromise. As the output of OP1 passes from high to low, C4/R17 produce a pulse that switches TR2 on. This charges C6 and a short positive pulse is passed to the flipping coil. For a low-to-high transition at the output of OP1, C5/R18 forces TR1 to conduct, discharging C6 and providing a negative current pulse through the coil. KMZ51 and KMZ52 both require flip current pulses of typically ±1A for a duration of 3µs. To drive that current controlled by the OP output, TR1 and TR2 should be Darlington transistors. For a complete SCU, the flipping generator is only required once and the flip coils of both sensors are connected in series. The function of decoupling network R21-C9 is described under supply voltage considerations.

For product development, it is recommended to use an improved flipping circuit like that shown in Figure 16. Here, an active current limiting provides, that the magnitude of the flip current pulses is independent of flip coil resistance. Thus, this circuit is insensitive to spread of flip resistance or supply voltage.

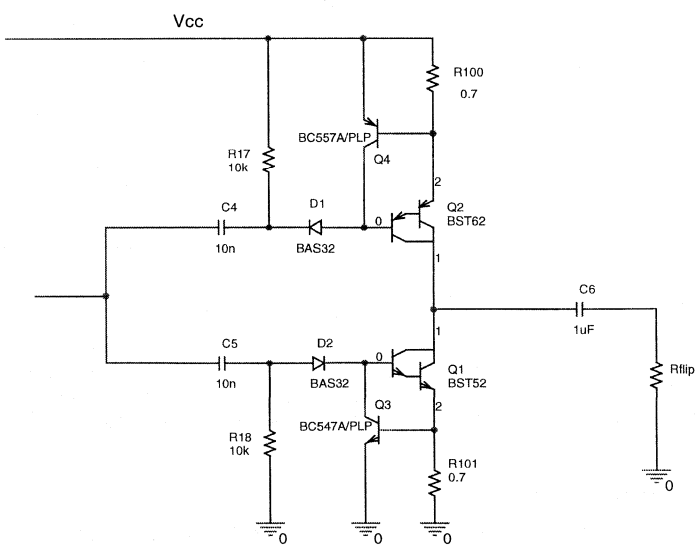

Figure 16 Flip circuit with active current limiting

5.5.3 Pre-amplifier (block 2)

The flipped sensor signal is amplified here by a factor of R4/Rbridge, where Rbridge is the resistance of the sensor bridge. Due to the electro-magnetic feedback used in this circuit, the pre-amp´s output will be virtually zero, when the closed loop control has settled. However, it should be provided that OP2 is operated in its linear range during transient processes of the closed loop control, e.g. after turn-on of the system. Thus, the pre-amplification should be set, such that OP2´s output is in its linear range, when the control loop is interrupted, even at maximum sensor signal plus max. offsets. An amplification of approximately 100 is a recommendable value.

5.5.4 Offset compensation (block 3)

The low pass filter around OP3 extracts the offset, which is the dc component of the flipped output signal (refer to Figure 12) and feeds it as negative feedback to OP2. The sensor offset is compensated this way. Principally, this could also be done by means of a capacitor between sensor and pre-amp, however the method shown here is preferable, as it compensates the offsets of both the sensor and OP2 simultaneously. This allows to use a low cost op-amp instead of a special low-offset type, thus reducing system cost. The determination of the filter cut-off frequency is a trade-off between smoothing of the output signal and response time.

5.5.5 Synchronous rectifier (block 4)

This block recovers the desired dc signal from the flipped ac signal. Provided that R7=R8=R9, this block performs an alternating +1 and –1 amplification, depending on the state of switch S1, which is controlled by the flipping generator. Thus, each time the output of OP2 changes polarity due to the flipping, this block causes an additional change of polarity, resulting in a rectification.

5.5.6 Integral controller (block 5)

This block forms the integral part of the PI-controller, built together with block 6 to drive the compensation coil for electro-magnetic feedback. An integral characteristic is required in the control loop, to force the remaining error - which is the sensor output signal - to zero. Dimensioning the time constant R10·C2 is a trade-off between response time and smoothness of output signal.

5.5.7 Compensation coil driver (block 6)

Forms the proportional part of the PI controller for electro-magnetic feedback including current source for the compensation coil. When the control loop has settled, i.e. when the compensation coil generates a field with equal magnitude and opposite sign to the respective earth´s field component, (Hex or Hey), the output voltage Vout is:

$$V_{out(x,y)} = H_{e(x,y)} \cdot \frac{R12}{Acomp} \qquad (9),$$

where Acomp is the field factor of the compensation coil (refer to the data sheet of KMZ5x). Equation (9) shows the desired effect of the electro-magnetic feedback: Vout is independent of sensor sensitivity and its temperature drift (KMZ52: typ. 0.31%/K). The temperature drifts of R12 and Acomp, which now affect the output voltage are significantly lower. Typical values are 0.02%/K down to 0.005% for standard or precision smd resistors and 0.01%/K for Acomp of the KMZ52. For ΔS compensation, Vout can be made adjustable by using a potentiometer for R12. Note, that due to the asymmetrical OPAMPs supply, Vout in (9) is the output voltage swing relative to Vref.

5.5.8 SCU without electro-magnetic feedback

If no temperature compensation of sensor sensitivity is required, the electro-magnetic feedback loop can be interrupted by omitting the compensation coil driver (block 6). Block 5 is still required as low pass filter in order to suppress flipping spikes on the signal line. However, a resistor R22 then needs to be connected in parallel to C2 in order to achieve a limited output voltage. The output voltage then is dependent on sensor sensitivity S and SCU amplification. Assuming that the synchronous rectifier (block 4) has an amplification magnitude of 1, the output voltage becomes:

$$V_{out(x,y)} = H_{e(x,y)} \cdot S \cdot \frac{R4}{R_{bridge}} \cdot \frac{R22}{R10} \qquad (10)$$

In this case, Vout can be adjusted by varying e.g. R22 or R10.

5.5.9 SCU with Microcontroller

Figure 17 shows a block diagram for an SCU, using a microcontroller. From the analogue circuitry shown in Figure 15, only the flip coil driver, pre-amps and - optionally - compensation coil drivers are required. The flipped sensor signals are fed to the µC via an A/D converter. It should be considered, that the resolution at this stage must be higher than the final compass accuracy. Principally the same considerations are valid for the D/A converter, driving the compensation coil driver. For a low-end compass, where accuracy is not critical, the internal 8 bit A/D converter of a low-cost µC could be sufficient. If higher accuracies are demanded, an external A/D converter with higher resolution can be the solution.

Offset compensation can be implemented as software, according to the equations shown in section 5.2. Further optional software features could be a control algorithm for electro-magnetic feedback or non-orthogonality compensation. Besides signal conditioning, the µC software will usually also perform the direction determination and further optional tasks, such as interference field calibration or true north calibration (see respective sections).

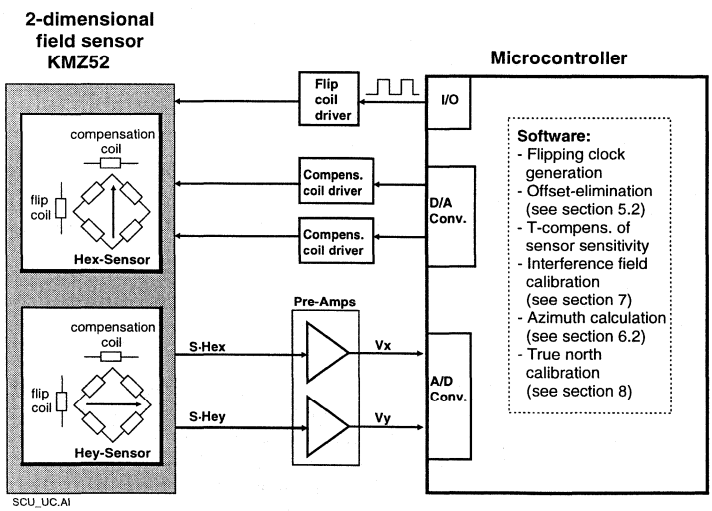

Figure 17 Signal conditioning circuit with microcontroller

6. DIRECTION DETERMINATION UNIT (DDU)

6.1 8-Segment Compass

If applications require a rough direction indication only, then a compass set-up is sufficient, which identifies the nearest of the eight cardinal or intermediate points (e.g. N, NW, S, SE, ...). This information can be gained from the SCU outputs without evaluating the arctan function in equation (1). Figure 18 shows the principle. Here the SCU output signals Vx and Vy are shown for a full clockwise rotation of the compass. By comparing the SCU signals with the thresholds Vt+ and Vt-, logic signals N', S', E', W' can be derived, which contain the desired information. Vt+ and Vt- are equal to +/-sin(22.5°). Figure 19 shows a circuit for the direction determination. As a display, e.g. LEDs can be driven by the respective outputs.

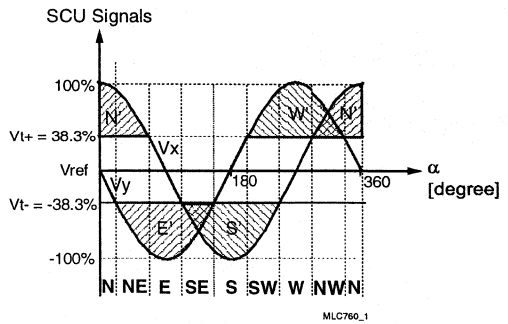

Figure 18 Direction determination for 8-segment compass

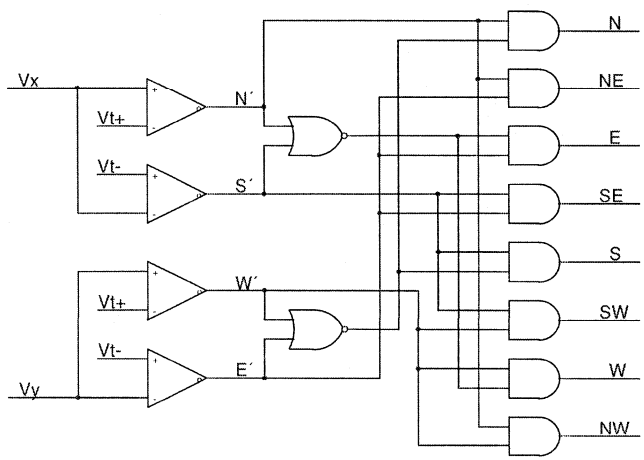

Figure 19 Circuit for 8-segment compass

6.2 High Resolution Compass

A compass with high accuracy is required for example in navigation systems. Here, the compass together with a measurement of the travelled distance are used to determine the actual position as long as no GPS signals can be received, e.g. while driving between high buildings.

If a direction information with high accuracy is required, e.g. 1 degree or better, then a microcontroller is required for evaluation of equation (1), where Hex and Hey have to be replaced by the SCU output voltages Vx and Vy respectively. It is assumed, that Vx and Vy are corrected with respect to offset, sensitivity difference and, if required, non-orthogonality. When implementing equation (1), it must be considered that the argument Vy/Vx has a pole at Vx = 0, and that the arctan function is uniquely defined only in the angular range of $-\pi/2$ to $+\pi/2$. Thus, the azimuth has to be computed, depending on the actual states of Vx and Vy:

$$
\begin{aligned}
&\alpha(Vx = 0, Vy > 0) = 270^\circ \\
&\alpha(Vx = 0, Vy < 0) = 90^\circ \\
&\alpha(Vx > 0, Vy > 0) = 360^\circ - (\arctan\frac{Vy}{Vx}) \cdot \frac{180^\circ}{\pi} \\
&\alpha(Vx > 0, Vy < 0) = -(\arctan\frac{Vy}{Vx}) \cdot \frac{180^\circ}{\pi} \\
&\alpha(Vx < 0) = 180^\circ - (\arctan\frac{Vy}{Vx}) \cdot \frac{180^\circ}{\pi}
\end{aligned}
\qquad (11)
$$

Equations (11) are based on the convention, that the azimuth is counted clockwise from north to the heading direction.

A very efficient way of computing trigonometric functions like arctan is the CORDIC (COordinate Rotating Digital Computing) algorithm. Its efficiency is based on the fact, that it only uses low-end functions like adding, shifting and reading of look-up tables. Basic information and implementation hints for the CORDIC algorithm can be found in the internet.

7. INTERFERENCE FIELD CALIBRATION

In practice, the earth field at the compass may be superimposed by other magnetic fields or distorted by nearby ferrous materials. An efficient compensation of such effects is required in order to achieve reliable azimuth readings.

As for any sensor system, only errors caused by deterministic interference sources can be compensated. In this case, deterministic means, that the interference source is at a fixed position relative to the compass and that its magnitude is constant versus time. Thus, as an example, a compass in a car could be compensated for the interference effects caused by the car body. On the other hand, a compass cannot be compensated for non-deterministic error signals, such as the field of another vehicle passing by. However, reading errors caused by such effects can usually be accepted, due to their momentary nature. To avoid misleading readings, a "low pass characteristic" may help, that suppresses the display of transient azimuth variations. Also a warning signal could be generated at the occurrence of such signals.

The influence of deterministic interference fields on a compass can be assessed by inspection of a test diagram as shown in Figure 20. The test diagram is a Lissajous figure, yielded by a 360° rotation of the compass and recording of the SCU output signals Vy versus Vx. Without any magnetic interference, the diagram appears as a circle, having its centre at (0,0) and a radius equal to the magnitude He of the earth field. All interference effects appear as a deviation from this shape. Basically, two kinds of interference can occur, called "hard iron effects" and "soft iron effects". "Hard iron effects" are caused by magnetized objects, which are at a fixed position with respect to the compass. These cause a magnetic field, which is vectorially added to the earth field. Thus, in the test diagram this effect appears as a shift of the circle´s centre to (Hix,Hiy), where Hix and Hiy are the components of the interference field. "Soft iron effects" occur due to distortion of the earth field by ferrous materials. This effect is dependent on compass angle. Therefore, it appears as a deformation of the circle in the test diagram. Figure 20 shows the effect of both hard iron and soft iron effects on the test diagram.

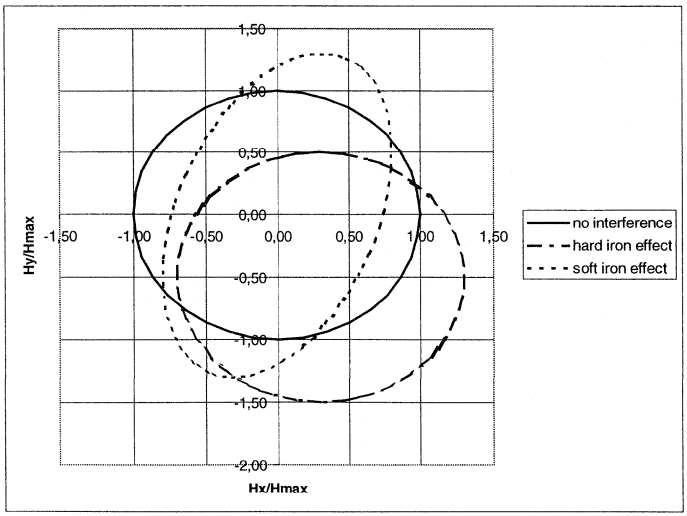

Figure 20 Typical test diagrams showing hard iron and soft iron effects

In practice, hard iron effects dominate over soft iron effects, provided the use of ferromagnetic materials near the compass can be avoided. To minimize the hard iron effects, a compass should never be installed near objects producing strong magnetic fields. As an example, loudspeaker magnets near the compass may produce

such strong fields, that the amplifiers of the SCU are overdriven. In this case, accurate measurement of the interference field and thus compensation are not possible.

Interference field compensation ideally means, to convert the shifted and/or deformed test diagram into a circle around the centre (0,0). Therefore, the interference field effect has to be measured and in the following, the compass readings have to be corrected considering the measurement results. Generally, this calibration procedure should be carried out individually for each compass. As an example, each individual car has its own "field signature". Even when mounting the same compass into the same environment again, e.g. after maintenance, it is recommended to carry out the calibration again. Thus, the calibration procedure should be simple, ideally automatical. Classical calibration methods, such as using a shielded room to measure the interference field effect without the earth field, or adjusting the compass reading to that of a reference compass, do not fulfill this requirement and will therefore not be discussed here.

Calibration methods become straight forward, if soft iron effects can be neglected compared to hard iron effects. As already pointed out, in this case only the components of a constant interference field have to be measured and compensated. In practice, soft iron effects are usually much weaker, provided there are no ferrous materials at or near the compass. In this case, satisfactory results may be achieved by using the "bidirectional calibration" method. Figure 21 illustrates the principle: Two measurements have to be carried out with the compass at the same location, but at a heading difference of 180°. For both measurements, the respective field components Hx and Hy have to be stored. Generally, the field at the compass is equal to the sum of earth field vector **He** and interference field vector **Hi**. After a compass rotation of 180°, **He** appears with equal magnitude but opposite sign, whereas **Hi** appears unchanged as its source is fixed with respect to the compass. Thus, the vector sum of both measurements **H1** + **H2** is:

$$\boldsymbol{H1}+\boldsymbol{H2}=\begin{pmatrix}H1x\\H1y\end{pmatrix}+\begin{pmatrix}H2x\\H2y\end{pmatrix}=\begin{pmatrix}Hex+Hix\\Hey+Hiy\end{pmatrix}+\begin{pmatrix}-Hex+Hix\\-Hey+Hiy\end{pmatrix}=\begin{pmatrix}2Hix\\2Hiy\end{pmatrix} \qquad (12)$$

Rearranging this vector equation, the interference field components as a function of the measured field components are yielded as:

$$Hix=\frac{1}{2}(H1x+H2x)$$
$$Hiy=\frac{1}{2}(H1y+H2y) \qquad (13)$$

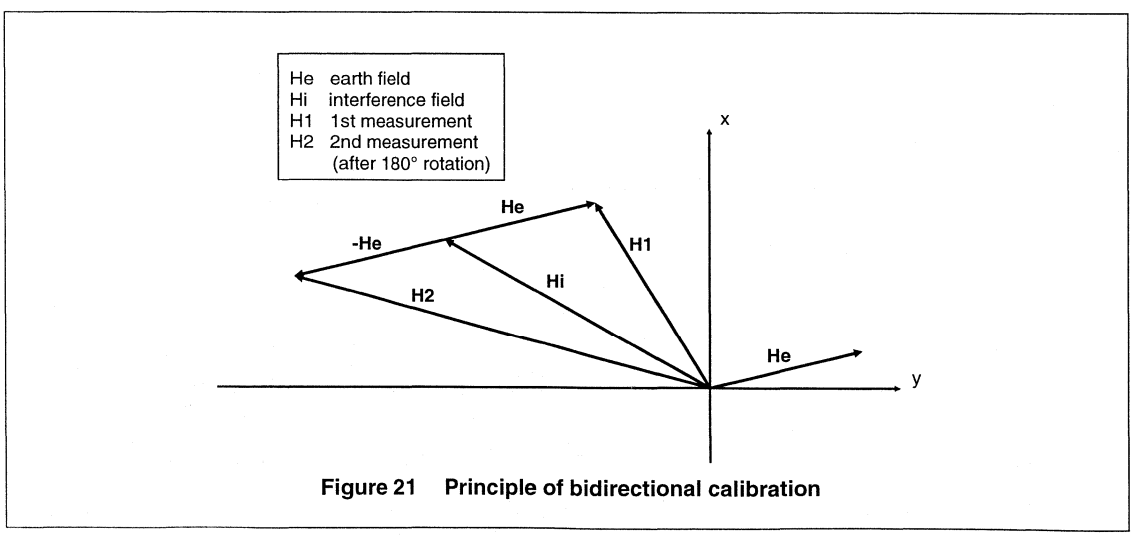

Figure 21 Principle of bidirectional calibration

Once the interference field components have been measured, their effect can be compensated by generating opposite field components -Hix and -Hiy at the respective sensors. Using Philips magnetoresistive sensors KMZ51 or KMZ52, this task can be fulfilled straight forward by applying appropriate currents to the compensation coils of the respective sensors. In systems using a microcontroller, the compensation can be done by subtraction of the interference field components from the respective sensor output signals.

The bidirectional calibration method can principally be implemented in an analog compass system. In that case, analog storage elements are required and a hardware implementation of equation (13). Using a microcontroller, the implementation of calibration procedures is generally simpler.

In applications, where not only hard iron effects, but also soft iron effects have to be compensated, more sophisticated calibration schemes have to be applied. These will not be covered by this application note, however a range of publications is available on that subject.

8. TRUE NORTH CALIBRATION

Once the azimuth has been measured with a compass, one has to be aware, that this indicates the heading direction relative to MAGNETIC north. However, in most practical cases, the heading direction relative to GEOGRAPHIC or TRUE north is required in order to allow navigation by means of a map. As the magnetic and geographic poles of the earth do not coincide, the direction of true north and magnetic north can deviate significantly from each other. This deviation is referred to as declination. Declination is defined as angle from true north to magnetic north. The value of declination varies with the position on earth and can be to the east or to the west. East declination means, that the magnetic north direction indicated by the compass is east of true north. Declination also varies over long periods of time, therefore only updated declination data should be used for compensation. Such data for locations world wide can be found at the web site of the National Geophysical Data Center NGDC [1].

In order to compensate for true north, the declination angle at the actual location has to be added to or subtracted from the azimuth reading of the compass. The appropriate operation depends on whether the declination is to the east or to the west.

A practical way for compensation of declination at a certain location or area would be to hold a compass in true north direction (i.e. along a road which exactly heads toward north). The azimuth reading now gives the declination value, that can be used furtheron for compensation.

9. TILT COMPENSATION

As pointed out in section 2, it is the horizontal (i.e. perpendicular to gravity) component of the geomagnetic field, that points to magnetic north. To measure this horizontal component, a compass system as described so far must be positioned, such that the sensitive axes of its field sensors are also in the horizontal plane. If however the compass is tilt, i.e. not held horizontally, a reading error occurs. The error magnitude depends on the tilt angle of the compass and on the inclination or dip angle of the earth´s field at the respective location.

Figure 22 helps to gain a basic understanding of the tilt effect and allows to derive the maximum tilt error. Here, x and y are the sensitive axes of the compass and the z-axis is normal to the compass plane. To simplify the illustration, the compass axes here are fixed, such that the x-y plane is parallel to the earth´s surface, whereas the tilt τ is "simulated" as a rotation of the earth´s field relative to the compass. A further simplification has been made, in that without tilt ($\tau = 0$) the y-axis coincides with the north-south direction and the x-axis coincides with the east-west direction. Thus, without tilt, the horizontal component of He has only a y-component and correctly points towards north. For a tilt along the north-south axis (i.e. with east-west as rotation axis), the horizontal component of He will vary in magnitude but will still point towards north. Thus, the tilt error is zero. If however a tilt along the east-west axis (i.e. with north-south as rotation axis) occurs, as indicated in the figure, the direction of He´s horizontal component deviates from north by an angle ε. For any tilt along an axis between north-south and east-west, the resulting error depends on the "tilt component" along the east-west axis. Therefore, a tilt along the east-west axis, as shown in Figure 22, causes the maximum error.

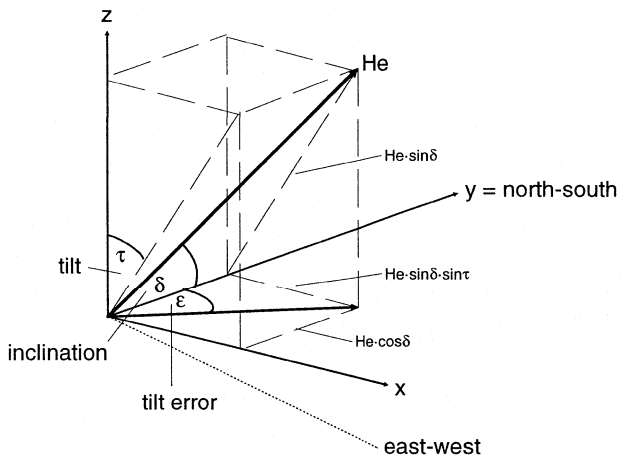

Figure 22 Tilt error

Derivation of the maximum tilt error ε from Figure 22 is straight forward:

$$\varepsilon_{max} = \arctan\frac{He \cdot \sin\delta \cdot \sin\tau_{east-west}}{He \cdot \cos\delta} = \arctan(\tan\delta \cdot \sin\tau_{east-west}) \qquad (14)$$

This equation is independent of heading direction, thus the simplification in Figure 22, that x = heading direction, causes no restriction. Equation (14) indicates, that the error increases with both inclination δ and tilt angle τ and that the error is zero, if inclination and/or tilt are zero. The maximum tilt error occurs for a tilt angle of 90°, where sinτ equals one and therefore the error reaches the magnitude of the inclination δ. Figure 23

shows tilt error versus tilt angle for two loactions on earth. Inclination values for locations world wide are available at [1].

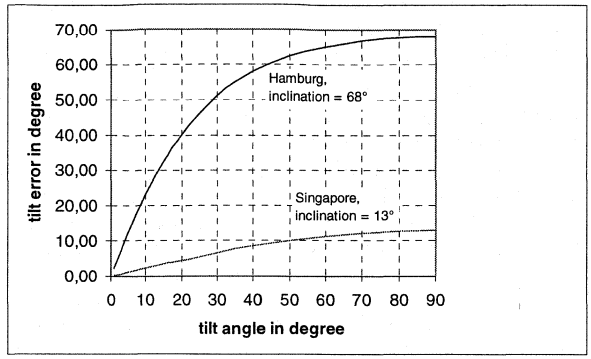

Figure 23 Tilt error magnitudes

A classical method for avoiding tilt errors is to put a compass into a liquid, which provides horizontal levelling of the compass due to gravity. This is often referred to as "mechanical gimbaling". However, as the compass here is not fixed within its housing, interference fields caused by this housing are no deterministic signals anymore and can therefore not be calibrated (refer to section 7).

Tilt error can be compensated without moving parts by converting the measured earth field components mathematically into the horizontal components. This technique is often referred to as "electronical gimbaling" and requires additional sensor elements:

- A third magnetic field sensor, as now all three cartesian vector components of the earth´s field, i.e. Hex, Hey, Hez have to be measured.
- Sensors for pitch and roll to detect the tilt status of the compass. Pitch and roll are terms coming from aviation. As shown in Figure 24, pitch refers to a tilt along the x or heading direction (= rotation around the y axis), whereas roll refers to a tilt along the y axis (= rotation around the x-axis).

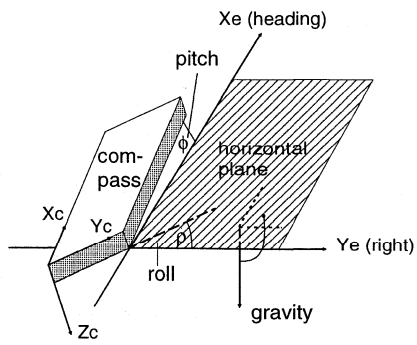

Figure 24 Definition of pitch and roll

The derivation of the horizontal earth field components Hxe, Hye from the measured field components Hxc, Hyc, Hzc requires a transformation between two rotated cartesian 3-D coordinate systems (refer to Figure 24). Equations (15) are the result of this transformation:

$$Hxe = Hxc \cdot \cos\phi - Hyc \cdot \sin\phi \cdot \sin\rho - Hzc \cdot \sin\phi \cdot \cos\rho$$
$$Hye = Hyc \cdot \cos\rho + Hzc \cdot \sin\rho \qquad (15)$$

Figure 25 gives a simplified block diagram for an electronically gimbaled compass system. Using Philips magnetoresistive sensors, the 3-axes field sensor system can be built up with a dual sensor KMZ52 for the x and y axes and a single sensor KMZ51 for the z axis. For pitch and roll sensing, gravity sensors as compact devices in IC packages are available, realized by combining micro-machining and integrated circuit technology.

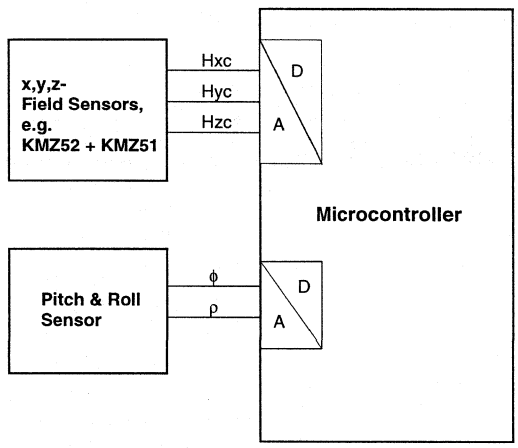

Figure 25 Electronically gimbaled compass

10. SYSTEM ACCURACY

Table 2 summarizes the main error influences on a compass system together with methods for calibration, as discussed in the respective sections of this paper. In all equations, α is the real azimuth.

Table 2 Summary of errors and calibration methods

Error source	Resulting azimuth error (α - $\alpha_{measured}$)	Calibration	See section
Offsets Vox and Voy at SCU outputs	$= \left\lvert \alpha - \arctan\frac{V_{max}\sin\alpha + V_{oy}}{V_{max}\cos\alpha + V_{ox}} \right\rvert$ $\approx 0.8° / \frac{V_{ox,y}}{V_{max}}[\%]$ Assumption: $V_{ox} = V_{oy}$	Continuous in-circuit calibration by flipping combined with electronic feedback or mathematical correction.	5.2, 5.5
Sensitivity difference ΔS between SCU channels	$= \left\lvert \alpha - \arctan\left[\left(1+\frac{\Delta S}{S}\right)\tan\alpha\right] \right\rvert$ $\approx 0.3° / \frac{\Delta S}{S}[\%]$	Trimming of SCU amplification to achieve equal amplitudes of Vout; if required, in-circuit T-drift compensation by electro-magnetic feedback.	5.3, 5.5
Non-orthogonality, i.e. sensors mounted at 90°±β	$= \left\lvert \alpha - \arctan\frac{\sin(\alpha+\beta)}{\cos\alpha} \right\rvert$ $\approx 1° / \beta[°]$	Measure β as phase difference between SCU output voltages and store it. Mathematical correction during operation.	5.4
Interference field Hix,Hiy ("hard iron" effect)	$= \left\lvert \alpha - \arctan\frac{H_e\sin\alpha + H_{iy}}{H_e\cos\alpha + H_{ix}} \right\rvert$ $\approx 0.8° / \frac{H_{ix,y}}{H_e}[\%]$	Determine interference fields, e.g. using bi-directional calibration method. Correction mathematically or using compensation coils.	7
Declination λ	$= \lambda[°]$	Shift zero-point of azimuth reading by λ.	8
Tilt τ	$= \arctan(\tan\delta \cdot \sin\tau_{east-west})$ δ: inclination angle	Continuous in-circuit calibration by using 3-dimensional compass, pitch and roll sensors and mathematical correction.	9

During trimming for compensation of ΔS, soft iron interference fields and tilt should be avoided, as these effects would also appear as a difference in SCU output amplitudes.

In systems using a microcontroller, further errors occur, mainly due to quantization and non-linearity of the A/D converter.

As the individual errors described above are random quantities and independent of each other, the total system error can be found by applying the error propagation law:

$$E_{tot} = \sqrt{E_1^2 + E_2^2 + \ldots + E_n^2} \qquad (16)$$

11. APPLICATION EXAMPLES

Following block diagrams represent ideas for the realization of complete compass systems. The functional blocks for signal conditioning and direction determination shown here have been described in earlier sections of this paper.

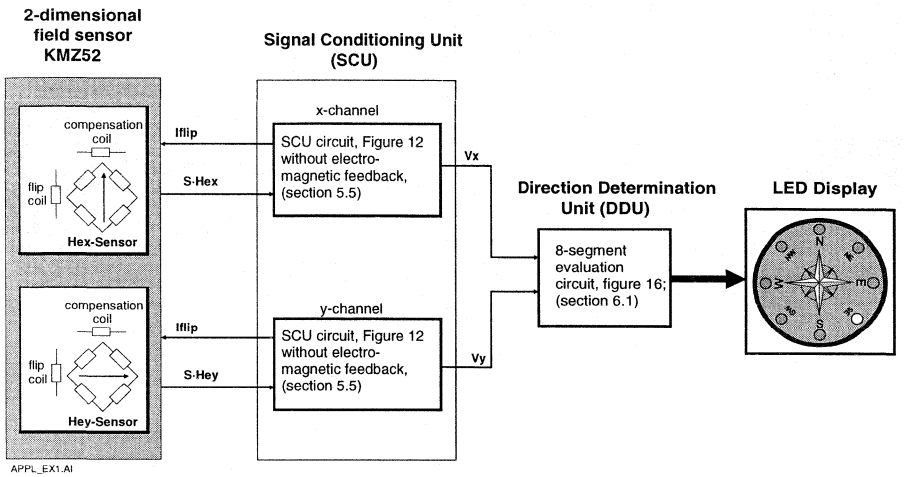

Figure 26 Analog 8-segment compass

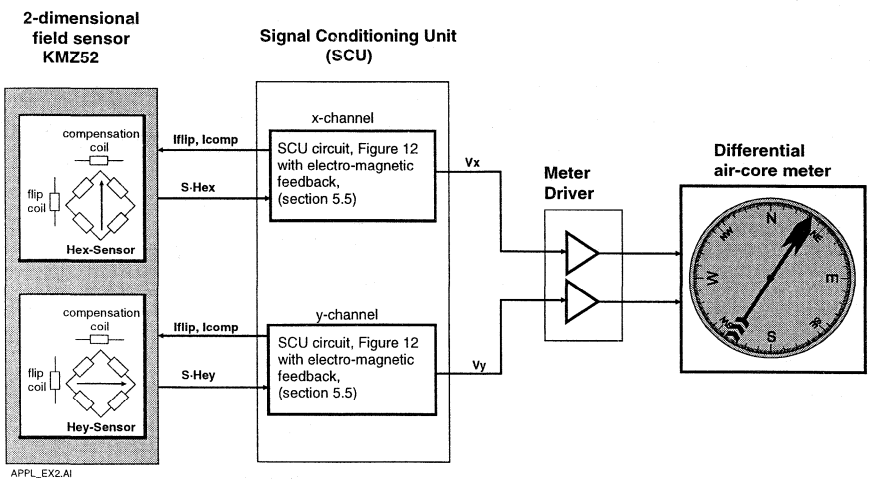

Figure 27 Analog high resolution compass

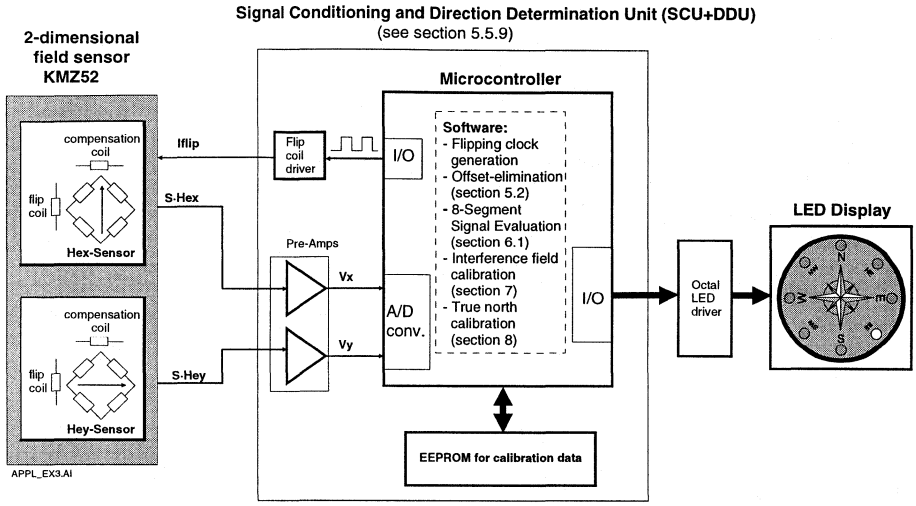

Figure 28 8-segment compass with microcontroller

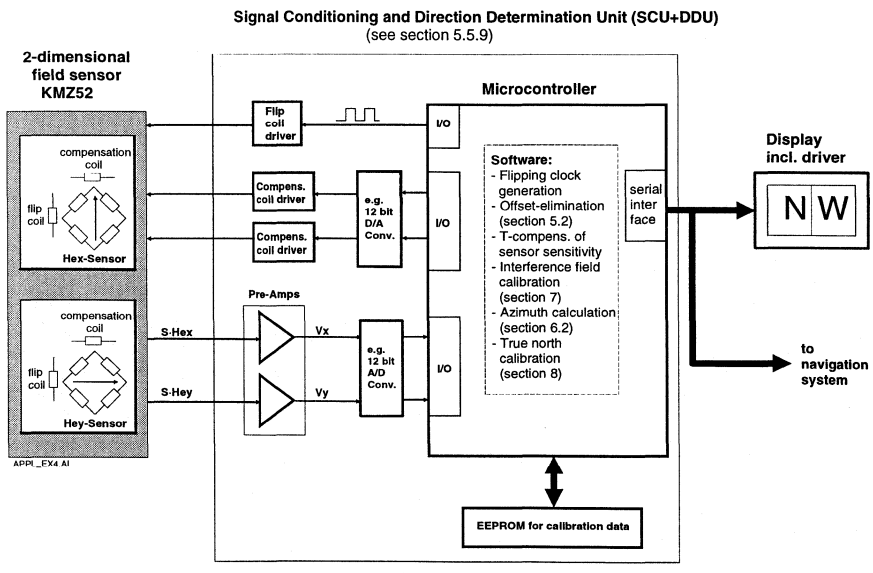

Figure 29 High-end compass with microcontroller

12. REFERENCES

[1] Status Report of Repeat Data At the WDC-A,
(Summary of data from geophysical observatories world wide)
http://www.ngdc.noaa.gov/seg/potfld/mrepeat1.shtml

[2] Data sheet: KMZ52 Magnetic Field Sensor
Philips Semiconductors

[3] Data Handbook SC17 including CD-ROM: Semiconductor Sensors
Philips Semiconductors, 1998

[4] Web site of Philips Semiconductors
http://www.philips.semiconductors.com/handbook/various_39.html

APPENDIX 1 List of abbreviations

H	magnetic field vector
H	magnetic field strength
He(x,y)	magnetic field strength of earth´s field (x,y component)
Hi(x,y)	magnetic field strength of interference field (x,y component)
S	sensitivity (of sensor element or SCU channel)
SCU	signal conditioning unit
DDU	direction determination unit
Voy,x	SCU offset voltage (x or y channel)
Vy,x	SCU output voltage (x or y channel)
ΔS	sensitivity difference between SCU channels
α	azimuth angle, exception: section 4: angle between current and magnetization within a magnetoresistive element
β	non-orthogonality of sensor system
δ	dip or inclination angle
ε	tilt error angle
ϕ	pitch angle
λ	declination angle
ρ	roll angle
τ	tilt angle

APPENDIX 2 Unit conversions

1 Tesla = 10^4 Gauss = 10^9 Gamma = $7{,}96 \cdot 10^5$ A/m

APPLICATION CIRCUIT

Signal conditioning unit for compass

Fig.36 shows a dimensioned circuit that provides the signal conditioning for both outputs of a KMZ52 (or two KMZ51), as required in a compass application.
The circuit delivers the output voltages Vx and Vy, which are proportional to the magnetic field measured in the x and y directions respectively.
The operational principal of the circuit is based on that described in section 5.

The circuit has the following characteristics:

- supply voltage 10 V
- flip frequency ≈ 500 Hz
- sensitivity ≈ 30 mV per A/m
- bandwidth ≈ 10 Hz.

For demonstration purposes, the circuit can be operated with or without electromagnetic feedback, depending on the state of switches S1 and S2.

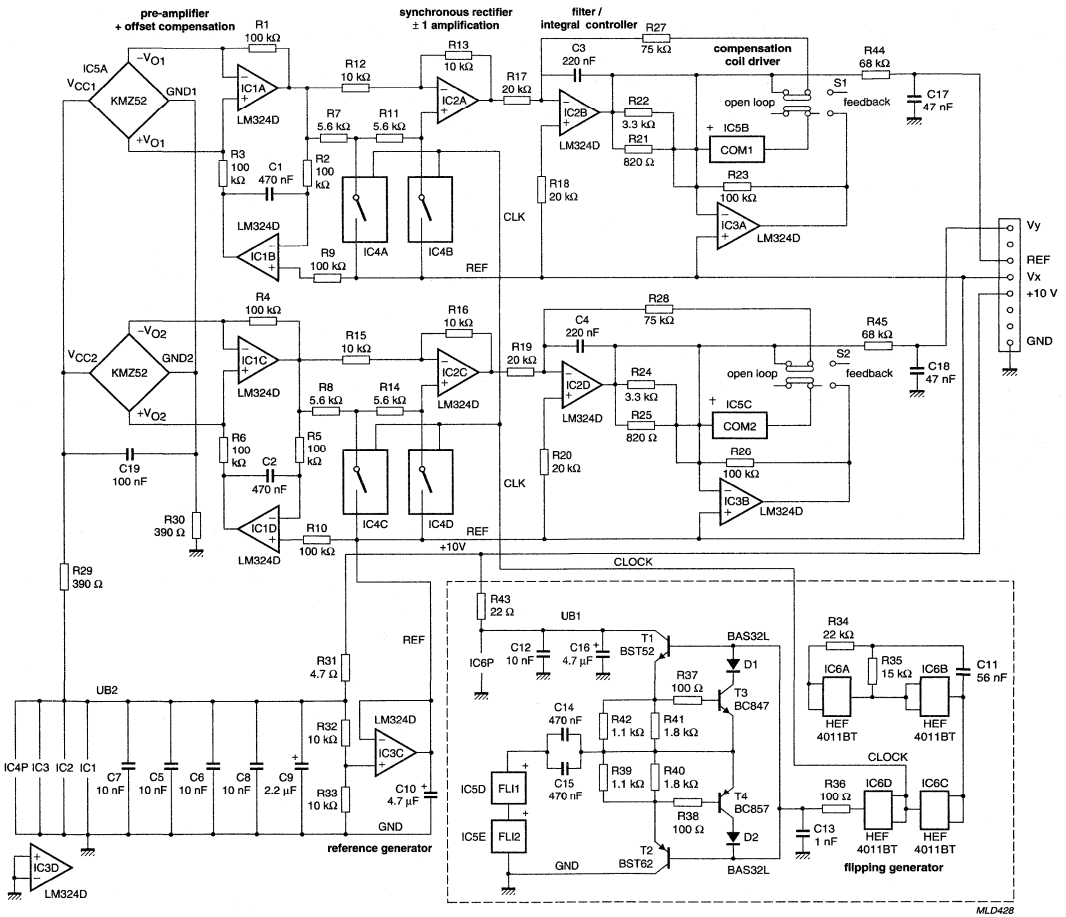

Fig.36 Application circuit diagram for signal conditioning unit for compass.

EXAMPLE 1

Earth geomagnetic field compensation in CRT's

The Earth's geomagnetic field has always caused problems for TV and monitor manufacturers, as it influences the trajectory of electrons in a CRT tube producing a horizontal tilt in the geometry and convergence error shifts. With the introduction of wide screen picture tubes, this problem has become unacceptable, especially with geometric test patterns and 16:9 aspect ratios. With the continuing goal of improving picture quality and allowing for varying magnetic fields in every part of the world, a compensation circuit was required to reduce this effect.

A simple one-dimensional solution is to wrap a DC-current carrying coil around the neck of the CRT to generate a magnetic field opposite to the Earth's field, cancelling the twist in the electrons path and reducing by approximately 50% the number of convergence errors.
This coil also has the additional advantage of compensating for any other extraneous electromagnetic field sources emanating from the TV such as the loudspeakers. By including a magnetoresistive sensor to detect the Earth field, the output from the sensor can be used to drive the compensation field, making adjustment automatic.

Although residual picture twist and North/South trapezoid errors can still be seen, a simple DC-shift in the compensation current will eliminate the picture twist and the addition of a vertical sawtooth (ramp) current, derived from the vertical deflection, will remove the N/S trapezoid.

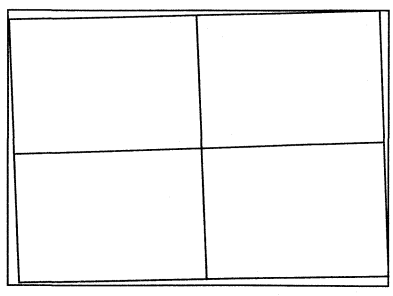

Fig.37 Geometry error - horizontal picture tilt.

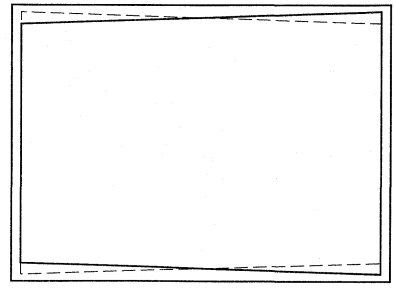

Fig.38 Geometry error - North/South trapezoid.

EXAMPLE 2

Traffic detection

As the number of vehicles using already congested roads steadily increases, traffic control systems are becoming necessary to avoid time consuming traffic jams. These systems monitor traffic flow, average speed and traffic density, allowing electronic road signs to control the flow and speed of traffic at known trouble spots. They also have the advantage of indicating possible incidents, where traffic speeds fall significantly below average on certain sections of road. Simple modifications to these systems allows them to be used to improve safety, and also to monitor ground traffic at airports.

Although highly sophisticated computer systems are used to analyse the various inputs in traffic systems, currently this input information is gained from inductive systems which have a number of disadvantages. The low sensitivity offered by inductive measuring systems requires large areas of road to be lifted and re-surfaced during installation. With their high power consumption, and the fact they produce very little information regarding the type of traffic passing over them, makes them both costly and inefficient. They are also rather unreliable due to road thermal stress.

As practically every vehicle manufactured contains a high number of ferromagnetic components, a measurable magnetic field specific to an individual model from every manufacturer can be detected, using weak field measurement techniques with magnetoresistive sensors. Even with the greater use of aluminium in manufacture and if the vehicle has been demagnetized, it will still create a measurable change in geomagnetic field strength and flux density.

Magnetoresistive sensors for magnetic field measurement

General

In comparison with inductive methods, with its high sensitivity magnetoresistive measuring can provide information on the passing vehicle type. Also, due to the sensor size and placement, systems can be easily and quickly installed in any stretch of road, or even by the side of the road, if necessary. Combined with almost negligible power consumption, this makes magnetoresistive control systems an inexpensive and highly efficient method of monitoring traffic levels.

MEASUREMENTS ON ROADS

A field test with three-dimensional sensor modules was set-up, firstly to measure the signals of different vehicles; and secondly, the relative occurrence of signal values of three vehicle categories (car, van and truck). For the first test, one module was placed in the road, under the vehicle and for comparison, a second module was placed at the side of the road. For the second test, which was performed 'live' on a street in Hamburg, Germany, the module could only be positioned at the side of the road.

The local geomagnetic field was calibrated to zero, so that only the disturbance in the field caused by the passing vehicle would be recorded. Figure 39 shows the spectra produced by an Opel Kadett.

The sensor modules also proved sensitive enough to detect and distinguish motorbikes (even with engine, frame and wheels being made of aluminium), which produced the following roadside spectra.

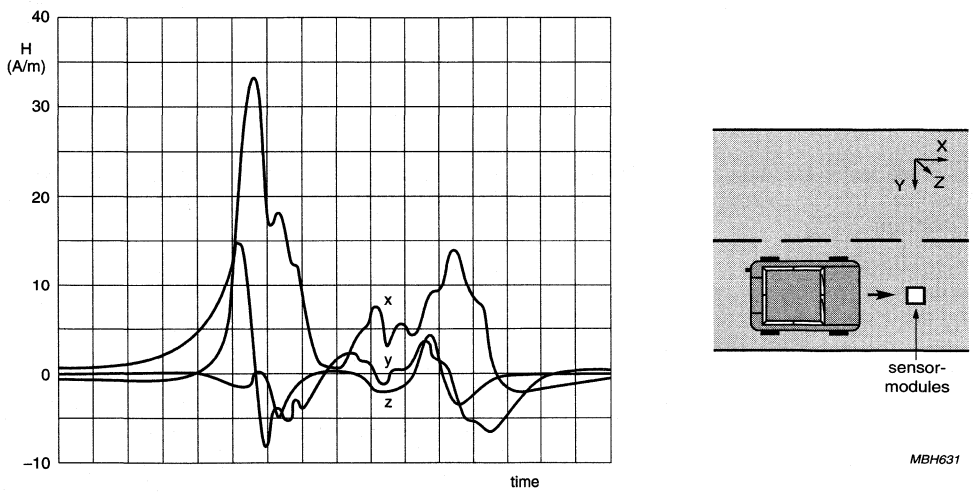

Fig.39 Spectra for an Opel Kadett from ground sensor.

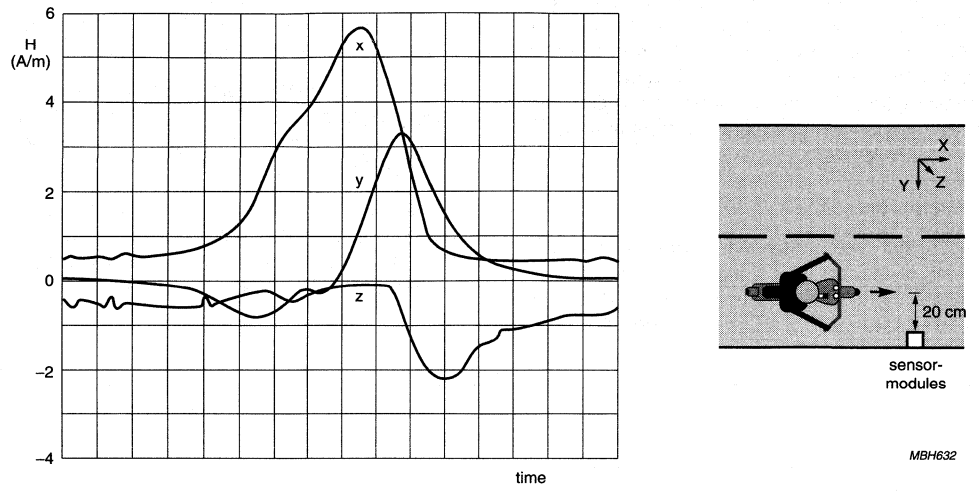

Fig.40 Spectra for a motorbike.

For the roadside test in Hamburg, the road was chosen at random and the maximum signal value was recorded for different vehicles, being grouped into cars, vans and trucks. The relative occurrence of signal values are shown in the following diagram.

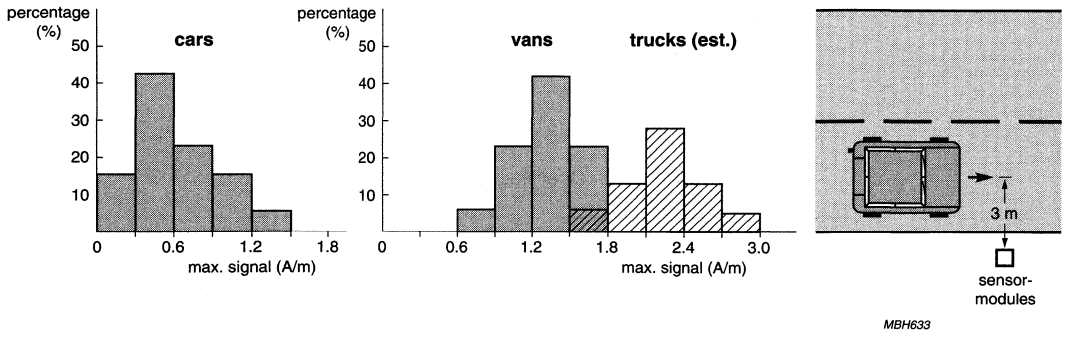

Fig.41 Distribution graphs of maximum signal versus occurrence.

The signals in each group seem to have a Gaussian distribution with a characteristic maximum (although in fact there were only three trucks, so the values for this group are an estimate).

AIRPORT GROUND TRAFFIC CONTROL

With the constant growth in air traffic around the world, one serious consideration in the improvement of safety and the ability to improve the handling capacity of airports, is the control of traffic on and around runways. Using a traffic control system, it is possible to introduce automatic guidance systems and prevent runway incursions even at heavily congested airports or under low visibility conditions, in accordance with regulations set-down by the internationally recognized authorities.

Although there are a number of possible sensor solutions, traffic systems using magnetoresistive technology have none of the drawbacks of existing radar, microwave, I/R, pressure, acoustic or inductive systems (see Table 6). They meet all of the functional and environmental restraints, such as large temperature ranges, insensitivity to climatic changes, low power consumption and, most of all, low cost, high reliability and ruggedness. They can also perform a range of signalling functions including detection of presence, recognition, classification, estimation of speed and deviation from path.

Table 6 Disadvantages of various sensors for airport ground traffic control units

Radar	Microwave barriers	Inductive sensors
• High costs • Reduced efficiency with large number of targets • Line of sight only • Complex target identification • Low resolution • Slow response times	• Cannot be installed flush with the ground • Creates new obstacles in surveyed area • Produce EM interference	• Low sensitivity and short range • Poor target information • High power consumption • Unreliable in harsh environments • Repairs require traffic to be stopped or diverted
Pressure sensors	**Acoustic sensors**	**I/R signalling**
• Frequent mechanical breakdowns when used in harsh environments • Associated ageing problems • Poor target identification	• Signal interference when used outdoor and due to weather conditions • Trade-off between sensitivity and range • Large power consumption	• Greatly affected by weather conditions • Complex target identification

EXAMPLE 3

Measurement of current

The principle of measuring current with a magnetoresistive sensor is straightforward. As a current, i, flows through a wire, it generates a magnetic field around it which is directly proportional to the current. By measuring the strength of this magnetic field with a magnetoresistive sensor, the current can thus be accurately determined.

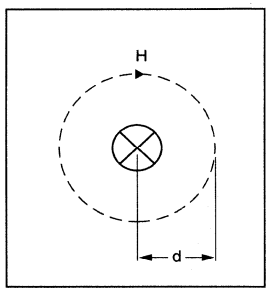

Fig.42 Diagram showing field direction in a current carrying wire.

The relationship between magnetic field strength H, current i and distance d is given by:

$$H = \frac{i}{2\pi d} \qquad (14)$$

Some calculated values of H for typical conditions are given in Table 7.

Table 7 Values for the magnetic field generated by a current carrying wire at various distances and currents

EXAMPLE	CURRENT (i)	DISTANCE (d)	MAGNETIC FIELD (H)
1	10 mA	0.5 mm	3.18 A/m
2	1 A	0.5 mm	318 A/m
3	1000 A	10 mm	15.9 kA/m

Table 7 clearly indicates that current measurement can involve measurement of weak or strong magnetic fields.

As the sensitivity of magnetoresistive sensors can easily be adjusted, using different set-ups and different electronics (refer to the selection guide in the General section), an individual sensor can be optimized for a specific current measurement application, a clear advantage over Hall effect sensors.

Set-ups with MR sensors allow current measurement without breaking the conductor or interfering with the circuit in any way, providing a distinct advantage over resistor based systems. They can be used for example, for measuring the current in a headlamp-failure detection system in motor vehicles or in clamp-on (non-contacting) meters, as used in the power industry.

The accuracy achievable in current measurement using magnetoresistive sensors is highly dependent on the specific application set-up. Factors which affect accuracy are mechanical tolerances (such as the distance between the sensor and the wire), temperature drift and the sensitivity of the conditioning electronics.

In any measurement set-up, there are always other magnetic fields present besides that generated by the current, such as the earth's magnetic field, and these interfere with the measurement. A more accurate measurement set-up uses two magnetic field sensors, to compensate for these external fields (see Fig.43).

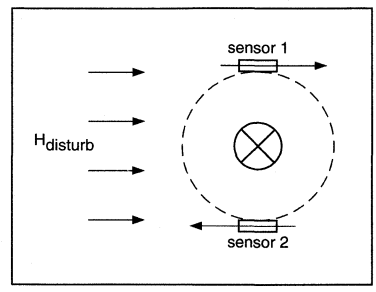

Fig.43 Diagram showing two sensors to measure current.

The first sensor detects both the interference field and the current-field in the positive direction, and the second sensor detects the interference field in the negative direction and the current-field in the positive direction. These two signals are added, cancelling out the interference field, leaving a signal that is representative of only the current-field.

This set-up works with homogeneous interference fields like that from the earth. Inhomogeneous fields, which will produce different interference fields inside the two sensors, will still affect the current measurement. This error can be minimized by keeping the distance between the sensors small. Large magnetic fields which fall outside the range of the sensors can also produce errors, so the size of external fields must be limited.

Another advantage of using two sensors, at a fixed distance apart, is that measurement is less sensitive to sensor-conductor distance. If the conductor is moved closer to the first sensor, then its distance from the second sensor is correspondingly increased and the effect is compensated. For small differences in distance between the conductor and sensors, sensitivity is nearly constant and the conductor need not be fixed in place. This method lends itself to measurement of current in free cables.

Table 8 summarizes the various advantages and disadvantages of one-sensor and two-sensor measurement set-ups as described above.

Table 8 Summary of advantages and disadvantages of typical measurement set-ups

CURRENT MEASUREMENT WITH TWO MAGNETIC FIELD SENSORS		CURRENT MEASUREMENT WITH ONE MAGNETIC FIELD SENSOR	
PROS	**CONS**	**PROS**	**CONS**
• no galvanic connection	• interference effects from inhomogeneous fields	• no galvanic connection	• effects of interference from external fields
• no breaking of the conductor	• errors generated from large external fields	• no breaking of the conductor	• sensitive to the sensor-conductor distance
• small physical dimensions		• small physical dimensions	
• reduced sensitivity to sensor-conductor distance			
• reduced interference effects from homogeneous fields			

For proper functionality of the set-ups shown in Fig.42 and Fig.43 it is important to limit disturbing fields in x-direction (perpendicular to sensitive direction) of the sensor. Thus 'flipping' of the sensor output characteristic (see section) can be prevented.

Applications where 'flipping' (respectively disturbing fields in x-direction) can not be prevented lead to a reversed sensor characteristic. This means for one and the same current (respectively magnetic field) the output voltage of the MR sensor bridge can be positive or negative, depending on the polarity of the magnetization of the permalloy. It is obvious that this phenomenon is unwanted, especially for DC current measurements. For AC current measurements, flipping may cause a frequency doubling at the output voltage of the MR sensor. This happens if the AC current to be measured also produces periodic magnetic field components in x-direction and therefore the sensor is flipped periodically.
To avoid 'flipping' of the transfer characteristic, it must be ensured that the magnetization of the permalloy is not reversed by disturbing fields in x-direction of the sensor. This can be achieved by applying a static magnetic field in x-direction, e.g. by gluing a permanent magnet to the sensor package. The magnitude of this stabilizing magnetic field in x-direction must be chosen properly, because on the one hand magnetic fields in x-direction avoid unwanted flipping, but on the other hand sensitivity of the sensor is reduced (see section 'Flipping').
A sophisticated solution for measuring DC currents, even with the presence of disturbing magnetic fields in x-direction and therefore flipping of the output characteristic, is to operate the sensor at its zero point. Such an arrangement in which the magnetic field generated by the current-carrying wire is compensated by a secondary circuit wrapped around a ferrite core can be seen in Fig 44.

At the 'null-field' point, detected by the sensor located in the air gap between the ends of the core, the magnitude of the current in the secondary circuit is a measure of the current in the main circuit.

Even if the sensor characteristic is reversed by disturbing magnetic fields in x-direction then the output voltage of the MR sensor bridge remains zero, because this operating point is equivalent to the point where the "normal" and "flipped" sensor characteristic intersect. Additionally this arrangement represents a more accurate way to measure DC currents, because any inaccuracies as a result of mechanical tolerances, temperature drift and slight non-linearity in the sensor characteristics are reduced.

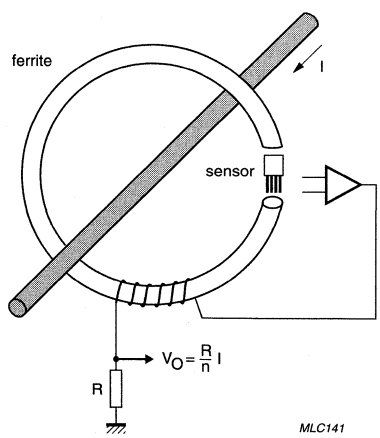

Fig.44 Current measurement using a compensating coil.

DEVICE DATA

Magnetic field sensor KMZ10A

DESCRIPTION

The KMZ10A is an extremely sensitive magnetic field sensor, employing the magnetoresistive effect of thin-film permalloy. Its properties enable this sensor to be used in a wide range of applications for navigation, current and field measurement, revolution counters, angular or linear position measurement and proximity detectors, etc.

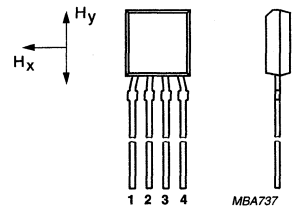

Fig.1 Simplified outline.

PINNING

PIN	SYMBOL	DESCRIPTION
1	$+V_O$	output voltage
2	GND	ground
3	$-V_O$	output voltage
4	V_{CC}	supply voltage

QUICK REFERENCE DATA

SYMBOL	PARAMETER	MIN.	TYP.	MAX.	UNIT
V_{CC}	bridge supply voltage	–	5	–	V
T_{bridge}	bridge operating temperature	–40	–	+150	°C
H_y	magnetic field strength	–0.5	–	+0.5	kA/m
H_x	auxiliary field	–	0.5	–	kA/m
S	sensitivity	–	16	–	$\frac{mV/V}{kA/m}$
R_{bridge}	bridge resistance	0.8	–	1.6	kΩ
V_{offset}	offset voltage	–1.5	–	+1.5	mV/V

CIRCUIT DIAGRAM

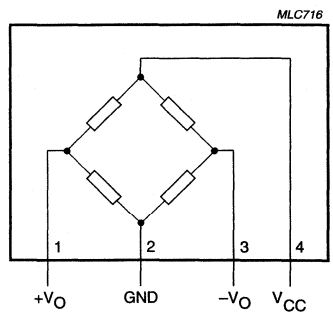

Fig.2 Simplified circuit diagram.

LIMITING VALUES

In accordance with the Absolute Maximum Rating System (IEC 134).

SYMBOL	PARAMETER	CONDITIONS	MIN.	MAX.	UNIT
V_{CC}	bridge supply voltage		–	9	V
P_{tot}	total power dissipation	up to T_{amb} = 134 °C	–	90	mW
T_{stg}	storage temperature	note 1	–65	+150	°C
T_{bridge}	bridge operating temperature		–40	+150	°C

Note

1. Maximum operating temperature of the thin-film permalloy.

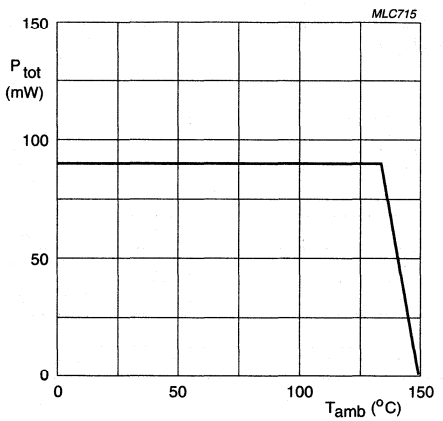

Fig.3 Power derating curve.

THERMAL CHARACTERISTICS

SYMBOL	PARAMETER	VALUE	UNIT
$R_{th\ j\text{-}a}$	thermal resistance from junction to ambient	180	K/W

CHARACTERISTICS

T_{amb} = 25 °C; H_x = 0.5 kA/m; notes 1 and 2; V_{CC} = 5 V unless otherwise specified.

SYMBOL	PARAMETER	CONDITIONS	MIN.	TYP.	MAX.	UNIT
H_y	magnetic field strength	note 2	−0.5	–	+0.5	kA/m
S	sensitivity	notes 2 and 3	13	–	19	$\frac{mV/V}{kA/m}$
TCV_O	temperature coefficient of output voltage	V_{CC} = 5 V; T_{amb} = −25 to +125 °C	–	−0.4	–	%/K
		I_{CC} = 3 mA; T_{amb} = −25 to +125 °C	–	−0.15	–	%/K
R_{bridge}	bridge resistance		0.8	–	1.6	kΩ
TCR_{bridge}	temperature coefficient of bridge resistance	T_{bridge} = −25 to +125 °C	–	0.25	–	%/K
V_{offset}	offset voltage		−1.5	–	+1.5	mV/V
TCV_{offset}	offset voltage drift	T_{bridge} = −25 to +125 °C	−6	–	+6	$\frac{\mu V/V}{K}$
FL	linearity deviation of output voltage	H_y = 0 to ±0.25 kA/m	–	–	0.8	%·FS
		H_y = 0 to ±0.4 kA/m	–	–	2.5	%·FS
		Hy = 0 to ±0.5 kA/m	–	–	4.0	%·FS
FH	hysteresis of output voltage		–	–	0.5	%·FS
f	operating frequency		0	–	1	MHz

Notes

1. Before first operation or after operation outside the SOAR (Fig.4) the sensor has to be reset by application of an auxiliary field H_x = 3 kA/m.
2. No disturbing field (H_d) allowed; for stable operation under disturbing conditions see Fig.4 (SOAR) and see Fig.5 for decrease of sensitivity.
3. $$S = \frac{(V_O \text{ at } H_y = 0.4\ kA/m) - (V_O \text{ at } H_y = 0)}{0.4 \times V_{CC}}.$$

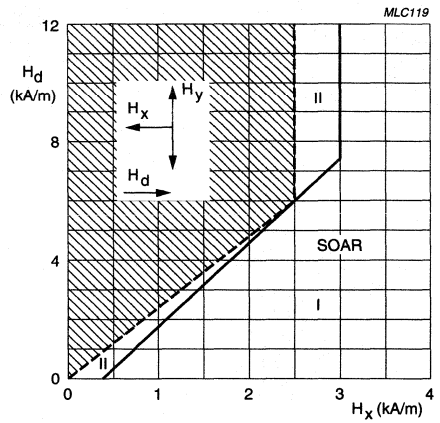

In applications with $H_x < 3$ kA/m, the sensor has to be reset, after leaving the SOAR, by an auxiliary field of $H_x = 3$ kA/m.

I = Region of permissible operation.

II = Permissible extension if $H_y < 0.15$ A/m.

Fig.4 Safe Operating Area (permissible disturbing field H_d as a component of auxiliary field H_x).

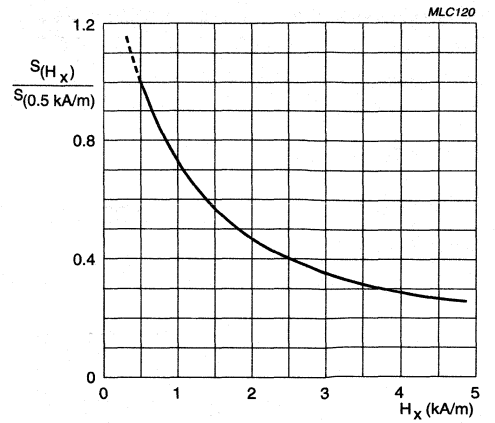

In applications with $H_x \leq 3$ kA/m, the sensor has to be reset by an auxiliary field of $H_x = 3$ kA/m before using.

Fig.5 Relative sensitivity (ratio of sensitivity at certain H_x and sensitivity at $H_x = 0.5$ kA/m).

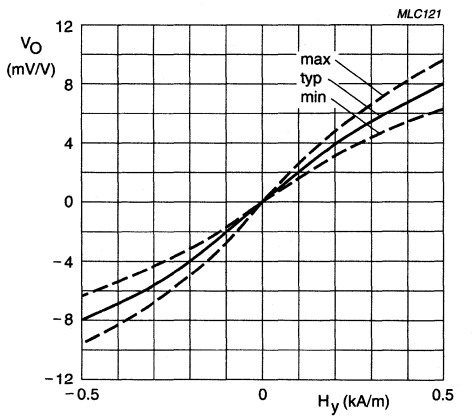

$H_x = 0.5$ kA/m; $T_{amb} = 25$ °C; $V_{offset} = 0$.

Fig.6 Sensor output characteristics.

PACKAGE OUTLINE

Plastic single-ended flat package; 4 in-line leads **SOT195**

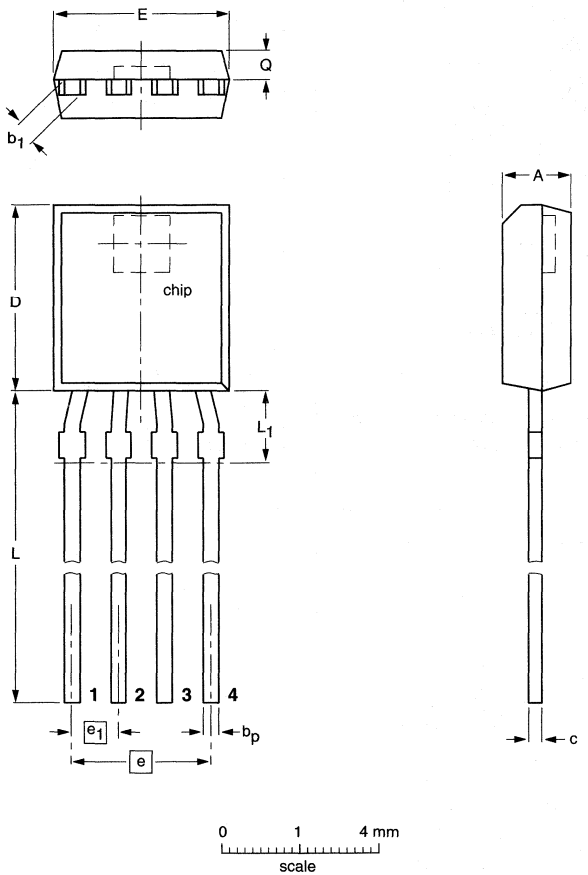

DIMENSIONS (mm are the original dimensions)

UNIT	A	b_p	b_1	c	D	E	e	e_1	L	L_1(1) max.	Q
mm	1.8 1.6	0.48 0.40	0.7 0.5	0.45 0.39	5.2 5.0	4.8 4.4	3.75	1.25	14.5 12.7	2	0.8 0.7

Notes

1. Terminal dimensions within this zone are uncontrolled to allow for flow of plastic and terminal irregularities.

OUTLINE VERSION	REFERENCES				EUROPEAN PROJECTION	ISSUE DATE
	IEC	JEDEC	EIAJ			
SOT195						97-06-02

Magnetic field sensor KMZ10A1

DESCRIPTION

The KMZ10A1 is an extremely sensitive magnetic field sensor, employing the magnetoresistive effect of thin-film permalloy. Its properties enable this sensor to be used in a wide range of applications such as navigation, current and earth magnetic field measurement etc. The special arrangement of the sensing chip allows the construction of coils for switching the auxiliary field (H_x) along the length axis of the sensor. The sensor can be operated at any frequency between DC and 1 MHz.

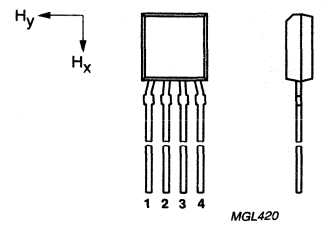

Fig.1 Simplified outline.

PINNING

PIN	SYMBOL	DESCRIPTION
1	$+V_O$	output voltage
2	GND	ground
3	$-V_O$	output voltage
4	V_{CC}	supply voltage

QUICK REFERENCE DATA

SYMBOL	PARAMETER	MIN.	TYP.	MAX.	UNIT
V_{CC}	DC supply voltage	–	5	–	V
H_y	magnetic field strength	–0.5	–	+0.5	kA/m
H_x	auxiliary field	–	0.5	–	kA/m
S	sensitivity	–	14	–	$\frac{mV/V}{kA/m}$
S_s	sensitivity (with switched H_x)	–	22	–	$\frac{mV/V}{kA/m}$
R_{bridge}	bridge resistance	0.85	–	1.75	kΩ
V_{offset}	offset voltage	–1.5	–	+1.5	mV/V

CIRCUIT DIAGRAM

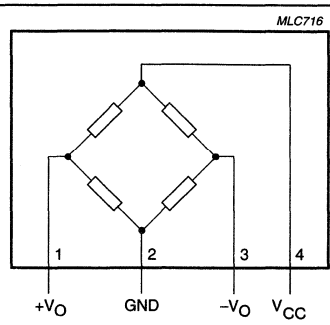

Fig.2 Simplified circuit diagram.

LIMITING VALUES

In accordance with the Absolute Maximum Rating System (IEC 134).

SYMBOL	PARAMETER	CONDITIONS	MIN.	MAX.	UNIT
V_{CC}	DC supply voltage		–	9	V
P_{tot}	total power dissipation	up to T_{amb} = 132 °C	–	100	mW
T_{stg}	storage temperature		−65	+150	°C
T_{bridge}	bridge operating temperature		−40	+150	°C

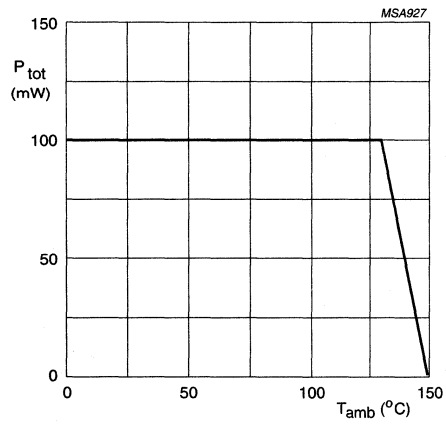

Fig.3 Power derating curve.

THERMAL CHARACTERISTICS

SYMBOL	PARAMETER	VALUE	UNIT
$R_{th\ j\text{-}a}$	thermal resistance from junction to ambient	180	K/W

CHARACTERISTICS

T_{amb} = 25 °C and H_x = 0.5 kA/m unless otherwise specified; see notes 1 and 2.

SYMBOL	PARAMETER	CONDITIONS	MIN.	TYP.	MAX.	UNIT
V_{CC}	DC supply voltage		–	5	–	V
H_y	operating range	note 2	–0.5	–	+0.5	kA/m
S	sensitivity	open circuit; notes 2 and 3	11	–	17	$\frac{mV/V}{kA/m}$
TCV_O	temperature coefficient of output voltage at constant supply voltage	V_{CC} = 5 V; T_{amb} = –25 to +125 °C	–	–0.4	–	%/K
VCV_O	temperature coefficient of output voltage at constant supply current	I_B = 3 mA; T_{amb} = –25 to +125 °C	–	–0.15	–	%/K
R_{bridge}	bridge resistance		0.85	–	1.75	kΩ
TCR_{bridge}	temperature coefficient of bridge resistance	T_j = –25 to +125 °C	–	0.25	–	%/K
V_{offset}	offset voltage		–1.5	–	+1.5	mV/V
TCV_{offset}	offset voltage drift	T_{bridge} = –25 to +125 °C	–6	–	+6	$\frac{\mu V/V}{K}$
FL	linearity deviation of output voltage	H_y = 0 to ±0.25 kA/m^{-1}	–	–	0.8	%·FS
		H_y = 0 to ±0.4 kA/m^{-1}	–	–	2.5	%·FS
		H_y = 0 to ±0.5 kA/m^{-1}	–	–	4.0	%·FS
FH	hysteresis of output voltage		–	–	0.5	%·FS
f	operating frequency		0	–	1	MHz
Characteristics with H_x = 0 (switched H_x, see note 4); V_{CC} = 5 V						
H_y	operating range	note 2	–0.05	–	+0.05	kA/m
S_s	sensitivity	slope between H_y = 0 and H_y = 40 A/m	14	–	27	$\frac{mV/V}{kA/m}$

Notes

1. Before first operation or after operation outside the SOAR (Fig.4) the sensor has to be reset by application of an auxiliary field H_x = 3 kA/m.
2. No disturbing field (H_d) allowed; for stable operation under disturbing conditions see Fig.4 (SOAR) and see Fig.5 for decrease of sensitivity.
3. Sensitivity measured as $\Delta V_O/\Delta H_y$ between H_y = 0 and H_y = 0.4 kA/m.
4. See application information.

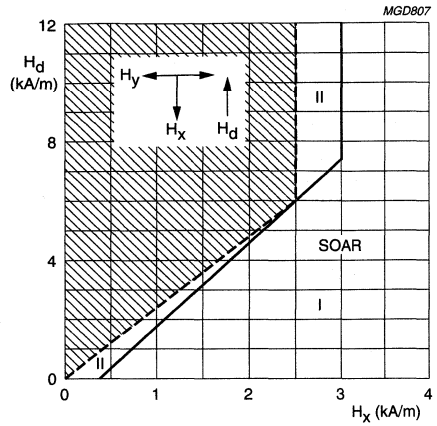

I = Region of permissible operation.

II = Permissible extension if $H_y < 0.05$ kA/m.

In applications with $H_x < 3$ kA/m, the sensor has to be reset, after leaving the SOAR, by an auxiliary field of $H_x = 3$ kA/m.

Fig.4 Safe Operating Area (permissible disturbing field H_d as a component of auxiliary field H_x).

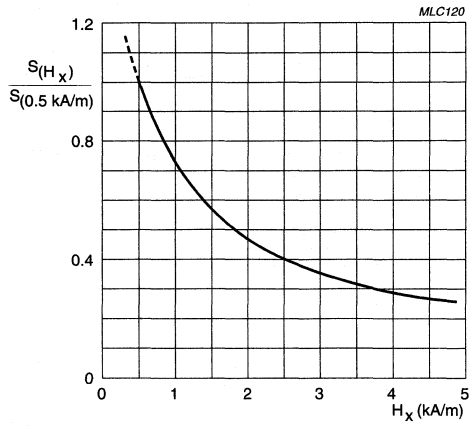

In applications with $H_x \leq 3$ kA/m, the sensor has to be reset by an auxiliary field of $H_x = 3$ kA/m before use.

Fig.5 Relative sensitivity (ratio of sensitivity at certain H_x and sensitivity at $H_x = 0.5$ kA/m).

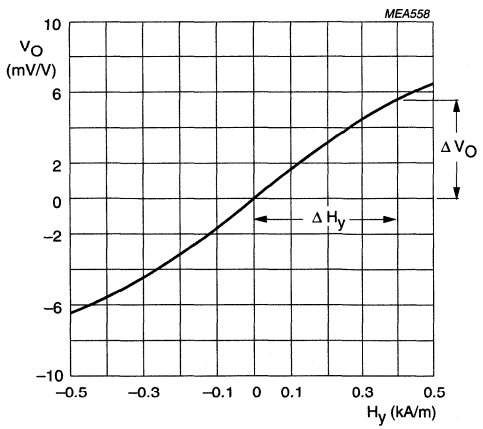

$H_x = 0.5$ kA/m; $T_{amb} = 25$ °C; $V_{offset} = 0$; $S = \Delta V_O / \Delta H_y$.

Fig.6 Sensor output characteristics.

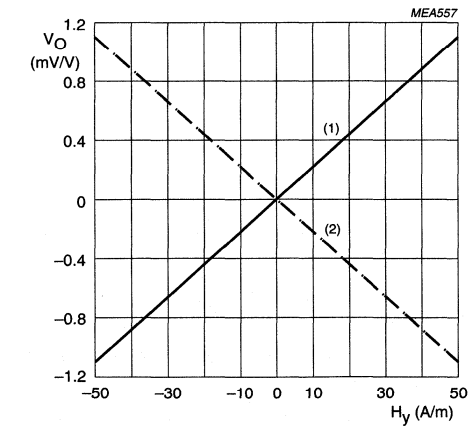

(1) Sensor reset with $H_x = 3$ kA/m.

(2) Sensor reset with $H_x = -3$ kA/m.

Fig.7 Output characteristic with $H_x = 0$ (switched H_x).

APPLICATION INFORMATION

A problem with measuring weak magnetic fields is that precision is limited by drift in both the sensor and amplifier offset. In these instances, it is possible to take advantage of the 'flipping' characteristics of the KMZ10 series to generate an output that is independent of offset. The sensor, located in a coil connected to a current pulse generator producing magnetic field pulses periodically reversed by alternate positive and negative going current pulses, is continually flipped from its normal to its reversed polarity and back again. The polarity of the offset however, remains unchanged, so the offset itself can be eliminated by passing the output signal through a filter circuit.

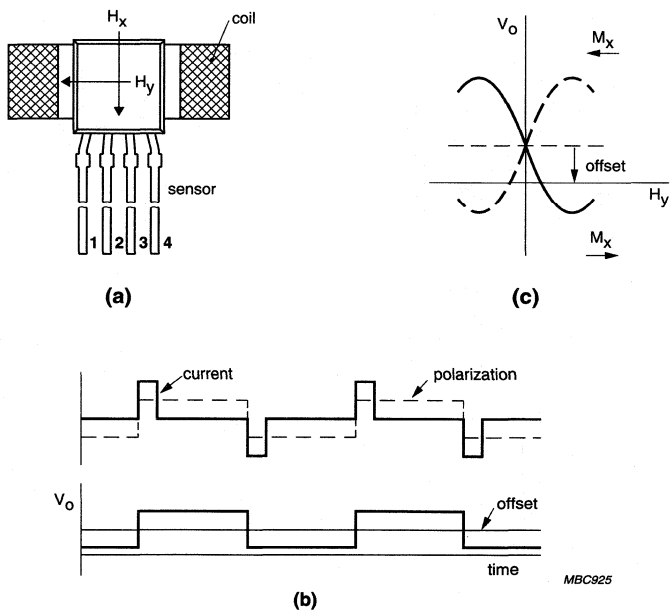

(a) Set-up.
(b) Pulse diagram.
(c) Sensor output characteristics.

Fig.8 Measuring weak magnetic fields with the KMZ10A1.

PACKAGE OUTLINE

Plastic single-ended flat package; 4 in-line leads **SOT195**

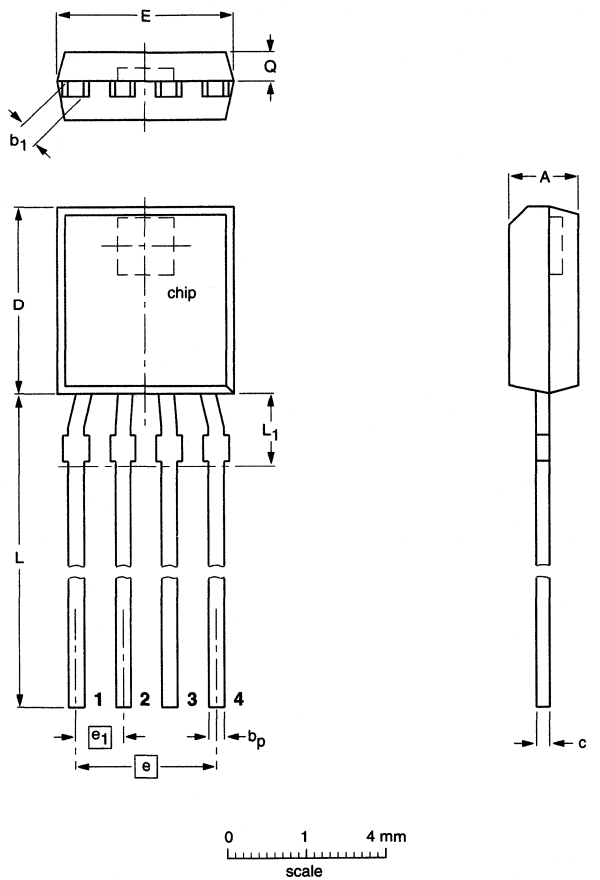

DIMENSIONS (mm are the original dimensions)

UNIT	A	b_p	b_1	c	D	E	e	e_1	L	L_1(1) max.	Q
mm	1.8 1.6	0.48 0.40	0.7 0.5	0.45 0.39	5.2 5.0	4.8 4.4	3.75	1.25	14.5 12.7	2	0.8 0.7

Notes

1. Terminal dimensions within this zone are uncontrolled to allow for flow of plastic and terminal irregularities.

OUTLINE VERSION	REFERENCES				EUROPEAN PROJECTION	ISSUE DATE
	IEC	JEDEC	EIAJ			
SOT195						97-06-02

Magnetic field sensor KMZ10B

DESCRIPTION

The KMZ10B is a sensitive magnetic field sensor, employing the magnetoresistive effect of thin-film permalloy. Its properties enable this sensor to be used in a wide range of applications for current and field measurement, revolution counters, angular or linear position measurement, proximity detectors, etc.

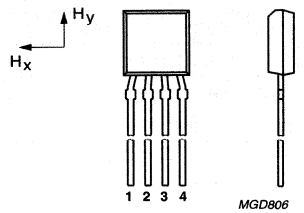

Fig.1 Simplified outline SOT195.

PINNING

PIN	SYMBOL	DESCRIPTION
1	$+V_O$	output voltage
2	GND	ground
3	$-V_O$	output voltage
4	V_{CC}	supply voltage

QUICK REFERENCE DATA

SYMBOL	PARAMETER	MIN.	TYP.	MAX.	UNIT
V_{CC}	bridge supply voltage	–	5	12	V
H_y	magnetic field strength	–2	–	+2	kA/m
H_x	auxiliary field	–	3	–	kA/m
S	sensitivity	–	4	–	$\frac{mV/V}{kA/m}$
R_{bridge}	bridge resistance	1.6	–	2.6	kΩ
V_{offset}	offset voltage	–1.5	–	+1.5	mV/V

CIRCUIT DIAGRAM

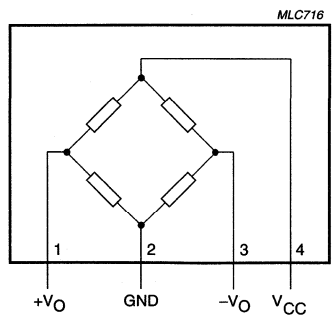

Fig.2 Simplified circuit diagram.

LIMITING VALUES

In accordance with the Absolute Maximum Rating System (IEC 134).

SYMBOL	PARAMETER	CONDITIONS	MIN.	MAX.	UNIT
V_{CC}	bridge supply voltage		–	12	V
P_{tot}	total power dissipation	up to T_{amb} = 130 °C	–	120	mW
T_{stg}	storage temperature		–65	+150	°C
T_{bridge}	bridge operating temperature		–40	+150	°C

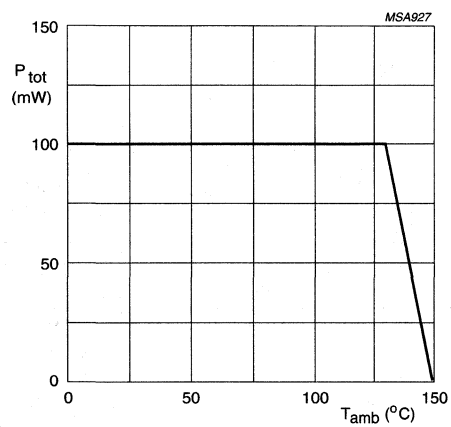

Fig.3 Power derating curve.

THERMAL CHARACTERISTICS

SYMBOL	PARAMETER	VALUE	UNIT
$R_{th\ j\text{-}a}$	thermal resistance from junction to ambient	180	K/W

CHARACTERISTICS

T_{amb} = 25 °C; H_x = 3 kA/m; note 1.

SYMBOL	PARAMETER	CONDITIONS	MIN.	TYP.	MAX.	UNIT
V_{CC}	bridge supply voltage		–	5	–	V
H_y	magnetic field strength		–2	–	+2	kA/m
S	sensitivity	open circuit, notes 2 and 3	3.2	–	4.8	$\frac{mV/V}{kA/m}$
TCV_O	temperature coefficient of output voltage	V_{CC} = 5 V; T_j = –25 to +125 °C	–	–0.4	–	%/K
		I_B = 3 mA; T_j = –25 to +125 °C	–	–0.1	–	%/K
R_{bridge}	bridge resistance		1.6	–	2.6	kΩ
TCR_{bridge}	temperature coefficient of bridge resistance	T_{bridge} = –25 to +125 °C	–	0.3	–	%/K
V_{offset}	offset voltage		–1.5	–	+1.5	mV/V
TCV_{offset}	offset voltage drift	T_j = –25 to +125 °C	–3	–	+3	$\frac{\mu V/V}{K}$
FL	linearity deviation of output voltage	H_y = 0 to ±1 kA/m	–	–	±0.5	%·FS
		H_y = 0 to ±1.6 kA/m	–	–	±1.7	%·FS
		H_y = 0 to ±2 kA/m	–	–	±2	%·FS
FH	hysteresis of output voltage		–	–	0.5	%·FS
f	operating frequency		0	–	1	MHz

Notes

1. In applications with H_x < 3 kA/m the sensor has to be reset before first operation by application of an auxiliary field H_x = 3 kA/m.
2. No disturbing field (H_d) allowed; for stable operation under disturbing conditions see Fig.4 (SOAR) and see Fig.5 for decrease of sensitivity.
3. $$S = \frac{(V_O \text{ at } H_y = 1.6\ kA/m) - (V_O \text{ at } H_y = 0)}{1.6 \times V_{CC}}.$$

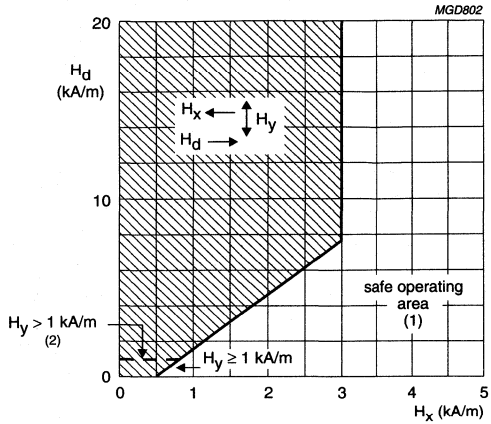

In applications with $H_x < 3$ kA/m, the sensor has to be reset, after leaving the SOAR, by an auxiliary field of $H_x = 3$ kA/m.

(1) Region of permissible operation.

(2) Permissible extension if $H_y < 1$ kA/m.

Fig.4 Safe Operating Area (permissible disturbing field H_d as a component of auxiliary field H_x).

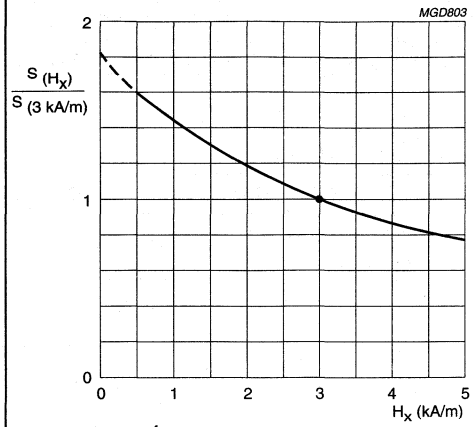

In applications with $H_x \leq 3$ kA/m, the sensor has to be reset by an auxiliary field of $H_x = 3$ kA/m before using.

Fig.5 Relative sensitivity (ratio of sensitivity at certain H_x and sensitivity at $H_x = 3$ kA/m).

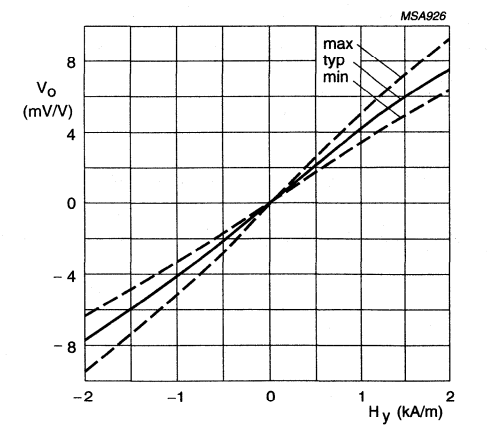

V_B = constant; $H_x = 3$ kA/m; $T_{amb} = 25$ °C; $V_{offset} = 0$.

Fig.6 Sensor output characteristics.

PACKAGE OUTLINE

Plastic single-ended flat package; 4 in-line leads **SOT195**

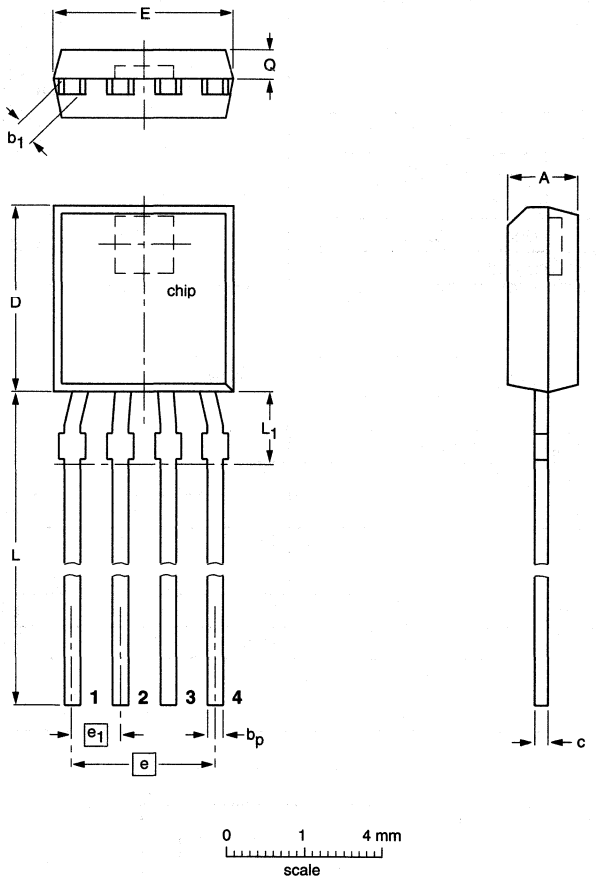

DIMENSIONS (mm are the original dimensions)

UNIT	A	b_p	b_1	c	D	E	e	e_1	L	L_1(1) max.	Q
mm	1.8 1.6	0.48 0.40	0.7 0.5	0.45 0.39	5.2 5.0	4.8 4.4	3.75	1.25	14.5 12.7	2	0.8 0.7

Notes

1. Terminal dimensions within this zone are uncontrolled to allow for flow of plastic and terminal irregularities.

OUTLINE VERSION	REFERENCES				EUROPEAN PROJECTION	ISSUE DATE
	IEC	JEDEC	EIAJ			
SOT195						97-06-02

Magnetic field sensor KMZ10C

DESCRIPTION

The KMZ10C is a magnetic field sensor, employing the magnetoresistive effect of thin-film permalloy. Its properties enable this sensor to be used in a wide range of applications for current and field measurement, revolution counters, angular or linear position measurement and proximity detectors, etc.

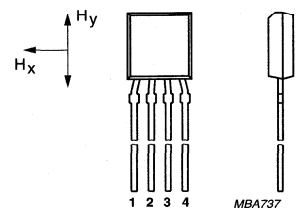

Fig.1 Simplified outline.

PINNING

PIN	SYMBOL	DESCRIPTION
1	$+V_O$	output voltage
2	GND	ground
3	$-V_O$	output voltage
4	V_{CC}	supply voltage

QUICK REFERENCE DATA

SYMBOL	PARAMETER	MIN.	TYP.	MAX.	UNIT
V_{CC}	DC supply voltage	–	5	–	V
T_{bridge}	bridge operating temperature	–40	–	+150	°C
H_y	magnetic field strength	–7.5	–	+7.5	kA/m
H_x	auxiliary field	–	3	–	kA/m
S	sensitivity	–	1.5	–	$\frac{mV/V}{kA/m}$
R_{bridge}	bridge resistance	1	–	1.8	kΩ
V_{offset}	offset voltage	–1.5	–	+1.5	mV/V

CIRCUIT DIAGRAM

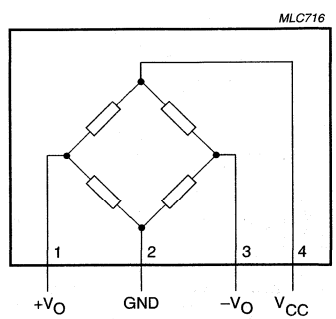

Fig.2 Simplified circuit diagram.

LIMITING VALUES

In accordance with the Absolute Maximum Rating System (IEC 134).

SYMBOL	PARAMETER	CONDITIONS	MIN.	MAX.	UNIT
V_{CC}	DC supply voltage		–	10	V
P_{tot}	total power dissipation	up to T_{amb} = 132 °C	–	100	mW
T_{stg}	storage temperature	note 1	−65	+150	°C
T_{bridge}	bridge operating temperature		−40	+150	°C

Note

1. Maximum operating temperature of the thin-film permalloy.

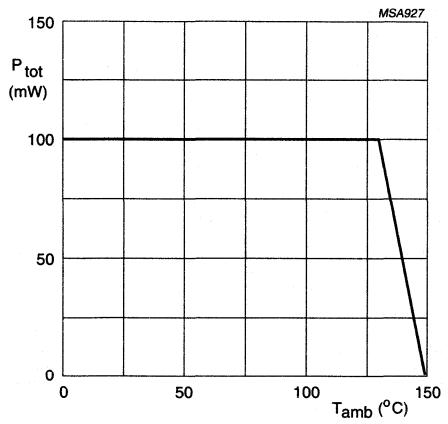

Fig.3 Power derating curve.

THERMAL CHARACTERISTICS

SYMBOL	PARAMETER	VALUE	UNIT
$R_{th\ j\text{-}a}$	thermal resistance from junction to ambient	180	K/W

CHARACTERISTICS

T_{amb} = 25 °C; H_x = 3 kA/m; note 1; V_{CC} = 5 V; unless otherwise specified.

SYMBOL	PARAMETER	CONDITIONS	MIN.	TYP.	MAX.	UNIT
H_y	magnetic field strength		−7.5	–	+7.5	kA/m
S	sensitivity	notes 1 and 2	1	–	2	$\frac{mV/V}{kA/m}$
TCV_O	temperature coefficient of output voltage	V_{CC} = 5 V; T_{amb} = −25 to +125 °C	–	−0.5	–	%/K
		I_{CC} = 3 mA; T_{amb} = −25 to +125 °C	–	−0.15	–	%/K
R_{bridge}	bridge resistance		1	–	1.8	kΩ
TCR_{bridge}	temperature coefficient of bridge resistance	T_{bridge} = −25 to +125 °C	–	0.35	–	%/K
V_{offset}	offset voltage		−1.5	–	+1.5	mV/V
TCV_{offset}	temperature coefficient of offset voltage	T_{bridge} = −25 to +125 °C	−2	–	+2	(μV/V)/K
FL	linearity deviation of output voltage	H_y = 0 to ±3.75 kA/m	–	–	0.8	%·FS
		H_y = 0 to ±6.0 kA/m	–	–	2.4	%·FS
		H_y = 0 to ±7.5 kA/m	–	–	2.7	%·FS
FH	hysteresis of output voltage		–	–	0.5	%·FS
f	operating frequency		0	–	1	MHz

Notes

1. In applications with H_x < 3 kA/m the sensor has to be reset before first operation by application of an auxiliary field H_x = 3 kA/m.
2. $S = \frac{(V_O \text{ at } H_y = 6\ kA/m) - (V_O \text{ at } H_y = 0)}{6 \times V_{CC}}$

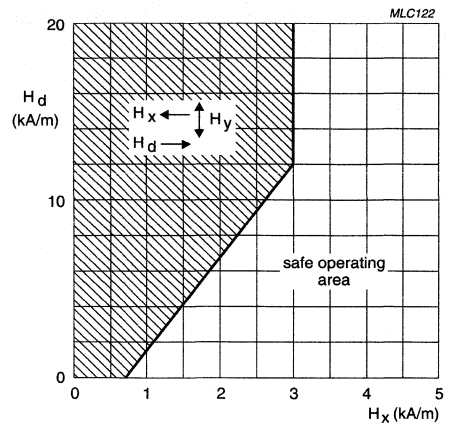

In applications with $H_x < 3$ kA/m, the sensor has to be reset, after leaving the SOAR, by an auxiliary field of $H_x = 3$ kA/m.

Fig.4 Safe Operating Area (permissible disturbing field H_d as a component of auxiliary field H_x).

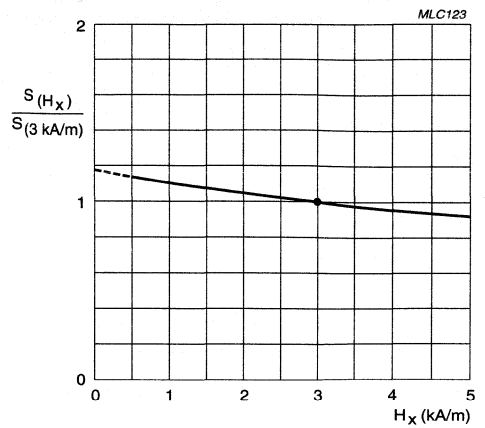

In applications with $H_x \leq 3$ kA/m, the sensor has to be reset by an auxiliary field of $H_x = 3$ kA/m before using.

Fig.5 Relative sensitivity (ratio of sensitivity at certain H_x and sensitivity at $H_x = 3$ kA/m).

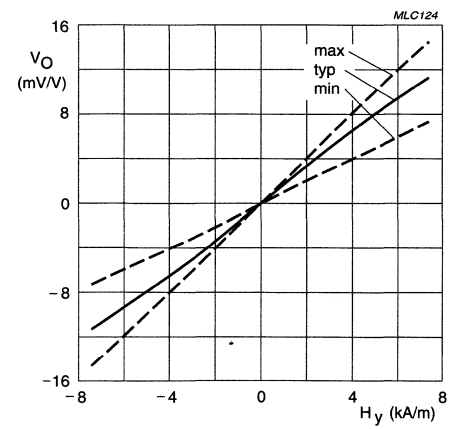

$H_x = 3$ kA/m; $T_{amb} = 25$ °C; $V_{offset} = 0$.

Fig.6 Sensor output characteristics.

PACKAGE OUTLINE

Plastic single-ended flat package; 4 in-line leads **SOT195**

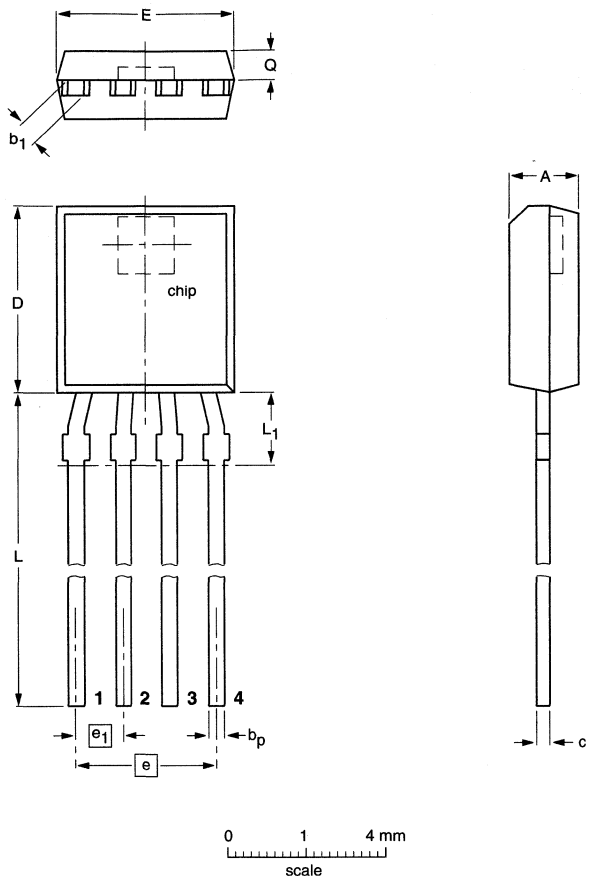

DIMENSIONS (mm are the original dimensions)

UNIT	A	b_p	b_1	c	D	E	e	e_1	L	L_1(1) max.	Q
mm	1.8 1.6	0.48 0.40	0.7 0.5	0.45 0.39	5.2 5.0	4.8 4.4	3.75	1.25	14.5 12.7	2	0.8 0.7

Notes

1. Terminal dimensions within this zone are uncontrolled to allow for flow of plastic and terminal irregularities.

OUTLINE VERSION	REFERENCES				EUROPEAN PROJECTION	ISSUE DATE
	IEC	JEDEC	EIAJ			
SOT195						97-06-02

Magnetic field sensor KMZ51

FEATURES

- High sensitivity
- Integrated compensation coil
- Integrated set/reset coil.

APPLICATIONS

- Navigation
- Current and earth magnetic field measurement
- Traffic detection.

DESCRIPTION

The KMZ51 is an extremely sensitive magnetic field sensor, employing the magnetoresistive effect of thin-film permalloy. The sensor contains one magnetoresistive Wheatstone bridge and integrated compensation and set/reset coils. The integrated compensation coil allows magnetic field measurement with current feedback loops to generate an output that is independent of drift in sensitivity. The orientation of sensitivity may be set or changed (flipped) by means of the integrated set/reset coil. A short current pulse should be applied to the compensation coil to recover (set) the sensor after exposure to strong disturbing magnetic fields. A negative current pulse will reset the sensor to reversed sensitivity. By use of periodically alternated flipping pulses and a lock-in amplifier, output is made independent of sensor and amplifier offset.

PINNING

PIN	SYMBOL	DESCRIPTION
1	$+I_{flip}$	flip coil
2	V_{CC}	bridge supply voltage
3	GND	ground
4	$+I_{comp}$	compensation coil
5	$-I_{comp}$	compensation coil
6	$-V_O$	bridge output voltage
7	$+V_O$	bridge output voltage
8	$-I_{flip}$	flip coil

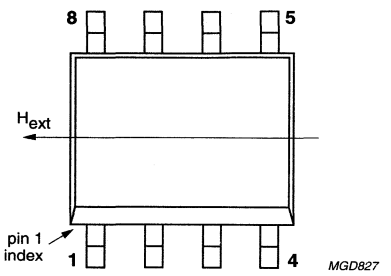

Fig.1 Simplified outline.

QUICK REFERENCE DATA

SYMBOL	PARAMETER	MIN.	TYP.	MAX.	UNIT
V_{CC}	bridge supply voltage	–	5	8	V
S	sensitivity (uncompensated)	12	16	–	$\frac{mV/V}{kA/m}$
V_{offset}	offset voltage	−1.5	–	+1.5	mV/V
R_{bridge}	bridge resistance	1	–	3	kΩ
R_{comp}	compensation coil resistance	100	170	300	Ω
A_{comp}	compensation coil field factor; note 1	19	22	25	$\frac{A/m}{mA}$

SYMBOL	PARAMETER	MIN.	TYP.	MAX.	UNIT
R_{flip}	flip coil resistance	1	2	3	Ω
$I_{flip\ (min)}$	minimum recommended flipping current; note 2	800	1000	1200	mA
$t_{flip\ (min)}$	minimum flip pulse duration; note 2	1	3	100	µs

Notes

1. The compensation coil generates a field $H_{comp} = A_{comp} \times I_{comp}$ in addition to the external field H_{ext}. Sensor output will become zero if $H_{ext} = -H_{comp}$.
2. Average power consumption of the flipping coil, defined by current, pulse duration and pulse repetition rate may not exceed the specified limit, see Chapter "Limiting values".

CIRCUIT DIAGRAM

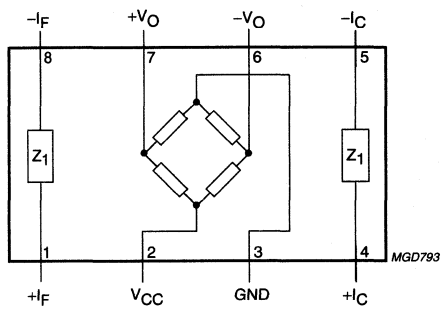

Fig.2 Simplified circuit diagram.

LIMITING VALUES

In accordance with the Absolute Maximum Rating System (IEC 60134).

SYMBOL	PARAMETER	MIN.	MAX.	UNIT
V_{CC}	bridge supply voltage	–	9	V
P_{tot}	total power dissipation	–	130	mW
T_{stg}	storage temperature	−65	+150	°C
T_{bridge}	bridge operating temperature	−40	+125	°C
I_{comp}	maximum compensation current	–	15	mA
$I_{flip\ (max)}$	maximum flipping current	–	1500	mA
$P_{flip\ (max)}$	maximum flipping power dissipation	–	50	mW
V_{isol}	voltage between isolated systems: flip coil and Wheatstone bridge; compensation coil and Wheatstone bridge; flip coil and compensation coil	–	60	V

THERMAL CHARACTERISTICS

SYMBOL	PARAMETER	VALUE	UNIT
$R_{th\ j\text{-}a}$	thermal resistance from junction to ambient	155	K/W

CHARACTERISTICS

T_{amb} = 25 °C unless otherwise specified.

SYMBOL	PARAMETER	CONDITIONS	MIN.	TYP.	MAX.	UNIT
V_{CC}	bridge supply voltage		–	5	8	V
H_y	operating range in sensitive direction		–0.2	–	+0.2	kA/m
H_x	operating range perpendicular to sensitive direction		–0.2	–	+0.2	kA/m
S	sensitivity	open circuit	12	16	–	$\frac{mV/V}{kA/m}$
TCS	temperature coefficient of sensitivity	T_s = –25 to +125 °C	–	0.31	–	%/K
TCV_O	temperature coefficient of output voltage	V_{CC} = 5 V; T_{amb} = –25 to +125 °C	–	–0.4	–	%/K
		I_{CC} 3 mA; T_{amb} = –25 to +125 °C	–	–0.1	–	%/K
R_{bridge}	bridge resistance	resistance pins 2 to 3	1	–	3	kΩ
TCR_{bridge}	temperature coefficient of bridge resistance	T_{bridge} = –25 to +125 °C	–	0.3	–	%/K
V_{offset}	offset voltage		–1.5	0	+1.5	mV/V
TCV_{offset}	temperature coefficient of offset voltage	T_{bridge} = –25 to +125 °C	–3	0	+3	$\frac{\mu V/V}{K}$
FH	hysteresis of output voltage		–	–	2	%FS
R_{comp}	resistance of compensation coil	resistance pins 4 to 5	100	170	300	Ω
A_{comp}	field factor of compensation coil		19	22	25	$\frac{A/m}{mA}$
R_{flip}	resistance of set/reset conductor	resistance pins 1 to 8	1	2	3	Ω
TCR_{flip}	temperature coefficient of resistance of set/reset coil	T_{flip} = –25 to +125 °C	–	0.39	–	%/K
I_{flip}	recommended flipping current for stable operation		±800	±1000	±1200	mA
t_{flip}	flip pulse duration		1	3	100	µs
R_{isol}	isolating resistance	resistance pins 1 to 2, 1 to 4 and 2 to 4	1	–	–	mΩ
V_{isol}	voltage between isolated systems	voltage pins 1 to 2, 1 to 4 and 2 to 4	–	–	50	V
f	operating frequency		0	–	1	MHz

PACKAGE OUTLINE

SO8: plastic small outline package; 8 leads; body width 3.9 mm **SOT96-1**

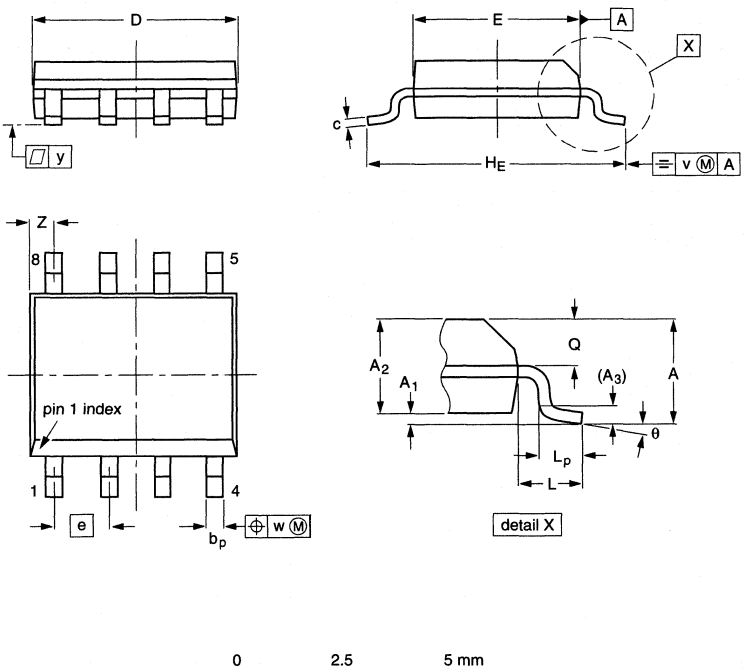

DIMENSIONS (inch dimensions are derived from the original mm dimensions)

UNIT	A max.	A_1	A_2	A_3	b_p	c	$D^{(1)}$	$E^{(2)}$	e	H_E	L	L_p	Q	v	w	y	$Z^{(1)}$	θ
mm	1.75	0.25 0.10	1.45 1.25	0.25	0.49 0.36	0.25 0.19	5.0 4.8	4.0 3.8	1.27	6.2 5.8	1.05	1.0 0.4	0.7 0.6	0.25	0.25	0.1	0.7 0.3	8° 0°
inches	0.069	0.010 0.004	0.057 0.049	0.01	0.019 0.014	0.0100 0.0075	0.20 0.19	0.16 0.15	0.050	0.244 0.228	0.041	0.039 0.016	0.028 0.024	0.01	0.01	0.004	0.028 0.012	

Notes

1. Plastic or metal protrusions of 0.15 mm maximum per side are not included.
2. Plastic or metal protrusions of 0.25 mm maximum per side are not included.

OUTLINE VERSION	REFERENCES				EUROPEAN PROJECTION	ISSUE DATE
	IEC	JEDEC	EIAJ			
SOT96-1	076E03	MS-012				~~97-05-22~~ 99-12-27

Magnetic Field Sensor KMZ52

FEATURES

- High sensitivity
- Integrated compensation coil
- Integrated set/reset coil.

APPLICATIONS

- Navigation
- Current and earth magnetic field measurement
- Traffic detection.

DESCRIPTION

The KMZ52 is an extremely sensitive magnetic field sensor, employing the magnetoresistive effect of thin-film permalloy. The sensor contains two magnetoresistive Wheatstone bridges physically offset from one another by 90° and integrated compensation and set/reset coils. The integrated compensation coils allow magnetic field measurement with current feedback loops to generate outputs that are independent of drift in sensitivity. The orientation of sensitivity may be set or changed (flipped) by means of the integrated set/reset coils. A short current pulse should be applied to the compensation coils to recover (set) the sensor after exposure to strong disturbing magnetic fields. A negative current pulse will reset the sensor to reversed sensitivity. By use of periodically alternated flipping pulses and a lock-in amplifier, the output is made independent of sensor and amplifier offset.

PINNING

SYMBOL	PIN	DESCRIPTION
$+I_{flip2}$	1	flip coil
V_{CC2}	2	bridge supply voltage
GND2	3	ground
$+I_{comp2}$	4	compensation coil
GND1	5	ground
$+I_{comp1}$	6	compensation coil
$-I_{comp1}$	7	compensation coil
$-V_{O1}$	8	bridge output voltage
$+V_{O1}$	9	bridge output voltage
$-I_{flip1}$	10	flip coil
$+I_{flip1}$	11	flip coil
V_{CC1}	12	bridge supply voltage
$-I_{comp2}$	13	compensation coil
$-V_{O2}$	14	bridge output voltage
$+V_{O2}$	15	bridge output voltage
$-I_{flip2}$	16	flip coil

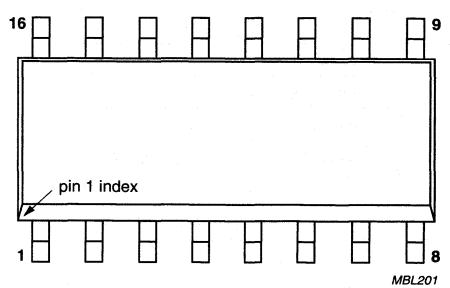

Fig.1 Simplified outline SOT109-1.

QUICK REFERENCE DATA

SYMBOL	PARAMETER	MIN.	TYP.	MAX.	UNIT
V_{CC}	bridge supply voltage	–	5	8	V
S	sensitivity (uncompensated)	12	16	–	$\frac{mV/V}{kA/m}$
V_{offset}	offset voltage per supply voltage	−1.5	0	+1.5	mV/V
R_{bridge}	bridge resistance	1	2	3	kΩ
R_{comp}	compensation coil resistance	100	170	300	Ω
A_{comp}	field factor of compensation coil; note 1	19	22	25	$\frac{A/m}{mA}$
R_{flip}	resistance of set/reset coil	1	2	3	Ω
I_{flip}	recommended flipping current for stable operation; note 2	±800	±1000	±1200	mA
t_{flip}	flip pulse duration; note 2	1	3	100	µs

Notes

1. The compensation coil generates a field $H_{comp} = A_{comp} \times I_{comp}$ in addition to the external field H_{ext}. Sensor output will become zero if $H_{ext} = H_{comp}$.
2. Average power consumption of the flipping coil, defined by current, pulse duration and pulse repetition rate may not exceed the specified limit, see Chapter "Limiting values".

LIMITING VALUES

In accordance with the Absolute Maximum System (IEC 60134).

SYMBOL	PARAMETER	MIN.	MAX.	UNIT
V_{CC}	bridge supply voltage	–	8	V
P_{tot}	total power dissipation	–	130	mW
T_{stg}	storage temperature	−65	+150	°C
T_{amb}	maximum operating temperature	−40	−125	°C
I_{comp}	maximum compensation current	–	15	mA
$I_{flip\ (max)}$	maximum flipping current	–	1500	mA
$P_{flip\ (max)}$	maximum flipping power dissipation	–	50	mW
V_{isol}	voltage between isolated systems: flip coil and Wheatstone bridge; compensation coil and Wheatsone bridge; flip coil and compensation coil	–	60	V

THERMAL CHARACTERISTICS

SYMBOL	PARAMETER	VALUE	UNIT
$R_{th\ j\text{-}a}$	terminal resistance from junction to ambient	105	K/W

CHARACTERISTICS

T_{bridge} = 25 °C; $V_{CC1} = V_{CC2}$ = 5 V; unless otherwise specified.

SYMBOL	PARAMETER	CONDITIONS	MIN.	TYP.	MAX.	UNIT
V_{CC}	bridge supply voltage	note 1	–	5	8	V
H	field strength operating range in sensor plane		–0.2	–	+0.2	kA/m
S	sensitivity	open circuit	12	16	–	$\frac{mV/V}{kA/m}$
TCS	temperature coefficient of sensitivity	T_s = –25 to +125 °C	–	0.31	–	%/K
k_{SX}	sensitivity synchronism	note 2	92	100	108	%
TCV_O	temperature coefficient of output voltage	V_{CC} = 5 V; T_{bridge} = –25 to +125 °C	–	–0.4	–	%/K
R_{bridge}	bridge resistance	note 3	1	2	3	kΩ
TCR_{bridge}	temperature coefficient of bridge resistance	T_{bridge} = –25 to +125 °C; note 4	–	0.3	–	%/K
V_{offset}	offset voltage per supply voltage		–1.5	0	+1.5	mV/V
TCV_{offset}	temperature coefficient of offset voltage	T_{bridge} = –25 to +125 °C; note 5	–3	0	+3	$\frac{\mu V/V}{K}$
FH	hysteresis of output voltage		–	–	2	%FS
R_{comp}	resistance of compensation coil	note 6	100	170	300	Ω
A_{comp}	field factor of compensation coil		19	22	25	$\frac{A/m}{mA}$
R_{flip}	resistance of set/reset coil	note 7	1	2	3	Ω
TCR_{flip}	temperature coefficient of resistance of set/reset coil	T_{flip} = –25 to +125 °C	–	0.39	–	%/K
I_{flip}	recommended flipping current for stable operation		±800	±1000	±1200	mA
t_{flip}	flip pulse duration		1	3	100	µs
R_{isol}	isolating resistance	note 8	1	–	–	MΩ
V_{isol}	voltage between isolated systems	note 8	–	–	50	V
R_{isol_dice}	isolating resistance between dice	die 1 to die 2	1	–	–	MΩ
f	operating frequency		0	–	1	MHz
α	angle die-to-die	note 9	88	90	92	deg
β	angle dice-to-package	note 9	–5	0	+5	deg

Notes

1. Due to the ratiometric output, the same supply voltage (V_{CC}) must be applied to both dice in one KMZ52 device.
2. $k_{SX} = 100 \times \frac{A_{comp1} \times S_1}{A_{comp2} \times S_2}\%$
3. Bridge resistance die 1: between pins 5 and 12; bridge resistance die 2: between pins 2 and 3.
4. $TCR_{bridge} = 100 \frac{R_{bridge(T_2)} - R_{bridge(T_1)}}{R_{bridge(T_1)}(T_2 - T_1)}$ Where T_1 = –25°C; T_2 = 125°C.

5. $TCV_{offset} = \frac{V_{offset(T_2)} - V_{offset(T_1)}}{(T_2 - T_1)}$ Where $T_1 = -25°C$; $T_2 = 125°C$.
6. Resistance of compensation coil die 1: between pins 6 and 7;
   resistance of compensation coil die 2: between pins 4 to 13.
7. Resistance of set/reset coil die 1: between pins 10 and 11;
   resistance of set/reset coil die 2: between pins 1 to 16.
8. Isolating resistance die 1: pins 7 and 8, 7 and 10 and 8 to 10;
   isolating resistance die 2: pins 1 to 2, 1 to 4 and 2 to 4.
9. Angle die-to-die: die 2 is turned by 90 ±2 degrees in anticlockwise direction with respect to die 1;
   angle dice-to-package: both dice in their fixed die-to-die position are tilted towards the package edges by 0 ±5 degrees.

APPLICATION INFORMATION

If the angle α between external magnetic field H and the long axis of the package is zero, H is parallel to the most sensitive direction of die 2 and perpendicular to the sensitive direction of die 1. A magnetic field turning clockwise (see Fig.2) thus yields an output proportional to cos α (V_{out2}) and an output proportional to sin α (V_{out1}).

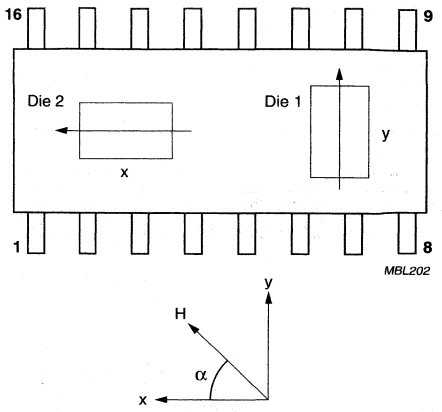

Fig.2 Angular relationship of dice.

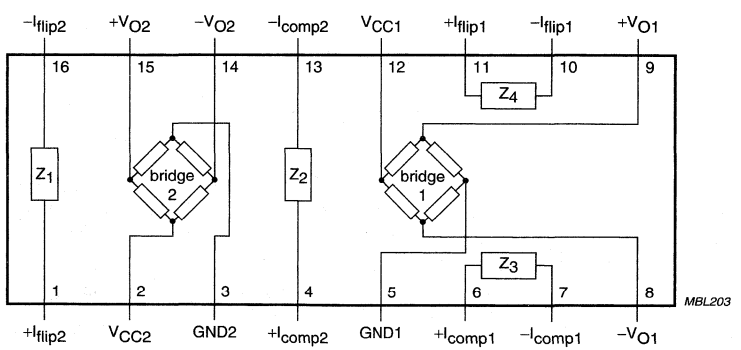

Fig.3 Simplified circuit diagram.

PACKAGE OUTLINE

SO16: plastic small outline package; 16 leads; body width 3.9 mm **SOT109-1**

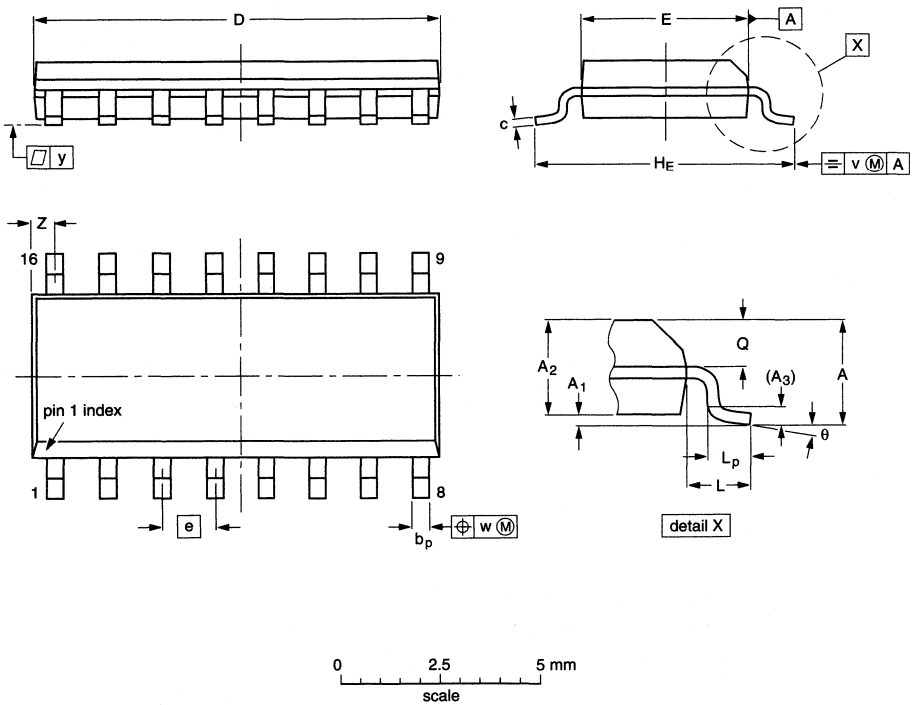

DIMENSIONS (inch dimensions are derived from the original mm dimensions)

UNIT	A max.	A_1	A_2	A_3	b_p	c	$D^{(1)}$	$E^{(1)}$	e	H_E	L	L_p	Q	v	w	y	$Z^{(1)}$	θ
mm	1.75	0.25 0.10	1.45 1.25	0.25	0.49 0.36	0.25 0.19	10.0 9.8	4.0 3.8	1.27	6.2 5.8	1.05	1.0 0.4	0.7 0.6	0.25	0.25	0.1	0.7 0.3	8° 0°
inches	0.069	0.010 0.004	0.057 0.049	0.01	0.019 0.014	0.0100 0.0075	0.39 0.38	0.16 0.15	0.050	0.244 0.228	0.041	0.039 0.016	0.028 0.020	0.01	0.01	0.004	0.028 0.012	

Note

1. Plastic or metal protrusions of 0.15 mm maximum per side are not included.

OUTLINE VERSION	REFERENCES				EUROPEAN PROJECTION	ISSUE DATE
	IEC	JEDEC	EIAJ			
SOT109-1	076E07	MS-012				~~97-05-22~~ 99-12-27

MAGNETORESISTIVE SENSORS FOR ROTATIONAL SPEED MEASUREMENT AND REFERENCE-/MARK DETECTION

APPLICATION NOTE

Rotational Speed Sensors KMI15/16

AN98087

Author(s):
Fritz Schmeißer, Klaus Dietmayer
Systems Laboratory Hamburg
Germany

Keywords

Rotational Speed Sensors
Contactless Speed Measurement
Magnetoresistive Sensors
Integrated Signal Conditioning

Date: 1999-01-11

Summary

The rotational speed sensors KMI 15/x and KMI 16/x make use of the magnetoresistive effect. They consist of the magnetoresistive sensor element, a permanent magnet fixed to this sensor and an integrated signal conditioning circuit. The magnetoresistive principle offers a number of advantages compared with Hall-Effect sensors or inductive sensors such as measurements down to zero speed and a better signal to noise ratio.

The integrated signal conditioning electronics of the sensor modules KMI 15/x or KMI 16/x amplifies the small output voltage of the sensor element and converts it to a digital output signal. This signal is either a rectangular modulation of the supply current for two-wire technology (KMI 15/x) or a switched output voltage with open collector (KMI 16/x). Both sensor modules meet high the requirements of the automotive industry regarding electromagnetic compatibility to line conducted and radiated interference. Although the KMI sensor modules are designed for automotive applications, they also can be used advantageous for rotational speed measurement and movement detection in a wide range of industrial applications.

Table of Contents

1. INTRODUCTION

The KMI 15/X and KMI 16/x are magnetoresistive sensor modules with an integrated signal conditioning electronics to provide a simple and cost effective solution for rotational speed measurements. Due to their compact design, they are simple to design-in and therefore time-to-market is significantly reduced.

The KMI sensor modules consist of the magnetoresistive sensor element, a permanent magnet fixed to this sensor and the integrated signal conditioning circuit designed in bipolar technology. Compared with other sensing techniques, the magnetoresistive technology has a number of practical advantages such as:

- Wide air gap due to high basic sensitivity of the magnetoresistive effect
- Wide operating frequency range, including zero speed detection
- Insensitive to vibration
- Wide operating temperature range
- High EMC

The KMI sensor modules provide two different interfaces to the application. The KMI 15/x sensor modules have an interface using a digital modulation of the supply current and therefore require only a two-wire connection to the application circuit. This current interface is recommended if signals have transmitted over longer distances. On the other hand, also a 3-pin open-collector version (KMI 16/x) is available in order to fit more easily in standard applications. The signal conditioning IC and the sensor element are physically separated to improve high temperature performance of the KMI sensors. This construction ensures that the sensor element can be exposed to higher temperatures than the IC and power dissipation of the IC will not cause inhomogeneous heat in the sensor element.

The first part of this report gives an introduction into the principles of rotational speed measurement using magnetoresistive sensors. Then the characteristics of the magnetoresistive element and the on-chip signal conditioning circuits are described in more detail. Correct mounting of the sensor is another item to be taken into account from the application point of view. Some hints are given for correct encapsulation, including the effects and failures caused by non-ideal mounting. Another important item is the EMC performance of the sensor modules for which test results are given. Finally, a proposal is made for an advanced application circuit.

2. ROTATIONAL SPEED MEASUREMENT USING MAGNETORESISTVE SENSORS

Rotational speed measurement using magnetoresistive sensors (MR-sensors) is achieved by counting ferromagnetic marks, such as teeth of a passive gear wheel or the number of magnetic elements of magnetised ring. Beside magnetoresistive sensors also the inductive sensors and Hall-Effect sensors can be used for this task. However, the magnetoresistive effect offers some essential advantages which should be mentioned briefly.

First, the output signal level of a MR sensor does not vary with rotation speed, as it is the case in inductive sensor systems. Inductive sensors show a direct relation between the rotational speed and the output amplitude and therefore require sophisticated electronics to evaluate the large signal voltage range, especially in applications requiring low jitters.

MR-sensors, in contrast, are characterised by the fact that the sensor is static and the output signal is generated by the bending of magnetic field lines according to the position of the target wheel. This principle is shown in Figure 1. As bending of the magnetic field lines also occurs when the target is not moving, MR-sensors can measure very slow rotations, even down to 0 Hz.

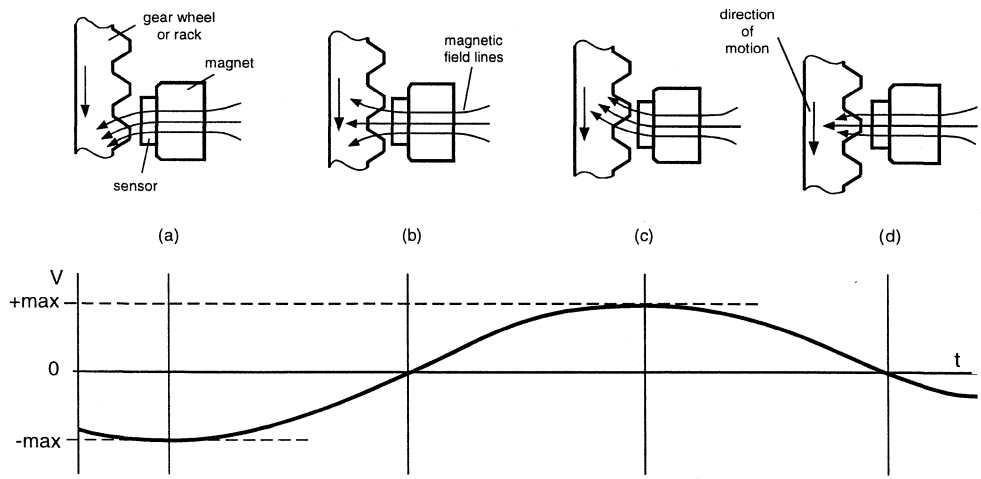

Figure 1: Sensor signal generation in MR-sensors

MR-sensors show larger output signals compared with Hall-Effect sensors as they have signal amplitudes of about 20 mV/kA/m. Hall-Effect sensors provide typically 0.4 mV/kA/m. The higher output voltage of the MR sensor means a much better signal to noise ratio of the sensor signal as well as improved EMC due to the higher signal levels. Moreover, it allows a much larger air gap between sensor and target at comparable target field strength. Consequently, also tolerances in the mechanical set-up and sensor housing may be larger, making the application simpler and reducing costs. Moreover, the necessary magnet is already attached to the sensor element, so that the KMI sensor modules are ready for use. Costs are further reduced as ferrite magnets can be used, rather than the expensive samarium cobalt magnets required for Hall-Effect sensors. All these advantages recommend MR-sensor modules for rotational speed measurements in a wide range of both automotive and industrial applications

The KMI sensor modules of Philips Semiconductors can also be used to measure direction of rotation. This requires two sensor modules placed to the target wheel at different positions. An extended signal conditioning electronic has to evaluate the phase difference between the signals of these two sensor modules.

3. MAGNETORESISTIVE ROTATIONAL SPEED SENSORS

3.1 The Magnetoresistive Sensor Element

3.1.1 The Magnetoresistive Effect

Magnetoresistive (MR) sensors make use of the magnetoresistive effect, the property of a current carrying magnetic material to change its resistivity in the presence of an external magnetic field. Figure 2 shows a strip of ferromagnetic material, called permalloy (20% Fe, 80% Ni).

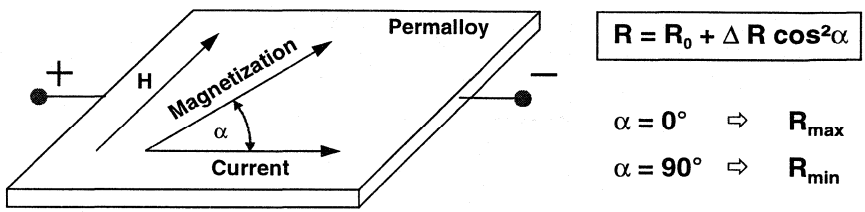

Figure 2: The magnetoresistive effect in permalloy

When no external magnetic field is present, the permalloy has an internal magnetisation vector parallel to the current. During deposition of the permalloy strip, a strong external magnetic field is applied parallel to the strip axis. This accentuates the inherent magnetic anisotropy of the strip and gives them a preferred magnetisation direction, so that even in the absence of an external magnetic field , the magnetisation will always tend to align with the strips. If an external magnetic field H is applied, parallel to the plane of the permalloy but perpendicular to the current flow, the internal magnetisation vector of the permalloy will rotate around an angle α. As a result, the resistance R of the permalloy will change as a function of the angle α, as given by:

$$R = R_0 + \Delta R \cdot \cos^2 \alpha$$

R_0 and ΔR are material parameters. ΔR is in the range of 2 to 3% of R_0.

3.1.2 Linearisation of Sensor Characteristic

It is obvious from this quadratic equation that the resistance to magnetic field relation is non-linear and in addition not unambiguous (compare with graph a) in Figure 4). To get a usable magnetic field sensor with a preferably linear characteristic, a more sophisticated design is necessary.

The magnetoresistive effect can be linearized by depositing aluminum stripes (called barber poles) on top of the permalloy strip at an angle of 45° to the strip axis. Figure 3 shows the principle. As aluminium has a much higher conductivity than permalloy, the effect of the barber pole is to rotate the current direction by 45°, effectively changing the angle between the magnetisation and the electrical current from α to (α - 45°). Graph b) in Figure 4 shows the impact on the sensor characteristic due to the barber pole structure.

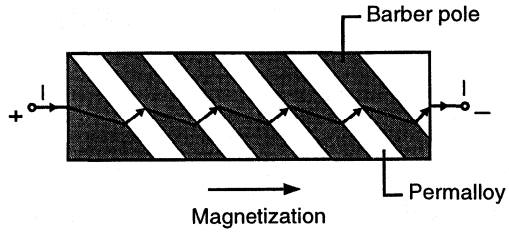

Figure 3: Linearization of the magnetoresistive effect

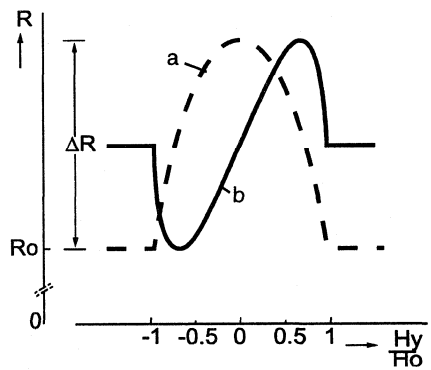

Figure 4: a) R-H characteristic of a standard sensor, b) R-H characteristic of barber pole sensors

To build up a complete sensor element, a Wheatstone bridge arrangement consisting of four magnetoresistive elements is used. In this arrangement, diagonal elements have barber poles of the same orientation. This means that one diagonal pair has barber poles orientated +45° to the strip axis, while the other pair has an orientation of -45°. This ensures a doubling of the output signal while still having an almost linear output signal. Moreover, the inherent temperature coefficients of the four bridge resistances are mutually compensated.

3.1.3 Flipping

Although the "flipping" of MR sensors does not affect the KMI sensor modules due to their stabilisation magnets, the effect should be mentioned for completeness.

The internal magnetisation of the sensor strip has two stable positions. So, if for any reason the sensor is influenced by a powerful magnetic field opposing the internal field, the magnetisation may switch or "flip" from its present direction into the opposite direction. As demonstrated in Figure 5 this leads to a reversal of the sensor characteristic. Consequently, to ensure stable operation, it must be avoided to operate the sensor in an environment where the sensor is subjected to strong negative external fields ("-Hx"). Preferably, a positive ("+Hx") auxiliary field of sufficient magnitude should be applied to prevent any likelihood of flipping within the intended operating range of Hy.

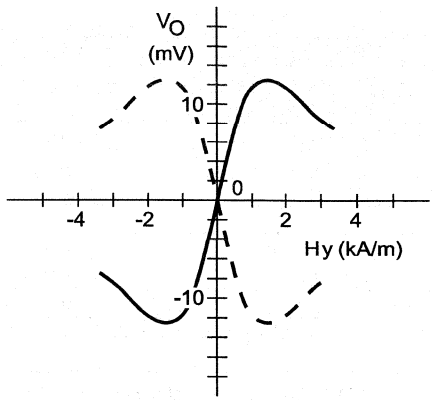

Figure 5: Reversal of sensor characteristic caused by flipping

For the sensor types KMI 15/1, KMI 15/4 and KMI 16/1, this stabilisation field is provided by a magnetic field component in x-direction of the operation magnet. This is field component is attained by an angled magnetisation (see Figure 7). The types KMI 15/2 and KMI 16/2 intended for active targets and therfore not requiring a magnet for operation, are fitted with a smaller auxiliary permanent magnet, magnetised in X-direction only.

3.2 Principle of Speed Measurement

The MR-sensor cannot directly measure rotational speed but is sensitive to the motion of toothed wheels made from ferrous material (passive targets) or rotating wheels having alternating magnetic poles (active targets).

3.2.1 Passive Targets Wheel

The principle of operation has already been briefly discussed in section 2. Figure 1 shows the general arrangement for a passive target wheel.

The sensor is fitted with a permanent magnet. Without a ferromagnetic target or a symmetric position of the toothed wheel, no component of the magnetic field would be in the sensitive direction (y-direction) and therefore the sensor output would be zero. For non-symmetric positions, for example if the passive target rotates in front of the sensor, the magnetic field is bent according to the actual wheel position and an alternating field component in the y-direction arises. This alternating field component is used to generate an output signal that varies according to the wheel position. The amplitude of the sensor output voltage depends on the magnetic field strength of the biasing magnet, the distance between sensor and target and, obviously, on the structure of the target. Large solid targets will give stronger signals at larger distances from the sensor than small targets.

The terms to describe the structure of a gear wheel are explained in TABLE 1 and Figure 6. Figure 7 shows the enlarged drawing of the complete sensor module for passive target wheels. The direction of magnetisation ensures a component of the magnetic field in x-direction to prevent the sensor from flipping (compare with section 0).

SYMBOL	DESCRIPTION	UNIT
DIN		
z	number of teeth	
d	Diameter	mm
m	module m= d / z	mm
p	pitch p = p m	mm
ASA		
PD	pitch diameter	inch
DP	diametric pitch DP = z/PD	1/inch
CP	circular pitch CP = p/DP	inch
For conversion from ASA to DIN : m = 25.4 mm/DP ; p = 25.4 x CP		

TABLE 1: Gear wheel dimensions

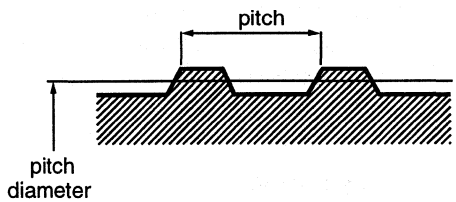

Figure 6: Gear wheel dimensions

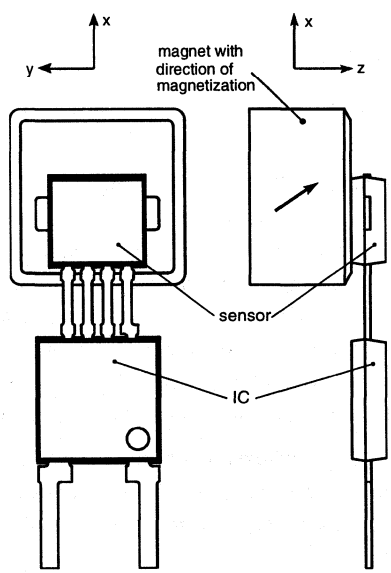

Figure 7: Component detail of the sensor KMI15/1 for passive target wheels

3.2.2 Active Target Wheel

In contrast to passive targets that are not magnetised, active targets show alternating magnetic poles as described in Figure 8. Here the target provides the "working" field and no magnet is required for operation. However, in order to prevent the sensor from, a small stabilisation magnet is still applied to the sensor. Figure 9 shows the KMI 15/2 sensor module intended for use with an active target wheel.

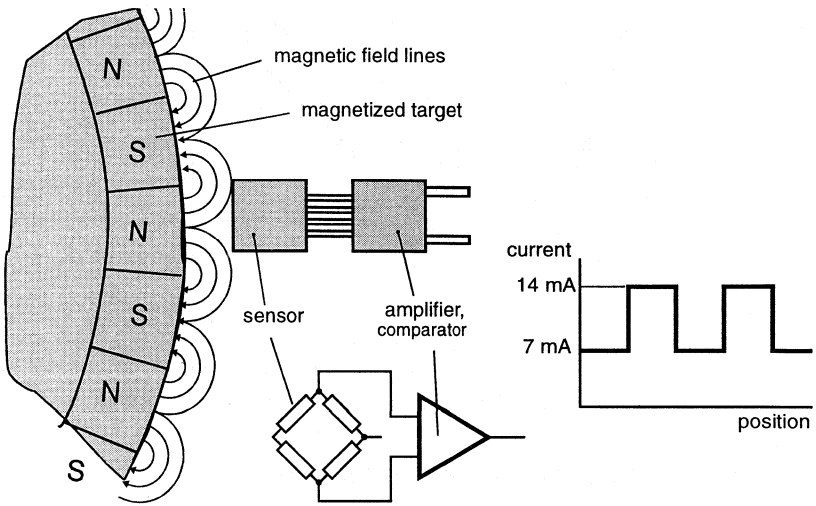

Figure 8: Rotational speed measurement using an active target wheel

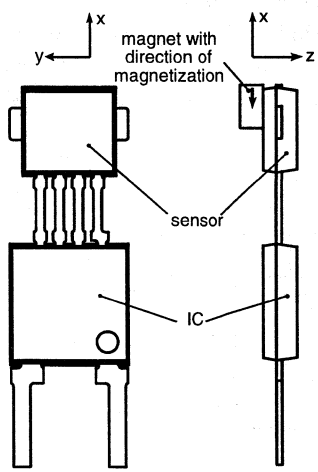

Figure 9: Component detail of the KMI 15/2

The structure of an active target can be expressed similarly to that for passive targets (see TABLE 1). In this case, a north-south magnetic pole pair represents a tooth-valley pair.

The achievable maximum sensing distance for an active wheel depends on the field strength and the structure of the magnetic poles. Figure 10 gives the relation between maximum air gap and pitch for typical plastoferrite rings. This graph was found by averaging measurement results of different target wheels.

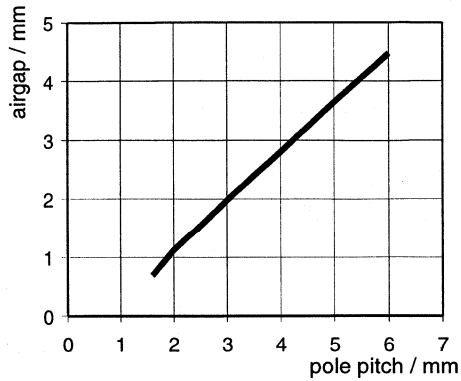

Figure 10: Maximum air gap versus pole pitch for active target wheels.

3.3 The Integrated Signal Conditioning Circuit

The rotational speed sensors KMI 15/x and KMI 16/x include an advanced bipolar signal conditioning circuitry. The KMI 16/x sensor modules provide an open collector output, while KMI 15/x sensor modules have a current interface that requires only two-wires to connect them in the application.

Figure 11 shows the block diagram of the KMI 15/x sensor modules, while the block diagram of the KMI 16/x modules is given in Figure 12. The only difference between both is that for the KMI16/x the switchable current source, which generates the modulated output current signal, is replaced by an open collector output. Moreover, the KMI 16/x sensors allow operation at 5V supply voltage and therfore directly provide a digital output at standard voltage levels.

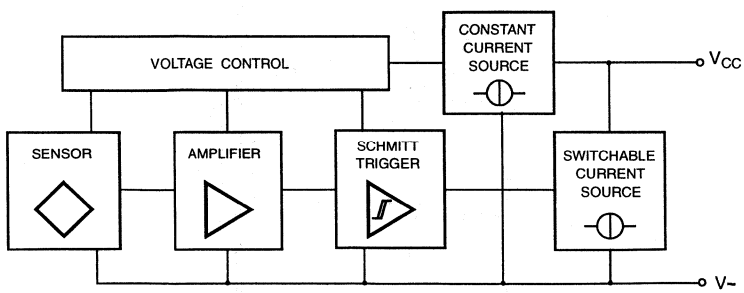

Figure 11: Block diagram of the KMI 15/x sensors with current interface

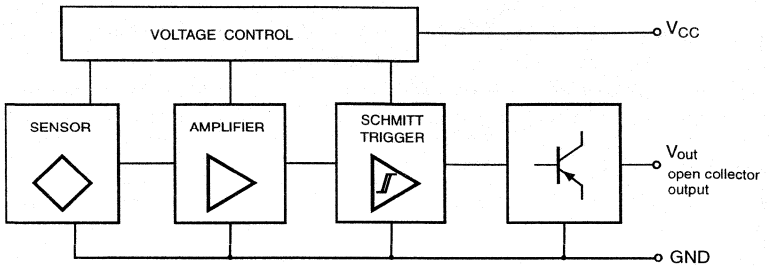

Figure 12: Block diagram of the KMI16/x sensors with open collector output.

Figure 13 shows a more detailed circuit diagram of the KMI 15/x sensor modules. After passing the EMC filter, the sensor signal is amplified and then digitised by a comparator. The comparator has a built-in hysteresis in order to avoid switching due to noise. The voltage control block is stabilised by a bandgap reference diode. It provides the 5 V power supply for the sensor, the amplifier and the comparator. The KMI 15/x modules use two current sources. One current source generates a basic current of 7 mA, which is used for the internal power supply. The current of the second, 7 mA current source is added when triggered by the digitised sensor signal. Thus, during operation, the output current, Icc, switches between 7 mA and 14 mA.

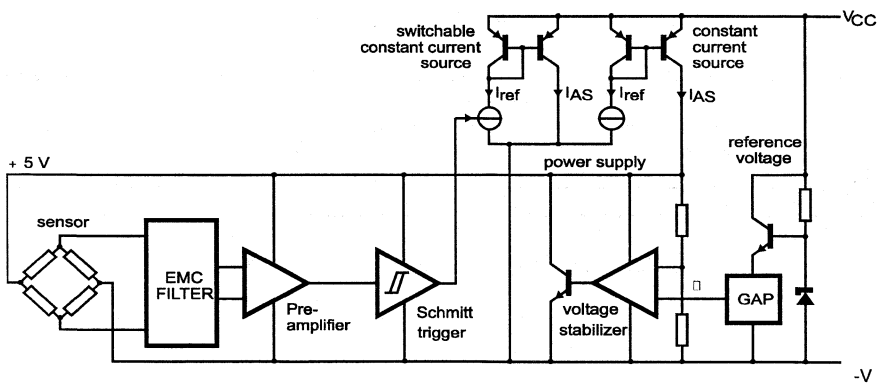

Figure 13: Sensor signal conditioning circuit of the KMI 15/x sensors

3.4 Product Overview

TABLE 2 gives an overview on the complete KMI family. As explained in the previous sections, the KMI 15/x types offer a current source output requiring only two wires for connection. The KMI 16/x sensors have separate signal outputs implemented as open collectors. For each of these interface types, there is at least one sensor module available for passive target wheels and another type for active target wheels. These sensor modules differ only by size and magnetisation direction of the magnet fitted to it.

Type	Interface	Target Wheel	Sensing Distance in mm	Package	Availability
KMI 15/1	Current source	Passive ferrom.	2.5	SOT453	Now
KMI 15/2	Current source	Magnetised	2.5	SOT453	Now
KMI 15/4	Current source	Passive ferrom.	2.0	SOT453	Now
KMI 16/1	Open collector	Passive ferrom.	2.5	SOT477	Now
KMI 16/2	Open collector	Magnetised	2.5	SOT477	Q1 '99

TABLE 2: Product overview

3.5 Limiting Electrical Conditions and Protection

The following Table 3 shows the limiting conditions for the KMI15 and KMI16.

Item	KMI16/x	KMI15/x	Remarks
Supply Voltage	4.5V to 16V	5.5V to 16V	
Load Dump Protection	Yes*	Yes*	*Max. 40V, 2s
Reverse Polarity	No	No	

Table 3: Limiting Conditions of KMI15 and KMI16

4. PROPERTIES OF THE SENSOR MODULES

4.1 Sensing Distance and Hysteresis

The sensing distance d is defined as the distance between the front of the sensor and the tips of the teeth, measured on the central axis of the magnet (see Figure 14). Above a certain value of d, Icc ceases to vary between 7 mA and 14 mA and remains constant at one of these values. The sensor signal, which decreases with larger sensing distances, has become too small to be recognised by the signal conditioning electronics.

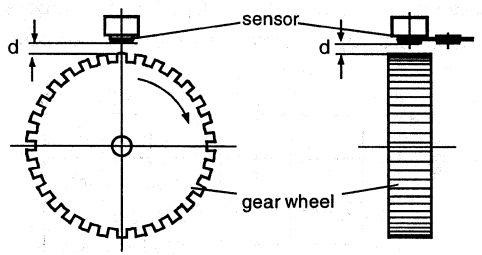

Figure 14: Definition of the sensing distance d

The KMI 15/x and KMI 16/x sensors are able to generate a stable digital output signal in a large range of sensing distances. They have a built-in hysteresis to avoid unwanted switching of the sensor due to

- Mechanical vibration of the sensor or the gear wheel
- Electrical interference
- Circuit oscillation at very low rotational speed

A larger hysteresis provides a better immunity to disturbances but, on the other hand, reduces the maximum sensing distance d, as the sensor signal must exceed the hysteresis levels to be recognised. Consequently, a compromise has to be found between hysteresis and sensing distance.

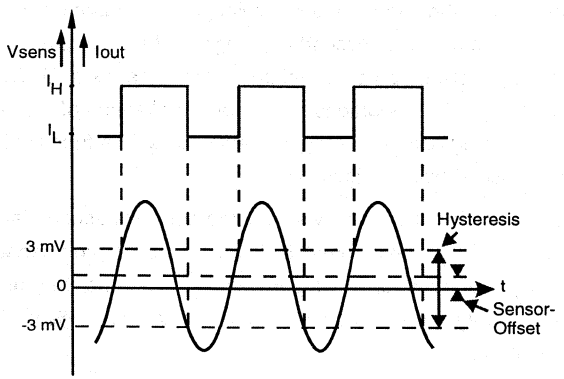

Figure 15: Sensor output voltage and hysteresis

For the KMI sensors, the hysteresis is set to +/- 3 mV at room temperature (see Figure 15). Consequently, the maximum attainable sensing distance is achieved when the sensor signal reaches the level of 6 mV peak-to-peak. Note that this limit assumes a zero sensor signal offset.

4.2 Temperature Coefficient

MR-sensors have negative temperature coefficients of about -0.4 %/K. This means that the amplitude of the sensor signal goes down at higher temperatures. Without compensation, or in other words, without an adaptation of the hysteresis levels, this effect would reduce the maximum sensing distance d at higher temperatures. Therefore the KMI sensor modules provide an automatic adaptation of the hysteresis levels with temperature. Figure 16 shows the residual temperature dependency of the maximum sensing distance.

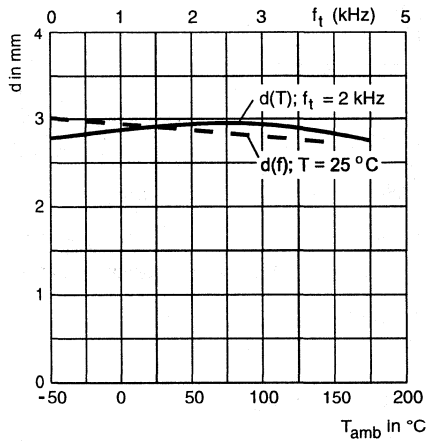

Figure 16: Maximum sensing distance d as a function of temperature and tooth frequency (KMI 15/1)

4.3 Eddy Currents

The movement of the ferromagnetic wheel in the magnetic field of the sensor system will induce eddy currents in the wheel. These eddy currents also cause a (secondary) magnetic field, superimposed to the operating field in the sensor. This secondary field generates an offset voltage in the sensor signal. The eddy currents and therefore the resulting offsets are nearly proportional to the rotational speed of the wheel. As a result, this effect slightly reduces the maximum sensing distance at higher frequencies. The function between rotational speed and maximum sensing distances is also shown in Figure 16.

The direction of the eddy currents and consequently sign of the generated secondary magnetic field depends on the direction of rotation. This means that the external field can increase or compensate a residual offset voltage of the sensor and therefore may cause a direction dependent change of the maximum achievable sensing distance. Consequently, also the duty cycle of the output signal of nominal 50% (without any offset) may slightly depend on the direction of movement.

4.4 Gear Wheel Structure

Finally the structure of the gear wheel itself will affect the maximum sensing distance. Figure 17 shows the variation of the maximum sensing distance d in dependence of the module m for a KMI15/1 sensor. Large solid targets will give stronger signals than small targets. In general, the "size" of the structure can be described as a relationship between wheel diameter and the number of teeth (see also TABLE 1: Gear wheel dimensions).

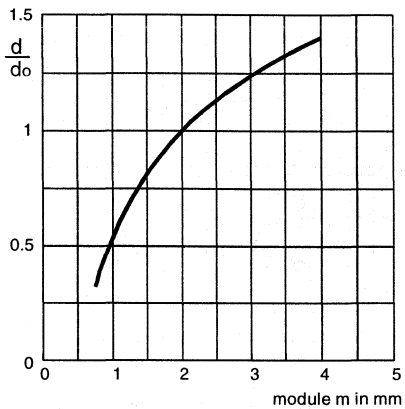

Figure 17: Normalised maximum sensing distance as a function of the module m for the KMI 15/1-sensor module

4.5 Position Tolerances

The optimum position of the sensor is symmetrical to the target wheel with respect to all degrees of freedom. Deviations from this position may reduce the amplitude of the MR-sensor output or increase signal offset, which, in consequence, reduces the maximum sensing distance. Significant larger or smaller values for the duty cycle of nominal 50% indicate that there is an additional offset caused by wrong mounting. There are three possible mounting errors that have to be taken into account:

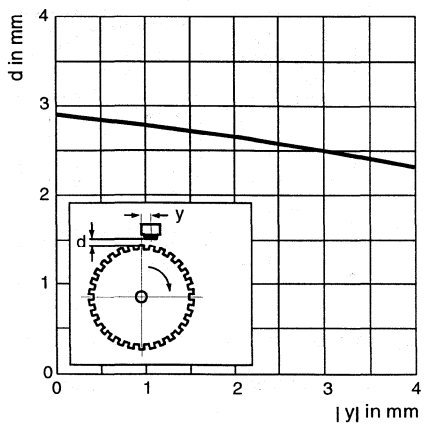

Figure 18: Sensing distance as a function of positional tolerance in the y-axis for a KMI15/1-sensor module.

The first possible error is a shift in y-direction relative to the optimum sensor position as defined in Figure 18. The graph in Figure 18 shows the sensing distance as a function of an y-axis shift. It is recommended to keep this shift smaller than 0.5 mm in order not to have a significant loss of performance.

The second effect to be taken into account is an angular error as defined in Figure 19. This error should be kept smaller than 1 degree for adequaete operation.

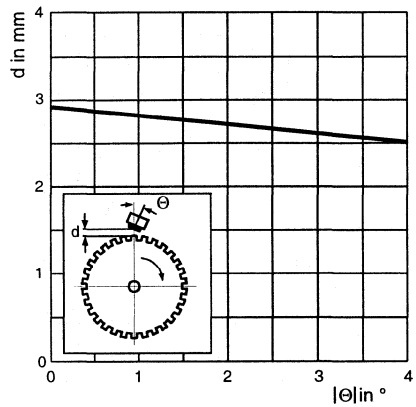

Figure 19: Sensing distance as a function of the angular error for the KMI15/1

An axial shift of the position in x-direction is not very critical with respect to the performance of the KMI sensor modules. Figure 20 shows the definition of this position error and gives some values for the KMI15/1. The graph is non-symmetrical due to the effect that a field component in x-direction already exist to prevent the sensor from flipping and this partitioning is changed by this position error. The optimum position is x = 0.

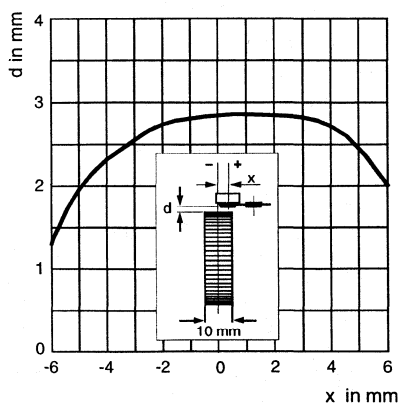

Figure 20: Sensing distance as a function of positional tolerance in the x-axis

A tilt in y-z plane has negligible impact on the sensing distance for angles less than 4°. Therefore, this error normally has not to be considered.

4.6 External Magnetic Fields

External magnetic fields if present are added to the operating field and therefore may cause an additional offset voltage. If this offset exceeds a certain limit (see e.g. Figure 15) an unacceptable change in duty cycle or even malfunction may occur. Sources of external magnetic fields are all kind of permanent magnets and electromagnetic devices like motors and relais, but also simple wires carrying high currents may cause significant magnetic fields. What level of disturbances is tolerable depends on the sensing distance required. In general, sensor modules should be mounted as far away as possible from all sources of magnetic fields. What external field strength is tolerated depends on the sensing distance required and therefore must be decided individually.

Another aspect to be taken into account is that very strong external fields may damage the sensor as they may permanently change the magnetisation of the attached permanent magnet. Magnetic fields up to a field strength of H = 5 kA/m are tolerated regarding this issue but already may significant influence the sensor performance.

5. ENCAPSULATION OF THE KMI SENSORS

5.1 Plastic Encapsulation

The KMI rotational speed sensor comes in special package patented by Philips that is predestined for customer specific encapsulation. Thanks to this package, the sensor modules are highly insensitive to mechanical stress. They can be easily built into a customised moulding, but some precautions should be taken into account to ensure full performance.

During plastic encapsulation the plastic material must not be injected directly to the MR-sensor or the integrated circuit because this may cause remaining mechanical stress in these parts. Furthermore it had to be ensured that the high temperature of the injected plastic material does not affect the durability of the gluing of the auxiliary magnet. High temperature and pressure could change the position of the magnet and therefore may damage the offset trimming.

The MR-sensor element is placed directly on the leadframe. Two reference points, which are part of this leadframe, can be used in the system design as reference mark. As the tolerances of the plastic encapsulation are no longer part of the overall tolerance calculation, this effect allows a precise sensor positioning and consequently a larger air gap.

Figure 21 shows the drawing of the lead frame with the reference points, the MR-sensor, the integrated signal conditioning circuit and the sensor package. The exact mechanical dimensions can be found in the current data book.

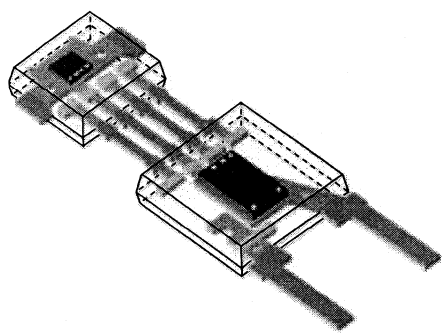

Figure 21: Construction and encapsulation of the KMI sensor modules.

5.2 Bending of Connection Pins

The electrical connections between the MR-sensor and the integrated circuit can be bent to adapt the sensor element position to the actual application. However, the maximum force to the connections between sensor element and IC must be limited to F=20 N in order not to destroy the device during this process.

The external connections to the supply pins should be fixed by clamping in order to avoid any tractive force to the leadframe in the sensor package. The maximum force allowed for this pins is F = 50 N.

The limiting values for bending are given in the following Figure 22.

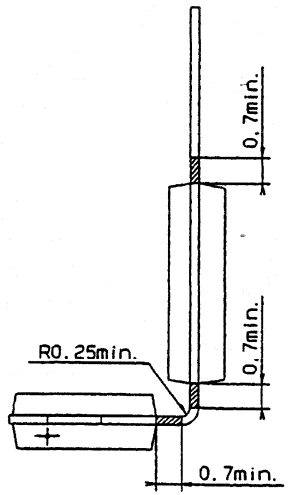

Figure 22: Limiting conditions for bending

6. APPLICATION CIRCUIT AND ELECTROMAGNETIC COMPATIBILITY

6.1 Test and Application Circuit

Figure 23 shows a test circuit to convert the current signal of the KMI 15/x sensor modules into a voltage. Figure 24 shows the respective circuit for the KMI16/x with open collector. Dependent on the actual conditions in the application, these simple circuits must be extended by protective components. An example for automotive applications is given in the next section.

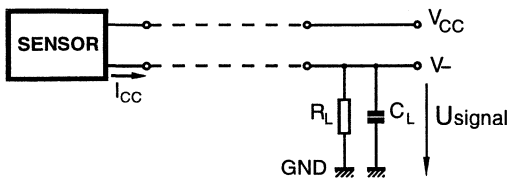

Figure 23: Test circuit for KMI15/x

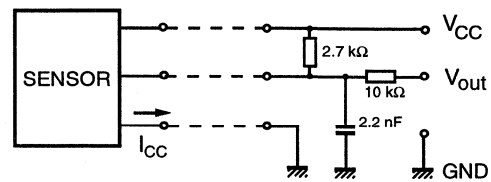

Figure 24: Test Circuit for KMI 16/x

6.2 Line Conducted Interferences

Figure 25 shows the recommended application circuit for KMI 15/x sensor modules in automotive applications. It adds some measures to improve electromagnetic compatibility. Spikes of positive or negative polarity are suppressed and also a protection against reverse polarity of the supply voltage is included.

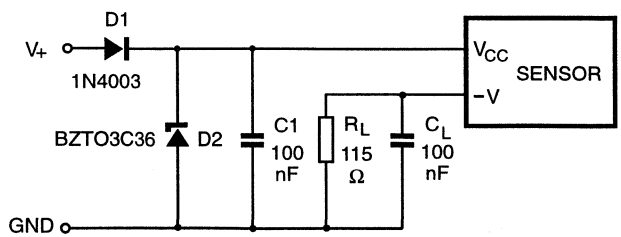

Figure 25: Recommended application circuit for the KMI15/x sensors

TABLE 4 lists the test results found for this circuit for line-conducted disturbances according to ISO 7637-1. It should be noted that this circuit does not protect the device against the "load dump pulse" (test pulse 5 according to ISO 7637-1). Protection against this pulse would require a special suppressor diode with sufficient energy absorption capability. However, as board nets of cars often already contain a central load dump protection that limits the pulse voltage to Vmax = 40 V, this kind of protection is not required in any case.

EMC REF. ISO 7637-1	MIN. (V)	MAX.(V)	Remarks	Severity class
Test pulse 1	-100	-	td = 2 ms	C
Test pulse 2	-	100	td = 0.2 ms	A
Test pulse 3a	-150	-	td = 0.1 µs	A
Test pulse 3b	-	100	td = 0.1 µs	A
Test pulse 4	-7	-	td = 130 ms	B
Test pulse 5		120	td = 400 ms	see text

TABLE 4: Test results regarding line conducted interferences

6.3 Radiated Interference

Any sensitive electronic system connected to other equipment by cables is exposed to electromagnetic disturbances. The KMI 15/x and KMI 16/x sensor modules provide RF-filter in the input stage to avoid negative effects on the system performance. The sensors were tested under standardised conditions in a "strip-line" according to ISO 11425-5. Tests were passed at a maximum field strength of E = 150 V/m with and without AM modulation (1kHz, 95%). Actual applications, however, may lead to different results due to special environment characteristics such as resonance effects. Therefore it is strongly recommended to do final tests regarding EMC in the application relevant environment.

6.4 Electrostatic Discharge

During handling and mounting electrostatic charges may affect the sensor pins and under extreme conditions even damage or destroy the sensor. Tests for electrostatic discharges (ESD) were conducted in line with IEC 801-2 to safeguard the handling capability of the KMI sensor modules. The IEC 801-2 test conditions were:

C = 150 pF, R = 150 Ω. V = 2 kV

These data are only valid for the supply pins, but no protective means are provided for the connections between sensor element and the IC. Common rules for handling electrostatic sensitive devices must be observed.

7. INTERFACE TO DIGITAL SIGNAL PROCESSING FOR KMI 15/X

7.1 General

The integrated rotational speed sensor KMI 15/x provides a modulated current. For subsequent digital signal processing, this current signal has to be converted to a ground referenced voltage signal, matching the logic levels of the processing unit. Additionally, the signal conditioning circuit should include a low pass filter in front of the comparator input and protective elements to suppress line conducted interference. Figure 26 shows the block diagram of a suitable application circuit. Details are discussed in the following sections.

Please note that the KMI16/x sensors already provide a digital output implemented as an open collector. As these modules can operate at 5V supply voltage, the standard level for digital systems, these types should be preferred in digital systems if the advantages of the two-wire current interface are not that important.

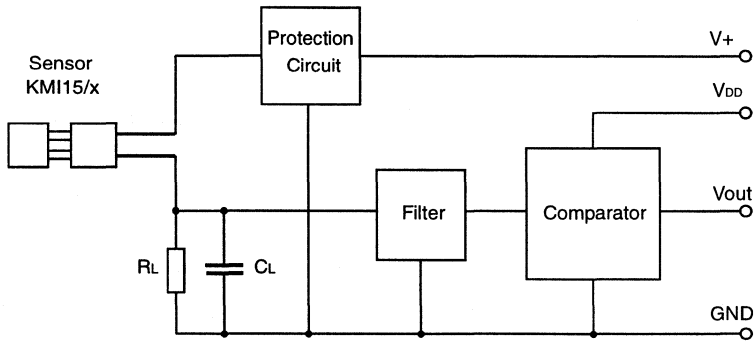

Figure 26: Block diagram of a suitable application circuit

Please note that the KMI16/x sensors already provide a digital output implemented as an open collector. As these modules can operate at 5V supply voltage, the standard level for digital systems, these types should be preferred in digital systems if the advantages of the two-wire current interface are not that important.

7.2 The Comparator

Figure 27 illustrates the output current levels regarding nominal values and specified tolerances.

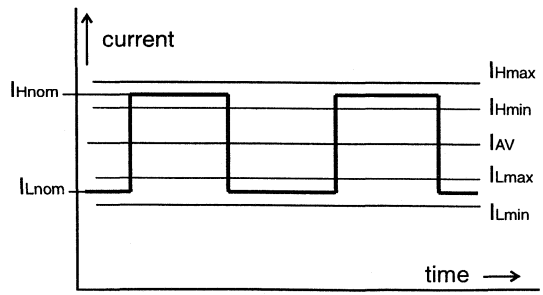

Figure 27: Current levels of the rectangular output signal

Using the recommended series resistor of 115 Ω, the current levels are converted into voltages as given in TABLE 5. Consequently, the comparator levels of a processing electronic must be set between V_{Hmin} and V_{Lmax} for reliable operation. This is ensured by using a reference level of V_{AV} . Additionally, a hysteresis should be implemented.

Symbols Current	Current in mA	voltage in V @ R = 115 Ω	Symbols Voltages
I_{Lmin}	5.6	0.64	V_{Lmin}
I_{Lnom}	7	0.81	V_{Lnom}
I_{Lmax}	8.4	0.97	V_{Lmax}
I_{AV}		1.13	V_{AV}
I_{Hmin}	11.2	1.29	V_{Hmin}
I_{Hnom}	14	1.61	V_{Hnom}
I_{Hmax}	16.8	1.93	V_{Hmax}

TABLE 5: Output current and voltage levels for R = 115 Ω

The complete circuit diagram proposed for such an application is depicted in Figure 28. The dimension is made assuming a 5V supply voltage (V_{DD}) for the comparator. The reference voltage V_{AV} is defined by voltage divider R5/R6. The voltage divider R9/R10, the feed back resistor R7 and the input resistors R2 and R3 determine the hysteresis of about +/- 50 mV.

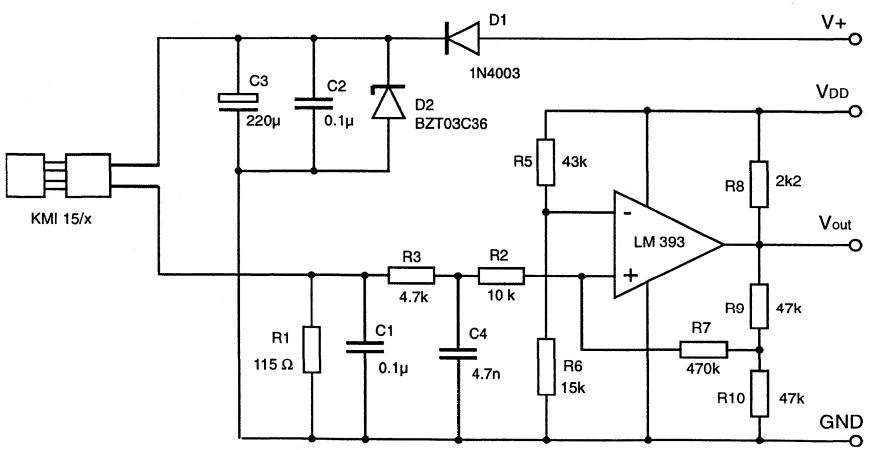

Figure 28: Complete application circuit for digital signal processing with the KMI 15/x sensor modules

7.3 Signal Filter

In addition to the parallel capacitor C1, a second lowpass filter is recommended to reduce RF interference. The example circuit in Figure 28 provides a first-order RC low pass filter for this task (R3, C4) with a cut off frequency of 10 kHz. This cut off frequency should be adapted according to the maximum signal frequency required in the application in order to achieve an optimum absorption of noise.

7.4 Protection Circuit

This part of the circuit has already be described in section 0. The series diode D1 protects the sensor and electronics against reverse polarity of the supply voltage and blocks negative interference pulses. The suppressor diode D2 limits positive interference pulses. Note that the specified type has not the capability to tolerate the load dump pulses. The capacitor C2 absorbs fast positive and negative interference pulses. The electrolytic capacitor C3 stores energy to supply the sensor during short supply voltage breakdown due to negative pulses.

8. OTHER APPLICATIONS

The primary application area of the KMI sensors is rotational speed measurement in automotive applications such as ABS, ASR or gearbox. However, the magnetoresistive rotational speed sensors of the KMI-family are not limited to automotive applications. Their characteristic recommends them for a wide range of general industrial applications. Another range of industrial applications is the detection of non-periodic or single events, where a movement can be transferred to a change of a magnetic field. Examples are:

- Proximity switch
- Position detector
- Limit switch
- Detection of electrical current levels

The common operating principle of these applications is that a moving ferromagnetic part, a moving permanent magnet or changes of the electrical current cause an alteration of the magnetic field measured by the MR sensor and, in consequence, forces an alteration of the output signal. The sensors of the KMI family offer simple, reliable and cost effective solutions also for this kind of applications.

DEVICE DATA

Integrated rotational speed sensor KMI15/1

FEATURES

- Digital current output signal
- Zero speed capability
- Wide air gap
- Wide temperature range
- Insensitive to vibration
- EMC resistant.

DESCRIPTION

The KMI15/1 sensor detects rotational speed of ferrous gear wheels and reference marks(1).
The sensor consists of a magnetoresistive sensor element, a signal conditioning integrated circuit in bipolar technology and a magnetized ferrite magnet.
The frequency of the digital current output signal is proportional to the rotational speed of a gear wheel.

CAUTION
Do not press two or more products together against their magnetic forces.

(1) The sensor contains a customized integrated circuit. Usage in hydraulic brake systems and in systems with active brake control is forbidden. For all other applications, higher temperature versions of up to 150 °C are available on request.

PINNING

PIN	DESCRIPTION
1	V_{CC}
2	V–

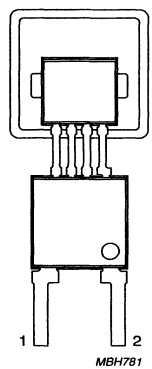

Fig.1 Simplified outline (SOT453B).

QUICK REFERENCE DATA

SYMBOL	PARAMETER	MIN.	TYP.	MAX.	UNIT
V_{CC}	DC supply voltage	–	12	–	V
$I_{CC\ (low)}$	current output signal low	–	7	–	mA
$I_{CC\ (high)}$	current output signal high	–	14	–	mA
d	sensing distance	0 to 2.5	0 to 2.9	–	mm
f_t	operating tooth frequency	0	–	25000	Hz
T_{amb}	ambient operating temperature	−40	–	+85	°C

LIMITING VALUES

In accordance with Absolute Maximum Rating System (IEC 60134).

SYMBOL	PARAMETER	CONDITIONS	MIN.	MAX.	UNIT
V_{CC}	DC supply voltage	T_{amb} = −40 to +85 °C; R_L = 115 Ω	−0.5	+16	V
T_{stg}	storage temperature		−40	+150	°C
T_{amb}	ambient operating temperature		−40	+85	°C
T_{sld}	soldering temperature	t ≤ 10 s	–	260	°C
	output short-circuit duration to GND		continuous		

CHARACTERISTICS

T_{amb} = 25 °C; V_{CC} = 12 V; d = 2.1 mm; f_t = 2 kHz; test circuit: see Fig.7; R_L = 115 Ω; sensor positioning: see Fig.15; gear wheel: module 2 mm; material 1.0715; unless otherwise specified.

SYMBOL	PARAMETER	CONDITIONS	MIN.	TYP.	MAX.	UNIT
$I_{CC\ (low)}$	current output signal low	see Figs 6 and 8	5.6	7	8.4	mA
$I_{CC\ (high)}$	current output signal high	see Figs 6 and 8	11.2	14	16.8	mA
t_r	output signal rise time	C_L = 100 pF; see Fig.9; 10 to 90% value	–	0.5	–	µs
t_f	output signal fall time	C_L = 100 pF; see Fig.9; 10 to 90% value	–	0.7	–	µs
t_d	switching delay time	between stimulation pulse (generated by a coil) and output signal	–	1	–	µs
f_t	operating tooth frequency	for both rotation directions	0	–	25000	Hz
d	sensing distance	see Fig.15 and note 1	0 to 2.5	0 to 2.9	–	mm
δ	duty cycle	see Fig.6	30	50	70	%

Note

1. High rotational speeds of wheels reduce the sensing distance due to eddy current effects (see Fig.17).

FUNCTIONAL DESCRIPTION

The KMI15/1 sensor is sensitive to the motion of ferrous gear wheels or reference marks. The functional principle is shown in Fig.3. Due to the effect of flux bending, the different directions of magnetic field lines in the magnetoresistive sensor element will cause an electrical signal. Because of the chosen sensor orientation and the direction of ferrite magnetization, the KMI15/1 is sensitive to movement in the 'y' direction in front of the sensor only (see Fig.2).

The magnetoresistive sensor element signal is amplified, temperature compensated and passed to a Schmitt trigger in the conditioning integrated circuit (Figs 4 and 5).
The digital output signal level (see Fig.6) is independent of the sensing distance within the measuring range (Fig.14).
A (2-wire) output current enables safe transfer of the sensor signal to the detecting circuit (see Fig.7).
The integrated circuit housing is separated from the sensor element housing to optimize the sensor behaviour at high temperatures.

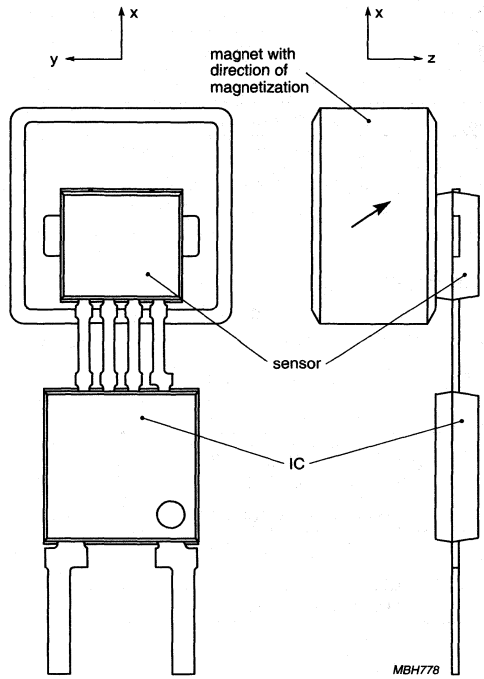

Fig.2 Component detail of the KMI15/1.

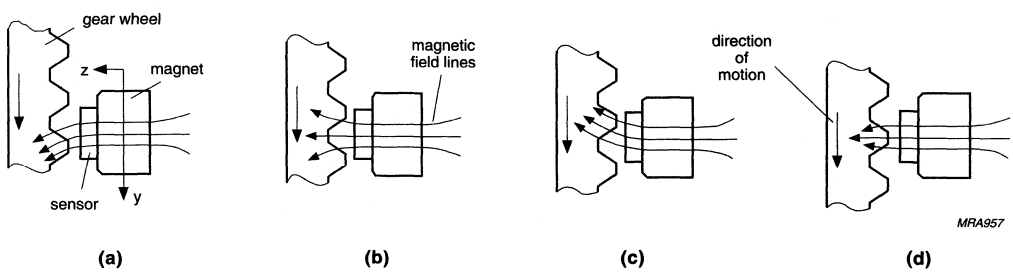

Fig.3 Functional principle.

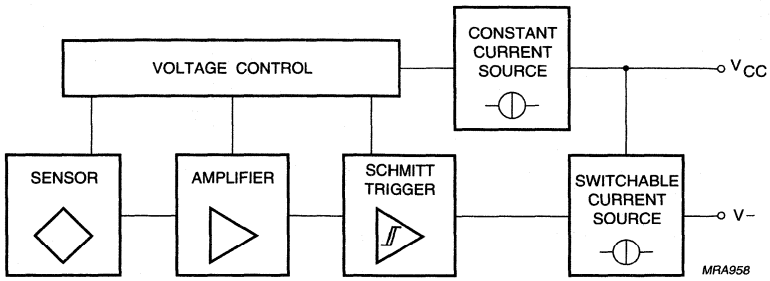

Fig.4 Block diagram.

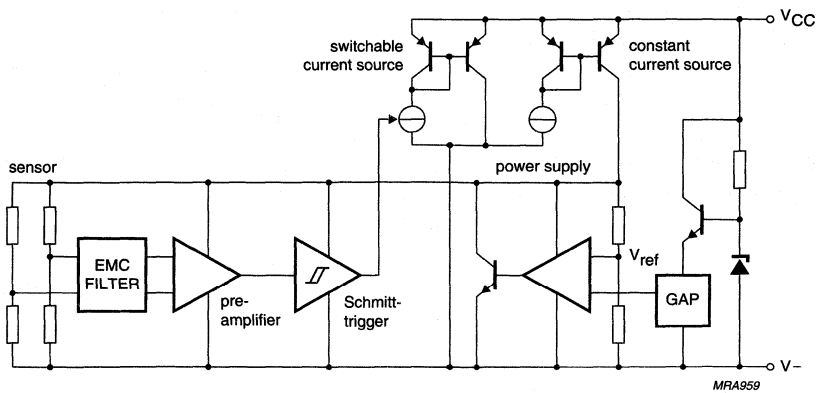

Fig.5 Simplified circuit diagram.

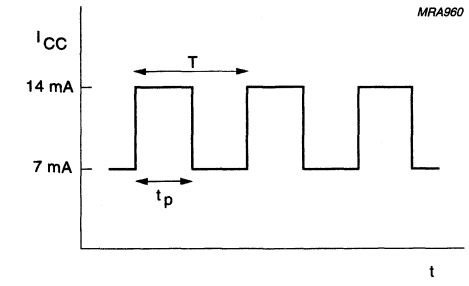

$$\delta = \frac{t_p}{T} \times 100\%$$

Fig.6 Output signal as a function of time.

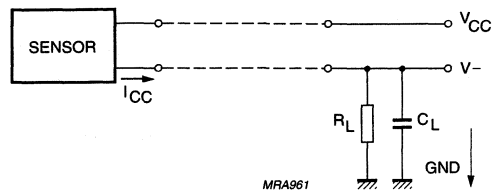

Fig.7 Test and application circuit.

APPLICATION INFORMATION

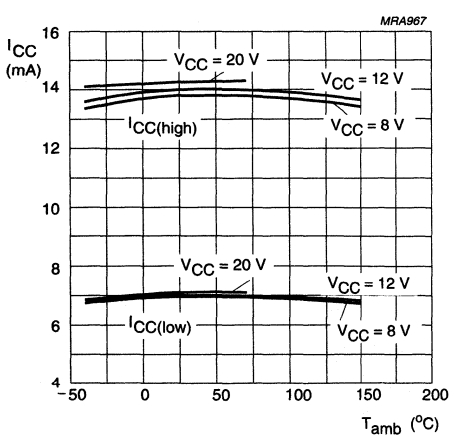

Fig.8 Output current levels as functions of ambient temperature; typical values.

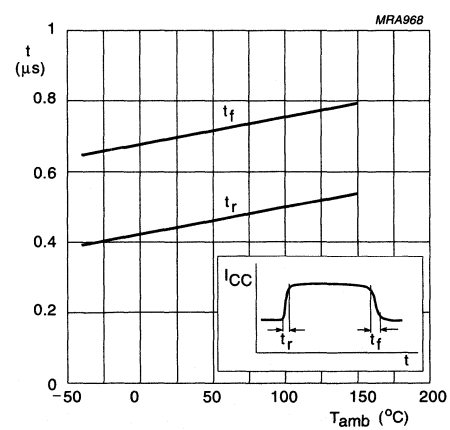

V_{CC} = 12 V; C_L = 100 pF; R_L = 115 Ω.

Fig.9 Output current switching times as functions of ambient temperature; typical values.

Mounting conditions

The recommended sensor position in front of a gear wheel is shown in Fig.15. The distance 'd' is measured between the sensor front and the tip of a gear wheel tooth.
The KMI15/1 senses ferrous indicators like gear wheels in the ± y direction only (no rotational symmetry of the sensor); see Fig.2. The effect of incorrect mounting positions on sensing distance is shown in Figs 11, 12 and 13. The symmetrical reference axis of the sensor corresponds to the axis of the ferrite magnet.

Environmental conditions

Due to eddy current effects the sensing distance depends on the tooth frequency (Fig.17). The influence of gear wheel module on the sensing distance is shown in Fig.16.

Gear Wheel Dimensions

SYMBOL	DESCRIPTION	UNIT
German DIN		
z	number of teeth	
d	diameter	mm
m	module m = d/z	mm
p	pitch p = π × m	mm
ASA; note1		
PD	pitch diameter (d in inch)	inch
DP	diametric pitch DP = z/PD	$inch^{-1}$
CP	circular pitch CP = π/DP	inch

Note

1. For conversion from ASA to DIN: m = 25.4 mm/DP; p = 25.4 mm × CP.

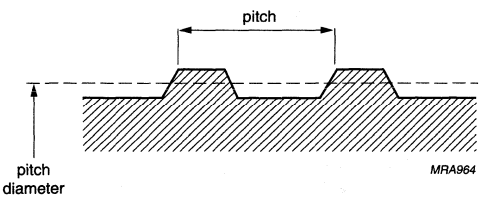

$$\text{module} = \frac{\text{pitch diameter}}{\text{number of teeth}}$$

pitch = module × π

Fig.10 Gear wheel dimensions.

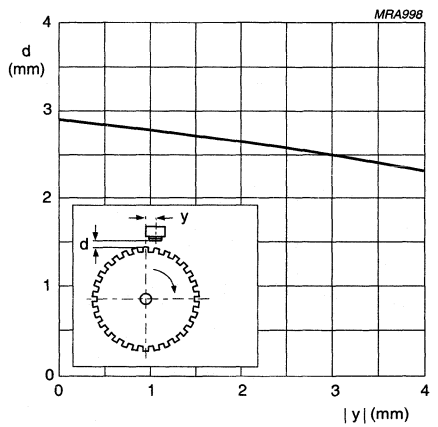

V_{CC} = 12 V; f_t = 2 kHz; module = 2 mm; pitch diameter = 100 mm.

Fig.11 Sensing distance as a function of positional tolerance in the y-axis; typical values.

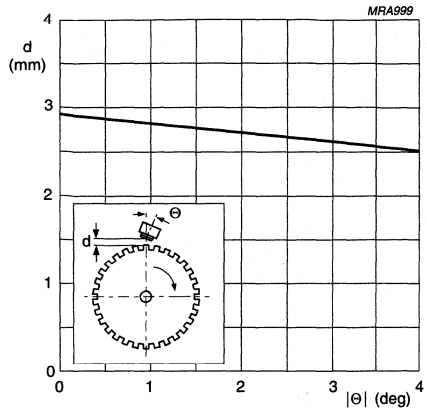

V_{CC} = 12 V; f_t = 2 kHz; module = 2 mm.

Fig.12 Sensing distance as a function of positional tolerance; typical values.

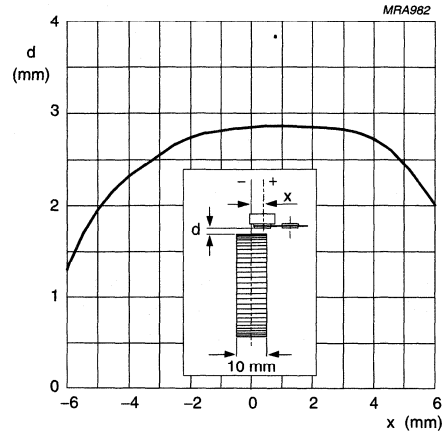

V_{CC} = 12 V; f_t = 2 kHz; module = 2 mm.

Fig.13 Sensing distance as a function of positional tolerance in the x-axis; typical values.

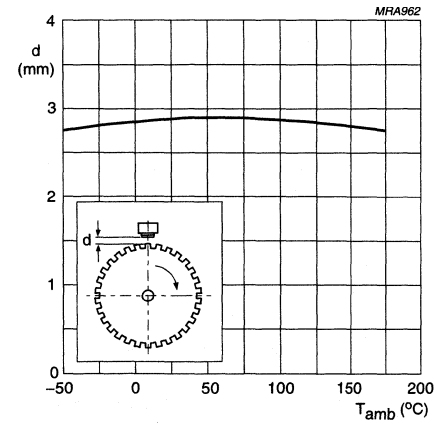

V_{CC} = 12 V; f_t = 2 kHz; module = 2 mm.

Fig.14 Sensing distance as a function of ambient temperature; typical values.

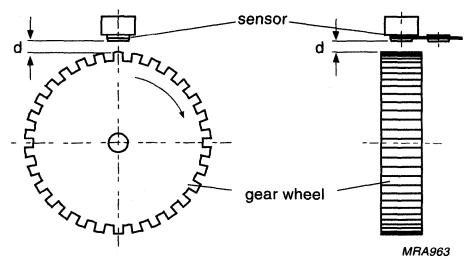

Fig.15 Sensor positioning.

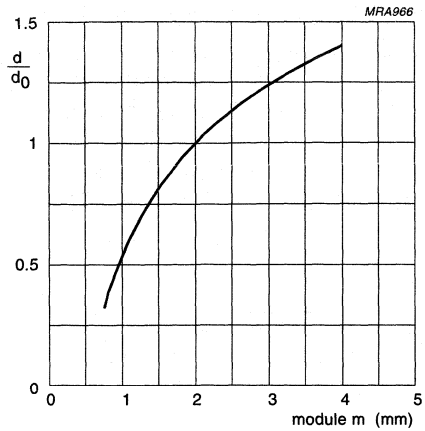

d_o = measuring distance for a gear wheel with module m = 2 mm.

Fig.16 Normalized maximum sensing distance as a function of gear wheel module; typical values.

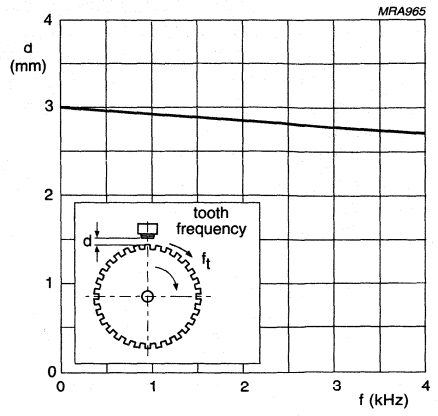

V_{CC} = 12 V; module = 2 mm.

Fig.17 Sensing distance as a function of tooth frequency; typical values.

EMC

Figure 18 shows a recommended application circuit for automotive applications (wheel sensing $f_t < 5$ kHz). It provides a protection interface to meet Electromagnetic Compatibility (EMC) standards and safeguard against voltage spikes. Table 1 lists the tests which are applicable to this circuit and the achieved class of functional status. Protection against 'load dump' (test pulse 5 according to *"DIN 40839"*) means a very high demand on the protection circuit and requires a suitable suppressor diode with sufficient energy absorption capability.

The board net often contains a central load dump protection that makes such a device in the protection circuit of the sensor module unnecessary.

Tests for electrostatic discharge (ESD) were conducted in line with *"IEC 801-2"* to demonstrate the KMI15/1's handling capabilities. The *"IEC 801-2"* test conditions were: C = 150 pF, R = 150 Ω, V = 2 kV.

Electromagnetic disturbances with fields up to 150 V/m and f = 1 GHz (ref. *"DIN 40839"*) have no influence on performance.

Table 1 EMC test results

EMC REF. DIN 40839	SYMBOL	MIN. (V)	MAX. (V)	REMARKS	CLASS
Test pulse 1	V_{LD}	−100	–	t_d = 2 ms	C
Test pulse 2	V_{LD}	–	100	t_d = 0.2 ms	A
Test pulse 3a	V_{LD}	−150	–	t_d = 0.1 µs	A
Test pulse 3b	V_{LD}	–	100	t_d = 0.1 µs	A
Test pulse 4	V_{LD}	−7	–	t_d = 130 ms	B
Test pulse 5	V_{LD}	–	120	t_d = 400 ms	B

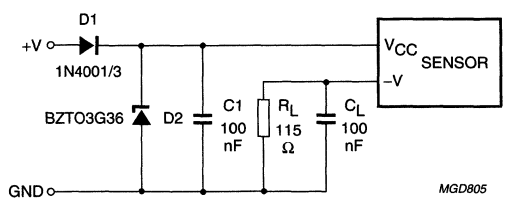

Fig.18 Test/application circuit for the KMI15/1.

PACKAGE OUTLINE

Plastic single-ended multi-chip package; magnetized ferrite magnet (8 x 8 x 4.5 mm); 4 interconnections; 2 in-line leads **SOT453B**

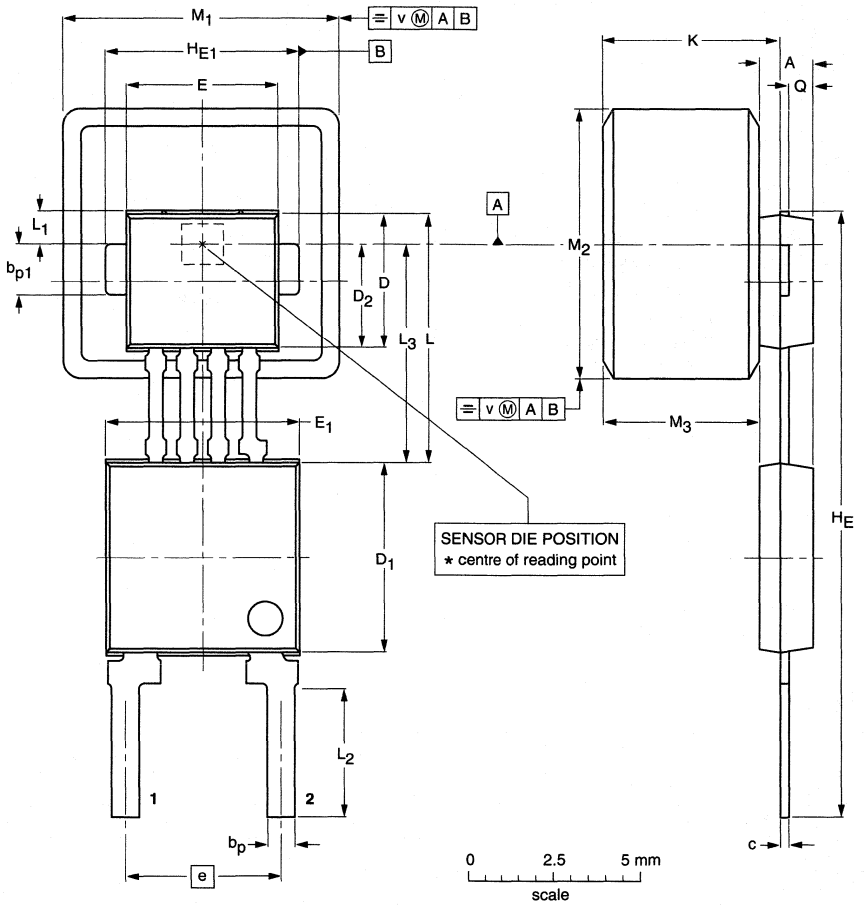

DIMENSIONS (mm are the original dimensions)

UNIT	A(1)	b_p	b_{p1}	c	D(2)	D_1(2)	D_2(2)	E(2)	E_1(2)	e	H_E	H_{E1}	K max.	L	L_1	L_2	L_3	M_1	M_2	M_3(1)	Q	v
mm	1.7 1.4	0.8 0.7	1.57 1.47	0.3 0.24	4.1 3.9	5.7 5.5	3.15 2.95	4.5 4.3	5.7 5.5	4.6 4.4	18.2 17.8	5.6 5.5	5.37	7.55 7.25	1.2 0.9	3.9 3.5	6.55 6.35	8.15 7.85	8.15 7.85	4.7 4.3	0.75 0.65	0.25

Notes

1. Glue thickness not included.
2. Plastic or metal protrusions of 0.15 mm maximum per side are not included.

OUTLINE VERSION	REFERENCES				EUROPEAN PROJECTION	ISSUE DATE
	IEC	JEDEC	EIAJ			
SOT453B						~~99-09-23~~ 00-08-31

Integrated rotational speed sensor KMI15/2

FEATURES

- Digital current output signal
- Zero speed capability
- Wide air gap
- Wide temperature range
- Insensitive to vibration
- EMC resistant.

DESCRIPTION

The KMI15/2 sensor detects (rotational) speed and reference mark detection of magnetized targets(1). The sensor consists of a magnetoresistive sensor element, a signal conditioning integrated circuit in bipolar technology and a magnetized ferrite magnet.
The frequency of the digital current output signal is proportional to the rotational speed of a gear wheel.

CAUTION
Do not press two or more products together against their magnetic forces.

(1) The sensor contains a customized integrated circuit. Usage in hydraulic brake systems and in systems with active brake control is forbidden. For all other applications, higher temperature versions of up to 150 °C are available on request.

PINNING

PIN	DESCRIPTION
1	V_{CC}
2	V–

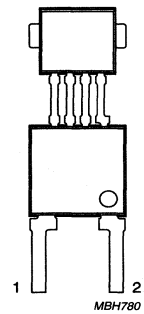

Fig.1 Simplified outline; (SOT453A).

QUICK REFERENCE DATA

SYMBOL	PARAMETER	MIN.	TYP.	MAX.	UNIT
V_{CC}	DC supply voltage	0.5	12	16	V
$I_{CC\ (low)}$	current output signal low	–	7	–	mA
$I_{CC\ (high)}$	current output signal high	–	14	–	mA
f_t	operating frequency	0	–	25000	Hz
T_{amb}	ambient operating temperature	–40	–	+85	°C

LIMITING VALUES

In accordance with Absolute Maximum Rating System (IEC 60134).

SYMBOL	PARAMETER	CONDITIONS	MIN.	MAX.	UNIT
V_{CC}	DC supply voltage	T_{amb} = −40 to +85 °C; R_L = 115 Ω	0.5	16	V
T_{stg}	storage temperature		−40	+150	°C
T_{amb}	operating ambient temperature		−40	+85	°C
T_{sld}	soldering temperature	t ≤ 10 s	–	260	°C
	output short-circuit duration to GND		continuous		

CHARACTERISTICS

T_{amb} = 25 °C; V_{CC} = 12 V; f_t = 2 kHz; test circuit: see Fig.7; R_L = 115 Ω.

SYMBOL	PARAMETER	CONDITIONS	MIN.	TYP.	MAX.	UNIT
$I_{CC\ (low)}$	current output signal low	see Fig.6	5.6	7.0	8.4	mA
$I_{CC\ (high)}$	current output signal high	see Fig.6	11.2	14.0	16.8	mA
t_r	output signal rise time	C_L = 100 pF; 10 to 90% value	–	0.5	–	µs
t_f	output signal fall time	C_L = 100 pF; 10 to 90% value	–	0.7	–	µs
t_d	switching delay time	between stimulation pulse (generated by a coil) and output signal	–	1	–	µs
f_t	operating frequency	for both rotation directions	0	–	25000	Hz
Hs_{LH}	magnetic switching field strength		0.05	0.3	0.8	kA/m
Hs_{HL}	magnetic switching field strength		0.05	0.3	0.8	kA/m
Hs	magnetic switching hysteresis		0.15	–	1.6	kA/m

FUNCTIONAL DESCRIPTION

The KMI15/2 sensor is sensitive to magnetic fields. The functional principle is shown in Fig.3. The field lines of a magnetized target are shown in Fig.3 as a straight target (it could also be circular e.g. for rotational speed measurement). If a sensor KMI15/2 is moved as shown in this field, either of the magnetic field components Hs_{HL} or Hs_{LH} is dominant, and forces the sensor to switch to either the high current (14 mA) or to the low current (7 mA). Oscillation of the sensor output signal is avoided by the implementation of a hysteresis into the signal conditioning electronic.

The MR sensor is stabilized by a permanent magnet applying a continuous magnetic field of ≥6 kA/m to the sensor. If the magnetic field given by the magnetized target errors like frequency doubling might occur. The magnetoresistive sensor element signal is amplified, temperature compensated and forwarded to a Schmitt-trigger in the conditioning integrated circuit (Figs 4 and 5). The digital output signal levels (Fig.6) are independent of the magnetic field condition.
A (2-wire) output current enables safe transfer of the sensor signal to the detecting circuit (Fig.7).
The integrated circuit housing is separated from the sensor element housing to optimize the sensor behaviour at high temperatures.

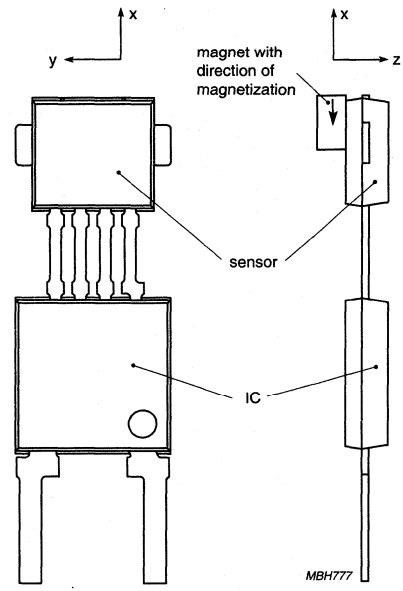

Fig.2 Component detail of the KMI15/2.

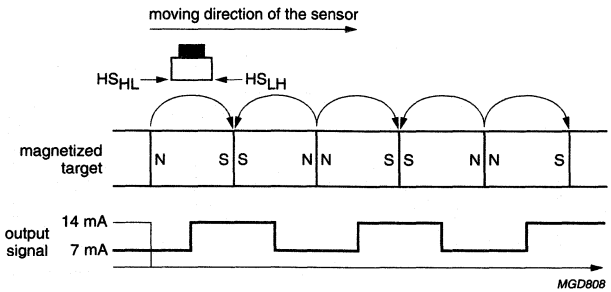

Fig.3 Functional principle of KMI15/2.

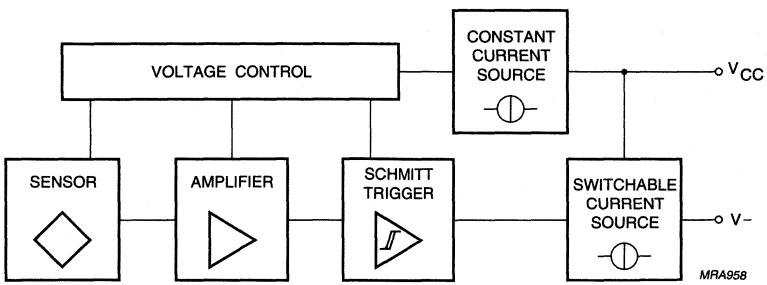

Fig.4 Block diagram.

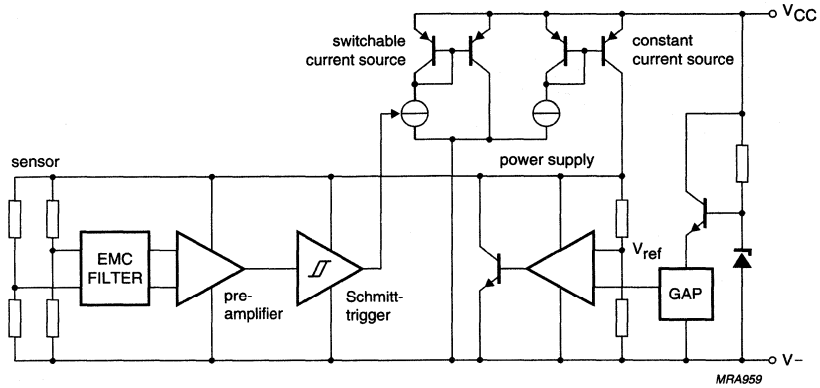

Fig.5 Simplified circuit diagram.

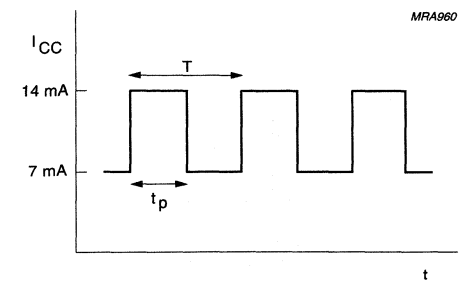

$$\delta = \frac{t_p}{T} \times 100\%$$

Fig.6 Output signal as a function of time.

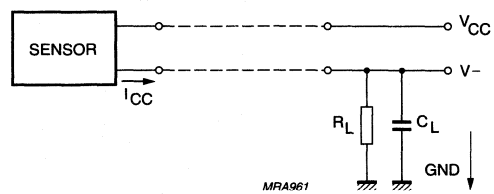

Fig.7 Test and application circuit.

PACKAGE OUTLINE

Plastic single-ended multi-chip package;
magnetized ferrite magnet (3.8 x 2 x 0.8 mm); 4 interconnections; 2 in-line leads **SOT453A**

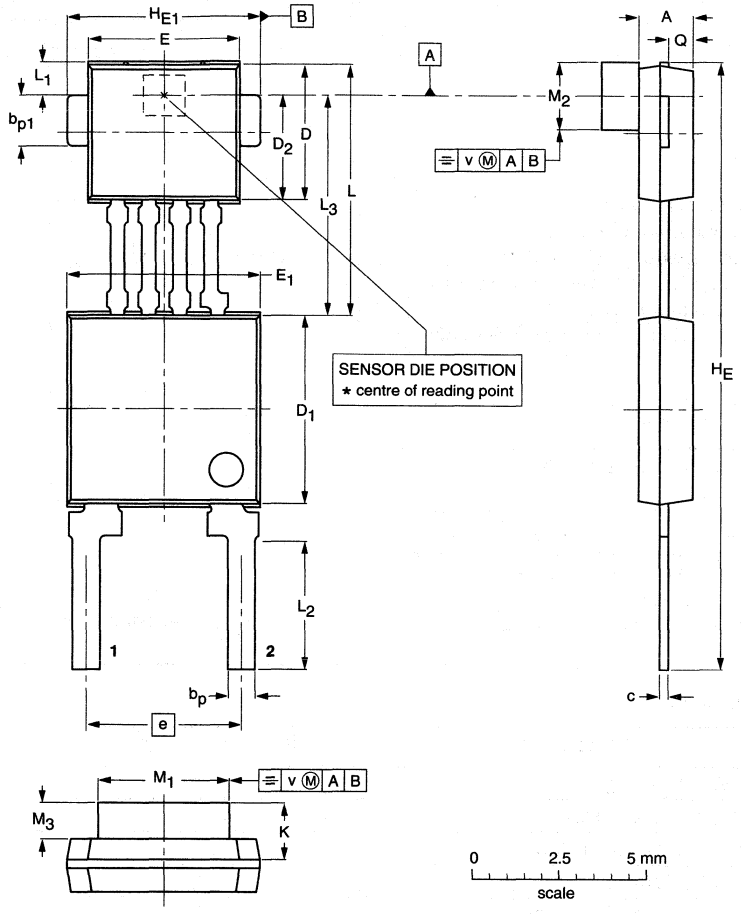

DIMENSIONS (mm are the original dimensions)

UNIT	A(1)	b_p	b_{p1}	c	D(2)	D_1(2)	D_2(2)	E(2)	E_1(2)	e	H_E	H_{E1}	K max.	L	L_1	L_2	L_3	M_1	M_2	M_3(1)	Q	v
mm	1.7 1.4	0.8 0.7	1.57 1.47	0.3 0.24	4.1 3.9	5.7 5.5	3.15 2.95	4.5 4.3	5.7 5.5	4.6 4.4	18.2 17.8	5.6 5.5	1.67	7.55 7.25	1.2 0.9	3.9 3.5	6.55 6.35	3.9 3.7	2.1 1.9	0.9 0.7	0.75 0.65	0.25

Notes

1. Glue thickness not included.
2. Plastic or metal protrusions of 0.15 mm maximum per side are not included.

OUTLINE VERSION	REFERENCES				EUROPEAN PROJECTION	ISSUE DATE
	IEC	JEDEC	EIAJ			
SOT453A						~~99-09-22~~ 00-08-31

Rotational speed sensor KMI15/4

FEATURES

- Digital current output signal
- Zero speed capability
- Wide air gap
- Wide temperature range
- Vibration insensitive
- EMC resistant.

DESCRIPTION

The KMI15/4 sensor detects rotational speed of ferrous gear wheels and reference marks(1).
The sensor consists of a magnetoresistive sensor element, a signal conditioning integrated circuit in bipolar technology and a ferrite magnet. The frequency of the digital current output signal is proportional to the rotational speed of a gear wheel.

CAUTION
Do not press two or more products together against their magnetic forces.

(1) The sensor contains a customized integrated circuit. Usage in hydraulic brake systems and in systems with active brake control is forbidden. For all other applications, higher temperature versions of up to 150 °C are available on request.

PINNING

PIN	DESCRIPTION
1	V_{CC}
2	V–

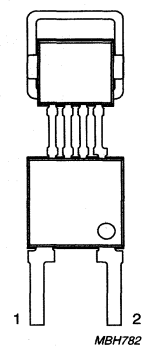

Fig.1 Simplified outline (SOT453C).

QUICK REFERENCE DATA

SYMBOL	PARAMETER	MIN.	TYP.	MAX.	UNIT
V_{CC}	DC supply voltage	–	12	–	V
T_{amb}	ambient operating temperature	–40	–	+85	°C
$I_{CC\ (low)}$	current output signal low	–	7	–	mA
$I_{CC\ (high)}$	current output signal high	–	14	–	mA
f_t	operating tooth frequency	0	–	25000	Hz
d	sensing distance	0 to 2.0	0 to 2.3	–	mm

LIMITING VALUES

In accordance with Absolute Maximum Rating System (IEC 60134).

SYMBOL	PARAMETER	CONDITIONS	MIN.	MAX.	UNIT
V_{CC}	DC supply voltage	T_{amb} = −40 to +85 °C; R_L = 115 Ω	−0.5	+16	V
T_{stg}	storage temperature		−40	+150	°C
T_{amb}	operating ambient temperature		−40	+85	°C
T_{sld}	soldering temperature	t ≤ 10 s	−	260	°C
	output short-circuit duration to GND		continuous		

CHARACTERISTICS

T_{amb} = 25 °C; V_{CC} = 12 V; d = 1.5 mm; f_t = 2 kHz; test circuit: see Fig.7; R_L = 115 Ω; sensor positioning: see Fig.15; gear wheel: module 2 mm; material 1.0715; unless otherwise specified.

SYMBOL	PARAMETER	CONDITIONS	MIN.	TYP.	MAX.	UNIT
$I_{CC\ (low)}$	current output signal low	see Figs 6 and 8	5.6	7	8.4	mA
$I_{CC\ (high)}$	current output signal high	see Figs 6 and 8	11.2	14	16.8	mA
t_r	output signal rise time	C_L = 100 pF; see Fig.9; 10 to 90% value	−	0.5	−	µs
t_f	output signal fall time	C_L = 100 pF; see Fig.9; 10 to 90% value	−	0.7	−	µs
t_d	switching delay time	between stimulation pulse (generated by a coil) and output signal	−	1	−	µs
f_t	operating tooth frequency	for both rotation directions	0	−	25000	Hz
d	sensing distance	see Fig.15 and note 1	0 to 2.0	0 to 2.3	−	mm
δ	duty cycle	see Fig.6	20	50	80	%

Note

1. High rotational speeds of wheels reduce the sensing distance due to eddy current effects (see Fig.17).

FUNCTIONAL DESCRIPTION

The KMI15/4 sensor is sensitive to the motion of ferrous gear wheels or reference marks. The functional principle is shown in Fig.3. Due to the effect of flux bending, the different directions of magnetic field lines in the magnetoresistive sensor element will cause an electrical signal. Because of the chosen sensor orientation and the direction of ferrite magnetization, the KMI15/4 is sensitive to movement in the 'y' direction in front of the sensor only (see Fig.2).

The magnetoresistive sensor element signal is amplified, temperature compensated and passed to a Schmitt-trigger in the conditioning integrated circuit (Figs 4 and 5). The digital output signal level (see Fig.6) is at a fixed level independent of the sensing distance. A (2-wire) output current enables safe sensor signal transport to the detecting circuit (see Fig.7). The integrated circuit housing is separated from the sensor element housing to optimize the sensor behaviour at high temperatures.

The strength of the magnetic field caused by the Ferroxdure 100 magnet in the different sensor directions, measured at the centre of the magnetoresistive bridge, is typically: H_x = 7 kA/m (auxiliary field) and H_z = 17 kA/m (perpendicular to the sensor surface). H_y is zero due to the trimming process.

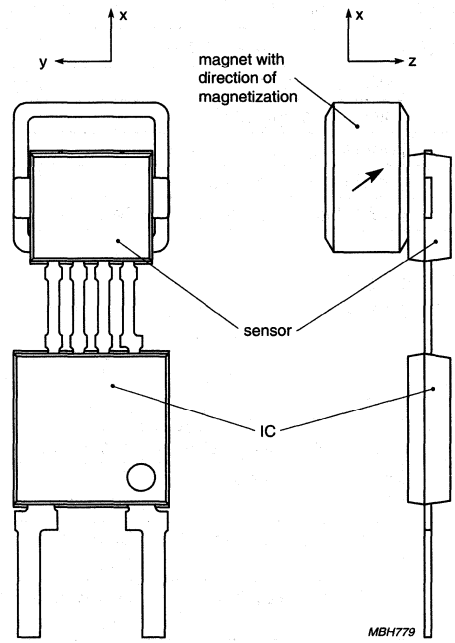

Fig.2 Component detail of the KMI15/4.

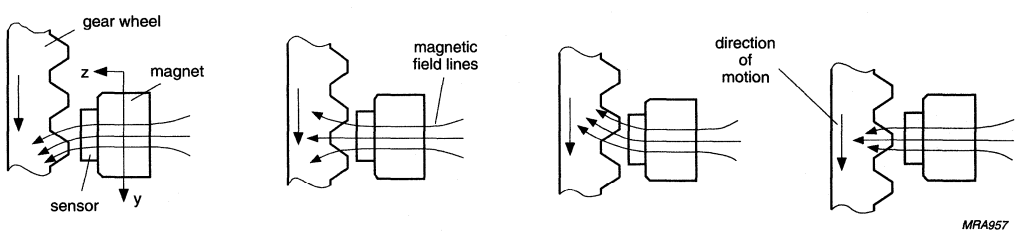

Fig.3 Functional principle.

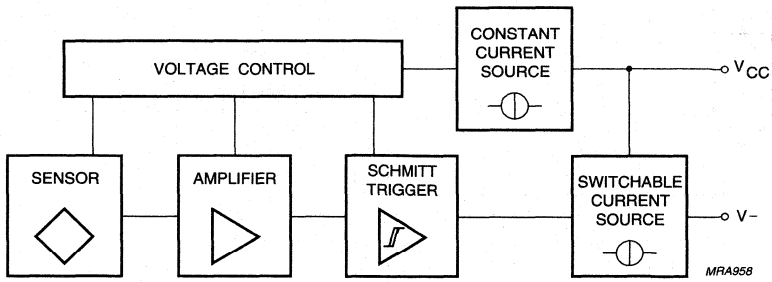

Fig.4 Block diagram.

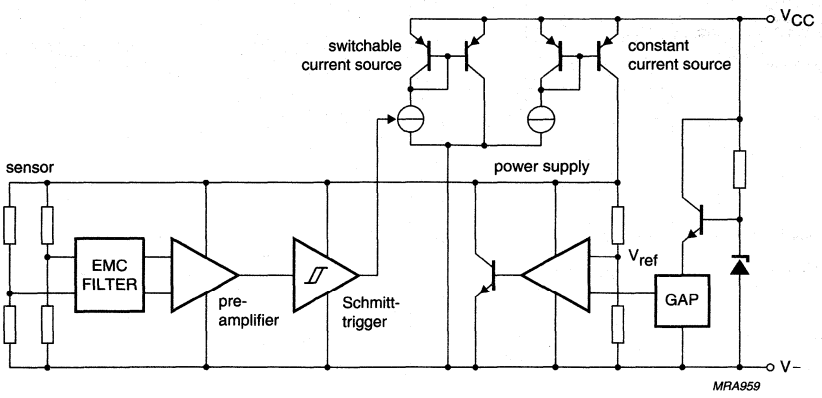

Fig.5 Simplified circuit diagram.

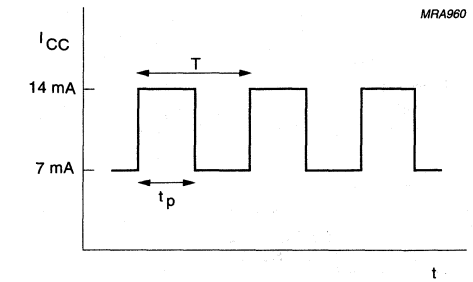

$$\delta = \frac{t_p}{T} \times 100\%$$

Fig.6 Output signal as a function of time.

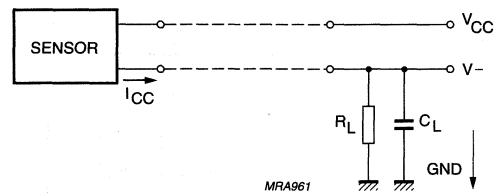

Fig.7 Test and application circuit.

APPLICATION INFORMATION

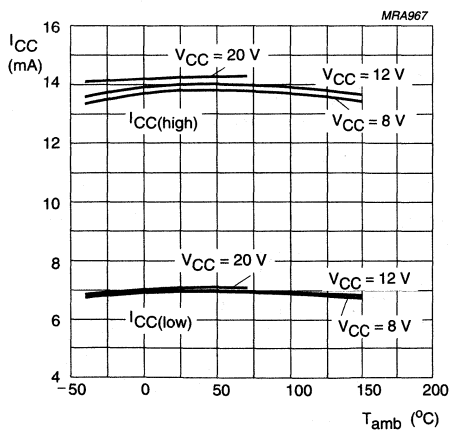

Fig.8 Output current levels as functions of ambient temperature; typical values.

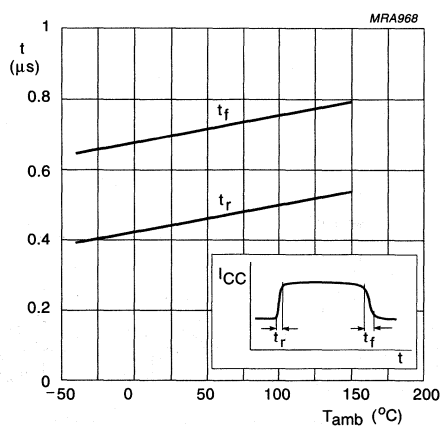

Fig.9 Output current switching times as functions of ambient temperature; typical values.

Mounting conditions

The recommended sensor position in front of a gear wheel is shown in Fig.15. Distance 'd' is measured between the sensor front and the tip of a gear wheel tooth. The KMI15/4 senses ferrous indicators like gear wheels in the ± y direction only (no rotational symmetry of the sensor); see Fig.2. The effect of incorrect mounting positions on sensing distance is shown in Figs 11, 12 and 13. The symmetrical reference axis of the sensor corresponds to the axis of the ferrite magnet.

Environmental conditions

Due to eddy current effects the sensing distance depends on the tooth frequency (see Fig.17). The influence of gear wheel module on the sensing distance is shown in Fig.16.

Gear Wheel Dimensions

SYMBOL	DESCRIPTION	UNIT
German DIN		
z	number of teeth	
d	diameter	mm
m	module m = d/z	mm
p	pitch p = π × m	mm
ASA; note1		
PD	pitch diameter (d in inch)	inch
DP	diametric pitch DP = z/PD	$inch^{-1}$
CP	circular pitch CP = π/DP	inch

Note

1. For conversion from ASA to DIN: m = 25.4 mm/DP; p = 25.4 mm × CP.

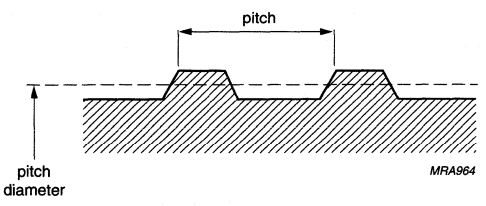

$$\text{module} = \frac{\text{pitch diameter}}{\text{number of teeth}}$$

$$\text{pitch} = \text{module} \times \pi$$

Fig.10 Gear wheel dimensions.

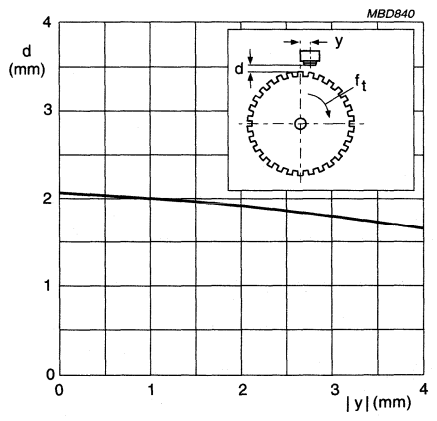

V_{CC} = 12 V; f_t = 2 kHz; module = 2 mm; pitch diameter = 100 mm.

Fig.11 Sensing distance as a function of positional tolerance in the y-axis; typical values.

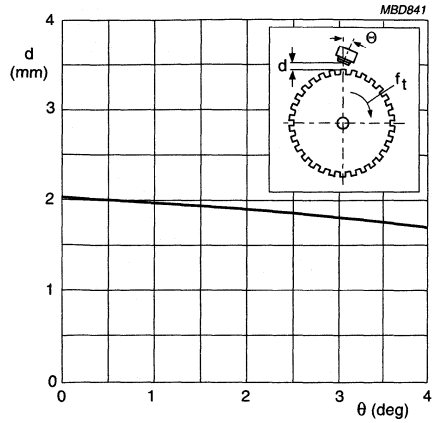

V_{CC} = 12 V; f_t = 2 kHz; module = 2 mm.

Fig.12 Sensing distance as a function of positional tolerance; typical values.

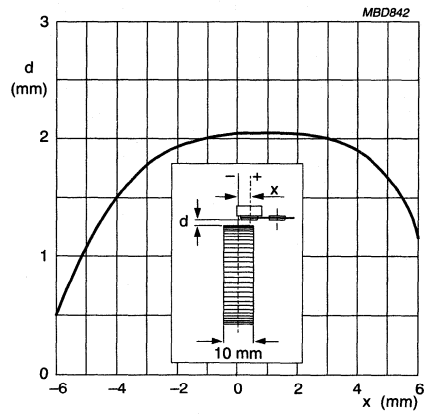

V_{CC} = 12 V; f_t = 2 kHz; module = 2 mm.

Fig.13 Sensing distance as a function of positional tolerance in the x-axis; typical values.

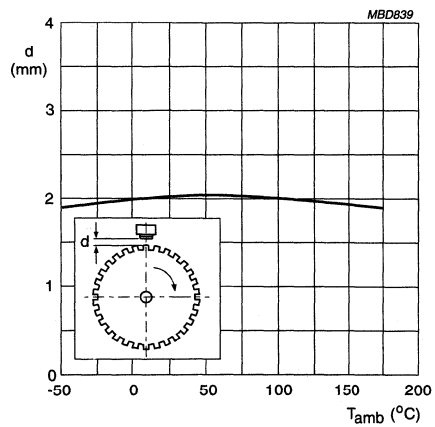

Fig.14 Typical sensing distance as a function of ambient temperature; typical values.

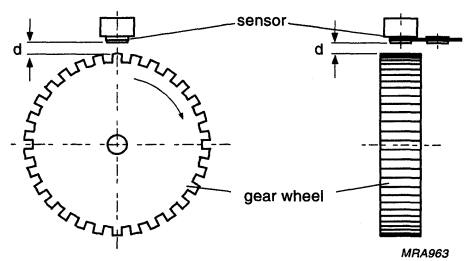

Fig.15 Sensor positioning.

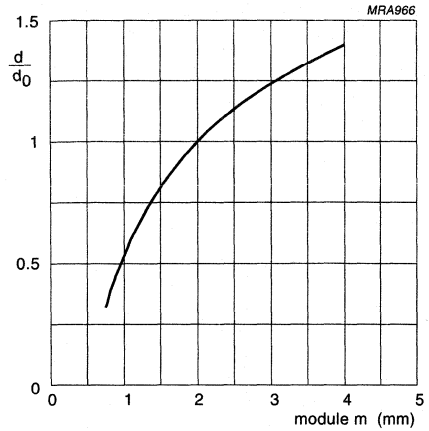

d_0 = sensing distance for gear wheel with module = 2 mm.

Fig.16 Normalized maximum sensing distance as a function of a gear wheel module; typical values.

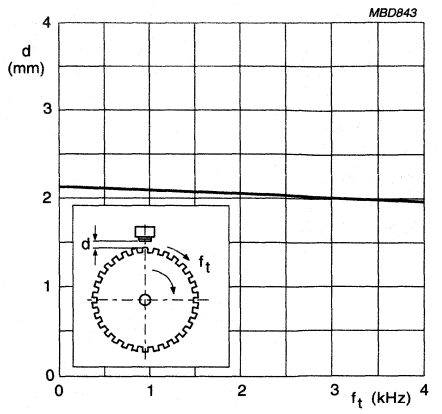

V_{CC} = 12 V; module = 2 mm.

Fig.17 Sensing distance as a function of tooth frequency; typical values.

EMC

Figure 18 shows a recommended application circuit for automotive applications (wheel sensing f_t < 5 kHz).
It provides a protection interface to meet Electromagnetic Compatibility (EMC) standards and safeguard against voltage spikes Table 1 lists the tests which are applicable to this circuit and the achieved class of functional status. Protection against 'load dump' (test pulse 5 according to *"DIN 40839"*) means a very high demand on the protection circuit and requires a suitable suppressor diode with sufficient energy absorption capability.

The board net often contains a central load dump protection that makes such a device in the protection circuit of the sensor module unnecessary.

Tests for electrostatic discharge (ESD) were conducted in line with *"IEC 801-2"* to demonstrate the KMI15/4's handling capabilities. The *"IEC 801-2"* test conditions were: C = 150 pF, R = 150 Ω, V = 2 kV.

Electromagnetic disturbances with fields up to 150 V/m and f = 1 GHz (ref. *"DIN 40839"*) have no influence on performance.

Table 1 EMC test results

EMC REF. DIN 40839	SYMBOL	MIN. (V)	MAX. (V)	REMARKS	CLASS
Test pulse 1	V_{LD}	−100	–	t_d = 2 ms	C
Test pulse 2	V_{LD}	–	100	t_d = 0.2 ms	A
Test pulse 3a	V_{LD}	−150	–	t_d = 0.1 µs	A
Test pulse 3b	V_{LD}	–	100	t_d = 0.1 µs	A
Test pulse 4	V_{LD}	−7	–	t_d = 130 ms	B
Test pulse 5	V_{LD}	–	120	t_d = 400 ms	B

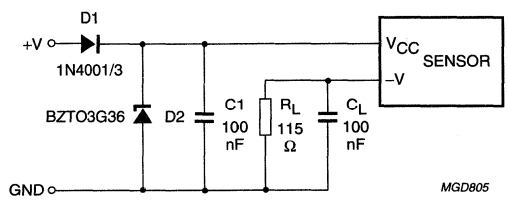

Fig.18 Test/application circuit for the KMI15/4.

PACKAGE OUTLINE

Plastic single-ended multi-chip package;
magnetized ferrite magnet (5.5 x 5.5 x 3 mm); 4 interconnections; 2 in-line leads **SOT453C**

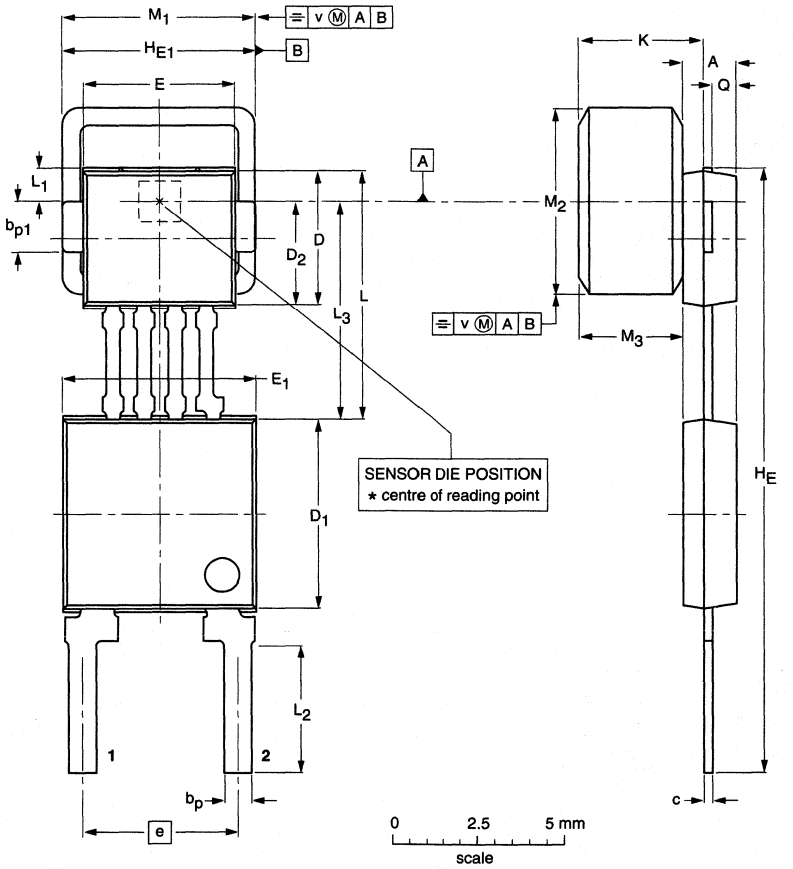

DIMENSIONS (mm are the original dimensions)

UNIT	A(1)	b_p	b_{p1}	c	D(2)	D_1(2)	D_2(2)	E(2)	E_1(2)	e	H_E	H_{E1}	K max.	L	L_1	L_2	L_3	M_1	M_2	M_3(1)	Q	v
mm	1.7 1.4	0.8 0.7	1.57 1.47	0.3 0.24	4.1 3.9	5.7 5.5	3.15 2.95	4.5 4.3	5.7 5.5	4.6 4.4	18.2 17.8	5.6 5.5	3.87	7.55 7.25	1.2 0.9	3.9 3.5	6.55 6.35	5.65 5.35	5.65 5.35	3.15 2.85	0.75 0.65	0.25

Notes

1. Glue thickness not included.
2. Plastic or metal protrusions of 0.15 mm maximum per side are not included.

OUTLINE VERSION	REFERENCES				EUROPEAN PROJECTION	ISSUE DATE
	IEC	JEDEC	EIAJ			
SOT453C						~~99-09-23~~ 00-08-31

Integrated rotational speed sensor KMI16/1

DESCRIPTION

The KMI16/1 sensor detects rotational speed of ferrous gear wheels and reference marks.

The sensor consists of a magnetoresistive sensor element, a signal conditioning integrated circuit in bipolar technology and a ferrite magnet.

The frequency of the digital current output signal is proportional to the rotational speed of the target wheel.

The open collector (OC) output allows for a high degree of flexibility in the design of subsequent conditioning electronics.

CAUTION
Do not press two or more products together against their magnetic forces. Do not expose products to strong magnetic fields of more than 30 kA/m.

PINNING

PIN	SYMBOL	DESCRIPTION
1	V_{CC}	DC supply voltage
2	V_{out}	open collector output
3	GND	ground

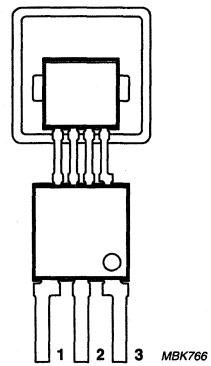

Fig.1 Simplified outline (SOT477B).

QUICK REFERENCE DATA

SYMBOL	PARAMETER	MIN.	TYP.	MAX.	UNIT
V_{CC}	DC supply voltage	4.5	5	16	V
I_{CC}	DC supply current (pin 1)	4	10	14	mA
V_{CEsat}	OC saturation voltage	–	–	1	V
d_{max}	maximum sensing distance	2.4	2.9	–	mm
f_t	operating tooth frequency	0	–	25000	Hz
T_{amb}	ambient operating temperature	–40	–	+150	°C

LIMITING VALUES

In accordance with the Absolute Maximum Rating System (IEC 60134)

SYMBOL	PARAMETER	CONDITIONS	MIN.	MAX.	UNIT
V_{CC}	DC operating supply voltage	T_{amb} = −40 to +150 °C	4.5	16	V
	voltage pin 1	T_{amb} = −40 to +150 °C; no wrong polarity protection	−0.5	+16	V
V_{out}	OC output voltage	T_{amb} = −40 to +150 °C; no wrong polarity protection; see Fig.5	−0.5	+16	V
$V_{out(max)}$	peak OC output voltage	T_{amb} = −40 to +40 °C; no wrong polarity protection; see Fig.5	−0.5	+26.5	V
$I_{out(max)}$	OC output current	T_{amb} = −40 to +150 °C	–	20	mA
$I_{out(off)}$	OC output leakage current	T_{amb} = −40 to +150 °C	–	100	µA
P_{tot}	total power dissipation	T_{amb} = −40 to +150 °C	–	200	mW
T_{sld}	soldering temperature	t ≤ 10 s	–	260	°C
T_{stg}	storage temperature		−65	+150	°C
T_{amb}	ambient operating temperature		−40	+150	°C

CHARACTERISTICS

T_{amb} = 25 °C; V_{CC} = 5 V; d = 1.9 mm; f_t = 2 kHz; test circuit see Fig.5; gear wheel: module 2.08 mm; material 9SMnPb28k; see Fig.6; centred sensor position; see notes 1, 2 and 3; unless otherwise specified.

SYMBOL	PARAMETER	CONDITIONS	MIN.	TYP.	MAX.	UNIT
I_{CC}	supply current (pin 1)	T_{amb} = −40 to +150 °C	4	10	14	mA
$V_{out\ (high)}$	OC output voltage high	OC = off state; T_{amb} = −40 to +150 °C	4.7	4.9	–	V
$V_{CE\ sat}$	OC saturation voltage	OC = on state; I_{out} = 20 mA	–	0.4	1	V
t_r	output signal rise time	10% to 90%	5	12	20	µs
t_f	output signal fall time	10% to 90%	0.1	0.4	10	µs
δ	duty cycle	T_{amb} = −40 to +150 °C	30	50	70	%
d_{min}	minimum sensing distance	T_{amb} = −40 to +150 °C	–	0.3	0.5	mm
d_{max}	maximum sensing distance	T_{amb} = −40 to +150 °C	2.4	2.9	–	mm

Notes

1. High rotational wheel speeds reduce the maximum sensing distance because of eddy currents, depending on target wheel dimensions and materials used.
2. Output pins are designed for electrostatic sensitivity for more than 2000 V according to Human Body Model (HBM); MIL-STD-883; method 3015.
3. EMC behaviour depends greatly on design of application circuit.

FUNCTIONAL DESCRIPTION

The KMI16/1 sensor is sensitive to the motion of ferrous gear wheels or reference marks. The functional principle is shown in Fig.3. Due to the effect of flux bending, the different directions of magnetic field lines in the magnetoresistive sensor element will cause an electrical signal. Because of the chosen sensor orientation and the direction of ferrite magnetization, the KMI16/1 is sensitive to movement in the 'y' direction in front of the sensor only (see Fig.2).

The magnetoresistive sensor element signal is amplified, temperature compensated and passed to a Schmitt trigger in the conditioning integrated circuit (see Fig.4). The digital output signal level is independent of the sensing distance within the measuring range (see Fig.10). A (3-wire) output current enables safe transfer of the sensor signal to the detecting circuit (see Fig.5). The integrated circuit housing is separated from the sensor element housing to optimize the sensor behaviour at high temperatures.

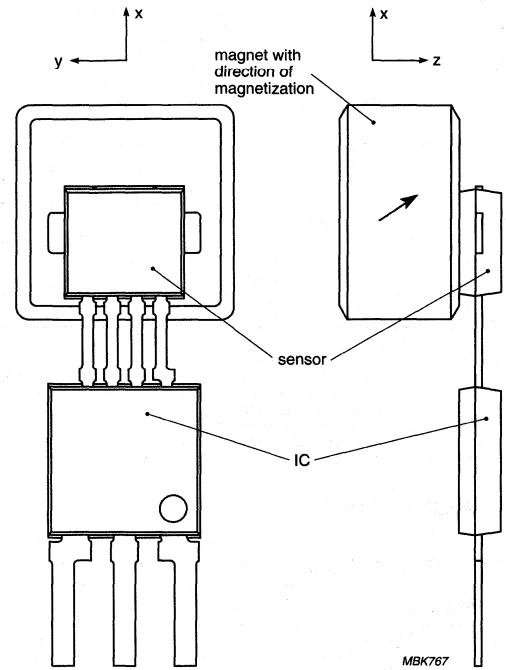

Fig.2 Component detail of the KMI16/1.

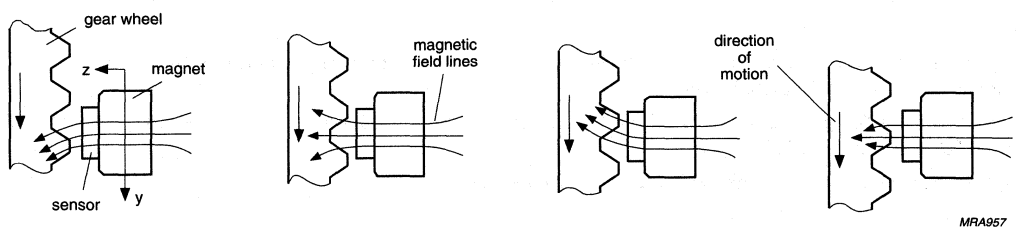

Fig.3 Functional principle.

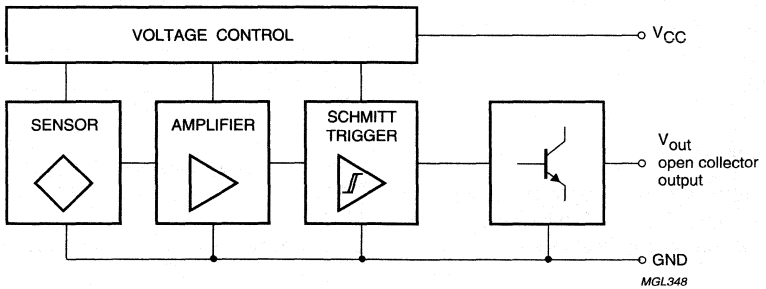

Fig.4 Block diagram.

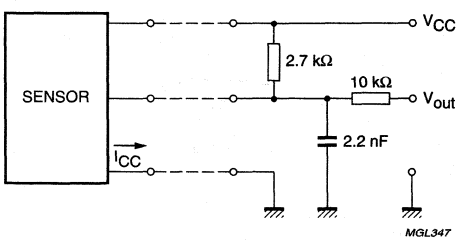

Fig.5 Test and application circuit.

APPLICATION INFORMATION

Mounting conditions

The recommended sensor position in front of a gear wheel is shown in Fig.11. The distance 'd' is measured between the sensor front and the tip of a gear wheel tooth. The KMI16/1 senses ferrous indicators like gear wheels in the 'y' direction only (no rotational symmetry of the sensor); see Fig.2. The effect of incorrect mounting positions on sensing distance is shown in Figs 7, 8 and 9. The symmetrical reference axis of the sensor corresponds to the axis of the ferrite magnet.

Environmental conditions

Due to eddy current effects the sensing distance depends on the tooth frequency (see Fig.13). The influence of the gear wheel module on the sensing distance is shown in Fig.12.

Gear Wheel Dimensions

SYMBOL	DESCRIPTION	UNIT
German DIN		
z	number of teeth	–
d	diameter	mm
m	module m = d/z	mm
p	pitch p = π × m	mm
ASA; note 1		
PD	pitch diameter (d in inch)	inch
DP	diametric pitch DP = z/PD	$inch^{-1}$
CP	circular pitch CP = π/DP	inch

Note

1. For conversion from ASA to DIN: m = 25.4 mm/DP; p = 25.4 mm × CP.

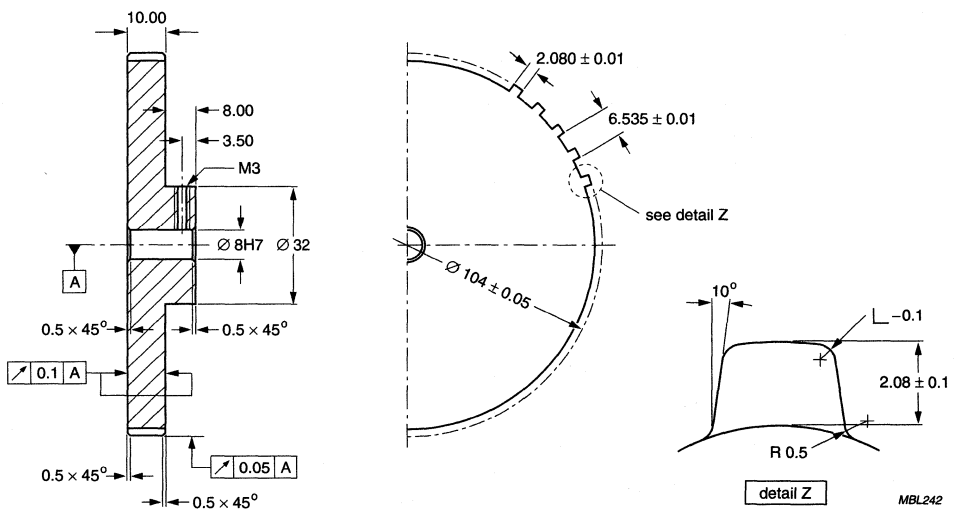

Fig.6 Gear wheel dimensions.

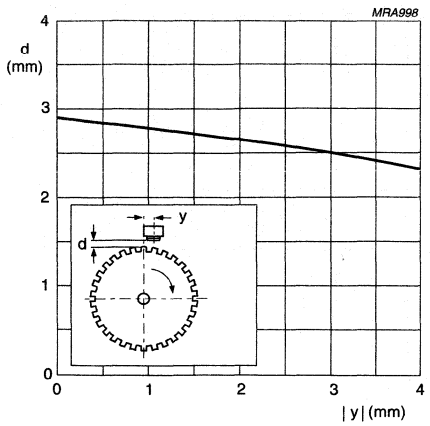

V_{CC} = 12 V; f_t = 2 kHz; module = 2 mm; pitch diameter = 100 mm.

Fig.7 Sensing distance as a function of positional tolerance in the y-axis; typical values.

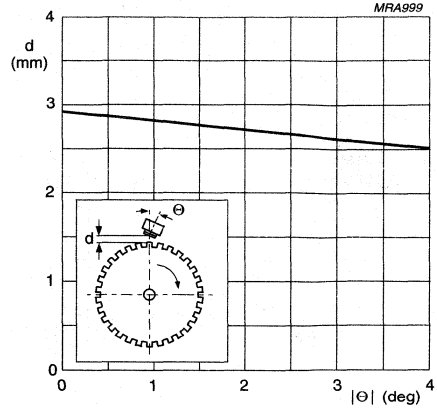

V_{CC} = 12 V; f_t = 2 kHz; module = 2 mm.

Fig.8 Sensing distance as a function of positional tolerance; typical values.

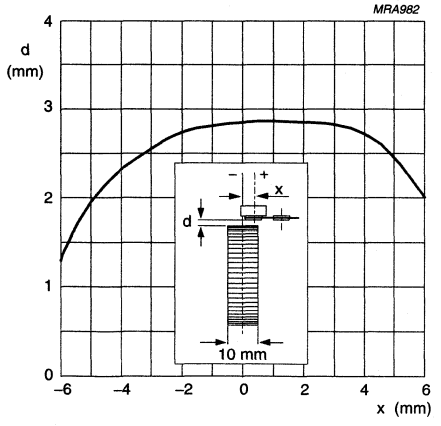

V_{CC} = 12 V; f_t = 2 kHz; module = 2 mm.

Fig.9 Sensing distance as a function of positional tolerance in the x-axis; typical values.

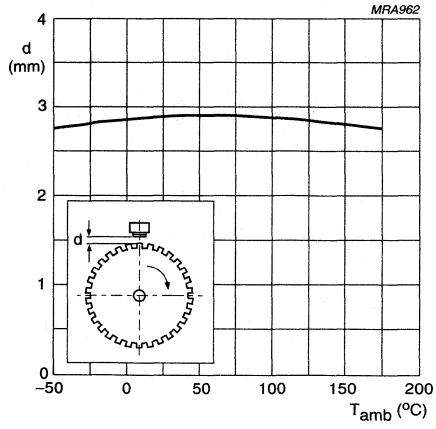

V_{CC} = 12 V; f_t = 2 kHz; module = 2 mm.

Fig.10 Sensing distance as a function of ambient temperature; typical values.

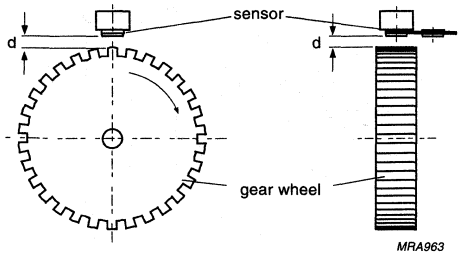

Fig.11 Sensor positioning.

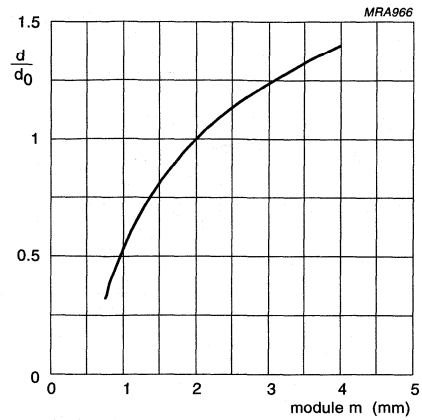

d_o = measuring distance for a gear wheel with module m = 2 mm.

Fig.12 Normalized maximum sensing distance as a function of gear wheel module; typical values.

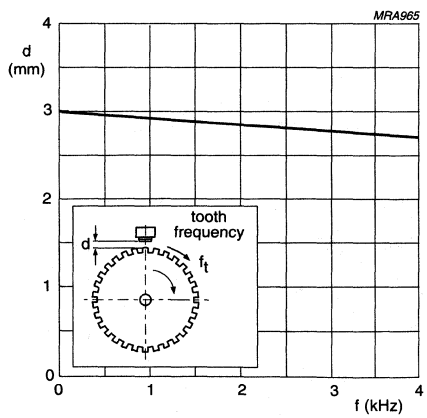

V_{CC} = 12 V; module = 2 mm.

Fig.13 Sensing distance as a function of tooth frequency; typical values.

PACKAGE OUTLINE

Plastic single-ended multi-chip package;
magnetized ferrite magnet (8 x 8 x 4.5 mm); 4 interconnections; 3 in-line leads **SOT477B**

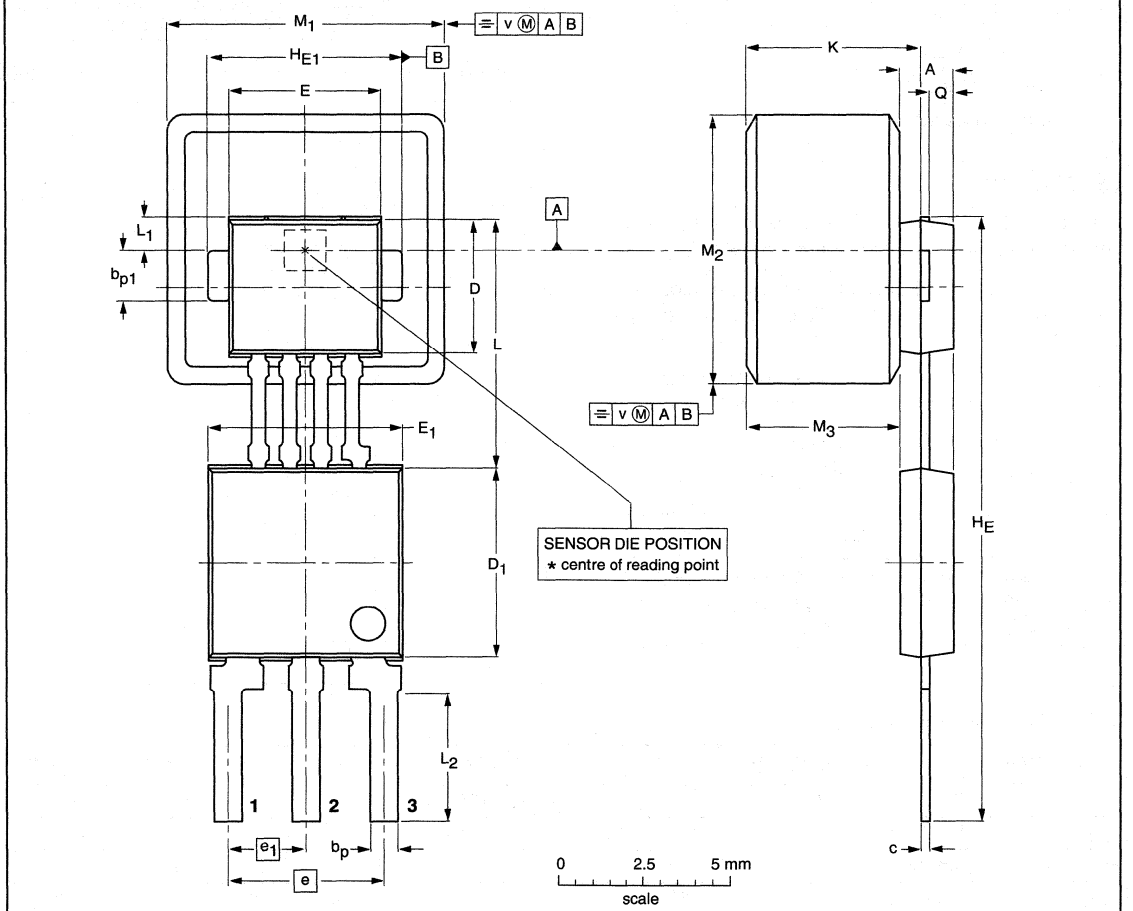

DIMENSIONS (mm are the original dimensions)

UNIT	A(1)	b_p	b_{p1}	c	D(2)	D_1(2)	E(2)	E_1(2)	e	e_1	H_E	H_{E1}	K max.	L	L_1	L_2	M_1	M_2	M_3(1)	Q	v
mm	1.7 1.4	0.8 0.7	1.57 1.47	0.3 0.24	4.1 3.9	5.7 5.5	4.5 4.3	5.7 5.5	4.6 4.4	2.35 2.15	18.2 17.8	5.6 5.5	5.37	7.55 7.25	1.2 0.9	3.9 3.5	8.15 7.85	8.15 7.85	4.7 4.3	0.75 0.65	0.25

Notes

1. Glue thickness not included.
2. Plastic or metal protrusions of 0.15 mm maximum per side are not included.

OUTLINE VERSION	REFERENCES				EUROPEAN PROJECTION	ISSUE DATE
	IEC	JEDEC	EIAJ			
SOT477B						~~99-09-23~~ 00-08-31

Integrated rotational speed sensor KMI18/2

FEATURES

- Open collector output
- For active target wheel application
- Wide air gap
- Zero speed capability
- Wide temperature range
- Insensitive to vibration.

DESCRIPTION

The KMI18/2 sensor detects rotational speed of active target wheels with magnetic reference marks.

It consists of a magnetoresistive sensor element, an integrated circuit for signal conditioning and a ferrite magnet.

The frequency of the digital voltage output signal is proportional to the rotational speed of the target wheel.

An open collector output gives high flexibility in the design of the subsequent signal conditioning electronics.

CAUTION
Do not press two or more products together against their magnetic forces. Do not expose products to strong magnetic fields of more than 30 kA/m.

PINNING

PIN	SYMBOL	DESCRIPTION
1	V_{CC}	DC supply voltage
2	OUT	open collector output
3	GND	ground

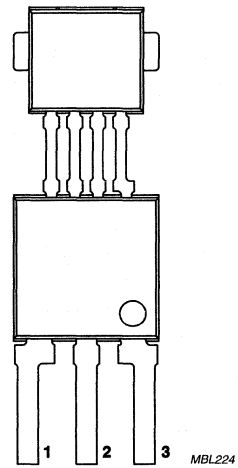

Fig.1 Simplified outline (SOT477A).

QUICK REFERENCE DATA

SYMBOL	PARAMETER	CONDITIONS	MIN.	TYP.	MAX.	UNIT
V_{CC}	DC supply voltage	T_{amb} = −40 to +150 °C	4.5	5	16.5	V
I_{CC}	DC supply current	V_{CC} = 5 V	6	7	10	mA
H_{yLH}	magnetic threshold for LH edge		100	250	400	A/m
H_{yHL}	magnetic threshold for HL edge		−400	−250	−100	A/m
T_{amb}	ambient operating temperature	V_{CC} = 5 V; note 1	−40	–	+150	°C

Note

1. Maximum power consumption according to power derating curve, see Fig.3.

LIMITING VALUES

In accordance with Absolute Maximum Rating System (IEC 60134); T_{amb} = –40 to +150 °C; see Fig.4.

SYMBOL	PARAMETER	CONDITIONS	MIN.	MAX.	UNIT
V_{CC}	DC supply voltage	not protected against incorrect polarity	–0.5	+16.5	V
V_{OUT}	output voltage	not protected against incorrect polarity	–0.5	+24	V
$I_{OUT(max)}$	maximum output current	low state; note 1	–	20	mA
$I_{OUT(high)}$	output leakage current	high state; note 2; see Fig.5	–	100	µA
		high state; note 2; see Fig.6	–	100	µA
P_{tot}	total power dissipation	V_{CC} = 16.5 V; I_{OUT} = 20 mA	–	300	mW
T_{amb}	ambient operating temperature	V_{CC} = 5 V	–40	+150	°C
T_{stg}	storage temperature		–40	+150	°C
T_{sld}	soldering temperature	t ≤ 10 s	–	260	°C

Notes

1. Low: transistor open (V_{CE} < 1 V).
2. High: transistor closed (V_{CE} > 4 V).

CHARACTERISTICS

T_{amb} = 26 ± 10 °C; V_{CC} = 5 V; f_{rm} = 0 to 25000 Hz; magnetic reading point according to 'Package outline'; unless otherwise specified.

SYMBOL	PARAMETER	CONDITIONS	MIN.	TYP.	MAX.	UNIT
Sensor characteristics						
H_{yLH}	magnetic trigger field strength (threshold) for LH-output edge	T_{amb} = 25 °C	100	250	400	A/m
		T_{amb} = –40 to +150 °C	–200	+250	+600	A/m
H_{yHL}	magnetic trigger field strength (threshold) for HL-output edge	T_{amb} = 25 °C	–400	–250	–100	A/m
		T_{amb} = –40 to +150 °C	–600	–250	+200	A/m
H_{y0}	magnetic offset		–150	–	+150	A/m
H_{yh}	magnetic trigger hysteresis		100	500	700	A/m
H_x	auxiliary magnetic field strength		5	8	10	kA/m
f_{rm}	frequency of magnetic reference marks		0	–	25000	Hz
Supply conditions						
I_{CC}	DC supply current	T_{amb} = 26 ± 10 °C; V_{CC} = 5 V	6.5	7.5	8.5	mA
		T_{amb} = –40 to +150 °C; V_{CC} = 5 V	6	7	10	mA
V_{CC}	DC supply voltage	T_{amb} = –40 to +150 °C	4.5	5	16.5	V
Signal output characteristics						
	transfer behaviour	change of magnetic reference field H_y	NS → HL SN → LH			
	power-on state		undefined			
I_{OUT}	output current	low state; note 1	0.1	–	20	mA

SYMBOL	PARAMETER	CONDITIONS	MIN.	TYP.	MAX.	UNIT
$I_{OUT(high)}$	output leakage current	high state; note 2; see Fig.6	–	–	100	µA
V_{OUT}	output saturation voltage	T_{amb} = –40 to +150 °C; low state; note 1				
		I_{OUT} = 1 mA	0.01	0.03	0.1	V
		I_{OUT} = 10 mA	0.1	0.2	0.5	V
		I_{OUT} = 20 mA	0.3	0.5	1	V
$t_{r(OUT)}$	output signal rise time	low 10% to high 90%; see Fig.7	5	12	20	µs
$t_{f(OUT)}$	output signal fall time	high 90% to low 10%; see Fig.7	0.05	0.5	1	µs
$t_{df(OUT)}$	output signal delay time of HL-edge		1.5	2.5	3.5	µs
$d_{tdf(OUT)}$	jitter	measured in harmonic magnetic field in y with $H_{y(max)}$ = 1 kA/m; normalized to cycle of one reference mark	0	–	0.15	%
Environmental conditions						
	external magnetic influence	note 3	–	–	30	kA/m
	ESD protection of sensor pins V_{CC}, OUT and GND	compliance to IEC 0801-2 (IV); note 4	2	–	–	kV
	ESD protection of internal pins B1, B2, B3 and B4	compliance to IEC 0801-2 (IV); note 5	0.3	–	–	kV
	EMC: compliance to ISO 11452-5	A; stripline; 300 V/m; 10 kHz to 400 MHz; 1500 mm				
	interference for pulse: ISO 7637; pulse 4	T = 25 °C; harmonic magnetic field in y with $H_{y(max)}$ = 1 kA/m and f_m = 50 Hz	function A			
Capacity of sensor shield						
C_S	shield capacity	B1 vs. B2 of MR bridge; f = 1 MHz; U_{osc} = 200 mV	37	43	48	pF

Notes

1. Low: transistor open (VCE < 1 V).
2. High: transistor closed (VCE > 4 V).
3. Higher magnetic fields could cause irreversible shifts of parameters.
4. Output pins are designed for electrostatic sensitivity with field strengths up to 2 kV according to Human Body Model (HBM), MIL-STD-883, Method 3015.
5. MR pins are designed for electrostatic sensitivity with field strengths up to 0.3 V according to Human Body Model (HBM), MIL-STD-883, Method 3015.

FUNCTIONAL DESCRIPTION

The KMI18/2 is sensitive to the rotation of an active target wheel with magnetic reference marks. The functional principle is shown in Fig.8. Because of the sensor layout and setup of the measuring system, only movements of reference marks in the y-direction will be sensed (coordinate system see Fig.2).

The electrical output signal of the sensor is amplified, temperature compensated and applied to a Schmitt trigger in the signal conditioning circuit (see Fig.9). An additional housing separates the conditioning circuitry from the magnetorestive sensor element, thereby ensuring optimal sensor performance at high temperatures.

The signal level of the digital output is independent from the sensing distance within the measuring range. Its frequency equals that of the reference marks on the target wheels(1).

An open collector voltage interface ensures accurate transmission (three wires) of the digital sensor signal to the subsequent signal conditioning electronics.

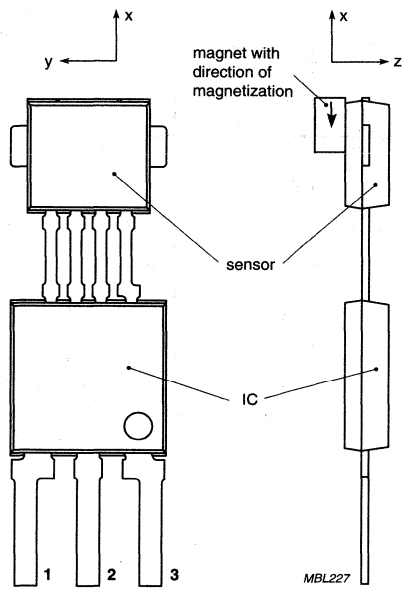

Fig.2 Component detail and coordinate system.

(1) See relevant application notes for specific target wheel data.

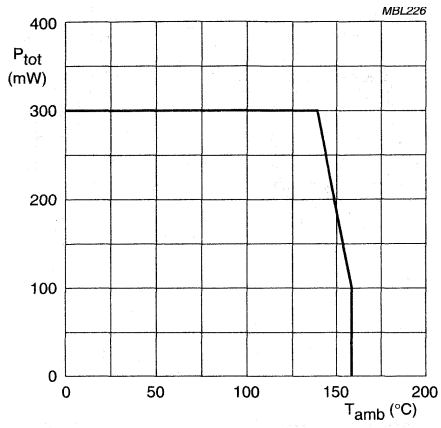

Fig.3 Power derating curve.

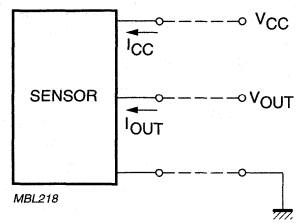

Fig.4 Supply and output.

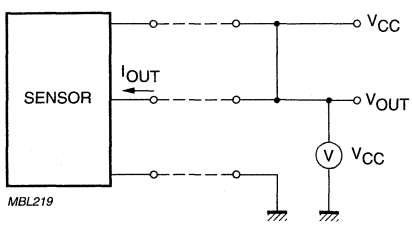

Fig.5 Leakage current test circuit: V_{CC} to OUT.

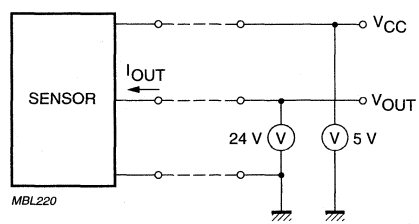

Fig.6 Leakage current test circuit: OUT to GND.

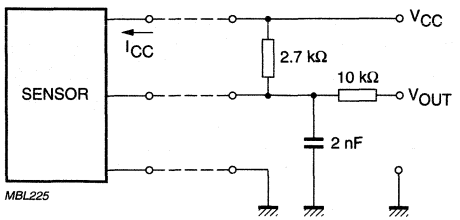

Fig.7 Test and application circuit with additional ceramic capacitor.

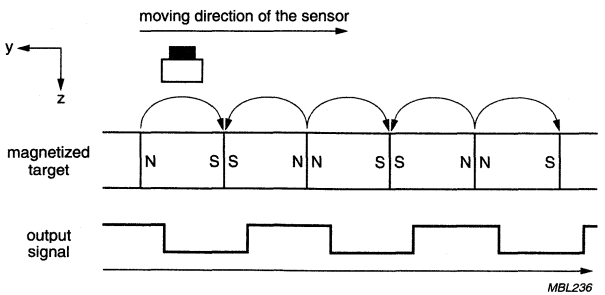

Fig.8 Functional principle.

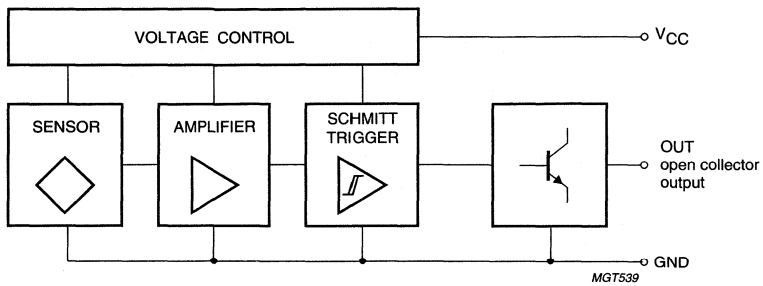

Fig.9 Block diagram.

PACKAGE OUTLINE

Plastic single-ended multi-chip package;
magnetized ferrite magnet (3.8 x 2 x 0.8 mm); 4 interconnections; 3 in-line leads **SOT477A**

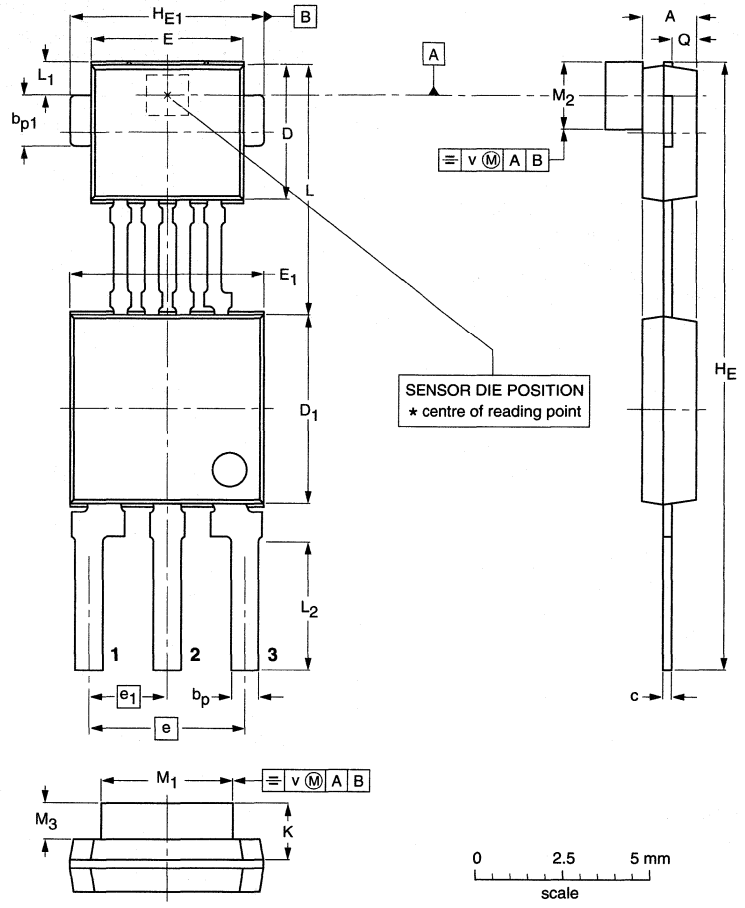

DIMENSIONS (mm are the original dimensions)

UNIT	A(1)	b_p	b_{p1}	c	D(2)	D_1(2)	E(2)	E_1(2)	e	e_1	H_E	H_{E1}	K max.	L	L_1	L_2	M_1	M_2	M_3(1)	Q	v
mm	1.7 1.4	0.8 0.7	1.57 1.47	0.3 0.24	4.1 3.9	5.7 5.5	4.5 4.3	5.7 5.5	4.6 4.4	2.35 2.15	18.2 17.8	5.6 5.5	1.67	7.55 7.25	1.2 0.9	3.9 3.5	3.9 3.7	2.1 1.9	0.9 0.75	0.75 0.65	0.25

Notes

1. Glue thickness not included.
2. Plastic or metal protrusions of 0.15 mm maximum per side are not included.

OUTLINE VERSION	REFERENCES				EUROPEAN PROJECTION	ISSUE DATE
	IEC	JEDEC	EIAJ			
SOT477A						00-08-31

Integrated rotational speed sensor KMI18/4

FEATURES

- Open collector output
- For active target wheel application
- Wide air gap
- Zero speed capability
- Wide temperature range
- Insensitive to vibration.

DESCRIPTION

The KMI18/4 sensor detects rotational speed of passive targets wheels with ferrous reference marks.

It consists of a magnetoresistive sensor element, an integrated circuit for signal conditioning and a ferrite magnet.

The frequency of the digital voltage output signal is proportional to the rotational speed of the target wheel (see Fig.3).

An open collector output gives high flexibility in the design of the subsequent signal conditioning.

CAUTION
Do not press two or more products together against their magnetic forces. Do not expose products to strong magnetic fields of more than 30 kA/m.

PINNING

PIN	SYMBOL	DESCRIPTION
1	V_{CC}	DC supply
2	OUT	open collector output
3	GND	ground

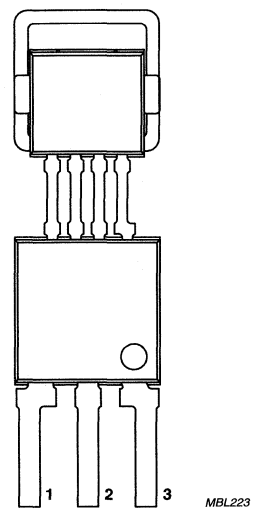

Fig.1 Simplified outline (SOT477C).

QUICK REFERENCE DATA

SYMBOL	PARAMETER	CONDITIONS	MIN.	TYP.	MAX.	UNIT
V_{CC}	DC supply voltage	T_{amb} = −40 to +150 °C	4.5	5	16.5	V
I_{CC}	DC supply current	V_{CC} = 5 V	6	7	10	mA
d_{max}	maximum sensing distance	gear wheel; see Fig.4	2.2	2.7	–	mm
d_{min}	minimum sensing distance	gear wheel; see Fig.4	–	–	0.3	mm
T_{amb}	ambient operating temperature	V_{CC} = 5 V; note 1	−40	–	+150	°C

Note

1. Maximum power consumption according to power derating curve, see Fig.5.

LIMITING VALUES

Limiting values in accordance with the Absolute Maximum Rating System (IEC 60134) for T_{amb} = −40 to +150 °C; see Fig.6.

SYMBOL	PARAMETER	CONDITIONS	MIN.	MAX.	UNIT
V_{CC}	DC supply voltage	not protected against incorrect polarity	−0.5	+16.5	V
V_{OUT}	output voltage	not protected against incorrect polarity	−0.5	+24	V
$I_{OUT(max)}$	maximum output current	low state; note 1	–	20	mA
$I_{OUT(high)}$	output leakage current	high state; note 2; see Fig.7	–	100	µA
		high state; note 2; see Fig.8	–	100	µA
P_{tot}	total power dissipation	V_{CC} = 16.5 V; I_{OUT} = 20 mA	–	300	mW
T_{amb}	ambient operating temperature	V_{CC} = 5 V	−40	+150	°C
T_{stg}	storage temperature		−40	+150	°C
T_{sld}	soldering temperature	t ≤ 10 s	–	260	°C

Notes

1. LOW: open collector output transistor open (V_{OUT} < 1 V).
2. HIGH: open collector output transistor closed (V_{OUT} > 4 V).

CHARACTERISTICS

T_{amb} = 26 ± 10 °C; V_{CC} = 5 V; f_{rm} = 0 to 25000 Hz; gear wheel according to Fig.4; magnetic reading point Fig.10 unless otherwise specified.

SYMBOL	PARAMETER	CONDITIONS	MIN.	TYP.	MAX.	UNIT
Sensor characteristics						
d_{max}	maximum sensing distance	T_{amb} = –40 to +150 °C	2.2	2.7	–	mm
d_{min}	minimum sensing distance	T_{amb} = –40 to +150 °C	–	–	0.3	mm
$\Delta\varphi$	repeatability of rotational angle	T_{amb}; f_{rm}; d; = constant	–	0.01	0.02	deg
H_{yLH}	magnetic trigger field strength (threshold) for LH-output edge	T_{amb} = –40 to +150 °C	–200	+300	+600	A/m
H_{yHL}	magnetic trigger field strength (threshold) for HL-output edge	T_{amb} = –40 to +150 °C	–600	–300	+200	A/m
H_{y0}	magnetic offset		–200	–	+200	A/m
H_{yh}	magnetic trigger hysteresis		100	500	700	A/m
H_x	auxiliary magnetic field strength		–11	–5.8	–3	kA/m
f_{rm}	frequency of magnetic reference marks		0	–	25000	Hz
Supply conditions						
I_{CC}	DC supply current	T_{amb} = 26 ± 10 °C; V_{CC} = 5 V	6.5	7.5	8.5	mA
		T_{amb} = –40 to +150 °C; V_{CC} = 5 V	6	7	10	mA
V_{CC}	DC supply voltage	T_{amb} = –40 to +150 °C;	4.5	5	16.5	V
Signal output characteristics						
	transfer behaviour	change of position of reference mark	see Fig.3			
	power-on state		undefined			
I_{OUT}	output current	low state; note 1	0.1	–	20	mA
$I_{OUT(high)}$	output leakage current	high state; note 2; see Fig.7	–	–	100	µA
V_{OUT}	output saturation voltage	T_{amb} = –40 to 150 °C; low state; note 1				
		I_{OUT} = 1 mA	0.01	0.03	0.1	V
		I_{OUT} = 10 mA	0.1	0.2	0.5	V
		I_{OUT} = 20 mA	0.3	0.5	1	V
t_{rOUT}	output signal rise time	low 10% to high 90%; see Fig.9	5	12	20	µs
t_{fOUT}	output signal fall time	high 90% to low 10%; see Fig.9	0.05	0.5	1	µs

SYMBOL	PARAMETER	CONDITIONS	MIN.	TYP.	MAX.	UNIT
t_{dfOUT}	output signal delay time of HL-edge		1.95	2.3	2.55	µs
		T_{amb} = (−40 to +150) °C	1.5	–	3.5	µs
d_{tdfOUT}	jitter of HL-edge	normalized to cycle of one reference mark; note 3	0	–	0.15	%
Environmental conditions						
	external magnetic influence	note 4	–	–	30	kA/m
	ESD protection of sensor pins V_{CC}, OUT and GND	compliance to IEC 0801-2 (IV); note 5	2	–	–	kV
	ESD protection of internal pins B1, B2, B3 and B4	compliance to IEC 0801-2 (IV); note 6	0.3	–	–	kV
	EMC: Compliance to ISO 11452-5	(A, stripline, 300 V/m, 10 kHz to 400 MHz, 1500 mm); note 7	–	–	–	
	interference for pulse: ISO 7637; pulse 4	T = 25 °C; note 7	function A			
Capacity of sensor shield						
C_s	shield capacity	B1 versus B2 of MR bridge; f = 1 MHz; U_{osc} = 200 mV	37	43	48	pF

Notes

1. LOW: open collector output transistor open (V_{OUT} < 1 V).
2. HIGH: open collector output transistor closed (V_{OUT} > 4 V).
3. Measured with harmonic magnetic field in 'y' with $H_{y\,max}$ = 1 kA/m and f_m = 10, 1000 and 8000 Hz.
4. Higher magnetic fields could cause irreversible shifts of parameters.
5. Output pins are designed for electrostatic sensitivity with field strengths up to 2 kV according to Human Body Model (HBM), MIL-STD-883, Method 3015.
6. MR pins are designed for electrostatic sensitivity with field strengths up to 0.3 kV according to Human Body Model (HBM), MIL-STD-883, Method 3015.
7. Measured with harmonic magnetic field in 'y' with $H_{y\,max}$ = 1 kA/m and f_m = 50 Hz.

FUNCTIONAL DESCRIPTION

The KMI18/4 is sensitive to the rotation of an passive target wheel with ferrous reference marks. The functional principle is shown in Fig.3. Because of the sensor layout and setup of the measuring system, only movements of reference marks in the y-direction will be sensed (coordinate system see Fig.2).

The electrical output signal of the sensor is amplified, temperature compensated and applied to a Schmitt trigger in the signal conditioning circuit (see Fig.11). An additional housing separates the conditioning circuitry from the magnetoresistive sensor element, thereby ensuring optimal sensor performance at high temperatures.

The signal level of the digital output is independent from the sensing distance within the measuring range. Its frequency equals that of the reference marks on the target wheels. Accuracy of the HL-edge, as a measure of the rotational angle, strongly depends on the properties of the chosen target wheel and the operating conditions.

An open collector voltage interface ensures accurate transmission (three wires) of the digital sensor signal to the subsequent signal conditioning electronics.

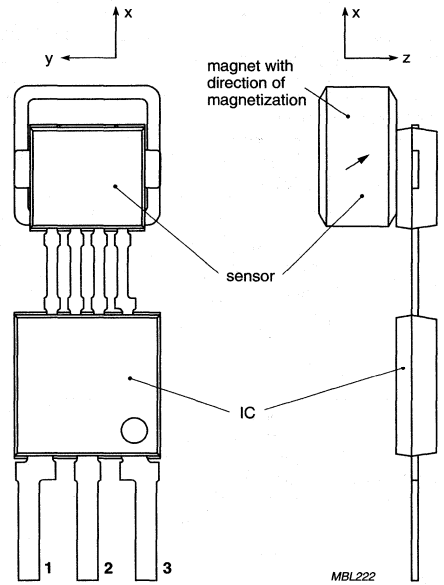

Fig.2 Component detail and coordinate system.

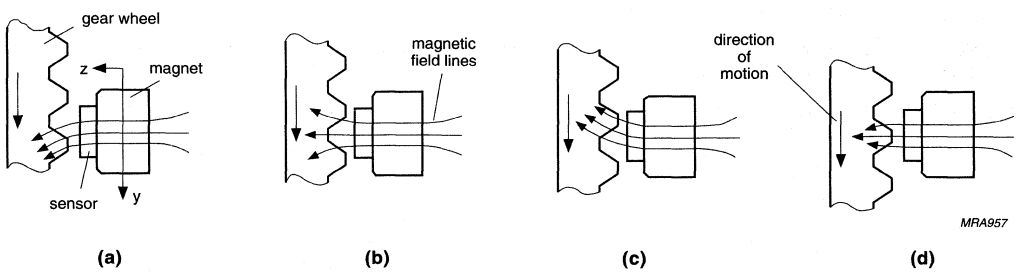

Fig.3 Functional principle.

Table 1 Gear wheel dimensions

SYMBOL	DESCRIPTION	VALUE	UNIT
German DIN			
z	number of teeth	50	
d	diameter	104	mm
m	module m = d/z	2.08	mm
p	pitch $\pi = p \times m$	6.53	mm
ASA			
PD	pitch diameter (d in inches)	4.09	inch
DP	diametric pitch DP = 25.4 mm/m	12.2	$inch^{-1}$
CP	circular pitch CP = p/25.4 mm	0.26	inch

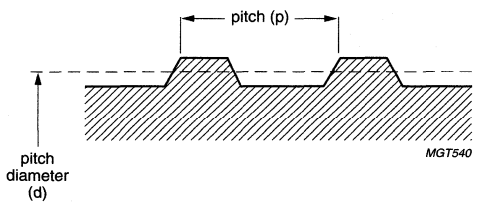

Material: 9SMnPb28k.

Fig.4 Gear wheel.

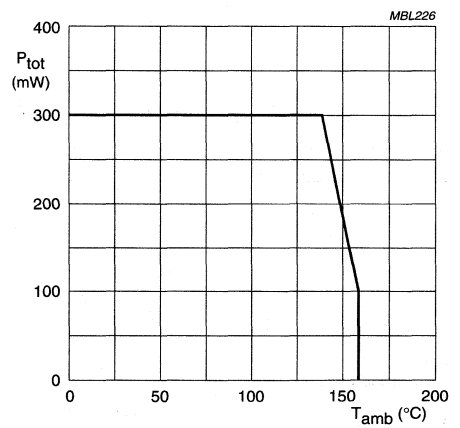

Fig.5 Power derating curve.

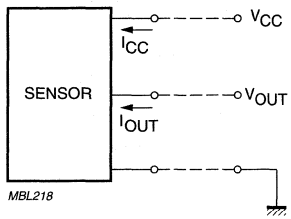

Fig.6 Supply and output.

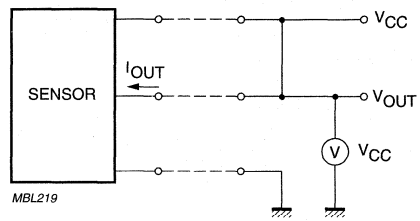

Fig.7 Leakage current test circuit: V_{CC} to OUT.

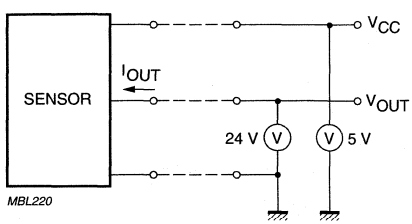

Fig.8 Leakage current test circuit: OUT to GND.

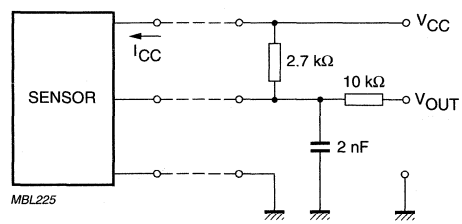

Fig.9 Test and application circuit with additional ceramic capacitor.

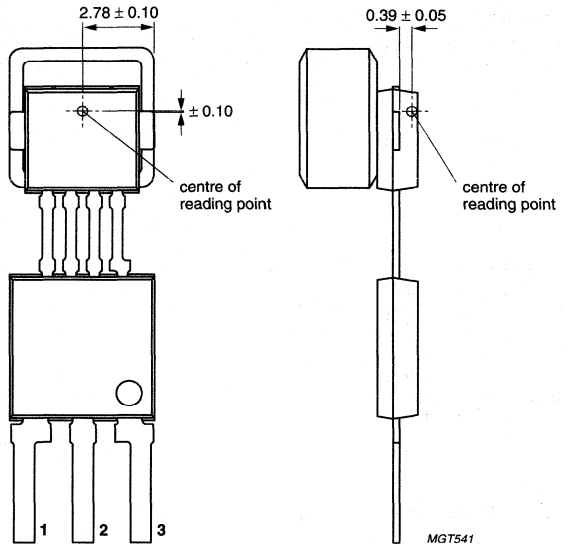

Fig.10 Definition of magnetic reading point.

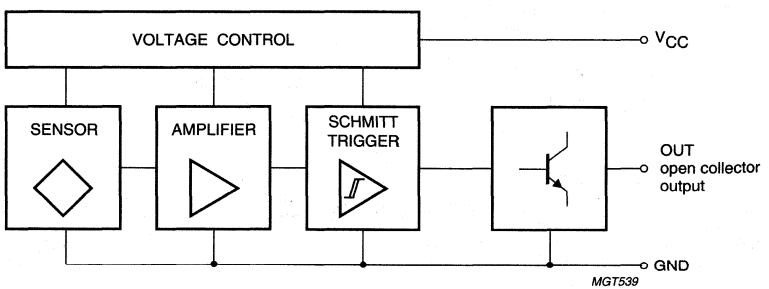

Fig.11 Block diagram.

PACKAGE OUTLINE

Plastic single-ended multi-chip package;
magnetized ferrite magnet (5.5 x 5.5 x 3 mm); 4 interconnections; 3 in-line leads **SOT477C**

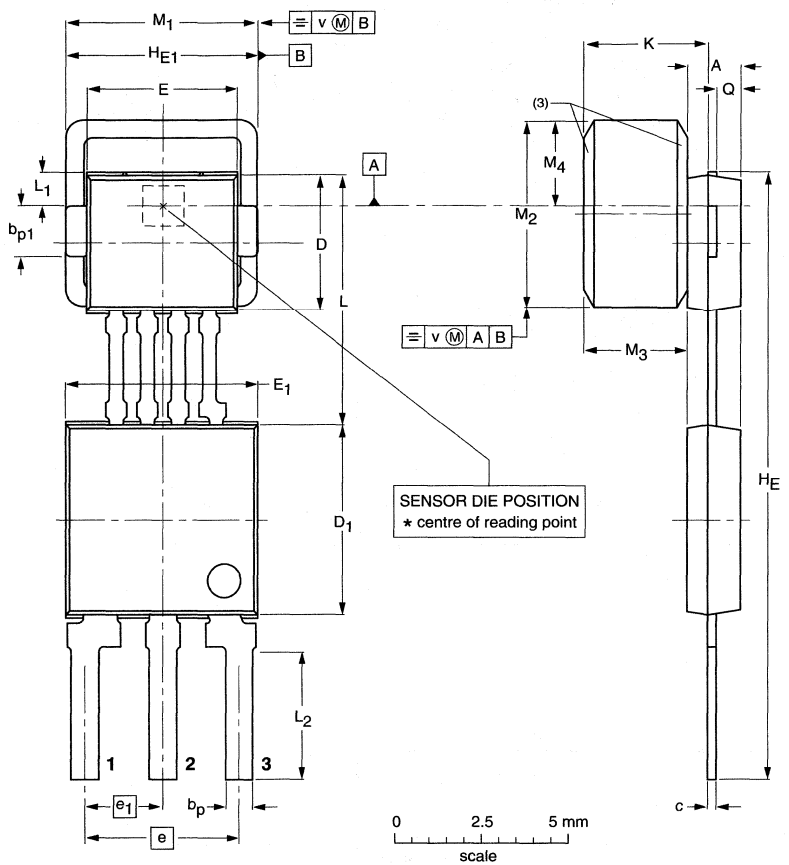

DIMENSIONS (mm are the original dimensions)

UNIT	A(1)	b_p	b_{p1}	c	D(2)	D_1(2)	E(2)	E_1(2)	e	e_1	H_E	H_{E1}	K max.	L	L_1	L_2	M_1	M_2	M_3(1)	M_4	Q	v
mm	1.7 1.4	0.8 0.7	1.57 1.47	0.3 0.24	4.1 3.9	5.7 5.5	4.5 4.3	5.7 5.5	4.6 4.4	2.35 2.15	18.2 17.8	5.6 5.5	3.87	7.55 7.25	1.2 0.9	3.9 3.5	5.65 5.35	5.65 5.35	3.05 2.95	2.6 2.4	0.75 0.65	0.25

Notes

1. Glue thickness not included.
2. Plastic or metal protrusions of 0.15 mm maximum per side are not included.
3. Magnet chamber optional.

OUTLINE VERSION	REFERENCES				EUROPEAN PROJECTION	ISSUE DATE
	IEC	JEDEC	EIAJ			
SOT477C						00-08-31

Rotational speed sensor for extended air gap application

KMI20/1

FEATURES

- Digital current output signal
- Digital offset compensation
- Extended air gap
- Zero speed capability
- Wide temperature range
- High tolerance to vibration
- EMC resistant
- Tolerant to positioning.

DESCRIPTION

The KMI20/1 is a sensitive rotational speed sensor for the application with ferrous gear wheels(1). The sensor consists of a magnetoresistive sensor element, a driver IC in BIMOS technology, a digital signal conditioning IC in a highly integrated CMOS technology and a magnetized ferrite magnet. The frequency of the digital current output signal is proportional to the rotational speed of a gear wheel.

CAUTION
Do not press two or more products together against their magnetic forces.

(1) The sensor contains customized integrated circuits. Usage in hydraulic brake systems and in systems with active brake control is forbidden. For all other applications, higher temperature versions of up to 150 °C are available on request.

PINNING

PIN	DESCRIPTION
1	V_{CC}
2	V–

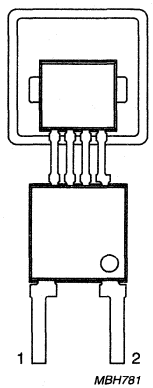

Fig.1 Simplified outline (SOT453B).

QUICK REFERENCE DATA

SYMBOL	PARAMETER	MIN.	TYP.	MAX.	UNIT
V_{CC}	DC supply voltage between leads 1 and 2	0	12	18	V
$I_{CC\ (low)}$	current output signal low	5.6	7	8.4	mA
$I_{CC\ (high)}$	current output signal high	11.2	14	16.8	mA
d	sensing distance	0 to 4	0 to 4.5	–	mm
f_t	operating tooth frequency	0	–	2500	Hz
T_{amb}	ambient operating temperature	–40	–	+85	°C

LIMITING VALUES

In accordance with Absolute Maximum Rating System (IEC 60134).

SYMBOL	PARAMETER	CONDITIONS	MIN.	MAX.	UNIT
V_{CC}	DC supply voltage	T_{amb} = –40 to +85 °C; R_L = 115 Ω	0	18	V
T_{stg}	storage temperature		–65	+150	°C
T_{amb}	operating ambient temperature		–40	+85	°C
T_{sld}	soldering temperature	t < 10 s	–	+260	°C
	output short-circuit duration	V_{CC} to GND (see Fig.7)	continuous		
	wrong polarity	T_{amb} = –40 to +65 °C; R_L = 115 Ω; note 1	continuous		

Note

1. With R_L = 115 Ω the device is continuously protected against wrong polarity of the DC supply voltage (V_{CC}) to GND (see Fig 7).

CHARACTERISTICS

T_{amb} = 25 °C; V_{CC} = 12 V; d = 2.1 mm; f_t = 2 kHz; test circuit: see Fig.7; R_L = 115 Ω; central sensor positioning: see Fig.9; gear wheel: module 2 mm; material 95MnPb28k; unless otherwise specified.

SYMBOL	PARAMETER	CONDITIONS	MIN.	TYP.	MAX.	UNIT
$I_{CC\ (low)}$	current output low	–40 to +85 °C; see Figs 7 and 9	5.6	7	8.4	mA
$I_{CC\ (high)}$	current output high	–40 to +85 °C; see Figs 7 and 9	11.2	14	16.8	mA
t_r	output signal rise time	C_L = 100 pF; see Fig.11; 10% to 90% value	–	0.5	–	µs
t_f	output signal fall time	C_L = 100 pF; see Fig.11; 90% to 10% value	–	0.5	–	µs
f_t	operating tooth frequency	for both rotational directions	0	–	2500	Hz
$d_{in\ 0\ Hz}$	sensing distance in initial mode for signals 0 Hz < f_t < 1 Hz	see Fig.9	0 to 2.5	0 to 2.9	–	mm
$d_{in\ 1\ Hz}$	sensing distance in initial mode for signals >1 Hz	see Fig.9	0 to 3.5	0 to 3.9	–	mm
d_{act}	sensing distance in active mode	see Fig.9	0 to 4.0	0 to 4.5	–	mm
$\delta_{in\ 0\ Hz}$	duty cycle in initial mode for signals >0 Hz	see Fig.5	20	50	80	%
$\delta_{in\ 1\ Hz}$	duty cycle in initial mode for signals >1 Hz	see Fig.5	20	50	80	%
δ_{act}	duty cycle in active mode	see Fig.5	40	50	60	%

Rotational speed sensor for extended air gap application

KMI20/1

FUNCTIONAL DESCRIPTION

The KMI20/1 is sensitive to the motion of ferrous gear wheels. The functional principle is shown in Fig.3. Due to the effect of flux bending, the different directions of magnetic field lines in the magnetoresistive sensor element will cause an electrical signal. Because of the chosen sensor orientation and the direction of ferrite magnetization the KMI20/1 is sensitive to movement in the 'y' direction in front of the sensor only (see Fig.2).

The KMI20/1 contains a magnetoresistive sensor element and two ICs: a Position Detector IC (PDIC) and a Line Driver IC (LDIC). The sensor signal is fed into the PDIC. The PDIC converts the signal to the digital domain, applies digital compensation and after additional processing converts it back to analogue. The LDIC contains two current sources (one constant, one switchable) and a voltage control unit (see Fig.4).

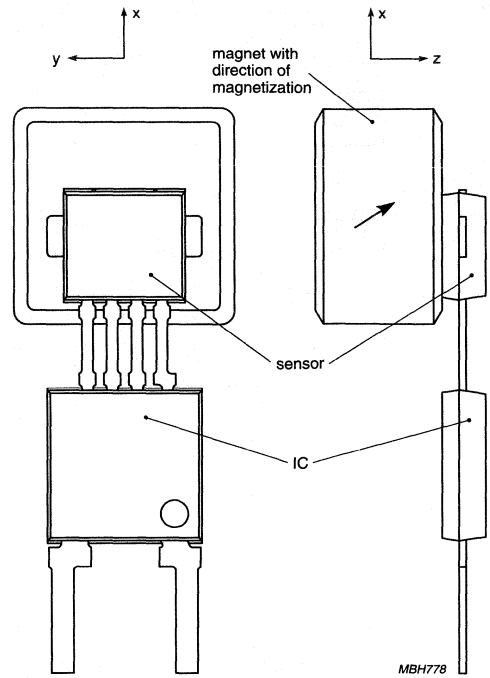

Fig.2 Component detail of the KMI20/1.

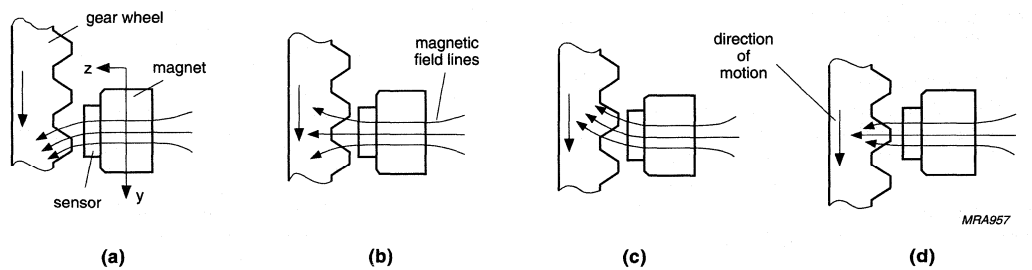

Fig.3 Functional principle.

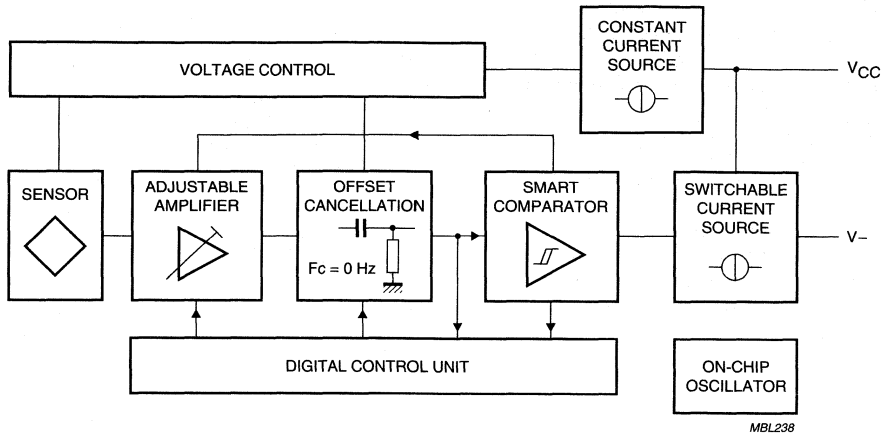

Fig.4 Block diagram.

Figure 5 shows the digital compensation function in algorithmic format. After power on the sensor system is running in INITIAL MODE 0 Hz. The sensor signal is preamplified but not offset compensated. The output signal represents the specified sensing distances (see Chapter "Characteristics") for every tooth of the wheel, totally speed independent. When $d_{in\ 0\ Hz} < d < d_{in\ 1\ Hz}$ the system must first detect the sensor signal amplitudes to compensate for the sensor offset (INITIAL MODE 1 Hz). An output signal is produced (first compensation run finished) at the latest after 11 wheel teeth, with a frequency above 1 Hz.

After detecting the teeth in initial mode the PDIC changes to ACTIVE MODE and the sensor signal is permanently offset compensated. The available sensing distance is increased to d_{act}. Quitting ACTIVE MODE is caused by power off or by the teeth frequency falling below 1 Hz. The system is locked into COMPENSATION MODE and continues to detect every wheel tooth down to zero speed.

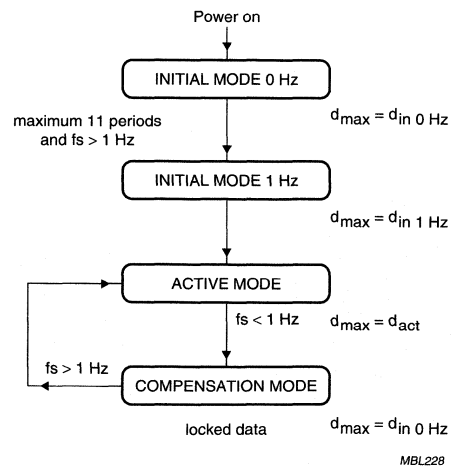

Fig.5 PDIC function algorithm.

Rotational speed sensor for extended air gap application

KMI20/1

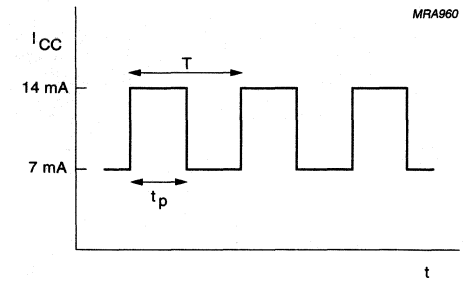

$$\delta = \frac{t_p}{T} \times 100\%$$

Fig.6 Output signal as a function of time.

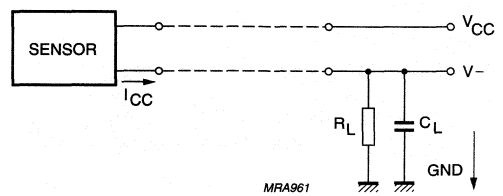

Fig.7 Test and application circuit.

Mounting conditions

The recommended sensor position in front of a gear wheel is shown in Fig.9. Distance 'd' is measured between the sensor front and the tip of a gear wheel tooth. The KMI20/1 senses ferrous indicators like gear wheels in the ±y direction only (no rotational symmetry of the sensor); see Fig.2. The symmetrical reference axis of the sensor corresponds to the axis of the ferrite magnet.

Gear wheel dimensions

SYMBOL	DESCRIPTION	UNIT
German DIN		
z	number of teeth	–
d	diameter	mm
m	module m = d/z	mm
p	pitch p = π × m	mm
ASA; note 1		
PD	pitch diameter (d in inch)	inch
DP	diametric pitch DP = z/PD	$inch^{-1}$
CP	circular pitch CP = π/DP	inch

Note

1. For conversion from ASA to DIN: m = 25.4 mm/DP; p = 25.4 mm × CP.

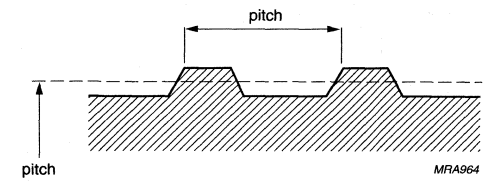

$$\text{module} = \frac{\text{pitch diameter}}{\text{number of teeth}}$$

$$\text{pitch} = \text{module} \times \pi$$

Fig.8 Gear wheel dimensions.

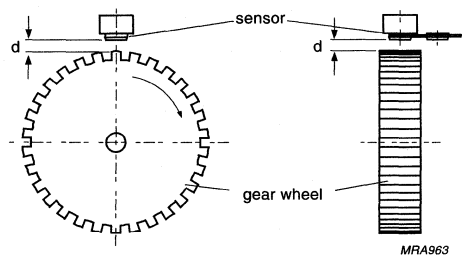

Centre die position: see Chapter "Package outline"

Fig.9 Sensor positioning.

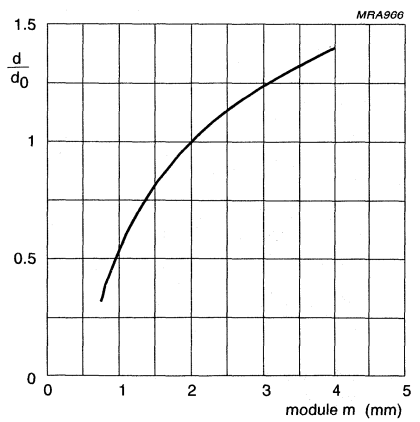

d_0 = measuring distance for a gear wheel with module m = 2 mm.

Fig.10 Normalized maximum sensing distance as a function of gear wheel module; typical values.

EMC

Figure 11 shows a recommended application circuit for automotive applications. It provides a protection interface to meet Electromagnetic Compatibility (EMC) standards and safeguard against voltage spikes. Table 1 lists the tests which are applicable to this circuit and the achieved class of functional status. Protection against 'load dump' (test pulses 5 according to *"DIN 40839"*) means a very high demand on the protection circuit and requires a suitable suppressor diode with sufficient energy absorption capability.

The board net often contains a central load dump protection that makes such a device in the protection circuit of the sensor module unneccesary.

Tests for ElectroStatic Discharge (ESD) were conducted in line with *"MIL Std. 883D, Method 3015.7"* to demonstrate the KMI20/1's handling capabilities. The test conditions were: C = 150 pF, R = 150 Ω and V = 4 kV.

Electromagnetic disturbances with fields up to 150 V/m and f = 1 GHz (ref. *"DIN 40839"*) have no influence on performance.

Table 1 EMC test results

EMC REF. DIN 40839	SYMBOL	MIN. (V)	MAX. (V)	REMARKS	CLASS
Test pulse 1	V_{LD}	−100	−	t_d = 2 ms	C
Test pulse 2	V_{LD}	−	100	t_d = 0.2 ms	A
Test pulse 3a	V_{LD}	−150	−	t_d = 0.1 µs	A
Test pulse 3b	V_{LD}	−	100	t_d = 0.1 µs	A
Test pulse 4	V_{LD}	−7	−	t_d = 130 ms	B
Test pulse 5	V_{LD}	−	120	t_d = 400 ms	B

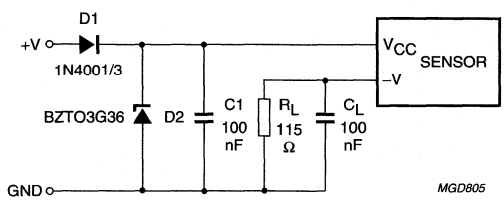

Fig.11 Test/application circuit for the KMI20/1.

PACKAGE OUTLINE

Plastic single-ended multi-chip package; magnetized ferrite magnet (8 x 8 x 4.5 mm); 4 interconnections; 2 in-line leads **SOT453B**

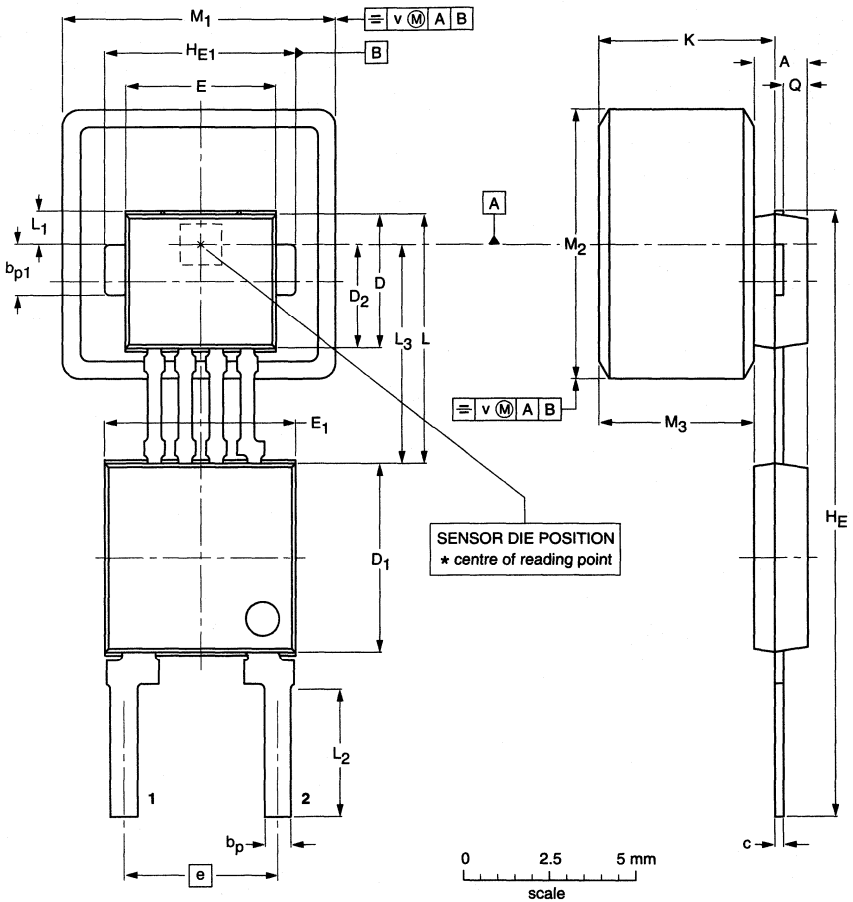

DIMENSIONS (mm are the original dimensions)

UNIT	A(1)	b_p	b_{p1}	c	D(2)	D_1(2)	D_2(2)	E(2)	E_1(2)	e	H_E	H_{E1}	K max.	L	L_1	L_2	L_3	M_1	M_2	M_3(1)	Q	v
mm	1.7 1.4	0.8 0.7	1.57 1.47	0.3 0.24	4.1 3.9	5.7 5.5	3.15 2.95	4.5 4.3	5.7 5.5	4.6 4.4	18.2 17.8	5.6 5.5	5.37	7.55 7.25	1.2 0.9	3.9 3.5	6.55 6.35	8.15 7.85	8.15 7.85	4.7 4.3	0.75 0.65	0.25

Notes

1. Glue thickness not included.
2. Plastic or metal protrusions of 0.15 mm maximum per side are not included.

OUTLINE VERSION	REFERENCES				EUROPEAN PROJECTION	ISSUE DATE
	IEC	JEDEC	EIAJ			
SOT453B						~~99-09-23~~ 00-08-31

Rotational speed sensor for extended air gap application

KMI20/2

FEATURES

- Digital current output signal
- Digital offset compensation
- Extended air gap
- Zero speed capability
- Wide temperature range
- High tolerance to vibration
- EMC resistant
- Tolerant to positioning.

DESCRIPTION

The KMI20/2 sensor detects rotational speed of magnetized targets(1).

The sensor consists of a magnetoresistive sensor element, a driver IC in BIMOS technology, a digital signal conditioning IC in highly integrated CMOS technology and a ferrite magnet. The frequency of the digital current output signal is proportional to the rotational speed of a magnetized wheel.

CAUTION
Do not press two or more products together against their magnetic forces.

(1) The sensor contains customized integrated circuits. Usage in hydraulic brake systems and in systems with active brake control is forbidden. For all other applications, higher temperature versions of up to 150 °C are available on request.

PINNING

PIN	SYMBOL
1	V_{CC}
2	V–

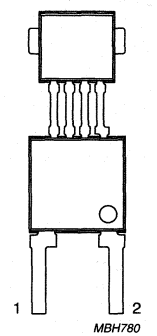

Fig.1 Simplified outline (SOT453A).

QUICK REFERENCE DATA

SYMBOL	PARAMETER	MIN.	TYP.	MAX.	UNIT
V_{CC}	DC supply voltage	0	12	18	V
$I_{CC\ (low)}$	current output signal low	5.6	7	8.4	mA
$I_{CC\ (high)}$	current output signal high	11.2	14	16.8	mA
f_t	operating tooth frequency	0	–	2500	Hz
T_{amb}	ambient operating temperature	–40	–	+85	°C

LIMITING VALUES

In accordance with the Absolute Maximum Rating System (IEC 60134).

SYMBOL	PARAMETER	CONDITIONS	MIN.	MAX.	UNIT
V_{CC}	DC supply voltage	T_{amb} = –40 to +85 °C; R_L = 115 Ω	0	18	V
T_{stg}	storage temperature		–65	+150	°C
T_{amb}	operating ambient temperature		–40	+85	°C
T_{sld}	soldering temperature	t < 10 s	–	260	°C
	output short-circuit duration to GND	see Fig.7	continuous		
	wrong polarity	T_{amb} = –40 to +65 °C, R_L = 115 Ω; note 1	continuous		

Note

1. With R_L = 115 Ω the device is continuously protected against wrong polarity of the DC supply voltage (V_{CC}) to GND; see Fig.7.

CHARACTERISTICS

T_{amb} = 25 °C; V_{CC} = 12 V; test circuit; see Fig.7; R_L = 115 Ω; unless otherwise specified.

SYMBOL	PARAMETER	CONDITIONS	MIN.	TYP.	MAX.	UNIT
$I_{CC\ (low)}$	current output low	–40 to +85 °C; see Fig.6	5.6	7	8.4	mA
$I_{CC\ (high)}$	current output high	–40 to +85 °C; see Fig.6	11.2	14	16.8	mA
t_r	output signal rise time	C_L = 100 pF; 10% to 90% value; see Fig.8	–	0.5	–	µs
t_f	output signal fall time	C_L = 100 pF; 90% to 10% value; see Fig.8	–	0.5	–	µs
f_t	operating tooth frequency	for both rotational directions	0	–	2500	Hz
$H_{yin\ 0\ Hz}$	magnetic hysteresis in initial mode	peak to peak	0.2	0.3	0.4	kA/m
$H_{yin(off)}$	magnetic offset in initial mode		–0.2	0	+0.2	kA/m
$H_{y(act)}$	magnetic hysteresis in active mode	percentage of last signal amplitude	30	–	45	%

FUNCTIONAL DESCRIPTION

The KMI20/2 is sensitive to magnetic fields. The functional principle is shown in Fig.3. The field lines of a magnetized target are shown as a straight target (it could also be circular e.g. for rotational speed measurement). The sensor is switched by the magnetic field components Hs_{LH} or Hs_{HL} either to low (7 mA) or to high (14 mA). Oscillation of the sensor is avoided by the implementation of a hysteresis in the signal conditioning circuit. Stability is ensured by the inclusion of a permanent magnet, the continuous magnetic field of which prevents frequency doubling in the sensor.

The KMI20/2 contains a magnetoresistive sensor element and two ICs: a Position Detector IC (PDIC) and a Line Driver IC (LDIC). The sensor signal is fed into the PDIC. The PDIC is the signal conditioning IC which includes A/D and D/A converters and a Schmitt trigger, and provides digital compensation. The LDIC contains two current sources (one constant and one switchable) and a voltage control unit (see Fig.4).

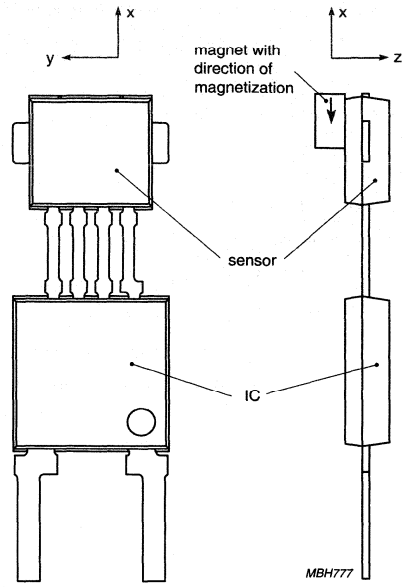

Fig.2 Component detail of the KMI20/2.

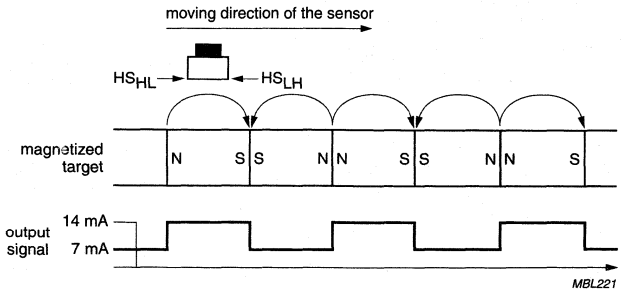

Fig.3 Functional principle of the KMI20/2.

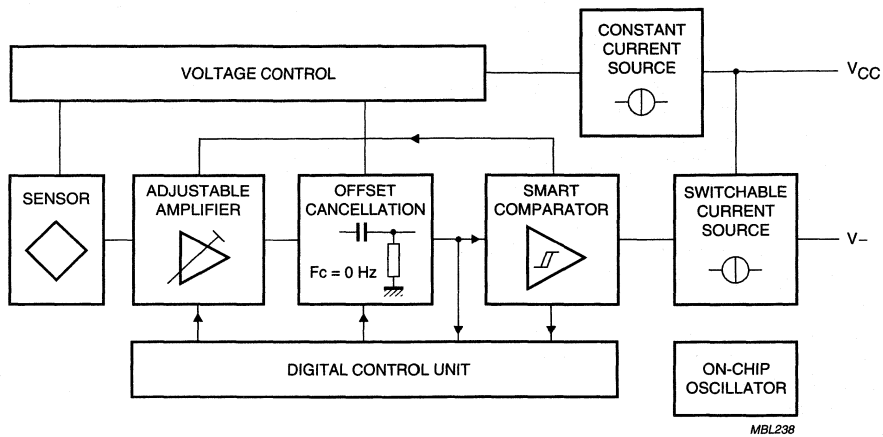

Fig.4 Block diagram.

Figure 5 shows the digital compensation function in algorithmic format. After power-on the sensor system is running in INITIAL MODE 0 Hz. The sensor signal is preamplified but not offset compensated. The output signal represents the specified magnetic field strength (see Chapter "Characteristics"), totally speed independent. When there is a magnetic offset the system must first detect the sensor signal amplitudes to compensate for it (INITIAL_MODE_1_Hz). An output signal is produced (first compensation run finished) at the latest after 11 magnetic field pairs with a frequency above 1 Hz have been sensed.

After detecting the fields in initial mode the PDIC changes to ACTIVE MODE. The sensor signal is permanently offset compensated. The hysteresis is now directly dependent on the last magnetic amplitude (30% to 45%, see Chapter "Characteristics") down to typically 50 A/m. Quitting ACTIVE MODE is caused by power off or by decreasing the magnetic field frequency below 1 Hz. The system is locked into COMPENSATION MODE and continues to detect every magnetic field down to zero speed.

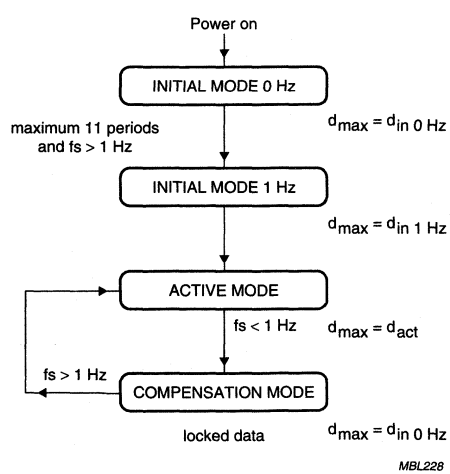

Fig.5 PDIC function algorithm.

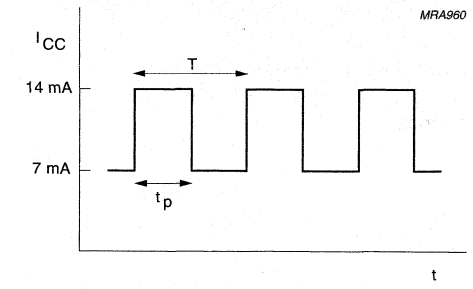

$$\delta = \frac{t_p}{T} \times 100\%$$

Fig.6 Output signal as a function of time.

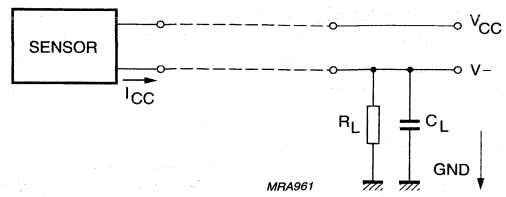

Fig.7 Test and application circuit.

EMC

Figure 8 shows a recommended application circuit for automotive applications. It provides a protection interface to meet Electromagnetic Compatibility (EMC) standards and safeguard against voltage spikes. Table 1 lists the tests which are applicable to this circuit and the achieved class of functional status. Protection against 'load dump' (test pulses 5 according to *"DIN 40839"*) means a very high demand on the protection circuit and requires a suitable suppressor diode with sufficient energy absorption capability.

The board net often contains a central load dump protection that makes such a device in the protection circuit of the sensor module unnecessary.

Tests for Electrostatic Discharge (ESD) were conducted in line with *"MIL Std. 883D, Method 3015.7"* to demonstrate the KMI20/2's handling capabilities. The test conditions were: C = 150 pF, R = 150 Ω and V = 4 kV.

Electromagnetic disturbances with fields up to 150 V/m and f = 1 GHz (ref. *"DIN 40839"*) have no influence on performance.

Table 1 EMC test results

EMC REF. DIN 40839	SYMBOL	MIN. (V)	MAX. (V)	REMARKS	CLASS
Test pulse 1	V_{LD}	−100	–	t_d = 2 ms	C
Test pulse 2	V_{LD}	–	100	t_d = 0.2 ms	A
Test pulse 3a	V_{LD}	−150	–	t_d = 0.1 µs	A
Test pulse 3b	V_{LD}	–	100	t_d = 0.1 µs	A
Test pulse 4	V_{LD}	−7	–	t_d = 130 ms	B
Test pulse 5	V_{LD}	–	120	t_d = 400 ms	B

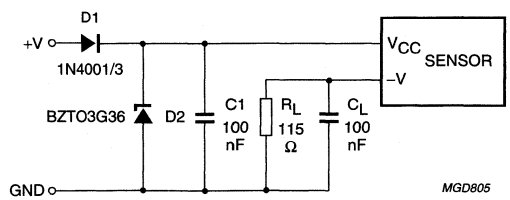

Fig.8 Test/application circuit for the KMI20/2.

Rotational speed sensor for extended air gap application

KMI20/2

PACKAGE OUTLINE

Plastic single-ended multi-chip package; magnetized ferrite magnet (3.8 x 2 x 0.8 mm); 4 interconnections; 2 in-line leads **SOT453A**

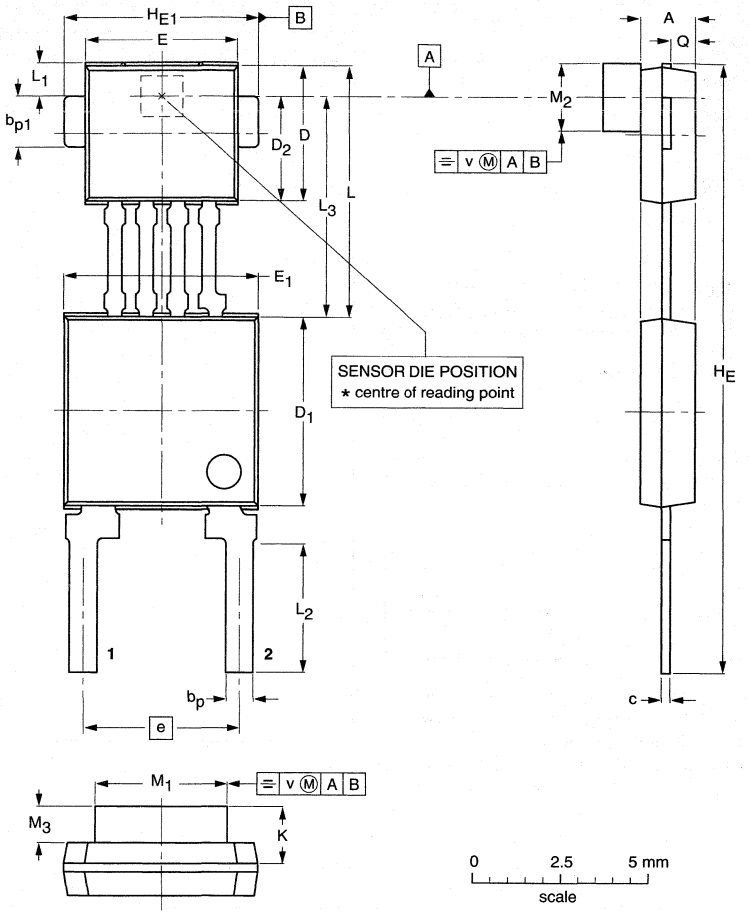

DIMENSIONS (mm are the original dimensions)

UNIT	A(1)	b_p	b_{p1}	c	D(2)	D_1(2)	D_2(2)	E(2)	E_1(2)	e	H_E	H_{E1}	K max.	L	L_1	L_2	L_3	M_1	M_2	M_3(1)	Q	v
mm	1.7 1.4	0.8 0.7	1.57 1.47	0.3 0.24	4.1 3.9	5.7 5.5	3.15 2.95	4.5 4.3	5.7 5.5	4.6 4.4	18.2 17.8	5.6 5.5	1.67	7.55 7.25	1.2 0.9	3.9 3.5	6.55 6.35	3.9 3.7	2.1 1.9	0.9 0.7	0.75 0.65	0.25

Notes

1. Glue thickness not included.
2. Plastic or metal protrusions of 0.15 mm maximum per side are not included.

OUTLINE VERSION	REFERENCES				EUROPEAN PROJECTION	ISSUE DATE
	IEC	JEDEC	EIAJ			
SOT453A						~~99-09-22~~ 00-08-31

Rotational speed sensor for extended air gap application

KMI20/4

FEATURES

- Digital current output signal
- Digital offset compensation
- Extended air gap
- Zero speed capability
- Wide temperature range
- High tolerance to vibration
- EMC resistant
- Tolerant to positioning.

DESCRIPTION

The KMI 20/4 is a sensitive rotational speed sensor designed for use in applications utilizing ferrous gear wheels(1).

The sensor consists of a magnetoresistive sensor element, a driver IC in BIMOS technology, a digital signal conditioning IC in highly integrated CMOS technology and a magnetized ferrite magnet. The frequency of the digital current output signal is proportional to the rotational speed of the gear wheel.

CAUTION
Do not press two or more products together against their magnetic forces.

(1) The sensor contains customized integrated circuits. Usage in hydraulic brake systems and in systems with active brake control is forbidden. For all other applications, higher temperature versions of up to 150 °C are available on request.

PINNING

PIN	SYMBOL
1	V_{CC}
2	V–

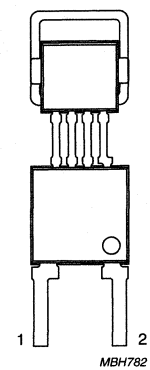

Fig.1 Simplified outline (SOT453C).

QUICK REFERENCE DATA

SYMBOL	PARAMETER	MIN.	TYP.	MAX.	UNIT
V_{CC}	DC supply voltage	0	12	18	V
$I_{CC\ (low)}$	current output signal low	5.6	7	8.4	mA
$I_{CC\ (high)}$	current output signal high	11.2	14	16.8	mA
d	sensing distance	0 to 3.6	0 to 4.1	–	mm
f_t	operating tooth frequency	0	–	2500	Hz
T_{amb}	ambient operating temperature	–40	–	+85	°C

LIMITING VALUES

In accordance with the Absolute Maximum Rating System (IEC 60134).

SYMBOL	PARAMETER	CONDITIONS	MIN.	MAX.	UNIT
V_{CC}	DC supply voltage	T_{amb} = −40 to +85 °C; R_L = 115 Ω	0	18	V
T_{stg}	storage temperature		−65	+150	°C
T_{amb}	operating ambient temperature		−40	+85	°C
T_{sld}	soldering temperature	t < 10 s	–	260	°C
	output short-circuit duration	V_{CC} to GND; see Fig.7	continuous		
	wrong polarity	T_{amb} = −40 to +65 °C, R_L = 115 Ω; note 1	continuous		

Note

1. With R_L = 115 Ω the device is continuously protected against wrong polarity of the DC supply voltage (V_{CC}) to GND (see Fig.7).

CHARACTERISTICS

T_{amb} = 25 °C; V_{CC} = 12 V; d = 1.7 mm; f_t = 2 kHz; test circuit; see Fig.7; R_L = 115 Ω; central sensor positioning: see Fig.9; gear wheel: module 2 mm; material 95MnPb28k; unless otherwise specified.

SYMBOLS	PARAMETER	CONDITIONS	MIN.	TYP.	MAX.	UNIT
$I_{CC\ (low)}$	current output low	−40 to +85 °C; see Figs 7 and 9	5.6	7	8.4	mA
$I_{CC\ (high)}$	current output high	−40 to +85 °C; see Figs 7 and 9	11.2	14	16.8	mA
t_r	output signal rise time	C_L = 100 pF; 10% to 90% value; see Fig.11	–	0.5	–	µs
t_f	output signal fall time	C_L = 100 pF; 90% to 10% value; see Fig.11	–	0.5	–	µs
f_t	operating tooth frequency	for both rotational directions	0	–	2500	Hz
$d_{in\ 0\ Hz}$	sensing distance in initial mode for signals 0 Hz < f_t < 1 Hz	see Fig.9	0 to 2.1	0 to 2.5	–	mm
$d_{in\ 1\ Hz}$	sensing distance in initial mode for signals >1 Hz	see Fig.9	0 to 3.1	0 to 3.5	–	mm
d_{act}	sensing distance in active mode	see Fig.9	0 to 3.6	0 to 4.1	–	mm
$\delta_{in\ 0\ Hz}$	duty cycle in initial mode for signals >0 Hz	see Fig.5	20	50	80	%
$\delta_{in\ 1\ Hz}$	duty cycle in initial mode for signals >1 Hz	see Fig.5	20	50	80	%
δ_{act}	duty cycle in active mode	see Fig.5	40	50	60	%

FUNCTIONAL DESCRIPTION

The KMI 20/4 is sensitive to the motion of ferrous gear wheels. The functional principle is shown in Fig.3. Due to the effect of flux bending, the different directions of magnetic field lines in the magnetoresistive sensor element will cause an electrical signal. Because of the chosen sensor orientation and the direction of ferrite magnetization the KMI20/4 is sensitive to movement in the 'y' direction in front of the sensor only (see Fig.2).

The KMI 20/4 contains a magnetoresistive sensor element and two ICs: a Position Detector IC (PDIC) and a Line Driver IC (LDIC). The sensor signal is fed into the PDIC. The PDIC converts the signal to the digital domain, applies digital compensation and after additional processing, converts it back to analogue. The LDIC contains two current sources (one constant, one switchable) and a voltage control unit (see Fig.4).

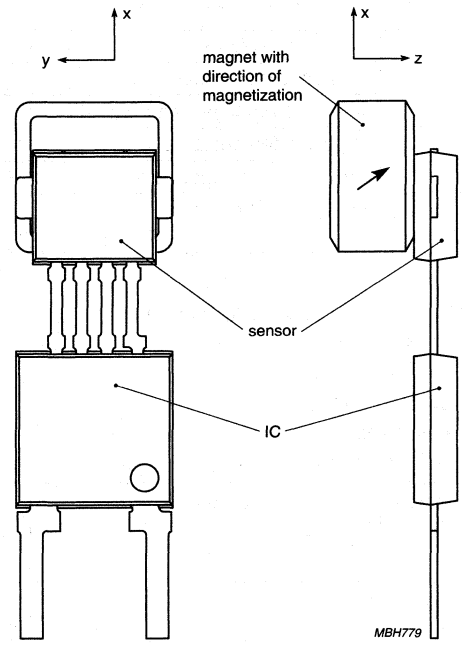

Fig.2 Component detail of the KMI20/4.

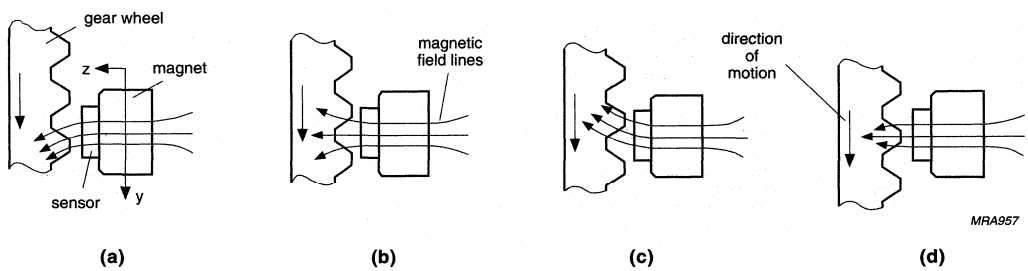

Fig.3 Functional principle.

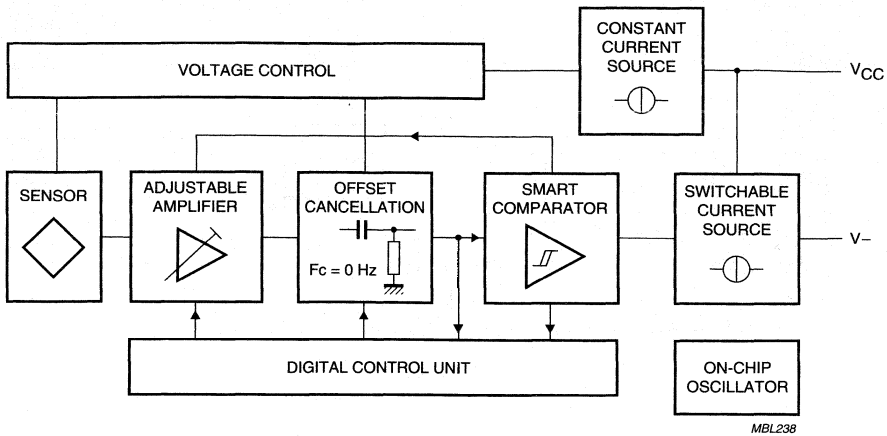

Fig.4 Block diagram.

Figure 5 shows the digital compensation function in algorithmic format. After power on the sensor system is running in INITIAL MODE 0 Hz. The sensor signal is preamplified but not offset compensated. The output signal represents the specified sensing distances (see Chapter "Characteristics") for every tooth of the wheel, totally speed independent. When $d_{in\ 0\ Hz} < d < d_{in\ 1\ Hz}$ the system must first detect the sensor signal amplitudes to compensate for the sensor offset (INITIAL MODE 1 Hz'). An output signal is produced (first compensation run finished) at the latest after 11 wheel teeth, with a frequency above 1 Hz.

After detecting the teeth in initial mode the PDIC changes to ACTIVE MODE and the sensor signal is permanently offset compensated. The available sensing distance is increased to d_{act}. Quitting ACTIVE MODE is caused by power off or by the teeth frequency falling below 1 Hz. The system is locked into COMPENSATION MODE and continues to detect every wheel tooth down to zero speed.

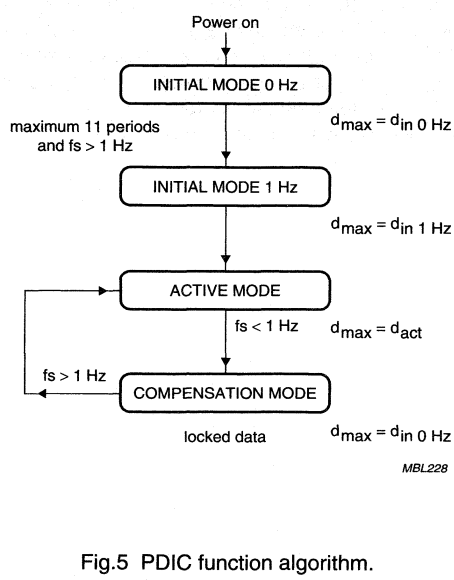

Fig.5 PDIC function algorithm.

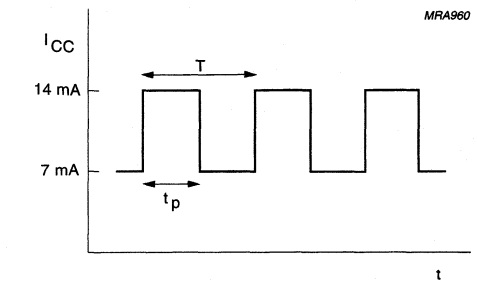

$$\delta = \frac{t_p}{T} \times 100\%$$

Fig.6 Output signal as a function of time.

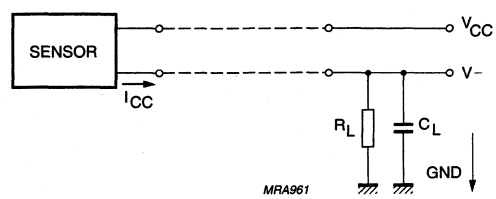

Fig.7 Test and application circuit.

Mounting conditions

The recommended sensor position in front of a gear wheel is shown in Fig.9. The distance 'd' is measured between the sensor front and the tip of a gear wheel tooth. The KMI20/4 senses ferrous indicators like gear wheels in the ±y direction only (no rotational symmetry of the sensor); see Fig.2. The symmetrical reference axis of the sensor corresponds to the axis of the ferrite magnet.

Gear wheel dimensions

SYMBOL	DESCRIPTION	UNIT
German DIN		
z	number of teeth	
d	diameter	mm
m	module m = d/z	mm
p	pitch p = π × m	mm
ASA; note 1		
PD	pitch diameter (d in inch)	inch
DP	diametric pitch DP = z/PD	$inch^{-1}$
CP	circular pitch CP = π/DP	inch

Note

1. For conversion from ASA to DIN: m = 25.4 mm/DP; p = 25.4 mm × CP.

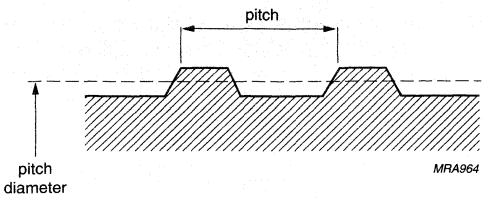

$$\text{module} = \frac{\text{pitch diameter}}{\text{number of teeth}}$$

$$\text{pitch} = \text{module} \times \pi$$

Fig.8 Gear wheel dimensions.

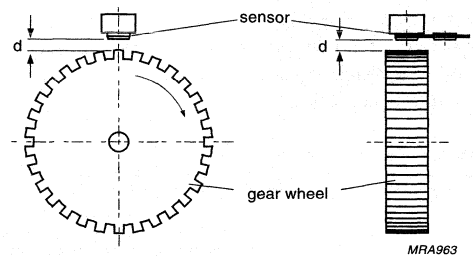

Center die position: see "Package outline".

Fig.9 Sensor positioning.

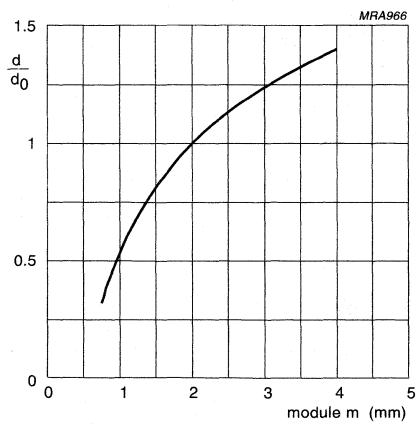

d_0 = measuring distance for a gear wheel with module m = 2 mm.

Fig.10 Normalized maximum sensing distance as a function of gear wheel module; typical values.

EMC

Figure 11 shows a recommended application circuit for automotive applications. It provides a protection interface to meet Electromagnetic Compatibility (EMC) standards and safeguard against voltage spikes. Table 1 lists the tests which are applicable to this circuit and the achieved class of functional status. Protection against 'load dump' (test pulses 5 according to *"DIN 40839"*) means a very high demand on the protection circuit and requires a suitable suppressor diode with sufficient energy absorption capability.

The board net often contains a central load dump protection that makes such a device in the protection circuit of the sensor module unnecessary.

Tests for Electrostatic Discharge (ESD) were conducted in line with *"MIL Std. 883D, Method 3015.7"* to demonstrate the KMI20_2's handling capabilities. The test conditions were: C = 150 pF, R = 150 Ω, V = 4 kV.

Electromagnetic disturbances with fields up to 150 V/m and f = 1 GHz (ref. *"DIN 40839"*) have no influence on performance.

Table 1 EMC test results

EMC REF. DIN 40839	SYMBOL	MIN. (V)	MAX. (V)	REMARKS	CLASS
Test pulse 1	V_{LD}	−100	−	t_d = 2 ms	C
Test pulse 2	V_{LD}	−	100	t_d = 0.2 ms	A
Test pulse 3a	V_{LD}	−150	−	t_d = 0.1 µs	A
Test pulse 3b	V_{LD}	−	100	t_d = 0.1 µs	A
Test pulse 4	V_{LD}	−7	−	t_d = 130 ms	B
Test pulse 5	V_{LD}	−	120	t_d = 400 ms	B

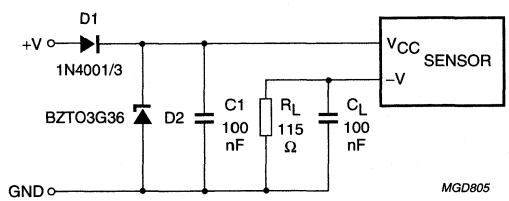

Fig.11 Test/application circuit for the KMI20/4.

Rotational speed sensor for extended air gap application

KMI20/4

PACKAGE OUTLINE

Plastic single-ended multi-chip package; magnetized ferrite magnet (5.5 x 5.5 x 3 mm); 4 interconnections; 2 in-line leads **SOT453C**

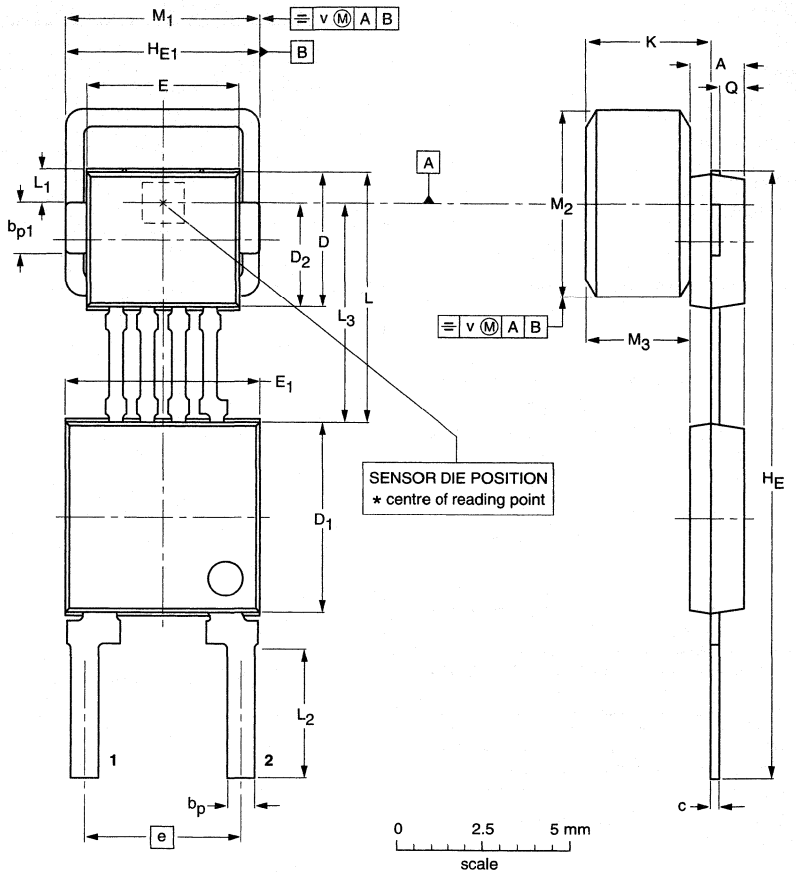

DIMENSIONS (mm are the original dimensions)

UNIT	A(1)	b_p	b_{p1}	c	D(2)	D_1(2)	D_2(2)	E(2)	E_1(2)	e	H_E	H_{E1}	K max.	L	L_1	L_2	L_3	M_1	M_2	M_3(1)	Q	v
mm	1.7 1.4	0.8 0.7	1.57 1.47	0.3 0.24	4.1 3.9	5.7 5.5	3.15 2.95	4.5 4.3	5.7 5.5	4.6 4.4	18.2 17.8	5.6 5.5	3.87	7.55 7.25	1.2 0.9	3.9 3.5	6.55 6.35	5.65 5.35	5.65 5.35	3.15 2.85	0.75 0.65	0.25

Notes

1. Glue thickness not included.
2. Plastic or metal protrusions of 0.15 mm maximum per side are not included.

OUTLINE VERSION	REFERENCES				EUROPEAN PROJECTION	ISSUE DATE
	IEC	JEDEC	EIAJ			
SOT453C						~~99-09-23~~ 00-08-31

Rotational speed sensor for extended air gap application and direction detection

KMI22/1

FEATURES

- Digital current output signal
- Digital offset compensation
- Extended air gap
- Zero speed capability
- Direction detection
- Digital output protocol
- Three level output signal
- Additional digital input pin
- Wide temperature range
- Insensitive to vibration
- EMC resistant
- Tolerant to positioning.

DESCRIPTION

The KMI22/1 is a sensitive rotational speed sensor for the application with ferrous gear wheels(1). The sensor consists of a magnetoresistive sensor element, a driver IC in BIMOS technology, a digital signal conditioning IC in highly integrated CMOS technology and a ferrite magnet. The digital two wire current output carries a signal proportional to the rotational speed of a gear wheel plus a digital protocol.

CAUTION
Do not press two or more products together against their magnetic forces.

(1) The sensor contains customized integrated circuits. Usage in hydraulic brake systems and in systems with active brake control is forbidden. For all other applications, higher temperature versions of up to 150 °C are available on request.

PINNING

PIN	DESCRIPTION
1	V_{CC}
2	V_{in}
3	V–

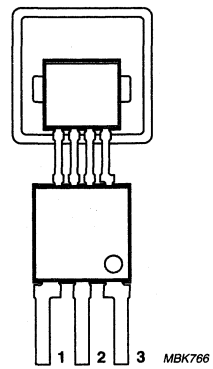

Fig.1 Simplified outline (SOT477B).

QUICK REFERENCE DATA

SYMBOL	PARAMETER	MIN.	TYP.	MAX.	UNIT
V_{CC}	DC supply voltage	0	12	18	V
I_{CCL}	current output signal low	5.6	7.0	8.4	mA
I_{CCPH}	current output signal protocol high	11.2	14	16.8	mA
I_{CCSH}	current output signal speed high	22.4	28	33.6	mA
V_{in}	input voltage pin 2	0	–	100	% V_{CC}
d	sensing distance	0 to 4	0 to 4.5	–	mm
f_r	operating tooth frequency	0	–	2500	Hz
T_{amb}	ambient operating temperature	–40	–	+85	°C

LIMITING VALUES

In accordance to the Absolute Maximum Rating System (IEC 60134).

SYMBOL	PARAMETER	CONDITIONS	MIN.	MAX.	UNIT
V_{CC}	DC supply voltage between leads 1 + 3	T_{amb} = –40 to +85 °C; R_L = 43 Ω; see Fig.12	0	18	V
V_{in}	input voltage pin 2	T_{amb} = –40 to + 85 °C	V–	V_{CC}	V
T_{stg}	storage temperature range		–65	+150	°C
T_{amb}	ambient operating temperature		–40	+85	°C
T_{sld}	soldering temperature	t < 10 s	–	260	°C
	output short-circuit duration	V_{CC} to GND (see Fig.12)	continuous		
	short-circuit duration	pin 2 to pin 1 and pin 2 to pin 3	continuous		
	wrong polarity	T_{amb} = –40 to +65 °C; R_L = 43 Ω; note 1	continuous		

Note

1. With R_L = 43 Ω the device is continuously protected against wrong polarity of DC supply voltage (V_{CC}) to GND; see Fig.12.

CHARACTERISTICS

T_{amb} = 25 °C; V_{CC} = 12 V; d = 2.1 mm; f_t = 2 kHz; test circuit: see Fig.12; R_L = 43 Ω; sensor positioning: see Fig.13; gear wheel: module 2 mm; material 1.0715; unless otherwise specified.

SYMBOL	PARAMETER	CONDITIONS	MIN.	TYP.	MAX.	UNIT
I_L	current output low	T = –40 to +85 °C; see Figs 6 and 8	5.6	7	8.4	mA
I_{PH}	current output protocol high	T = –40 to +85 °C; see Figs 6 and 8;	11.2	14	16.8	mA
I_{SH}	current output speed high	T = –40 to +85 °C; see Figs 6 and 8;	22.4	28	33.6	mA
t_r	output signal rise time	C_L = 100 pF; 10 to 90% value	–	0.5	–	µs
t_f	output signal fall time	C_L = 100 pF; 90 to 10% value	–	0.5	–	µs
f_t	operating tooth frequency	for both rotation directions T = –40 to +85 °C	0	–	2500	Hz
$d_{in\ 0\ Hz}$	sensing distance in initial mode for signals > 0 Hz	see Fig.13	0 to 2.5	0 to 2.9	–	mm
$d_{in\ 1\ Hz}$	sensing distance in initial mode for signals > 1 Hz	see Fig.13	0 to 3.5	0 to 3.9	–	mm
d_{dir}	sensing distance for safe direction detection	see Fig.13	0 to 3	0 to 3.4	–	mm
d_{act}	sensing distance in active mode	see Fig.13	0 to 4	0 to 4.5	–	mm
$\delta_{in\ 0\ Hz}$	duty cycle in initial mode for signals > 0 Hz	T = –40 to +85 °C; see Fig.5	20	50	80	%
$\delta_{in\ 1\ Hz}$	duty cycle in initial mode for signals > 1 Hz	T = –40 to +85 °C; see Fig.5	20	50	80	%
δ_{act}	duty cycle in active mode	T = –40 to +85 °C; see Fig.5	40	50	60	%

Rotational speed sensor for extended air gap application and direction detection

KMI22/1

FUNCTIONAL DESCRIPTION

The KMI22/1 is sensitive to the motion of ferrous gear wheels. The functional principle is shown in Fig.3. Due to the effect of flux bending the different directions of magnetic field lines in the magnetoresistive sensor element will cause an electrical signal. Because of the chosen sensor orientation and the direction of ferrite magnetization the KMI22/1 is sensitive to movement in the 'y' direction in front of the sensor only (see Fig.2).

The KMI22/1 contains a magnetoresistive sensor element and two ICs: a Position Detector IC (PDIC) and a Line Driver IC (LDIC). The sensor signal is fed into the PDIC which converts the signal to the digital domain, applies digital compensation and additional processing. The LDIC contains three current sources (one constant, two switchable), a voltage control unit and a level shifter to provide the signal V_{in} to the PDIC (see Fig.4). The digital output from the device is the combination of the speed pulse and an 8-bit data protocol.

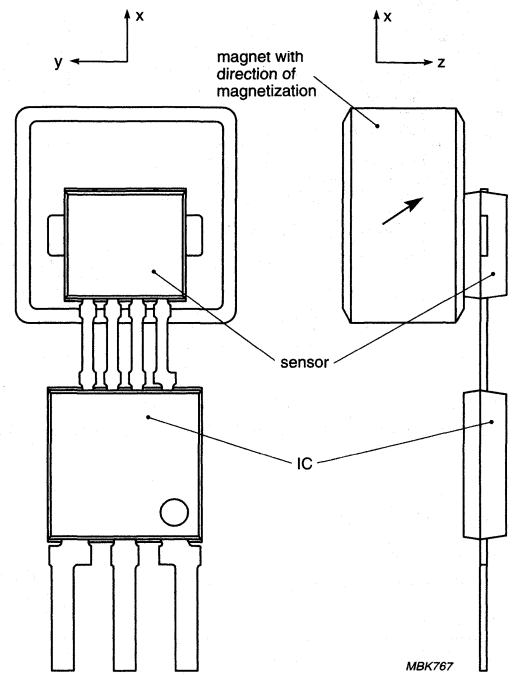

Fig.2 Component detail of the KMI22/1.

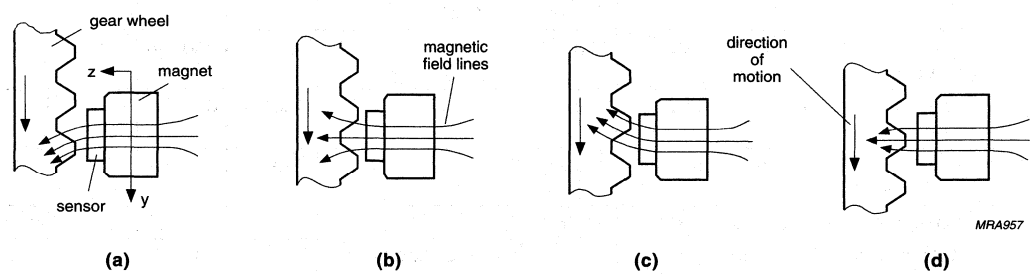

Fig.3 Functional principle.

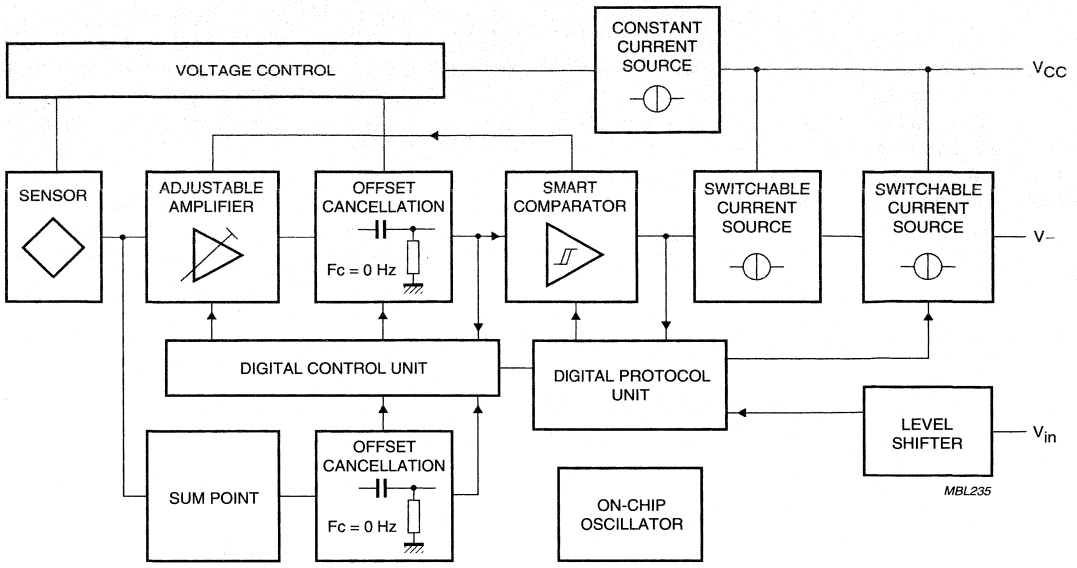

Fig.4 Block diagram.

Figure 5 shows the digital compensation function in algorithmic format. After power on the sensor system is running in INITIAL MODE 0 Hz. The sensor signal is preamplified but not offset compensated. The output signal represents the specified sensing distances (see Chapter "Characteristics") for every tooth of the wheel, totally speed independent.

When $d_{in\ 0\ Hz} < d < d_{in\ 1\ Hz}$ the system must first detect the sensor signal amplitudes to compensate for the sensor offset INITIAL MODE 1 Hz. An output signal is produced (first compensation run finished) latest after 11 wheel teeth, with a frequency above 1 Hz have been sensed.

After detecting the teeth in initial mode the PDIC changes to the ACTIVE MODE and the sensor signal is permanently offset compensated. The available sensing distance is increased to d_{act}. Quitting ACTIVE MODE is caused by power off or by the teeth frequency falling below 1 Hz. The system is locked into COMPENSATION MODE and continues to detect every wheel tooth down to zero speed.

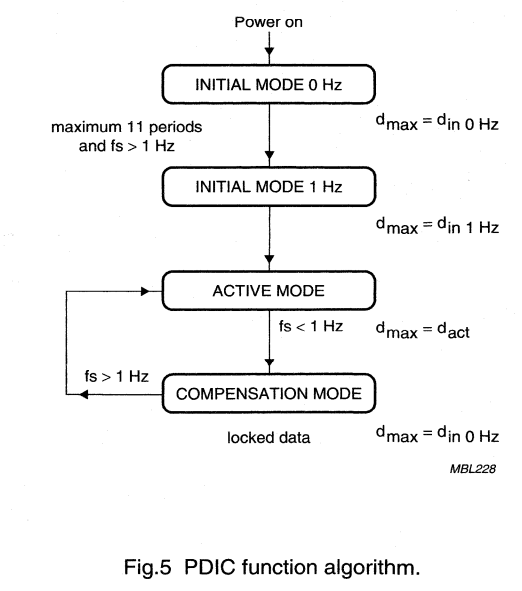

Fig.5 PDIC function algorithm.

Output signal

The output signal is shown in Fig.6. The signal contains a speed signal and an 8-bit protocol following the speed signal. This serial transmission, using the Manchester Code to encode the bits, is realized by modulating the 3-level output current of the sensor system. A short pulse of the highest current level I_{SH} represents the gear wheel structure, whereas the protocol bits are coded by using the protocol current level I_{PH}.

Definition of the protocol data bit value

Figure 7 shows the definition of the protocol data bit value. The protocol data bit has the bit length t_d. It is split into two half signal parts by the current edge in the middle of the data bit. Data bit HIGH is defined by the rising current edge from I_L to I_{PH}. Data bit LOW is defined by the falling current edge. Any data bit without a current edge at its middle is invalid.

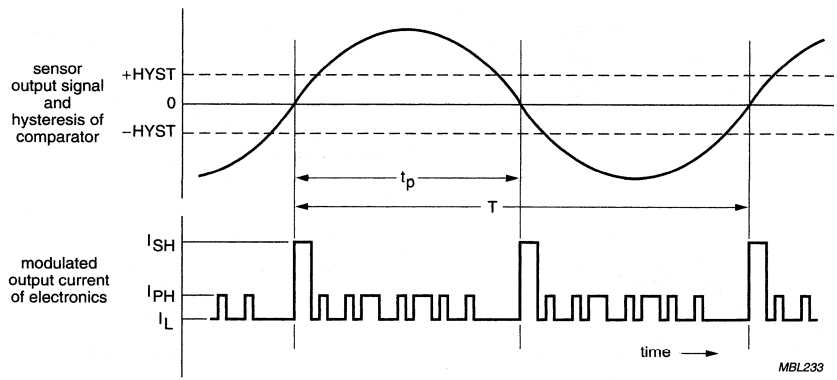

$$\delta = \frac{t_p}{T} \times 100\%$$

Fig.6 Output signal.

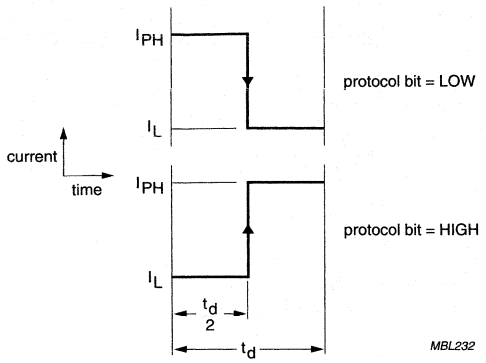

Fig.7 Definition of protocol data bit value.

Timing of the data

The data timing is shown in Figs 8 and 9.

OPERATION AT NORMAL SPEED

The wheel speed pulse is generated whenever a rising or falling edge of the wheel signal is detected. The pulse length is t_s. Following the wheel speed pulse a pre-bit is sent. It is always low and has the length t_p.

After the pre-bit the sensor logic begins to transfer the data protocol bits. The data protocol transferred by the sensor logic consists of 9 data bits (8 data bits and a parity bit; see Table 3). The data bit is length t_d and must contain a current edge its middle.

Following the data protocol bits an end bit with length $0.5 \times t_d$ is transferred. The end bit is always low, switching the current output to I_L until the arrival of the next wheel speed pulse leading edge.

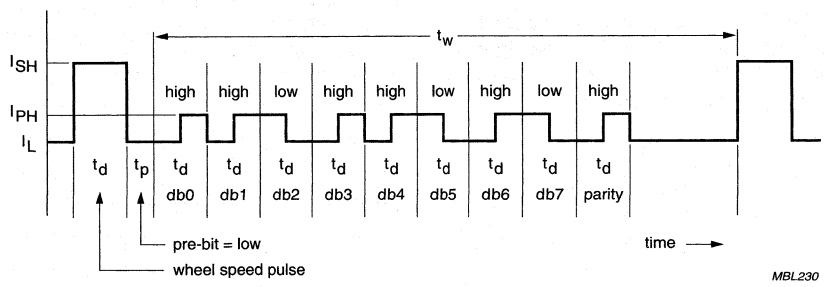

Fig.8 Timing diagram of data protocol at normal wheel speed.

OPERATION AT VERY LOW SPEED

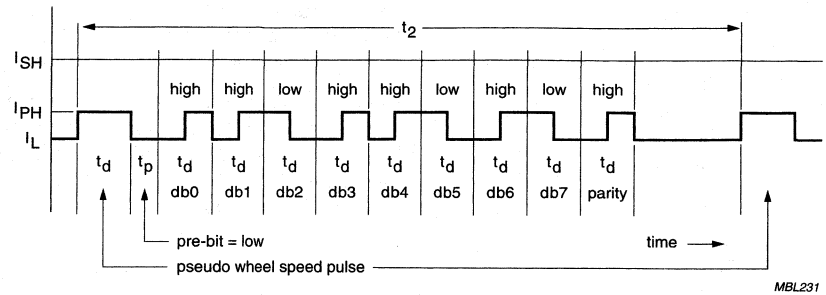

Fig.9 Timing diagram of data protocol at very low speed.

In the event that no wheel speed pulse is detected during time t_2 the protocol transfer is executed as described previously, except that a pseudo wheel speed pulse with protocol level high of I_{PH} instead of I_{SH} is substituted for the wheel speed pulse (see Fig.9).

TIMING AT HIGH SPEED

The pulse width of data bits t_d is fixed, whereas the time interval between wheel speed pulses is not. The higher the speed of the wheel, the shorter the period t_w, therefore not all data bits can be transferred at high wheel speed.

In this situation, calculations are made based on the current wheel speed pulse interval (n) to determine how many will fit into this window. This data is then used to determine the number of data bits that will be transferred during the next wheel speed pulse interval (n + 2), as shown in Table 1.

During time interval n + 2 the sensor current output consists of the wheel speed pulse, pre-bit, data bits (less than 9 bits; see Table 1), and the end bit data.

Referring to Table 1 it can be seen that the minimum number of data bits that will be transferred during period n + 2 is 2. If 3 or less data bits are to be transferred, the end bit length will be reduced to 0.

Table 1 Calculation of the number of protocol bits

MAXIMUM NUMBER OF t_d IN THE CURRENT TIME INTERVAL n (t_w)	PROTOCOL BITS FOR TIME INTERVAL n + 2
<5	2
5	3
6	4
7	5
8	6
9	7
10	8
>10	8

PULSE AND PROTOCOL DEFINITIONS

Table 2 Pulse and protocol timing

T_{amb} = −40 to +85 °C; V_{CC} = 12 V; test circuit: see Fig.12; R_L = 43 Ω; unless otherwise specified.

SYMBOL	PARAMETER	CONDITIONS	MIN.	TYP.	MAX.	UNIT
t_s	speed signal pulse width	see Figs 8 and 9	40	50	60	µs
t_p	pre-bit pulse width	see Figs 8 and 9	20	25	30	µs
t_d	data pulse width	see Figs 8 and 9	40	50	60	µs
t_2	time between pseudo speed pulses	see Fig.9	120	150	180	ms

Table 3 Definition of data bits

DATA BIT	SYMBOL	DESCRIPTION	REMARK
0	AR	air gap reserve	logic 1 when distance too large; note 1
1	M	mode state	logic 1 when in initial mode, 0 when in active mode
2	V_{in}	digital input state	logic 1 when V_{in} = low; default
3	VDR	validity direction recognition	logic 1 when direction bit is valid; note 2
4	DR	direction recognition	logic 1 when direction is positive (see Fig.10)
5	SD0	sensing distance bit 0	reflects actual sensing distance; LSB; note 3; Fig.10
6	SD1	sensing distance bit 1	reflects actual sensing distance; note 3; Fig.10
7	SD2	sensing distance bit 2	reflects actual sensing distance; MSB; note 3; Fig.10
8	P	parity	'high' for even parity: P = XOR (data 0, data 1 to data 7)

Notes

1. Air gap reserve: this bit of the protocol indicates that the processed signal amplitude is smaller than twice the minimum allowed signal amplitude (see Fig.10). If this bit is flagged then the air gap is nearly used up, which means that the sensor system will stop working for a further reduction of the signal amplitude.
2. Correct direction recognition is guaranteed for sensing distance: see Chapter "Characteristics".
3. Bits SD0 to SD2: These bits are used to quantify the signal amplitude and therefore the air gap can be divided into 8 sections (see Fig.10). For a temperature sweep over the complete specified range the air gap information may change by 2 LSBs due to the temperature coefficient of the sensor signal amplitude.

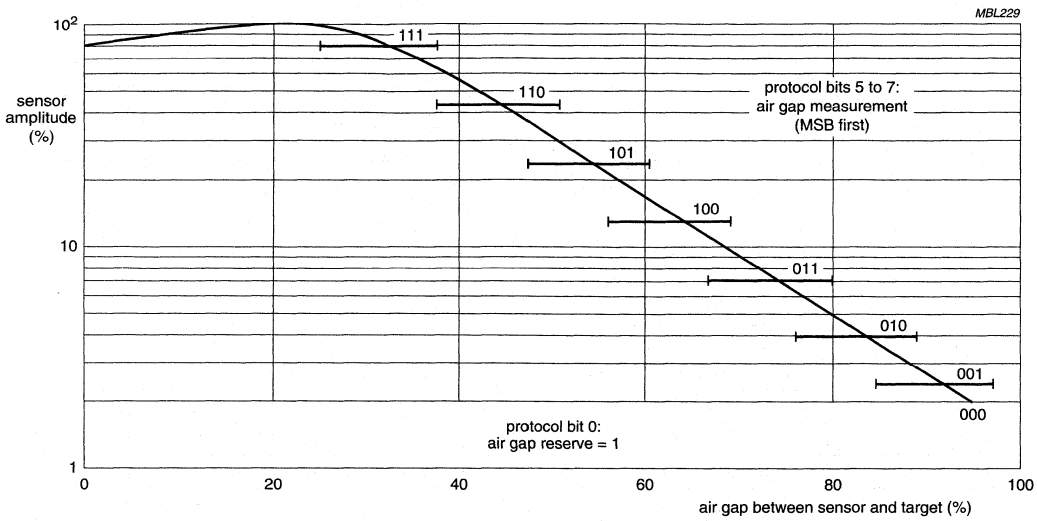

Fig.10 Sensor amplitude versus air gap.

Mounting conditions

The recommended sensor position in front of a gear wheel is shown in Fig.13. The distance 'd' is measured between the sensor front and the tip of a gear wheel tooth. The KMI22/1 senses ferrous indicators like gear wheels in the y direction only (no rotational symmetry of the sensor); see Fig.2. The symmetrical reference axis of the sensor corresponds to the axis of the ferrite magnet.

Table 4 Gear wheel dimensions

SYMBOL	DESCRIPTION	UNIT
German DIN		
z	number of teeth	
d	diameter	mm
m	module m = d/z	mm
p	pitch π = p × m	mm
ASA; note 1		
PD	pitch diameter (d in inches)	inch
DP	diametric pitch DP = z/PD	$inch^{-1}$
CP	circular pitch CP = π/DP	inch

Note

1. For conversion from ASA to DIN: m = 25.4 mm/DP; p = 25.4 mm × CP.

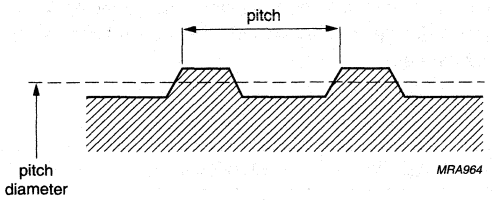

$$\text{module} = \frac{\text{pitch diameter}}{\text{number of teeth}}$$

$$\text{pitch} = \text{module} \times \pi$$

Fig.11 Gear wheel dimensions.

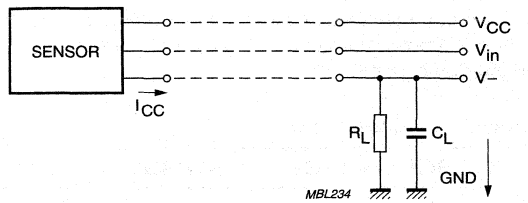

Fig.12 Test and application circuit.

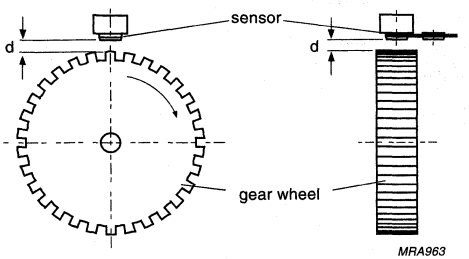

Centre die position: see Chapter "Package outline".

Fig.13 Sensor positioning.

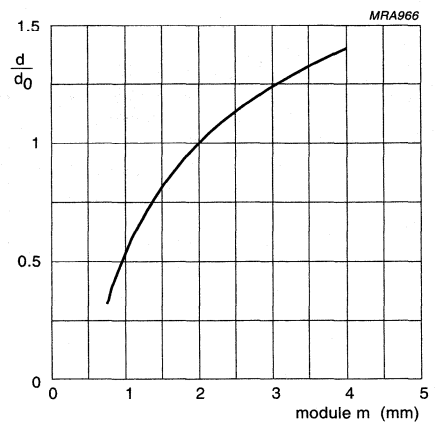

d_0 = measuring distance for a gear wheel with module m = 2 mm.

Fig.14 Normalized maximum sensing distance as a function of gear wheel module; typical values.

EMC

Figure 15 shows a recommended application circuit for automotive applications. It provides a protection interface to meet Electromagnetic Compatibility (EMC) standards and safeguard against voltage spikes. Table 5 lists the tests which are applicable to this circuit and the achieved class of functional status. Protection against 'load dump' (test pulses 5 according to *"DIN 40839"*) means a very high demand on the protection circuit and requires a suitable suppressor diode with sufficient energy absorption capability.

The board net often contains a central load dump protection that makes such a device in the protection circuit of the sensor module unnecessary.

Tests for electrostatic discharge (ESD) were conducted in line with *"IEC 801-2"* to demonstrate the KMI22/1's handling capabilities. The *"IEC 801-2"* test conditions were: C = 150 pF, R = 150 Ω, V = 4 kV.

Electromagnetic disturbances with fields up to 150 V/m and f = 1 GHz (ref. *"DIN 40839"*) have no influence on performance.

Table 5 EMC test results

EMC REF. DIN 40839	SYMBOL	MIN. (V)	MAX. (V)	REMARKS	CLASS
Test pulse 1	V_{LD}	−100	–	t_d = 2 ms	C
Test pulse 2	V_{LD}	–	100	t_d = 0.2 ms	A
Test pulse 3a	V_{LD}	−150	–	t_d = 0.1 µs	A
Test pulse 3b	V_{LD}	–	100	t_d = 0.1 µs	A
Test pulse 4	V_{LD}	−7	–	t_d = 130 ms	B
Test pulse 5	V_{LD}	–	120	t_d = 400 ms	B

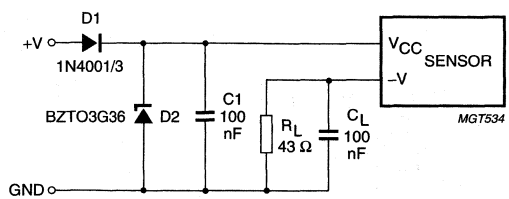

Fig.15 EMC: test and application circuit.

Rotational speed sensor for extended air gap application and direction detection

KMI22/1

PACKAGE OUTLINE

Plastic single-ended multi-chip package; magnetized ferrite magnet (8 x 8 x 4.5 mm); 4 interconnections; 3 in-line leads **SOT477B**

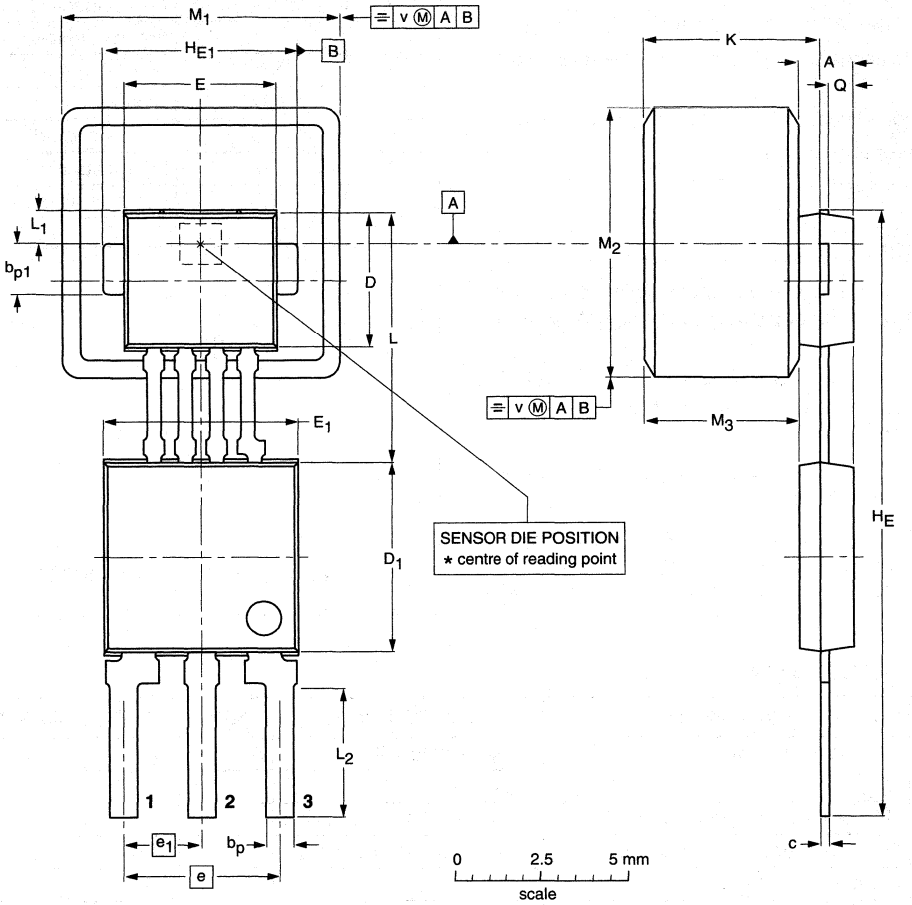

DIMENSIONS (mm are the original dimensions)

UNIT	$A^{(1)}$	b_p	b_{p1}	c	$D^{(2)}$	$D_1{}^{(2)}$	$E^{(2)}$	$E_1{}^{(2)}$	e	e_1	H_E	H_{E1}	K max.	L	L_1	L_2	M_1	M_2	$M_3{}^{(1)}$	Q	v
mm	1.7 1.4	0.8 0.7	1.57 1.47	0.3 0.24	4.1 3.9	5.7 5.5	4.5 4.3	5.7 5.5	4.6 4.4	2.35 2.15	18.2 17.8	5.6 5.5	5.37	7.55 7.25	1.2 0.9	3.9 3.5	8.15 7.85	8.15 7.85	4.7 4.3	0.75 0.65	0.25

Notes

1. Glue thickness not included.
2. Plastic or metal protrusions of 0.15 mm maximum per side are not included.

OUTLINE VERSION	REFERENCES				EUROPEAN PROJECTION	ISSUE DATE
	IEC	JEDEC	EIAJ			
SOT477B						~~99-09-23~~ 00-08-31

Trigger amplifier with two wire current interface UZZ7000T

FEATURES

- Differential input trigger amplifier
- Designed for signal conditioning of magnetoresistive sensor bridges
- Two wire 7 and 14 mA current interface
- Stabilized voltage supply source for external sensor bridges
- Comparator with temperature controlled hysteresis
- Wide temperature range
- Max. 19 V supply.

PINNING

PIN	SYMBOL	DESCRIPTION
1	SA	positive differential input
2	n.c.	not connected
3	n.c.	not connected
4	VAC	current output and supply
5	GND	ground
6	n.c.	not connected
7	VP	bridge supply
8	SB	negative differential input

DESCRIPTION

The UZZ7000T is a differential input amplifier circuit with a trigger mechanism for application with magnetoresistive sensor bridges.

It is equipped with a two wire current interface. The polarity of an input voltage difference triggers the circuit supply current between 7 and 14 mA.

The device also includes a voltage regulator for supply to an external sensor bridge.

An on-chip temperature sensor adapts the comparator hysteresis to the temperature dependent sensitivity of typical magnetoresistive sensors, such as the Philips KMZ family types.

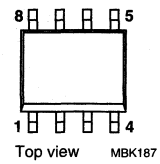

Fig.1 Simplified outline SOT96-1.

QUICK REFERENCE DATA

SYMBOL	PARAMETER	CONDITIONS	MIN.	TYP.	MAX.	UNIT
V_{VAC}	DC supply voltage	T_{amb} = −40 to +60 °C	5.5	12	19	V
		T_{amb} = −40 to +150 °C	–	–	15	V
$I_{VAC(L)}$	DC supply and output current	V_{VAC} = 12 V; V_{in} > 0; note 1	–	7	–	mA
$I_{VAC(H)}$	DC supply and output current	V_{VAC} = 12 V; V_{in} < 0; note 1	–	14	–	mA
V_{VP}	DC bridge supply voltage		–	4.9	–	V
I_{VP}	bridge supply current capability	V_{VP} > 4.7 V	–	–	−4.3	mA
T_{amb}	ambient operating temperature	V_{CC} = 12 V; note 2	−40	–	+150	°C

Notes

1. $V_{in} = V_{SA} - V_{SB}$.
2. Maximum power consumption according to power derating curve, see Fig.2.

LIMITING VALUES

In accordance with the Absolute Maximum Rating System (IEC 60134).

SYMBOL	PARAMETER	CONDITIONS	MIN.	MAX.	UNIT
V_{VAC}	DC supply voltage	not protected against incorrect polarity			
		T_{amb} = −40 to +60 °C	−0.5	+19	V
		T_{amb} = −40 to +150 °C	–	15	V
V_{SA}	maximum input voltage range	$t \leq 5$ s; T_{amb} = 26 ± 10 °C	−0.5	7	V
V_{SB}	maximum input voltage range	$t \leq 5$ s; T_{amb} = 26 ± 10 °C	−0.5	7	V
P_{tot}	total power dissipation	note 1	–	320	mW
T_{amb}	ambient operating temperature	V_{CC} = 12 V; note 1	−40	+150	°C
T_{stg}	storage temperature		−40	+150	°C

Note

1. Maximum power consumption according to power derating curve, see Fig.2.

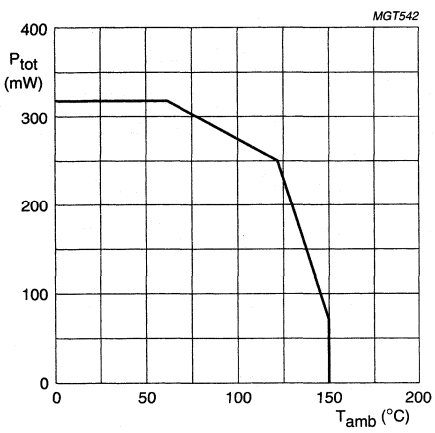

Fig.2 Power derating curve.

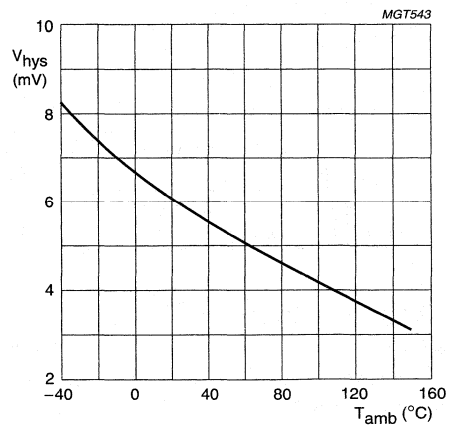

Fig.3 Hysteresis voltage as a function of temperature.

CHARACTERISTICS

T_{amb} = 26 °C; V_{VAC} = 12 V; unless otherwise specified.

SYMBOL	PARAMETER	CONDITIONS	MIN.	TYP.	MAX.	UNIT
Supply conditions						
$I_{VAC(L)}$	DC supply current	T_{amb} ± 10 °C	5.6	7	8.4	mA
$I_{VAC(H)}$	DC supply current	T_{amb} ± 10 °C	11.2	14	16.8	mA
V_{VAC}	DC supply voltage	T_{amb} = −40 to +150 °C	5.5	12	15	V
Signal input characteristics						
f_{rm}	input frequency range		0	–	25000	Hz
V_{SA}	maximum input voltage range		−0.5	–	7	V
	operating input voltage range		2.4	–	2.6	V
V_{SB}	maximum input voltage range		−0.5	–	7	V
	operating input voltage range		2.4	–	2.6	V
V_{OFF}	input offset voltage	T_{amb} ± 10 °C	−2.1	–	2.1	mV
I_{BIAS}	input bias current	V_{SA} - V_{SB} = 0	0.14	0.5	1.6	µA
I_{OFF}	input offset current	V_{SA} - V_{SB} = 0	−75	–	75	nA
V_{HYS}	input hysteresis voltage	at T_{amb}; notes 1 and 2	5.4	6	6.9	mV
Bridge supply output characteristics						
V_{VP}	DC bridge supply voltage		4.7	4.9	5	V
I_{VP}	DC bridge supply current		–	–	−4.3	mA
Environmental conditions						
	ESD protection of output pins VAC and GND	compliance to IEC 0801-2 (IV); note 3	2	–	–	kV
	ESD protection of sensor interface pins SA, SB and VP	compliance to IEC 0801-2 (IV); note 4	0.3	–	–	kV

Notes

1. Input hysteresis voltage is the difference between higher and lower switching point referred to input.
2. Temperature dependence of voltage hysteresis; see Fig.3.
3. Output pins are designed for electrostatic sensitivity with field strengths up to 2 kV according to Human Body Model (HBM), MIL-STD-883, method 3015.
4. Differential input pins are designed for electrostatic sensitivity with field strengths up to 0.3 kV according to Human Body Model (HBM), MIL-STD-883, method 3015.

FUNCTIONAL DESCRIPTION

The UZZ7000 is a differential input trigger amplifier with a two wire interface and sensor supply regulator. It is designed for application with magnetoresistive sensor bridges. The block diagram is shown in Fig.4

The circuitry includes a voltage regulator for supply to an external sensor bridge.

An on-chip temperature sensor adapts the comparator hysteresis to the temperature dependent sensitivity of a typical magnetoresistive sensor from the Philips MR-Sensor KMZ families.

The UZZ7000T device and the connected sensor bridge are supplied from a two wire current interface. The digital output is directly related to the differential voltage input between pins SA and SB which switches the constant current source between 7 and 14 mA.

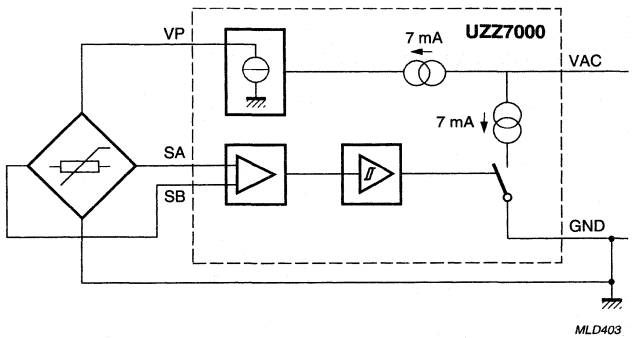

Fig.4 Block diagram.

PACKAGE OUTLINE

SO8: plastic small outline package; 8 leads; body width 3.9 mm **SOT96-1**

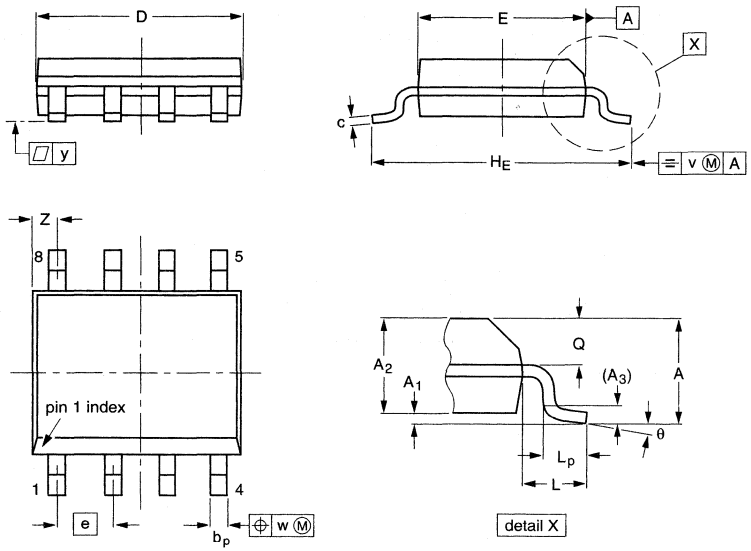

DIMENSIONS (inch dimensions are derived from the original mm dimensions)

UNIT	A max.	A_1	A_2	A_3	b_p	c	$D^{(1)}$	$E^{(2)}$	e	H_E	L	L_p	Q	v	w	y	$Z^{(1)}$	θ
mm	1.75	0.25 0.10	1.45 1.25	0.25	0.49 0.36	0.25 0.19	5.0 4.8	4.0 3.8	1.27	6.2 5.8	1.05	1.0 0.4	0.7 0.6	0.25	0.25	0.1	0.7 0.3	8° 0°
inches	0.069	0.010 0.004	0.057 0.049	0.01	0.019 0.014	0.0100 0.0075	0.20 0.19	0.16 0.15	0.050	0.244 0.228	0.041	0.039 0.016	0.028 0.024	0.01	0.01	0.004	0.028 0.012	

Notes

1. Plastic or metal protrusions of 0.15 mm maximum per side are not included.
2. Plastic or metal protrusions of 0.25 mm maximum per side are not included.

OUTLINE VERSION	REFERENCES				EUROPEAN PROJECTION	ISSUE DATE
	IEC	JEDEC	EIAJ			
SOT96-1	076E03	MS-012				~~97-05-22~~ 99-12-27

Trigger amplifier with open collector output UZZ7001T

FEATURES

- Differential input trigger amplifier
- Designed for signal conditioning of magnetoresistive sensor bridges
- Open collector output
- Stabilized voltage supply source for external sensor bridges
- Comparator with temperature controlled hysteresis
- Wide temperature range
- Max. 16.5 V supply.

PINNING

PIN	SYMBOL	DESCRIPTION
1	SA	positive differential input
2	n.c.	not connected
3	n.c.	not connected
4	V_{CC}	supply
5	OUT	open collector output
6	GND	ground
7	VP	bridge supply
8	SB	negative differential input

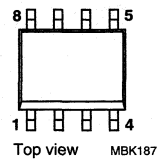

Fig.1 Simplified outline SOT96-1.

DESCRIPTION

The UZZ7001T is a differential input amplifier circuit with a trigger mechanism for application with magnetoresistive sensor bridges.

It is equipped with an open collector output and a voltage regulator for supply to an external sensor bridge.

An on-chip temperature sensor adapts the comparator hysteresis to the temperature dependent sensitivity of a typical magnetoresistive sensor such as the Philips KMZ family types.

QUICK REFERENCE DATA

SYMBOL	PARAMETER	CONDITIONS	MIN.	TYP.	MAX.	UNIT
V_{CC}	DC supply voltage	T_{amb} = –40 to +150 °C	4.5	5	16.5	V
I_{CC}	DC supply current	V_{CC} = 5 V	–	7.5	–	mA
V_{VP}	DC bridge supply voltage		–	3.3	–	V
I_{VP}	DC bridge supply current		–	–	–3	mA
T_{amb}	ambient operating temperature	V_{CC} = 5 V; note 1	–40	–	+150	°C

Note

1. Maximum power consumption according to power derating curve, see Fig.2.

LIMITING VALUES

In accordance with the Absolute Maximum Rating System (IEC 60134).

SYMBOL	PARAMETER	CONDITIONS	MIN.	MAX.	UNIT
V_{CC}	DC supply voltage	not protected against incorrect polarity	−0.5	+16.5	V
V_{SA}	maximum input voltage range	$t \leq 5$ s; $T_{amb} = 26 \pm 10$ °C	−0.5	tbf	V
V_{SB}	maximum input voltage range	$t \leq 5$ s; $T_{amb} = 26 \pm 10$ °C	−0.5	tbf	V
V_{OUT}	output voltage	not protected against incorrect polarity	−0.5	24	V
$I_{OUT(L)}$	maximum output current	low state; note 1	–	20	mA
$I_{OUT(H)}$	output leakage current	high state; notes 2 and 3	–	100	µA
$I_{OUT(rev)}$	maximum reverse current	$t \leq 5$ s; $T_{amb} = 26 \pm 10$ °C	–	tbf	mA
P_{tot}	total power dissipation	$V_{CC} = 16.5$ V; $I_{OUT} = 20$ mA; note 4	–	300	mW
T_{amb}	ambient operating temperature	$V_{CC} = 5$ V	−40	+150	°C
T_{stg}	storage temperature		−40	+150	°C
T_{sld}	soldering temperature	$t \leq 10$ s	–	260	°C

Notes

1. Low state: output transistor closed ($V_{OUT} < 1$ V; $V_{SA} > V_{SB}$).
2. High state: output transistor open ($V_{OUT} > 4$ V; $V_{SA} < V_{SB}$).
3. $V_{OUT} = 16.5$ V.
4. Maximum power consumption according to power derating curve, see Fig.2.

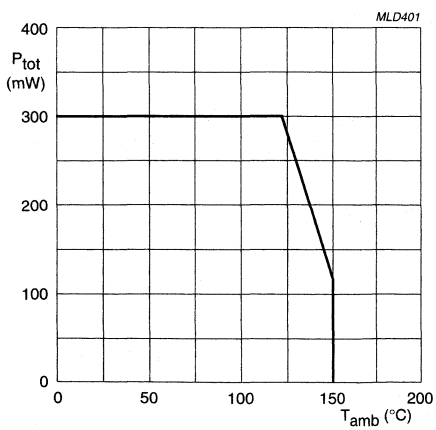

Fig.2 Power derating curve.

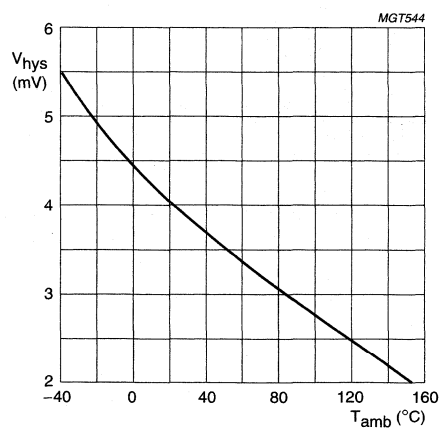

Fig.3 Hysteresis voltage as a function of temperature.

CHARACTERISTICS

T_{amb} = 26 °C; V_{CC} = 5 V; unless otherwise specified.

SYMBOL	PARAMETER	CONDITIONS	MIN.	TYP.	MAX.	UNIT
Supply conditions						
V_{CC}	DC supply voltage	T_{amb} = −40 to +150 °C	4.5	5	16.5	V
I_{CC}	DC supply current	T_{amb} = 26 ± 10 °C; V_{CC} = 5 V	6.5	7.5	8.5	mA
		T_{amb} = −40 to +150 °C; V_{CC} = 5 V	6	7.5	10	mA
Signal input characteristics						
f_{rm}	input frequency range		0	–	25000	Hz
V_{SA}	maximum input voltage range		−0.5	–	tbf	V
	operating input voltage range		1.4	1.65	1.9	V
V_{SB}	maximum input voltage range		−0.5	–	tbf	V
	operating input voltage range		1.4	1.65	1.9	V
V_{OFF}	input offset voltage		−2.1	–	2.1	mV
I_{BIAS}	input bias current	V_{CC} = 16.5 V; V_{SA} - V_{SB} = 0	0.1	–	1	µA
I_{OFF}	input offset current	V_{SA} - V_{SB} = 0	−75	–	75	nA
V_{HYS}	input hysteresis voltage	notes 1 and 2	3	4	7	mV
Signal output characteristics						
V_P	DC bridge supply voltage		3.1	3.3	3.5	V
I_P	DC bridge supply current		–	–	−3	mA
$I_{OUT(L)}$	output current	low state; note 3	-	–	20	mA
$I_{OUT(H)}$	output leakage current	high state; notes 4 and 5	-	–	1.1	µA
V_{OUT}	output saturation voltage	T_{amb} = −40 to +150 °C; low state; note 3				
		I_{OUT} = 10 mA	0.15	–	0.5	V
		I_{OUT} = 20 mA	0.3	–	1	V
t_r	output signal rise time	low 10% to high 90%; note 6	5	12	20	µs
t_f	output signal fall time	high 90% to low 10%; note 6	0.05	0.5	1	µs
t_{df}	output signal HL-delay		1.84	2.3	2.76	µs
		T_{amb} = −40 to +150 °C	1.5	–	3.5	µs
Environmental conditions						
	ESD protection of output pins V_{CC}, OUT and GND	compliance to IEC 0801-2 (IV); note 7	2	–	–	kV
	ESD protection of sensor interface pins SA, SB and VP	compliance to IEC 0801-2 (IV); note 8	0.3	–	–	kV

Notes

1. Input hysteresis voltage is the difference between higher and lower switching point referred to input.
2. Temperature dependence of voltage hysteresis; see Fig.3.
3. Low state: output transistor closed (V_{OUT} < 1 V; V_{SA} > V_{SB}).
4. High state: output transistor open (V_{OUT} > 4 V; V_{SA} < V_{SB}).

5. V_{OUT} = 16.5 V.
6. See Fig.5 test circuit.
7. Output pins are designed for electrostatic sensitivity with field strengths up to 2 kV according to Human Body Model (HBM), MIL-STD-883, method 3015.
8. Differential input pins are designed for electrostatic sensitivity with field strengths up to 0.3 kV according to Human Body Model (HBM), MIL-STD-883, method 3015.

FUNCTIONAL DESCRIPTION

The UZZ7001 is a differential input trigger amplifier circuit designed for application with magnetoresistive sensor bridges. The block diagram is shown in Fig.4.

The circuit contains an open collector output stage and a voltage regulator for supply to an external sensor bridge.

An on-chip temperature sensor adapts the comparator hysteresis to the temperature dependent sensitivity of a typical magnetoresistive sensor from the Philips-MR. Sensor KMZ family.

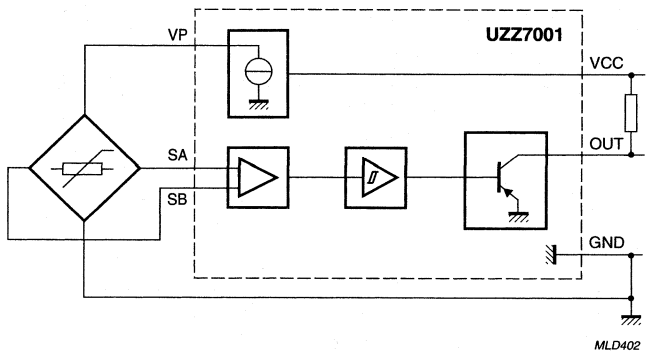

Fig.4 Circuit block diagram.

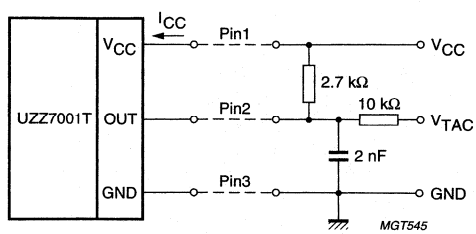

Fig.5 Test and application circuit.

PACKAGE OUTLINE

SO8: plastic small outline package; 8 leads; body width 3.9 mm **SOT96-1**

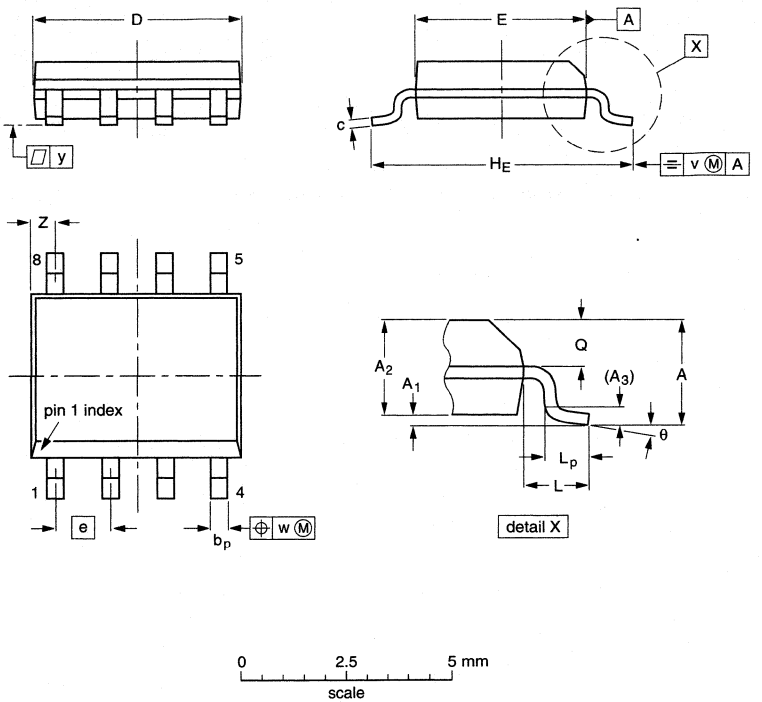

DIMENSIONS (inch dimensions are derived from the original mm dimensions)

UNIT	A max.	A_1	A_2	A_3	b_p	c	$D^{(1)}$	$E^{(2)}$	e	H_E	L	L_p	Q	v	w	y	$Z^{(1)}$	θ
mm	1.75	0.25 0.10	1.45 1.25	0.25	0.49 0.36	0.25 0.19	5.0 4.8	4.0 3.8	1.27	6.2 5.8	1.05	1.0 0.4	0.7 0.6	0.25	0.25	0.1	0.7 0.3	8° 0°
inches	0.069	0.010 0.004	0.057 0.049	0.01	0.019 0.014	0.0100 0.0075	0.20 0.19	0.16 0.15	0.050	0.244 0.228	0.041	0.039 0.016	0.028 0.024	0.01	0.01	0.004	0.028 0.012	

Notes

1. Plastic or metal protrusions of 0.15 mm maximum per side are not included.
2. Plastic or metal protrusions of 0.25 mm maximum per side are not included.

OUTLINE VERSION	REFERENCES				EUROPEAN PROJECTION	ISSUE DATE
	IEC	JEDEC	EIAJ			
SOT96-1	076E03	MS-012				~~97-05-22~~ 99-12-27

MAGNETORESISTIVE SENSORS FOR ANGLE MEASUREMENT

APPLICATION NOTE

Contactless Angle Measurement using KMZ41 and UZZ9000

AN00023

Author(s):

Klaus Dietmayer

Marcus Weser

Systems Laboratory Hamburg, Germany

Keywords

UZZ9000

KMZ41

Contactless Angle Measurement

Magnetoresistive Sensors

Date: 24 March 2000

Contactless Angle Measurement Using KMZ41 and UZZ9000

Application Note AN00023

Summary

This report describes how to build a MR based measurement system using the magnetoresistive sensor KMZ41 and the sensor signal conditioning IC UZZ9000 available from Philips Semiconductors.

The first section gives an introduction into MR technology. It is shown that the magnetoresistive effect is naturally an angular effect recommending its use for angle measurement applications. The next sections describe the basic function of a system consisting of the sensor KMZ41 and the sensor signal conditioning IC UZZ9000. The KMZ41 sensor comprises two Wheatstone bridges on one substrate. This gives a very good matching of mechanical and electrical properties. The signal conditioning IC UZZ9000 is optimised for the usage with the KMZ41 but can also be used in conjunction with any other sensor providing two sinusoidal signals with 90°-phase shift, such as resolver applications, Hall sensors and GMR sensor. This mixed signal IC provides an analog, ratiometric output signal that allows a direct replacement of present potentiometer solutions. The input angular range can be adjusted between 0° to 30° and 0° to 180° in steps of 10°. Also, the zero point of the mechanical angle is user programmable between +/- 5° in steps of 0.5°. Both KMZ41 and UZZ9000 are specified between -40°C to +150°C for normal operation.

The last section describes the non-ideal cases and their impact on system accuracy. The error analysis based on a 3-Sigma confidence interval shows that the absolute accuracy is better than 0.6° in a temperature range from -40°C to +85°C. This corresponds to an relative error better than 0.4% referred to 180° full scale. At 150°C, the maximum absolute error is better than 1.2°. The resolution of the measurement system is better than 0.1° at all temperatures. If a field strength of 100 kA/m (1250 Gauss) is used for the magnetic system, then the hysteresis lies within the resolution and is therefore not measurable.

Contactless Angle Measurement Using KMZ41 and UZZ9000

Application Note AN00023

Contents

Contactless Angle Measurement using KMZ41 and UZZ9000

Application Note AN00023

1. INTRODUCTION

Magnetoresistive sensors (MR sensors) of Philips Semiconductors make use of the fact that the electrical resistance of certain ferromagnetic alloys, such as permalloy, is influenced by external magnetic fields. This solid state magnetoresistive effect - or anisotropic magnetoresistance (AMR) - is easily realised in thin film technology, allowing the production of precise but also cost-effective sensors.

As the magnetoresistive effect is naturally an angular effect, its utilization for contactless angle measurement systems fits perfectly. The underlying principle is simple: the electrical resistance of the permalloy strip changes with the angle between the internal magnetization vector in the strip and the vector of electrical current flowing through it. Consequently, to achieve accurate measurements, the only condition to be met is that the internal magnetization vector of the permalloy must directly follow an external magnetic field vector. This is ensured when using an external field strength much higher than the internal magnetization. As this strong external field saturates the sensor, the actual field strength has no impact on the measurements. Only the direction of the field is evaluated. This leads to the following advantages of magnetoresitive angle measurement systems:

- Independence of magnetic drift during life time.
- Independence of magnetic drift with temperature.
- Independence of mechanical assembly tolerances.
- Independence of mechanical shifts caused by thermal stress.

Moreover, the small offset drift of the sensor signals requires no compensation for temperature effects, which simplifies implementation.

Additionally, MR based systems show the same advantages as all other contactless measurement systems; they are free of wear and they can be completely encapsulated making the sensor modules robust regarding contamination and mechanical destruction. All these advantages recommend magnetoresistive angle measurement systems for applications requiring very robust and precise but also cost-effective solutions. This, for example, is the case in all automotive applications.

To support users who want to build up a contactless angle measurement system, Philips Semiconductors provides a two-chip solution consisting of the magnetoresistive sensor KMZ41 and the sensor signal conditioning IC UZZ9000. The UZZ9000 was designed for the usage with the KMZ41 and therefore provides an optimised interface to this sensor. It has a standard analog output that operates ratiometrically with respect to supply voltage. Consequently, this two-chip system may directly replace present potentiometer solutions.

The intention of this paper is to provide the necessary background information for system design. After giving a short introduction in the MR technology for angle measurement and discussing basics of possible system set-ups, both the KMZ41 and the UZZ9000 are described in more detail. Besides electrical characteristics and functional behaviour, main items are the correct choice of the magnet

arrangement and the trimming procedure to compensate the static offsets of the sensor. The last section describes non-ideal cases and their impact on system accuracy. A proposal is made how to calculate the achievable system accuracy under different system constraints.

2. MAGNETORESISTVE SENSOR TECHNOLOGY FOR ANGLE MEASUREMENT

Magnetoresistive (MR) sensors make use of the magnetoresistive effect, the property of a current carrying magnetic material to change its resistance in the presence of an external magnetic field. Figure 1 shows a strip of ferromagnetic material, called permalloy.

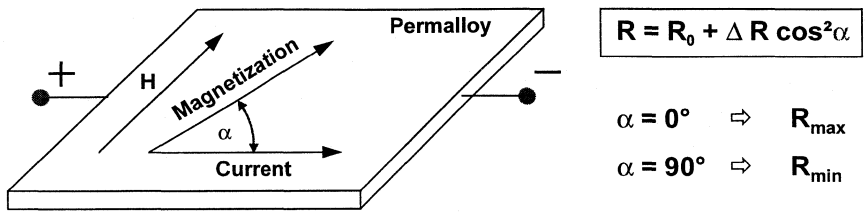

Figure 1: The magnetoresistive effect in permalloy

Assume that, when no external magnetic field is present, the permalloy has an internal magnetization vector M parallel to the current flow ($\alpha = 0$). If an external magnetic field H is applied, parallel to the plane of the permalloy but perpendicular to the current flow, the internal magnetization vector of the permalloy will rotate around an angle α. As a result, the resistance R of the permalloy will change as a function of the rotation angle α, as given by:

$$R = R_0 + \Delta R_0 \cos^2 \alpha \qquad (1)$$

R_0 and ΔR_0 are material constants. To achieve an optimum sensor characteristics, Philips use Ni19Fe81, which has a high R_0 value and low magnetostriction. With this material, ΔR_0 is in the order of 2 to 3%. It is obvious from this quadratic equation that the resistance to magnetic field relation is non-linear. It becomes also clear that the magnetoresistive effect is naturally an angular effect recommending its utilisation for angle measurement applications. Here the external magnetic field carries the measurement information between sensor and physical value to be measured.

Having this principle of operation in mind, it becomes clear that the precondition to achieve accurate measurements is that the internal magnetization vector M must directly follow the vector H of the external field. This can be achieved by applying an external field H much higher than the internal field of approximately 3 kA/m. When using the KMZ41 for angle measurement, it is recommended to provide an external field of at least

$$H \geq 100 \text{ kA/m} \quad (1250 \text{ Gauss}). \qquad (2)$$

In that case the two vectors M and H are virtually parallel to each other.

Normally, the external magnetic field is generated by permanent magnets, e.g. SmCo types. Figure 2 shows a basic set-up, where the angular position of a rotating shaft is measured with the help of the permanent magnet fixed to it.

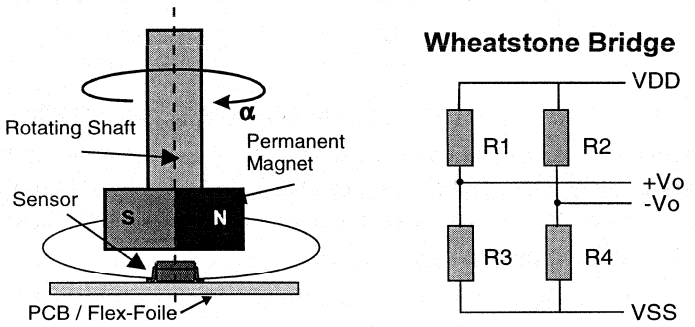

Figure 2 Basic arrangement of sensor and magnet for contactless angle measurement.

The magnetoresistive angle sensors of Philips Semiconductors are etched on a silicon substrate, with four permalloy strips arranged in a Wheatstone bridge configuration. According to the basic relationship given by Equation (1), the differential output signal (+Vo, -Vo) of such a Wheatstone bridge is proportional to $\sin 2\alpha$. This means that a sensor comprising one Wheatstone bridge can measure an angular range of 90°. This is visualised in Figure 3.

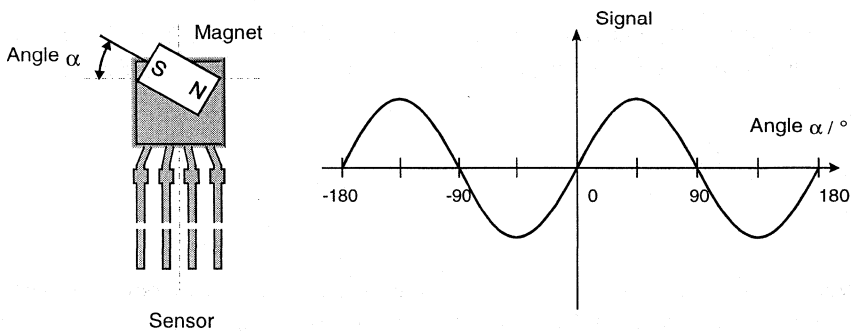

Figure 3: Output signal from a single Wheatstone bridge sensor

Apart from the limited angular range, the single bridge sensor shows another disadvantage regarding signal evaluation. As the signal amplitude changes with temperature, the output signal of the sensor forces the user to implement a temperature compensation. This is avoided when using a two-bridge arrangement combined with a signal evaluation explained below. Figure 4 shows the principle.

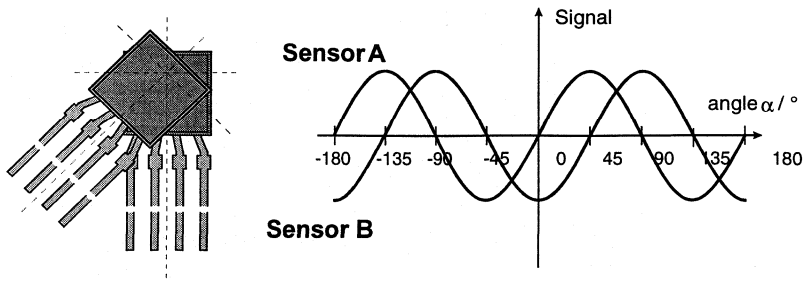

Figure 4 Output signal from a double Wheatstone bridge sensor (KMZ41)

The two sensor bridges are positioned at an offset angle of 45° to each other. In this arrangement, the two output signals show an electrical phase shift of 90°. The two signals are therefore proportional to $\sin 2\alpha$ and $\cos 2\alpha$, respectively. It can be proved easily that these two signals now allow an evaluation of a 180° angular range.

Even in this arrangement, the signal amplitudes will change with temperature. However, both bridges are processed in the same thin film process steps on the same substrate and they will therefore show very similar characteristic. Assuming that both output signals have no offsets or offsets have been compensated previously, the output signals can be described mathematically as follows:

$$X(\alpha,T) = X_0(T)\sin 2\alpha \tag{3}$$

$$Y(\alpha,T) = Y_o(T)\cos 2\alpha \tag{4}$$

Assuming further that the amplitudes of both signals are really identical ($X_0 = Y_0$), the unknown angle α can be determined without any error from the signals *X* and *Y* as given by Equation (5):

$$\alpha = \frac{1}{2}\arctan\left(\frac{X}{Y}\right) \tag{5}$$

This result does not depend on the absolute amplitude of the signals. Consequently, temperature measurement and compensation of the temperature effects is not required.

Of course, due to the non-ideal manufacturing process, a real sensor will not show the ideal behaviour assumed above. A detailed discussion of these non-ideal cases and their impact on system accuracy can be found in section 7.

3. SYSTEM OVERVIEW

An angle measurement system requires one sensor KMZ41 and one sensor signal evaluation IC UZZ9000. Figure 5 shows the block diagrams of both components:

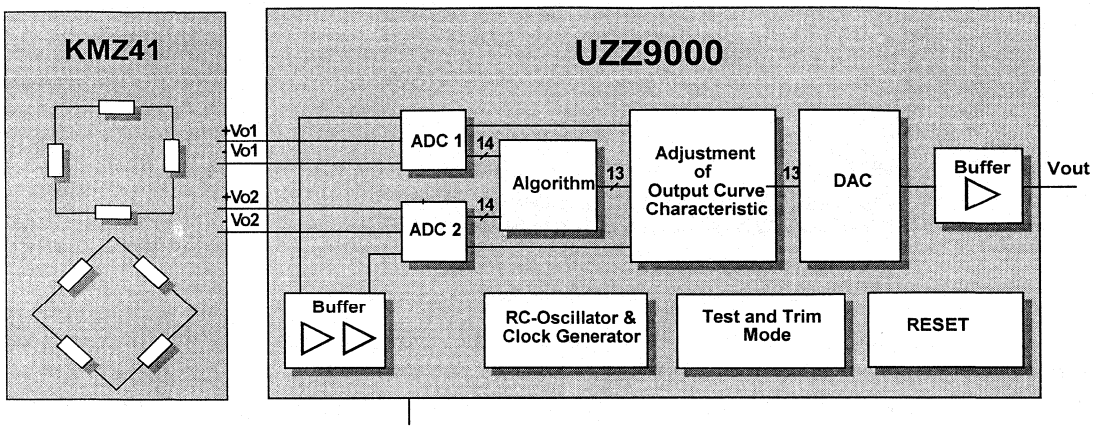

Figure 5: Block diagram of the two-chip measurement system

The differential sensor signals +/-Vo1 and +/-Vo2 of the KMZ41 are sampled by the UZZ9000 input stage and then are converted into the digital domain. This conversion is done with the help of two separate but simultaneously clocked Sigma-Delta AD converter (4). The digital representations of the two signals are then used to calculate the angle. For this calculation the CORDIC algorithm is used. CORDIC is nothing else than an iterative way to calculate the inverse tangent function of both signals without extensive numerical overhead. Details of the CORDIC algorithm can be found in reference (3).

Afterwards, the current angle represented as a 13-bit digital value is converted back into the analog domain. The output characteristic of the DA converter is shown in Figure 6. This DA converter, as well as the ADCs in the input stage, operates ratiometric to the analog supply voltage (VDDA, VSSA). This means that all analog signals are represented as a fraction of this analog supply voltage. **Note that due to this ratiometric operation, the same analog voltage as used for the UZZ9000 must supply the KMZ41 sensor.** This guarantees that variations of the supply voltage will have no impact on system accuracy.

As can be seen from Figure 6, the mechanical angular range is linearly converted into analog voltages between 5.5% and 94.5% VDDA. This output voltage range represents the normal operation mode. Below and above this valid range lie diagnostic areas. The output signal enters these areas only in cases of errors. An error condition occurs due to a shortcircuit of the output VOUT to the supply voltage or ground, or if the magnet has been lost and no valid input signals are available.

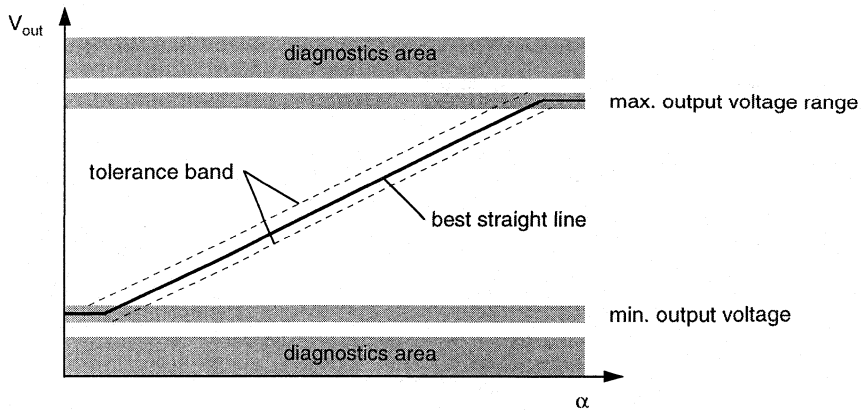

Figure 6: UZZ9000 output characteristic

To adapt the UZZ9000 to different application requirements, the mechanical input angular range can be adjusted between 0° to 30° and 0° to 180° in steps of 10°. This function adapts the fixed output voltage range to the different possible input ranges to reduce the absolute angular error of the DAC and thus the overall system error. Moreover, even the zero point of the output curve can be adjusted in the range of +/-5° to compensate for tolerances. Both settings are derived from an analog voltage the user must provide at special pins of the UZZ9000 during reset. Details on how to adjust the UZZ9000 to different angular ranges and zero point offsets can be found in section 5

As mentioned before, the sinusoidal input signals coming from the KMZ41 may have a static offset that must be compensated to get accurate results. This compensation is done separately for each channel by providing an analog voltage to special pins of the UZZ9000. These voltages (OFF1, OFF2) must be provided continuously during operation as compensation is done real time and not stored at system start. As KMZ41 and UZZ9000 are not sold as one unit, the user is responsible for providing the correct compensation voltages. Due to the ratiometric nature, the offset voltages must be referenced from the same analog voltage VDDA, for example, using a laser trimmable resistor divider. The UZZ9000 provides some special functions for the trimming process, which are described in section 5.

Apart from the features described above, the UZZ9000 provides an on-chip RC-Oscillator generating the clock for the IC's state machine. Consequently, no external clock reference is required for system operation. Moreover, the UZZ9000 has a power-down and power-up reset with build-in hysteresis. This reset block automatically generates a reset signal during power-on or if the save voltage range is left.

4. SENSOR KMZ41

The magnetoresitive sensor KMZ41 of Philips Semiconductors has been designed for angle measurement applications, preferably in combination with the signal conditioning IC UZZ9000. The application relevant items are discussed in the following sections. The KMZ41 properties affecting the system accuracy are discussed in section 7. Please refer to the latest data sheet to get actual specification data of the KMZ41.

4.1 Layout of the KMZ41 Sensor

The KMZ41 comprises two complete Wheatstone bridges made on the same substrate in thin film technology. Therefore both bridges show a very good matching regarding electrical and mechanical properties. Figure 7 shows the layout of the sensor.

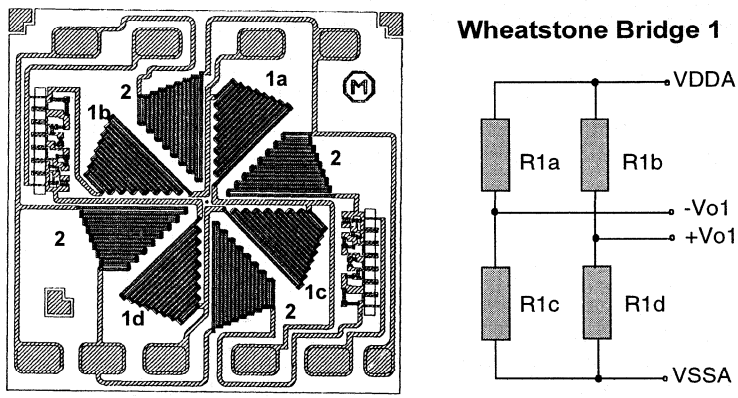

Figure 7: Layout of the double bridge sensor KMZ41.
1a to 1d indicate the sensitive elements of Wheatstone bridge 1

Moreover, the different sensitive elements of Wheatstone bridge 1 are marked. Both bridges have separate connections for supply voltage. The die size of the KMZ41 is about 1.5 mm^2 with a sensitive area of about 1 mm^2.

In order not to influence the external magnetic field and therefore the accuracy of measurements, the lead frame of the KMZ41 is made without use of ferrous material. **Please note that with respect to a good system design it is also important not to place elements consisting of ferrous material very close to the KMZ41.**

4.2 Input and Output Signals

The KMZ41 is housed in a SO8 package. The pinning is given in TABLE 1.

TABLE 1: Pinning of the KMZ41

Pin	Symbol	Type*	Description
1	-Vo1	A	negative output voltage of bridge 1
2	-Vo2	A	negative output voltage of bridge 2
3	Vcc2	A	supply voltage bridge 2
4	Vcc1	A	supply voltage bridge 1
5	+Vo1	A	positive output voltage of bridge 1
6	+Vo2	A	positive output voltage of bridge 2
7	GND2	A	Ground bridge 2
8	GND1	A	Ground bridge 1

* A = analog pin, D = digital pin

Apart from the two separate supplies, the KMZ41 provides two differential signal lines for each Wheatstone bridge. The following discussion assumes that the external magnetic field is strong enough to saturate the sensor. This ensures that each bridge of the KMZ41 has a sinusoidal output voltage as given in Figure 8.

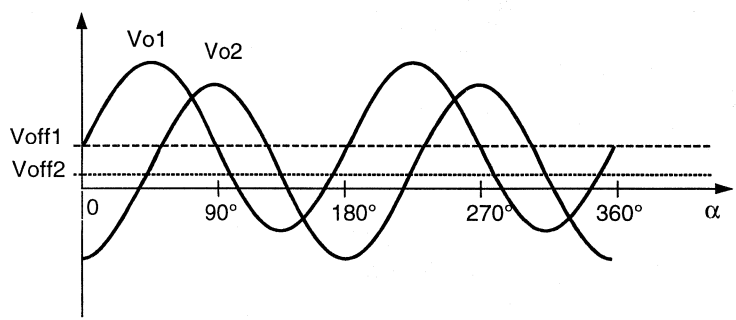

Figure 8: Output signals of the KMZ41

Ideally, these signals would have no static DC offset. However, static offsets cannot be completely avoided due to manufacturing tolerances. As these DC-offsets Voff1 and Voff2 affect the system accuracy, they must be compensated by the signal conditioning IC. The UZZ9000 provides special build-in functions for this task. Please note that Figure 8 is drawn exaggerated to emphasize the effect, the actual sensor has much smaller offsets.

The amplitudes of the output signals depend on both the supply voltage and the ambient temperature. Because of the ideal thermal coupling, the temperature coefficients of both bridges are almost identical. The MR effect exhibits a negative temperature coefficient. This means that with higher temperatures, the signal amplitude decreases and vice versa. A short example demonstrates this effect:

The typical temperature coefficient (TCVpeak) for the KMZ41 is -0.31 % / K. Consequently, based on a known peak voltage at room temperature, the peak voltage at any other temperature T can be calculated as follows:

$$Vpeak_T = Vpeak_{25°C} * \left(1 + (T - 25°C) * \frac{TCVo}{100\%}\right) \quad (6)$$

To give an example, the peak voltage of the KMZ41 at room temperature and 5V supply is typically $Vpeak_{25°C}$ = 78 mV. Consequently, at T = 125 °C, a peak voltage of $Vpeak_{125°C}$ = 53.8 mV can be expected. At -40°C, however, the peak voltage increases to $Vpeak_{-40°C}$ = 93.7 mV. This effect does not affect the system accuracy when using the signal processing implemented in the UZZ9000.

Besides the signal amplitude, also the DC offset drifts with temperature. However, this offset drift is so small that it needs no compensation in normal applications. The offset drift and its impact on system accuracy is discussed in section 7.

4.3 Magnets and Magnet Arrangements

It is recommended to use the KMZ41 in a magnetic field saturating the sensor. This is guaranteed when the field strength is above 100 kA/m in the sensitive area of the sensor.

The most simple magnet arrangement is that of a block magnet rotating directly above the KMZ41 as depicted in Figure 2. The effective magnetic field strength of such a block magnet arrangement depends on the distance between magnet and sensor, magnet size and magnet material. Because of strong field requirements, the usage of rare earth magnets such as SmCo or NeFeB is recommended.

Figure 9 shows the field strength of three sample magnets as a function of the distance between magnet and the top of the sensor package. It becomes clear that only the SmCo type achieves field strengths of 100 KA/m and more for distances below 0.8 mm. Its dimension of 8x3x7.5 has been chosen due to economic aspects and is used in several applications. Stronger fields allowing larger distances, this can be achieved easily when using thicker but more expensive magnets, e.g. a SmCo 8x4x7.5. Please note that the underlined dimension characterises the direction of magnetization.

In low-end applications, however, a low system price may be more important than excellent system accuracy. As a consequence, here it may be adequate to use cheaper magnets not saturating the sensor, e.g. FXD types. The additional error induced by this measure is discussed in section 7.

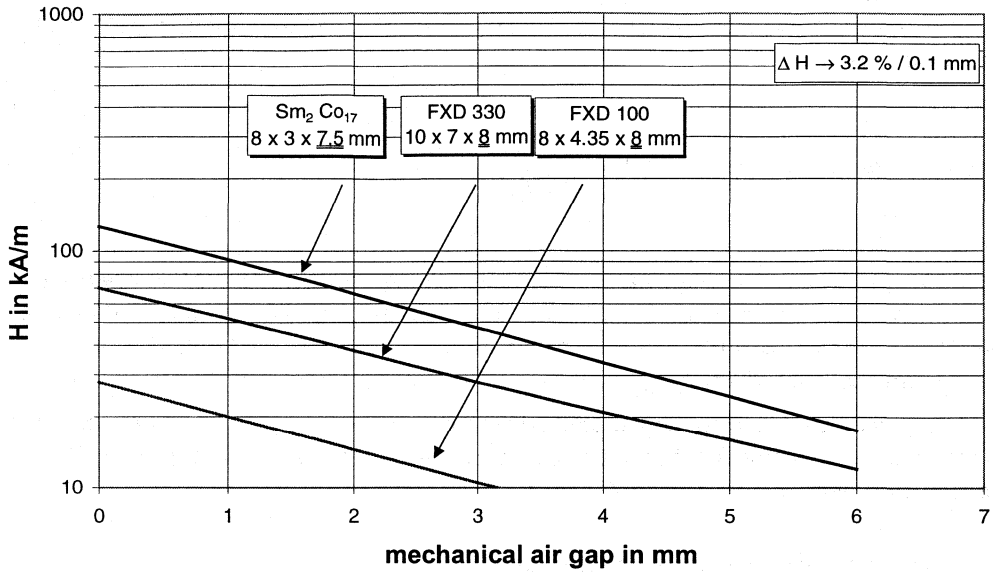

Figure 9: Field strength in the sensitive plane of the KMZ41 in dependence of the air gap between the top of the sensor package and the block magnet. The underlined dimension characterises the direction of magnetization.

4.4 Other Mechanical Set-ups

The usage of a block magnet rotating above the sensor is only one simple possibility for a magnetic system set-up. Meanwhile, several application specific solutions were built. These set-ups use flux rings and flux guides. The targets of optimisation are:

- Concentration of the magnetic field in order to allow the usage of weaker magnets.
- Making the magnetic field homogenous in a wider range to tolerate larger mounting tolerances.
- Shielding of the primary field against external fields.

Figure 10 shows the general arrangement of such a magnetic system. The inner walls of the flux ring carry the permanent magnets. This unit rotates around the fixed sensor. Such a magnet arrangement (diameters, dimensions of the flux ring and the magnets) must be dimensioned application-specific. A final solution will be a compromise between system accuracy and system costs.

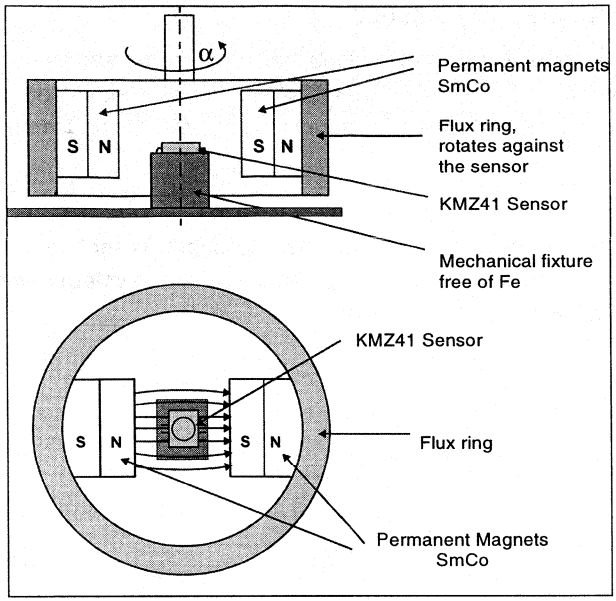

Figure 10: Mechanical set-up using a flux ring for shielding against external fields and 2 permanent magnets generating a homogenous field inside the ring

5. SIGNAL CONDITIONING IC UZZ9000

The UZZ9000 is a mixed signal IC for angle calculation. It combines two sinusoidal signals (sine and cosine) into one single linear output signal. The UZZ9000 can be used in conjunction with any sensor that encodes a mechanical angle into two sinusoidal signals with 90° phase shift.

5.1 General Description

The basic operation of the UZZ9000 has already been described in section 3. Within this section, some more details should be addressed that might be useful for a system designer. The detailed block diagram of the UZZ9000 is given in Figure 11.

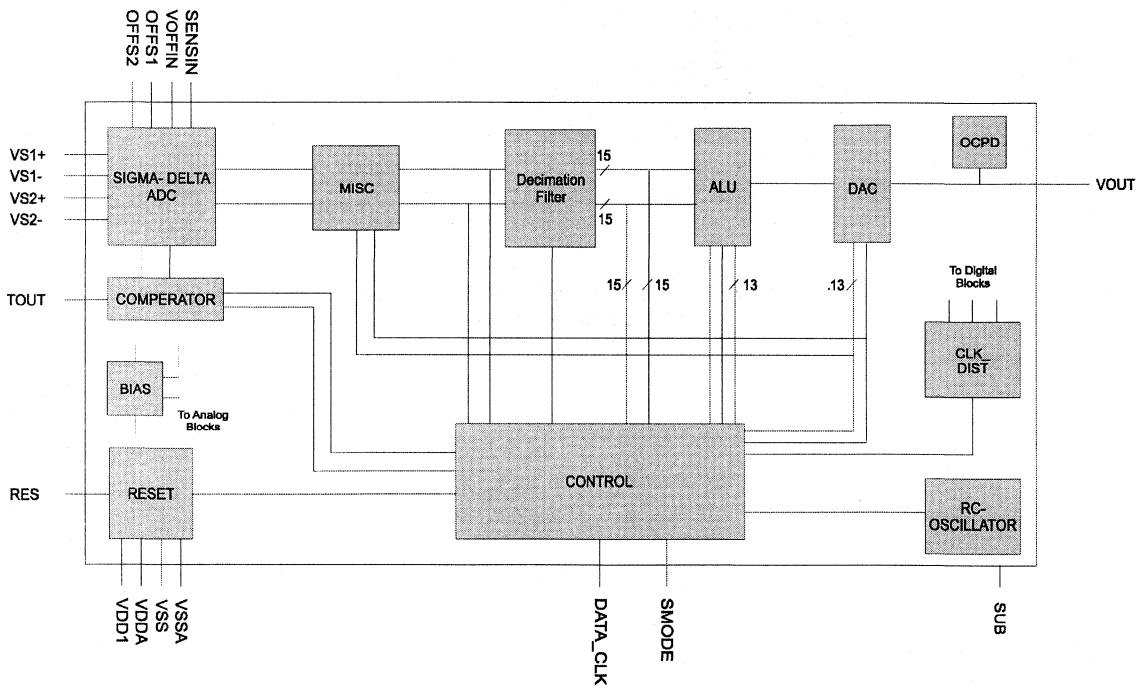

Figure 11: Detailed block diagram of the UZZ9000

The following list gives a short description of the relevant blocks.

1. The **ADC** block contains two Sigma Delta AD converters, a sensor offset correction circuitry and the circuitry required for the sensitivity adjustment and offset adjustment of the chip output voltage curve.

2. **DF** stands for the two digital low pass decimation filter which convert the low resolution high speed bit stream coming from the Sigma Delta converters into a low speed digital word.
3. The **ALU** block derives an angle value from the two digital inputs using the CORDIC algorithm
4. The **DAC** converts the digital output of the ALU block to an analog output voltage.
5. The block **CNTRL** provides the clock and the control signals for the chip
6. The **COMP** block generates binary output signals used for sensor trimming.
7. The **RESET** block supplies a reset signal during power-up and power-down when the power supply is below a certain value
8. The **OSC** unit generates the master clock

On entering the IC, the analog measurement signals are converted to digital data by an ADC. The ADC is a Sigma-Delta modulator, employing a 4th order continuous time architecture, with an over-sampling ratio of 128 to achieve high resolution. The output of the converter is a digital bit-stream at the over-sampling frequency of typically 500 kHz. The bit stream is fed into a decimation filter which performs both low pass filtering and down-sampling. There are two input channels of the IC, each of which has its own ADC and decimation filter. The two decimation filter outputs are digital words of 15-bit at a lower frequency of typically 3.9 kHz. This is the typical sampling frequency of the sensor system. The digital representations of the two signals are then used to calculate the current angle. This calculation is done using the so-called CORDIC algorithm. The angle is represented with a 13-bit resolution. A resistive-string DAC converts this digital data into an analog voltage output.

The UZZ9000 has an overall accuracy better than 0.45°. This limit holds at all angular ranges up to 180° and over the specified ambient temperature range of -40°C to +150°C. Details of timing, input and output characteristic and the trimming process are discussed in the following sections. The following TABLE 13 gives the pinning of the UZZ9000 that comes in a standard SO24 package.

TABLE 2: Pinning of the UZZ9000

Pin	Symbol	I/O*	Type*	Description
1	+Vo2	I	A	positive output voltage of sensor 2 (Wheatstone bridge 2)
2	+Vo1	I	A	positive output voltage of sensor 1 (Wheatstone bridge 1)
3	VDD	S	A	digital supply
4	VSS	S	A	digital ground
5	VSSA	S	A	analog ground
6	RES	I	D	resets the digital part of the UZZ9000, pin is active high. If not used, pin can be left unconnected (internal pull-down resistor) or connect it to ground.
7	TEST1	I	D	used for production tests, can be left unconnected (internal

Pin	Symbol	I/O*	Type*	Description
				pull-down resistor) or connect it to ground
8	TEST2	O	D	used for production tests, must be left unconnected
9	DATA_CLK	I	D	data clock, used when setting the UZZ9000 into trim mode, can be left unconnected (internal pull-down resistor) or connect it to ground
10	SMODE	I	D	serial mode programmer, used when setting UZZ9000 into trim mode, can be left unconnected (internal pull-down resistor) or connect it to ground
11	TEST3	O	D	used for production tests, must be left unconnected
12	VOUT	O	A	Voltage output connected to the DAC that converts the digital representation of the angle into the analog domain (normal operation mode), or to diagnostic voltages (in the case of an error).
13	SENSIN	I	A	Trimming input for sensitivity (different angular ranges) of the output curve.
14	VOFFIN	I	A	Trimming input for zero point adjustment of the output curve.
15	OFF2	I	A	offset trimming input for sensor 2 (Wheatstone bridge 2)
16	OFF1	I	A	offset trimming input for sensor 1 (Wheatstone bridge 1)
17	VDDA	S	A	analog supply
18	VSSA	S	A	analog ground
19	TEST4	I	D	used for production tests, can be left unconnected (internal pull-down resistor) or connect it to ground
20	TEST5	I	D	used for production tests, can be left unconnected because of an internal pull-down resistor or connect it to ground
21	VDD	S	A	digital supply
22	TOUT	O	D	used in trim mode, gives the offset corrected signal of sensor 1 or sensor 2, must be left unconnected in application
23	-Vo2	I	A	negative output voltage of sensor 2 (Wheatstone bridge 2)
24	-Vo1	I	A	negative output voltage of sensor 1 (Wheatstone bridge 1)

* A = analog pin, D = digital pin, S = supply, I = input, O = output

5.2 Characteristics of Input and Output Signals

The input stage of the UZZ9000 expects sinusoidal signals. The electrical characteristics of these signals are defined in TABLE 3. These values correspond to the KMZ41 sensor specification.

TABLE 3: Limits of the UZZ9000 input signals

Parameter	Min	Max	Units
Analog supply voltage	4.5	5.5	V
Differential input voltage range (peak voltage) referred to analog supply voltage (including any offset)	+/- 6.6*	+/- 28	mV / V
Differential input voltage offset referred to analog supply voltage	-2	+2	mV / V
Common mode range referred to the analog supply voltage	490	510	mV / V

* If signals of both channels are below this limit at the same time, the magnet lost error condition becomes active (see section 5.6).

The output stage of the UZZ9000 is able to drive any external output load as defined in TABLE 4. Please note that an external pull-up or pull-down resistor is not required for applications as those resistors are already provided on-chip.

TABLE 4: Limits for the output load of the UZZ9000

Parameter	Symbol	Min	Nom	Max	Units
Output load pull down	R_{Lpd}	2.5			kΩ
Output load pull up (+6V to +14V)	R_{Lpu}	5			kΩ
Output capacitance *	C_L		0.05	200	nF

* If the output capacitance is greater than 50 pF (nominal value), a resistor of R >= 300 Ω has to be connected in series with the output to ensure stability of the output stage. As this affects the accuracy, the capacitive load should be limited to the nominal value.

The valid output voltage range for a valid angle is nominally 5.5% to 95% VDDA. Above and below this range is the diagnostic region. This region is discussed further in section 5.5. TABLE 5 and Figure 12 describe the details of the output curve characteristic.

TABLE 5: Partitions of the UZZ9000 output curve

Parameter	Symbol	Min	Nom	Max	Units
Normal operating range:					
Min Value	$V_{Out\_N\_Min}$	5.0	5.5	6.0	% VDDA
Max Value	$V_{Out\_N\_Max}$	94.0	94.5	95.0	% VDDA
Lower diagnostic range:	V_{Out_DL}	0		4	% VDDA
Upper diagnostic range:	V_{Out_DU}	96		100	% VDDA

As can be seen from Figure 12, the mechanical input angular range between $\alpha 1$ and $\alpha 2$ is linearly converted to output voltages between 5.5% VDDA and 94.5% VDDA. The best straight line is the ideal output characteristic of the UZZ9000. The tolerance band in Figure 12 indicates the limits in which the actual output curve may be found.

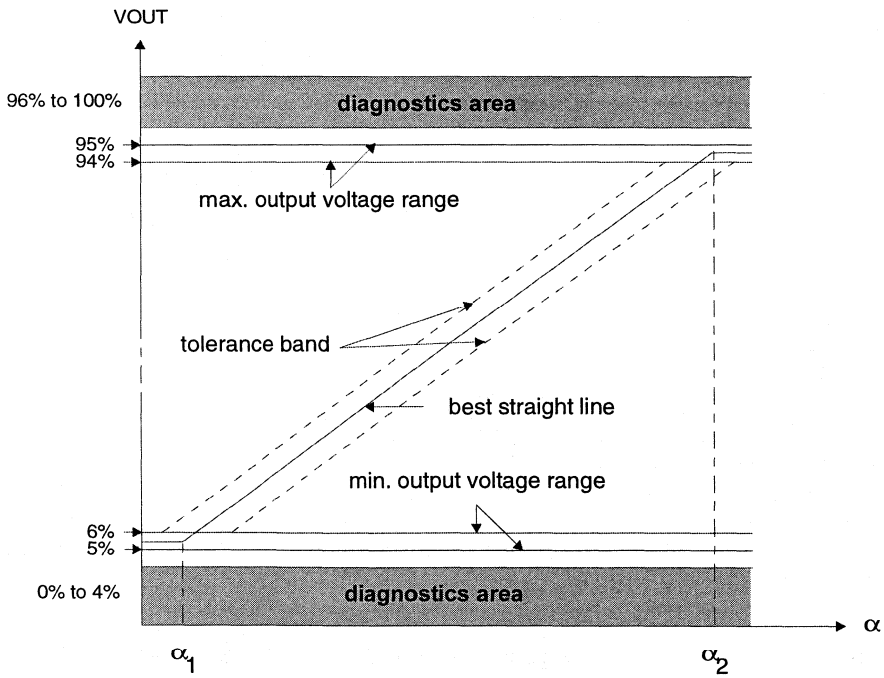

Figure 12: Detailed output curve characteristic of the UZZ9000

The maximum overall angular error under any specified conditions is guaranteed to be less than 0.45°. Assuming an angular range of 180°, the output voltage error is calculated as follows:

$$E_{180°} < \frac{0.45°}{180°}(94.5-5.5)\,\%\,\mathrm{VDDA} = 0.22\,\%\,\mathrm{VDDA} \qquad (7)$$

It becomes clear that this output voltage error directly depends on the chosen angular range. The absolute angular error, however, is approximately the same in every angular range.

5.3 Adjusting the Angular Range and the Zero Point Offset

In order to fit to different applications, the mechanical input angular range of the UZZ9000 and the zero point of the output curve are user programmable. This section describes how to select a certain mode.

5.3.1 Changes of the Output Curve Characteristic

By changing the angular range, the output curve is manipulated as shown in Figure 13. Without any zero point offset, the sensitive part starts at mechanically 0° ($\alpha 1 = 0°$). When using a KMZ41 sensor, the maximum angular range $\Delta\alpha$ is 0° to 180°. For the UZZ9000, smaller angular ranges can be set. In this case, $\alpha 2$ becomes smaller than 180° and the output curve is clipped at this position. The location of discontinuity X_D (change from lower to upper clipping area) depends on the adjusted range and can be calculated as follows:

$$X_D = \Delta\alpha + \frac{180° - \Delta\alpha}{2} \qquad (8)$$

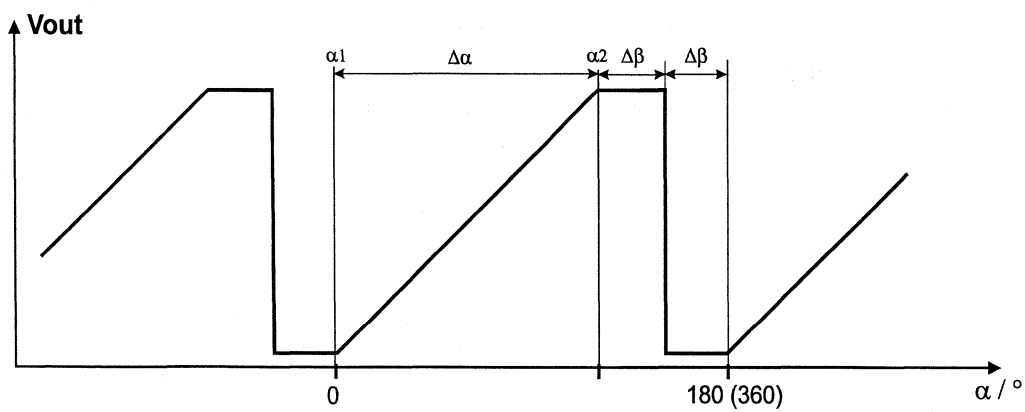

Figure 13: Output curve for different angular ranges. Note that when using MR-sensors (KMZ41), the signal period is 0° to 180° as the signals are proportional to sin2α and cos2α.

In order to compensate tolerances, the zero point of the output curve can be shifted by +/- 5° in steps of 0.5°. The effect of this measure is shown in Figure 14. Now α1 is no longer identical with mechanically 0°, but with the zero point shift X_{off}. Consequently, the location of discontinuity X_D calculates according to Equation (9):

$$X_D = x_{Off} + \Delta\alpha + \frac{180° - \Delta\alpha}{2} \quad (9)$$

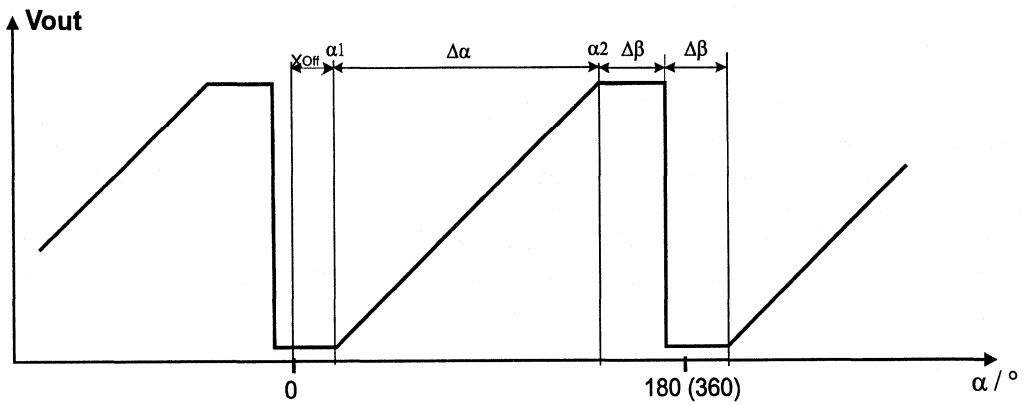

Figure 14: Output curve for different angular ranges including a zero point offset. Note that when using MR-sensors (KMZ41), the signal period is 0° to 180° as the signals are proportional to sin2α and cos2α.

5.3.2 How to Set a Certain Angular Range

To select one of 16 different angular ranges, an external voltage (see TABLE 6) has to be applied to pin 13 of the UZZ9000 (SENSIN). During the IC's initialization phase, which directly follows power-on reset or an external reset, this voltage is read and then converted into the digital domain. The digital value is stored until the next reset state occurs. Consequently, the angular range cannot be changed during normal operation but is still fixed after initialization phase.

Please note that the voltage at pin 13 must be ratiometric to VDDA and also stable over temperature and lifetime. This is ensured, for instance, when providing this voltage via a (trimmable) resistor divider connected to VDDA, which is the analog supply of the UZZ9000. The following TABLE 6 defines the fractions of the supply voltage VDDA that must be fed to pin 13 to select a certain range. Please note that when using the 30° angular range, a constant zero point offset of 15° is added. Consequently, when using the 30° range, the zero point offset can be programmed between 10° and 20° only (see next section).

TABLE 6: Definition of voltages to set one of the UZZ9000 angular ranges

Angular Range	Min	Nom	Max	Units
0° to 30°(*)	33,47	33,73	33,99	% VDDA
0° to 40°	35,69	35,95	36,21	% VDDA
0° to 50°	37,91	38,17	38,43	% VDDA
0° to 60°	40,14	40,40	40,66	% VDDA
0° to 70°	42,36	42,62	42,88	% VDDA
0° to 80°	44,58	44,84	45,10	% VDDA
0° to 90°	46,80	47,06	47,32	% VDDA
0° to 100°	49,02	49,28	49,54	% VDDA
0° to 110°	51,25	51,51	51,77	% VDDA
0° to 120°	53,47	53,73	53,99	% VDDA
0° to 130°	55,69	55,95	56,21	% VDDA
0° to 140°	57,91	58,17	58,43	% VDDA
0° to 150°	60,13	60,39	60,65	% VDDA
0° to 160°	62,36	62,62	62,88	% VDDA
0° to 170°	64,58	64,84	65,10	% VDDA
0° to 180°	66,80	67,06	67,32	% VDDA

(*) When choosing the angular range from 0° to 30°, a constant zero point offset of 15° is added.

5.3.3 How to Set a Zero Point Offset

To adjust the zero point offset or to set it to 0°, an external voltage has to be applied to the UZZ9000 at pin 14 (VOFFIN). The function is similar to the one described in the previous section: After reset the voltage is read, converted into the digital domain and then stored until another reset state occurs. Consequently, the zero point offset cannot be adjusted without a reset.

As said before, it is recommended to use a resistor divider connected to VDDA to generate this voltage. TABLE 7 defines the allowed voltage ranges as a percentage of the supply VDDA.

TABLE 7: Definition of the voltages to select a certain zero point offset

Zero Point Offset	Min	Nom	Max	Units
-5°	33,47	33,73	33,99	% VDDA
-4.5°	35,14	35,40	35,66	% VDDA
-4°	36,80	37,06	37,32	% VDDA
-3.5°	38,47	38,73	38,99	% VDDA
-3°	40,13	40,39	40,65	% VDDA
-2.5°	41,80	42,06	42,32	% VDDA
-2°	43,47	43,73	43,99	% VDDA
-1.5°	45,13	45,39	45,65	% VDDA
-1°	46,80	47,06	47,32	% VDDA
-0.5°	48,46	48,72	48,98	% VDDA
0.0°	50,13	50,39	50,65	% VDDA
0.5°	51,80	52,06	52,32	% VDDA
1.0°	53,46	53,72	53,98	% VDDA
1.5°	55,13	55,39	55,65	% VDDA
2.0°	56,79	57,05	57,31	% VDDA
2.5°	58,46	58,72	58,98	% VDDA
3.0°	60,13	60,39	60,65	% VDDA
3.5°	61,79	62,05	62,31	% VDDA
4.0°	63,46	63,72	63,98	% VDDA
4.5°	65,12	65,38	65,64	% VDDA
5.0°	66,79	67,05	67,31	% VDDA

5.4 Offset Trimming

To achieve a linear output characteristic, it is necessary to adapt the offsets of the two input signals to the input stage of the UZZ9000. For this reason a sensor offset cancellation procedure was implemented in the UZZ9000 which is started by sending a special serial data protocol to the UZZ9000. This trimming procedure is required for both input signals.

5.4.1 Trim Interface

The serial interface used to switch the UZZ9000 into trim mode consists of the two terminals SMODE (pin 10) and DATA_CLK (pin 9). The structure of this protocol is shown in Figure 15.

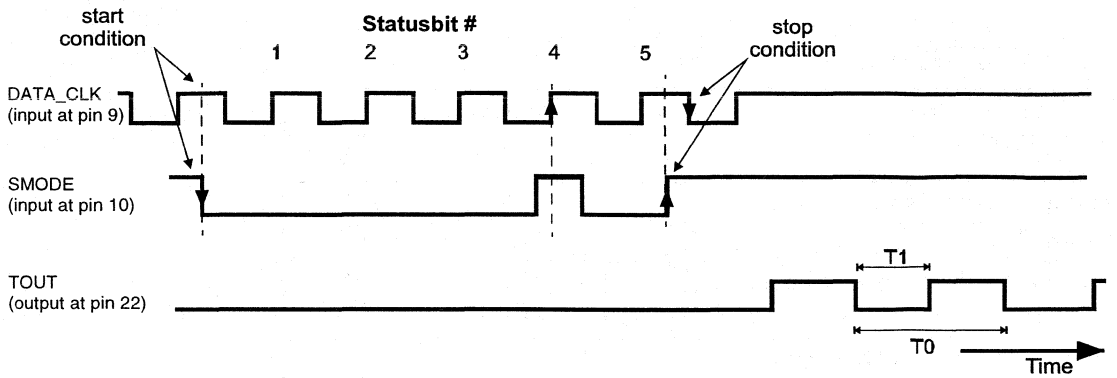

Figure 15: Protocol used to set the UZZ9000 into trim mode.

All signal levels at DATA_CLK and SMODE must be chosen according to the requirements listed in TABLE 8. Because of the asynchronous protocol, the following points have to be taken into account:

The protocol starts with a falling edge at SMODE, which must occur at a high level of the DATA_CLK. The next five bits are used for coding of the message send to the UZZ9000. They are transferred via SMODE and are sampled with the rising edge of DATA_CLK. During the fifth high level output of DATA_CLK (counted from the start condition onwards), a rising edge must appear at SMODE and afterwards DATA_CLK has to change one more time to low level in order to successfully complete the protocol.

TABLE 8: Definition of the trim interface signals

Parameter	Min	Nom	Max	Unit
supply voltage VDD of UZZ9000	4.5	5.0	5.5	V
low level of DATA_CLK, SMODE	0		5	%VDD
high level of DATA_CLK, SMODE	95		100	%VDD
rise and fall time of signal edges of DATA_CLK and SMODE (from 10% VDD to 90% VDD and vice versa)	8			ns
Frequency of DATA_CLK	0.1		1	MHz

5.4.2 How to Enter the Trim Mode

The status bits to be transmitted to the UZZ9000 are shown in TABLE 9. Also please note that a complete protocol has to be sent to return to normal operation. Another possibility to leave the trim mode is to reset the device.

TABLE 9: Programming of trim modes

Mode	Status Bits				
	1	**2**	**3**	**4**	**5**
enter trim mode for sensor input channel 1	0	0	0	1	0
enter trim mode for sensor input channel 2	0	0	1	0	0
leave trim mode for either input channels	0	0	0	0	0

After entering one of the trim modes, a square wave output is visible at the terminal TOUT (pin 22) provided there is a dynamic input signal.

5.4.3 Offset Calibration

To make use of the build-in trimming procedure of the UZZ9000, it is necessary to generate dynamic sensor signals at its inputs. When the KMZ41 is used, a rotating permanent magnet in front of the sensor can easily generate these input signals. The principle of this set-up is shown in Figure 16.

Please note that the absolute rotational speed of the permanent magnet is not that important but it must be constant over time. Please further note that the rotational axis of the motor and magnet must be aligned exactly with the center of the KMZ41 package as shown in Figure 16. It is not necessary to use the same magnet for both trimming and application, but after trimming, the KMZ41 and UZZ9000 must be treated as one unit. The trimming procedure is as follows.

When the UZZ9000 has been switched to trim mode and sinusoidal sensor voltages are applied to its inputs, then the terminal TOUT (pin 22) immediately shows a square wave signal. This square wave signal has the same frequency as the sensor signal and a duty cycle T1/T0 as shown in Figure 15 previously.

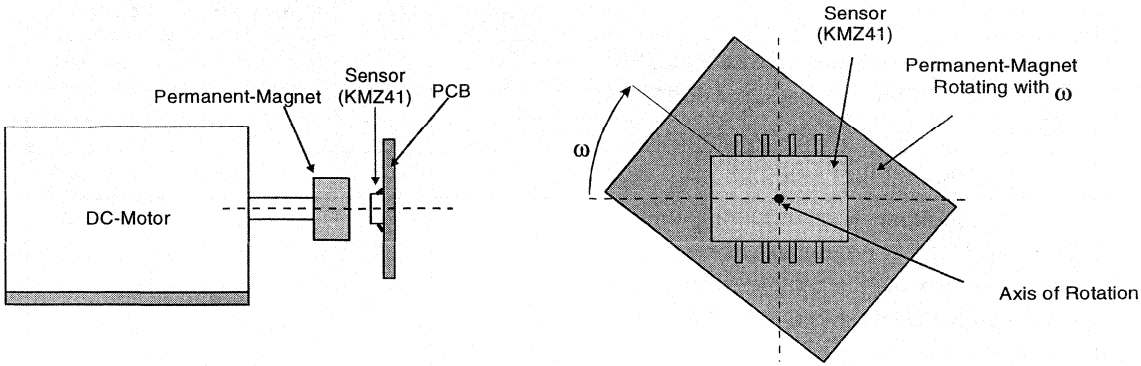

Figure 16: Proposal for a mechanical set-up to trim the UZZ9000

At a duty cycle of 50%, the offset for the selected channel is virtually eliminated. Therefore, the voltage at OFF1 (PIN16, channel 1) or OFF2 (PIN15, channel 2), respectively, has to be adjusted until this target is achieved. The trimming voltages OFF1 and OFF2 must be ratiometric to the UZZ9000 VDDA supply and must not vary more than 0.1 % VDDA with temperature and over lifetime. As already proposed for adjusting the angular ranges and zero point offset, these properties can be ensured, for example, when using a trimmable resistor divider connected to VDDA.

When building up an automatic trimming station for mass production, it is recommended to firstly determine the actual trim voltage to be fed to OFF1 and OFF2 as a fraction of VDDA. Afterwards, the resistor dividers are trimmed according to the requirements found. This procedure will be much faster compared with trying to trim the resistors step by step to get 50% duty cycle. In practice, laser trimmable resistors used for both divider elements have shown good results. Using resistors of the same material is important to get a similar temperature coefficient. Please note that for duty cycle measurements, the measuring device should be set into averaging mode in order to eliminate the influence of short spikes or noise. TABLE 10 summarises the recommended trim parameters:

TABLE 10: Definitions and recommendations of trim parameters

Parameter	Symbol	Min	Nom	Max	Unit
Frequency of the motor	fo	20		30	s^{-1}
Frequency of the sensor input signals (KMZ41)	2 fo	40		60	Hz
Stability of the rotational speed over one signal period	Δf			0.05	% fo
Limits for the duty cycle of nominal 50% during trimming		49.96		50.04	%

Parameter	Symbol	Min	Nom	Max	Unit
Variation of the voltages provided at OFF1 and OFF2 with temperature and during lifetime				0.1	%VDDA
Voltage range for OFF1 and OFF2		33.3		66.7	%VDDA
Input signal offset range to be aligned by OFF1 and OFF2. Values are referred to VDDA. The min value corresponds to the min value for OFF1 and OFF2 (33.3% VDDA), and vice versa.		-2		2	mV / V

Example:

The following example serves to demonstrate the meaning of these limits and allows the calculation of the system accuracy if other values are applied.

Assuming sinusoidal sensor signals with the amplitude *A*, then the relation between an DC offset Δx and the measured duty cycle T1/T0 is as follows:

$$\Delta x = A\sin(\pi \cdot (0.5 + T1/T0)) \tag{10}$$

At room temperature and 5V supply voltage, the typical signal amplitude *A* of the KMZ41 is 78 mV. Consequently, at a duty cycle of 50.04% (or 49.96%) the remaining offset voltage is:

$$\Delta x = 78\ mV \sin(\pi \cdot (0.5 + 0.5004)) = -0.098\ mV \tag{11}$$

As a result, the remaining offset is 0.13% referred to the signal amplitude of 78 mV. The angular error caused by this offset is discussed in section 7.

The other parameter specified is the drift of the voltages applied to OFF1 and OFF2 with temperature and over lifetime. It is specified to be less than 0.1% VDDA. The maximum voltage range for OFF1 and OFF2 is 33.3 % VDDA which is used to align the input signal offset range of +/- 2 mV / V. Consequently, changes of OFF1 or OFF2 by 0.1% VDDA will cause offset voltages Δx of:

$$\Delta x = \frac{0.1\%\ \text{VDDA}}{33.3\%\ \text{VDDA}} \cdot 2 \cdot 2\ \text{mV / V} = 0.012\ \text{mV / V} \tag{12}$$

At a supply voltage of 5V, the offset voltage caused by the drift of OFF1 and OFF2 is 0.06 mV for each channel. The resulting angular error due to this offset is discussed in section 7.

5.5 Reset

During reset, the output of the UZZ9000 VOUT is forced to nominal 5.5 % VDDA. This is the minimum value of normal operation.

In addition to the external reset pin (pin 6), the UZZ9000 provides an internal power-up / power-down reset logic which supervises the supply voltage continuously. When the supply voltage increases and reaches a safe level, reset becomes inactive and the device starts initialization after a nominal delay of 100 us. This is to ensure settling of all analog and digital sections. When the supply voltage leaves the safe voltage level, the device is reset immediately. This internal reset logic can be over-ridden by the external pin RES (pin 6) in all modes and at any time. The reset pin RES (pin 6) is active high. It is internally pulled down to VSS and therefore does not have to be connected if the function is not required.

As the UZZ9000 has two different voltage supplies, the power-up and power-down reset operates as follows:

1. **Power-Up**

VDD or VDDA	<= 3.3 V	reset active
VDD and VDDA	>= 4.3 V	reset not active, reset will switch from high to low after a delay of 100 us.

2. **Power-Down**

VDD or VDDA	<= 3.3 V	reset active
VDD and VDDA	>= 4.2 V	reset not active, device active

If the supply voltage rises, the device is switched into active mode as soon as VDD *AND* VDDA reach the power-up switching level, which lies between 3.3 V and 4.3 V, and the delay of about 100 us has elapsed. In contrast, if the supply voltage at VDD *OR* VDDA goes below the power-down limit, which lies between 3.3 V and 4.2 V, reset becomes active immediately. Due to possible ripples on the supply voltage, a hysteresis of 100 mV is implemented between the power-up and power-down switching voltage levels. The following TABLE 11 summarises the specified limits.

TABLE 11: Definitions of switching levels of the build-in reset logic

Parameter	Min	Nom	Max	Unit
Switching voltage for falling VDDA OR VDD	3.3		4.2	V
Switching Hysteresis		0.1		V

Parameter	Min	Nom	Max	Unit
Switching voltage for rising VDDA AND VDD	3.3		4.3	V
Delay for starting the initialization of the UZZ9000 when VDD AND VDDA have risen above the power-up switching level		100		us

5.6 Diagnostic

The UZZ9000 provides some powerful diagnostics features that allow the user to recognize certain failures of the device or system. A failure has occurred when the output voltage VOUT lies above or below the normal operation range (see Figure 12). Either one of the diagnostic areas is reached during any of the following conditions:

1. Short circuit between VOUT and VSS (R < 1 Ω)
2. Short circuit between VOUT and VDD (R < 1 Ω)
3. Disconnection of VDD when the load is pulled down
4. Disconnection of VSS when the load is pulled up
5. Invalid input signal from the sensor, e.g. Magnet Lost. This failure is assumed when the offset corrected input signal of sensor 1 AND sensor 2 is below +/- 15 mV (tolerance +/- 5%).

In the output buffer block, the internal pull-up and pull-down resistors guarantee that VOUT will be pulled to one of the power supplies when the other supply is disconnected and so VOUT reaches the diagnostic region even in the case when there is no output load.

If the external load is a pull-down resistor, then the device will go into the diagnostic area if VDD is disconnected, but not if VSS is disconnected. Similarly, if the load is a pull-up resistor, then the device will go into the diagnostic area if VSS is disconnected, but not if VDD is disconnected. **Note that there is no need to connect an output load to the UZZ9000.**

After recovering from short circuit to ground or supply voltage, the chip returns to the normal operation mode without any damage. There is no time limitation regarding short circuit of VOUT.

5.7 Measurements Dynamics

The UZZ9000 provides an on-chip RC Oscillator that generates the clock for the whole device. Consequently, no external clock supply is required for the measurement system.

The nominal clock frequency of the on-chip oscillator is 4 MHz at room temperature. It varies over temperature. At -40°C, the clock frequency may reduce down to 2.8 MHz. At higher temperatures, however, a frequency up to 5.2 MHz may occur. Consequently, this influences the dynamics of measurements. From the application point of view, two different effects have to be distinguished: The system delay, which means how long it takes until a changed input signal is recognized at the output, and the measurement update rate.

The system delay is mainly caused by the settling time of the low pass decimation filter, which depends on the maximum frequency content (shape) of the input signals and the clock frequency. The following maximum values can be expected for the entire system delay (see TABLE 12):

TABLE 12: System delay and update rates of the UZZ9000

Parameter / Conditions	Min	Typ	Max	Unit
System delay defined as the time passes by until 95% of the final value is reached:				
- Max. signal frequency < 200Hz			0.6	ms
- Transients (Step response)			1.2	ms
Measurement update rate:				
- -40°C	0.37			ms
- 25°C (room temperature)		0.26		ms
- 150°C			0.20	ms

The measurement update rate, however, is directly related to the oscillator frequency. At room temperature, a new value is available every 0.26 ms. When looking at the entire temperature range of the UZZ9000, update rates between 0.37 ms and 0.2 ms are possible (see TABLE 12).

6. SCHEMATICS FOR CONNECTING KMZ41 AND UZZ9000

6.1 Single Measurement System

As shown in Figure 5, four wires are required to connect KMZ41 and UZZ9000. For these connections, both chips provide terminals with identical names. The corresponding pin numbers are listed in TABLE 13.

TABLE 13: Pinning of the KMZ41 and UZZ9000 signal lines

	-Vo1	+Vo1	-Vo2	+Vo2
KMZ41 (SO 8)	Pin 1	Pin 5	Pin 2	Pin 6
UZZ9000 (SO 24)	Pin 24	Pin 2	Pin 23	Pin 1

Connecting these pins name by name, e.g. Pin 1 of the KMZ41 with Pin 24 of the UZZ9000 etc., results in the following output characteristic:

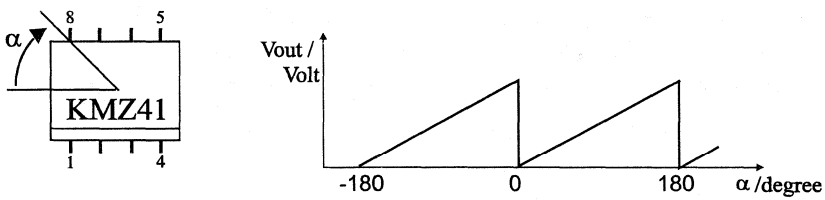

Figure 17: Definition of mechanical angle and the resulting output curve characteristic when using the standard connection between KMZ41 and UZZ9000

In some applications, however, it might be useful to shift the output curve. This can be easily achieved in steps of 45° by changing the pin connections between KMZ41 and UZZ9000. The different possibilities are listed in Figure 18.

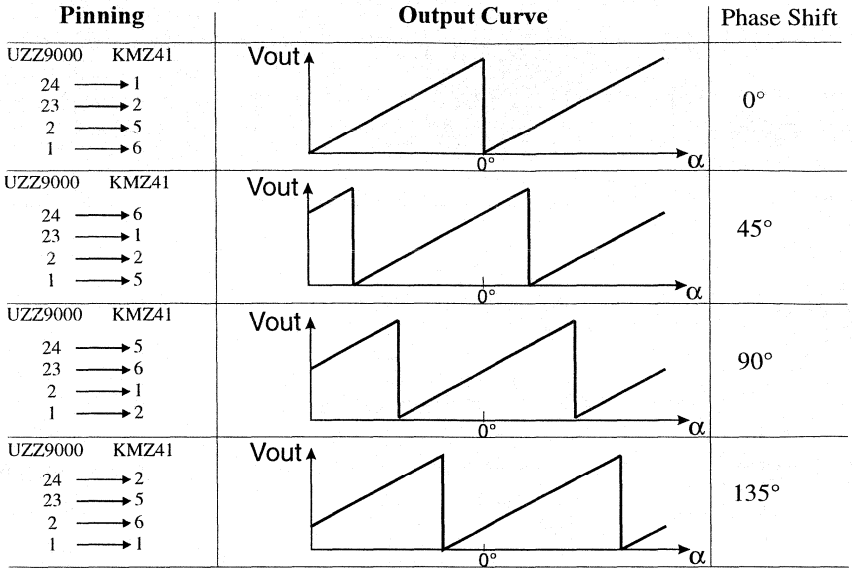

Figure 18: Possible connections between KMZ41 and UZZ9000 giving different zero point shifts of the output curve

6.2 Fault Tolerant Systems

In safety relevant applications it might become necessary to have two or more independent measurement systems for the same physical value. If using two independent KMZ41 sensors and two UZZ9000 in 180° angular range, a simple plausibility check can be made when having an anti-parallel output curve characteristic. This holds because then the sum of both output values is always 95% VDDA, independent of the actual angle. Please note that this easy control method is limited to the 180° angular range. If using other angular ranges, this check requires a more complex signal evaluation.

In general, there are two possibilities to achieve an anti-parallel output curve. These are explained in the following figures. In the first arrangement shown in Figure 19, the two sensors are mounted at the same position but opposite to each other (using the front and backside of one PCB or Flex Foil). Because of this mirror arrangement, the desired output characteristic is achieved by connecting both sensors in the standard way.

Conversely, when mounting the sensors on top of one another as shown in Figure 20, the connections have to be changed. In addition to these examples, many other output characteristics are achievable by applying the different configurations discussed in the previous section.

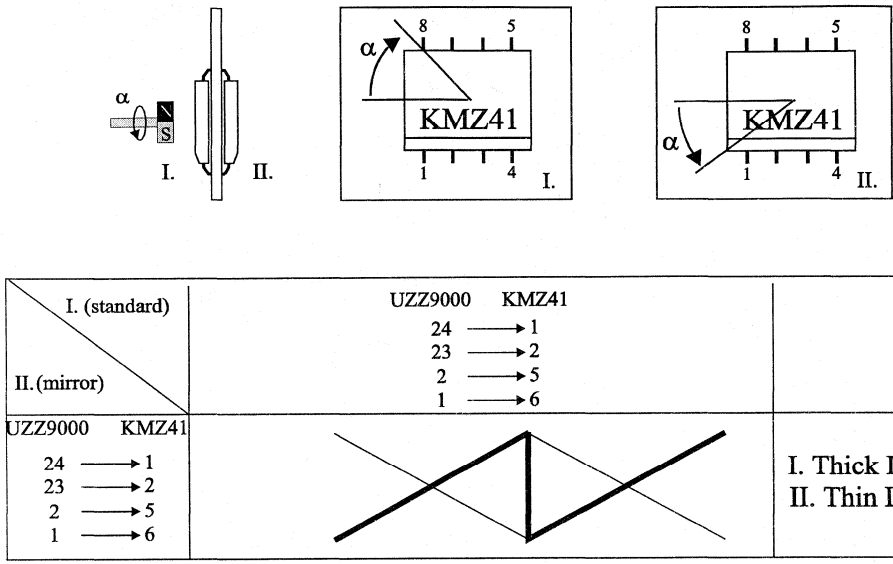

Figure 19: Two KMZ41 sensors mounted on opposite sides of one PCB (mirror arrangement).

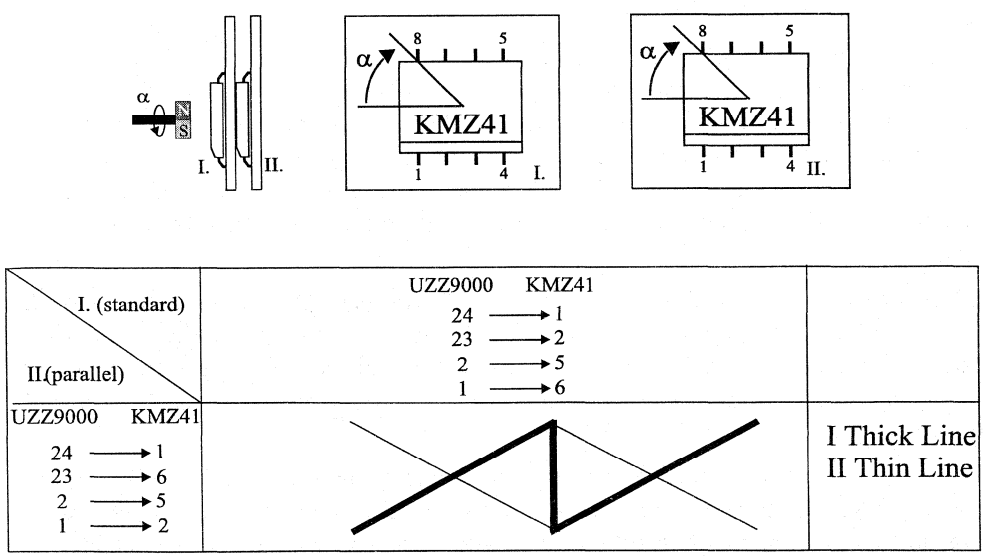

Figure 20: Two KMZ41 sensors mounted on top of one another (parallel arrangement)

6.3 Typical Application Circuit

Figure 21 shows a typical application circuit.

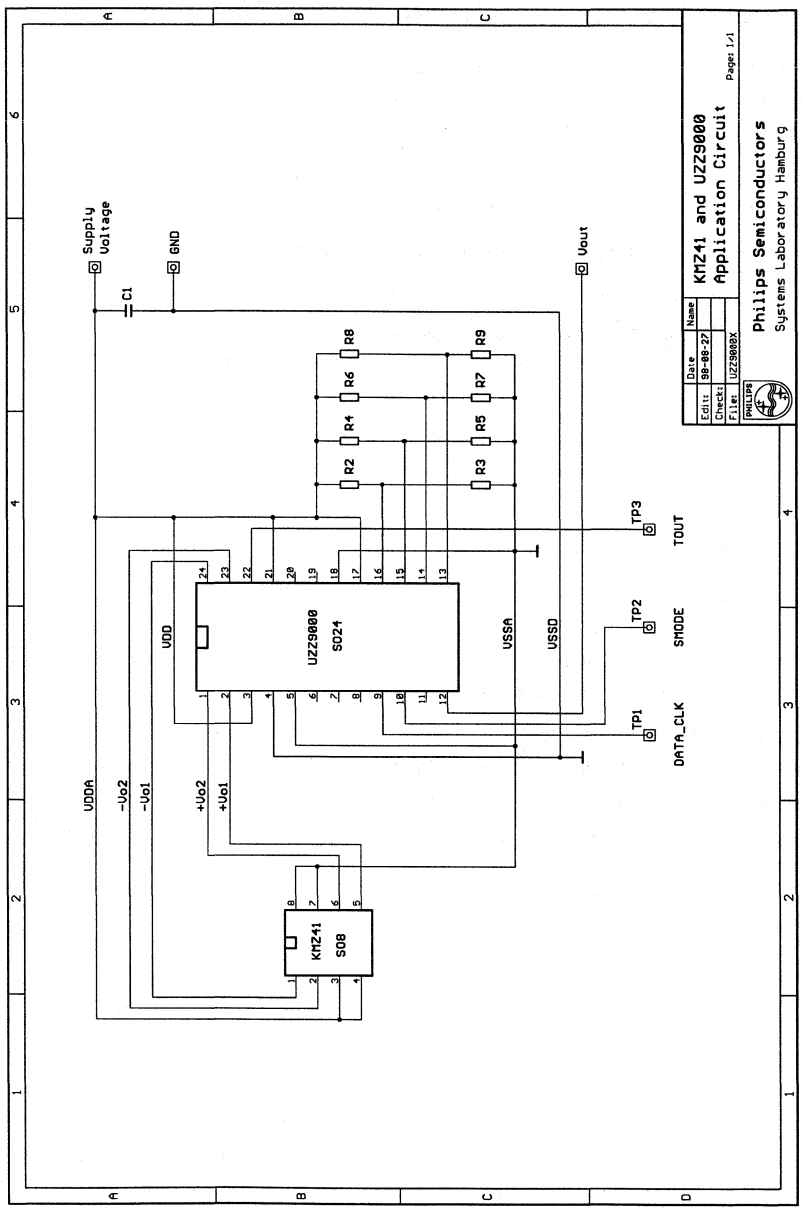

Figure 21: Schematics of a typical application circuit

7 SYSTEM ACCURACY

7.1 Sensor KMZ41

There are three different errors that may be caused by non-adequate magnetic field arrangements. These are:

- Form deviations of the sensor signals (no sinusoidal shape) and hysteresis of the sensor response if the magnetic field H does not saturate the sensor.
- Form deviations of the sensor signals caused by a non-symmetrical sensor to magnet arrangement (inhomogeneous magnetic field).
- Influence of external magnetic fields influencing the primary field used for measurements.

The influence of external fields can not be described in general as these effects depend on the actual measurement set-up. Therefore this item is not discussed within this paper. The only possibility to get rid of external fields or to limit its impact is to use some kind of a magnetic shielding as discussed in section 4.

In addition to these magnetic effects, there are some non-ideal properties of the KMZ41 sensor affecting the system accuracy. These are discussed in section 7.1.3.

7.1.1 Less Magnetic Field Strength

A complete saturation of the sensor would require the usage of an infinite magnetic field. Consequently, a complete saturation is impossible in practice and errors caused by fewer magnetic fields have to be taken into account. The magnetic field strength, which is proposed in this paper, is a compromise between the remaining error and magnet costs.

Insufficient magnetic field show two effects. The first one is the signal form error caused by a non-sinusoidal shape of the output signals (see Figure 22). Figure 23 shows the shape of the resulting measurement error. Due to its geometrical nature, the maximum and minimum values will always occur at the same locations for every sensor. Maximum values occur at the mechanical angles of 11.25°, 33.75°, 56.25°, 78.75°, 101.25°, 123.75°, 146.25° and 168.25°. No measurement errors occur at 22.5°, 45°, 67.5°, 90°, 112.5°, 135°, 157.5° and 180°.

Figure 24 shows the relation between the magnetic field strength H and the maximum peak error E_{Form} that may occur. At the recommended magnetic field strength of 100 kA/m, the measurement error is less than 0.04° and therefore negligible. The signal form error is reversible and does not depend on the history, as it is the case for hysteresis effects.

Hysteresis effects become visible if the angle turns back and forth over larger angular ranges as shown in Figure 25. The positions where these errors occur depend on the direction of movement. If fields become stronger, the hysteresis zones shrink to smaller areas around the positions 0°, 45°, 90° and 135°. Figure 24 also gives the maximum error caused by hysteresis effects. These are less than the errors caused by the signal form error.

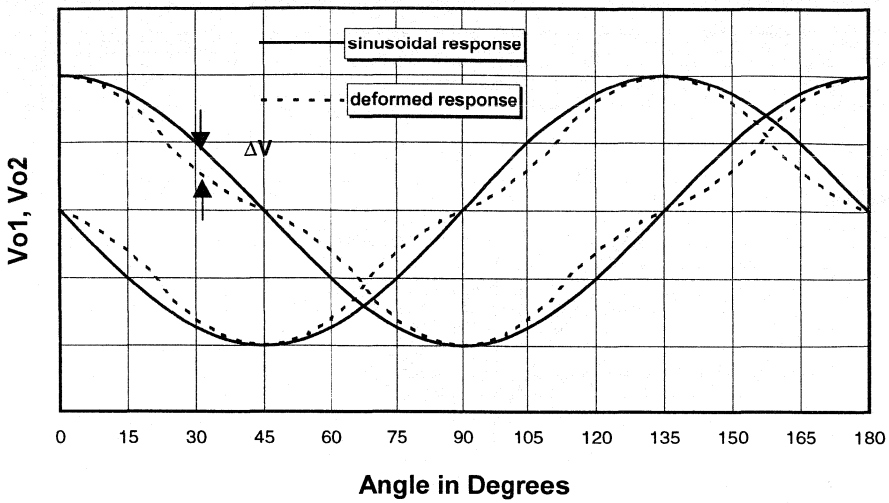

Figure 22: Signal form error of KMZ41 output signals caused by too low magnetic field not saturating the sensor

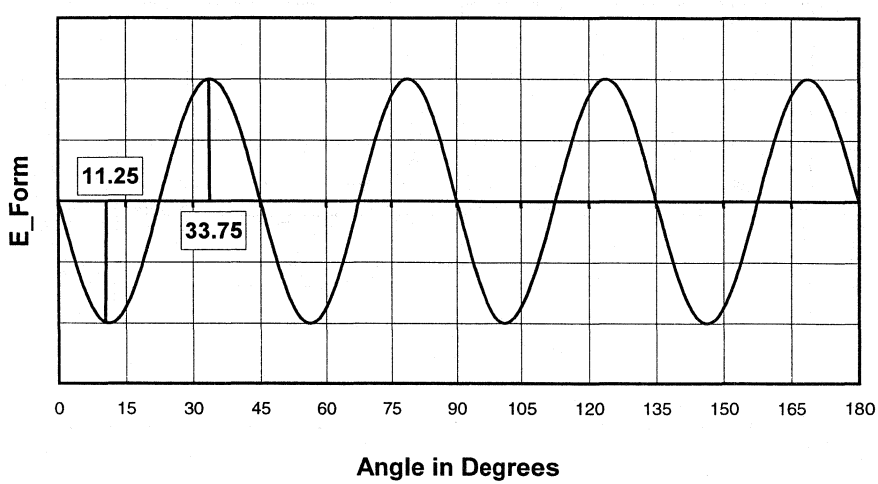

Figure 23: Shape of the measurement errors caused by the non-ideal sensor signals given in Figure 22.

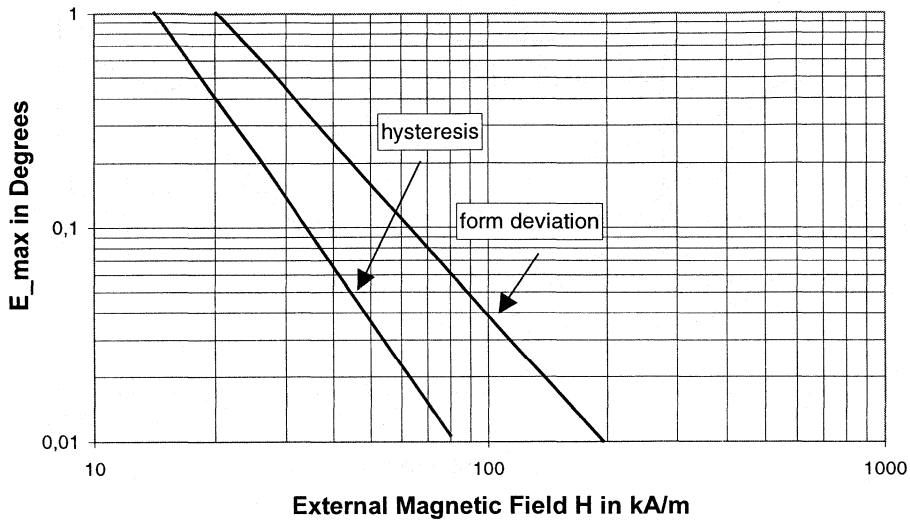

Figure 24: Maximum measurement error caused by signal form error and hysteresis

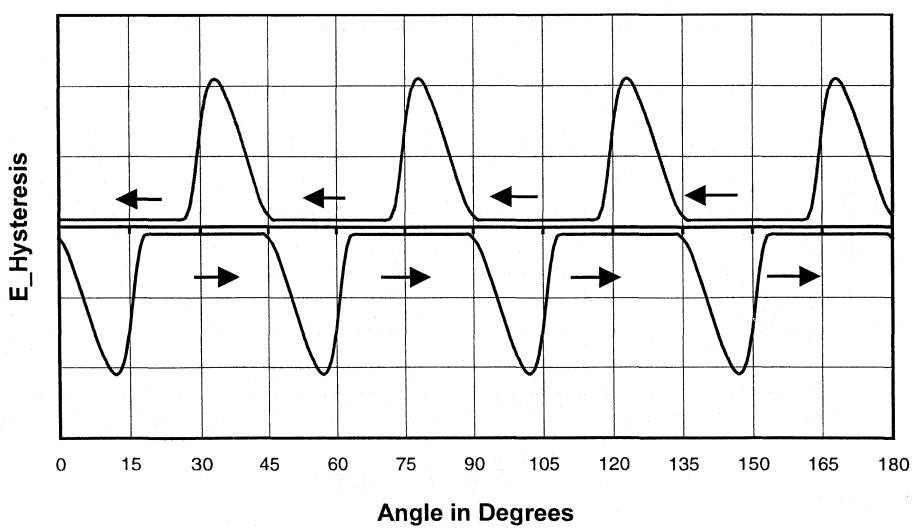

Figure 25: Shape of the measurement error caused by hysteresis

It is obvious that the measurement error caused by signal form errors and hysteresis can be neglected when using a magnetic field around 100 kA/m.

Another argument for using strong magnetic fields is the lower impact of external magnetic fields. This is especially an issue when using an unshielded magnet set-up. Here, even the very small magnetic earth field of about 30 A/m causes measurement errors. To give a rough estimation, an earth field perpendicular to the measurement field of 100 kA/m would cause a maximum error of 0.017°. Ten times this error would occur when operating at 10 kA/m, and this is not negligible.

7.1.2 Effects of Inhomogeneous Magnetic Fields

The sensor signal will get deformed even if sensor and magnet are not precisely aligned, which also may cause measurement errors. The reason for these deformations is that then the sensitive part of the sensor is not completely placed in the homogeneous part of the magnetic field, or, in other words, the relevant part of the magnetic field used for measurements has become inhomogeneous. As the actual angular error resulting from an inhomogeneous field depends on the specific set-up, it can not be calculated in general. However, for the simple block magnet arrangement discussed before, a rule of thumb can be used.

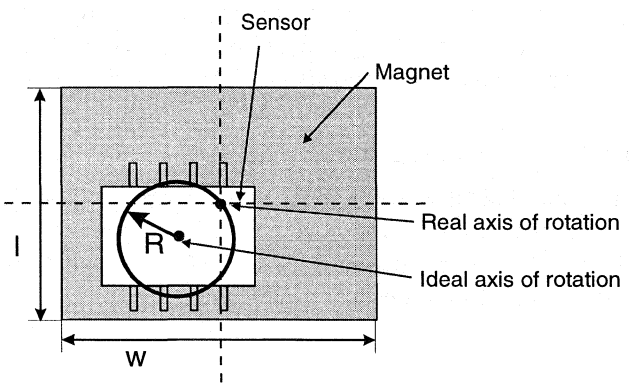

Figure 26: Definition of parameters for calculating the angular error caused by an inhomogeneous field.

Assuming the magnet arrangement depicted in Figure 2, the resulting maximum angular error can be estimated as given in Equation (10):

$$E_{\text{Inhomogenoeus}} = C \cdot R^2 \qquad (13)$$

with: $C = \frac{320°}{(w+l)^2}$ Magnet Constant

R Radius of the circle in which the centre of the magnet lies (see Figure 26). The midpoint of this circle is identical with the ideal axis of rotation

w Width of the magnet

l Length of the magnet

Note that w and l describe the magnet surface faced to the sensor. For the above mentioned magnets (see Figure 9), w and l are approximately 8 mm and thus $C \approx 1.25°/\mathrm{mm}^2$. Consequently, a radius R of 1 mm (the magnet is positioned 1 mm apart from the ideal position) can cause maximum errors up to 1.25°. As a result, small mounting tolerances are strongly recommended when using a simple block magnet arrangement. However, enlarging the magnet will reduce this error at the expense of higher magnet costs.

Please note that this error calculation is only applicable for the block magnet arrangement. When looking at more complex magnetic designs, e.g. the one depicted in Figure 10, a customised solution must be found. Normally, when carefully designing such a complex magnetic circuit, higher mounting tolerances are possible.

Also a non-parallel position of the sensor surface and magnet surface causes errors due to an inhomogeneous magnetic field in the sensitive area of the sensor. But as long as this deviation can be limited to the range of 1° to 2°, the resulting measurement error is negligible. Consequently, the achievable precision regarding parallel mounting should not be a limiting factor.

7.1.3 Non-Ideal Properties of the Components

Due to production scatter, the KMZ41 does not generate ideal output signals but shows some variations in performance. Since continuous improvement is the target of this sensor, please refer to the latest data sheet of the KMZ41 to get current data. In the following sections, the different effects and their impact on system accuracy are described in general.

Offset and Offset Drift

The sinusoidal output signals of the KMZ41 may show offsets that limit the accuracy of the system. From the application point of view, the offset of each channel can be subdivided into two parts: a constant portion, which is virtually eliminated by trimming, and a portion that changes with temperature but needs no compensation because it is very small. Note that the temperature dependent portion is zero at the temperature where the sensor system was trimmed. Introducing an offset into the mathematical description of both signals gives:

$$X = X_0 \sin 2\alpha + \Delta x \quad (14)$$

$$Y = Y_o \cos 2\alpha + \Delta y \quad (15)$$

The absolute angular error caused by offsets is also a function of the actual angle. It is calculated as follows:

$$E_{Offset}(\alpha, \Delta x, \Delta y) = \left| \alpha - \frac{1}{2} \arctan\left(\frac{X_0 \sin 2\alpha + \Delta x}{Y_0 \cos 2\alpha + \Delta y} \right) \right| \quad (16)$$

If both channels have the same offsets ($\Delta x = \Delta y$) , the maximum angular error is:

$$E_{Offset\_Max} = 0.4° / \% \text{ Amplitude} \quad (17)$$

This means that an offset of 1% referred to the amplitude ($X_0 / \Delta x = Y_0 / \Delta y = 1\%$) results in a maximum angular error of 0.4°. Please note that both signal amplitude and offset vary with temperature. Please also note that the angular positions where these maximum errors occur are not fixed but depend on the constellation of Δx to Δy. As these values change from part to part, locations with less errors can not be determined in general.

If only one channel shows an offset but the other is ideal, the worst case value of Equation (14) is reduced by the factor $1/\sqrt{2}$.

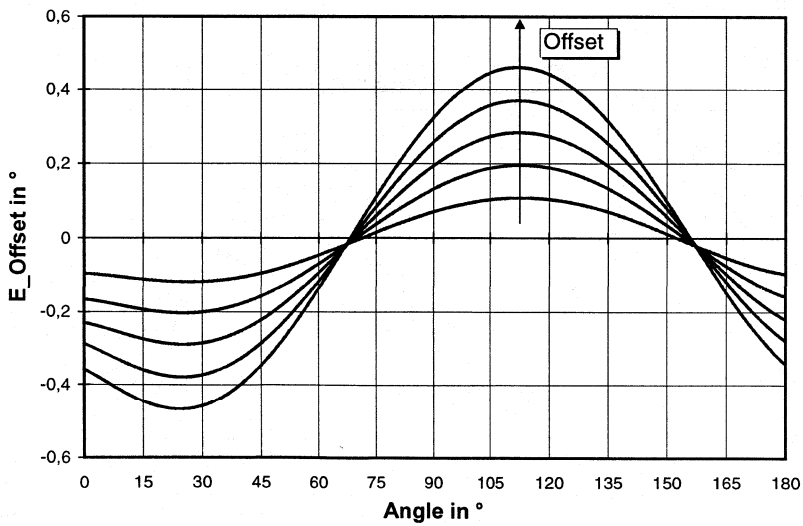

Figure 27: Typical shape of the error curve caused by signal offsets

Figure 27 shows the typical shape of the measurement error over the entire angular range. The error curve has a period of 180° what makes it distinguishable from other error shapes discussed below.

Different Signal Amplitudes

Although processed at the same time and on the same silicon substrate, both Wheatstone bridges may show slightly different signal amplitudes. The angular error caused by this effect is as follows:

$$E_{Amplitude}(\alpha, A) = \left| \alpha - \frac{1}{2} \arctan\left(A \frac{\sin 2\alpha}{\cos 2\alpha} \right) \right| \tag{18}$$

with: $A = \frac{X_0}{Y_0}$ Ratio of the signal amplitudes

The maximum error due to differences of signal amplitudes is:

$$E_{Amplitude\_max} = 0.158° / \% \ . \tag{19}$$

This means that differences between the signal amplitudes of 1% will cause a maximum angular error of 0.158°. In contrast to the offset errors, this error function shows a period of 90°. Moreover, the positions where maximum errors occur will not change significantly with A. Figure 28 shows the typical shape of the output curve.

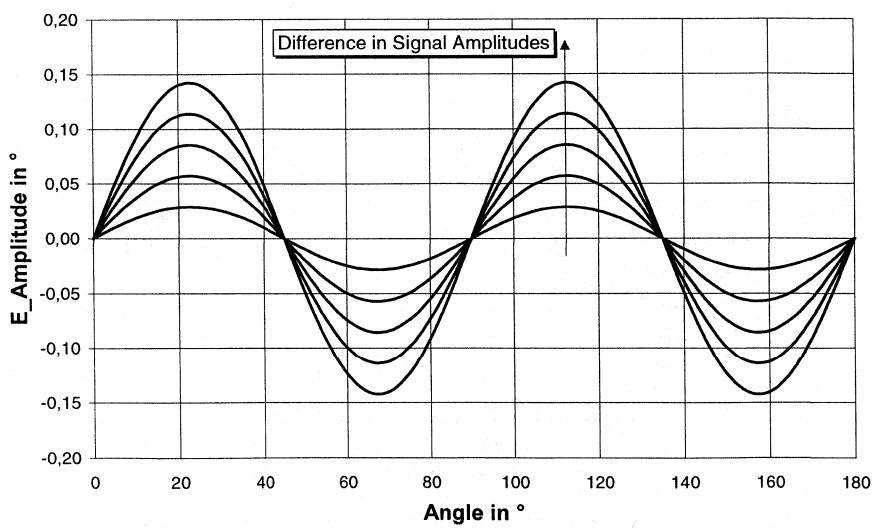

Figure 28: Typical shape of the error curve caused by different signal amplitudes.

Phase Difference between Channels

The last item to be thought of is a phase error between both channels. This means that the phase between signal *X* and *Y* is not exactly 90° over the entire angular range. Introducing this error into the mathematical description of the signal gives:

$$X = X_0 \sin(2\alpha + \Delta\beta(\alpha)) \tag{20}$$

$$Y = Y_o \cos 2\alpha \tag{21}$$

Note that the phase shift is a function of the actual angle α and therefore may not be constant over the entire angular range. The resulting angular error can be calculated as follows:

$$E_{Phase}(\alpha, \Delta\beta) = \left| \alpha - \frac{1}{2} \arctan\left(\frac{\sin(2\alpha + \Delta\beta(\alpha))}{\cos 2\alpha} \right) \right| \tag{22}$$

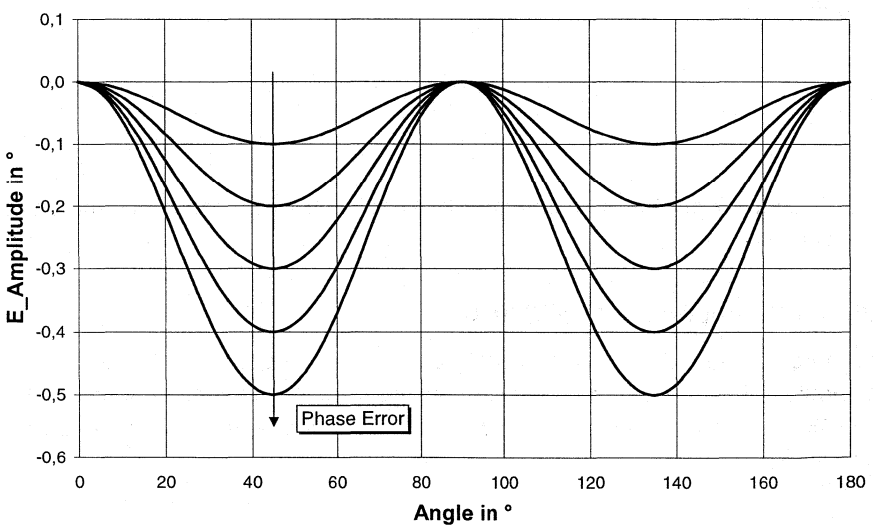

Figure 29: Typical shape of an error curve caused by phase errors.

Assuming a constant phase error, the maximum measurement error that may occur is:

$$E_{Phase\_Max} = 0.5° / ° \text{ Phase Shift} \tag{23}$$

This means that a phase shift of 1° results in a maximum angular error of 0.5°. Figure 29 shows the shape of the corresponding error function.

7.1.4 Discussion of Different Effects

When looking at the different effects discussed before, it makes sense to distinguish between errors that can be omitted when carefully designing a system and others to which the designer has no control.

The errors caused by insufficient magnetic fields are negligible when using a suitable magnet system. Therefore they must only be included in the error budget, if weaker magnets should be used in order to reduce costs. The same argumentation holds with respect to the mechanical mounting tolerances. If accuracy is important, the magnet system can be designed to provide a larger homogeneous area, allowing mounting tolerances without any impact on system accuracy. In turn, when a simple block magnet is used, mounting tolerances can be limited to reasonable values of, for example, 0.1 mm eccentricity or less.

Consequently, only errors caused by offset, different signal amplitudes and phase shift between the two channels should be taken into account. As process scatters cause these errors, it is adequate to use a statistical calculation of the overall error for the KMZ41. This can be formulated mathematically as given in Equation (24):

$$E_{KMZ41\_Max} = \sqrt{E^2_{Offset\_Max} + E^2_{Amplitude\_Max} + E^2_{Phase\_Max}} \quad (24)$$

In order to get the overall error for the measurement system the errors caused by the UZZ9000 have to be added to this value.

7.2 Signal Conditioning IC UZZ9000

There are several blocks in the UZZ9000 that may cause errors, e.g. the ADC, the ALU and the DAC. These errors should not be discussed in detail. An analysis shows that the accuracy of the UZZ9000 is better than 0.45° in any case. This value holds over the entire specified temperature range and at all angular ranges provided.

$$E_{Signal\_Max} < 0.45° \quad (25)$$

This worst case value is true for the 180° angular range of the UZZ9000. In smaller angular ranges, however, the absolute error caused by the DAC becomes smaller because then the whole output voltage range is matched to that smaller range. But as this does not significantly reduce the overall

error of the UZZ9000, for simplicity, the worst case value should be used for error calculations to be on the safe side.

Additionally, the accuracy and stability of the trimming voltage has to be taken into account. An estimate of the remaining offset error after trimming can be determined according to the following procedure (compare with section 5.4):

1. Determine the maximum voltage error of the resistor divider used for offset compensation with temperature and over lifetime according to Equation (12).
2. Determine the achievable accuracy with the trimming equipment according to Equation (11).
3. Add both values to get the remaining offset.

Example:

Assume that the resistor divider guarantees an accuracy better than 0.2 % VDDA with temperature and over lifetime (compare with Table 10). This means that the maximum offset voltage due to this effect would be less than 0.12 mV at 5V supply voltage (see Equation (12)).

Moreover, the measurement and trimming equipment may guarantee a duty cycle between 49.96% and 50.04%. According to Equation (11), the remaining offset voltage would be less than 0.1 mV at 5V supply voltage. Consequently, the DC offset voltage caused by non-ideal trimming is:

$$U_{Offset\_Trim} = 0.12\ \text{mV} + 0.1\ \text{mV} = 0.22\ \text{mV} \tag{26}$$

This resulting angular error E_{Trim} has to be added to the value resulting from offset drift of the KMZ41. Consequently, the overall error budget for the UZZ9000 is:

$$E_{UZZ9000\_Max} = \sqrt{E^2_{Signal\_Max} + E^2_{Trim}} \tag{27}$$

7.3 Application Example for Error Calculation

The following example serves to demonstrate a way to calculate the minimum accuracy that can be expected from a MR based measurement system under certain system constraints. The component specific data are taken from the current specification of the KMZ41 and UZZ9000 (see references (1) and (2)). As these devices are targets to continuous improvement, please refer to the latest data sheets to get data presently valid.

The system data assumed and the component data used are as follows:

- Temperature range required for the system: -40°C to 85°C
- Temperature while trimming: 25°C
- Maximum phase error between channels: 0.5°
- Maximum error of amplitude synchronism (k): 0.5 %
- Offset Drift (TCVoffset): 2 µV / V / K
- Constant offset due to non-ideal trimming: 0.2 mV
- Supply voltage: 5 V
- Signal amplitude KMZ41: 78 mV @ 25°C
- Temperature coefficient of peak voltage (TCVpeak): -0.31 % / K

The temperature during trimming is 25°C and therefore lies in the middle of the required operating temperature range. Consequently, the maximum change of temperature referred to this trimming temperature is about 60°C.

Nevertheless the upper limit of the operating temperature range of 85°C is more critical because the signal amplitude decreases with higher temperatures and therefore the percentage of offset to be taken into account increases. With the given data, the maximum offset voltage at 85°C is:

$$U_{Offset\_Max} = 2\ \mu V/V/°C \cdot 5V \cdot 60\ °C = 0.60\ mV \tag{28}$$

The amplitude of the signal at 85°C is 63.5 mV which is calculated using Equation (6) (TCVpeak = -0.31 % / K). As a result, the maximum offset caused by offset drift is:

$$Offset_{Max} = \frac{0.60\ mV}{63.5\ mV} 100\% = 0.94\% \tag{29}$$

The graph in Figure 30 shows the results of this calculation at other temperatures. For example, the offset drift to be taken into account at 125°C would be 1.7 %. At the maximum temperature of 150°C, 2.6 % offset may occur.

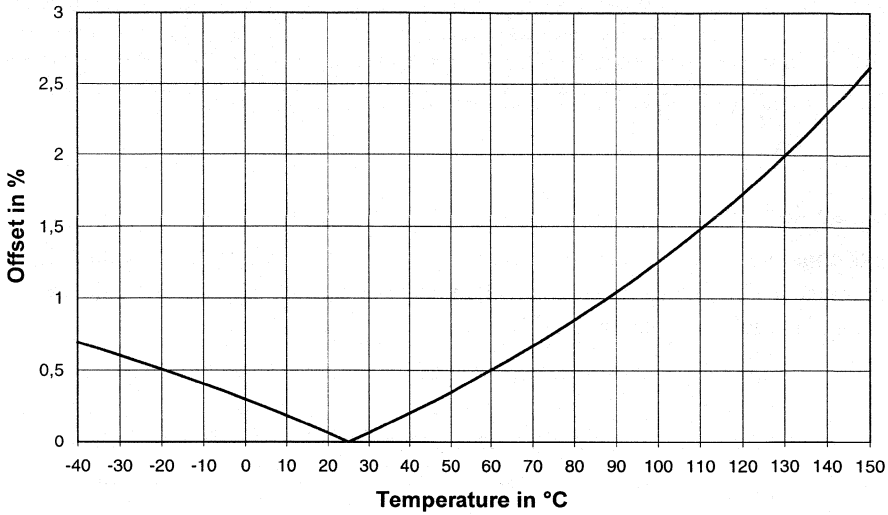

Figure 30: Offset drift at different maximum temperatures assuming the data defined in the text.

The maximum angular error caused by this offset drift can be calculated according to Equation (17). An offset of 0.94% corresponds to a maximum angular error of

$$E_{Offset\_Max} = 0.94\% \cdot 0.4°/\% = 0.38°. \tag{30}$$

In addition to offset drift, the trim error adds another portion. With the given remaining offset voltage of 0.2 mV after trimming, the evaluation of Equation (17) and Equation (29) results in:

$$E_{Trim} = \frac{0.2\,\mathrm{mV}}{63.5\,\mathrm{mV}} \cdot 0.4°/\% = 0.13° \tag{31}$$

Similarly, the maximum phase error and the maximum amplitude error can be calculated according to Equation (19) and Equation (23). The results are:

$$E_{Amplitude\_Max} = 0.5\,\% \cdot 0.158°/\% = 0.08° \tag{32}$$

$$E_{Phase\_Max} = 0.5° \cdot 0.5°/° = 0.25° \tag{33}$$

This gives an overall error of

$$E_{Max} = \sqrt{E_{Offset\_Max}^2 + E_{Trim}^2 + E_{Phase\_Max}^2 + E_{Amplitude\_Max}^2 + E_{Signal\_Max}^2}$$
$$= \sqrt{0.38^2 + 0.13^2 + 0.25^2 + 0.08^2 + 0.45^2}\ ° = 0.66° \quad (34)$$

As a result, an accuracy better than 0.7° can be expected under the given constraints.

Please note that due to the input of 3-Sigma values, this result is a 3-Sigma value also and thus typical accuracy will be significantly higher than calculated here. When using the 180° angular range, the relative error would be less than 0.4 %.

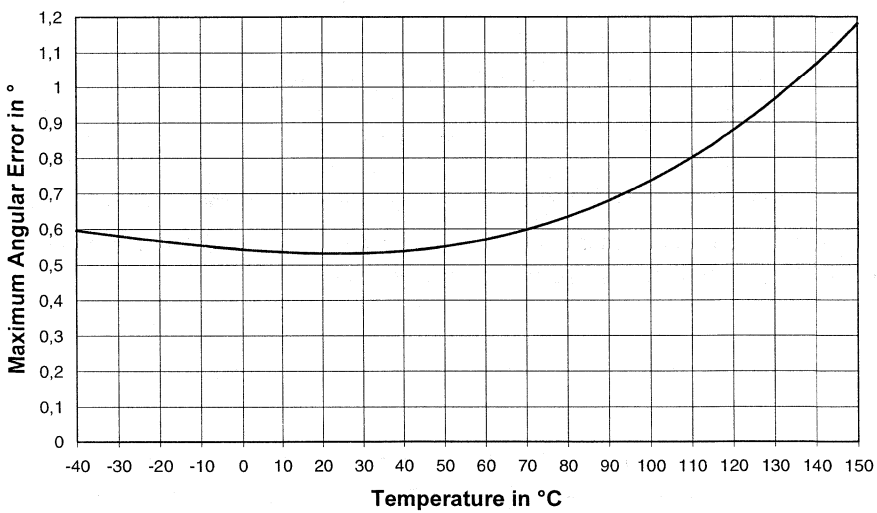

Figure 31: Maximum absolute angular error over temperature assuming the system data given in the example described in the text. The graph shows 3-Sigma values.

Similar calculations can be carried out for other temperature ranges. The result is shown in Figure 31. At 150°C, for example, a maximum error of 1.2° may occur. Again, this is a 3-Sigma value and therefore typical accuracy would be much better than calculated here.

8. REFERENCES

[1] KMZ41, Tentative Specification, Philips Semiconductors, August 1998

[2] UZZ9000 Sensor Conditioning Electronics, Objective Specification, Data Sheet, File under Discrete Semiconductors Data Book, SC17, Philips Semiconductors, 1998-08-20

[3] G. C. Giels: A 540 MHz 10-bit Polar to Cartesian Converter. IEEE Journal of Solid-States Circuits, Vol. 26, No 11, Nov. 1991, pp. 1645-1650.

[4] E. v. d. Zwan: Low Power CMOS Sigma-Delta A/D converters for speech coding. Philips Research, Nat. Lab. Technical Note NR. 230/95, 1995

[5] E. Hogenauer: An Economical Class of Digital Filters for Decimation and interpolation. IEEE Trans ASSP-29, No.2, April 1981, pp. 155-162

APPLICATION NOTE

Contactless Angle Measurement using KMZ41 and UZZ9001

AN00004

Author(s):

Klaus Dietmayer

Marcus Weser

Systems Laboratory Hamburg, Germany

Keywords

UZZ9001

KMZ41

Contactless Angle Measurement

Magnetoresistive Sensors

Digital Interface

Date: 17. January 2000

Contactless Angle Measurement Using KMZ41 and UZZ9001

Application Note AN00004

Summary

This report describes how to build a MR based measurement system using the magnetoresistive sensor KMZ41 and the sensor signal conditioning IC UZZ9001 available from Philips Semiconductors. The UZZ9001 is very similar to the UZZ9000 described in the Application note AN98097. Instead of the analog signal output, the UZZ9001 provides an SPI (serial digital) interface to the application. Moreover, the UZZ9001 operates in 180° mode only and provides no possibility to adjust the mechanical offset.

The first section gives an introduction into MR technology. It is shown that the magnetoresistive effect is naturally an angular effect recommending its use for angle measurement applications. The next sections describe the basic function of a system consisting of the sensor KMZ41 and the sensor signal conditioning IC UZZ9001. The KMZ41 sensor comprises two Wheatstone bridges on one substrate. This gives a very good matching of mechanical and electrical properties. The signal conditioning IC UZZ9001 is optimised for the usage with the KMZ41 but can also be used in conjunction with any other sensor providing two sinusoidal signals with 90°-phase shift, such as resolver applications, Hall sensors and GMR sensors. This mixed signal IC provides a serial digital output from which the angle information can be read digitally with 13-bit resolution. Both KMZ41 and UZZ9001 are specified between -40°C to +150°C for normal operation.

The last section describes the non-ideal cases and their impact on system accuracy. The error analysis based on a 3-Sigma confidence interval shows that the absolute accuracy is better than 0.6° in a temperature range from -40°C to +85°C. This corresponds to an relative error better than 0.4% referred to 180° full scale. At 150°C, the maximum absolute error is better than 1.2°. The resolution of the measurement system is better than 0.1° at all temperatures. Provided the field strength of 100 kA/m (1250 Gauss) is used for the magnetic system, the hysteresis lies within the resolution and is therefore not measurable.

Contactless Angle Measurement Using KMZ41 and UZZ9001

Application Note AN00004

Contents

Contactless Angle Measurement Using KMZ41 and UZZ9001

Application Note AN00004

Contactless Angle Measurement using KMZ41 and UZZ9001

Application Note AN00004

1 INTRODUCTION

Magnetoresistive sensors (MR sensors) of Philips Semiconductors make use of the fact that the electrical resistance of certain ferromagnetic alloys, such as permalloy, is influenced by external magnetic fields. This solid state magnetoresistive effect - or anisotropic magnetoresistance (AMR) - is easily realised in thin film technology, allowing the production of precise but also cost-effective sensors.

As the magnetoresistive effect is naturally an angular effect, its utilization for contactless angle measurement systems fits perfectly. The underlying principle is simple: the electrical resistance of the permalloy strip changes with the angle between the internal magnetization vector in the strip and the vector of electrical current flowing through it. Consequently, to achieve accurate measurements, the only condition to be met is that the internal magnetization vector of the permalloy must directly follow an external magnetic field vector. This is ensured when using an external field strength much higher than the internal magnetization. As this strong external field saturates the sensor, the actual field strength has no impact on the measurements. Only the direction of the field is evaluated. This leads to the following advantages of magnetoresitive angle measurement systems:

- Independence of magnetic drift during life time.
- Independence of magnetic drift with temperature.
- Independence of mechanical assembly tolerances.
- Independence of mechanical shifts caused by thermal stress.

Moreover, the small offset drift of the sensor signals requires no compensation for temperature effects, which simplifies implementation.

Additionally, MR based systems show the same advantages as all other contactless measurement systems; they are free of wear and they can be completely encapsulated making the sensor modules robust regarding contamination and mechanical destruction. All these advantages recommend magnetoresistive angle measurement systems for applications requiring very robust and precise but also cost-effective solutions. This, for example, is the case in all automotive applications.

To support users who want to build up a contactless angle measurement system, Philips Semiconductors provides a two-chip solution consisting of the magnetoresistive sensor KMZ41 and the sensor signal conditioning IC UZZ9000 (analog output) and UZZ9001 (digital output). The ICs were designed for the usage with the KMZ41 and therefore provide an optimised interface to this sensor.

The intention of this paper is to provide the necessary background information for system design. After giving a short introduction in the MR technology for angle measurement and discussing basics of possible system set-ups, both the KMZ41 and the UZZ9001 are described in more detail. Besides electrical characteristics and functional behaviour, main items are the correct choice of the magnet arrangement and the trimming procedure to compensate the static offsets of the sensor. The last

section describes non-ideal cases and their impact on system accuracy. A proposal is made how to calculate the achievable system accuracy under different system constraints.

2 MAGNETORESISTVE SENSOR TECHNOLOGY FOR ANGLE MEASUREMENT

Magnetoresistive (MR) sensors make use of the magnetoresistive effect, the property of a current carrying magnetic material to change its resistance in the presence of an external magnetic field. Figure 1 shows a strip of ferromagnetic material, called permalloy.

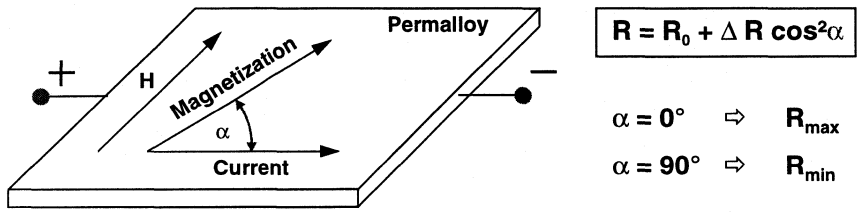

Figure 1: The magnetoresistive effect in permalloy

Assume that, when no external magnetic field is present, the permalloy has an internal magnetization vector M parallel to the current flow ($\alpha = 0$). If an external magnetic field H is applied, parallel to the plane of the permalloy but perpendicular to the current flow, the internal magnetization vector of the permalloy will rotate around an angle α. As a result, the resistance R of the permalloy will change as a function of the rotation angle α, as given by:

$$R = R_0 + \Delta R_0 \cos^2 \alpha \qquad (1)$$

R_0 and ΔR_0 are material constants. To achieve an optimum sensor characteristics, Philips use Ni19Fe81, which has a high R_0 value and low magnetostriction. With this material, ΔR_0 is in the order of 2 to 3%. It is obvious from this quadratic equation that the resistance to magnetic field relation is non-linear. It becomes also clear that the magnetoresistive effect is naturally an angular effect recommending its utilisation for angle measurement applications. Here the external magnetic field carries the measurement information between sensor and physical value to be measured.

Having this principle of operation in mind, it becomes clear that the precondition to achieve accurate measurements is that the internal magnetization vector M must directly follow the vector H of the external field. This can be achieved by applying an external field H much higher than the internal field of approximately 3 kA/m. When using the KMZ41 for angle measurement, it is recommended to provide an external field of at least

$$H \geq 100 \text{ kA/m} \quad (1250 \text{ Gauss}). \qquad (2)$$

In that case the two vectors M and H are virtually parallel to each other.

Normally, the external magnetic field is generated by permanent magnets, e.g. SmCo types. Figure 2 shows a basic set-up, where the angular position of a rotating shaft is measured with the help of the permanent magnet fixed to it.

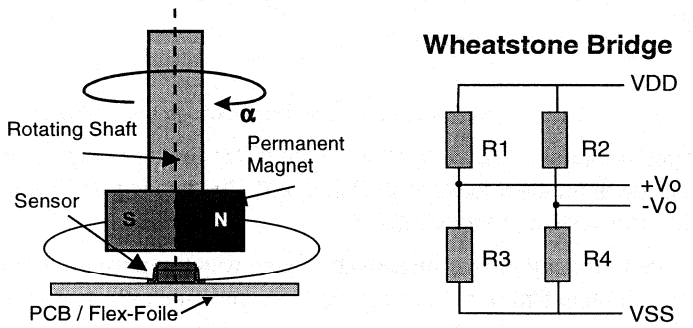

Figure 2 Basic arrangement of sensor and magnet for contactless angle measurement.

The magnetoresistive angle sensors of Philips Semiconductors are etched on a silicon substrate, with four permalloy strips arranged in a Wheatstone bridge configuration. According to the basic relationship given by Equation (1), the differential output signal (+Vo, -Vo) of such a Wheatstone bridge is proportional to $\sin 2\alpha$. This means that a sensor comprising one Wheatstone bridge can measure an angular range of 90°. This is visualised in Figure 3.

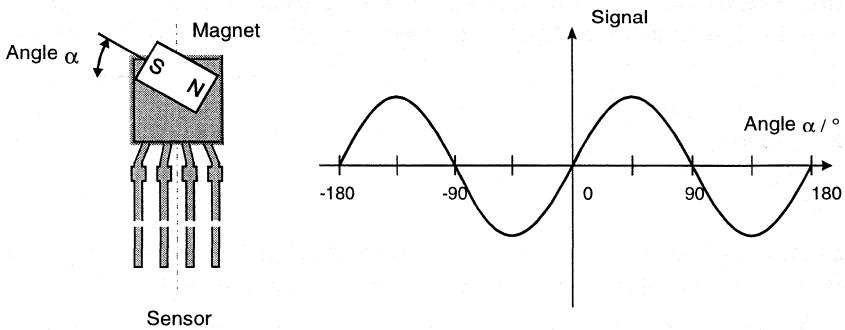

Figure 3: Output signal from a single Wheatstone bridge sensor

Apart from the limited angular range, the single bridge sensor shows another disadvantage regarding signal evaluation. As the signal amplitude changes with temperature, the output signal of the sensor forces the user to implement temperature compensation. This is avoided when using a two-bridge arrangement combined with a signal evaluation explained below. Figure 4 shows the principle.

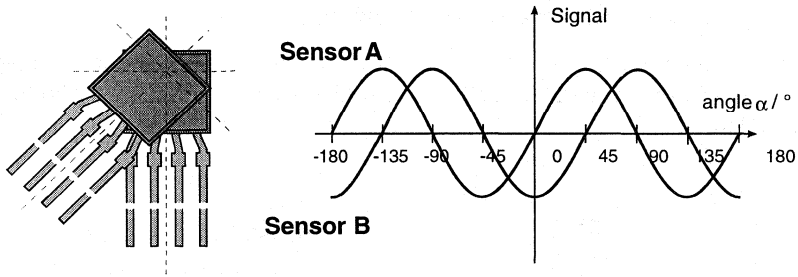

Figure 4 Output signal from a double Wheatstone bridge sensor (KMZ41)

The two sensor bridges are positioned at an offset angle of 45° to each other. In this arrangement, the two output signals show an electrical phase shift of 90°. The two signals are therefore proportional to $\sin 2\alpha$ and $\cos 2\alpha$, respectively.

Even in this arrangement, the signal amplitudes will change with temperature. However, both bridges are processed in the same thin film process steps on the same substrate and they will therefore show very similar characteristic. Assuming that both output signals have no offsets or offsets have been compensated previously, the output signals can be described mathematically as follows:

$$X(\alpha,T) = X_0(T)\sin 2\alpha \tag{3}$$

$$Y(\alpha,T) = Y_o(T)\cos 2\alpha \tag{4}$$

Assuming further that the amplitudes of both signals are really identical ($X_0 = Y_0$), the unknown angle α can be determined without any error from the signals *X* and *Y* as given by Equation (5):

$$\alpha = \frac{1}{2}\arctan\left(\frac{X}{Y}\right) \tag{5}$$

This result does not depend on the absolute amplitude of the signals. Consequently, temperature measurement and compensation of the temperature effects is not required.

Of course, due to the non-ideal manufacturing process, a real sensor will not show the ideal behaviour assumed above. A detailed discussion of these non-ideal cases and their impact on system accuracy can be found in section 7.

3 SYSTEM OVERVIEW

An angle measurement system requires one sensor KMZ41 and one sensor signal evaluation IC UZZ9001. Figure 5 shows the block diagrams of both components:

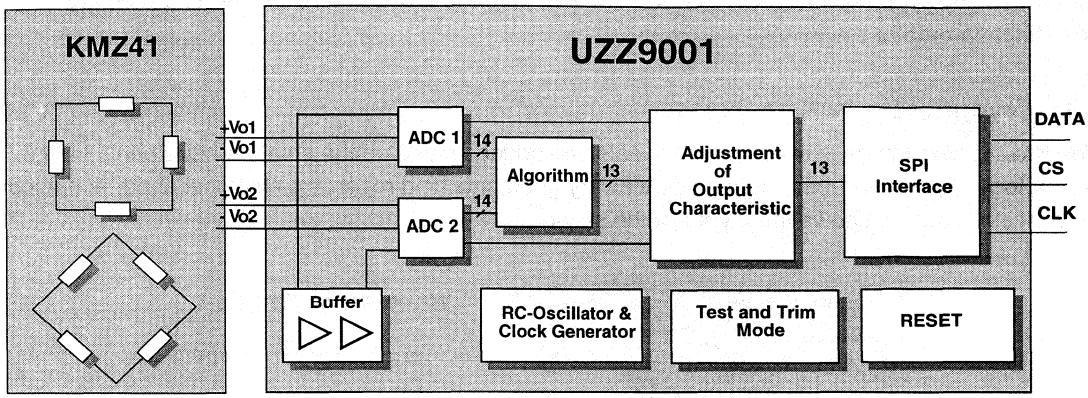

Figure 5: Block diagram of the two-chip measurement system

The differential sensor signals +/-Vo1 and +/-Vo2 of the KMZ41 are sampled by the UZZ9001 input stage and then are converted into the digital domain. This conversion is done with the help of two separate but simultaneously clocked Sigma-Delta AD converter [4]. The digital representations of the two signals are then used to calculate the angle. For this calculation the CORDIC algorithm is used. CORDIC is nothing else than an iterative way to calculate the inverse tangent function of both signals without extensive numerical overhead. Details of the CORDIC algorithm can be found in reference [3]. Afterwards, the current angle represented as a 13-bit digital value can be read from the SPI.

As mentioned before, the sinusoidal input signals coming from the KMZ41 may have a static offset that must be compensated to get accurate results. This compensation is done separately for each channel by providing an analog voltage to special pins of the UZZ9001. These voltages (OFF1, OFF2) must be provided continuously during operation as compensation is done real time and not stored at system start. As KMZ41 and UZZ9001 are not sold as one unit, the user is responsible for providing the correct compensation voltages. The UZZ9001 provides some special functions for the trimming process, which are described in section 5.

Apart from the features described above, the UZZ9001 provides an on-chip RC-Oscillator generating the clock for the IC's state machine. Consequently, no external clock reference is required for system operation. Moreover, the UZZ9001 has a power-down and power-up reset with build-in hysteresis. This reset block automatically generates a reset signal during power-on or if the save voltage range is left.

4 SENSOR KMZ41

The magnetoresitive sensor KMZ41 of Philips Semiconductors has been designed for angle measurement applications, preferably in combination with the signal conditioning IC UZZ9001. The application relevant items are discussed in the following sections. The KMZ41 properties affecting the system accuracy are discussed in section 7. Please refer to the latest data sheet to get actual specification data of the KMZ41.

4.1 Layout of the KMZ41 Sensor

The KMZ41 comprises two complete Wheatstone bridges made on the same substrate in thin film technology. Therefore both bridges show a very good matching regarding electrical and mechanical properties. Figure 6 shows the layout of the sensor.

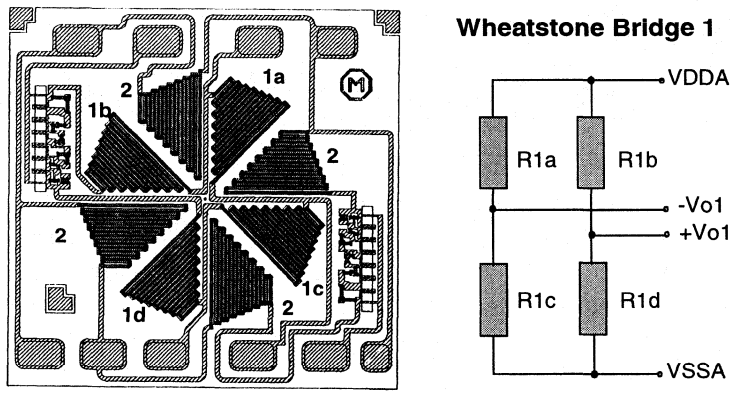

Figure 6: Layout of the double bridge sensor KMZ41.
1a to 1d indicate the sensitive elements of Wheatstone bridge 1

Moreover, the different sensitive elements of Wheatstone bridge 1 are marked. Both bridges have separate connections for supply voltage. The die size of the KMZ41 is about 1.5 mm^2 with a sensitive area of about 1 mm^2.

In order not to influence the external magnetic field and therefore the accuracy of measurements, the lead frame of the KMZ41 is made without use of ferrous material. **Please note that with respect to a good system design it is also important not to place elements consisting of ferrous material very close to the KMZ41.**

4.2 Input and Output Signals

The KMZ41 is housed in a SO8 package. The pinning is given in TABLE 1.

TABLE 1: Pinning of the KMZ41

Pin	Symbol	Type*	Description
1	-Vo1	A	negative output voltage of bridge 1
2	-Vo2	A	negative output voltage of bridge 2
3	Vcc2	A	supply voltage bridge 2
4	Vcc1	A	supply voltage bridge 1
5	+Vo1	A	positive output voltage of bridge 1
6	+Vo2	A	positive output voltage of bridge 2
7	GND2	A	Ground bridge 2
8	GND1	A	Ground bridge 1

* A = analog pin, D = digital pin

Apart from the two separate supplies, the KMZ41 provides two differential signal lines for each Wheatstone bridge. The following discussion assumes that the external magnetic field is strong enough to saturate the sensor. This ensures that each bridge of the KMZ41 has a sinusoidal output voltage as given in Figure 7.

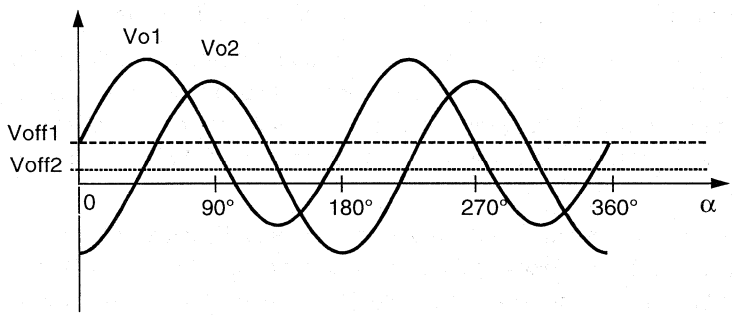

Figure 7: Output signals of the KMZ41

Ideally, these signals would have no static DC offset. However, static offsets cannot be completely avoided due to manufacturing tolerances. As these DC-offsets Voff1 and Voff2 affect the system accuracy, they must be compensated by the signal conditioning IC. The UZZ9001 provides special build-in functions for this task. Please note that Figure 7 is drawn exaggerated to emphasize the effect, the actual sensor has much smaller offsets.

The amplitudes of the output signals depend on both the supply voltage and the ambient temperature. Because of the ideal thermal coupling, the temperature coefficients of both bridges are almost identical. The MR effect exhibits a negative temperature coefficient. This means that with higher temperatures, the signal amplitude decreases and vice versa. A short example demonstrates this effect:

The typical temperature coefficient (TCVpeak) for the KMZ41 is -0.31 % / K. Consequently, based on a known peak voltage at room temperature, the peak voltage at any other temperature T can be calculated as follows:

$$Vpeak_T = Vpeak_{25°C} * \left(1 + (T - 25°C) * \frac{TCVpeak}{100\%}\right) \quad (6)$$

To give an example, the peak voltage of the KMZ41 at room temperature and 5V supply is typically $Vpeak_{25°C}$ = 78 mV. Consequently, at T = 125 °C, a peak voltage of $Vpeak_{125°C}$ = 53.8 mV can be expected. At -40°C, however, the peak voltage increases to $Vpeak_{-40°C}$ = 93.7 mV. This effect does not affect the system accuracy when using the signal processing implemented in the UZZ9001.

Besides the signal amplitude, also the DC offset drifts with temperature. However, this offset drift is so small that it needs no compensation in normal applications. The offset drift and its impact on system accuracy are discussed in section 7.

4.3 Magnets and Magnet Arrangements

It is recommended to use the KMZ41 in a magnetic field saturating the sensor. This is guaranteed when the field strength is above 100 kA/m in the sensitive area of the sensor.

The most simple magnet arrangement is that of a block magnet rotating directly above the KMZ41 as depicted in Figure 2. The effective magnetic field strength of such a block magnet arrangement depends on the distance between magnet and sensor, magnet size and magnet material. Because of strong field requirements, the usage of rare earth magnets such as SmCo or NeFeB is recommended.

Figure 8 shows the field strength of three sample magnets as a function of the distance between magnet and the top of the sensor package. It becomes clear that only the SmCo type achieves field strengths of 100 KA/m and more for distances below 0.8 mm. Its dimension of 8x3x7.5 has been chosen due to economic aspects and is used in several applications. Stronger fields allowing larger distances, this can be achieved easily when using thicker but more expensive magnets, e.g. a SmCo 8x4x7.5. Please note that the underlined dimension characterises the direction of magnetization.

In low-end applications, however, a low system price may be more important than excellent system accuracy. As a consequence, here it may be adequate to use cheaper magnets not saturating the sensor, e.g. FXD types. The additional error induced by this measure is discussed in section 7.

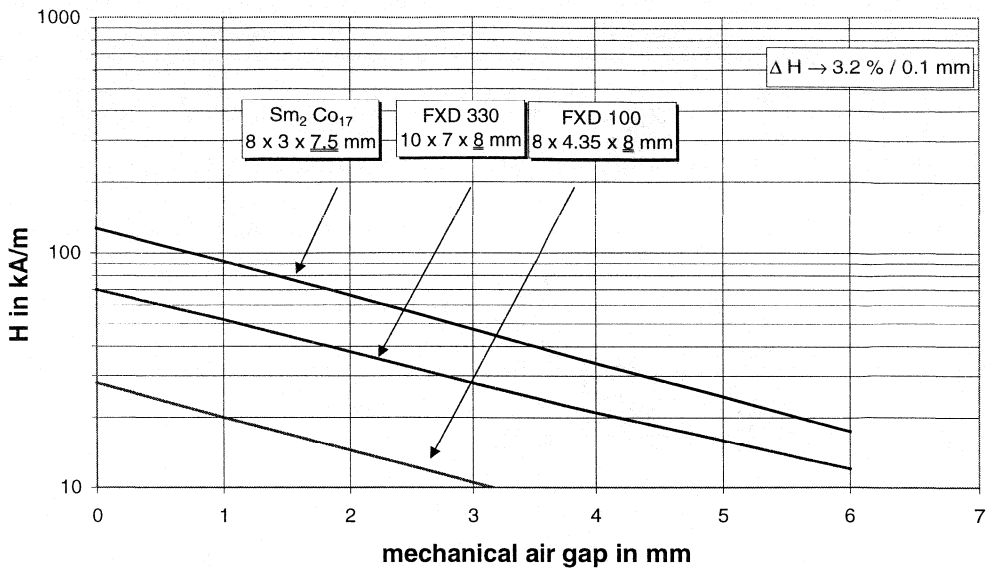

Figure 8: Field strength in the sensitive plane of the KMZ41 in dependence of the air gap between the top of the sensor package and the block magnet. The underlined dimension characterises the direction of magnetization.

4.4 Other Mechanical Set-ups

The usage of a block magnet rotating above the sensor is only one simple possibility for a magnetic system set-up (Figure 2). Meanwhile, several application specific solutions were built. These set-ups use flux rings and flux guides. Figure 9 shows the general arrangement of such a magnetic system. The inner walls of the flux ring carry the permanent magnets. This unit rotates around the fixed sensor (for example KMZ41). The two permanent magnets generate a more homogenous field inside the ring than the basic arrangement as shown in Figure 2. The additional use of the flux ring makes a shielding against external fields possible.

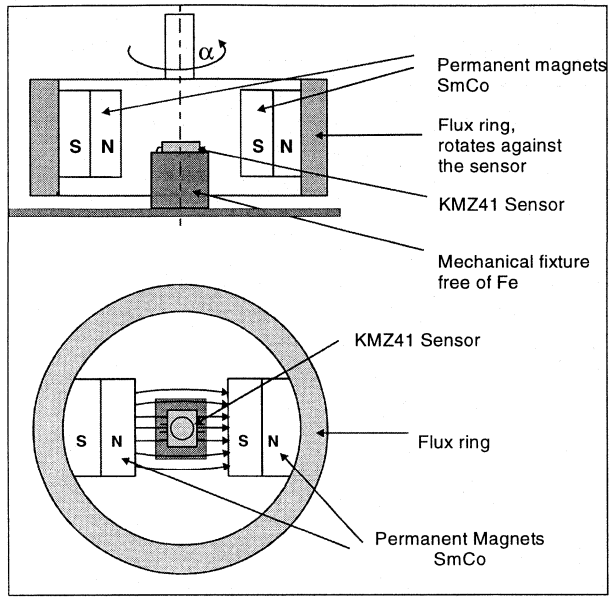

Figure 9: Mechanical set-up with two-permanent magnets and a flux ring

Simulation results of different magnetic arrangements are shown in

- Figure 10 (two-magnet arrangement),
- Figure 11 (four-magnet arrangement) and
- Figure 12 (ring-magnet arrangement).

Each Figure shows the simulated flux lines in dependence of the magnet arrangement. In each arrangement the same magnetic flux ring and magnetic material is applied (SmCo). The magnetic arrangements produce different magnetic fields with respect to strength and homogeneity.

It is obvious that the ring-magnet arrangement has the most homogeneous magnetic field in comparison to the other magnet arrangements. The arrangement with two-magnets seems to be more inhomogeneous as the four-magnet arrangement.

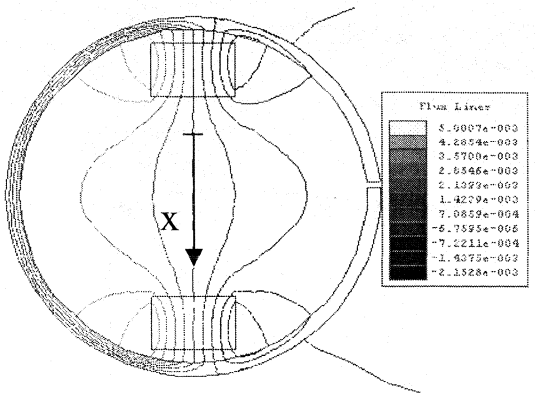

Figure 10: Flux lines of a two-magnet arrangement

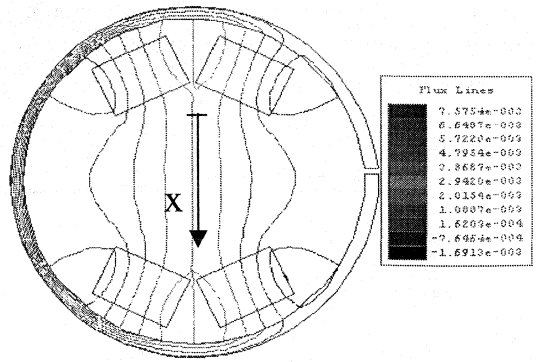

Figure 11: Flux lines of a four-magnet arrangement.

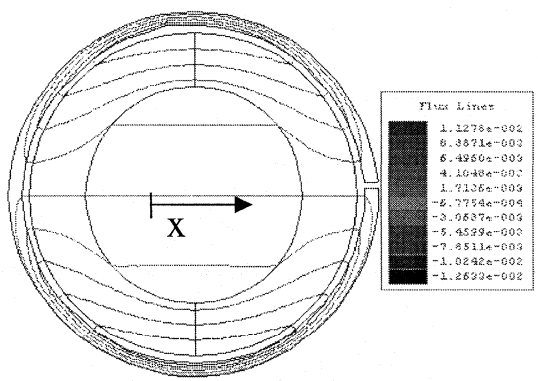

Figure 12: Flux lines of a ring-magnet arrangement

Figure 13 shows the simulated magnetic field strength H of these magnetic arrangements. The relevant position (X-Position) for the sensor is also shown in Figure 10 to Figure 12.

The ring-magnet arrangement generates the most homogeneous magnetic field in comparison to the other magnetic arrangements. The arrangement of four-magnets achieves a little bit more inhomogeneous result as the ring magnet. The simulated magnetic field strength reaches a value up to $H_{Simulation}$ = 180 kA/m and is quite similar between both magnetic arrangements. Overall the four-magnet arrangement can be an alternative to the ring-magnet arrangement.

The two-magnet arrangement achieves a significant lower magnetic field strength. At the relevant sensor position a magnetic field strength of $H_{Simulation}$ = 105 kA/m is achieved. The parabolic curve is disadvantageous in comparison to the homogeneous magnetic field of the ring-magnet. Therefore

this solution can be a compromise between the system accuracy and the system costs. The mechanical set-up for this simulation is shown in Figure 9.

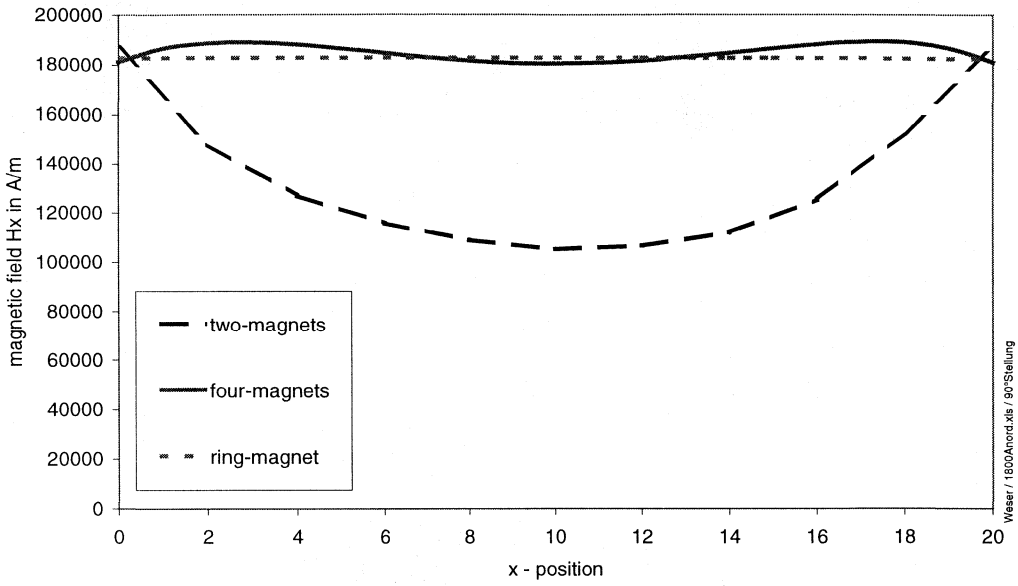

Figure 13: Simulation of the magnetic field strength $H_{simulated}$ for different magnet arrangements (two-, four-magnet and ring-magnet arrangement)

Therefore the magnet arrangement (diameters, dimensions of the flux ring and the magnets) must be dimensioned application-specific. The mean targets of optimisation are:

- Concentration of the magnetic field in order to allow the usage of weaker magnets (ferrite instead of rare earth).
- Making the magnetic field homogenous in a wider range to tolerate larger mounting tolerances.
- Shielding of the primary field against external fields.

A final solution will be a compromise between system accuracy and system costs.

5 SIGNAL CONDITIONING IC UZZ9001

The UZZ9001 is a signal IC for angle calculation. It combines two sinusoidal signals (sine and cosine) into one digital output signal. The UZZ9001 can be used in conjunction with any sensor that encodes a mechanical angle into two sinusoidal signals with 90° phase shift. The UZZ9001 is very similar to the UZZ9000, which is described in the Application note AN98097. Instead of the analog signal output, the UZZ9001 provides a digital output. The digital output stage implements the Motorola Serial Peripheral Interface (SPI). Moreover, the UZZ9001 operates in 180° mode only and provides no possibility to adjust the mechanical offset like the UZZ9000. The UZZ9001 has an overall accuracy better than 0.35° assuming ideal inputs. This limit holds over the specified ambient temperature range of -40°C to +150°C. The Pinning of the UZZ9001, the input and output characteristic and the trimming process are discussed in the following sections.

5.1 General Description

The basic operation of the UZZ9001 has already been described in section 3. Within this section, some more details should be addressed that might be useful for a system designer. The detailed block diagram of the UZZ9001 is given in Firgue 14.

The following list gives a short description of the relevant blocks.

1. The **ADC** block contains two Sigma Delta AD converters for the sensor signals and a sensor offset correction circuitry.
2. **DF** stands for the two digital low pass decimation filter which convert the low resolution high speed bit stream coming from the Sigma Delta converters into a low speed digital word.
3. The **ALU** block derives an angle value from the two digital inputs using the CORDIC algorithm.
4. The **SPI** converts the digital angle value from parallel into serial data, which can be clocked out by the user.
5. The block **CNTRL** provides the clock and the control signals for the chip.
6. The **COMP** block generates binary output signals used for sensor trimming.
7. The **RESET** block supplies a reset signal during power-up and power-down when the power supply is below a certain value.
8. The **OSC** unit generates the master clock

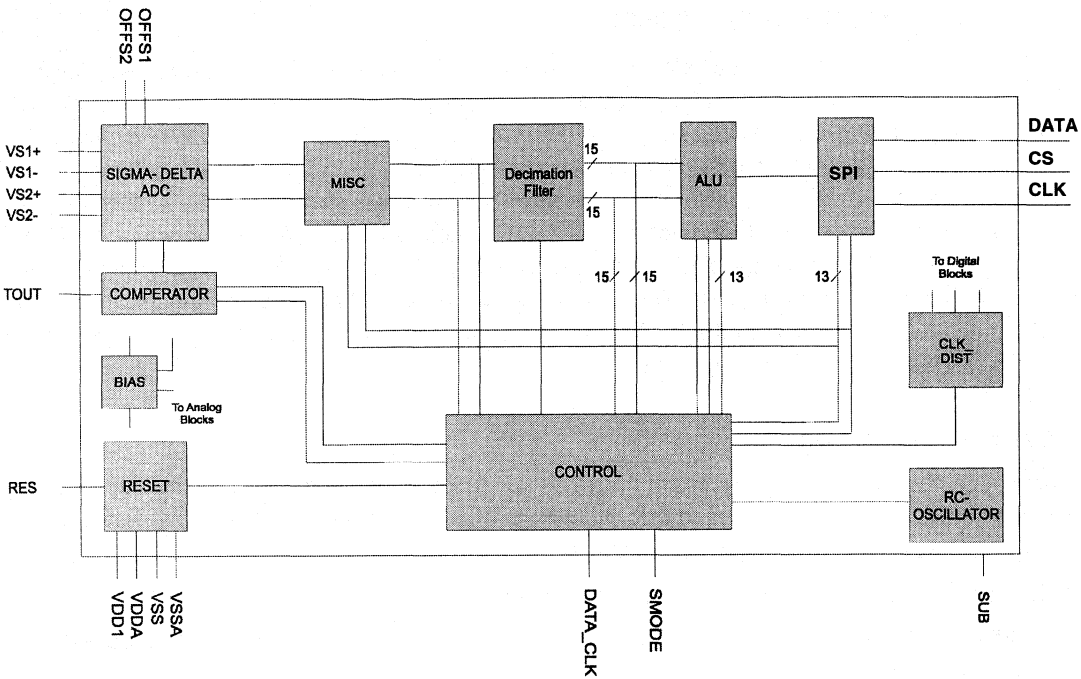

Firgue 14: Detailed block diagram of the UZZ9001

On entering the IC, the analog measurement signals are converted to digital data by an ADC. The ADC is a Sigma-Delta modulator, employing a 4th order continuous time architecture, with an over-sampling ratio of 128 to achieve high resolution. The output of the converter is a digital bit-stream at the over-sampling frequency of typically 500 kHz. The bit stream is fed into a decimation filter, which performs both low-pass filtering and down sampling. There are two input channels of the IC, each of which has its own ADC and decimation filter. The two decimation filter outputs are digital words of 15-bit at a lower frequency of typically 3.9 kHz. This is the typical sampling frequency of the sensor system. The digital representations of the two signals are then used to calculate the current angle. This calculation is done using the so-called CORDIC algorithm. The angle is represented with a 13-bit resolution accessible via the SPI (Serial Peripheral Interface).

The SPI is a byte-orientated synchronous serial master-slave bus system. The UZZ9001 has a SPI that operates in slave mode only. A configuration of the UZZ9001 via the SPI is not possible and therefore an input data line is not required.

The general arrangement of such a basic slave SPI interface is shown in Figure 15. All signals are related to the common VSS line (digital ground). Only a master SPI module (Electronic Control Unit, ECU) can initiate transmissions. Therefore, the start of the transmission is indicated by setting the CS pin to logical low (signal is active low), by the master module. Then the master module can "clock out"

the required data from the shift register. This transfer mode and details of the timing are specified in section "Serial Peripheral Interface (SPI)".

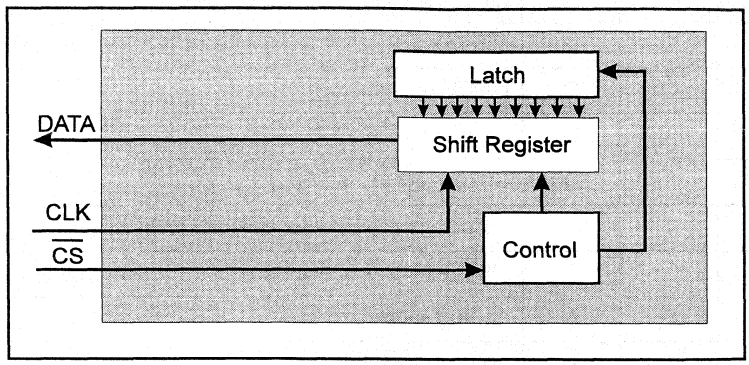

Figure 15: Slave-SPI Block Diagram

5.2 Pinning of the UZZ9001

The following **Table 2** gives the pinning of the UZZ9001 that comes in a standard SO24 package.

Table 2 Pinning of the UZZ9001

Pin	Symbol	I/O*	Type*	Description
1	+Vo2	I	A	positive output voltage of sensor 2 (Wheatstone bridge 2)
2	+Vo1	I	A	positive output voltage of sensor 1 (Wheatstone bridge 1)
3	VDD	S	A	digital supply
4	VSS	S	A	digital ground
5	VSSA	S	A	analog ground
6	RES	I	D	resets the digital part of the UZZ9001, pin is active high. If not used, pin can be left unconnected (internal pull-down resistor) or connect it to ground.
7	TEST1	I	D	used for production tests, can be left unconnected (internal pull-down resistor) or connect it to ground
8	TEST2	O	D	used for production tests, must be left unconnected
9	DATA_CLK	I	D	data clock, used when setting the UZZ9001 into trim mode, can be left unconnected (internal pull-down resistor) or connect it to ground
10	SMODE	I	D	serial mode programmer, used when setting UZZ9001 into

Pin	Symbol	I/O*	Type*	Description
				trim mode, can be left unconnected (internal pull-down resistor) or connect it to ground
11	TEST3	O	D	used for production tests, must be left unconnected
12	DATA	O	D	DATA pin of the SPI.
13	CLK	I	D	Data clock of the SPI.
14	CS	I	D	Chip Select of the SPI.
15	OFF2	I	A	offset trimming input for sensor 2 (Wheatstone bridge 2)
16	OFF1	I	A	offset trimming input for sensor 1 (Wheatstone bridge 1)
17	VDDA	S	A	analog supply
18	VSSA	S	A	analog ground
19	TEST4	I	D	used for production tests, can be left unconnected (internal pull-down resistor) or connect it to ground
20	TEST5	I	D	used for production tests, can be left unconnected because of an internal pull-down resistor or connect it to ground
21	VDD	S	A	digital supply
22	TOUT	O	D	used in trim mode, gives the offset corrected signal of sensor 1 or sensor 2, must be left unconnected in application
23	-Vo2	I	A	negative output voltage of sensor 2 (Wheatstone bridge 2)
24	-Vo1	I	A	negative output voltage of sensor 1 (Wheatstone bridge 1)

* A = analog pin, D = digital pin, S = supply, I = input, O = output

5.3 Characteristics of the Input Signals

The input stage of the UZZ9001 expects two sinusoidal signals (section 4.2). The electrical characteristics of these signals are defined in TABLE 3. These values correspond to the KMZ41 sensor specification.

TABLE 3: Limits of the UZZ9001 input signals

Parameter	Min	Max	Units
Analog supply voltage	4.5	5.5	V
Differential input voltage range (peak voltage)	+/- 6.6*	+/- 28	mV / V

Parameter	Min	Max	Units
referred to analog supply voltage (including any offset)			
Differential input voltage offset referred to analog supply voltage	-2	+2	mV / V
Common mode range referred to the analog supply voltage	490	510	mV / V

* If signals of both channels are below this limit at the same time, the magnet lost error condition becomes active (see section 5.6).

5.4 Characteristic of the Output Signal (SPI-Pins)

The digital output signal of the UZZ9001 is coded in 14 bits named D13 to D0. Within these 14 bits, the coding of the angle uses 13 bits (D12 to D0). One bit (D13) is reserved to indicate error and diagnostic conditions.

The 14 data bits (D13-D0) are arranged in 2 Bytes as shown in Figure 16. D13 is the MSB of the sensor signal and D0 is the LSB of the sensor signal. Byte 2, which is sent first, contains the data bits D13 to D7 and additionally the parity bit P2 which is added to allow the recognition of disturbed messages. P2 gives the ODD Parity of the data bits D13 to D7 and has to be evaluated by the master module.

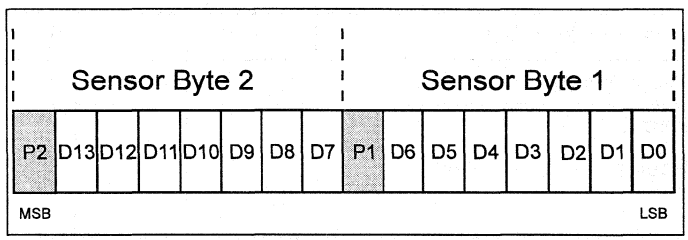

Figure 16: Coding of the digital output

Similar, Byte 1 comprises data bits D6 to D0 and the parity bit P1, which gives the ODD Parity of the data, bits D6 to D0. The ODD parity is chosen to detect failure modes where the DATA pin is short-circuit to GND or VDD or where the connection between DATA out of the slave and DATA in of the master is interrupted (e.g. broken wire).

The error and diagnostic conditions are indicated by D13 = 1 (logical high). In this case, the last two bits (D0 and D1) specify the error case. All other bits (D3 - D12) still shows the current measurement value. Consequently, the two least significant bits are lost for the measurement representation, which results in 11-bit resolution in error and diagnosis cases. Whether the measurement value is reliable or

not depends on the special error case and has to be evaluated by the master unit. The coding is specified in Table 4.

Table 4: Coding of error and diagnostic cases

D1	D0	Case	Measurement value reliable	Comments / Remarks
0	0	No valid value presently available due to RESET	No	
0	1	Magnet Lost	No	
1	0	reserved	-	
1	1	reserved	-	

The output stage of the UZZ9001 (DATA pin) is able to drive any external output load as defined in TABLE 5. This output changes from direct connection to VSS to output active (driver active) in dependence of the CS line.

TABLE 5: Static Operating Characteristics of the DATA Pin

Symbol	Parameter	Min	Nom	Max	Units
V_{OL}	Output voltage "LO"			0.4	V
V_{OH}	Output voltage "HI"	V_{DD} - 0.8		V_{DD}	V
I_O	Output current (Peak Driver Capability)			10	mA
C_{OUT}	Output capacitance (Note1)		150		pF

Note 1: C_{OUT} should chosen adequately in combination with a resistance in order to limit I_O during switching to the specified maximum value

The requirements of the other digital signals (CLK and CS pins) of the SPI are given in **Table 6**. This signals are input signals of the SPI and necessary for the digital output signal on the DATA Pin.

Table 6 Static Operating Characteristics of CLK and CS Pins

Symbol	Parameter	Min	Typ	Max	Unit
V_{IL}	Input voltage "LO"	0		0.3 * V_{DD}	V

V_{IH}	Input voltage "HI"	0.7 * V_{DD}		V_{DD}	V
I_I	Input current		10		uA
C_{IN}	Input capacitance		10		pF

5.5 Serial Peripheral Interface (SPI)

This chapter gives a general overview on the pin characteristics, their interrelationships and timing requirements.

5.5.1 CS Pin

The Electronic Control Unit (ECU) selects the UZZ9001 via the CS pin, which is active low. Whenever the pin is in a logic low state, the DATA pin output driver is enabled allowing data to be transferred from the UZZ9001 to the ECU. Consequently, on the falling edge of the CS signal, the DATA output driver changes from fixed connection to Vss into active mode which means it drives the actual data bit level onto the DATA line. CS is active (low) during data transmission. With the leading edge of CS, DATA changes again from active state to fixed connection to Vss. Additionally the edges on the CS line are used to up-date the SPI Shift Register content.

5.5.2 CLK Pin

The system clock (CLK) clocks the internal shift registers of the UZZ9001. With every falling edge of CLK, the register is shifted by one position and therefore the next data bit level is driven on the DATA line. The bit level is sampled (by the master) at the next leading edge of the CLK signal. Due to synchronisation requirements of the internal logic of the UZZ9001 and to ensure correct SPI timing conditions, the CLK pin must be held on a constant "logical high" level whenever a transition of the CS signal occurs. The master unit provides the timing of the CS and CLK Signal, therefore the designer of the ECU is responsible for meeting these timing requirements. Details of the SPI Timing are specified in section "SPI-Timing" (5.5.4).

5.5.3 DATA Pin

The serial output (DATA) pin is the output from the shift register. It operates as push-pull driver. If CS is not active, the pin is connected to Vss. An external serial resistor will limit the current if inadvertently the line is connected to VDD. The DATA pin remains in this state until the CS pin goes to a logic low state. When CS is active then the DATA pin push-pull output driver is activated and drives the present data bit level onto the bus line.

5.5.4 SPI-Timing

As a slave node the UZZ9001 provides only one operation mode. With respect to Motorola SPI devices, this mode is selected by setting CPHA = 1 and CPOL = 1.

In this transfer mode the data bits are sampled by the master unit using the leading edge of the clock, as shown in Figure 17. The falling edge indicates that the next data bit has to be provided by the slave device (shift operation).

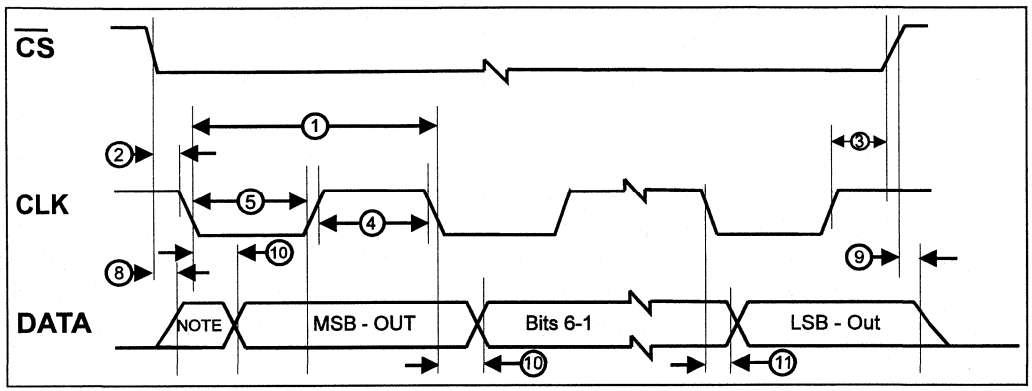

NOTE: Not defined data, normally LSB of character previously transmitted

Figure 17: UZZ9001 SPI Interface Timing

The timing requirements of the SPI interface are given in the following table:

TABLE 7: SPI-Timing:

Diagram Number	Parameter	Symbol	Min	Max	Unit	Remarks / Test Conditions
	Operating Frequency	f_{op}	DC	1	MHz	
1	Cycle Time	t_{cyc}	1	-	us	
2	Enable Lead Time	t_{Lead}	15		ns	Determined by master module
3	Enable Lag Time	t_{Lag}	15		ns	Determined by master module
4	Clock High Time	t_{clk_high}	100	-	ns	Determined by master module
5	Clock Low Time	t_{clk_low}	100	-	ns	Determined by master module
8	Access Time	t_{acc}	0	20	ns	Time to data active

Diagram Number	Parameter	Symbol	Min	Max	Unit	Remarks / Test Conditions
						from fixed V_{SS} state
9	Disable Time	t_{dis}	-	25	ns	Hold time to fixed V_{SS} state
10	Data Valid Time (After Clock Edge)	t_v	-	40	ns	With 100 pF on all SPI pins
11	Data Hold Time (Output, After Clock Edge)	t_h	5	-	ns	
	Transmission Delay (Time between the leading edge of CS until the next falling edge)	t_{Delay}	1.2		us	

Another advantage of the chosen operation mode is that the CS pin has not to be toggled between the transmission of more than one byte. This lightens the two byte operation of the UZZ9001 as explained below. The timing of the CS line during transmission of the two sensor bytes is shown in Figure 18.

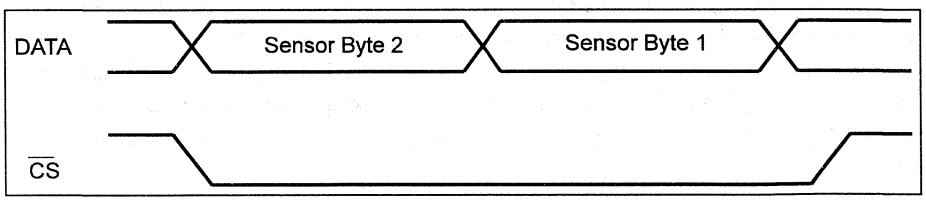

Figure 18: Timing of the CS Line

The transmission may be stopped by the user at any time. A leading edge at the CS pin will initialise the SPI Shift Register allowing the start of a complete new transmission. If the CS line is held low (active) during stop of transmission, the stopped transmission can be continued without loss of data.

5.6 Offset Trimming

For a correct output signal, it is necessary to adapt the offsets of the two input signals to the input stage of the UZZ9001. For this reason a sensor offset cancellation procedure was implemented in the

UZZ9001 which is started by sending a special serial data protocol to the UZZ9001. This trimming procedure is required for both input signals.

5.6.1 Trim Interface

The serial interface used to switch the UZZ9001 into trim mode consists of the two terminals SMODE (pin 10) and DATA_CLK (pin 9). The structure of this protocol is shown in Figure 19.

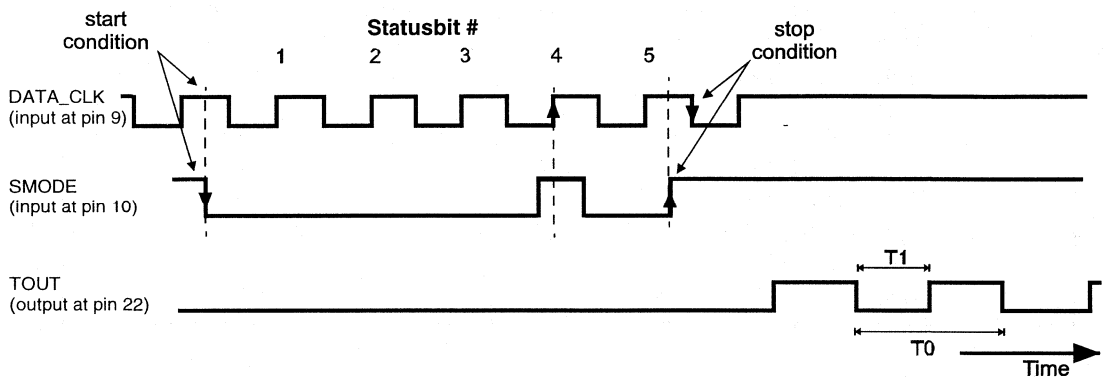

Figure 19: Protocol used to set the UZZ9001 into trim mode.

All signal levels at DATA_CLK and SMODE must be chosen according to the requirements listed in TABLE 8. Because of the asynchronous protocol, the following points have to be taken into account:

The protocol starts with a falling edge at SMODE, which must occur at a high level of the DATA_CLK. The next five bits are used for coding of the message send to the UZZ9001. They are transferred via SMODE and are sampled with the rising edge of DATA_CLK. During the fifth high level output of DATA_CLK (counted from the start condition onwards), a rising edge must appear at SMODE and afterwards DATA_CLK has to change one more time to low level in order to successfully complete the protocol.

TABLE 8: Definition of the trim interface signals

Parameter	Min	Nom	Max	Unit
supply voltage VDD of UZZ9001	4.5	5.0	5.5	V
low level of DATA_CLK, SMODE	0		5	%VDD
high level of DATA_CLK, SMODE	95		100	%VDD
rise and fall time of signal edges of DATA_CLK and SMODE (from 10% VDD to 90% VDD and	8			ns

Parameter	Min	Nom	Max	Unit
vice versa)				
Frequency of DATA_CLK	0.1		1	MHz

5.6.2 How to Enter the Trim Mode

The status bits to be transmitted to the UZZ9001 are shown in TABLE 9. Also please note that a complete protocol has to be sent to return to normal operation. Another possibility to leave the trim mode is to reset the device.

TABLE 9: Programming of trim modes

Mode	Status Bits				
	1	2	3	4	5
enter trim mode for sensor input channel 1	0	0	0	1	0
enter trim mode for sensor input channel 2	0	0	1	0	0
leave trim mode for either input channels	0	0	0	0	0

After entering one of the trim modes, a square wave output is visible at the terminal TOUT (pin 22) provided there is a dynamic input signal.

5.6.3 Offset Calibration

To make use of the build-in trimming procedure of the UZZ9001, it is necessary to generate dynamic sensor signals at its inputs. When the KMZ41 is used, a rotating permanent magnet in front of the sensor can easily generate these input signals. The principle of this set-up is shown in Figure 20.

Please note that the absolute rotational speed of the permanent magnet is not that important but it must be constant over time. Please further note that the rotational axis of the motor and magnet must be aligned exactly with the center of the KMZ41 package as shown in Figure 20. It is not necessary to use the same magnet for both trimming and application, but after trimming, the KMZ41 and UZZ9001 must be treated as one unit. The trimming procedure is as follows.

When the UZZ9001 has been switched to trim mode and sinusoidal sensor voltages are applied to its inputs, then the terminal TOUT (pin 22) immediately shows a square wave signal. This square wave

signal has the same frequency as the sensor signal and a duty cycle T1/T0 as shown in Figure 19 previously.

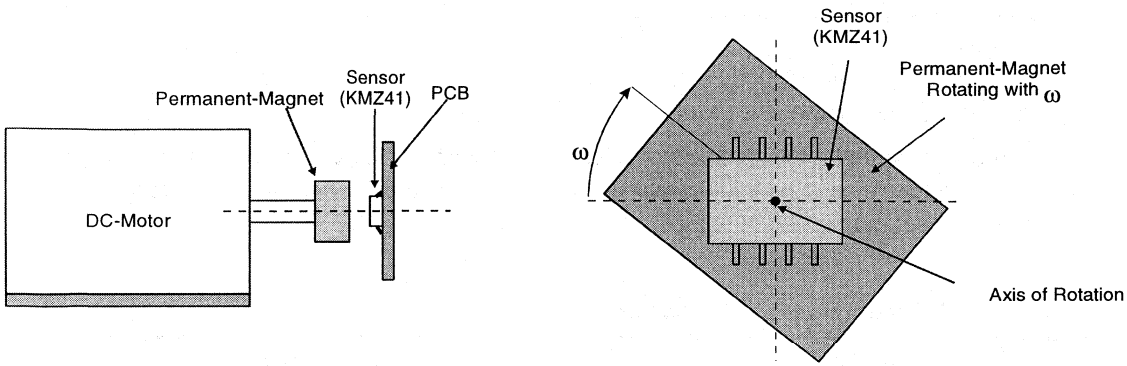

Figure 20: Proposal for a mechanical set-up to trim the UZZ9001

At a duty cycle of 50%, the offset for the selected channel is virtually eliminated. Therefore, the voltage at OFF1 (PIN16, channel 1) or OFF2 (PIN15, channel 2), respectively, has to be adjusted until this target is achieved. The trimming voltages OFF1 and OFF2 must be ratiometric to the UZZ9001 VDDA supply and must not vary more than 0.1 % VDDA with temperature and over lifetime. As already proposed for adjusting the angular ranges and zero point offset, these properties can be ensured, for example, when using a trimmable resistor divider connected to VDDA.

When building up an automatic trimming station for mass production, it is recommended to firstly determine the actual trim voltage to be fed to OFF1 and OFF2 as a fraction of VDDA. Afterwards, the resistor dividers are trimmed according to the requirements found. This procedure will be much faster compared with trying to trim the resistors step by step to get 50% duty cycle. In practice, laser trimmable resistors used for both divider elements have shown good results. Using resistors of the same material is important to get a similar temperature coefficient. Please note that for duty cycle measurements, the measuring device should be set into averaging mode in order to eliminate the influence of short spikes or noise. TABLE 10 summarises the recommended trim parameters:

TABLE 10: Definitions and recommendations of trim parameters

Parameter	Symbol	Min	Nom	Max	Unit
Frequency of the motor	fo	20		30	s^{-1}
Frequency of the sensor input signals (KMZ41)	2 fo	40		60	Hz
Stability of the rotational speed over one signal period	Δf			0.05	% fo

Parameter	Symbol	Min	Nom	Max	Unit
Limits for the duty cycle of nominal 50% during trimming		49.96		50.04	%
Variation of the voltages provided at OFF1 and OFF2 with temperature and during lifetime				0.1	%VDDA
Voltage range for OFF1 and OFF2		33.3		66.7	%VDDA
Input signal offset range to be aligned by OFF1 and OFF2. Values are referred to VDDA. The min value corresponds to the min value for OFF1 and OFF2 (33.3% VDDA), and vice versa.		-2		2	mV / V

Example:

The following example serves to demonstrate the meaning of these limits and allows the calculation of the system accuracy if other values are applied.

Assuming sinusoidal sensor signals with the amplitude *A*, then the relation between an DC offset Δx and the measured duty cycle T1/T0 is as follows:

$$\Delta x = A \sin(\pi \cdot (0.5 + T1/T0)) \quad (7)$$

At room temperature and 5V supply voltage, the typical signal amplitude *A* of the KMZ41 is 78 mV. Consequently, at a duty cycle of 50.04% (or 49.96%) the remaining offset voltage is:

$$\Delta x = 78\ mV \sin(\pi \cdot (0.5 + 0.5004)) = -0.098\ mV \quad (8)$$

As a result, the remaining offset is 0.13% referred to the signal amplitude of 78 mV. The angular error caused by this offset is discussed in section 7.

The other parameter specified is the drift of the voltages applied to OFF1 and OFF2 with temperature and over lifetime. It is specified to be less than 0.1% VDDA. The maximum voltage range for OFF1 and OFF2 is 33.3 % VDDA which is used to align the input signal offset range of +/- 2 mV / V. Consequently, changes of OFF1 or OFF2 by 0.1% VDDA will cause offset voltages Δx of:

$$\Delta x = \frac{0.1\%\ \mathrm{VDDA}}{33.3\%\ \mathrm{VDDA}} \cdot 2 \cdot 2\ \mathrm{mV/V} = 0.012\ \mathrm{mV/V} \quad (9)$$

At a supply voltage of 5V, the offset voltage caused by the drift of OFF1 and OFF2 is 0.06 mV for each channel. The resulting angular error due to this offset is discussed in section 7.

5.7 Reset

In addition to the external reset pin (pin 6), the UZZ9001 provides an internal power-up / power-down reset logic which supervises the supply voltage continuously. When the supply voltage increases and reaches a safe level, reset becomes inactive and the device starts initialization after a nominal delay of 100 us. This is to ensure settling of all analog and digital sections. When the supply voltage leaves the safe voltage level, the device is reset immediately. This internal reset logic can be over-ridden by the external pin RES (pin 6) in all modes and at any time. The reset pin RES (pin 6) is active high. It is internally pulled down to VSS and therefore does not have to be connected if the function is not required.

As the UZZ9001 has two different voltage supplies, the power-up and power-down reset operates as follows:

1. **Power-Up**

VDD or VDDA	<= 2.8 V	reset active
VDD and VDDA	>= 4.5 V	reset not active, reset will switch from high to low after a delay of 100 us.

2. **Power-Down**

VDD or VDDA	<= 2.8 V	reset active
VDD and VDDA	>= 4.4 V	reset not active, device active

If the supply voltage rises, the device is switched into active mode as soon as VDD *AND* VDDA reach the power-up switching level, which lies between 2.8 V and 4.5 V, and the delay of about 100 us has elapsed. In contrast, if the supply voltage at VDD *OR* VDDA goes below the power-down limit, which lies between 2.8 V and 4.4 V, reset becomes active immediately. Due to possible ripples on the supply voltage, a hysteresis of at least 100 mV is implemented between the power-up and power-down switching voltage levels. The following TABLE 11 summarises the specified limits.

TABLE 11: Definitions of switching levels of the build-in reset logic

Parameter	Min	Typ	Max	Unit
Switching voltage for falling VDDA OR VDD	2.8		4.4	V

Parameter	Min	Typ	Max	Unit
Switching Hysteresis		0. 3		V
Switching voltage for rising VDDA AND VDD	2.8		4.5	V
Delay for starting the initialization of the UZZ9001 when VDD AND VDDA have risen above the power-up switching level		100		us

5.8 Measurements Dynamics

The UZZ9001 provides an on-chip RC Oscillator that generates the clock for the whole device. Consequently, no external clock supply is required for the measurement system.

The nominal clock frequency of the on-chip oscillator is 4 MHz at room temperature. It varies over temperature. At -40°C, the clock frequency may reduce down to 2.3 MHz. At higher temperatures, however, a frequency up to 5.7 MHz may occur. Consequently, this influences the dynamics of measurements. From the application point of view, two different effects have to be distinguished: The system delay, which means how long it takes until a changed input signal is recognized at the output, and the measurement update rate.

The system delay is mainly caused by the settling time of the low pass decimation filter, which depends on the maximum frequency content (shape) of the input signals and the clock frequency. The following maximum values can be expected for the entire system delay (see TABLE 12):

TABLE 12: System delay and update rates of the UZZ9001

Parameter / Conditions	Min	Typ	Max	Unit
System delay defined as the time passes by until 95% of the final value is reached:				
- Max. signal frequency < 200Hz			0.6	ms
- Transients (Step response)			1.2	ms
Measurement update rate:				
- -40°C	0.45			ms
- 25°C (room temperature)		0.26		ms
- 150°C			0.18	ms

The measurement update rate, however, is directly related to the oscillator frequency. At room temperature, a new value is available every 0.26 ms. When looking at the entire temperature range of the UZZ9001, update rates between 0.45 ms and 0.18 ms are possible (see TABLE 12).

5.9 Typical Application Circuit

Figure 21 shows a typical application circuit.

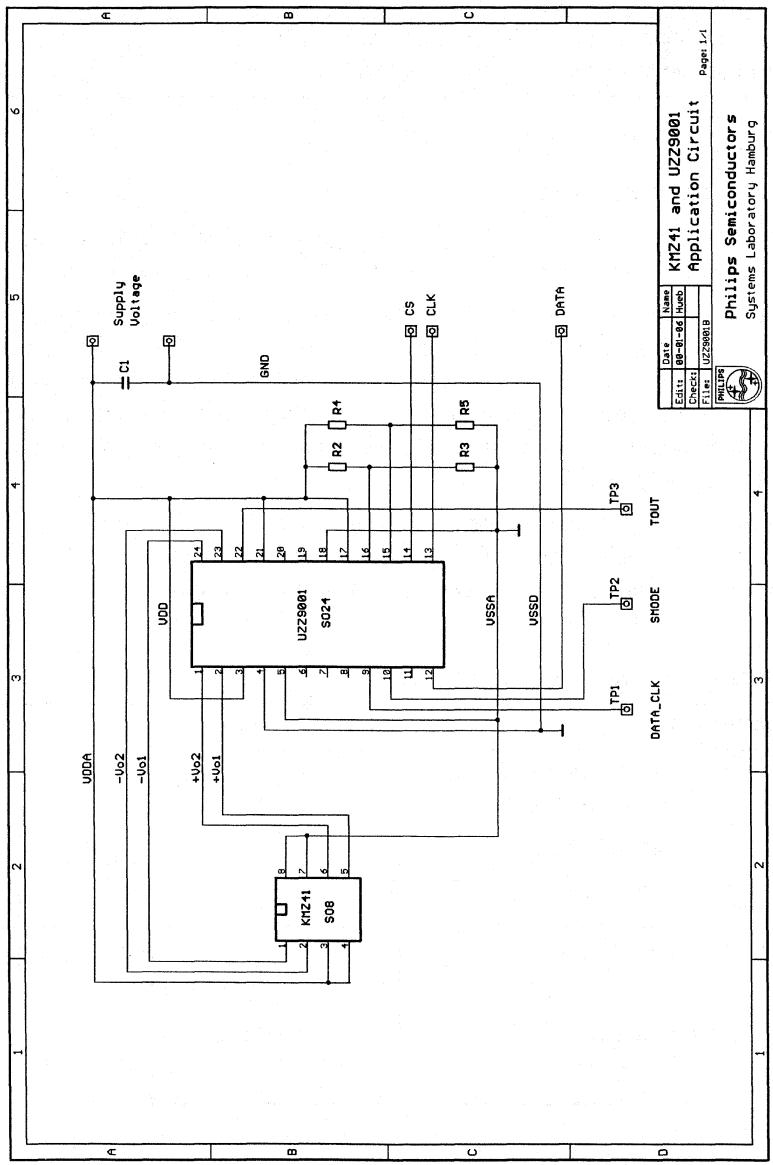

Figure 21: Schematics of a typical application circuit

6 SYSTEM ACCURACY

6.1 Sensor KMZ41

There are three different errors that may be caused by non-adequate magnetic field arrangements. These are:

- Form deviations of the sensor signals (no sinusoidal shape) and hysteresis of the sensor response if the magnetic field H does not saturate the sensor.
- Form deviations of the sensor signals caused by a non-symmetrical sensor to magnet arrangement (inhomogeneous magnetic field).
- Influence of external magnetic fields influencing the primary field used for measurements.

The influence of external fields can not be described in general as these effects depend on the actual measurement set-up. Therefore this item is not discussed within this paper. The only possibility to get rid of external fields or to limit its impact is to use some kind of a magnetic shielding as discussed in section 4.

In addition to these magnetic effects, there are some non-ideal properties of the KMZ41 sensor affecting the system accuracy. These are discussed in section 7.1.3.

6.1.1 Less Magnetic Field Strength

A complete saturation of the sensor would require the usage of an infinite magnetic field. Consequently, a complete saturation is impossible in practice and errors caused by fewer magnetic fields have to be taken into account. The magnetic field strength, which is proposed in this paper, is a compromise between the remaining error and magnet costs.

Insufficient magnetic field has two effects. The first one is the signal form error caused by a non-sinusoidal shape of the output signals (see Figure 22). Figure 23 shows the shape of the resulting measurement error. Due to its geometrical nature, the maximum and minimum values will always occur at the same locations for every sensor. Maximum values occur at the mechanical angles of 11.25°, 33.75°, 56.25°, 78.75°, 101.25°, 123.75°, 146.25° and 168.25°. No measurement errors occur at 22.5°, 45°, 67.5°, 90°, 112.5°, 135°, 157.5° and 180°.

Figure 24 shows the relation between the magnetic field strength H and the maximum peak error E_{Form} that may occur. At the recommended magnetic field strength of 100 kA/m, the measurement error is less than $E_{Form} = 0.04°$ and therefore negligible. The signal form error is reversible and does not depend on the history, as it is the case for hysteresis effects.

Hysteresis effects become visible if the angle turns back and forth over larger angular ranges as shown in Figure 25. The positions where these errors occur depend on the direction of movement. If fields become stronger, the hysteresis zones shrink to smaller areas around the positions 0°, 45°, 90° and 135°. Figure 24 also gives the maximum error caused by hysteresis effects. These are less than the errors caused by the signal form error.

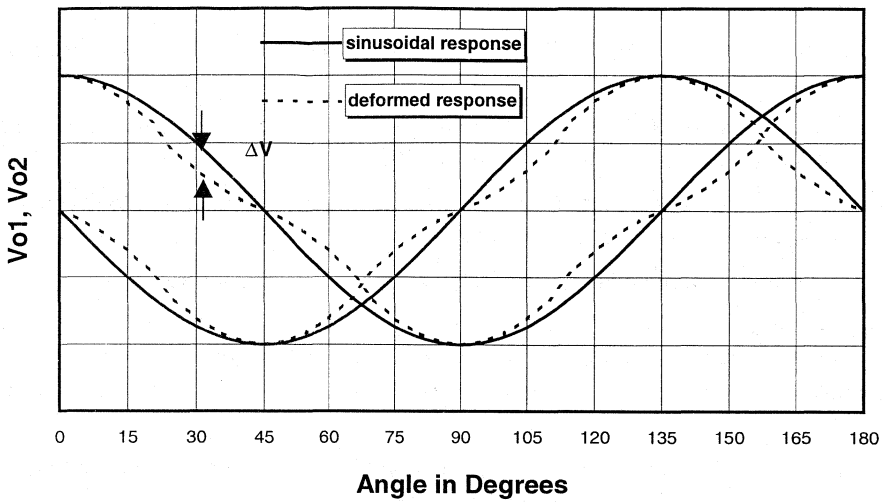

Figure 22: Signal form error of KMZ41 output signals caused by too low magnetic field not saturating the sensor

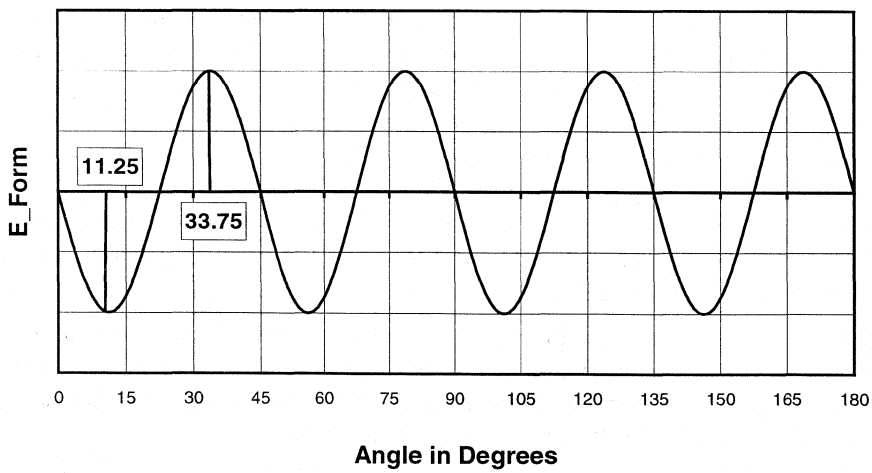

Figure 23: Shape of the measurement errors caused by the non-ideal sensor signals given in Figure 22.

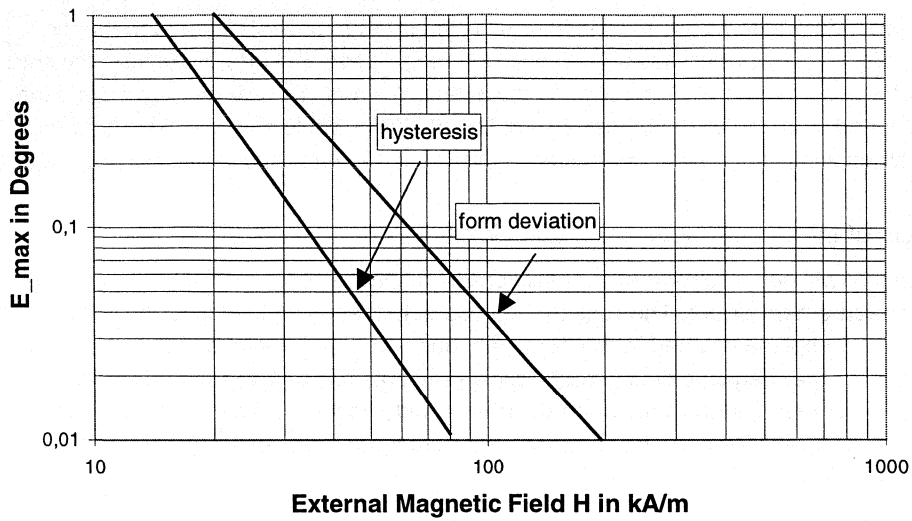

Figure 24: Maximum measurement error caused by signal form error and hysteresis

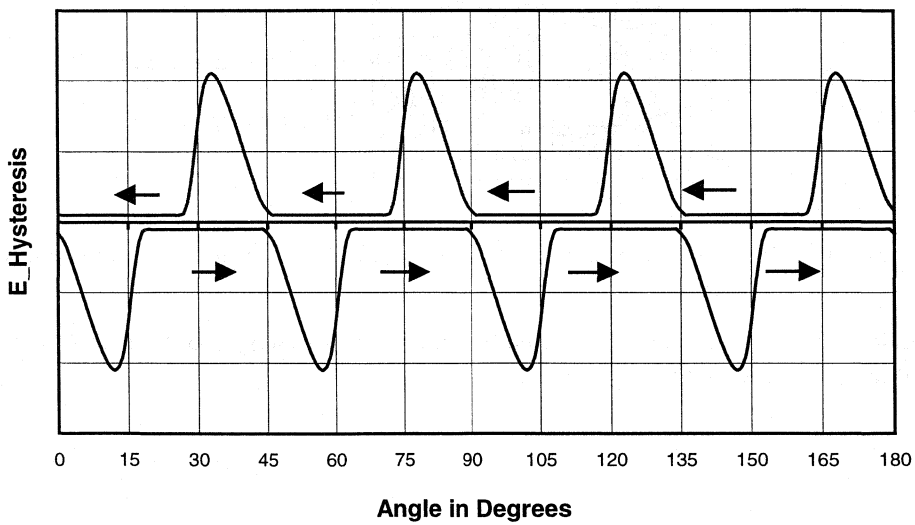

Figure 25: Shape of the measurement error caused by hysteresis

It is obvious that the measurement error caused by signal form errors and hysteresis can be neglected when using a magnetic field around 100 kA/m.

Another argument for using strong magnetic fields is the lower impact of external magnetic fields. This is especially an issue when using an unshielded magnet set-up. Here, even the very small magnetic earth field of about 30 A/m causes measurement errors. To give a rough estimation, an earth field perpendicular to the measurement field of 100 kA/m would cause a maximum error of 0.017°. Ten times this error would occur when operating at 10 kA/m, and this is not negligible.

6.1.2 Effects of Inhomogeneous Magnetic Fields

The sensor signal will get deformed even if sensor and magnet are not precisely aligned, which also may cause measurement errors. The reason for these deformations is that then the sensitive part of the sensor is not completely placed in the homogeneous part of the magnetic field, or, in other words, the relevant part of the magnetic field used for measurements has become inhomogeneous. As the actual angular error resulting from an inhomogeneous field depends on the specific set-up, it can not be calculated in general. However, for the simple block magnet arrangement discussed before, a rule of thumb can be used.

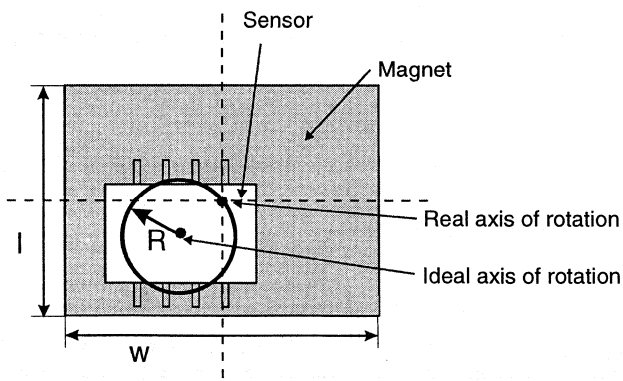

Figure 26: Definition of parameters for calculating the angular error caused by an inhomogeneous field.

Assuming the magnet arrangement depicted in Figure 2, the resulting maximum angular error can be estimated as given in Equation (10):

$$E_{\text{Inhomogeneous}} = C \cdot R^2 \qquad (10)$$

with: $C = \dfrac{320°}{(w+l)^2}$ Magnet Constant

R	Radius of the circle in which the centre of the magnet lies (see Figure 26). The midpoint of this circle is identical with the ideal axis of rotation
w	Width of the magnet
l	Length of the magnet

Note that w and l describe the magnet surface faced to the sensor. For the above mentioned magnets (see Figure 8), w and l are approximately 8 mm and thus $C \approx 1.25°/\text{mm}^2$. Consequently, a radius R of 1 mm (the magnet is positioned 1 mm apart from the ideal position) can cause maximum errors up to 1.25°. As a result, small mounting tolerances are strongly recommended when using a simple block magnet arrangement. However, enlarging the magnet will reduce this error at the expense of higher magnet costs.

Please note that this error calculation is only applicable for the block magnet arrangement. When looking at more complex magnetic designs, e.g. the one depicted in Figure 9, a customised solution must be found. Normally, when carefully designing such a complex magnetic circuit, higher mounting tolerances are possible.

Also a non-parallel position of the sensor surface and magnet surface causes errors due to an inhomogeneous magnetic field in the sensitive area of the sensor. But as long as this deviation can be limited to the range of 1° to 2°, the resulting measurement error is negligible. Consequently, the achievable precision regarding parallel mounting should not be a limiting factor.

6.1.3 Non-Ideal Properties of the Components

Due to production scatter, the KMZ41 does not generate ideal output signals but shows some variations in performance. Since continuous improvement is the target of this sensor, please refer to the latest data sheet of the KMZ41 to get current data. In the following sections, the different effects and their impact on system accuracy are described in general.

6.1.3.1 Offset and Offset Drift

The sinusoidal output signals of the KMZ41 may show offsets that limit the accuracy of the system. From the application point of view, the offset of each channel can be subdivided into two parts: a constant portion, which is virtually eliminated by trimming, and a portion that changes with temperature but needs no compensation because it is very small. Note that the temperature dependent portion is zero at the temperature where the sensor system was trimmed. Introducing an offset into the mathematical description of both signals gives:

$$X = X_0 \sin 2\alpha + \Delta x \tag{11}$$

$$Y = Y_0 \cos 2\alpha + \Delta y \tag{12}$$

The absolute angular error caused by offsets is also a function of the actual angle. It is calculated as follows:

$$E_{Offset}(\alpha, \Delta x, \Delta y) = \left| \alpha - \frac{1}{2} \arctan\left(\frac{X_0 \sin 2\alpha + \Delta x}{Y_0 \cos 2\alpha + \Delta y} \right) \right| \quad (13)$$

If both channels have the same offsets ($\Delta x = \Delta y$) , the maximum angular error is:

$$E_{Offset\_Max} = 0.4° / \% \text{ Amplitude} \quad (14)$$

This means that an offset of 1% referred to the amplitude ($X_0 / \Delta x = Y_0 / \Delta y = 1\%$) results in a maximum angular error of 0.4°. Please note that both signal amplitude and offset vary with temperature. Please also note that the angular positions where these maximum errors occur are not fixed but depend on the constellation of Δx to Δy. As these values change from part to part, locations with less errors can not be determined in general.

If only one channel shows an offset but the other is ideal, the worst case value of Equation (14) is reduced by the factor $1/\sqrt{2}$.

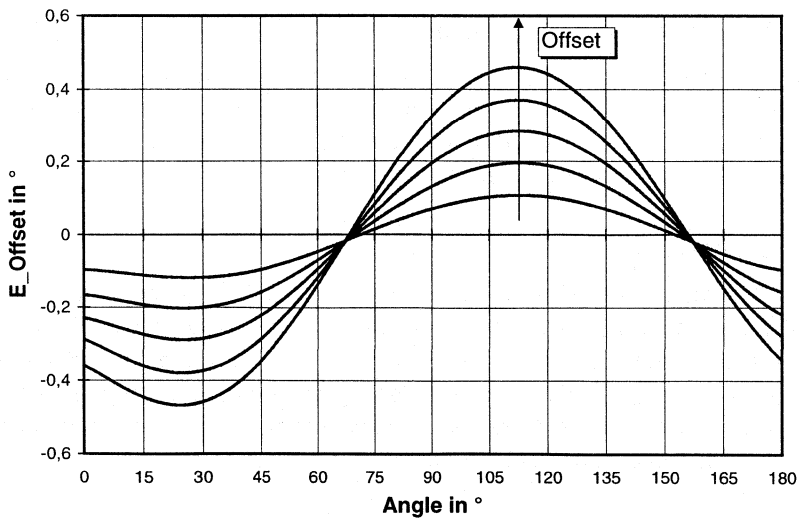

Figure 27: Typical shape of the error curve caused by signal offsets

Figure 27 shows the typical shape of the measurement error over the entire angular range. The error curve has a period of 180° what makes it distinguishable from other error shapes discussed below.

6.1.3.2 Different Signal Amplitudes

Although processed at the same time and on the same silicon substrate, both Wheatstone bridges may show slightly different signal amplitudes. The angular error caused by this effect is as follows:

$$E_{Amplitude}(\alpha, A) = \left| \alpha - \frac{1}{2} \arctan\left(A \frac{\sin 2\alpha}{\cos 2\alpha} \right) \right| \tag{15}$$

with: $A = \frac{X_0}{Y_0}$ Ratio of the signal amplitudes

The maximum error due to differences of signal amplitudes is:

$$E_{Amplitude\_max} = 0.158° / \% \ . \tag{16}$$

This means that differences between the signal amplitudes of 1% will cause a maximum angular error of 0.158°. In contrast to the offset errors, this error function shows a period of 90°. Moreover, the positions where maximum errors occur will not change significantly with A. Figure 28 shows the typical shape of the output curve.

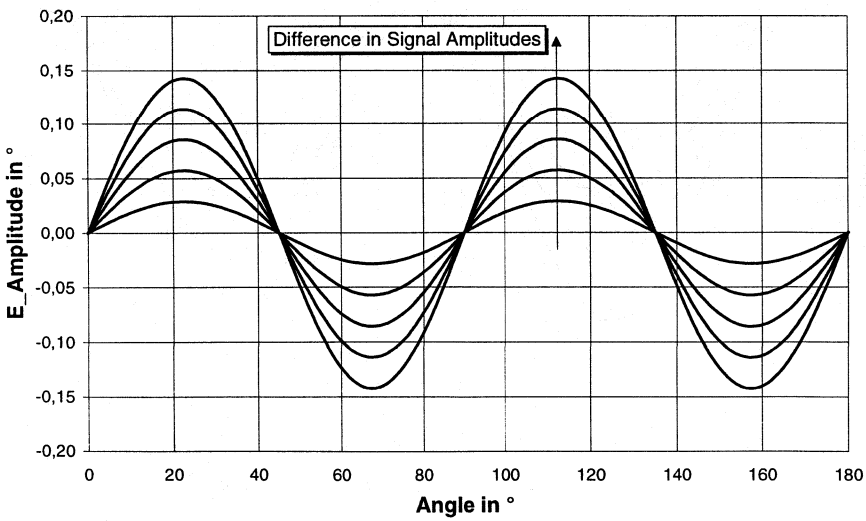

Figure 28: Typical shape of the error curve caused by different signal amplitudes.

6.1.3.3 Phase Difference between Channels

The last item to be thought of is a phase error between both channels. This means that the phase between signal *X* and *Y* is not exactly 90° over the entire angular range. Introducing this error into the mathematical description of the signal gives:

$$X = X_0 \sin(2\alpha + \Delta\beta(\alpha)) \tag{17}$$

$$Y = Y_o \cos 2\alpha \tag{18}$$

Note that the phase shift is a function of the actual angle α and therefore may not be constant over the entire angular range. The resulting angular error can be calculated as follows:

$$E_{Phase}(\alpha, \Delta\beta) = \left| \alpha - \frac{1}{2} \arctan\left(\frac{\sin(2\alpha + \Delta\beta(\alpha))}{\cos 2\alpha} \right) \right| \tag{19}$$

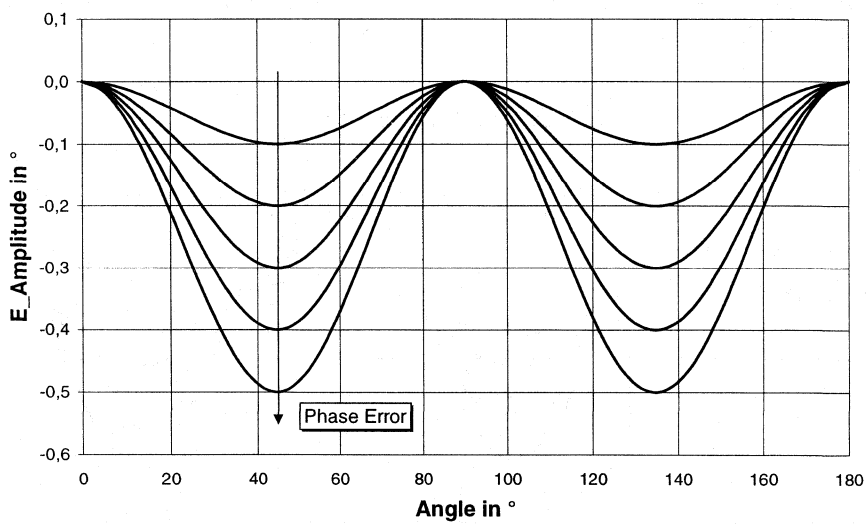

Figure 29: Typical shape of an error curve caused by phase errors.

Assuming a constant phase error, the maximum measurement error that may occur is:

$$E_{Phase\_Max} = 0.5° / ° \text{ Phase Shift} \tag{20}$$

This means that a phase shift of 1° results in a maximum angular error of 0.5°. Figure 29 shows the shape of the corresponding error function.

7.1.4 Discussion of Different Effects

When looking at the different effects discussed before, it makes sense to distinguish between errors that can be omitted when carefully designing a system and others to which the designer has no control.

The errors caused by insufficient magnetic fields are negligible when using a suitable magnet system. Therefore they must only be included in the error budget, if weaker magnets should be used in order to reduce costs. The same argumentation holds with respect to the mechanical mounting tolerances. If accuracy is important, the magnet system can be designed to provide a larger homogeneous area, allowing mounting tolerances without any impact on system accuracy. In turn, when a simple block magnet is used, mounting tolerances can be limited to reasonable values of, for example, 0.1 mm eccentricity or less.

Consequently, only errors caused by offset, different signal amplitudes and phase shift between the two channels should be taken into account. As process scatters cause these errors, it is adequate to use a statistical calculation of the overall error for the KMZ41. This can be formulated mathematically as given in Equation (24):

$$E_{KMZ41\_Max} = \sqrt{E^2_{Offset\_Max} + E^2_{Amplitude\_Max} + E^2_{Phase\_Max}} \quad (21)$$

In order to get the overall error for the measurement system the errors caused by the UZZ9001 have to be added to this value.

6.2 Signal Conditioning IC UZZ9001

There are several blocks in the UZZ9001 that may cause errors, e.g. the ADC and the ALU. These errors should not be discussed in detail. An analysis shows that the accuracy of the UZZ9001 is better than 0.35° in any case. This value holds over the entire specified temperature range and at all angular ranges provided.

$$E_{Signal\_Max} < 0.45° \quad (22)$$

This worst case value is true for the 180° angular range of the UZZ9001. In smaller angular ranges, however, the absolute error caused by the DAC becomes smaller because then the whole output voltage range is matched to that smaller range. But as this does not significantly reduce the overall

error of the UZZ9001, for simplicity, the worst case value should be used for error calculations to be on the safe side.

Additionally, the accuracy and stability of the trimming voltage has to be taken into account. An estimate of the remaining offset error after trimming can be determined according to the following procedure (compare with section 5.4):

1. Determine the maximum voltage error of the resistor divider used for offset compensation with temperature and over lifetime according to Equation (12).
2. Determine the achievable accuracy with the trimming equipment according to Equation (11).
3. Add both values to get the remaining offset.

Example:

Assume that the resistor divider guarantees an accuracy better than 0.2 % VDDA with temperature and over lifetime (compare with Table 10). This means that the maximum offset voltage due to this effect would be less than 0.12 mV at 5V supply voltage (see Equation (12)).

Moreover, the measurement and trimming equipment may guarantee a duty cycle between 49.96% and 50.04%. According to Equation (11), the remaining offset voltage would be less than 0.1 mV at 5V supply voltage. Consequently, the DC offset voltage caused by non-ideal trimming is:

$$U_{Offset\_Trim} = 0.12\ \text{mV} + 0.1\ \text{mV} = 0.22\ \text{mV} \tag{23}$$

This resulting angular error E_{Trim} has to be added to the value resulting from offset drift of the KMZ41. Consequently, the overall error budget for the UZZ9001 is:

$$E_{UZZ9000\_Max} = \sqrt{E_{Signal\_Max}^2 + E_{Trim}^2} \tag{24}$$

6.3 Application Example for Error Calculation

The following example serves to demonstrate a way to calculate the minimum accuracy that can be expected from a MR based measurement system under certain system constraints. The component specific data are taken from the current specification of the KMZ41 and UZZ9001 (see references (1) and (2)). As these devices are targets to continuous improvement, please refer to the latest data sheets to get data presently valid.

The system data assumed and the component data used are as follows:

- Temperature range required for the system: -40°C to 85°C
- Temperature while trimming: 25°C
- Maximum phase error between channels: 0.5°
- Maximum error of amplitude synchronism (k): 0.5 %
- Offset Drift (TCVoffset): 2 µV / V / K
- Constant offset due to non-ideal trimming: 0.2 mV
- Supply voltage: 5 V
- Signal amplitude KMZ41: 78 mV @ 25°C
- Temperature coefficient of peak voltage (TCVpeak): -0.31 % / K

The temperature during trimming is 25°C and therefore lies in the middle of the required operating temperature range. Consequently, the maximum change of temperature referred to this trimming temperature is about 60°C.

Nevertheless the upper limit of the operating temperature range of 85°C is more critical because the signal amplitude decreases with higher temperatures and therefore the percentage of offset to be taken into account increases. With the given data, the maximum offset voltage at 85°C is:

$$U_{Offset\_Max} = 2\ \mu V/V/°C \cdot 5V \cdot 60\ °C = 0.60\ mV \tag{25}$$

The amplitude of the signal at 85°C is 63.5 mV which is calculated using Equation (6) (TCVpeak = -0.31 % / K). As a result, the maximum offset caused by offset drift is:

$$Offset_{Max} = \frac{0.60\ mV}{63.5\ mV} 100\% = 0.94\% \tag{26}$$

The graph in Figure 30 shows the results of this calculation at other temperatures. For example, the offset drift to be taken into account at 125°C would be 1.7 %. At the maximum temperature of 150°C, 2.6 % offset may occur.

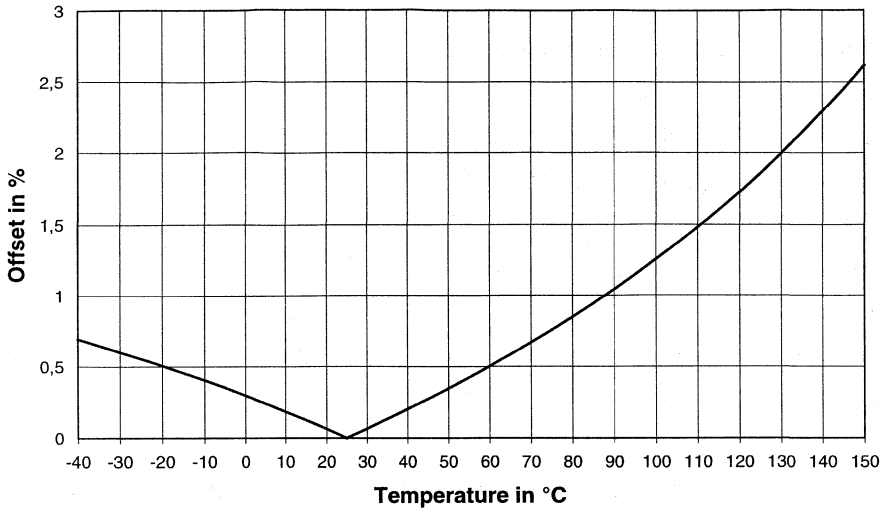

Figure 30: Offset drift at different maximum temperatures assuming the data defined in the text.

The maximum angular error caused by this offset drift can be calculated according to Equation (17). An offset of 0.94% corresponds to a maximum angular error of

$$E_{Offset\_Max} = 0.94\% \cdot 0.4°/\% = 0.38°. \tag{27}$$

In addition to offset drift, the trim error adds another portion. With the given remaining offset voltage of 0.2 mV after trimming, the evaluation of Equation (17) and Equation (29) results in:

$$E_{Trim} = \frac{0.2\,\text{mV}}{63.5\,\text{mV}} \cdot 0.4°/\% = 0.13° \tag{28}$$

Similarly, the maximum phase error and the maximum amplitude error can be calculated according to Equation (19) and Equation (23). The results are:

$$E_{Amplitude\_Max} = 0.5\,\% \cdot 0.158°/\% = 0.08° \tag{29}$$

$$E_{Phase\_Max} = 0.5° \cdot 0.5°/° = 0.25° \tag{30}$$

This gives an overall error of

$$E_{Max} = \sqrt{E^2_{Offset\_Max} + E^2_{Trim} + E^2_{Phase\_Max} + E^2_{Amplitude\_Max} + E^2_{Signal\_Max}}$$
$$= \sqrt{0.38^2 + 0.13^2 + 0.25^2 + 0.08^2 + 0.35^2}\ ° = 0.59° \quad (31)$$

As a result, an accuracy better than 0.6° can be expected under the given constraints.

Please note that due to the input of 3-Sigma values, this result is a 3-Sigma value also and thus typical accuracy will be significantly higher than calculated here. When using the 180° angular range, the relative error would be less than 0.4 %.

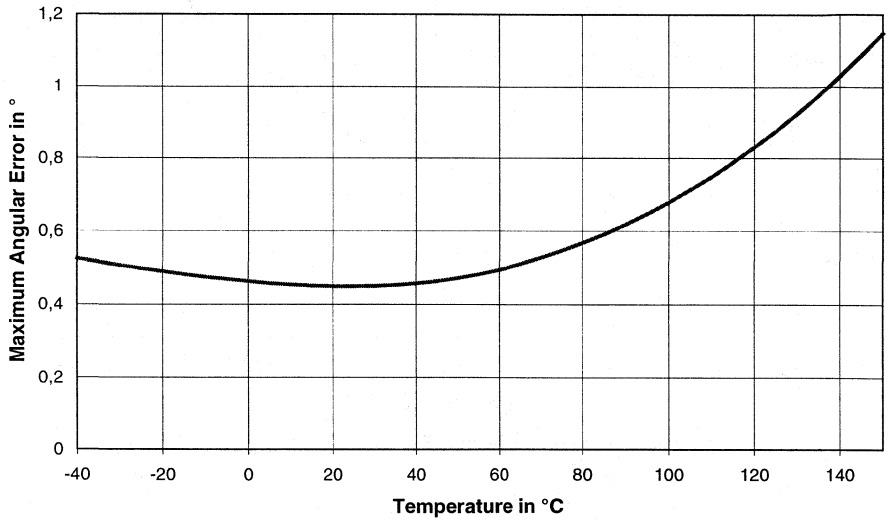

Figure 31: Maximum absolute angular error over temperature assuming the system data given in the example described in the text. The graph shows 3-Sigma values.

Similar calculations can be carried out for other temperature ranges. The result is shown in Figure 31. At 150°C, for example, a maximum error of 1.2° may occur. Again, this is a 3-Sigma value and therefore typical accuracy would be much better than calculated here.

The error E_{System} describes the angle error of the hole measuring system. Therefore, the errors $E_{inhomogenoeus}$ and E_{Form} must be included (section 6.1.2). The overall error E_{System} can be calculated as follows:

$$E_{System} = \sqrt{E^2_{Max} + E^2_{Inhomogenoeus} + E^2_{Form}} \quad (32)$$

The error $E_{inhomogenoeus}$ has very often the highest component in the error calculation. This means the effects of inhomogeneous magnetic fields are resulting in high angle errors (see section 6.1.2). Therefore small mounting tolerances are strongly recommend when using a simple block magnet arrangement (see Figure 2). Lower angle errors at higher mounting tolerances are expected with magnetic arrangements shown in section 4.4. An application specific solution must found between system accuracy and system costs.

A measured angle error E_{System} is given in Figure 32. It shows that the angle error can be lower than 0.25° by a proper magnetic arrangement.

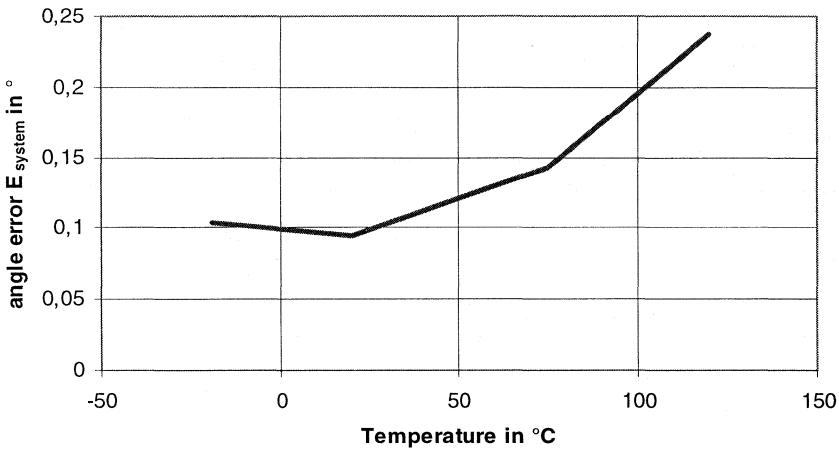

Figure 32: Measured angle error E_{system} for a typical set-up

7 REFERENCES

[1] KMZ41, Tentative Specification, Philips Semiconductors, August 1998

[2] UZZ9001 Sensor Conditioning Electronics, Objective Specification, Data Sheet, File under Discrete Semiconductors Data Book, SC17, Philips Semiconductors, 1998-08-20

[3] G. C. Giels: A 540 MHz 10-bit Polar to Cartesian Converter. IEEE Journal of Solid-States Circuits, Vol. 26, No 11, Nov. 1991, pp. 1645-1650.

[4] E. v. d. Zwan: Low Power CMOS Sigma-Delta A/D converters for speech coding. Philips Research, Nat. Lab. Technical Note NR. 230/95, 1995

[5] E. Hogenauer: An Economical Class of Digital Filters for Decimation and interpolation. IEEE Trans ASSP-29, No.2, April 1981, pp. 155-162

[6] K. Dietmayer: Contactless Angle Measurement using KMZ41 and UZZ9000, Philips Semiconductors, Application Note AN98097, 16.12.1998

DEVICE DATA

Programmable angle sensor KMA200

FEATURES

- Magnetic field angular sensing
- Resolution 0.1 °
- Accuracy better than 0.6 °
- Maximum angular range 0° to 180 °
- Programmable angle range
- Temperature range from –40 to +125 °C
- User programmable EEPROM
- Ratiometric analog output
- 13-bit digital output
- Bi-directional digital interface (SPI)
- Adjustable zero point offset
- On-line diagnosis for all main functional blocks
- Switch-off function at durable over voltage
- Temperature control
- Pre-calibrated delivery.

DESCRIPTION

The KMA200 is a programmable angle sensor, employing the magnetoresistive effect of thin film permalloy for sensing the angle between an external magnetic field in the sensor plane and the sensor. The sensor consists of two galvanic separated wheatstone bridges and an integrated circuit.

The KMA200 is user programmable. This allows user specific adjustment of the angular range and zero point and the storage of a 32-bit identifier. The data is held permanently in an EEPROM.

The device can be programmed to work either in analog or digital (SPI) output. One of three different analog output characteristics may be selected. The implemented on-line diagnosis monitors the input and output signals as well as the data processing. Deviations from and failures of the angle value are indicated in the output signal. Overall temperature control is implemented.

PINNING

PIN	SYMBOL	DESCRIPTION
1	VDD	supply voltage
2	DATA/VOUT1	data I/O, analog output
3	CLK/VOUT2	data clock, analog output
4	GND	ground
5	CS	chip select (used for data transfer I/O)

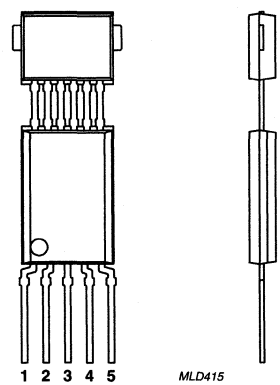

Fig.1 Simplified outline (SOT637).

QUICK REFERENCE DATA

SYMBOL	PARAMETER	MIN.	TYP.	MAX.	UNIT
V_{DD}	operating voltage	4.5	5	5.5	V
I_{DD}	supply current	–	10	–	mA
RES	resolution	–	0.1	–	deg
A_{80}	accuracy in temperature range –40 to +80 °C; note 1	–	–	0.6	deg
A_{125}	accuracy in temperature range –40 to +125 °C; note 1	–	–	1.2	deg
T_{amb}	ambient temperature	–40	–	+125	°C
f_{op}	operating frequency of the SPI; note 2	–	–	1	MHz

Notes

1. In (homogenous) magnetic field at saturation field strength.
2. With optimized application circuit.

LIMITING VALUES

In accordance with the Absolute Maximum Rating System (IEC 60134)

SYMBOL	PARAMETER	MIN.	MAX.	UNIT
V_{DD}	operating voltage	–0.3	+18	V
V_{pin}	voltage at all external pins	–0.3	+18	V
T_{stg}	storage temperature	–40	+125	°C
T_{amb}	ambient operating temperature	–40	+125	°C

FUNCTIONAL DESCRIPTION

The KMA200 consists of an MR sensor element and a signal conditioning IC as shown in Fig.2.
The sensor element produces two sinusoidal signals with a phase shift of 90 °C depending on the angular orientation of a stimulating magnetic field to the input of the IC.
The sinusoidal voltages are applied to the IC where they are converted into a linear representation of the angular value by means of two 13 bit ADC's and a ROM code controlled data processing unit.

Sensor voltage offset compensation, zero point and angular range adjustment, on-line diagnosis and the selection of different output characteristics is also incorporated.

Offset and configuration parameters are stored in a user programmable EEPROM that is accessed via a serial programming interface (SPI).

Either an analog or digital data output may be selected.

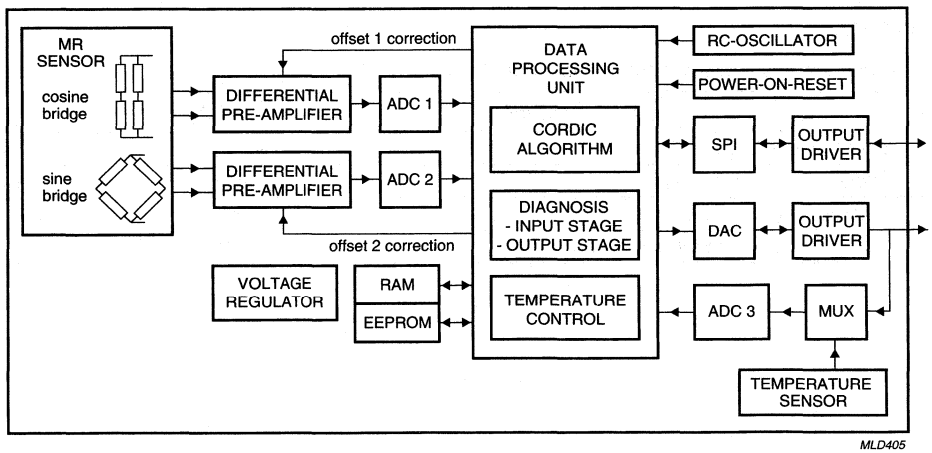

Fig.2 Functional block diagram.

Output signal

The KMA200 supplies two output pins. They are set to work either in digital or analog output mode, depending on the user defined control word stored in the EEPROM.

In the analog output mode the measured angle value is converted into a linear voltage value that is ratiometric to the supply voltage V_{DD}.

This voltage is driven by the standard output stage to pin VOUT1. Supporting redundancy requirements, the same value is fed to a second output stage that is connected to pin VOUT2. This second output stage is programmable to one of three different output characteristics (Mode 1, Mode 2 or inoperative output).
The analog output voltage range codes linear angles value and diagnostic information as well.

A valid angle value is nominally mapped to an output voltage range of 5% to 95% V_{DD} at the standard output VOUT1 (see Fig.3) and the second output VOUT2 if it is set to operate in Mode 1 (see Fig.4). In Mode 2 (see Fig.5) the valid output range at pin VOUT2 is nominally 5% to 50% V_{DD}.

Output voltages above or below these ranges are used for diagnostics.

Setting the KMA200 output characteristics

OUTPUT CHARACTERISTICS		PIN ASSIGNMENT		MODE SETTING		
MODE	TYPE	VOUT1/DATA	VOUT2/DATA	CTL2	CTL1	CTL0
Mode 1	analog	standard	inverted	tbf	tbf	tbf
Mode 2	analog	standard	half range	tbf	tbf	tbf
Mode 3	analog	standard	high resistance	tbf	tbf	tbf
Mode 4	digital	serial clock (SPI)	serial clock (SPI)	tbf	tbf	tbf
Mode 5	digital	25	serial clock (SPI)	tbf	tbf	tbf

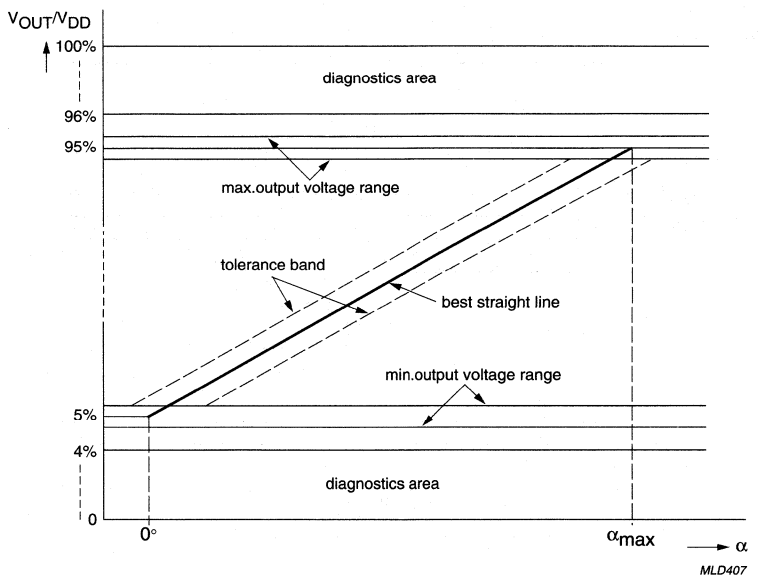

Fig.3 Standard analog output mode.

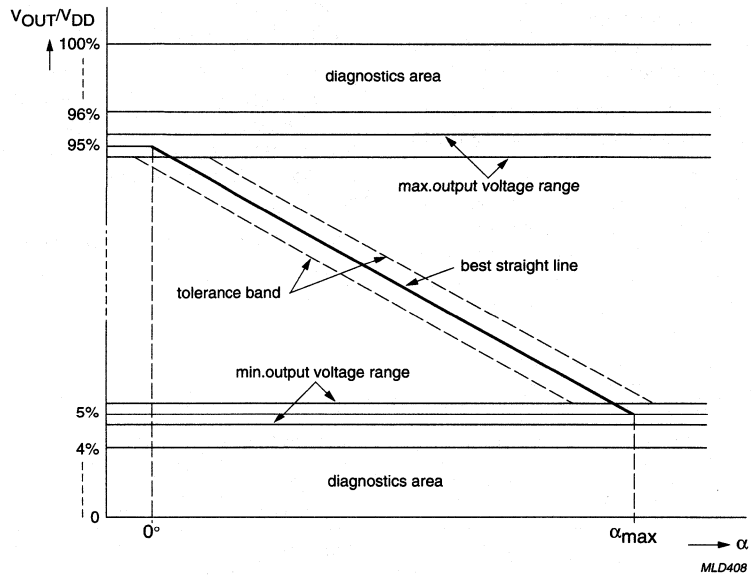

Fig.4 Inverted analog output mode (Mode 1).

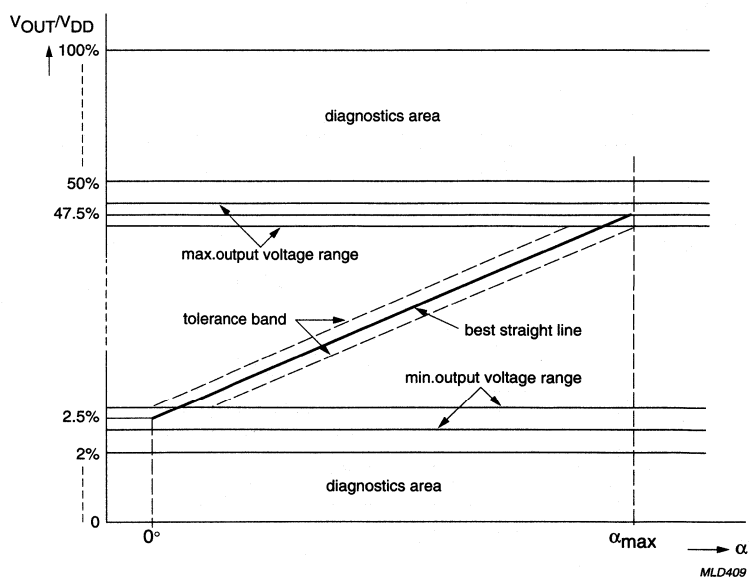

Fig.5 Half range analog output mode (Mode 2).

Digital output (SPI)

The serial programmable interface is compatible with the Motorola SPI specification. The sensor signal comprises 14 bits (D13 to D0) as shown in Fig.6. Bits D12 to D0 are used for the coding the angle value while D13 is reserved for indicating error and diagnostic conditions as defined below. The 14 data bits are arranged in 2 bytes. D13 is the MSB of the sensor signal and D0 is the LSB of the sensor signal. Byte 2, which is sent first, contains data bits D13 to D7 and the parity bit P2 which is added to allow the recognition of disturbed messages. P2 gives the ODD parity of data bits D13 to D7. Similarly, byte 1 comprises data bits D6 to D0 and parity bit P1, which gives the ODD parity of data bits D6 to D0.

The ODD parity is chosen to detect failure modes where the DATA pin is short-circuit to GND or V_{DD} or where the connection between DATA out of the slave and DATA in of the master is interrupted (e.g. broken wire).

The error and diagnostic conditions are indicated by D13 = 1 (active high). In an error situation the last two bits (D1 and D0) contain the error code. All other bits (D12 to D3) still show the current measurement value, but as the last two bits are lost for measurement representation the resolution is reduced to 11 bit. Whether the measurement value is reliable or not depends on the special error case and has to be evaluated by the master unit.

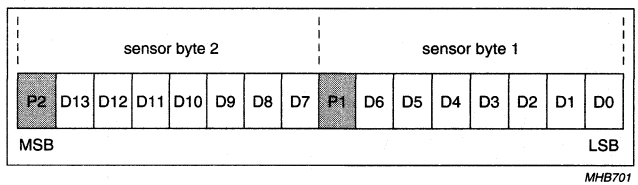

Fig.6 Digital output coding.

Further development

It is planned to develop a downgraded derivative of this angular measurement system. The accuracy and resolution of the angular measurement will remain the same, but some diagnostic features will not be implemented. The device will be usable in a limited temperature range up to 120 °C. Furthermore the downgraded device will not provide a protection against over voltage, so max. supply voltage is limited to 6 V. A standard SMD package will be used.

PACKAGE OUTLINE

Plastic single-ended multi-chip package; 6 interconnections; 5 in-line leads **SOT637**

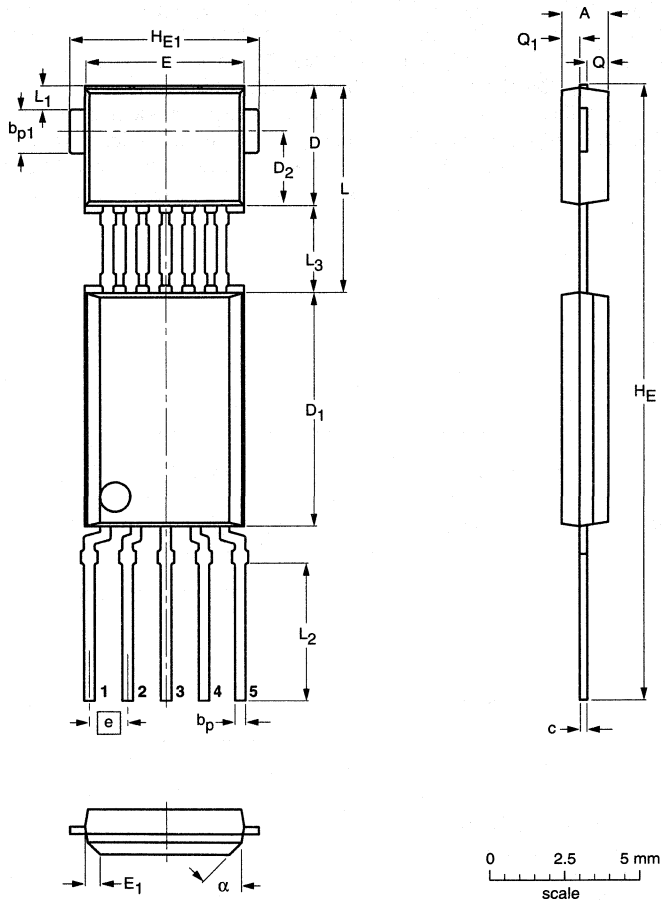

DIMENSIONS (mm are the original dimensions)

UNIT	A	b_p	b_{p1}	c	$D^{(1)}$	$D_1{}^{(1)}$	$D_2{}^{(1)}$	$E^{(1)}$	E_1	e	H_E	H_{E1}	L	L_1	L_2 min.	L_3	Q	Q_1	α
mm	1.65 1.45	0.41 0.34	1.57 1.47	0.30 0.24	4.1 3.9	8.1 7.9	2.55	5.45 5.25	0.5	1.27	21.2 20.8	6.35 6.25	7.1 6.9	0.85 0.75	4.75	3.1 2.9	0.75 0.65	0.65 0.55	45°

Note

1. Plastic or metal protrusions of 0.15 mm maximum per side are not included.

OUTLINE VERSION	REFERENCES				EUROPEAN PROJECTION	ISSUE DATE
	IEC	JEDEC	EIAJ			
SOT637						00-08-31

Magnetic field sensor KMZ41

DESCRIPTION

The KMZ41 is a sensitive magnetic field sensor, employing the magnetoresistive effect of thin-film permalloy. The sensor contains two galvanic separated Wheatstone bridges. Its properties enable this sensor to be used in angle measurement applications under strong field conditions. A rotating magnetic field strength > 40 kA/m (recommended field strength > 100 kA/m) in the x-y plane will deliver a sinusoidal output signal. The sensor can be operated at any frequency between DC and 1 MHz.

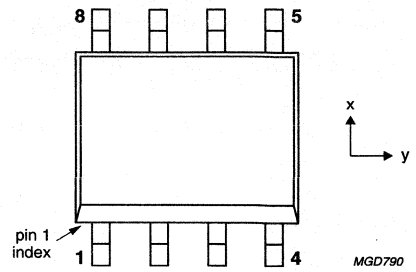

Fig.1 Simplified outline SOT96-1.

PINNING

PIN	SYMBOL	DESCRIPTION
1	$-V_{O1}$	output voltage bridge 1
2	$-V_{O2}$	output voltage bridge 2
3	V_{CC2}	supply voltage bridge 2
4	V_{CC1}	supply voltage bridge 1
5	$+V_{O1}$	output voltage bridge 1
6	$+V_{O2}$	output voltage bridge 2
7	GND2	ground 2
8	GND1	ground 1

QUICK REFERENCE DATA

SYMBOL	PARAMETER	MIN.	TYP.	MAX.	UNIT
V_{CC1}	bridge supply voltage	–	5	9	V
V_{CC2}	bridge supply voltage	–	5	9	V
S	sensitivity (α_1 = 45°; α_2 = 0°)	2.44	2.72	3.00	mV/°
R_{bridge}	bridge resistance	2	2.5	3	kΩ
$V_{offset1}$	offset voltage	–2	–	+2	mV/V
$V_{offset2}$	offset voltage	–2	–	+2	mV/V

CIRCUIT DIAGRAM

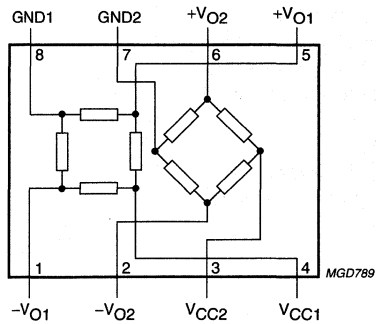

Fig.2 Simplified circuit diagram.

LIMITING VALUES

In accordance with the Absolute Maximum Rating System (IEC 60134).

SYMBOL	PARAMETER	CONDITIONS	MIN.	MAX.	UNIT
V_{CC}	bridge supply voltage		–	9	V
P_{tot}	total power dissipation		–	90	mW
T_{stg}	storage temperature		−65	+150	°C
T_{bridge}	bridge operating temperature		−40	+150	°C

THERMAL CHARACTERISTICS

SYMBOL	PARAMETER	VALUE	UNIT
$R_{th\ j\text{-}a}$	thermal resistance from junction to ambient	155	K/W

CHARACTERISTICS

T_{amb} = 25 °C; $H_{rotation}$ = 100 kA/m; V_{CC1} = 5 V; V_{CC2} = 5 V unless otherwise specified.

SYMBOL	PARAMETER	CONDITIONS	MIN.	TYP.	MAX.	UNIT
V_{CC1}	bridge supply voltage		–	5	9	V
V_{CC2}	bridge supply voltage		–	5	9	V
S	sensitivity	open circuit, note 1; α = 0° (bridge 2); α = 45° (bridge 1)	2.44	2.72	3.00	mV/°
$V_{peak\ 1}$	peak voltage	note 2; see Fig.4	70	78	86	mV
$V_{peak\ 2}$	peak voltage	note 2; see Fig.4	70	78	86	mV
TCV_{peak}	temperature coefficient of peak voltage	T_{amb} = –40 to +150 °C; note 3	–0.25	–0.31	–0.37	%/K
R_{bridge}	bridge resistance	note 4	2	2.5	3	kΩ
TCR_{bridge}	temperature coefficient of bridge resistance	T_{bridge} = –40 to +150 °C note 5	0.3	0.32	0.34	%/K
V_{offset}	offset voltage	see Fig.4	–2	–	+2	mV/V
TCV_{offset}	temperature coefficient of offset voltage	T_{bridge} = –40 to +150 °C note 6; see Fig.4	–2	–	+2	$\frac{\mu V/V}{K}$
ΔV_{offset}	maximum change of offset voltage within temperature range	T_{amb} = –40 to +100 °C; note 7; see Fig.3	–0.2	0	+0.14	mV/V
		T_{amb} = –40 to +150 °C; note 7; see Fig.3	–0.28	0	+0.22	mV/V
FH	hysteresis of output voltage	note 8	0	0.01	0.04	%FS
ω	amplitude angular velocity	note 9	0	25000	t.b.f	°/s
k	amplitude synchronism	note 10	99.5	100	100.5	%
TCk	temperature coefficient of amplitude synchronism	T_{amb} = –40 to +150 °C note 11	–0.002	0	0.002	%/K
$\Delta\alpha$	angular inaccuracy	note 12	0	0.1	0.25	deg

Notes

1. Sensitivity changes with angle due to sinusoidal output.
2. $V_{peak} = |(V_{out\ max} - V_{offset})|$.
3. $TCV_{peak} = 100 \frac{V_{peak(T_2)} - V_{peak(T_1)}}{V_{peak(T1)}(T_2 - T_1)}$ Where T_1 = –40°C; T_2 = 150°C.
4. Bridge resistance between pins 8 and 4, pins 7 and 3, pins 5 and 1, pins 6 and 2.
5. $TCR_{bridge} = 100 \frac{R_{bridge(T_2)} - R_{bridge(T_1)}}{R_{bridge(T_1)}(T_2 - T_1)}$ Where T_1 = –40°C; T_2 = 150°C.
6. $TCV_{offset} = \frac{V_{offset(T_2)} - V_{offset(T_1)}}{(T_2 - T_1)}$ Where T_1 = –40°C; T_2 = 150°C.
7. $\Delta V_{offset} = (V_{offset}(T) - V_{offset}(T = 25\ °C)$.

8. $$FH_1 = 100 \left| \frac{V_{O1(67.5°)135° \Rightarrow 45°} - V_{O1(67.5°)45° \Rightarrow 135°}}{2 \times V_{peak1}} \right|$$

$$FH_2 = 100 \left| \frac{V_{O2(22.5°)90° \Rightarrow 0°} - V_{O2(22.5°)0° \Rightarrow 90°}}{2 \times V_{peak2}} \right|$$

9. No change in V_O; no distortion of sinusoidal output; tested up to 25000 °/s maximum.

10. $k = \frac{V_{peak1}}{V_{peak2}} \cdot 100$.

11. $TCk = 100 \frac{(k_{T2} - k_{T1})}{k_{T1}(T_2 - T_1)}$ Where $T_1 = -40°C$; $T_2 = 150°C$.

12. $\Delta\alpha = |\alpha_{real} - \alpha_{measured}|$ without offset voltage influences.

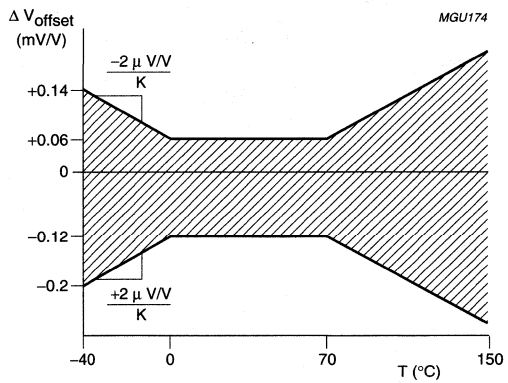

(1) 0 = initial offset voltage per supply voltage.
(2) Typical drift of the offset voltage per supply voltage remains inside shaded area of graph.

Fig.3 Supply voltage offset voltage as a function of temperature.

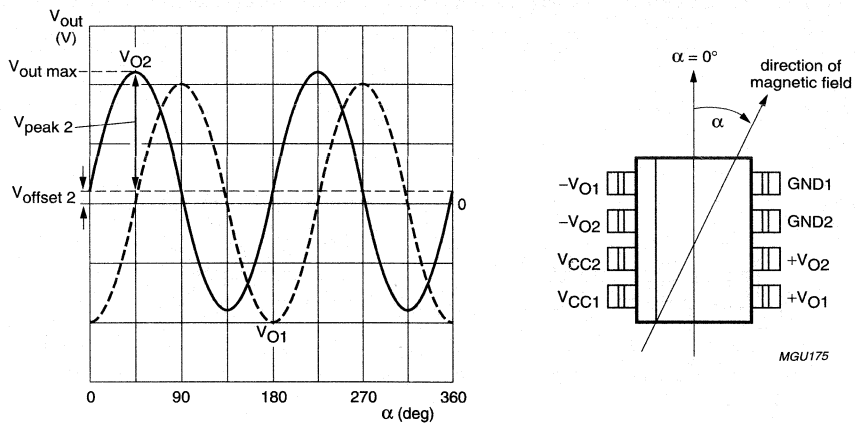

Fig.4 Output signals related to the direction of the magnetic field.

PACKAGE OUTLINE

SO8: plastic small outline package; 8 leads; body width 3.9 mm **SOT96-1**

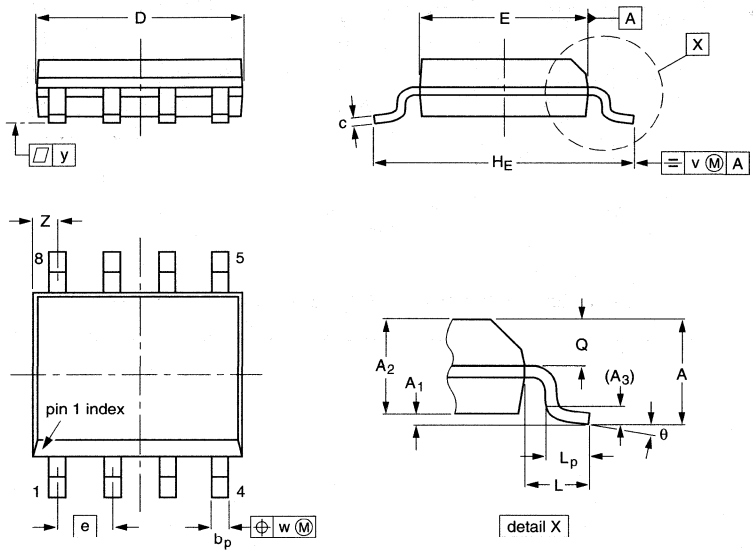

DIMENSIONS (inch dimensions are derived from the original mm dimensions)

UNIT	A max.	A_1	A_2	A_3	b_p	c	$D^{(1)}$	$E^{(2)}$	e	H_E	L	L_p	Q	v	w	y	$Z^{(1)}$	θ
mm	1.75	0.25 0.10	1.45 1.25	0.25	0.49 0.36	0.25 0.19	5.0 4.8	4.0 3.8	1.27	6.2 5.8	1.05	1.0 0.4	0.7 0.6	0.25	0.25	0.1	0.7 0.3	8° 0°
inches	0.069	0.010 0.004	0.057 0.049	0.01	0.019 0.014	0.0100 0.0075	0.20 0.19	0.16 0.15	0.050	0.244 0.228	0.041	0.039 0.016	0.028 0.024	0.01	0.01	0.004	0.028 0.012	

Notes

1. Plastic or metal protrusions of 0.15 mm maximum per side are not included.
2. Plastic or metal protrusions of 0.25 mm maximum per side are not included.

OUTLINE VERSION	REFERENCES				EUROPEAN PROJECTION	ISSUE DATE
	IEC	JEDEC	EIAJ			
SOT96-1	076E03	MS-012				~~97-05-22~~ 99-12-27

Magnetic field sensor KMZ43

DESCRIPTION

The KMZ43 is a sensitive magnetic field sensor, employing the magnetoresistive effect of thin-film permalloy. The sensor contains two galvanic separated Wheatstone bridges, with a relative angular displacement of 45°.

A rotating magnetic field in the x-y plane will produce two independent sinusoidal output signals, one a function of +cos(2α) and the second a function of +sin(2α), α being the angle between sensor and field direction (see Fig.3). Unlike the KMZ41[1], which needs a saturation field strength of 100 kA/m, the KMZ43 is suited to high precision angle measurement applications under low field conditions (saturation field strength 25 kA/m).

The sensor can be operated at any frequency between DC and 1 MHz.

(1) The KMZ41 delivers a +sin(2α) and a −cos(2α) signal.

PINNING

PIN	SYMBOL	DESCRIPTION
1	$-V_{O1}$	output voltage bridge 1
2	$-V_{O2}$	output voltage bridge 2
3	V_{CC2}	supply voltage bridge 2
4	V_{CC1}	supply voltage bridge 1
5	$+V_{O1}$	output voltage bridge 1
6	$+V_{O2}$	output voltage bridge 2
7	GND2	ground 2
8	GND1	ground 1

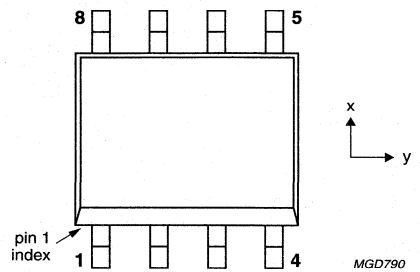

Fig.1 Simplified outline SOT96-1.

QUICK REFERENCE DATA

SYMBOL	PARAMETER	MIN.	TYP.	MAX.	UNIT
V_{CC1}	operating voltage	–	5	9	V
V_{CC2}	operating voltage	–	5	9	V
S	sensitivity (a_2 = 0°, a_1 = 135°)	2.1	2.3	2.5	mV/°
$V_{offset1}$	offset voltage per supply voltage	−2	–	+2	mV/V
$V_{offset1}$	offset voltage per supply voltage	−2	–	+2	mV/V
R_{bridge}	bridge resistance	3.2	3.7	4.2	kΩ

CIRCUIT DIAGRAM

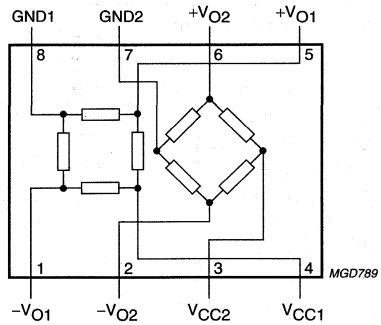

Fig.2 Simplified circuit diagram.

LIMITING VALUES

In accordance with the Absolute Maximum Rating System (IEC 60134).

SYMBOL	PARAMETER	MIN.	MAX.	UNIT
V_{CC1}	operating voltage	–	9	V
V_{CC2}	operating voltage	–	9	V
P_{tot}	total power dissipation	–	45	mW
T_{stg}	storage temperature range	−65	+150	°C
T_{amb}	operating temperature range	−40	+150	°C

THERMAL CHARACTERISTICS

SYMBOL	PARAMETER	CONDITIONS	VALUE	UNIT
$R_{th\ j\text{-}a}$	thermal resistance from junction to ambient	in free air	155	K/W

CHARACTERISTICS

T_{amb} = 25 °C and $H_{rotation}$ = 25 kA/m, V_{CC1} = 5 V; V_{CC2} = 5 V unless otherwise specified.

SYMBOL	PARAMETER	CONDITIONS	MIN.	TYP.	MAX.	UNIT
V_{CC}	bridge supply voltage		–	5	9	V
S	sensitivity	open circuit; note 1 a = 0° (bridge 2) a = 135° (bridge 1)	2.1	2.3	2.5	mV/°
V_{peak1}	peak voltage	note 2; see Fig.3	60	66	72	mV
V_{peak2}	peak voltage	note 2; see Fig.3	60	66	72	mV
TCV_{peak}	temperature coefficient of peak voltage	T_{amb} = –40 to +150 °C; note 3	–0.27	–0.29	–0.31	%/K
R_{bridge}	bridge resistance	note 4	3.2	3.7	4.2	kΩ
TCR_{bridge}	temperature coefficient of bridge resistance	T_{amb} = –40 to +150 °C; note 5	0.29	0.31	0.34	%/K
V_{offset}	offset voltage per supply voltage	see Fig.3	–2	0	+2	mV/V
TCV_{offset}	temperature coefficient of offset voltage per supply voltage	T_{amb} = –40 to +150 °C; note 6; see Fig.3	–1	0	+1	(μV/V)/K
FH	hysteresis of output voltage	note 7	–	0	0.02	%FS
ω	operating angular velocity		0	–	1 MHz	°/s
k	amplitude synchronism	note 8	99.5	100	100.5	%
TCk	temperature coefficient of amplitude synchronism	T_{amb} = –40 to +150 °C; note 9	–0.002	0	–0.002	%/K
Δα	angular inaccuracy	note 10	–	0	0.1	deg

Notes

1. Sensitivity changes with angle due to sinusoidal output.
2. $V_{peak} = |(V_{out\ max} - V_{offset})|$.
3. $TCV_{peak} = 100 \dfrac{V_{peak(T_2)} - V_{peak(T_1)}}{V_{peak(T1)}(T_2 - T_1)}$ Where T_1 = –40°C; T_2 = 150°C.
4. Bridge resistance between pins 8 and 4, pins 7 and 3, pins 5 and 1, pins 6 and 2.
5. $TCR_{bridge} = 100 \dfrac{R_{bridge(T_2)} - R_{bridge(T_1)}}{R_{bridge(T_1)}(T_2 - T_1)}$ Where T_1 = –40°C; T_2 = 150°C.
6. $TCV_{offset} = \dfrac{V_{offset(T_2)} - V_{offset(T_1)}}{(T_2 - T_1)}$ Where T_1 = –40°C; T_2 = 150°C.

7. $$FH_1 = 100 \left| \frac{V_{O1(67.5°)135° \Rightarrow 45°} - V_{O1(67.5°)45° \Rightarrow 135°}}{2 \times V_{peak1}} \right|$$

$$FH_2 = 100 \left| \frac{V_{O2(22.5°)90° \Rightarrow 0°} - V_{O2(22.5°)0° \Rightarrow 90°}}{2 \times V_{peak2}} \right|$$

8. $k = \frac{V_{peak1}}{V_{peak2}} \cdot 100$.

9. $TCk = 100 \frac{(k_{T2} - k_{T1})}{k_{T1}(T_2 - T_1)}$ Where $T_1 = -40°C$; $T_2 = 150°C$.

10. $\Delta\alpha = |\alpha_{real} - \alpha_{measured}|$ without offset voltage influences.

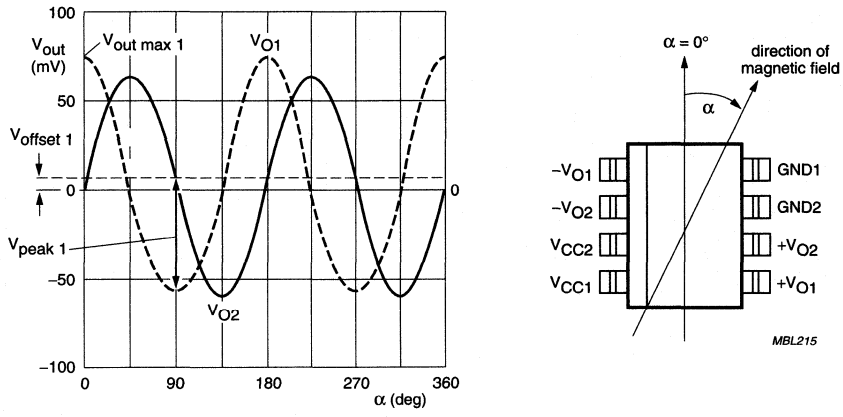

Fig.3 Output signals related to the direction of the magnetic field.

PACKAGE OUTLINE

SO8: plastic small outline package; 8 leads; body width 3.9 mm **SOT96-1**

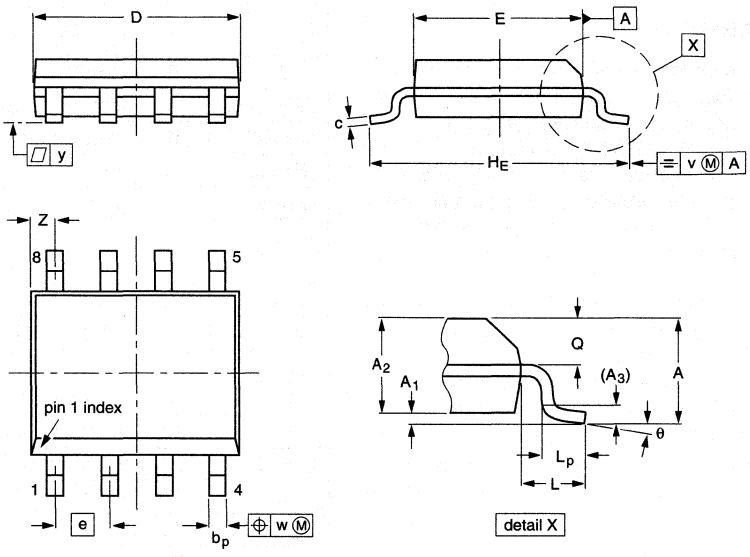

DIMENSIONS (inch dimensions are derived from the original mm dimensions)

UNIT	A max.	A_1	A_2	A_3	b_p	c	$D^{(1)}$	$E^{(2)}$	e	H_E	L	L_p	Q	v	w	y	$Z^{(1)}$	θ
mm	1.75	0.25 0.10	1.45 1.25	0.25	0.49 0.36	0.25 0.19	5.0 4.8	4.0 3.8	1.27	6.2 5.8	1.05	1.0 0.4	0.7 0.6	0.25	0.25	0.1	0.7 0.3	8° 0°
inches	0.069	0.010 0.004	0.057 0.049	0.01	0.019 0.014	0.0100 0.0075	0.20 0.19	0.16 0.15	0.050	0.244 0.228	0.041	0.039 0.016	0.028 0.024	0.01	0.01	0.004	0.028 0.012	

Notes

1. Plastic or metal protrusions of 0.15 mm maximum per side are not included.
2. Plastic or metal protrusions of 0.25 mm maximum per side are not included.

OUTLINE VERSION	REFERENCES				EUROPEAN PROJECTION	ISSUE DATE
	IEC	JEDEC	EIAJ			
SOT96-1	076E03	MS-012				~~97-05-22~~ 99-12-27

Sensor Conditioning Electronic UZZ9000

FEATURES

- One chip fully integrated signal conditioning IC
- Accuracy better than 1° together with KMZ41 in 100° angle range
- Temperature range from –40 to 150 °C
- Adjustable angle range
- Adjustable zero point.

GENERAL DESCRIPTION

The UZZ9000 is an integrated circuit that combines two sinusoidal signals (sine and cosine) into one single linear output signal. When used in conjunction with the magnetoresistive sensor KMZ41 it provides a measurement system for angles up to 180°. The UZZ9000 can also be used for other applications in which an angle has to be calculated from a sine and a cosine signal.
A typical application would be any kind of resolver application.
The two input signals are converted into the digital domain with two separate AD-converters. A CORDIC algorithm performs the inverse tangent transformation. Since today's applications typically require analog output signals (e.g. potentiometers), the resulting signal is transferred back to the analog domain.
The UZZ9000 enables the user to set both the angle range and the zero point offset. These ranges are set by external voltage dividers.

PINNING

SYMBOL	PIN	DESCRIPTION
$+V_{O2}$	1	sensor 2 positive differential input
$+V_{O1}$	2	sensor 1 positive differential input
V_{DD2}	3	digital supply voltage
V_{SS}	4	digital ground
GND	5	analog ground
RST	6	reset of the digital part; note 1
TEST1	7	for production test; note 1
TEST2	8	note 2
DATA_CLK	9	trim-mode data-clock; note 1
SMODE	10	serial mode programmer; note 1
TEST3	11	note 2
V_{OUT}	12	output voltage
Var	13	angle-range input set
V_{offin}	14	offset input set
OFFS2	15	offset trimming input sensor 2
OFFS1	16	offset trimming input sensor 1
V_{DDA}	17	analog supply voltage
GND	18	analog ground
TEST4	19	for production test; note 1
TEST5	20	for production test; note 1
V_{DD1}	21	digital supply voltage
T_{out}	22	test output
$-V_{O2}$	23	sensor 2 negative differential input
$-V_{O1}$	24	sensor 1 negative differential input

Notes

1. Connected to ground.
2. Pin to be left unconnected.

QUICK REFERENCE DATA

SYMBOL	PARAMETER	CONDITIONS	MIN.	TYP.	MAX.	UNIT
V_{DDA}	supply voltage	note 1	4.5	5	5.5	V
V_{DD1}	supply voltage	note 1	4.5	5	5.5	V
V_{DD2}	supply voltage	note 1	4.5	5	5.5	V
I_{CCtot}	total supply current		–	13	15	mA
A	angle range	in 10° steps with KMZ41	30	–	180	deg
A	accuracy	with ideal input signal; range = 100°	±0.45	–	–	deg

Note

1. V_{DDA}, V_{DD1} and V_{DD2} must be connected to the same supply voltage.

LIMITING VALUES

In accordance with the Absolute Maximum Rating System (IEC 60134).

SYMBOL	PARAMETER	CONDITIONS	MIN.	MAX.	UNIT
V_{DDA}	supply voltage		−0.3	+6	V
V_{DD1}	supply voltage		−0.3	+6	V
V_{DD2}	supply voltage		−0.3	+6	V
V_{pin}	voltage at all pins		−0.3	V_{DD}	V
T_{stg}	storage temperature		−55	+150	°C
T_j	operating temperature	125 to 150 °C; max 200 hours	−40	+150	°C

THERMAL CHARACTERISTICS

SYMBOL	PARAMETER	VALUE	UNIT
$R_{th\ j\text{-}a}$	thermal resistance from junction to ambient	80	K/W

ESD SENSITIVITY

SYMBOL	PARAMETER	CONDITIONS	VALUE	UNIT
ESD	ESD sensitivity	human body model	2	kV
		machine model	±150	V

ELECTRICAL CHARACTERISTICS

T_{amb} = −40 to +150 °C; V_{DD} = 4.5 to 5.5 V; typical characteristics for T_{amb} = 25 °C and V_{DD} = 5 V unless otherwise specified.

SYMBOL	PARAMETER	CONDITIONS	MIN.	TYP.	MAX.	UNIT
V_{DDA}	supply voltage		4.5	5	5.5	V
V_{DD1}	supply voltage		4.5	5	5.5	V
V_{DD2}	supply voltage		4.5	5	5.5	V
I_{DD}	supply current	without load	–	10	15	mA
$(+V_O)-(-V_O)$	differential input voltage	referred to V_{DD}	±6.6	–	±28	mV/V
	common mode range	referred to V_{DD}	490	–	510	mV/V
	lost magnet threshold	referred to V_{DD}	–	3	–	mV/V
f_{ext}	external clock frequency	for trim interface	0.1	–	1	MHz
f_{int}	internal clock frequency	T_j = −40 to 150 °C	2.3	4	5.7	MHz
C_{load}	output load		–	–	50	pF
		with series resistance >300 Ω	–	–	200	nF
V_{reset}	switching voltage threshold for power on/off	between falling and rising V_{DD}	2.8	–	4.5	V
	hysteresis		–	0.3	–	
V_{out}	output voltage range for valid ranges	lower bound	5	–	6	% V_{DD}
		upper bound	94	–	95	% V_{DD}
V_d	diagnostic area	for irregular input signal	0	–	4	% V_{DD}
			96	–	100	% V_{DD}
A	accuracy	with ideal input signal; range = 100°	±0.45	–	–	degree
Res	resolution	range = 100°	0.1	–	–	degree
t_{on}	power up time		–	–	20	ms
t_r	response time	to 95% of final value	–	0.7	1.2	ms
V_{LM}	sensor voltage	lost magnet threshold	12	15	20	mV

FUNCTIONAL DESCRIPTION

The UZZ9000 is a mixed signal IC for angle measurement systems. The UZZ9000 has been designed for the double sensor KMZ41. It combines two analog signals (sine and cosine) into a linear output signal. The analog measurement signals on the IC input are converted to digital data by two ADC's. Each ADC is a Sigma-Delta modulator employing a 4th order continuous time architecture with an over-sampling ratio of 128 to achieve high resolution. The converter output is a digital bit-stream with an over-sampling frequency of typically 500 kHz. The bit-stream is fed into a decimation filter which performs both low pass filtering and down-sampling. The IC has two input channels each of which has its own ADC and decimation filter. The two decimation filter outputs are 15-bit digital words at a lower frequency of typically 3.9 kHz which is the typical sampling frequency of the sensor system. The digital representations of the two signals are then used to calculate the current angle by the ALU. This calculation is carried out using the so-called CORDIC algorithm. The angle is represented by a 13-bit resolution. A DAC converts the digital signal back to the analog domain.

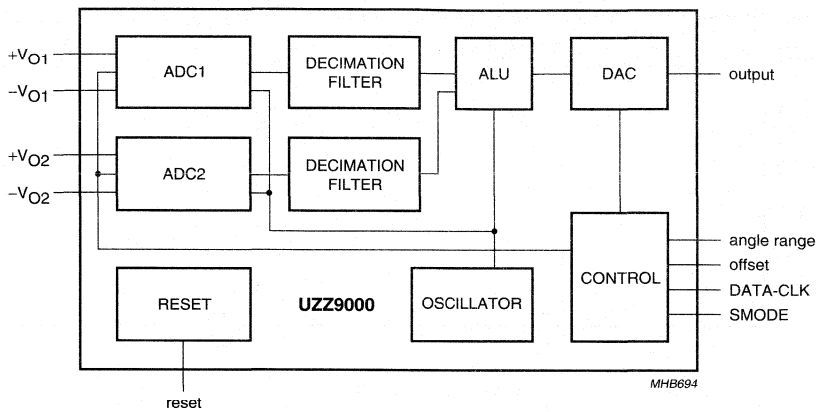

Fig.1 Block diagram.

The following list gives a short description of the relevant block functions:

1. The ADC block contains two Sigma Delta AD converters, sensor offset correction circuitry and the circuitry required for the sensitivity and offset adjustment of the chip output voltage curve.
2. The decimation filter block comprises two digital low pass decimation filters convert the low resolution high speed bit stream output from the ADC's into a low speed digital word.
3. The ALU block derives an angle value from the two digital inputs using the CORDIC algorithm.
4. The DAC converts the output of the ALU block to an analog signal.
5. The CONTROL block provides the clock and the control signals for the chip.
6. The RESET block supplies a reset signal during power-up and power-down when the power supply is below a certain value.
7. The Oscillator generates the master clock.

Angle range selection

In order to accommodate varying applications, both the mechanical input angular range of the UZZ9000 and the zero point of the output curve are user programmable. This section describes how to select a desired mode.
The output curve is adjusted by changing the angular range as shown in Fig.2. Without any zero point offset, the ramp-up starts at mechanical 0° ($\alpha 1 = 0°$). When using a KMZ41 sensor, the maximum angular range $\Delta\alpha$ is 0° to 180°. For the UZZ9000, smaller angular ranges can be set. In this case, $\alpha 2$ becomes smaller than 180° and the output curve is clipped at this position. The location of discontinuity X_D (change from lower to upper clipping area) depends on the adjusted range and can be calculated as follows:

$$X_D = \Delta\alpha + \frac{180° - \Delta\alpha}{2}$$

In order to compensate for tolerances, the zero point of the output curve can be shifted by ±5° in steps of 0.5°. The effect of this measure is shown in Fig.3. Now $\alpha 1$ is no longer identical with mechanical 0°, but with the zero point shift X_{off}. Consequently, the location of discontinuity X_D can be calculated as follows:

$$X_D = x_{off} + \Delta\alpha + \frac{180° - \Delta\alpha}{2}$$

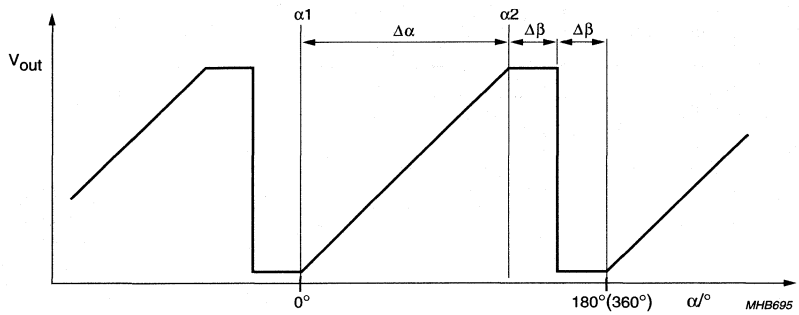

When using MR sensors (KMZ41), the signal period is 0° to 180° as the signals are proportional to sin2α and cos2α.

Fig.2 Output curve for different angular ranges.

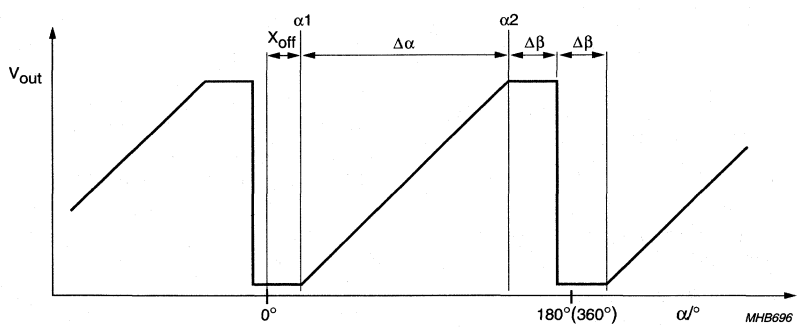

When using MR sensors (KMZ41), the signal period is 0° to 180° as the signals are proportional to sin2α and cos2α.

Fig.3 Output curve for different angular ranges including a zero point offset.

Angle range setting

To select one of 16 different angular ranges, an external voltage (see Table 1) must be applied to pin 13 of the UZZ9000 (Var). During the ICs initialisation phase, which directly follows power-on reset or an external reset, this voltage is read and then converted into the digital domain. The digital value is stored until the next reset state occurs. Consequently, the angular range cannot be changed during normal operation but is still fixed after initialisation phase. Note that the voltage at pin 13 must be ratiometric to V_{DDA} and also stable over temperature and lifetime. This is ensured, for instance, when providing this voltage via a (trimmable) resistor divider connected to V_{DDA}, which is the analog supply of the UZZ9000. The following defines the % value of the supply voltage V_{DDA} that must be supplied to pin 13 to select a certain range. When using the 30° angular range, a constant zero point offset of 15° is added. Consequently, when using the 30° range, the zero point offset can be programmed between 10° and 20° only (see Zero point offset setting).

Table 1 Definition of voltages to set UZZ9000 angular ranges

ANGULAR RANGE (°)	MIN. (%)	NOM. (%)	MAX. (%)	UNIT (%)
0 to 30	33.47	33.73	33.99	V_{DDA}
0 to 40	35.69	35.95	36.21	V_{DDA}
0 to 50	37.91	38.17	38.43	V_{DDA}
0 to 60	40.14	40.40	40.66	V_{DDA}
0 to 70	42.36	42.62	42.88	V_{DDA}
0 to 80	44.58	44.84	45.10	V_{DDA}
0 to 90	46.80	47.06	47.32	V_{DDA}
0 to 100	49.02	49.28	49.54	V_{DDA}
0 to 110	51.25	51.51	51.77	V_{DDA}
0 to 120	53.47	53.73	53.99	V_{DDA}
0 to 130	55.69	55.95	56.21	V_{DDA}
0 to 140	57.91	58.17	58.43	V_{DDA}
0 to 150	60.13	60.39	60.65	V_{DDA}
0 to 160	62.36	62.62	62.88	V_{DDA}
0 to 170	64.58	64.84	65.10	V_{DDA}
0 to 180	66.80	67.06	67.32	V_{DDA}

Zero point offset setting

To adjust the zero point offset or to set it to 0°, an external voltage has to be applied to the UZZ9000 at pin 14 (VOFFIN). The function is similar to that described previously. After reset the voltage is read, converted into the digital domain and then stored until another reset state occurs. Consequently, the zero point offset cannot be adjusted without a reset. It is recommended to use a resistor divider connected to V_{DDA} to generate this voltage. Table 2 defines the allowed voltage ranges as a percentage of the supply V_{DDA}.

Table 2 Definition of voltages to set a certain zero point offset

ZERO POINT OFFSET (°)	MIN. (%)	NOM. (%)	MAX. (%)	UNIT (%)
–5	33.47	33.73	33.99	V_{DDA}
–4.5°	35.14	35.40	35.66	V_{DDA}
–4°	36.80	37.06	37.32	V_{DDA}
–3.5°	38.47	38.73	38.99	V_{DDA}
–3°	40.13	40.39	40.65	V_{DDA}
–2.5°	41.80	42.06	42.32	V_{DDA}
–2°	43.47	43.73	43.99	V_{DDA}
–1.5 °	45.13	45.39	45.65	V_{DDA}
–1°	46.80	47.06	47.32	V_{DDA}
–0.5°	48.60	48.72	48.98	V_{DDA}
0°	50.13	50.39	50.65	V_{DDA}
0.5°	51.80	52.06	52.32	V_{DDA}
1°	53.46	53.72	53.98	V_{DDA}
1.5°	64.58	55.39	55.65	V_{DDA}
2°	56.79	57.05	57.31	V_{DDA}
2.5°	58.46	58.72	58.98	V_{DDA}
3°	60.13	60.39	60.65	V_{DDA}
3.5°	61.79	62.05	62.31	V_{DDA}
4°	63.46	63.72	63.98	V_{DDA}
4.5°	65.12	65.38	65.64	V_{DDA}
5°	66.79	67.05	67.31	V_{DDA}

Offset trimming

To achieve a linear output characteristic, it is necessary to adapt the offsets of the two input signals to the input stage of the UZZ9000. For this reason a sensor offset cancellation procedure has been implemented in the UZZ9000 which is started by sending a special serial data protocol to the UZZ9000. This trimming procedure is required for both input signals.

Trim interface

The serial interface used to switch the UZZ9000 into trim mode consists of the two terminals SMODE (pin 10) and DATA_CLK (pin 9). The structure of this protocol is shown in Fig.4.
All signal levels at DATA_CLK and SMODE must be selected according to the requirements listed in Table 3. The following points must be taken into account with regard to the asynchronous protocol.
The protocol starts with a falling edge at the SMODE, which must occur at a high DATA_CLK level. The following five bits are used to code the message sent to the UZZ9000. They are transferred via the SMODE and are sampled with the rising edge of the DATA_CLK. During the fifth high level output of DATA_CLK (counted from the start condition onwards), a rising edge must appear at the SMODE and the DATA_CLK follows this with one more change to low level in order to successfully complete the protocol.

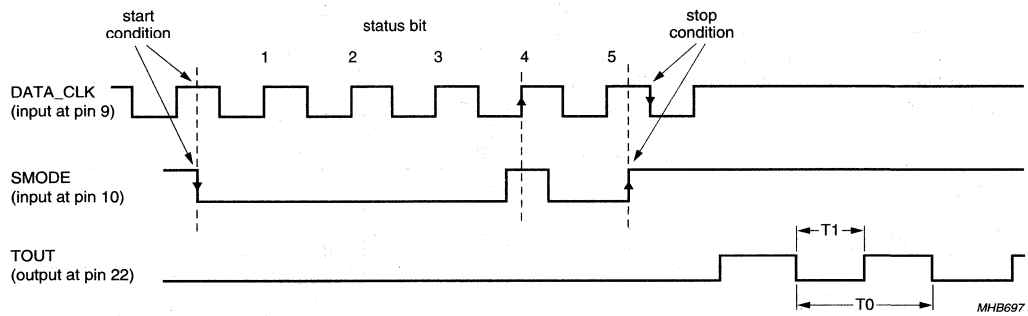

Fig.4 Protocol used to set UZZ9000 into trim mode.

Table 3 Definition of the trim interface signals

PARAMETER	MIN.	NOM.	MAX.	UNIT
UZZ9000 supply voltage	4.5	5	5.5	V
low level of DATA_CLK, SMODE	0	–	5	$\%V_{DD}$
high level of DATA_CLK, SMODE	95	–	100	$\%V_{DD}$
rise and fall time of DATA_CLK and SMODE signal edges (10 to 90% V_{DD}) and (90 to 10% V_{DD})	8	–	–	ns
DATA_CLK frequency	0.1	–	1	MHz

How to enter the trim mode

The status bits to be transmitted to the UZZ9000 are shown in Table 4. Note that a complete protocol has to be sent before normal operation can be resumed. The trim mode can also be exited by resetting the device. After entering one of the trim modes and provided there is a dynamic input signal, a square wave output is visible at the terminal T_{OUT} (pin 22).

Table 4 Programming of trim modes

MODE	STATUS BITS				
	1	2	3	4	5
enter trim mode for sensor input channel 1	0	0	0	1	0
enter trim mode for sensor input channel 2	0	0	1	0	0
leave trim mode for either input channel	0	0	0	0	0

Reset

In addition to the external reset pin (pin 6), the UZZ9001 provides an internal power-up/ power-down reset logic which continuously monitors the supply voltage. When the supply voltage increases and reaches a safe level, reset becomes inactive and the device starts initialization. When the supply voltage exceeds the safe voltage level, the device is reset immediately. This internal reset logic can be over-ridden by the external pin RES (pin 6) in all modes and at any time. The reset pin RES (pin 6) is active when in the high position. It is internally pulled to ground and therefore need not be connected if the function is not required.

Diagnostic

The UZZ9000 provides powerful diagnostics features that allow the user to recognize certain failures of the device or system. A failure will occur when the output voltage V_{OUT} either rises above or falls below the normal operation range. Either one of the diagnostic areas is reached during any of the following conditions

1. Short circuit between V_{OUT} and GND ($R < 1\ \Omega$).
2. Short circuit between V_{OUT} and V_{DD} ($R < 1\ \Omega$).
3. Disconnection of V_{DD} when the load is pulled down.
4. Disconnection of GND when the load is pulled up.
5. Invalid input signal from the sensor, e.g. Magnet Lost. This failure is assumed when the offset corrected input signal of sensor 1 and sensor 2 is below ±15 mV.

The internal pull-up and pull-down resistors in the output buffer block ensure that V_{OUT} will be pulled to one of the power supplies when the other supply is disconnected so V_{OUT} reaches the diagnostic region even when there is no output load. If the external load is a pull-down resistor, then the device enters into the diagnostic area if V_{DD} is disconnected, but not if V_{SS} is disconnected. Similarly, if the load is a pull-up resistor, then the device will enter the diagnostic area if V_{SS} is disconnected, but not if V_{DD} is disconnected. It is not necessary to connect an output load to the UZZ9000. After recovering from short circuit to ground or supply voltage, the chip returns undamaged to the normal operation mode. There is no time limitation regarding short circuit of V_{OUT}.

Measurement dynamics

The UZZ9000 includes an on-chip RC Oscillator that generates the clock for the whole device. Consequently, no external clock supply is required for the measurement system. The nominal clock frequency of the on-chip oscillator is 4 MHz at room temperature. It varies with temperature change. At –40 °C the clock frequency may decrease to 2.3 MHz. At higher temperatures however, a frequency up to 5.7 MHz may be reached. This influences the dynamics of measurements. From an application point of view, two different effects have to be distinguished: The system delay, which means how long it takes until a changed input signal is recognized at the output, and the measurement update rate. The system delay is mainly caused by the settling time of the low pass decimation filter, which depends on the maximum frequency content (shape) of the input signals and the clock frequency. The following maximum values can be expected for the entire system delay. The measurement update rate, however, is directly related to the oscillator frequency. At room temperature, a new value is available every 0.26 ms. When taking the entire temperature range into account, update rates between 0.45 and 0.18 ms are possible. (see Table 5).

Table 5 System delay and update rates of the UZZ9000

PARAMETER	MIN.	TYP.	MAX.	UNIT
system delay (time elapsed until 95% of the final value is reached)				
max. signal frequency < 200 MHz	–	–	0.6	ms
transients (step response)	–	–	1.2	ms
measurement update rate				
–40 °C	0.45	–	–	ms
25 °C (room temperature)	–	0.26	–	ms
150 °C	–	–	0.18	ms

PACKAGE OUTLINE

SO24: plastic small outline package; 24 leads; body width 7.5 mm SOT137-1

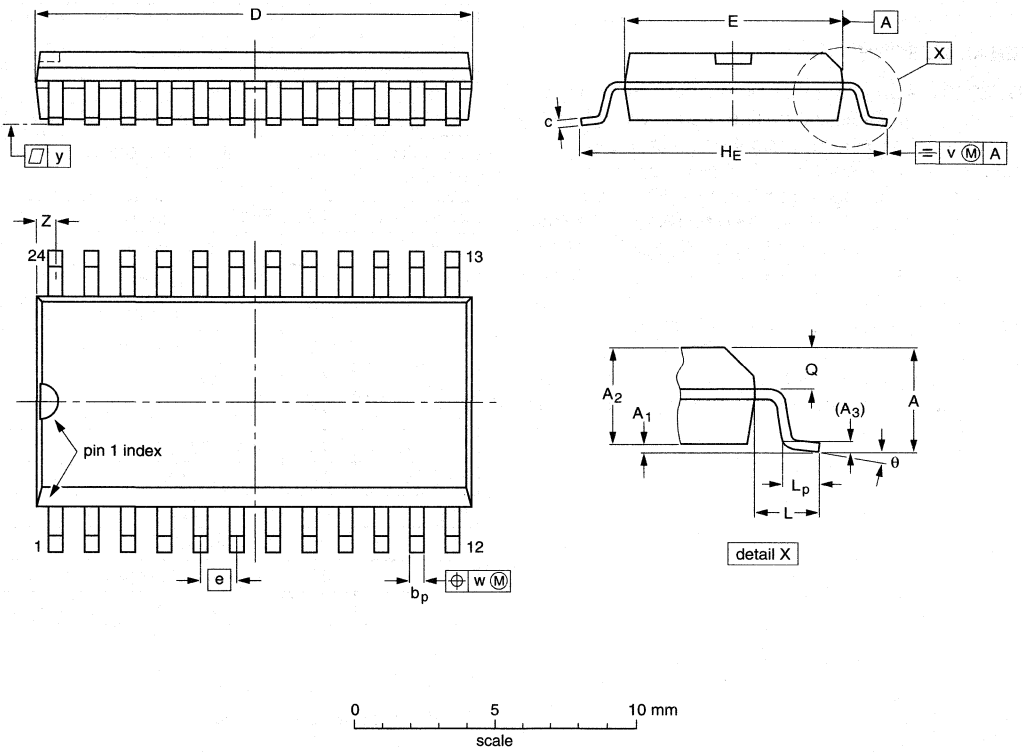

DIMENSIONS (inch dimensions are derived from the original mm dimensions)

UNIT	A max.	A_1	A_2	A_3	b_p	c	$D^{(1)}$	$E^{(1)}$	e	H_E	L	L_p	Q	v	w	y	$Z^{(1)}$	θ
mm	2.65	0.30 0.10	2.45 2.25	0.25	0.49 0.36	0.32 0.23	15.6 15.2	7.6 7.4	1.27	10.65 10.00	1.4	1.1 0.4	1.1 1.0	0.25	0.25	0.1	0.9 0.4	8° 0°
inches	0.10	0.012 0.004	0.096 0.089	0.01	0.019 0.014	0.013 0.009	0.61 0.60	0.30 0.29	0.050	0.419 0.394	0.055	0.043 0.016	0.043 0.039	0.01	0.01	0.004	0.035 0.016	

Note

1. Plastic or metal protrusions of 0.15 mm maximum per side are not included.

OUTLINE VERSION	REFERENCES				EUROPEAN PROJECTION	ISSUE DATE
	IEC	JEDEC	EIAJ			
SOT137-1	075E05	MS-013				~~97-05-22~~ 99-12-27

Sensor Conditioning Electronic UZZ9001

FEATURES

- One chip angle sensor output signal conditioning
- 180° angle range with KMZ41
- Accuracy better than 1° together with KMZ41
- Temperature range from –40 to +150 °C
- SPI protocol
- SO24 package.

GENERAL DESCRIPTION

The UZZ9001 is an integrated circuit that combines two sinusoidal signals (sine and cosine) into one single linear output signal. These signals might come from the magnetoresistive sensor KMZ41. This results in a measurement system for angles up to 180°. The integrated circuit UZZ9001 can also be used for all other applications in which an angle has to be calculated from a sine and cosine signal. A typical application would be any kind of resolver application.
The two input signals are converted into the digital domain with two separate AD converters. A CORDIC algorithm performs the inverse tangent transformation. The output stage implements the Motorola Serial Peripheral Interface (SPI) protocol.

PINNING

SYMBOL	PIN	DESCRIPTION
$+V_{O2}$	1	sensor 2 positive differential input
$+V_{O1}$	2	sensor 1 positive differential input
V_{DD2}	3	digital supply voltage
V_{SS}	4	digital ground
GND	5	analog ground
RST	6	reset of the digital part; note 1
TEST1	7	for production test; note 1
TEST2	8	note 2
DATA_CLK	9	trim-mode data-clock; note 1
SMODE	10	serial mode programmer; note 1
TEST3	11	note 2
data	12	SPI data output
CLK	13	SPI data clock in
CS	14	SPI chip select
OFFS2	15	offset trimming input sensor 2
OFFS1	16	offset trimming input sensor 1
V_{DDA}	17	analog supply voltage
GND	18	analog ground
TEST4	19	for production test; note 1
TEST5	20	for production test; note 1
V_{DD1}	21	digital supply voltage
T_{out}	22	test output
$-V_{O2}$	23	sensor 2 negative differential input
$-V_{O1}$	24	sensor 1 negative differential input

Notes

1. Connected to ground.
2. Pin to be left unconnected.

QUICK REFERENCE DATA

SYMBOL	PARAMETER	CONDITIONS	MIN.	TYP.	MAX.	UNIT
V_{DDA}	supply voltage	note 1	4.5	5	5.5	V
V_{DD1}	supply voltage	note 1	4.5	5	5.5	V
V_{DD2}	supply voltage	note 1	4.5	5	5.5	V
I_{CCtot}	total supply current	no output load	–	5	15	mA
Res	resolution		–	13	–	bit
A	accuracy	with ideal input signal	±0.35	–	–	deg
$I_{data-out}$	peak output current		–	–	10	mA

Note

1. V_{DDA}, V_{DD1} and V_{DD2} must be connected to the same supply voltage.

LIMITING VALUES

In accordance with the Absolute Maximum Rating System (IEC 60134).

SYMBOL	PARAMETER	CONDITIONS	MIN.	MAX.	UNIT
V_{DDA}	supply voltage		−0.3	+6	V
V_{DD1}	supply voltage		−0.3	+6	V
V_{DD2}	supply voltage		−0.3	+6	V
V_{pin}	voltage at all pins		−0.3	V_{DD}	V
T_{stg}	storage temperature		−55	+150	°C
T_{amb}	operating temperature	125 to 150 °C; max 200 hours	−40	+150	°C

THERMAL CHARACTERISTICS

SYMBOL	PARAMETER	VALUE	UNIT
$R_{th\ j\text{-}a}$	thermal resistance from junction to ambient	80	K/W

ESD SENSITIVITY

SYMBOL	PARAMETER	CONDITIONS	VALUE	UNIT
ESD	ESD sensitivity	human body model	2	kV
		machine model	±150	V

ELECTRICAL CHARACTERISTICS

T_{amb} = −40 to +150 °C; V_{DD} = 4.5 to 5.5 V; typical characteristics for T_{amb} = 25 °C and V_{DD} = 5 V unless otherwise specified.

SYMBOL	PARAMETER	CONDITIONS	MIN.	TYP.	MAX.	UNIT
V_{DDA}	supply voltage		4.5	5	5.5	V
V_{DD1}	supply voltage		4.5	5	5.5	V
V_{DD2}	supply voltage		4.5	5	5.5	V
I_{DD}	supply current	without load	–	5	15	mA
$(+V_O)-(-V_O)$	differential input voltage	referred to V_{DD}	±6.6	–	±28	mV/V
	common mode range	referred to V_{DD}	490	–	510	mV/V
	lost magnet threshold	referred to V_{DD}	–	3	–	mV/V
f_{ext}	external clock frequency	for trim interface	0.1	–	1	MHz
f_{int}	internal clock frequency		2.3	4	5.7	MHz
I_o	data output	constant current	–	–	1	mA
		peak current	–	–	10	mA
V_{reset}	switching voltage threshold	between falling and rising V_{DD}	2.8	–	4.5	V
	hysteresis		–	0.3	–	V
A	accuracy	with ideal input signal	±0.35	–	–	degree
Res	resolution		–	13	–	bit
t_{on}	power up time		–	–	20	ms
t_r	response time	to 95% of final value	–	0.7	1.2	ms
V_{ID}	digital input voltage	LO signal	0	–	0.3 x V_{DD}	V
		HI signal	0.7 x V_{DD}	–	V_{DD}	V
V_{OD}	digital output voltage	LO signal	–	–	0.4	V
		HI signal	V_{DD} −0.8	–	–	V
V_{LM}	sensor voltage	lost magnet threshold	12	15	20	mV

FUNCTIONAL DESCRIPTION

The UZZ9001 is a mixed signal IC for angle measurement systems. It combines two analog signals (sine and cosine) into a linear output signal. The output stage implements the Motorola Serial Peripheral Interface (SPI) protocol. The UZZ9001 has been designed for use with the double sensor KMZ41.

The analog measurement signals on the IC input are converted to digital data with two ADC's. The ADC's are a Sigma-Delta modulator employing a 4th order continuous time architecture with an over-sampling ratio of 128 to achieve high resolution. The converter output is a digital bitstream with an over-sampling frequency of typically 500 kHz.

The bitstream is fed into a decimation filter which performs both low pass filtering and down-sampling. The IC has two input channels each of which has its own ADC and decimation filter. The two decimation filter outputs are 15-bit digital words at a lower frequency of typically 3.9 kHz which is the typical sampling frequency of the sensor system. The digital representations of the two signals are then used to calculate the current angle. This calculation is carried out using the so-called CORDIC algorithm. The angle is represented with a 13-bit resolution. An SPI compatible interface converts the output word to the serial peripheral interface protocol.

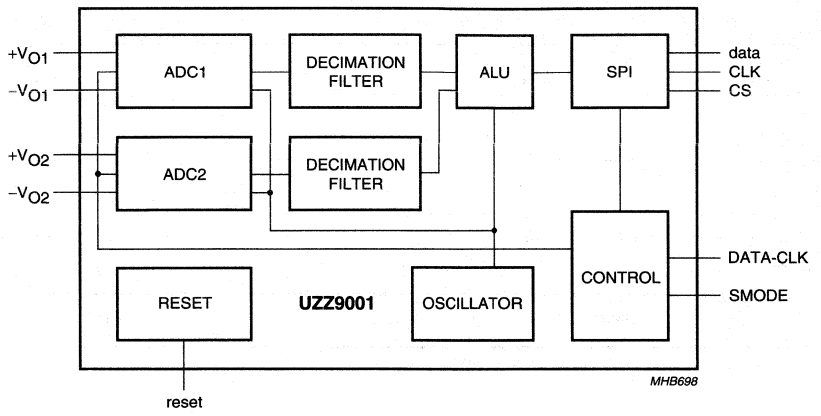

Fig.1 Block diagram.

The following list gives a short description of the relevant block functions:

1. The ADC block contains two Sigma Delta AD converters, sensor offset correction circuitry and the circuitry required for the sensitivity and offset adjustment of the chip output voltage curve.
2. Two digital low pass decimation filters convert the low resolution high speed bit stream coming from the ADC Sigma Delta converters into a low speed digital word.
3. The ALU block derives an angle value from the two digital inputs using the CORDIC algorithm.
4. The SPI converts the output of the ALU block to a SPI compatible 16 bit word.
5. The CONTROL block provides the clock and the control signals for the chip.
6. The RESET block supplies a reset signal during power-up and power-down when the power supply is below a certain value.
7. The Oscillator unit generates the master clock.

Serial Peripheral interface (SPI)

The UZZ9001 provides an interface to SPI compatible devices, and as a slave node functions in one operational mode only. For Motorola SPI devices, this mode is selected by setting CPHA to 1 and CPOL to 1. In this transfer mode, data bits are sampled by the master using the leading edge of the clock as shown in Figure 2. The falling edge indicates that the next data bit has to be provided by the slave device (shift operation).
An advantage of this mode is that the CS input toggles only once between every two sensor data bytes (see Fig.3). Data transmission can be stopped by the user at any time. The leading edge of the CS input initialises the SPI shift register allowing the start of a complete new transmission. If the CS line is held active low during stop of transmission, resumption of transmission can be made without loss of data

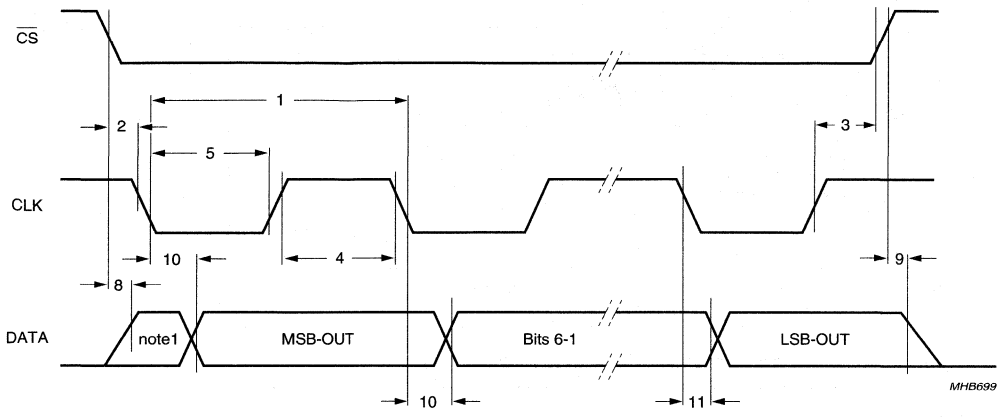

(1) Not defined data, normally LSB of character previously transmitted.

Fig.2 UZZ9001 SPI timing.

Table 1 SPI-Timing

DIAGRAM NUMBER	PARAMETER	SYMBOL	MIN.	MAX.	UNIT	REMARKS/TEST CONDITIONS
1	cycle time	t_{cyc}	1	–	µs	
2	enable lead time	t_{lead}	15	–	ns	determined by master module
3	enable lag time	t_{lag}	15	–	ns	determined by master module
4	clock high time	t_{clk_high}	100	–	ns	determined by master module
5	clock low time	t_{clk_low}	100	–	ns	determined by master module
8	access time	t_{acc}	0	20	ns	time to data active from fixed V_{SS} state
9	disable time	t_{dis}	–	25	ns	hold time to fixed V_{SS} state
10	data valid time (after clock edge)	t_v	–	40	ns	with 100 pF on all SPI pins
11	data hold time (output, after clock edge)	t_h	5	–	ns	
	operating frequency	f_{op}	–	1	MHz	
	transmission delay (time between the leading edge of CS until the next falling edge)	t_{delay}	1.2	–	µs	

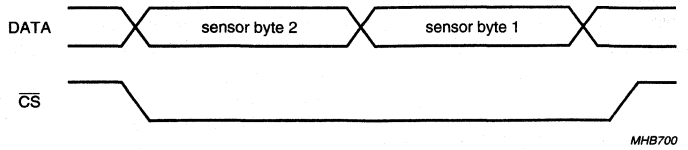

Fig.3 CS Line timing.

Sensor signal coding

The sensor signal comprises 14 bits (D13 to D0) as shown in Fig.4. Bits D12 to D0 are used for the coding of the angle while D0 is reserved to indicate error and diagnostic conditions as defined below. The 14 data bits are arranged in 2 Bytes. D13 is the MSB of the sensor signal and D0 is the LSB of the sensor signal. Byte 2, which is sent first, contains data bits D13 to D7 and additionally the parity bit P2 which is included for the recognition of interrupted messages. P2 gives the ODD parity of data bits D13 to D7 and has to be evaluated by the master module.Similarly, Byte 1 comprises data bits D6 to D0 and parity bit P1, which gives the ODD parity of data bits D6 to D0. The internal coding of angle values is as follows:

$$00\ 0000\ 0000\ 0000_B = 0°, 180°$$

$$\underset{D13}{01}\ 1111\ 1111\ \underset{D0}{1111_B} = (2^{13}-1)\frac{180°}{2^{13}} \approx 179.978$$

During normal operation, bit D13 is active low. Each increment represents an angle value

of: $\alpha_{inc} = \frac{180°}{2^{13}} \approx 0.022°$

The error and diagnostic conditions are indicated by D13 = 1 (active high). In an error situation the last two bits (D0 and D1) specify the error code (see Table 2). All other bits (D3 to D12) still show the current measurement value, but as the last two bits are lost for measurement representation the resolution is reduced to 11 bit.

Table 2 Error and diagnostic cases coding

D1	D0	CASE	MEASUREMENT VALUE RELIABLE
0	0	no valid value presently available due to RESET	no
0	1	magnet lost	no
1	0	reserved	–
1	1	reserved	–

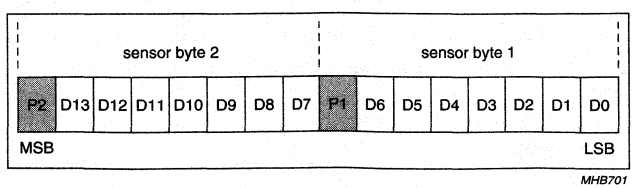

Fig.4 Sensor signal coding.

Magnet lost condition

If both offset corrected input signal of sensor 1 and sensor 2 are below the lost magnet threshold then the failure 'Magnet lost' is assumed.

Offset trimming

To achieve a linear output characteristic, it is necessary to shift the offsets of the two input signals to the input stage of the UZZ9001. For this reason a sensor offset cancellation procedure has been implemented in the UZZ9001 which is started by sending a special serial data protocol to the UZZ9001. This trimming procedure is required for both input signals.

Trim interface

The UZZ9001 trim mode serial interface consists of the two terminals SMODE (pin 10) and DATA_CLK (pin 9). The structure of this protocol is shown in Figure 5. All signal levels of DATA_CLK and SMODE must lie within the ranges set out in Table 3. The protocol starts with a falling edge at the SMODE, which must occur at a high DATA_CLK level. The following five bits are used to code the message sent to the UZZ9001. They are transferred via the SMODE and are sampled with the rising edge of the DATA_CLK. During the fifth high level output of DATA_CLK (counted from the start condition onwards), a rising edge must appear at the SMODE and the DATA_CLK follows this with one more change to low level in order to successfully complete the protocol.

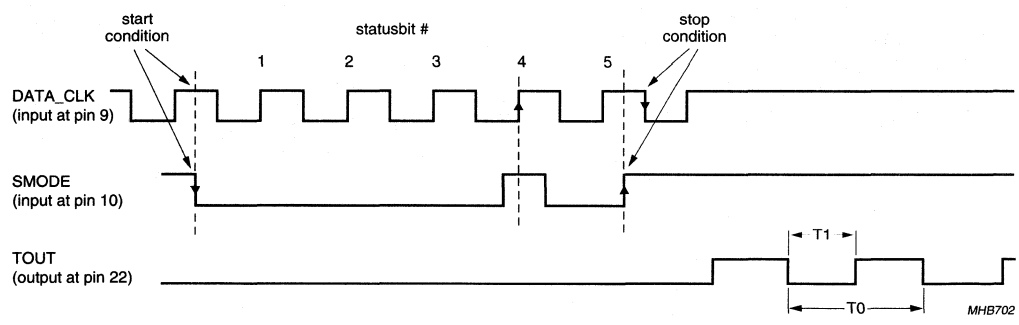

Fig.5 Protocol used to set UZZ9001 into trim mode.

Table 3 Definition of the trim interface signals

PARAMETER	MIN.	MAX.	UNIT
low level of DATA_CLK, SMODE	0	5	$\%V_{DD}$
high level of DATA_CLK, SMODE	95	100	$\%V_{DD}$
rise and fall time of DATA_CLK and SMODE signal edges (10 to 90% V_{DD}) and (90 to 10% V_{DD})	8	–	ns
DATA_CLK frequency	0.1	1	MHz

Table 4 Programming of trim modes

MODE	STATUS BITS				
	1	2	3	4	5
enter trim mode for sensor input channel 1	0	0	0	1	0
enter trim mode for sensor input channel 2	0	0	1	0	0
leave trim mode for either input channel	0	0	0	0	0

How to enter the trim mode

Details of voltage levels and timing of the status bits to be transmitted to the UZZ9001 are given in Table 3. Note that a complete protocol has to be sent before normal operation can be resumed. The trim mode can also be exited by resetting the device. After entering one of the trim modes and provided there is a dynamic input signal there will be a square wave output at the terminal T_{OUT} (pin 22).

Reset

In addition to the external reset pin (pin 6), the UZZ9001 provides an internal power-up/ power-down reset logic which continuously monitors the supply voltage. When the supply voltage increases and reaches a safe level, reset becomes inactive and the device starts initialization. When the supply voltage exceeds the safe voltage level, the device is reset immediately. This internal reset logic can be over-ridden in all modes and at any time by applying an external active high command to the RES input pin (pin 6) in all modes and at any time. The reset pin RES (pin 6). This pin is internally pulled to ground and therefore need not be connected if the function is not required.

Measurement dynamics

The UZZ9001 includes an on-chip RC Oscillator that generates the clock for the whole device. Consequently, no external clock supply is required for the measurement system. The nominal clock frequency of the on-chip oscillator is 4 MHz at room temperature. It varies with temperature change. At –40 °C the clock frequency may decrease to 2.3 MHz. At higher temperatures however, a frequency up to 5.7 MHz may occur. This influences the dynamics of measurements. From an application point of view, two different effects have to be distinguished. The system delay, which means how long it takes until a changed input signal is recognized at the output, and the measurement update rate. The system delay is mainly caused by the settling time of the low pass decimation filter, which depends on the maximum frequency content (shape) of the input signals and the clock frequency. The following maximum values can be expected for the entire system delay. The measurement update rate, however, is directly related to the oscillator frequency. At room temperature, a new value is available every 0.26 ms. When taking the entire temperature range into account, update rates between 0.45 and 0.18 ms are possible. (see Table 5)

Table 5 System delay and update rates of the UZZ9001

PARAMETER	MIN.	TYP.	MAX.	UNIT
System delay (time elapsed until 95% of the final value is reached)				
max. signal frequency < 200 MHz	–	–	0.6	ms
transients (step response)	–	–	1.2	ms
Measurement update rate				
–40 °C	0.45	–	–	ms
+25 °C (room temperature)	–	0.26	–	ms
+150 °C	–	–	0.18	ms

APPLICATION INFORMATION

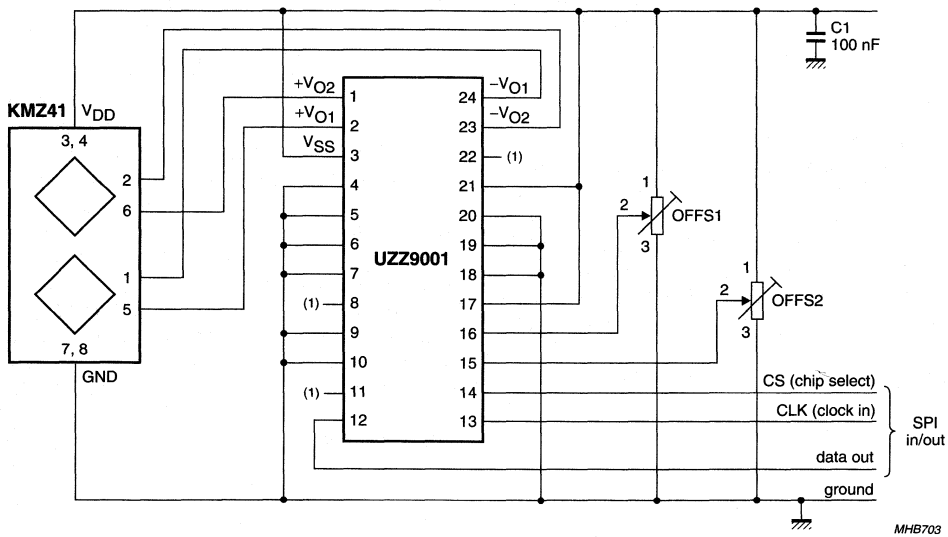

(1) For test applications pin to be left unconnected.

Fig.6 UZZ9001 trim mode configuration.

PACKAGE OUTLINE

SO24: plastic small outline package; 24 leads; body width 7.5 mm **SOT137-1**

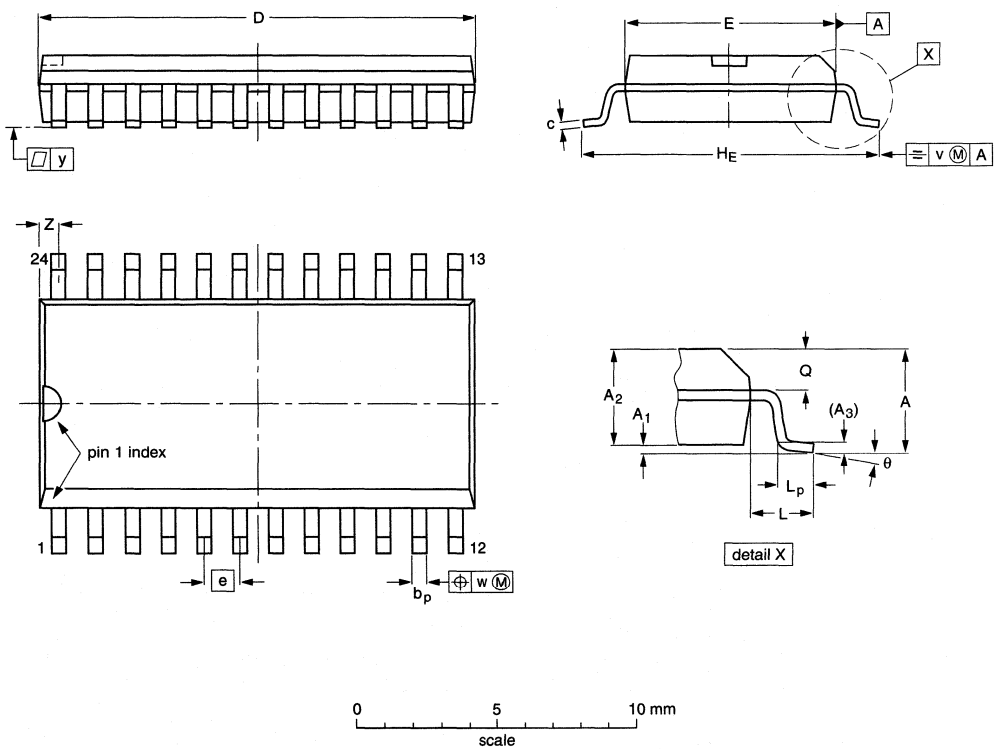

DIMENSIONS (inch dimensions are derived from the original mm dimensions)

UNIT	A max.	A_1	A_2	A_3	b_p	c	$D^{(1)}$	$E^{(1)}$	e	H_E	L	L_p	Q	v	w	y	$Z^{(1)}$	θ
mm	2.65	0.30 0.10	2.45 2.25	0.25	0.49 0.36	0.32 0.23	15.6 15.2	7.6 7.4	1.27	10.65 10.00	1.4	1.1 0.4	1.1 1.0	0.25	0.25	0.1	0.9 0.4	8° 0°
inches	0.10	0.012 0.004	0.096 0.089	0.01	0.019 0.014	0.013 0.009	0.61 0.60	0.30 0.29	0.050	0.419 0.394	0.055	0.043 0.016	0.043 0.039	0.01	0.01	0.004	0.035 0.016	

Note

1. Plastic or metal protrusions of 0.15 mm maximum per side are not included.

OUTLINE VERSION	REFERENCES				EUROPEAN PROJECTION	ISSUE DATE
	IEC	JEDEC	EIAJ			
SOT137-1	075E05	MS-013				~~97-05-22~~ 99-12-27

SILICON SENSORS FOR TEMPERATURE MEASUREMENT

GENERAL

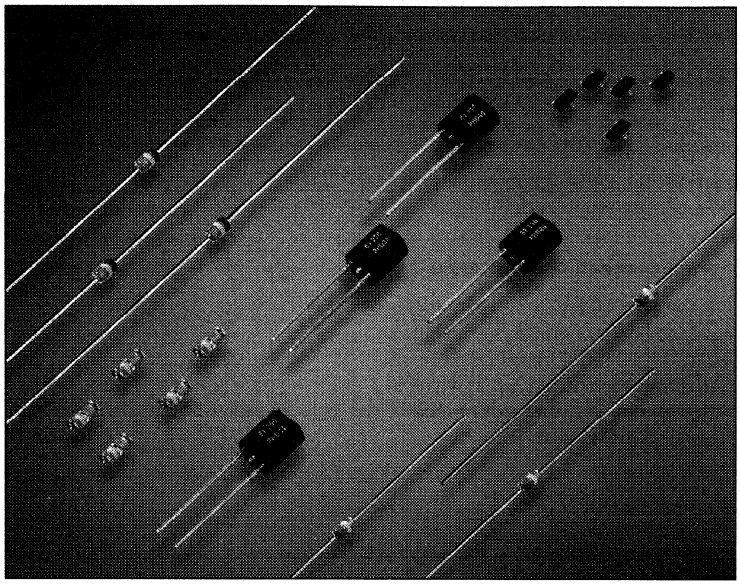

With their high accuracy and excellent long term stability, the KTY series of silicon sensors in spreading resistor technology provide an attractive alternative to the more conventional sensors based on NTC or PTC technology. Their main advantages are:

- Long term stability
- Si batch process based technology
- Virtual linear characteristics.

Table 1 Drifts of Si Sensors
After 10000 hours permanent operation with nominal operating current at maximum operating temperature.

TYPE	TYPICAL DRIFT (K)	MAXIMUM DRIFT (K)
KTY81-1 KTY82-1	0.20	0.50
KTY81-2 KTY82-2	0.20	0.80
KTY83	0.15	0.40

The properties of our temperature sensors are based on those of the chemical element silicon, and therefore sensor behaviour is as stable as this chemical element. This means that temperature drifts during the lifetime of the products are negligible. In recent tests this has been verified, when sensors operating at their maximum operating temperature for 10000 hours (equivalent to 1.14 years) have shown typical drifts of 0.2 K with a maximum of 0.4 K to 0.8 K.

Long term stability

Assuming that the sensor is typically used at half of the specified maximum temperature, our Si sensor will have a low drift as described in Table 1 for at least 450000 hours (equals 51 years). This calculation is based on the Arrenius equation (activation energy = 0.7 eV).

Si batch process products

Because our products are based on Si technology, we indirectly benefit from progress in this field, due to development of microprocessors and computer memory etc. Additionally, this indirect benefit also extends to encapsulation technology, where the trend is towards miniaturization and high volume manufacture.

Virtual linear characteristics

Si temperature sensors show a virtually linear characteristic compared to the exponential characteristic of NTCs (see Fig.2). This means that Si temperature sensors have a TK (temperature coefficient) which is nearly constant over the complete temperature range. This characteristic can be ideally exploited when the sensor is used to provide, for example, temperature compensation for a microprocessor with integrated A/D converter.

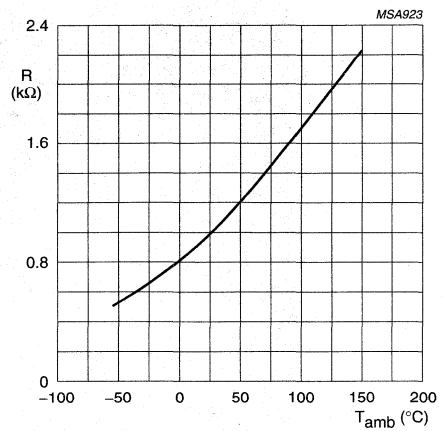

Fig.2 Characteristic of KTY81.

Construction of the sensor: spreading resistance principle

The construction of the basic sensor chip is shown in Fig.3. The chip size is ≈500 × 500 × 240 μm. The upper plane of the chip is covered by an SiO_2 insulation layer, in which a metallized hole with a diameter of ≈20 μm has been cut out. The entire bottom plane is metallized.

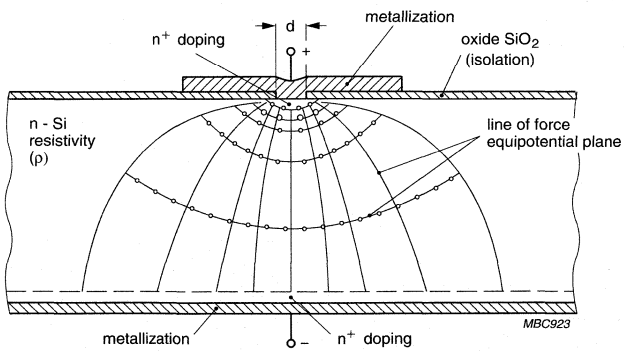

The top plane is provided with a circular metal contact; the entire bottom plane is metallized.

$R \approx \frac{\rho}{\pi} \times \frac{1}{d}$.

Fig.3 Section through the crystal showing the spreading resistance principle and the electrode arrangement.

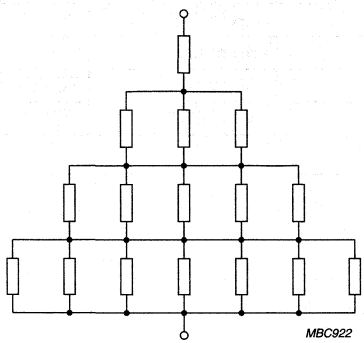

Fig.4 Equivalent circuit symbolically representing the spreading resistance principle shown in Fig.3.

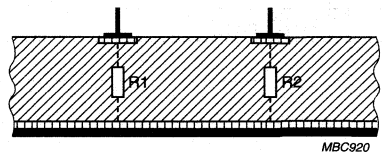

Fig.5 Setup consisting of two single sensors connected in series, but with opposite polarity.

This arrangement provides a conical current distribution through the crystal, hence the name 'spreading resistance' (see Fig.4). A major advantage of this arrangement is that the dependency of the sensor resistance on manufacturing tolerances is significantly reduced. The dominant part of the resistance is determined by the area close to the metallization hole which makes the setup independent of the Si crystal dimension tolerances. An n^+ region, diffused into the crystal beneath the metallization reduces barrier-layer effects at the metal-semiconductor junctions.

Figure 5 shows a second arrangement, effectively consisting of two single sensors connected in series, but with opposite polarity, which has the advantage of providing a resistance that is independent of current direction. This is in contrast to the single-sensor arrangement of Fig.3, which, for larger currents and temperatures above 100 °C, gives a resistance that varies slightly with the current direction.

Normally, silicon temperature sensors have a temperature limit of ≈150 °C, imposed by the intrinsic semiconductor properties of silicon. If, however, the single-sensor device is biased with its metal contact positive, the onset of intrinsic semiconductor behaviour is shifted to a higher temperature. This stems from the fact that a positive voltage on the gold contact severely depletes the hole concentration in the upper n^+ diffusion layer, and so effectively insulates holes spontaneously generated within the body of the crystal due to its intrinsic nature. As a result the holes are prevented from contributing to the total current, and hence from affecting the resistance.

The twin-sensor arrangement shown in Fig.5 has been applied in the KTY81 and KTY82 series. These sensors, in SOD70 (KTY81) and SOT23 (KTY82) packages (Figs 6 and 7), are therefore polarity independent.

The KTY83/84 series use the more basic single-sensor arrangement. The simplicity of this arrangement allows the sensors to be produced in the compact SOD68; DO-34 package. (Fig 8). In addition to simplicity, another important advantage of the single-sensor device is the potential for operation at temperatures up to 300 °C. The KTY84 makes use of this property, being specifically designed for operation at temperatures up to 300 °C. Table 2 provides an overview of product key characteristics.

Table 2 Overview of product - key characteristics

FAMILY TYPE	R_{25} (Ω)	AVAILABLE TOLERANCE (ΔR)	T_{oper} RANGE (°C)	PACKAGE
KTY81-1	1000	±1% up to ±5%	−55 to 150	SOD70
KTY81-2	2000	±1% up to ±5%	−55 to 150	SOD70
KTY82-1	1000	±1% up to ±5%	−55 to 150	SOT23
KTY82-2	2000	±1% up to ±5%	−55 to 150	SOT23
KTY83-1	1000	±1% up to ±5%	−55 to 175	SOD68 (DO-34)
KTY84-1	1000 (R_{100})	±3% up to ±5%	−40 to 300	SOD68 (DO-34)

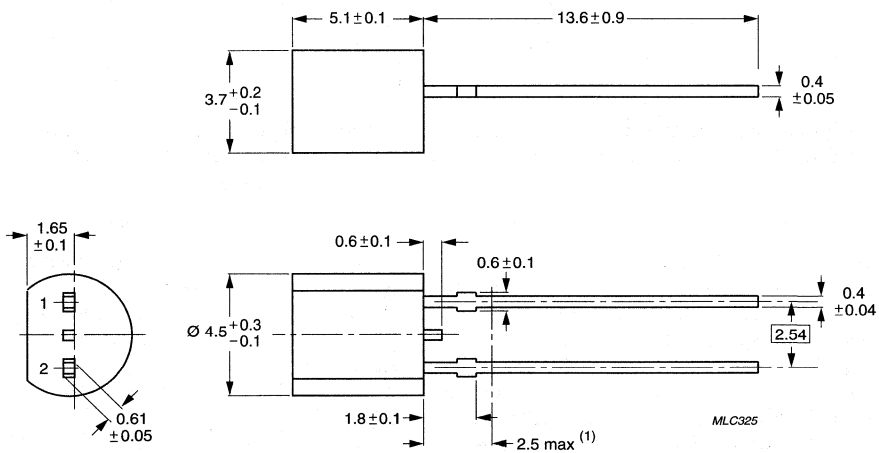

(1) Terminal dimensions within this zone are uncontrolled to allow for flow of plastic and terminal irregularities.

Fig.6 Outline of the KTY81 (SOD70).

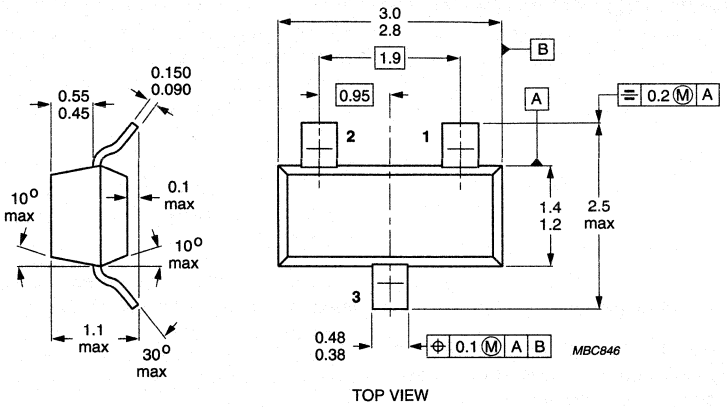

Fig.7 Outline of the KTY82 (SOT23).

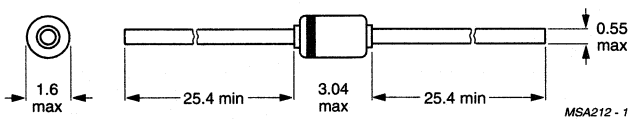

The marking band indicates the negative connector.

Fig.8 Outline of the KTY83/84 (SOD68; DO34).

TEMPERATURE DEPENDENCY

For the KTY83 series of temperature sensors, the mathematical expression for the sensor resistance 'R_T' as a function of temperature is given by:

$$R_T = R_{ref}[1 + A(T - T_{ref}) + B(T - T_{ref})^2] \quad (1)$$

where:

R_T is resistance at temperature T

R_{ref} is the nominal resistance at the reference temperature (T_{ref})

T_{ref} is referee temperature (100 °C for the KTY84, 25 °C for all other types)

A, B are type-dependent coefficients.

For the KTY81/82/84 series, the slope of the characteristic curve decreases slightly in the upper temperature range above a certain temperature T_I (point of inflection). Therefore, an additional term in equation (1) becomes necessary:

$$R_T = R_{ref}[1 + A(T - T_{ref}) + B(T - T_{ref})^2 - C(T - T_I)^D]$$

where:

T_I is temperature above which the slope of the characteristic curve starts to decrease (point of inflection).

C, D are type-dependent coefficients.

C is 0 for $T < T_I$.

For the types previously mentioned, the type-dependent constants 'A', 'B', 'C' and 'D', as well as 'T_I', are given in Table 3.

For high-precision applications, e.g. microcontroller-based control systems, the above expressions and the values in Table 3 can be used to generate a calibration table to store in a ROM for look-up and linear interpolation. Data for maximum expected temperature error is supplied separately in the related data sheets. The calculations are based on both specified resistance ratios (R_{25}/R_{100} and R_{25}/R_{-55}) and the basic resistance spread at 25 °C.

If a microcontroller is not used, the slight deviation from linearity can easily be compensated using a parallel resistor (if a constant current source is used), a series resistor (if a constant voltage source is used) or a suitable combination of both. This is discussed in the Section "Linearization".

Table 3 Type dependent constants

SENSOR TYPE	A (K^{-1})	B (K^{-2})	C[1] (K^{-D})	D	T_I (°C)
KTY81-1	7.874×10^{-3}	1.874×10^{-5}	3.42×10^{-8}	3.7	100
KTY81-2	7.874×10^{-3}	1.874×10^{-5}	1.096×10^{-6}	3.0	100
KTY82-1	7.874×10^{-3}	1.874×10^{-5}	3.42×10^{-8}	3.7	100
KTY82-2	7.874×10^{-3}	1.874×10^{-5}	1.096×10^{-6}	3.0	100
KTY83	7.635×10^{-3}	1.731×10^{-5}	–	–	–
KTY84	6.12×10^{-3}	1.1×10^{-5}	3.14×10^{-8}	3.6	250

Note

1. For $T < T_I$: C = 0.

RESISTANCE/TEMPERATURE CHARACTERISTICS

Manufacturing tolerances

Silicon temperature sensors are normally produced to quite fine tolerances: 'ΔR' between ±0.5% and ±2%. Figure 9 illustrates how these tolerances are specified. The tolerance on resistance quoted in our data sheets is given by the resistance spread 'ΔR' measured at 25 °C.

Because of spread in the slope of the resistance characteristics, 'ΔR' will increase each side of the 25 °C point, to produce the butterfly curve shown in Fig.9. To give an indication of this spread in slope, we also quote the ratio of resistance at two other temperatures (–55 °C and 100 °C) to the nominal resistance at 25 °C, i.e. 'R_{-55}/R_{25}' and 'R_{100}/R_{25}'; for the KTY84, we quote 'R_{25}/R_{100}' and 'R_{250}/R_{100}'. A table giving the ΔR tolerances is included in each of the Temperature Sensor data sheets.

The user, however, is usually more interested in the maximum expected temperature error '$\pm\Delta T$'. We also provide this in the data sheets as a graph showing 'ΔT' as a function of 'T'. For the high temperature sensor KTY84, we specify the resistance spread at 100 °C.

The relation between the tolerance of the resistance of the sensor and the resulting accuracy of the temperature measurement is given by the temperature coefficient, Fig.9 shows a typical situation. In the range between –40 °C and +150 °C the temperature coefficient varies between about 1 (–40 °C) and about 0.35 (+150 °C). From this graph the relation between the expected resistance tolerance and the resulting temperature error can easily be derived. The calculated maximum temperature error is given in the form of a table in every data sheet.

Current dependency of sensor resistance

The resistance of silicon temperature sensors is dependent on the operating current. In applications with an operating current deviating from the nominal current, a deviation of sensor resistance from the nominal values has to be taken into account.

For any application, an operating current ≥0.1 mA is recommended. For lower operating currents, the current dependency is additionally influenced by temperature.

For any application with operating currents above the nominal values, it should be noted, that an additional error caused by self-heating effects will influence the measurement accuracy.

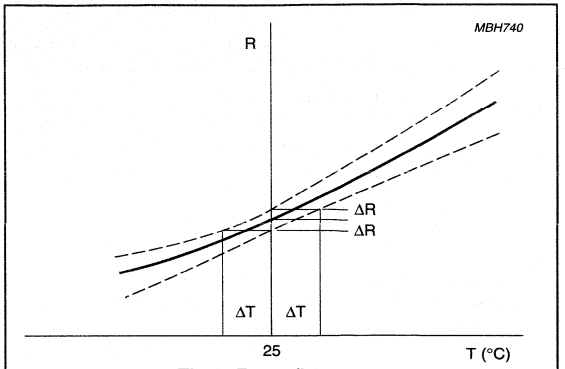

Fig.9 Butterfly curve.

Polarity of current

KTY83 and 84 sensors are marked with a coloured band to indicate polarity. The published characteristics of the sensors will only be obtained if the current polarity is correct. In events where the current polarity is incorrect, the curve $R = f(T_{amb})$ differs in the upper temperature range significantly from the published form.
Note: Light, especially infrared light, also has an influence on the sensor characteristics when the current polarity is incorrect.

Linearization

The resistance/temperature characteristics of the silicon temperature sensors are nearly linear, but in some applications further linearization becomes necessary, e.g. control systems requiring high accuracy.

A simple way to do this is to shunt the sensor resistance 'R_T' with a fixed resistor 'R_L' (see Fig.10a). The resistance '$R_L \times R_T/(R_L + R_T)$' of the parallel combination then effectively becomes a linear function of temperature, and the output voltage 'V_T' of the linearized circuit can be used to regulate the control system.

If the circuit is powered by a constant-voltage source (see Fig.10b), a linearization resistor R_L can be connected in series with the sensor. The voltages across the sensor and across the resistor will then again be approximately linear functions of temperature.

The value of the series or parallel resistor depends on the required operating temperature range of the sensor.
A method for finding this resistance is described below, giving zero temperature error at three equidistant points T_a, T_b and T_c.

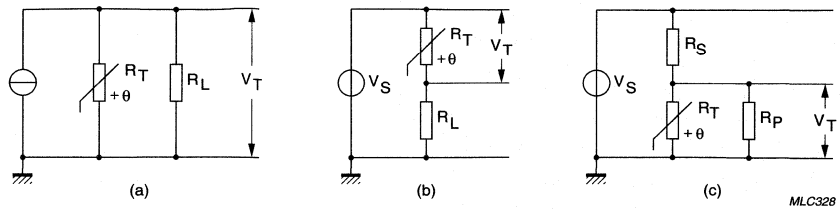

(a) With a resistor 'R_L' shunted across the sensor.
(b) With a resistor 'R_L' in series with the sensor and system powered by a constant-voltage source.
(c) With a series 'R_S' and parallel resistor 'R_P' and system powered by a constant-voltage source.

Fig.10 Linearization of sensor characteristics.

Consider the parallel arrangement. With the resistance of the sensor at three points R_a, R_b and R_c, the requirement for linearity at the three points is:

$$\frac{R_L \times R_a}{R_L + R_a} - \frac{R_L \times R_b}{R_L + R_b} = \frac{R_L \times R_b}{R_L + R_b} - \frac{R_L \times R_c}{R_L + R_c}$$

so

$$R_L = \frac{R_b \times (R_a + R_c) - 2R_a \times R_c}{R_a + R_c - 2R_b}.$$

The same resistor will also be suitable for the series arrangement.

In practice, a current source is too expensive and a fixed supply voltage, e.g. 5 or 12 V is used for a specific operating current, e.g. 1 or 0.1mA. In this case, linearization can be achieved by a series/parallel resistor combination to the sensor (see Fig.10c). The resistance of the parallel combination (R_P, R_T) and series resistor R_S is equal to the optimum linearization resistor R_L, calculated previously. Starting with the value of resistor R and with the desired current I_S through the sensor at a reference temperature T (preferably in the middle of the measured range), the resistor R_S and R_P can be calculated as follows:

$$\text{series resistor: } R_S = \frac{V_S}{I_S \times \left(\frac{R_T}{R_L} + 1\right)}$$

$$\text{parallel resistor: } R_P = \frac{1}{\frac{1}{R_L} - \frac{1}{R_S}}.$$

As an example, Fig.11 shows the deviation from linearity to be expected from a nominal KTY81 sensor, linearized over the temperature range 0 to 100 °C with a linearizing resistance of $R_L = 2870\ \Omega$.

Figure 18 shows an application example using a series/parallel combination for the KTY81 ($I_S = 1$ mA).

Effect of tolerances on linearized sensor characteristics

In practical applications with an arbitrary sensor, the total uncertainty in the sensor reading will be a combination of spread due to manufacturing tolerances and linearization errors.

As an example, Fig.13 shows the combined effects of manufacturing tolerances and linearization errors for the KTY81 sensor linearized over the temperature range 0 to 100 °C. Calibration of the subsequent circuitry (op-amp, control circuitry, etc.) can reduce this error significantly.

Figure 14 shows the temperature error of the system with (linear) output circuitry calibrated at 50 °C, and Fig.15 shows the error of the same system calibrated at 0 and 100 °C.

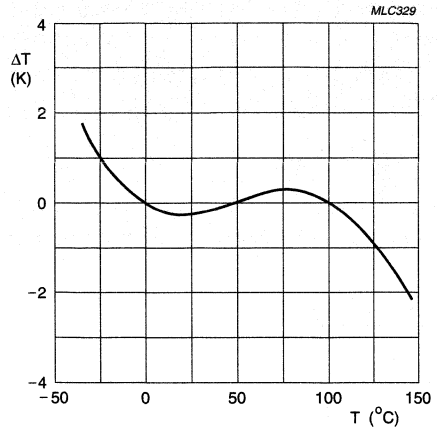

Sensor linearized over the temperature range 0 to 100 °C (linearizing resistance 2870 Ω).

Fig.11 Linearization error 'ΔT' to be expected from a nominal KTY81 sensor.

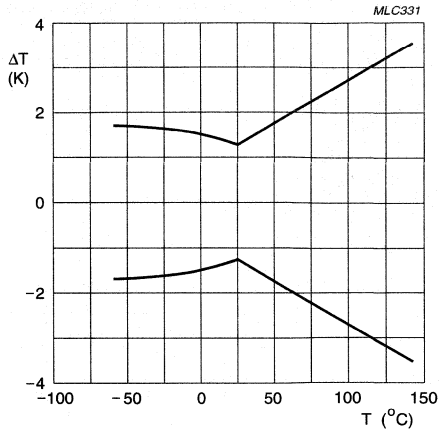

Fig.12 Maximum temperature error 'ΔT' due to manufacturing tolerances expected of a KTY81-1 sensor.

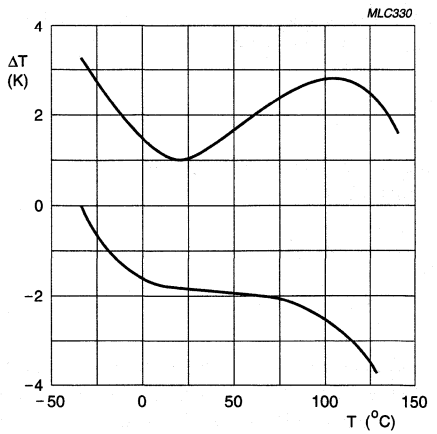

Fig.13 Combined effects of manufacturing tolerances and linearization errors for the KTY81 sensor.

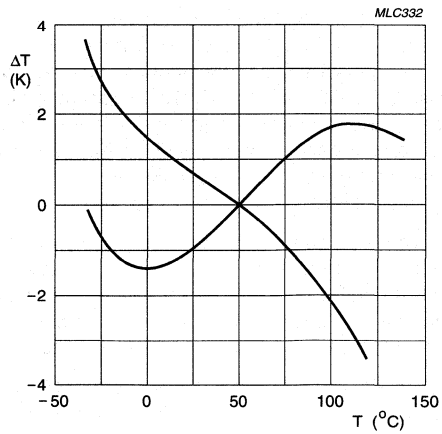

Fig.14 Maximum expected temperature error of a KTY81-1 sensor plus linearization resistor calibrated at 50 °C.

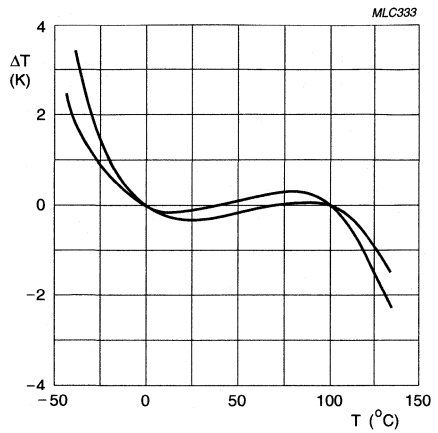

Fig.15 Error of a KTY81-1 sensor (same system as Fig.14) calibrated at 0 and 100 °C.

TEMPERATURE COMPENSATION

In many applications, it is necessary to compensate for the temperature dependency of electronic circuitry. For example, the sensitivity of many magnetic field sensors has a linear drift with temperature. To compensate for this drift, a temperature sensor with linear characteristics is required. The temperature sensors of the KTY series are well suited for this purpose and can be used for compensation of both positive and negative drift.

In many events, as with the magnetoresistive sensor KMZ10B, the temperature drift is negative. For this sensor, two circuits in SMD-technology, which include temperature compensation, are described below. The formulae given can be used to adapt the circuits to other conditions.

Figure 16 shows a simple setup using a single op-amp (NE5230D). The circuit provides the following facilities:

- Compensation of the **average** (sensor-to-sensor) sensitivity drift with temperature via a negative feedback loop incorporating a KTY82-210 silicon temperature sensor
- Offset adjustment by means of potentiometers 'R1' and 'R2'
- Gain adjustment by means of potentiometer 'R7'.

The temperature sensor is part of the amplifier's feedback loop and thus increases the amplification with increasing temperature.

With the resistor as shown in Fig.16 the temperature dependent amplification 'A' is given by:

$$A = \frac{R7}{R4 + \frac{R_B}{2}}\left(1 + 2\frac{R_T}{R_S}\right) \qquad (2)$$

and the temperature coefficient of the amplification can be calculated to be:

$$TC_A = \frac{R_T \times TC_{KTY}}{R_T + \frac{R_S}{2}}$$

with:

R_T = temperature dependent resistance of the KTY82.

TC_{KTY} = temperature coefficient of the KTY82 at reference temperature (0.79 %/K at 25 °C).

R_B = bridge resistance of the magnetoresistive sensor.

The temperature coefficient of amplification must be equal and opposite to the magnetic field sensor's 'TC' of sensitivity.

The value of the resistor 'R_S', which determines the positive 'TC' of the amplification is:

$$R_S = 2 \times R_T\left(\frac{TC_{KTY}}{TC_A} - 1\right).$$

The resistance of the feedback resistor can be derived from equation (2):

$$R7 = R4 \times \left(\frac{A}{1 + 2\frac{R_T}{R_S}}\right).$$

The temperature dependent values 'R_T' and 'A' are taken for a certain reference temperature, usually 25 °C, but in other applications a different reference temperature may be more suitable.

Figure 17 shows an example with a commonly used instrumentation amplifier. The circuit can be divided into two stages: a differential amplifier stage that produces a symmetrical output signal derived from the

magnetoresistive sensor, and an output stage that also provides a reference to ground for the amplification stage.

To compensate the negative sensor drift, the amplification is again given an equal but positive temperature coefficient by means of a KTY81-110 silicon temperature sensor in the feedback loop of the differential amplifier.

The amplification of the input stage ('OP1' and 'OP2') is given by:

$$A1 = 1 + \frac{R_T + R_B}{R_A}$$

and the amplification of the complete amplifier by:

$$A = A1 \times \frac{R14}{R10}.$$

The positive temperature coefficient of the amplification is:

$$TC_A = \frac{R_T \times TC_{KTY}}{R_A + R_B + R_T}.$$

For the given negative 'TC' of the magnetoresistive sensor and the required amplification of the input stage 'A1', the resistance 'R_A' and 'R_B' can be calculated by:

$$R_B = R_T \times \left(\frac{TC_{KTY}}{TC_A} \times \left(1 - \frac{1}{A1}\right) - 1 \right)$$

$$R_A = \frac{R_T + R_B}{A1 - 1}.$$

The circuit provides for adjustment of gain and offset voltage of the magnetic-field sensor. The calculated resistance 'R_A' consists of the fixed resistor 'R5' and trimming resistor 'R6' provided for amplification adjustment. Amplification adjustment only negligibly influences the 'TC' of the amplifier. The output stage 'OP3' gives an output voltage of $^2/_5$ of the supply voltage (2 V for V_S = 5 V) for zero output voltage of the magnetic field sensor and an output voltage of ±1 V for V_S = 5 V. For other supply voltages the circuit has a ratiometric behaviour.

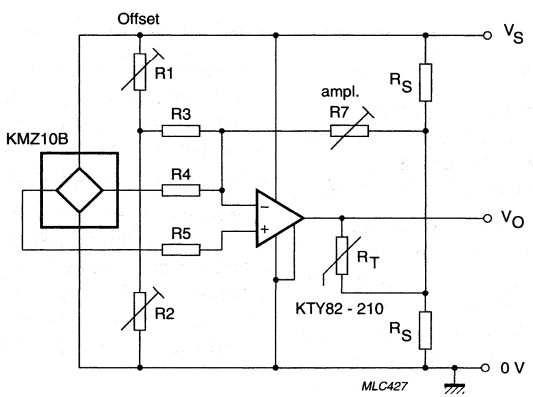

Example: A = 50 (typ.), TC_A = 0.004 K^{-1}.

Fig.16 Temperature compensation circuit.

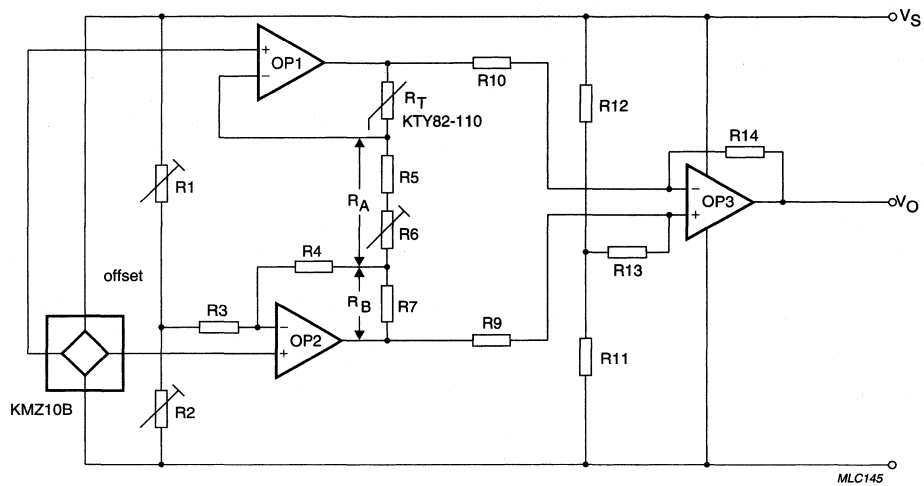

Example: A = 50 (typ.), TC_A = 0.004 K^{-1}.

Fig.17 KMZ10B evaluation circuit with instrumentation amplifier.

TYPICAL APPLICATION CIRCUIT

Figure 18 shows a typical and versatile temperature measuring circuit using silicon temperature sensors. This example is designed for the KTY81-110 (or the KTY82-110) and a temperature range from 0 to 100 °C.

With resistors 'R1' and 'R2', the sensor forms one arm of a bridge, the other arm being formed by resistor 'R3', potentiometer 'P1' and resistor 'R4'. The values of 'R1' and 'R2' are chosen to supply the sensor with the proper current of ≈1 mA, and to linearize the sensor characteristic over the temperature range of interest: in this event, between 0 and 100 °C. Over this temperature range, the output voltage V_O will vary linearly between $0.2V_S$ and $0.6V_S$, i.e. between 1 V and 3 V for a supply of V_S = 5 V.

To calibrate the circuit, adjust 'P1' to set 'V_O' to 1 V, with the sensor at 0 °C. Then, at a temperature of 100 °C, adjust 'P2' to set 'V_O' to the corresponding output voltage, in this example 3 V. With this circuit, adjustment of 'P2' has no effect on the zero adjustment.

The measurement accuracy obtained by this two-point calibration is shown in Fig.15. If the application can tolerate a temperature deviation of ±2 K at the temperature extremes (see Fig.14), costs can be reduced by replacing 'P2' with a 1.8 kΩ fixed resistor and adjusting 'V_O' at one temperature (the middle of the range, for example), using 'P1'.

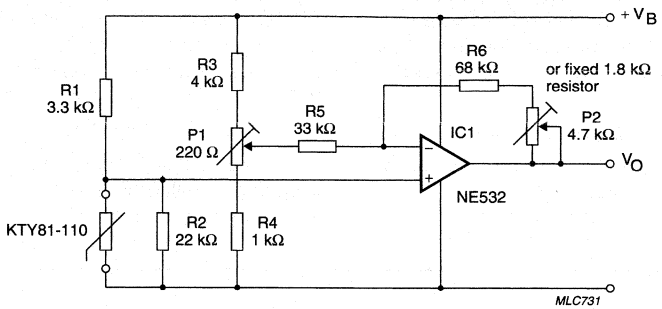

A KTY82-110 sensor would be equally suitable.
Temperature range 0 to 100 °C; $V_O = 0.2V_S$ to $0.6V_S$.
For $V_S = 5$ V: $V_O = 1$ to 3 V.
All resistors metal film; tolerance ±1%.

Fig.18 Temperature measuring circuit using a KTY81-110 sensor.

HIGH TEMPERATURE MEASUREMENT WITH KTY84

The operating range of silicon temperature sensors normally is limited to about 150 °C (an exception is the KTY83 with an upper temperature limit of 175 °C). This is due to the temperature stability of the package and the increasing intrinsic conductivity of the silicon die above 150 °C. The measuring range of the KTY84 silicon temperature sensors, however, is extended up to 300 °C.

The SOD68 (DO-34) diode housing together with special contacts between leads and sensor die give the necessary temperature resistivity for the package. The influence of the intrinsic conductivity can be suppressed by a sufficiently high operating current flowing in the correct direction.

Figure 19 shows the nominal characteristic for the recommended operating current of 2 mA and the effect of operating the sensor with a lower, and especially, a reverse current. The sensor resistance at the high temperature end makes it impossible to draw the current of 2 mA through the sensor in a common bridge circuit as in the previously suggested circuits. This is due to the usually limited supply voltage and the fact that the value of the series resistor may not be less than the linearization resistor of ≈5 kΩ. A solution is to supply the sensor by a constant current source.

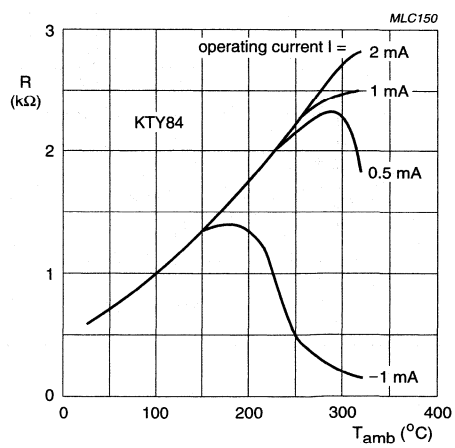

Fig.19 Sensor characteristic of the KTY84.

Figure 20 gives an example with internal voltage stabilization, a supply voltage of 8 to 24 V and for the full measuring range up to 300 °C. Operational amplifier 'OP1' and transistor 'TR1' form a current source to feed the temperature sensor. 'OP2' amplifies the bridge signal to the output voltage range. The circuit provides adjustment for a 'zero point'; 100 °C equals V_O = 2 V ('P1'), and full range ('P2').

A second example for a KTY84 evaluation circuit takes into consideration that in some electronic systems a supply voltage of only 5 V may be used. Under such circumstances it would be impossible to obtain the recommended current of 2 mA. A compromise is suggested by the circuit in Fig.21. A low drop current source supplies the temperature sensor and the linearization resistor. The maximum attainable current at 300 °C is 1.5 mA. This value is below the nominal operating current, but as Fig.19 shows, at up to 250 °C this will not cause any additional measuring error. Between 250 °C and 300 °C, however, a slightly decreasing slope of the sensor characteristic has to be taken into account.

The KTY84 silicon temperature sensor is a reliable and cost effective alternative to more expensive options such as Pt100-resistors or thermocouplers.

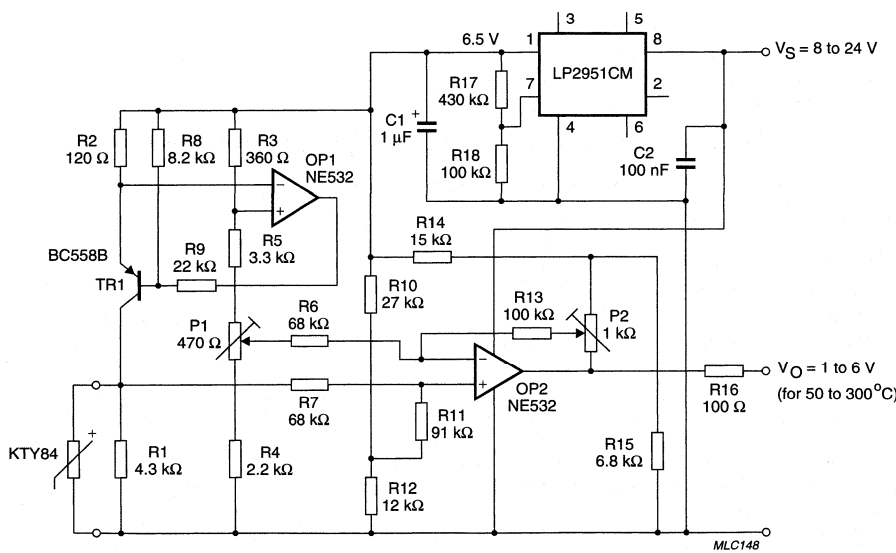

Fig.20 Evaluation circuit for KTY 84 with voltage regulation.

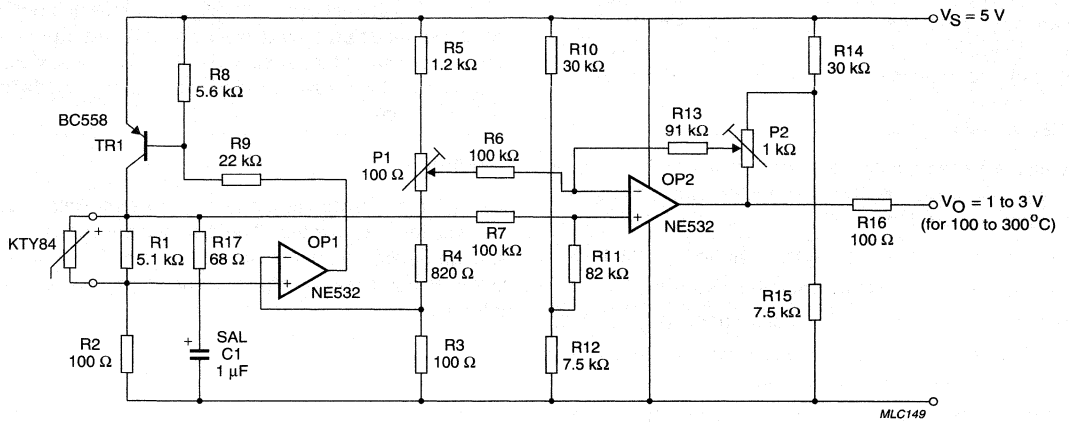

Fig.21 KTY84 evaluation circuit for 5 V power supply.

A/D CONVERTER TEMPERATURE COMPENSATION

When an A/D converter is integrated with a microcontroller, temperature compensation is required.

Figure 22 shows a suitable configuration, using a KTY81-210 temperature sensor in series with linearization resistor R_S. This voltage divider provides a linear temperature dependent voltage V_T of between 1.127 V and 1.886 V over the range 0 to 100 °C. This voltage is used as a reference for the A/D converter. The linear slope 'S' of V_T = 7.59 mV/ K.

ADDITIONAL TEMPERATURE SENSOR APPLICATIONS

Philips temperature sensors are also suitable for use in a number of other applications, for which information can be supplied on request:

- Electronic circuit protection
- Protection for power supplies
- Domestic appliances
- The white goods industry
- The automotive industry.

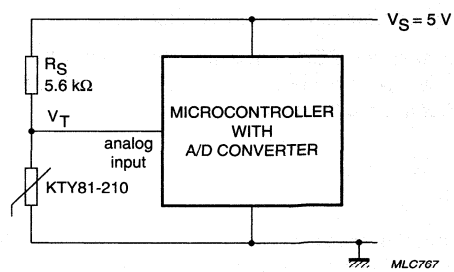

Fig.22 Temperature compensation for A/D converters.

MOUNTING AND HANDLING RECOMMENDATIONS

Mounting

KTY81

When potting techniques for KTY81 sensors are used for assembling, care has to be taken to ensure that mechanical stress and temperature development during curing of epoxy resin do not overstress the devices.

KTY83 AND 84

Excessive forces applied to a sensor may cause serious damage. To avoid this, the following recommendations should be adhered to:

- No perpendicular forces must be applied to the body
- During bending, the leads must be supported
- Bending close to the body must be done very carefully
- Axial forces to the body can influence the accuracy of the sensor and should be avoided
- These sensors can be mounted on a minimum pitch of 5 mm (2E).

Handling

ELECTROSTATIC DISCHARGE (ESD) SENSITIVITY

Electrostatic discharges above a certain energy can lead to irreversible changes of the sensor characteristic. In extreme events, sensors can even be destroyed. In accordance with the test methods described in IEC 47 (CO)955, temperature sensors are classified as sensitive components with respect to ESD. During handling (testing, transporting, fitting), the common rules for handling of ESD sensitive components should be observed.

If necessary, the ESD sensitivity in the practical application can be further reduced by connecting a 10 nF capacitor in parallel to the sensor.

Soldering

KTY81

The common rules for soldering components in TO-92 packages should be observed.

KTY 82

The common rules for soldering SMD components in SOT23 packages should be observed.

KTY83

Avoid any force on the body or leads during, or just after, soldering. Do not correct the position of an already soldered sensor by pushing, pulling or twisting the body. Prevent fast cooling after soldering. For hand soldering, where mounting is not on a printed-circuit board, the soldering temperature should be <300 °C, the soldering time <3 s and the distance between body and soldering point >1.5 mm. For hand soldering, dip, wave or other bath soldering, mounted on a printed-circuit board, the soldering temperature should be <300 °C, the soldering time <5 s and the distance between body and soldering point >1.5 mm.

Welding

The KTY84 sensors are manufactured with nickel plated leads suitable for welding. The distance between the body and the welding point should be >0.5 mm. Care should be taken to ensure that welding current never passes through the sensor.

TAPE AND REEL PACKAGING

Tape and reel packaging meets the feed requirements of automatic pick and place equipment. It is also an ideal shipping container.

Table 4 Packaging quantities

TYPE	PACKAGE OUTLINE	PACKAGING METHOD	SPQ	PQ	12NC NUMBER XXXX XXX XX...
KTY81	SOD70	bulk pack	500	4000	112
		reel pack, radial	2000	10000	116
KTY82	SOT23	bulk pack	500	25000	212
		reel pack, SMD low profile 7"	3000	3000	215
		reel pack, SMD low profile 11¼"	10000	10000	235
KTY83, 84	SOD68 (DO-34)	reel pack axial 52 mm	10000	10000	113
		ammopack axial small size	1000	1000	153

DEVICE DATA

Silicon temperature sensors KTY81-1 series

DESCRIPTION

The temperature sensors in the KTY81-1 series have a positive temperature coefficient of resistance and are suitable for use in measurement and control systems. The sensors are encapsulated in the SOD70 leaded plastic package.

Tolerances of 0.5% or other special selections are available on request.

PINNING

PIN	DESCRIPTION
1	electrical contact
2	electrical contact
3	not to be connected to a potential

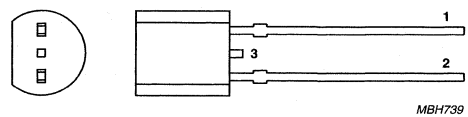

Fig.1 Simplified outline (SOD70).

MARKING

TYPE NUMBER	CODE
KTY81-110	110
KTY81-120	120
KTY81-121	121
KTY81-122	122
KTY81-150	150
KTY81-151	151
KTY81-152	152

QUICK REFERENCE DATA

SYMBOL	PARAMETER	CONDITIONS	MIN.	MAX.	UNIT
R_{25}	sensor resistance	T_{amb} = 25 °C; I_{cont} = 1 mA			
	KTY81-110		990	1010	Ω
	KTY81-120		980	1020	Ω
	KTY81-121		980	1000	Ω
	KTY81-122		1000	1020	Ω
	KTY81-150		950	1050	Ω
	KTY81-151		950	1000	Ω
	KTY81-152		1000	1050	Ω
T_{amb}	ambient operating temperature		−55	+150	°C

LIMITING VALUES

In accordance with the Absolute Maximum Rating System (IEC 60134).

SYMBOL	PARAMETER	CONDITIONS	MIN.	MAX.	UNIT
I_{cont}	continuous sensor current	in free air; T_{amb} = 25 °C	–	10	mA
		in free air; T_{amb} = 150 °C	–	2	mA
T_{amb}	ambient operating temperature		–55	+150	°C

CHARACTERISTICS

T_{amb} = 25 °C, in liquid, unless otherwise specified.

SYMBOL	PARAMETER	CONDITIONS	MIN.	TYP.	MAX.	UNIT
R_{25}	sensor resistance	I_{cont} = 1 mA				
	KTY81-110		990	–	1010	Ω
	KTY81-120		980	–	1020	Ω
	KTY81-121		980	–	1000	Ω
	KTY81-122		1000	–	1020	Ω
	KTY81-150		950	–	1050	Ω
	KTY81-151		950	–	1000	Ω
	KTY81-152		1000	–	1050	Ω
TC	temperature coefficient		–	0.79	–	%/K
R_{100}/R_{25}	resistance ratio	T_{amb} = 100 °C and 25 °C	1.676	1.696	1.716	
R_{-55}/R_{25}	resistance ratio	T_{amb} = –55 °C and 25 °C	0.480	0.490	0.500	
τ	thermal time constant; note 1	in still air	–	30	–	s
		in still liquid; note 2	–	5	–	s
		in flowing liquid; note 2	–	3	–	s
	rated temperature range		–55	–	+150	°C

Notes

1. The thermal time constant is the time taken for the sensor to reach 63.2% of the total temperature difference. For example, if a sensor with a temperature of 25 °C is moved to an environment with an ambient temperature of 100 °C, the time for the sensor to reach a temperature of 47.4 °C is the thermal time constant.
2. Inert liquid, e.g. FC43 manufactured by the 3M company.

Table 1 Ambient temperature, corresponding resistance, temperature coefficient and maximum expected temperature error for KTY81-110 and KTY81-120

I_{cont} = 1 mA.

AMBIENT TEMPERATURE		TEMP. COEFF.	KTY81-110				KTY81-120			
(°C)	(°F)	(%/K)	RESISTANCE (Ω)			TEMP. ERROR (K)	RESISTANCE (Ω)			TEMP. ERROR (K)
			MIN.	TYP.	MAX.		MIN.	TYP.	MAX.	
–55	–67	0.99	475	490	505	±3.02	470	490	510	±4.02
–50	–58	0.98	500	515	530	±2.92	495	515	535	±3.94
–40	–40	0.96	552	567	582	±2.74	547	567	588	±3.78
–30	–22	0.93	609	624	638	±2.55	603	624	645	±3.62
–20	–4	0.91	669	684	698	±2.35	662	684	705	±3.45
–10	14	0.88	733	747	761	±2.14	726	747	769	±3.27
0	32	0.85	802	815	828	±1.91	793	815	836	±3.08
10	50	0.83	874	886	898	±1.67	865	886	907	±2.88
20	68	0.80	950	961	972	±1.41	941	961	982	±2.66
25	77	0.79	990	1000	1010	±1.27	980	1000	1020	±2.54
30	86	0.78	1029	1040	1051	±1.39	1018	1040	1061	±2.68
40	104	0.75	1108	1122	1136	±1.64	1097	1122	1147	±2.97
50	122	0.73	1192	1209	1225	±1.91	1180	1209	1237	±3.28
60	140	0.71	1278	1299	1319	±2.19	1265	1299	1332	±3.61
70	158	0.69	1369	1392	1416	±2.49	1355	1392	1430	±3.94
80	176	0.67	1462	1490	1518	±2.8	1447	1490	1532	±4.3
90	194	0.65	1559	1591	1623	±3.12	1543	1591	1639	±4.66
100	212	0.63	1659	1696	1733	±3.46	1642	1696	1750	±5.05
110	230	0.61	1762	1805	1847	±3.83	1744	1805	1865	±5.48
120	248	0.58	1867	1915	1963	±4.33	1848	1915	1982	±6.07
125	257	0.55	1919	1970	2020	±4.66	1899	1970	2040	±6.47
130	266	0.52	1970	2023	2077	±5.07	1950	2023	2097	±6.98
140	284	0.45	2065	2124	2184	±6.28	2043	2124	2205	±8.51
150	302	0.35	2145	2211	2277	±8.55	2123	2211	2299	±11.43

Table 2 Ambient temperature, corresponding resistance, temperature coefficient and maximum expected temperature error for KTY81-121 and KTY81-122

I_{cont} = 1 mA.

AMBIENT TEMPERATURE		TEMP. COEFF.	KTY81-121				KTY81-122			
(°C)	(°F)	(%/K)	RESISTANCE (Ω)			TEMP. ERROR (K)	RESISTANCE (Ω)			TEMP. ERROR (K)
			MIN.	TYP.	MAX.		MIN.	TYP.	MAX.	
−55	−67	0.99	471	485	500	±3.02	480	495	510	±3.02
−50	−58	0.98	495	510	524	±2.92	505	520	535	±2.92
−40	−40	0.96	547	562	576	±2.74	558	573	588	±2.74
−30	−22	0.93	603	617	632	±2.55	615	630	645	±2.55
−20	−4	0.91	662	677	691	±2.35	676	690	705	±2.35
−10	14	0.88	726	740	754	±2.14	741	755	769	±2.14
0	32	0.85	794	807	820	±1.91	810	823	836	±1.91
10	50	0.83	865	877	889	±1.67	883	895	907	±1.67
20	68	0.80	941	951	962	±1.41	960	971	982	±1.41
25	77	0.79	980	990	1000	±1.27	1000	1010	1020	±1.27
30	86	0.78	1018	1029	1041	±1.39	1039	1050	1062	±1.39
40	104	0.75	1097	1111	1125	±1.64	1120	1134	1148	±1.64
50	122	0.73	1180	1196	1213	±1.91	1204	1221	1238	±1.91
60	140	0.71	1266	1286	1305	±2.19	1291	1312	1332	±2.19
70	158	0.69	1355	1378	1402	±2.49	1382	1406	1430	±2.49
80	176	0.67	1447	1475	1502	±2.8	1477	1505	1533	±2.8
90	194	0.65	1543	1575	1607	±3.12	1574	1607	1639	±3.12
100	212	0.63	1642	1679	1716	±3.46	1676	1713	1750	±3.46
110	230	0.61	1745	1786	1828	±3.83	1780	1823	1865	±3.83
120	248	0.58	1849	1896	1943	±4.33	1886	1934	1982	±4.33
125	257	0.55	1900	1950	2000	±4.66	1938	1989	2041	±4.66
130	266	0.52	1950	2003	2056	±5.07	1989	2044	2098	±5.07
140	284	0.45	2044	2103	2162	±6.28	2085	2146	2206	±6.28
150	302	0.35	2124	2189	2254	±8.55	2167	2233	2299	±8.55

Table 3 Ambient temperature, corresponding resistance, temperature coefficient and maximum expected temperature error for KTY81-150 and KTY81-151

I_{cont} = 1 mA.

AMBIENT TEMPERATURE		TEMP. COEFF.	KTY81-150				KTY81-151			
(°C)	(°F)	(%/K)	RESISTANCE (Ω)			TEMP. ERROR (K)	RESISTANCE (Ω)			TEMP. ERROR (K)
			MIN.	TYP.	MAX.		MIN.	TYP.	MAX.	
−55	−67	0.99	456	490	524	±7.04	456	478	499	±4.52
−50	−58	0.98	479	515	550	±6.99	480	502	524	±4.45
−40	−40	0.96	530	567	605	±6.91	530	553	576	±4.3
−30	−22	0.93	584	624	663	±6.84	584	608	632	±4.16
−20	−4	0.91	642	684	725	±6.77	642	667	691	±4.01
−10	14	0.88	703	747	791	±6.69	704	729	753	±3.84
0	32	0.85	769	815	861	±6.61	770	794	819	±3.67
10	50	0.83	838	886	934	±6.51	839	864	889	±3.48
20	68	0.80	912	961	1010	±6.41	912	937	962	±3.28
25	77	0.79	950	1000	1050	±6.35	950	975	1000	±3.18
30	86	0.78	987	1040	1093	±6.55	988	1014	1040	±3.33
40	104	0.75	1064	1122	1181	±6.97	1064	1094	1124	±3.64
50	122	0.73	1143	1209	1274	±7.4	1144	1178	1212	±3.97
60	140	0.71	1226	1299	1371	±7.85	1227	1266	1305	±4.31
70	158	0.69	1313	1392	1472	±8.31	1314	1357	1401	±4.67
80	176	0.67	1402	1490	1577	±8.79	1404	1453	1501	±5.05
90	194	0.65	1495	1591	1687	±9.29	1497	1551	1606	±5.43
100	212	0.63	1591	1696	1801	±9.81	1593	1654	1714	±5.84
110	230	0.61	1690	1805	1919	±10.4	1692	1759	1827	±6.3
120	248	0.58	1791	1915	2039	±11.28	1792	1867	1942	±6.94
125	257	0.55	1840	1970	2099	±11.91	1842	1920	1999	±7.38
130	266	0.52	1889	2023	2158	±12.72	1891	1973	2055	±7.94
140	284	0.45	1980	2124	2269	±15.21	1982	2071	2161	±9.63
150	302	0.35	2057	2211	2365	±20.09	2059	2156	2252	±12.88

Table 4 Ambient temperature, corresponding resistance, temperature coefficient and maximum expected temperature error for KTY81-152

I_{cont} = 1 mA.

AMBIENT TEMPERATURE			KTY81-152			
(°C)	(°F)	(%/K)	RESISTANCE (Ω)			TEMP. ERROR (K)
			MIN.	TYP.	MAX.	
−55	−67	0.99	480	502	525	±4.52
−50	−58	0.98	505	528	551	±4.45
−40	−40	0.96	558	582	606	±4.3
−30	−22	0.93	614	639	664	±4.16
−20	−4	0.91	675	701	726	±4.01
−10	14	0.88	740	766	792	±3.84
0	32	0.85	809	835	861	±3.67
10	50	0.83	882	908	934	±3.48
20	68	0.80	959	985	1011	±3.28
25	77	0.79	1000	1025	1050	±3.18
30	86	0.78	1038	1066	1093	±3.33
40	104	0.75	1119	1150	1182	±3.64
50	122	0.73	1203	1239	1275	±3.97
60	140	0.71	1290	1331	1372	±4.31
70	158	0.69	1381	1427	1473	±4.67
80	176	0.67	1476	1527	1578	±5.05
90	194	0.65	1573	1631	1688	±5.43
100	212	0.63	1674	1738	1802	±5.84
110	230	0.61	1779	1850	1921	±6.3
120	248	0.58	1884	1963	2041	±6.94
125	257	0.55	1937	2019	2101	±7.38
130	266	0.52	1988	2074	2160	±7.94
140	284	0.45	2084	2178	2271	±9.63
150	302	0.35	2165	2266	2367	±12.88

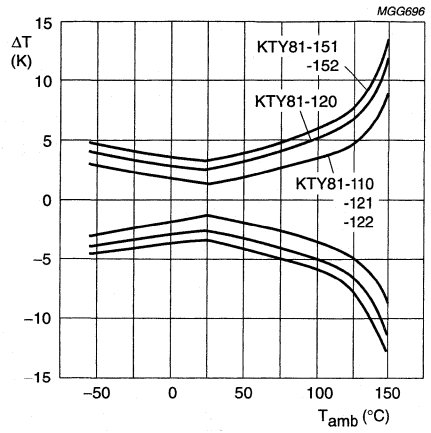

Fig.2 Maximum expected temperature error (ΔT).

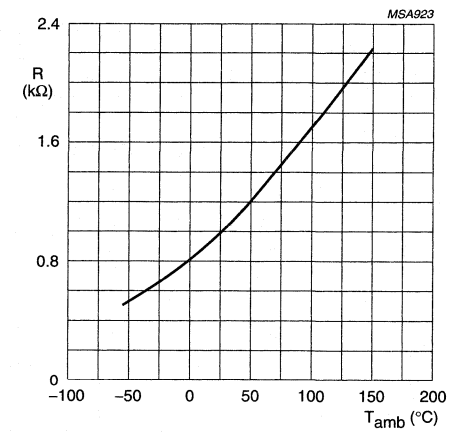

I_{cont} = 1 mA.

Fig.3 Sensor resistance as a function of ambient temperature; average values.

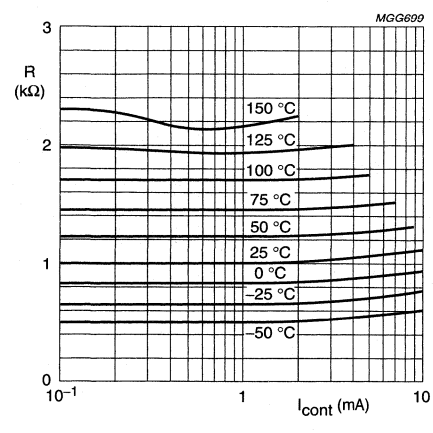

To keep the temperature error low, an operating current of I_{cont} = 1 mA is recommended for temperatures above 100 °C.

Fig.4 Sensor resistance as a function of operating current.

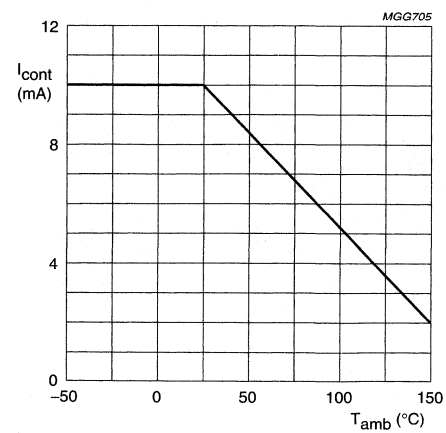

Fig.5 Maximum operating current for safe operation.

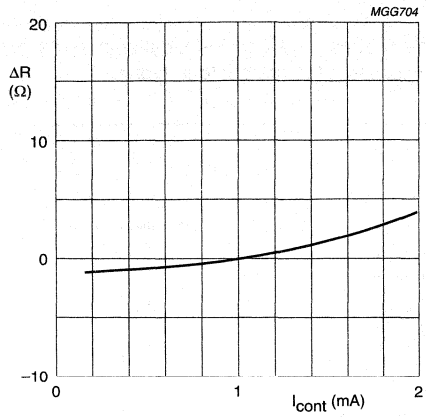

T_{amb} = 25 °C.

Fig.6 Deviation of sensor resistance as a function of operating current in still liquid.

APPLICATION INFORMATION

SYMBOL	PARAMETER	CONDITIONS	TYP.	UNIT
ΔR_{25}	drift of sensor resistance at 25 °C	10000 hours continuous operation; T_{amb} = 150 °C	1.6	Ω

PACKAGING

Sensors in SOD70 encapsulation are delivered in bulk packaging and also in reel packaging for automatic placement on hybrid circuits and printed-circuit boards (see Figs 7 and 8).

Note: Types in bulk packaging have a lead-to-lead distance of 2.54 millimetres. The lead-to-lead distance of types packaged on reel is 5.08 millimetres for spread lead types and 2.54 millimetres for straight lead types.

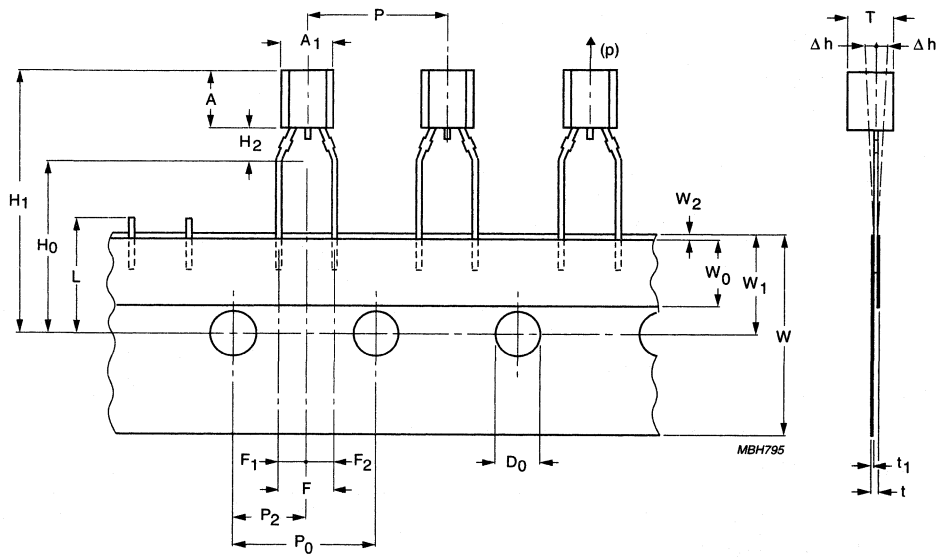

Fig.7 Configuration of bandolier: spread leads.

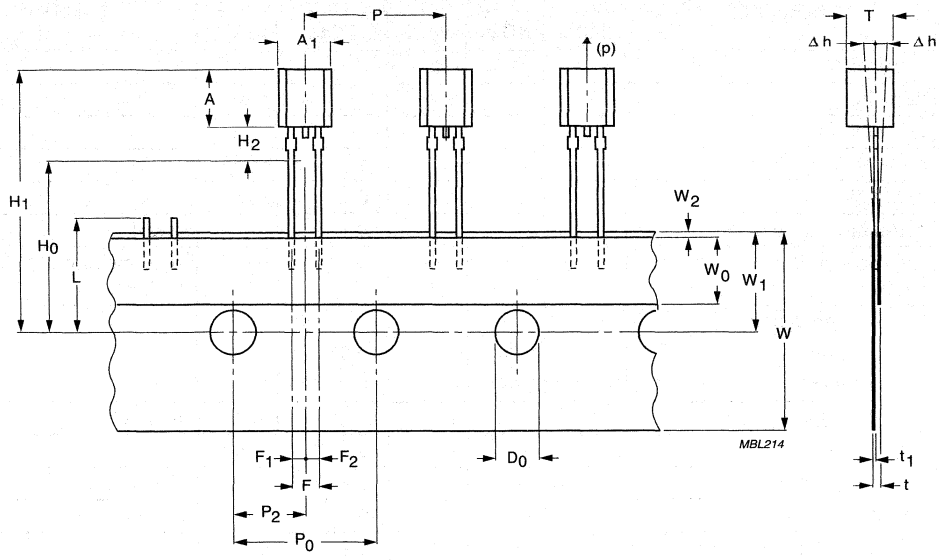

Fig.8 Configuration of bandolier: straight leads.

Table 5 Tape specification

SYMBOL	DIMENSION	SPECIFICATIONS					REMARKS
		MIN.	NOM.	MAX.	TOL.	UNIT	
A_1	body width	4.4	–	4.8	–	mm	
A	body height	5	–	5.2	–	mm	
T	body thickness	3.6	–	4.2	–	mm	
P	pitch of component	–	12.7	–	±1	mm	
P_0	feed hole pitch	–	12.7	–	±0.3	mm	
	cumulative pitch error	–	–	–	±0.1		note 1
P_2	feed hole centre to component centre	–	6.35	–	±0.4	mm	to be measured at bottom of clinch
F	lead-to-lead distance						
	spread leads	–	5.08	–	+0.6/–0.2	mm	
	straight leads	–	2.54	–	+0.6/–0.2	mm	
Δh	component alignment	–	0	1	–	mm	at top of body
W	tape width	–	18	–	±0.5	mm	
W_0	hold-down tape width	–	6	–	±0.2	mm	
W_1	hole position	–	9	–	+0.7/–0.5	mm	
W_2	hold-down tape position	–	0.5	–	±0.2	mm	
H_0	lead wire clinch height	–	16.5	–	±0.5	mm	
H_1	component height	–	–	23.25	–	mm	
L	length of snipped leads	–	–	11	–	mm	
D_0	feed hole diameter	–	4	–	±0.2	mm	
t	total tape thickness	–	–	1.2	–	mm	t_1 = 0.3 to 0.6
F_1, F_2	lead to snipped lead distance						
	spread leads	–	2.54	–	+0.4/–0.2	mm	
	straight leads	–	1.27	–	+0.4/–0.2	mm	
H_2	clinch height	–	2.5	–	+0.5/0	mm	
(p)	pull-out force	6	–	–	–	N	

Note

1. Measured over 20 devices.

PACKAGE OUTLINE

Plastic near cylindrical single-ended package; 2 in-line leads **SOD70**

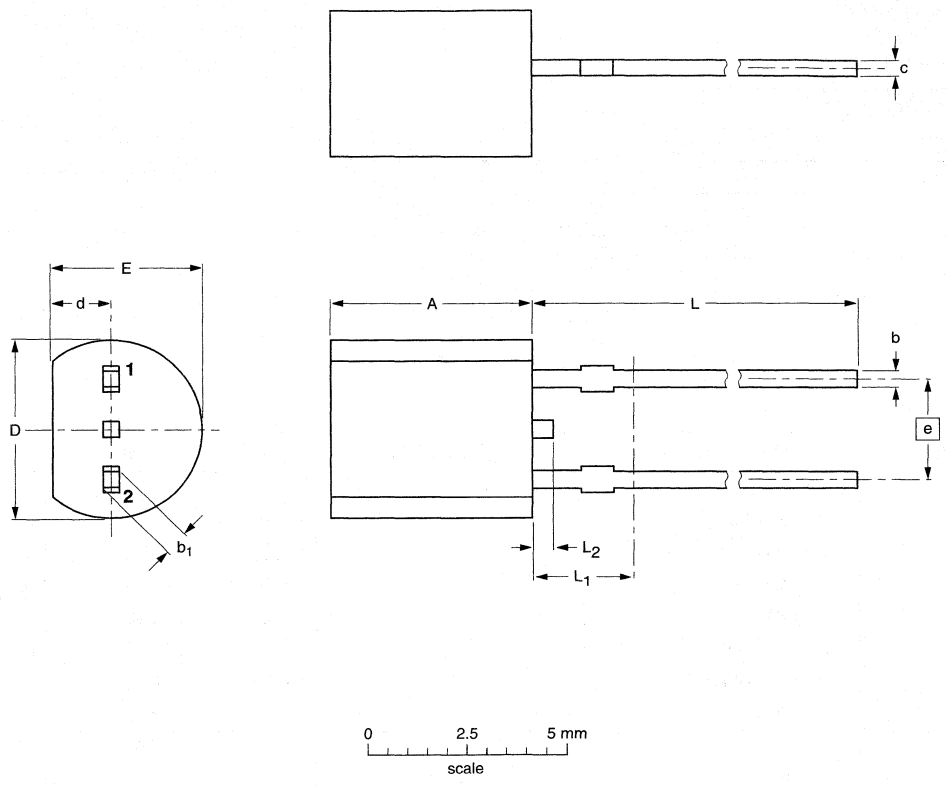

DIMENSIONS (mm are the original dimensions)

UNIT	A	b	b_1	c	D	d	E	e	L	L_1(1) max.	L_2
mm	5.2 5.0	0.48 0.40	0.66 0.56	0.45 0.40	4.8 4.4	1.7 1.4	4.2 3.6	2.54	14.5 12.7	2.5	0.7 0.5

Note

1. Terminal dimensions within this zone are uncontrolled to allow for flow of plastic and terminal irregularities.

OUTLINE VERSION	REFERENCES				EUROPEAN PROJECTION	ISSUE DATE
	IEC	JEDEC	EIAJ			
SOD70						98-05-25

Silicon temperature sensors KTY81-2 series

DESCRIPTION

The temperature sensors in the KTY81-2 series have a positive temperature coefficient of resistance and are suitable for use in measurement and control systems. The sensors are encapsulated in the SOD70 leaded plastic package.

Tolerances of 0.5% or other special selections are available on request.

PINNING

PIN	DESCRIPTION
1	electrical contact
2	electrical contact
3	not to be connected to a potential

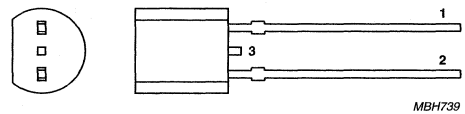

Fig.1 Simplified outline (SOD70).

MARKING

TYPE NUMBER	CODE
KTY81-210	210
KTY81-220	220
KTY81-221	221
KTY81-222	222
KTY81-250	250
KTY81-251	251
KTY81-252	252

QUICK REFERENCE DATA

SYMBOL	PARAMETER	CONDITIONS	MIN.	MAX.	UNIT
R_{25}	sensor resistance	T_{amb} = 25 °C; I_{cont} = 1 mA			
	KTY81-210		1980	2020	Ω
	KTY81-220		1960	2040	Ω
	KTY81-221		1960	2000	Ω
	KTY81-222		2000	2040	Ω
	KTY81-250		1900	2100	Ω
	KTY81-251		1900	2000	Ω
	KTY81-252		2000	2100	Ω
T_{amb}	ambient operating temperature		−55	+150	°C

LIMITING VALUES

In accordance with the Absolute Maximum Rating System (IEC 60134).

SYMBOL	PARAMETER	CONDITIONS	MIN.	MAX.	UNIT
I_{cont}	continuous sensor current	in free air; T_{amb} = 25 °C	–	10	mA
		in free air; T_{amb} = 150 °C	–	2	mA
T_{amb}	ambient operating temperature		−55	+150	°C

CHARACTERISTICS

T_{amb} = 25 °C, in liquid, unless otherwise specified.

SYMBOL	PARAMETER	CONDITIONS	MIN.	TYP.	MAX.	UNIT
R_{25}	sensor resistance	I_{cont} = 1 mA				
	KTY81-210		1980	–	2020	Ω
	KTY81-220		1960	–	2040	Ω
	KTY81-221		1960	–	2000	Ω
	KTY81-222		2000	–	2040	Ω
	KTY81-250		1900	–	2100	Ω
	KTY81-251		1900	–	2000	Ω
	KTY81-252		2000	–	2100	Ω
TC	temperature coefficient		–	0.79	–	%/K
R_{100}/R_{25}	resistance ratio	T_{amb} = 100 °C and 25 °C	1.676	1.696	1.716	
R_{-55}/R_{25}	resistance ratio	T_{amb} = −55 °C and 25 °C	0.480	0.490	0.500	
τ	thermal time constant; note 1	in still air	–	30	–	s
		in still liquid; note 2	–	5	–	s
		in flowing liquid; note 2	–	3	–	s
	rated temperature range		−55	–	+150	°C

Notes

1. The thermal time constant is the time taken for the sensor to reach 63.2% of the total temperature difference. For example, if a sensor with a temperature of 25 °C is moved to an environment with an ambient temperature of 100 °C, the time for the sensor to reach a temperature of 72.4 °C is the thermal time constant.
2. Inert liquid, e.g. FC43 manufactured by the 3M company.

Table 1 Ambient temperature, corresponding resistance, temperature coefficient and maximum expected temperature error for KTY81-210 and KTY81-220

I_{cont} = 1 mA.

AMBIENT TEMPERATURE		TEMP. COEFF.	KTY81-210				KTY81-220			
(°C)	(°F)	(%/K)	RESISTANCE (Ω)			TEMP. ERROR (K)	RESISTANCE (Ω)			TEMP. ERROR (K)
			MIN.	TYP.	MAX.		MIN.	TYP.	MAX.	
−55	−67	0.99	951	980	1009	±3.02	941	980	1019	±4.02
−50	−58	0.98	1000	1030	1059	±2.92	990	1030	1070	±3.94
−40	−40	0.96	1105	1135	1165	±2.74	1094	1135	1176	±3.78
−30	−22	0.93	1218	1247	1277	±2.55	1205	1247	1289	±3.62
−20	−4	0.91	1338	1367	1396	±2.35	1325	1367	1410	±3.45
−10	14	0.88	1467	1495	1523	±2.14	1452	1495	1538	±3.27
0	32	0.85	1603	1630	1656	±1.91	1587	1630	1673	±3.08
10	50	0.83	1748	1772	1797	±1.67	1730	1772	1814	±2.88
20	68	0.80	1901	1922	1944	±1.41	1881	1922	1963	±2.66
25	77	0.79	1980	2000	2020	±1.27	1960	2000	2040	±2.54
30	86	0.78	2057	2080	2102	±1.39	2036	2080	2123	±2.68
40	104	0.75	2217	2245	2272	±1.64	2194	2245	2295	±2.97
50	122	0.73	2383	2417	2451	±1.91	2359	2417	2475	±3.28
60	140	0.71	2557	2597	2637	±2.19	2531	2597	2663	±3.61
70	158	0.69	2737	2785	2832	±2.49	2709	2785	2860	±3.94
80	176	0.67	2924	2980	3035	±2.8	2894	2980	3065	±4.3
90	194	0.65	3118	3182	3246	±3.12	3086	3182	3278	±4.66
100	212	0.63	3318	3392	3466	±3.46	3284	3392	3500	±5.05
110	230	0.59	3523	3607	3691	±3.93	3487	3607	3728	±5.61
120	248	0.53	3722	3817	3912	±4.7	3683	3817	3950	±6.59
125	257	0.49	3815	3915	4016	±5.26	3775	3915	4055	±7.31
130	266	0.44	3901	4008	4114	±6	3861	4008	4154	±8.27
140	284	0.33	4049	4166	4283	±8.45	4008	4166	4325	±11.46
150	302	0.20	4153	4280	4407	±14.63	4110	4280	4450	±19.56

Table 2 Ambient temperature, corresponding resistance, temperature coefficient and maximum expected temperature error for KTY81-221 and KTY81-222

I_{cont} = 1 mA.

AMBIENT TEMPERATURE		TEMP. COEFF.	KTY81-221				KTY81-222			
(°C)	(°F)	(%/K)	RESISTANCE (Ω)			TEMP. ERROR (K)	RESISTANCE (Ω)			TEMP. ERROR (K)
			MIN.	TYP.	MAX.		MIN.	TYP.	MAX.	
−55	−67	0.99	941	970	999	±3.02	960	990	1020	±3.02
−50	−58	0.98	990	1019	1049	±2.92	1010	1040	1070	±2.92
−40	−40	0.96	1094	1123	1153	±2.74	1116	1146	1176	±2.74
−30	−22	0.93	1205	1235	1264	±2.55	1230	1260	1290	±2.55
−20	−4	0.91	1325	1354	1382	±2.35	1352	1381	1410	±2.35
−10	14	0.88	1452	1480	1508	±2.14	1481	1510	1538	±2.14
0	32	0.85	1587	1613	1640	±1.91	1619	1646	1673	±1.91
10	50	0.83	1730	1754	1779	±1.67	1765	1790	1815	±1.67
20	68	0.80	1882	1903	1924	±1.41	1920	1941	1963	±1.41
25	77	0.79	1960	1980	2000	±1.27	2000	2020	2040	±1.27
30	86	0.78	2037	2059	2081	±1.39	2078	2100	2123	±1.39
40	104	0.75	2195	2222	2250	±1.64	2239	2267	2295	±1.64
50	122	0.73	2360	2393	2426	±1.91	2407	2441	2475	±1.91
60	140	0.71	2531	2571	2611	±2.19	2582	2623	2664	±2.19
70	158	0.69	2710	2757	2804	±2.49	2764	2812	2860	±2.49
80	176	0.67	2895	2950	3005	±2.8	2953	3009	3065	±2.8
90	194	0.65	3086	3150	3214	±3.12	3149	3214	3279	±3.12
100	212	0.63	3285	3358	3431	±3.46	3351	3426	3501	±3.46
110	230	0.59	3488	3571	3655	±3.93	3558	3643	3728	±3.93
120	248	0.53	3684	3779	3873	±4.7	3759	3855	3951	±4.7
125	257	0.49	3776	3876	3976	±5.26	3853	3955	4056	±5.26
130	266	0.44	3862	3967	4073	±6	3940	4048	4155	±6
140	284	0.33	4009	4125	4241	±8.45	4090	4208	4326	±8.45
150	302	0.20	4112	4237	4363	±14.63	4195	4323	4451	±14.63

Table 3 Ambient temperature, corresponding resistance, temperature coefficient and maximum expected temperature error for KTY81-250 and KTY81-251

I_{cont} = 1 mA.

AMBIENT TEMPERATURE		TEMP. COEFF.	KTY81-250				KTY81-251			
(°C)	(°F)	(%/K)	RESISTANCE (Ω)			TEMP. ERROR (K)	RESISTANCE (Ω)			TEMP. ERROR (K)
			MIN.	TYP.	MAX.		MIN.	TYP.	MAX.	
−55	−67	0.99	911	980	1049	±7.04	913	956	999	±4.52
−50	−58	0.98	959	1030	1101	±6.99	960	1004	1048	±4.45
−40	−40	0.96	1060	1135	1210	±6.91	1061	1106	1152	±4.3
−30	−22	0.93	1168	1247	1327	±6.84	1169	1216	1263	±4.16
−20	−4	0.91	1283	1367	1451	±6.77	1285	1333	1381	±4.01
−10	14	0.88	1407	1495	1583	±6.69	1408	1457	1507	±3.84
0	32	0.85	1538	1630	1721	±6.61	1539	1589	1639	±3.67
10	50	0.83	1677	1772	1867	±6.51	1678	1728	1778	±3.48
20	68	0.80	1824	1922	2021	±6.41	1825	1874	1923	±3.28
25	77	0.79	1900	2000	2100	±6.35	1900	1950	2000	±3.18
30	86	0.78	1974	2080	2185	±6.55	1975	2028	2080	±3.33
40	104	0.75	2127	2245	2362	±6.97	2129	2189	2248	±3.64
50	122	0.73	2287	2417	2547	±7.4	2289	2357	2425	±3.97
60	140	0.71	2453	2597	2741	±7.85	2455	2532	2609	±4.31
70	158	0.69	2626	2785	2943	±8.31	2628	2715	2802	±4.67
80	176	0.67	2805	2980	3154	±8.79	2807	2905	3003	±5.05
90	194	0.65	2990	3182	3374	±9.29	2993	3102	3212	±5.43
100	212	0.63	3182	3392	3602	±9.81	3185	3307	3429	±5.84
110	230	0.59	3379	3607	3836	±10.65	3382	3517	3652	±6.45
120	248	0.53	3569	3817	4065	±12.25	3573	3721	3870	±7.53
125	257	0.49	3658	3915	4173	±13.45	3662	3817	3973	±8.33
130	266	0.44	3741	4008	4274	±15.06	3745	3907	4070	±9.4
140	284	0.33	3883	4166	4450	±20.49	3887	4062	4237	±12.96
150	302	0.20	3982	4280	4578	±34.35	3987	4173	4359	±22.02

Table 4 Ambient temperature, corresponding resistance, temperature coefficient and maximum expected temperature error for KTY81-252

I_{cont} = 1 mA.

AMBIENT TEMPERATURE		TEMP. COEFF.	KTY81-252			
(°C)	(°F)	(%/K)	RESISTANCE (Ω)			TEMP. ERROR (K)
			MIN.	TYP.	MAX.	
−55	−67	0.99	959	1005	1050	±4.52
−50	−58	0.98	1009	1055	1102	±4.45
−40	−40	0.96	1115	1163	1211	±4.3
−30	−22	0.93	1229	1278	1328	±4.16
−20	−4	0.91	1351	1401	1452	±4.01
−10	14	0.88	1480	1532	1584	±3.84
0	32	0.85	1618	1670	1723	±3.67
10	50	0.83	1764	1817	1869	±3.48
20	68	0.80	1919	1970	2022	±3.28
25	77	0.79	2000	2050	2100	±3.18
30	86	0.78	2077	2132	2187	±3.33
40	104	0.75	2238	2301	2364	±3.64
50	122	0.73	2406	2478	2549	±3.97
60	140	0.71	2581	2662	2743	±4.31
70	158	0.69	2763	2854	2946	±4.67
80	176	0.67	2951	3054	3157	±5.05
90	194	0.65	3147	3262	3376	±5.43
100	212	0.63	3349	3477	3605	±5.84
110	230	0.59	3556	3697	3839	±6.45
120	248	0.53	3756	3912	4068	±7.53
125	257	0.49	3850	4013	4177	±8.33
130	266	0.44	3937	4108	4278	±9.4
140	284	0.33	4087	4271	4455	±12.96
150	302	0.20	4191	4387	4583	±22.02

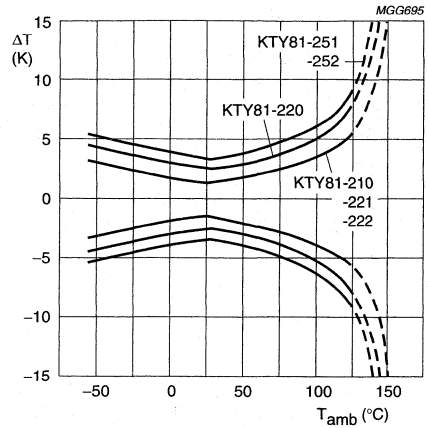

Fig.2 Maximum expected temperature error (ΔT).

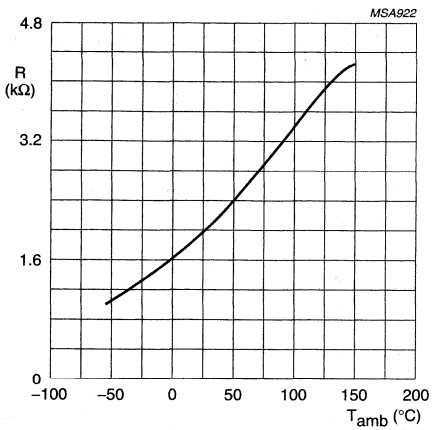

I_{cont} = 1 mA.

Fig.3 Sensor resistance as a function of ambient temperature; average values.

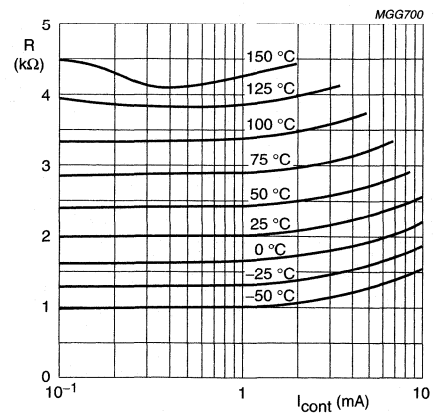

To keep the temperature error low, an operating current of I_{cont} = 1 mA is recommended for temperatures above 100 °C.

Fig.4 Sensor resistance as a function of operating current.

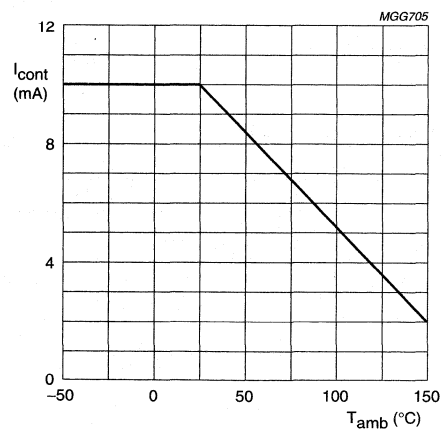

Fig.5 Maximum operating current for safe operation.

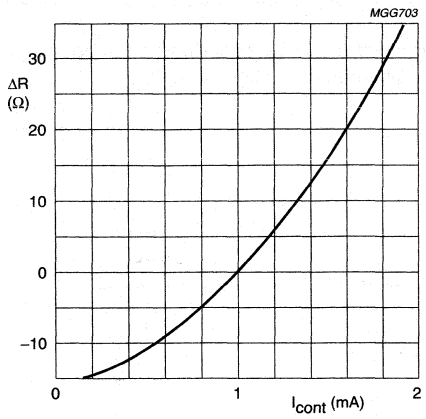

T_{amb} = 25 °C.

Fig.6 Deviation of sensor resistance as a function of operating current in still liquid.

APPLICATION INFORMATION

SYMBOL	PARAMETER	CONDITIONS	TYP.	UNIT
ΔR_{25}	drift of sensor resistance at 25 °C	10000 hours continuous operation; T_{amb} = 150 °C	3.2	Ω

PACKAGING

Sensors in SOD70 encapsulation are delivered in bulk packaging, and also reel packaging for automatic placement on hybrid circuits and printed-circuit boards (see Figs 7 and 8).

Note: Types in bulk packaging have a lead-to-lead distance of 2.54 millimetres. The lead-to-lead distance of types packaged on reel is 5.08 millimetres for spread lead types and 2.54 millimetres for straight lead types.

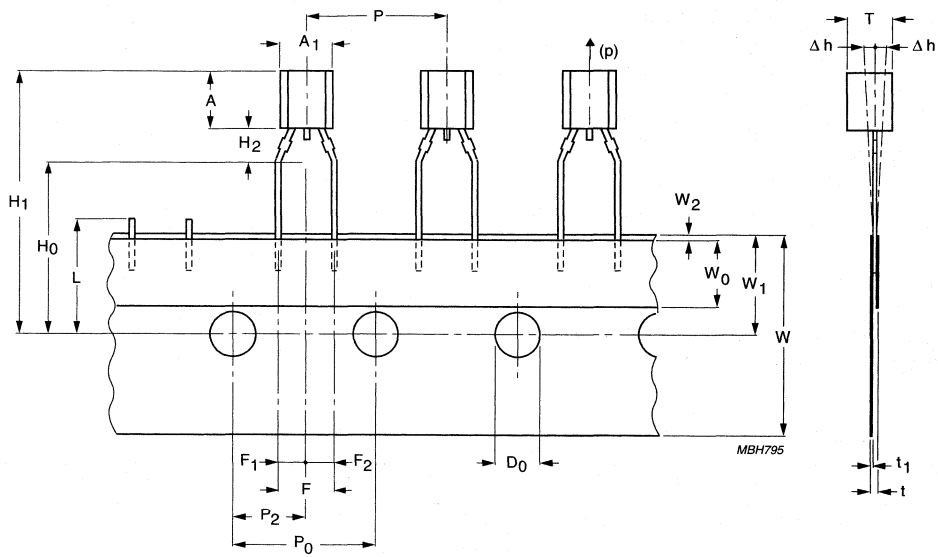

Fig.7 Configuration of bandolier: spread leads.

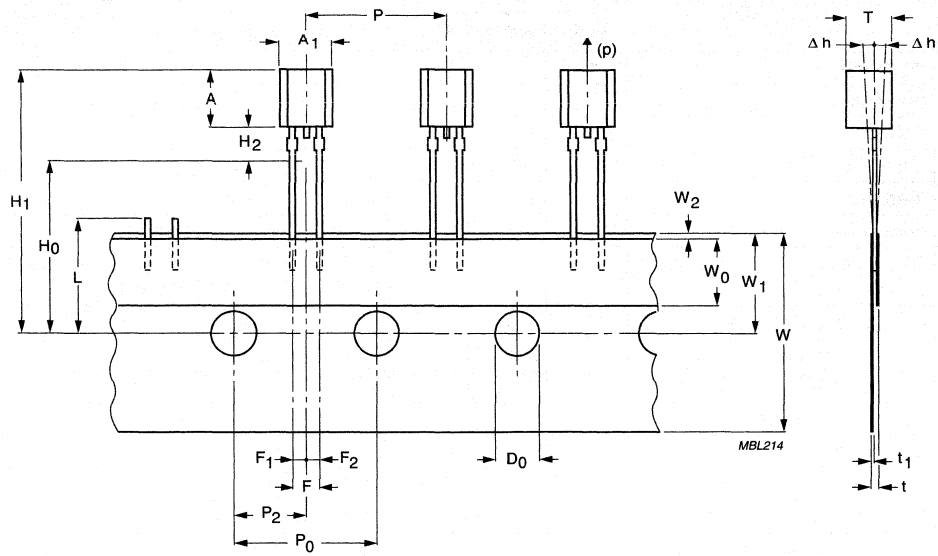

Fig.8 Configuration of bandolier: straight leads.

Table 5 Tape specification

SYMBOL	DIMENSION	SPECIFICATIONS					REMARKS
		MIN.	NOM.	MAX.	TOL.	UNIT	
A_1	body width	4.4	–	4.8	–	mm	
A	body height	5	–	5.2	–	mm	
T	body thickness	3.6	–	4.2	–	mm	
P	pitch of component	–	12.7	–	±1	mm	
P_0	feed hole pitch	–	12.7	–	±0.3	mm	
	cumulative pitch error	–	–	–	±0.1		note 1
P_2	feed hole centre to component centre	–	6.35	–	±0.4	mm	to be measured at bottom of clinch
F	lead-to-lead distance						
	spread leads	–	5.08	–	+0.6/–0.2	mm	
	straight leads	–	2.54	–	+0.6/–0.2	mm	
Δh	component alignment	–	0	1	–	mm	at top of body
W	tape width	–	18	–	±0.5	mm	
W_0	hold-down tape width	–	6	–	±0.2	mm	
W_1	hole position	–	9	–	+0.7/–0.5	mm	
W_2	hold-down tape position	–	0.5	–	±0.2	mm	
H_0	lead wire clinch height	–	16.5	–	±0.5	mm	
H_1	component height	–	–	23.25	–	mm	
L	length of snipped leads	–	–	11	–	mm	
D_0	feed hole diameter	–	4	–	±0.2	mm	
t	total tape thickness	–	–	1.2	–	mm	t_1 = 0.3 to 0.6
F_1, F_2	lead to snipped lead distance						
	spread leads	–	2.54	–	+0.4/–0.2	mm	
	straight leads	–	1.27	–	+0.4/–0.2	mm	
H_2	clinch height	–	2.5	–	+0.5/0	mm	
(p)	pull-out force	6	–	–	–	N	

Note

1. Measured over 20 devices.

PACKAGE OUTLINE

Plastic near cylindrical single-ended package; 2 in-line leads **SOD70**

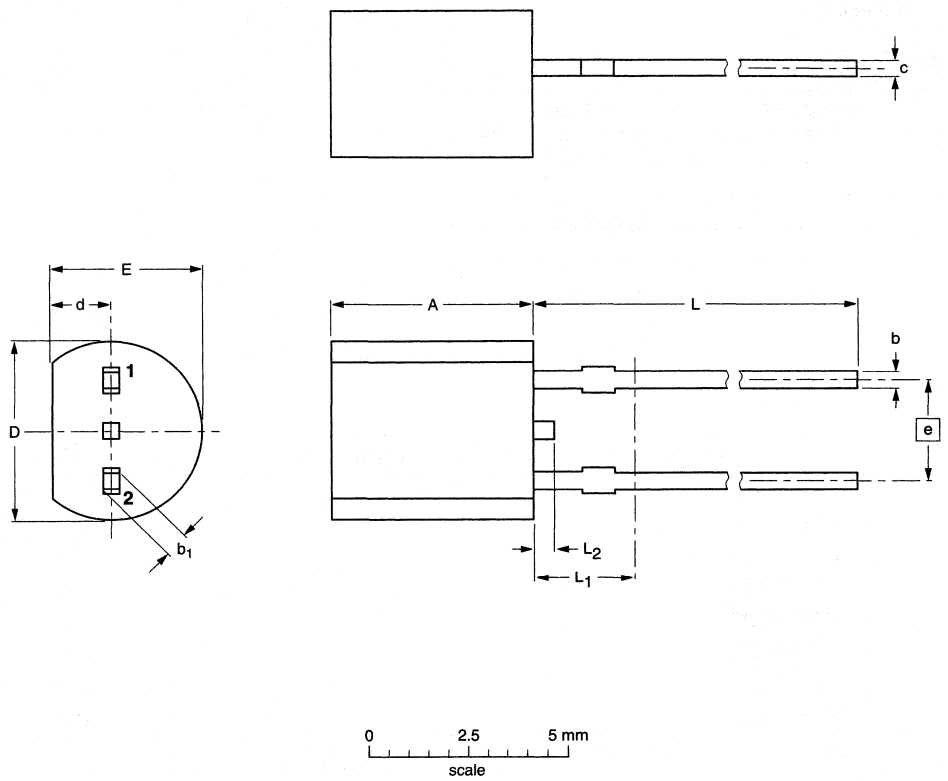

DIMENSIONS (mm are the original dimensions)

UNIT	A	b	b_1	c	D	d	E	e	L	L_1(1) max.	L_2
mm	5.2 5.0	0.48 0.40	0.66 0.56	0.45 0.40	4.8 4.4	1.7 1.4	4.2 3.6	2.54	14.5 12.7	2.5	0.7 0.5

Note

1. Terminal dimensions within this zone are uncontrolled to allow for flow of plastic and terminal irregularities.

OUTLINE VERSION	REFERENCES				EUROPEAN PROJECTION	ISSUE DATE
	IEC	JEDEC	EIAJ			
SOD70						98-05-25

Silicon temperature sensors KTY82-1 series

DESCRIPTION

The temperature sensors in the KTY82-1 series have a positive temperature coefficient of resistance and are suitable for use in measurement and control systems. The sensors are encapsulated in the small plastic SMD SOT23 package.

Tolerances of 0.5% or other special selections are available on request.

MARKING

TYPE NUMBER	CODE
KTY82-110	110
KTY82-120	120
KTY82-121	121
KTY82-122	122
KTY82-150	150
KTY82-151	151
KTY82-152	152

PINNING

PIN	DESCRIPTION
1	electrical contact
2	electrical contact
3	substrate (must remain potential free)

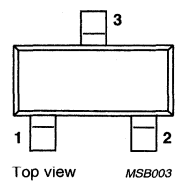

Fig.1 Simplified outline (SOT23).

QUICK REFERENCE DATA

SYMBOL	PARAMETER	CONDITIONS	MIN.	MAX.	UNIT
R_{25}	sensor resistance	T_{amb} = 25 °C; I_{cont} = 1 mA			
	KTY82-110		990	1010	Ω
	KTY82-120		980	1020	Ω
	KTY82-121		980	1000	Ω
	KTY82-122		1000	1020	Ω
	KTY82-150		950	1050	Ω
	KTY82-151		950	1000	Ω
	KTY82-152		1000	1050	Ω
T_{amb}	ambient operating temperature		−55	+150	°C

LIMITING VALUES

In accordance with the Absolute Maximum Rating System (IEC 134).

SYMBOL	PARAMETER	CONDITIONS	MIN.	MAX.	UNIT
I_{cont}	continuous sensor current	in free air; T_{amb} = 25 °C	−	10	mA
		in free air; T_{amb} = 150 °C	−	2	mA
T_{amb}	ambient operating temperature		−55	+150	°C

CHARACTERISTICS

T_{amb} = 25 °C, in liquid, unless otherwise specified.

SYMBOL	PARAMETER	CONDITIONS	MIN.	TYP.	MAX.	UNIT
R_{25}	sensor resistance	I_{cont} = 1 mA				
	KTY82-110		990	–	1010	Ω
	KTY82-120		980	–	1020	Ω
	KTY82-121		980	–	1000	Ω
	KTY82-122		1000	–	1020	Ω
	KTY82-150		950	–	1050	Ω
	KTY82-151		950	–	1000	Ω
	KTY82-152		1000	–	1050	Ω
TC	temperature coefficient		–	0.79	–	%/K
R_{100}/R_{25}	resistance ratio	T_{amb} = 100 °C and 25 °C	1.676	1.696	1.716	
R_{-55}/R_{25}	resistance ratio	T_{amb} = −55 °C and 25 °C	0.480	0.490	0.500	
τ	thermal time constant; note 1	in still air	–	7	–	s
		in still liquid; note 2	–	1	–	s
		in flowing liquid; note 2	–	0.5	–	s
	rated temperature range		−55	–	+150	°C

Notes

1. The thermal time constant is the time taken for the sensor to reach 63.2% of the total temperature difference. For example, if a sensor with a temperature of 25 °C is moved to an environment with an ambient temperature of 100 °C, the time for the sensor to reach a temperature of 72.4 °C is the thermal time constant.
2. Inert liquid, e.g. FC43 manufactured by the 3M company.

Table 1 Ambient temperature, corresponding resistance, temperature coefficient and maximum expected temperature error for KTY82-110 and KTY82-120

I_{cont} = 1 mA.

AMBIENT TEMPERATURE		TEMP. COEFF.	KTY82-110				KTY82-120			
(°C)	(°F)	(%/K)	RESISTANCE (Ω)			TEMP. ERROR (K)	RESISTANCE (Ω)			TEMP. ERROR (K)
			MIN.	TYP.	MAX.		MIN.	TYP.	MAX.	
−55	−67	0.99	475	490	505	±3.02	470	490	510	±4.02
−50	−58	0.98	500	515	530	±2.92	495	515	535	±3.94
−40	−40	0.96	552	567	582	±2.74	547	567	588	±3.78
−30	−22	0.93	609	624	638	±2.55	603	624	645	±3.62
−20	−4	0.91	669	684	698	±2.35	662	684	705	±3.45
−10	14	0.88	733	747	761	±2.14	726	747	769	±3.27
0	32	0.85	802	815	828	±1.91	793	815	836	±3.08
10	50	0.83	874	886	898	±1.67	865	886	907	±2.88
20	68	0.80	950	961	972	±1.41	941	961	982	±2.66
25	77	0.79	990	1000	1010	±1.27	980	1000	1020	±2.54
30	86	0.78	1029	1040	1051	±1.39	1018	1040	1061	±2.68
40	104	0.75	1108	1122	1136	±1.64	1097	1122	1147	±2.97
50	122	0.73	1192	1209	1225	±1.91	1180	1209	1237	±3.28
60	140	0.71	1278	1299	1319	±2.19	1265	1299	1332	±3.61
70	158	0.69	1369	1392	1416	±2.49	1355	1392	1430	±3.94
80	176	0.67	1462	1490	1518	±2.8	1447	1490	1532	±4.3
90	194	0.65	1559	1591	1623	±3.12	1543	1591	1639	±4.66
100	212	0.63	1659	1696	1733	±3.46	1642	1696	1750	±5.05
110	230	0.61	1762	1805	1847	±3.83	1744	1805	1865	±5.48
120	248	0.58	1867	1915	1963	±4.33	1848	1915	1982	±6.07
125	257	0.55	1919	1970	2020	±4.66	1899	1970	2040	±6.47
130	266	0.52	1970	2023	2077	±5.07	1950	2023	2097	±6.98
140	284	0.45	2065	2124	2184	±6.28	2043	2124	2205	±8.51
150	302	0.35	2145	2211	2277	±8.55	2123	2211	2299	±11.43

Table 2 Ambient temperature, corresponding resistance, temperature coefficient and maximum expected temperature error for KTY82-121 and KTY82-122

I_{cont} = 1 mA.

AMBIENT TEMPERATURE		TEMP. COEFF.	KTY82-121				KTY82-122			
(°C)	(°F)	(%/K)	RESISTANCE (Ω)			TEMP. ERROR (K)	RESISTANCE (Ω)			TEMP. ERROR (K)
			MIN.	TYP.	MAX.		MIN.	TYP.	MAX.	
−55	−67	0.99	471	485	500	±3.02	480	495	510	±3.02
−50	−58	0.98	495	510	524	±2.92	505	520	535	±2.92
−40	−40	0.96	547	562	576	±2.74	558	573	588	±2.74
−30	−22	0.93	603	617	632	±2.55	615	630	645	±2.55
−20	−4	0.91	662	677	691	±2.35	676	690	705	±2.35
−10	14	0.88	726	740	754	±2.14	741	755	769	±2.14
0	32	0.85	794	807	820	±1.91	810	823	836	±1.91
10	50	0.83	865	877	889	±1.67	883	895	907	±1.67
20	68	0.80	941	951	962	±1.41	960	971	982	±1.41
25	77	0.79	980	990	1000	±1.27	1000	1010	1020	±1.27
30	86	0.78	1018	1029	1041	±1.39	1039	1050	1062	±1.39
40	104	0.75	1097	1111	1125	±1.64	1120	1134	1148	±1.64
50	122	0.73	1180	1196	1213	±1.91	1204	1221	1238	±1.91
60	140	0.71	1266	1286	1305	±2.19	1291	1312	1332	±2.19
70	158	0.69	1355	1378	1402	±2.49	1382	1406	1430	±2.49
80	176	0.67	1447	1475	1502	±2.8	1477	1505	1533	±2.8
90	194	0.65	1543	1575	1607	±3.12	1574	1607	1639	±3.12
100	212	0.63	1642	1679	1716	±3.46	1676	1713	1750	±3.46
110	230	0.61	1745	1786	1828	±3.83	1780	1823	1865	±3.83
120	248	0.58	1849	1896	1943	±4.33	1886	1934	1982	±4.33
125	257	0.55	1900	1950	2000	±4.66	1938	1989	2041	±4.66
130	266	0.52	1950	2003	2056	±5.07	1989	2044	2098	±5.07
140	284	0.45	2044	2103	2162	±6.28	2085	2146	2206	±6.28
150	302	0.35	2124	2189	2254	±8.55	2167	2233	2299	±8.55

Table 3 Ambient temperature, corresponding resistance, temperature coefficient and maximum expected temperature error for KTY82-150 and KTY82-151

I_{cont} = 1 mA.

AMBIENT TEMPERATURE		TEMP. COEFF.	KTY82-150				KTY82-151			
(°C)	(°F)	(%/K)	RESISTANCE (Ω)			TEMP. ERROR (K)	RESISTANCE (Ω)			TEMP. ERROR (K)
			MIN.	TYP.	MAX.		MIN.	TYP.	MAX.	
−55	−67	0.99	456	490	524	±7.04	456	478	499	±4.52
−50	−58	0.98	479	515	550	±6.99	480	502	524	±4.45
−40	−40	0.96	530	567	605	±6.91	530	553	576	±4.3
−30	−22	0.93	584	624	663	±6.84	584	608	632	±4.16
−20	−4	0.91	642	684	725	±6.77	642	667	691	±4.01
−10	14	0.88	703	747	791	±6.69	704	729	753	±3.84
0	32	0.85	769	815	861	±6.61	770	794	819	±3.67
10	50	0.83	838	886	934	±6.51	839	864	889	±3.48
20	68	0.80	912	961	1010	±6.41	912	937	962	±3.28
25	77	0.79	950	1000	1050	±6.35	950	975	1000	±3.18
30	86	0.78	987	1040	1093	±6.55	988	1014	1040	±3.33
40	104	0.75	1064	1122	1181	±6.97	1064	1094	1124	±3.64
50	122	0.73	1143	1209	1274	±7.4	1144	1178	1212	±3.97
60	140	0.71	1226	1299	1371	±7.85	1227	1266	1305	±4.31
70	158	0.69	1313	1392	1472	±8.31	1314	1357	1401	±4.67
80	176	0.67	1402	1490	1577	±8.79	1404	1453	1501	±5.05
90	194	0.65	1495	1591	1687	±9.29	1497	1551	1606	±5.43
100	212	0.63	1591	1696	1801	±9.81	1593	1654	1714	±5.84
110	230	0.61	1690	1805	1919	±10.4	1692	1759	1827	±6.3
120	248	0.58	1791	1915	2039	±11.28	1792	1867	1942	±6.94
125	257	0.55	1840	1970	2099	±11.91	1842	1920	1999	±7.38
130	266	0.52	1889	2023	2158	±12.72	1891	1973	2055	±7.94
140	284	0.45	1980	2124	2269	±15.21	1982	2071	2161	±9.63
150	302	0.35	2057	2211	2365	±20.09	2059	2156	2252	±12.88

Table 4 Ambient temperature, corresponding resistance, temperature coefficient and maximum expected temperature error for KTY82-152

I_{cont} = 1 mA.

AMBIENT TEMPERATURE		TEMP. COEFF.	KTY82-152			
(°C)	(°F)	(%/K)	RESISTANCE (Ω)			TEMP. ERROR (K)
			MIN.	TYP.	MAX.	
−55	−67	0.99	480	502	525	±4.52
−50	−58	0.98	505	528	551	±4.45
−40	−40	0.96	558	582	606	±4.3
−30	−22	0.93	614	639	664	±4.16
−20	−4	0.91	675	701	726	±4.01
−10	14	0.88	740	766	792	±3.84
0	32	0.85	809	835	861	±3.67
10	50	0.83	882	908	934	±3.48
20	68	0.80	959	985	1011	±3.28
25	77	0.79	1000	1025	1050	±3.18
30	86	0.78	1038	1066	1093	±3.33
40	104	0.75	1119	1150	1182	±3.64
50	122	0.73	1203	1239	1275	±3.97
60	140	0.71	1290	1331	1372	±4.31
70	158	0.69	1381	1427	1473	±4.67
80	176	0.67	1476	1527	1578	±5.05
90	194	0.65	1573	1631	1688	±5.43
100	212	0.63	1674	1738	1802	±5.84
110	230	0.61	1779	1850	1921	±6.3
120	248	0.58	1884	1963	2041	±6.94
125	257	0.55	1937	2019	2101	±7.38
130	266	0.52	1988	2074	2160	±7.94
140	284	0.45	2084	2178	2271	±9.63
150	302	0.35	2165	2266	2367	±12.88

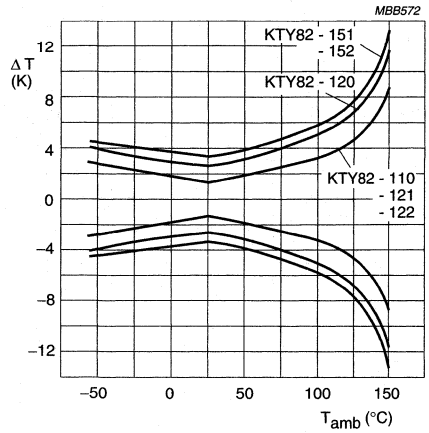

Fig.2 Maximum expected temperature error (ΔT).

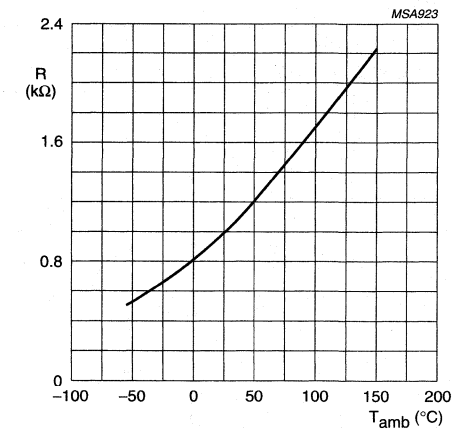

I_{cont} = 1 mA.

Fig.3 Sensor resistance as a function of ambient temperature; average values.

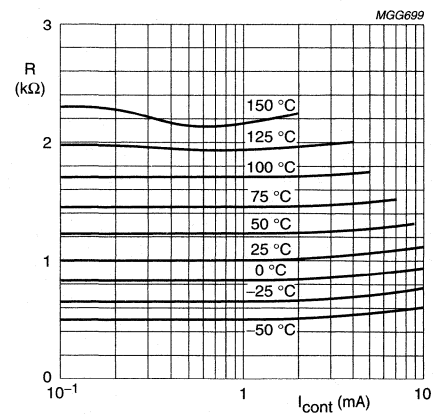

To keep the temperature error low, an operating current of I_{cont} = 1 mA is recommended for temperatures above 100 °C.

Fig.4 Sensor resistance as a function of operating current.

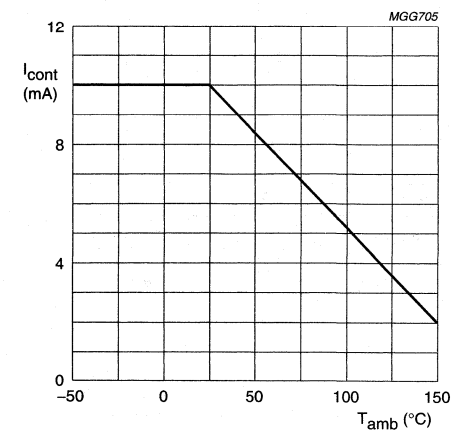

Fig.5 Maximum operating current for safe operation.

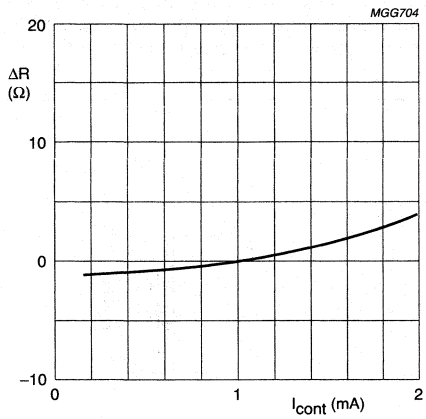

T_{amb} = 25 °C.

Fig.6 Deviation of sensor resistance as a function of operating current in still liquid.

APPLICATION INFORMATION

SYMBOL	PARAMETER	CONDITIONS	TYP.	UNIT
ΔR_{25}	drift of sensor resistance at 25 °C	10000 hours continuous operation; T_{amb} = 150 °C	1.6	Ω

PACKAGING

Tape specification

Sensors in SOT23 encapsulation are delivered in reel packaging for automatic placement on hybrid circuits and printed-circuit boards. The devices are placed with the mounting side downwards in the compartments.

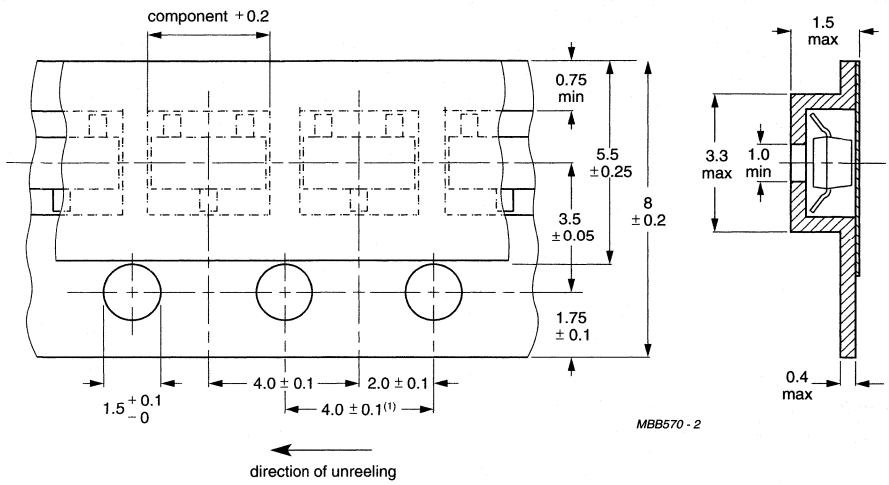

Dimension in mm.

(1) Tolerance over any 10 pitches: ±0.2 mm.

Fig.7 Configuration of bandolier.

PACKAGE OUTLINE

Plastic surface mounted package; 3 leads **SOT23**

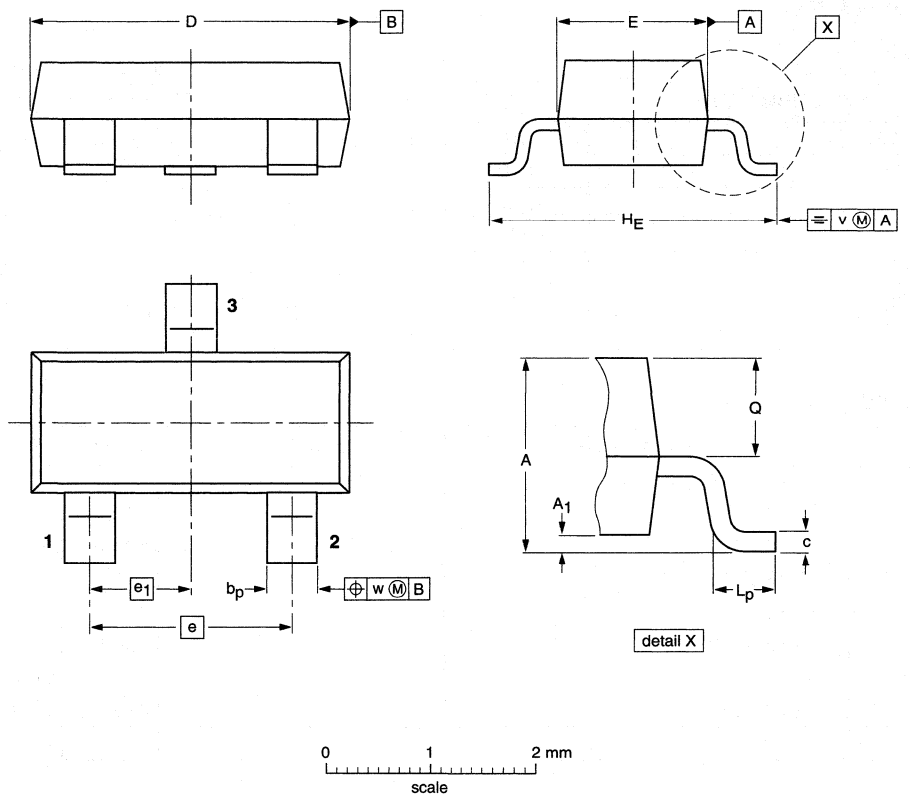

DIMENSIONS (mm are the original dimensions)

UNIT	A	A_1 max.	b_p	c	D	E	e	e_1	H_E	L_p	Q	v	w
mm	1.1 0.9	0.1	0.48 0.38	0.15 0.09	3.0 2.8	1.4 1.2	1.9	0.95	2.5 2.1	0.45 0.15	0.55 0.45	0.2	0.1

OUTLINE VERSION	REFERENCES				EUROPEAN PROJECTION	ISSUE DATE
	IEC	JEDEC	EIAJ			
SOT23		TO-236AB				~~97-02-28~~ 99-09-13

Silicon temperature sensors KTY82-2 series

DESCRIPTION

The temperature sensors in the KTY82-2 series have a positive temperature coefficient of resistance and are suitable for use in measurement and control systems. The sensors are encapsulated in the small plastic SMD SOT23 package.

Tolerances of 0.5% or other special selections are available on request.

PINNING

PIN	DESCRIPTION
1	electrical contact
2	electrical contact
3	substrate (must remain potential free)

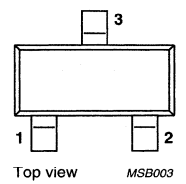

Fig.1 Simplified outline (SOT23).

MARKING

TYPE NUMBER	CODE
KTY82-210	210
KTY82-220	220
KTY82-221	221
KTY82-222	222
KTY82-250	250
KTY82-251	251
KTY82-252	252

QUICK REFERENCE DATA

SYMBOL	PARAMETER	CONDITIONS	MIN.	MAX.	UNIT
R_{25}	sensor resistance	T_{amb} = 25 °C; I_{cont} = 1 mA			
	KTY82-210		1980	2020	Ω
	KTY82-220		1960	2040	Ω
	KTY82-221		1960	2000	Ω
	KTY82-222		2000	2040	Ω
	KTY82-250		1900	2100	Ω
	KTY82-251		1900	2000	Ω
	KTY82-252		2000	2100	Ω
T_{amb}	ambient operating temperature		−55	+150	°C

LIMITING VALUES

In accordance with the Absolute Maximum Rating System (IEC 134).

SYMBOL	PARAMETER	CONDITIONS	MIN.	MAX.	UNIT
I_{cont}	continuous sensor current	in free air; T_{amb} = 25 °C	–	10	mA
		in free air; T_{amb} = 150 °C	–	2	mA
T_{amb}	ambient operating temperature		−55	+150	°C

CHARACTERISTICS

T_{amb} = 25 °C, in liquid, unless otherwise specified.

SYMBOL	PARAMETER	CONDITIONS	MIN.	TYP.	MAX.	UNIT
R_{25}	sensor resistance	I_{cont} = 1 mA				
	KTY82-210		1980	–	2020	Ω
	KTY82-220		1960	–	2040	Ω
	KTY82-221		1960	–	2000	Ω
	KTY82-222		2000	–	2040	Ω
	KTY82-250		1900	–	2100	Ω
	KTY82-251		1900	–	2000	Ω
	KTY82-252		2000	–	2100	Ω
TC	temperature coefficient		–	0.79	–	%/K
R_{100}/R_{25}	resistance ratio	T_{amb} = 100 °C and 25 °C	1.676	1.696	1.716	
R_{-55}/R_{25}	resistance ratio	T_{amb} = −55 °C and 25 °C	0.480	0.490	0.500	
τ	thermal time constant; note 1	in still air	–	7	–	s
		in still liquid; note 2	–	1	–	s
		in flowing liquid; note 2	–	0.5	–	s
	rated temperature range		−55	–	+150	°C

Notes

1. The thermal time constant is the time taken for the sensor to reach 63.2% of the total temperature difference. For example, if a sensor with a temperature of 25 °C is moved to an environment with an ambient temperature of 100 °C, the time for the sensor to reach a temperature of 72.4 °C is the thermal time constant.
2. Inert liquid, e.g. FC43 manufactured by the 3M company.

Table 1 Ambient temperature, corresponding resistance, temperature coefficient and maximum expected temperature error for KTY82-210 and KTY82-220

I_{cont} = 1 mA.

AMBIENT TEMPERATURE		TEMP. COEFF.	KTY82-210				KTY82-220			
(°C)	(°F)	(%/K)	RESISTANCE (Ω)			TEMP. ERROR (K)	RESISTANCE (Ω)			TEMP. ERROR (K)
			MIN.	TYP.	MAX.		MIN.	TYP.	MAX.	
−55	−67	0.99	951	980	1009	±3.02	941	980	1019	±4.02
−50	−58	0.98	1000	1030	1059	±2.92	990	1030	1070	±3.94
−40	−40	0.96	1105	1135	1165	±2.74	1094	1135	1176	±3.78
−30	−22	0.93	1218	1247	1277	±2.55	1205	1247	1289	±3.62
−20	−4	0.91	1338	1367	1396	±2.35	1325	1367	1410	±3.45
−10	14	0.88	1467	1495	1523	±2.14	1452	1495	1538	±3.27
0	32	0.85	1603	1630	1656	±1.91	1587	1630	1673	±3.08
10	50	0.83	1748	1772	1797	±1.67	1730	1772	1814	±2.88
20	68	0.80	1901	1922	1944	±1.41	1881	1922	1963	±2.66
25	77	0.79	1980	2000	2020	±1.27	1960	2000	2040	±2.54
30	86	0.78	2057	2080	2102	±1.39	2036	2080	2123	±2.68
40	104	0.75	2217	2245	2272	±1.64	2194	2245	2295	±2.97
50	122	0.73	2383	2417	2451	±1.91	2359	2417	2475	±3.28
60	140	0.71	2557	2597	2637	±2.19	2531	2597	2663	±3.61
70	158	0.69	2737	2785	2832	±2.49	2709	2785	2860	±3.94
80	176	0.67	2924	2980	3035	±2.8	2894	2980	3065	±4.3
90	194	0.65	3118	3182	3246	±3.12	3086	3182	3278	±4.66
100	212	0.63	3318	3392	3466	±3.46	3284	3392	3500	±5.05
110	230	0.59	3523	3607	3691	±3.93	3487	3607	3728	±5.61
120	248	0.53	3722	3817	3912	±4.7	3683	3817	3950	±6.59
125	257	0.49	3815	3915	4016	±5.26	3775	3915	4055	±7.31
130	266	0.44	3901	4008	4114	±6	3861	4008	4154	±8.27
140	284	0.33	4049	4166	4283	±8.45	4008	4166	4325	±11.46
150	302	0.20	4153	4280	4407	±14.63	4110	4280	4450	±19.56

Table 2 Ambient temperature, corresponding resistance, temperature coefficient and maximum expected temperature error for KTY82-221 and KTY82-222

I_{cont} = 1 mA.

AMBIENT TEMPERATURE		TEMP. COEFF.	KTY82-221				KTY82-222			
(°C)	(°F)	(%/K)	RESISTANCE (Ω)			TEMP. ERROR (K)	RESISTANCE (Ω)			TEMP. ERROR (K)
			MIN.	TYP.	MAX.		MIN.	TYP.	MAX.	
−55	−67	0.99	941	970	999	±3.02	960	990	1020	±3.02
−50	−58	0.98	990	1019	1049	±2.92	1010	1040	1070	±2.92
−40	−40	0.96	1094	1123	1153	±2.74	1116	1146	1176	±2.74
−30	−22	0.93	1205	1235	1264	±2.55	1230	1260	1290	±2.55
−20	−4	0.91	1325	1354	1382	±2.35	1352	1381	1410	±2.35
−10	14	0.88	1452	1480	1508	±2.14	1481	1510	1538	±2.14
0	32	0.85	1587	1613	1640	±1.91	1619	1646	1673	±1.91
10	50	0.83	1730	1754	1779	±1.67	1765	1790	1815	±1.67
20	68	0.80	1882	1903	1924	±1.41	1920	1941	1963	±1.41
25	77	0.79	1960	1980	2000	±1.27	2000	2020	2040	±1.27
30	86	0.78	2037	2059	2081	±1.39	2078	2100	2123	±1.39
40	104	0.75	2195	2222	2250	±1.64	2239	2267	2295	±1.64
50	122	0.73	2360	2393	2426	±1.91	2407	2441	2475	±1.91
60	140	0.71	2531	2571	2611	±2.19	2582	2623	2664	±2.19
70	158	0.69	2710	2757	2804	±2.49	2764	2812	2860	±2.49
80	176	0.67	2895	2950	3005	±2.8	2953	3009	3065	±2.8
90	194	0.65	3086	3150	3214	±3.12	3149	3214	3279	±3.12
100	212	0.63	3285	3358	3431	±3.46	3351	3426	3501	±3.46
110	230	0.59	3488	3571	3655	±3.93	3558	3643	3728	±3.93
120	248	0.53	3684	3779	3873	±4.7	3759	3855	3951	±4.7
125	257	0.49	3776	3876	3976	±5.26	3853	3955	4056	±5.26
130	266	0.44	3862	3967	4073	±6	3940	4048	4155	±6
140	284	0.33	4009	4125	4241	±8.45	4090	4208	4326	±8.45
150	302	0.20	4112	4237	4363	±14.63	4195	4323	4451	±14.63

Table 3 Ambient temperature, corresponding resistance, temperature coefficient and maximum expected temperature error for KTY82-250 and KTY82-251

I_{cont} = 1 mA.

AMBIENT TEMPERATURE		TEMP. COEFF.	KTY82-250				KTY82-251			
(°C)	(°F)	(%/K)	RESISTANCE (Ω)			TEMP. ERROR (K)	RESISTANCE (Ω)			TEMP. ERROR (K)
			MIN.	TYP.	MAX.		MIN.	TYP.	MAX.	
−55	−67	0.99	911	980	1049	±7.04	913	956	999	±4.52
−50	−58	0.98	959	1030	1101	±6.99	960	1004	1048	±4.45
−40	−40	0.96	1060	1135	1210	±6.91	1061	1106	1152	±4.3
−30	−22	0.93	1168	1247	1327	±6.84	1169	1216	1263	±4.16
−20	−4	0.91	1283	1367	1451	±6.77	1285	1333	1381	±4.01
−10	14	0.88	1407	1495	1583	±6.69	1408	1457	1507	±3.84
0	32	0.85	1538	1630	1721	±6.61	1539	1589	1639	±3.67
10	50	0.83	1677	1772	1867	±6.51	1678	1728	1778	±3.48
20	68	0.80	1824	1922	2021	±6.41	1825	1874	1923	±3.28
25	77	0.79	1900	2000	2100	±6.35	1900	1950	2000	±3.18
30	86	0.78	1974	2080	2185	±6.55	1975	2028	2080	±3.33
40	104	0.75	2127	2245	2362	±6.97	2129	2189	2248	±3.64
50	122	0.73	2287	2417	2547	±7.4	2289	2357	2425	±3.97
60	140	0.71	2453	2597	2741	±7.85	2455	2532	2609	±4.31
70	158	0.69	2626	2785	2943	±8.31	2628	2715	2802	±4.67
80	176	0.67	2805	2980	3154	±8.79	2807	2905	3003	±5.05
90	194	0.65	2990	3182	3374	±9.29	2993	3102	3212	±5.43
100	212	0.63	3182	3392	3602	±9.81	3185	3307	3429	±5.84
110	230	0.59	3379	3607	3836	±10.65	3382	3517	3652	±6.45
120	248	0.53	3569	3817	4065	±12.25	3573	3721	3870	±7.53
125	257	0.49	3658	3915	4173	±13.45	3662	3817	3973	±8.33
130	266	0.44	3741	4008	4274	±15.06	3745	3907	4070	±9.4
140	284	0.33	3883	4166	4450	±20.49	3887	4062	4237	±12.96
150	302	0.20	3982	4280	4578	±34.35	3987	4173	4359	±22.02

Table 4 Ambient temperature, corresponding resistance, temperature coefficient and maximum expected temperature error for KTY82-252

I_{cont} = 1 mA.

AMBIENT TEMPERATURE		TEMP. COEFF.	KTY82-252			
(°C)	(°F)	(%/K)	RESISTANCE (Ω)			TEMP. ERROR (K)
			MIN.	TYP.	MAX.	
−55	−67	0.99	959	1005	1050	±4.52
−50	−58	0.98	1009	1055	1102	±4.45
−40	−40	0.96	1115	1163	1211	±4.3
−30	−22	0.93	1229	1278	1328	±4.16
−20	−4	0.91	1351	1401	1452	±4.01
−10	14	0.88	1480	1532	1584	±3.84
0	32	0.85	1618	1670	1723	±3.67
10	50	0.83	1764	1817	1869	±3.48
20	68	0.80	1919	1970	2022	±3.28
25	77	0.79	2000	2050	2100	±3.18
30	86	0.78	2077	2132	2187	±3.33
40	104	0.75	2238	2301	2364	±3.64
50	122	0.73	2406	2478	2549	±3.97
60	140	0.71	2581	2662	2743	±4.31
70	158	0.69	2763	2854	2946	±4.67
80	176	0.67	2951	3054	3157	±5.05
90	194	0.65	3147	3262	3376	±5.43
100	212	0.63	3349	3477	3605	±5.84
110	230	0.59	3556	3697	3839	±6.45
120	248	0.53	3756	3912	4068	±7.53
125	257	0.49	3850	4013	4177	±8.33
130	266	0.44	3937	4108	4278	±9.4
140	284	0.33	4087	4271	4455	±12.96
150	302	0.20	4191	4387	4583	±22.02

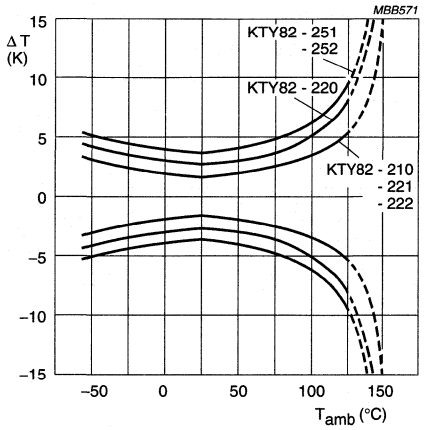

Fig.2 Maximum expected temperature error (ΔT).

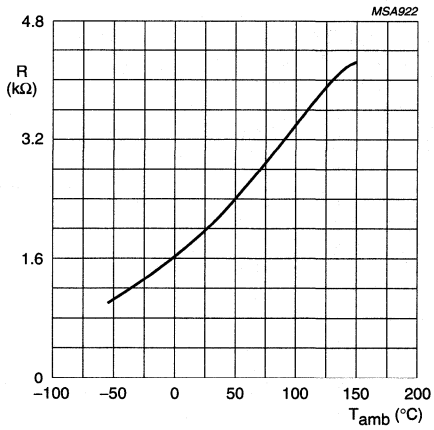

I_{cont} = 1 mA.

Fig.3 Sensor resistance as a function of ambient temperature; average values.

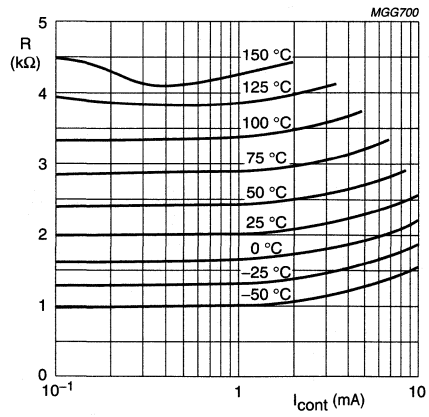

To keep the temperature error low, an operating current of I_{cont} = 1 mA is recommended for temperatures above 100 °C.

Fig.4 Sensor resistance as a function of operating current.

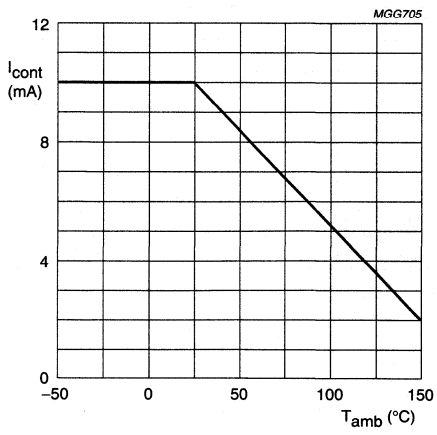

Fig.5 Maximum operating current for safe operation.

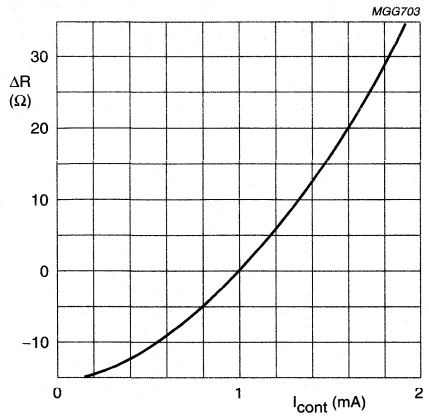

T_{amb} = 25 °C.

Fig.6 Deviation of sensor resistance as a function of operating current in still liquid.

APPLICATION INFORMATION

SYMBOL	PARAMETER	CONDITIONS	TYP.	UNIT
ΔR_{25}	drift of sensor resistance at 25 °C	10000 hours continuous operation; T_{amb} = 150 °C	3.2	Ω

PACKAGING

Tape specification

Sensors in SOT23 encapsulation are delivered in reel packaging for automatic placement on hybrid circuits and printed-circuit boards. The devices are placed with the mounting side downwards in the compartments.

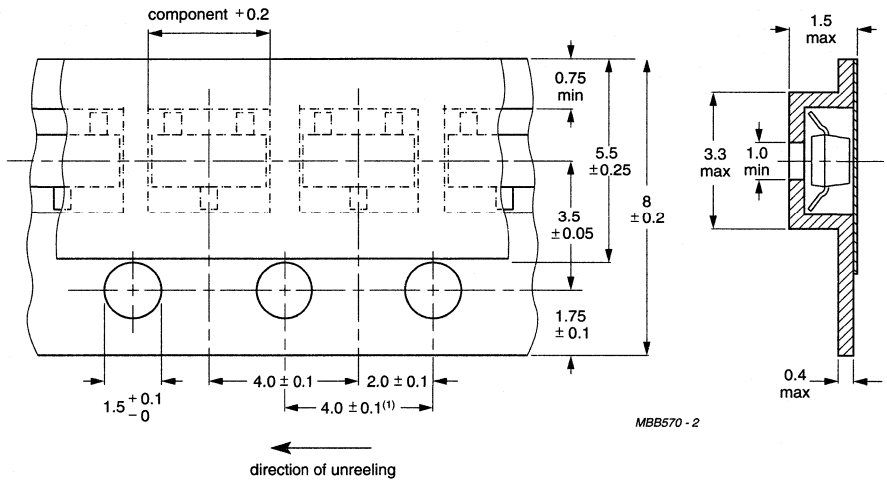

Dimension in mm.

(1) Tolerance over any 10 pitches: ±0.2 mm.

Fig.7 Configuration of bandolier.

PACKAGE OUTLINE

Plastic surface mounted package; 3 leads **SOT23**

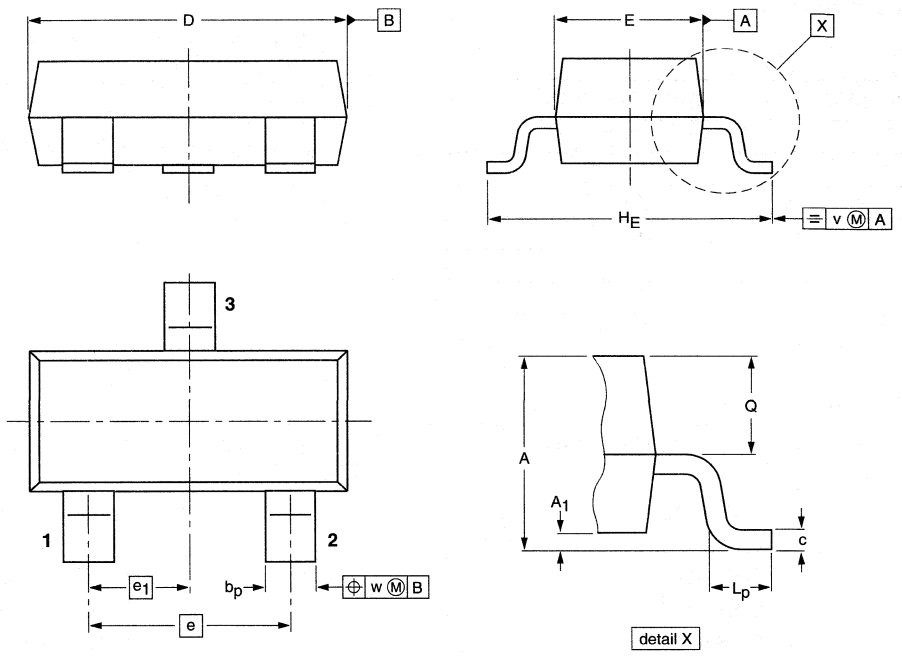

DIMENSIONS (mm are the original dimensions)

UNIT	A	A_1 max.	b_p	c	D	E	e	e_1	H_E	L_p	Q	v	w
mm	1.1 0.9	0.1	0.48 0.38	0.15 0.09	3.0 2.8	1.4 1.2	1.9	0.95	2.5 2.1	0.45 0.15	0.55 0.45	0.2	0.1

OUTLINE VERSION	REFERENCES				EUROPEAN PROJECTION	ISSUE DATE
	IEC	JEDEC	EIAJ			
SOT23		TO-236AB				~~97-02-28~~ 99-09-13

Silicon temperature sensors KTY83-1 series

DESCRIPTION

The temperature sensors in the KTY83-1 series have a positive temperature coefficient of resistance and are suitable for use in measurement and control systems. The sensors are encapsulated in the SOD68 (DO-34) package.

Tolerances of 0.5% or other special selections are available on request.

The black band indicates the negative connection.
The marking provides type identity.
The sensor must be operated with the lower potential at the marked connection.

Fig.1 Simplified outline (SOD68; DO34).

MARKING

TYPE NUMBER	MARKING CODE
KTY83-110	KTY83A
KTY83-120	KTY83C
KTY83-121	KTY83D
KTY83-122	KTY83E
KTY83-150	KTY83H
KTY83-151	KTY83K
KTY83-152	KTY83N

QUICK REFERENCE DATA

SYMBOL	PARAMETER	CONDITIONS	MIN.	MAX.	UNIT
R_{25}	sensor resistance	T_{amb} = 25 °C; I_{cont} = 1 mA			
	KTY83-110		990	1010	Ω
	KTY83-120		980	1020	Ω
	KTY83-121		980	1000	Ω
	KTY83-122		1000	1020	Ω
	KTY83-150		950	1050	Ω
	KTY83-151		950	1000	Ω
	KTY83-152		1000	1050	Ω
T_{amb}	ambient operating temperature		–55	+175	°C

LIMITING VALUES

In accordance with the Absolute Maximum Rating System (IEC 60134).

SYMBOL	PARAMETER	CONDITIONS	MIN.	MAX.	UNIT
I_{cont}	continuous sensor current	in free air; T_{amb} = 25 °C	–	10	mA
		in free air; T_{amb} = 175 °C	–	2	mA
T_{amb}	ambient operating temperature		–55	+175	°C

CHARACTERISTICS

T_{amb} = 25 °C, in liquid, unless otherwise specified.

SYMBOL	PARAMETER	CONDITIONS	MIN.	TYP.	MAX.	UNIT
R_{25}	sensor resistance	I_{cont} = 1 mA				
	KTY83-110		990	–	1010	Ω
	KTY83-120		980	–	1020	Ω
	KTY83-121		980	–	1000	Ω
	KTY83-122		1000	–	1020	Ω
	KTY83-150		950	–	1050	Ω
	KTY83-151		950	–	1000	Ω
	KTY83-152		1000	–	1050	Ω
TC	temperature coefficient		–	0.76	–	%/K
R_{100}/R_{25}	resistance ratio	T_{amb} = 100 °C and 25 °C	1.65	1.67	1.69	
R_{-55}/R_{25}	resistance ratio	T_{amb} = −55 °C and 25 °C	0.49	0.50	0.51	
τ	thermal time constant; note 1	in still air	–	20	–	s
		in still liquid; note 2	–	1	–	s
		in flowing liquid; note 2	–	0.5	–	s
	rated temperature range		−55	–	+175	°C

Notes

1. The thermal time constant is the time taken for the sensor to reach 63.2% of the total temperature difference. For example, if a sensor with a temperature of 25 °C is moved to an environment with an ambient temperature of 100 °C, the time for the sensor to reach a temperature of 72.4 °C is the thermal time constant.
2. Inert liquid, e.g. FC43 manufactured by the 3M company.

Table 1 Ambient temperature, corresponding resistance, temperature coefficient and maximum expected temperature error for KTY83-110 and KTY83-120

I_{cont} = 1 mA.

AMBIENT TEMPERATURE		TEMP. COEFF.	KTY83-110				KTY83-120			
(°C)	(°F)	(%/K)	RESISTANCE (Ω)			TEMP. ERROR (K)	RESISTANCE (Ω)			TEMP. ERROR (K)
			MIN.	TYP.	MAX.		MIN.	TYP.	MAX.	
−55	−67	0.97	485	500	515	±3.08	480	500	520	±4.11
−50	−58	0.96	510	525	540	±2.99	504	525	545	±4.04
−40	−40	0.93	562	577	592	±2.81	556	577	598	±3.88
−30	−22	0.91	617	632	647	±2.62	611	632	654	±3.72
−20	−4	0.88	677	691	706	±2.42	670	691	713	±3.56
−10	14	0.85	740	754	768	±2.2	732	754	776	±3.37
0	32	0.83	807	820	833	±1.97	798	820	841	±3.18
10	50	0.80	877	889	902	±1.72	868	889	910	±2.97
20	68	0.78	951	962	973	±1.45	942	962	983	±2.74
25	77	0.76	990	1000	1010	±1.31	980	1000	1020	±2.62
30	86	0.75	1027	1039	1050	±1.44	1017	1039	1060	±2.77
40	104	0.73	1105	1118	1132	±1.7	1093	1118	1143	±3.07
50	122	0.71	1185	1202	1219	±1.98	1173	1202	1231	±3.39
60	140	0.69	1268	1288	1309	±2.27	1255	1288	1321	±3.73
70	158	0.67	1355	1379	1402	±2.58	1341	1379	1416	±4.08
80	176	0.65	1445	1472	1500	±2.9	1430	1472	1515	±4.44
90	194	0.63	1537	1569	1601	±3.24	1522	1569	1617	±4.82
100	212	0.61	1633	1670	1707	±3.59	1617	1670	1723	±5.22
110	230	0.60	1732	1774	1816	±3.95	1714	1774	1834	±5.63
120	248	0.58	1834	1882	1929	±4.34	1815	1882	1948	±6.06
125	257	0.57	1886	1937	1987	±4.53	1867	1937	2006	±6.28
130	266	0.57	1939	1993	2046	±4.73	1919	1993	2066	±6.5
140	284	0.55	2047	2107	2167	±5.14	2026	2107	2188	±6.96
150	302	0.54	2158	2225	2292	±5.57	2136	2225	2314	±7.43
160	320	0.52	2272	2346	2420	±6.02	2249	2346	2444	±7.92
170	338	0.51	2389	2471	2553	±6.47	2364	2471	2578	±8.43
175	347	0.51	2449	2535	2621	±6.71	2423	2535	2646	±8.68

Table 2 Ambient temperature, corresponding resistance, temperature coefficient and maximum expected temperature error for KTY83-121 and KTY83-122

I_{cont} = 1 mA.

AMBIENT TEMPERATURE		TEMP. COEFF.	KTY83-121				KTY83-122			
(°C)	(°F)	(%/K)	RESISTANCE (Ω)			TEMP. ERROR (K)	RESISTANCE (Ω)			TEMP. ERROR (K)
			MIN.	TYP.	MAX.		MIN.	TYP.	MAX.	
–55	–67	0.97	480	495	510	±3.08	490	505	520	±3.08
–50	–58	0.96	505	519	534	±2.99	515	530	545	±2.99
–40	–40	0.93	556	571	586	±2.81	567	583	598	±2.81
–30	–22	0.91	611	626	641	±2.62	624	639	654	±2.62
–20	–4	0.88	670	685	699	±2.42	684	698	713	±2.42
–10	14	0.85	732	746	760	±2.2	747	762	776	±2.2
0	32	0.83	799	812	825	±1.97	815	828	842	±1.97
10	50	0.80	868	880	893	±1.72	886	898	911	±1.72
20	68	0.78	942	953	963	±1.45	961	972	983	±1.45
25	77	0.76	980	990	1000	±1.31	1000	1010	1020	±1.31
30	86	0.75	1017	1028	1039	±1.44	1038	1049	1060	±1.44
40	104	0.73	1094	1107	1121	±1.7	1116	1130	1144	±1.7
50	122	0.71	1173	1190	1206	±1.98	1197	1214	1231	±1.98
60	140	0.69	1256	1276	1295	±2.27	1281	1301	1322	±2.27
70	158	0.67	1341	1365	1388	±2.58	1368	1392	1416	±2.58
80	176	0.65	1430	1458	1485	±2.9	1459	1487	1515	±2.9
90	194	0.63	1522	1554	1585	±3.24	1553	1585	1617	±3.24
100	212	0.61	1617	1653	1690	±3.59	1650	1687	1724	±3.59
110	230	0.60	1715	1756	1798	±3.95	1750	1792	1834	±3.95
120	248	0.58	1816	1863	1910	±4.34	1853	1900	1948	±4.34
125	257	0.57	1867	1917	1967	±4.53	1905	1956	2007	±4.53
130	266	0.57	1920	1973	2025	±4.73	1959	2012	2066	±4.73
140	284	0.55	2027	2086	2145	±5.14	2068	2128	2188	±5.14
150	302	0.54	2137	2203	2269	±5.57	2180	2247	2314	±5.57
160	320	0.52	2249	2323	2396	±6.02	2295	2370	2444	±6.02
170	338	0.51	2365	2446	2527	±6.47	2413	2496	2578	±6.47
175	347	0.51	2424	2509	2595	±6.71	2473	2560	2647	±6.71

Table 3 Ambient temperature, corresponding resistance, temperature coefficient and maximum expected temperature error for KTY83-150 and KTY83-151

I_{cont} = 1 mA.

AMBIENT TEMPERATURE		TEMP. COEFF.	KTY83-150				KTY83-151			
(°C)	(°F)	(%/K)	RESISTANCE (Ω)			TEMP. ERROR (K)	RESISTANCE (Ω)			TEMP. ERROR (K)
			MIN.	TYP.	MAX.		MIN.	TYP.	MAX.	
−55	−67	0.97	465	500	535	±7.19	466	487	509	±4.92
−50	−58	0.96	489	525	561	±7.16	489	512	534	±4.56
−40	−40	0.93	539	577	615	±7.1	539	562	586	±4.42
−30	−22	0.91	592	632	673	±7.04	593	617	641	±4.28
−20	−4	0.88	649	691	734	±6.97	650	674	699	±4.12
−10	14	0.85	710	754	798	±6.9	710	735	760	±3.96
0	32	0.83	774	820	866	±6.81	774	799	824	±3.79
10	50	0.80	842	889	937	±6.72	842	867	892	±3.59
20	68	0.78	913	962	1012	±6.61	914	938	963	±3.39
25	77	0.76	950	1000	1050	±6.55	950	975	1000	±3.27
30	86	0.75	986	1039	1091	±6.76	987	1013	1039	±3.43
40	104	0.73	1060	1118	1177	±7.19	1061	1090	1120	±3.76
50	122	0.71	1137	1202	1267	±7.63	1138	1172	1206	±4.1
60	140	0.69	1217	1288	1360	±8.1	1218	1256	1295	±4.45
70	158	0.67	1300	1379	1457	±8.58	1301	1344	1387	±4.83
80	176	0.65	1386	1472	1559	±9.07	1387	1435	1484	±5.21
90	194	0.63	1475	1569	1664	±9.59	1476	1530	1584	±5.62
100	212	0.61	1566	1670	1773	±10.12	1568	1628	1688	±6.04
110	230	0.60	1661	1774	1887	±10.66	1663	1730	1796	±6.47
120	248	0.58	1759	1882	2004	±11.282	1761	1835	1908	±6.92
125	257	0.57	1809	1937	2064	±11.51	1811	1888	1966	±7.15
130	266	0.57	1859	1993	2126	±11.8	1862	1943	2024	±7.38
140	284	0.55	1963	2107	2251	±12.4	1965	2054	2143	±7.87
150	302	0.54	2069	2225	2380	±13.01	2072	2169	2267	±8.36
160	320	0.52	2178	2346	2514	±13.64	2181	2288	2394	±8.87
170	338	0.51	2290	2471	2652	±14.28	2293	2409	2525	±9.4
175	347	0.51	2347	2535	2722	±14.61	2350	2471	2592	±9.67

Table 4 Ambient temperature, corresponding resistance, temperature coefficient and maximum expected temperature error for KTY83-152

I_{cont} = 1 mA.

AMBIENT TEMPERATURE		TEMP. COEFF.	KTY83-152			
(°C)	(°F)	(%/K)	RESISTANCE (Ω)			TEMP. ERROR (K)
			MIN.	TYP.	MAX.	
−55	−67	0.97	489	512	536	±4.92
−50	−58	0.96	514	538	561	±4.56
−40	−40	0.93	567	591	616	±4.42
−30	−22	0.91	623	648	673	±4.28
−20	−4	0.88	683	709	734	±4.12
−10	14	0.85	747	773	799	±3.96
0	32	0.83	814	840	867	±3.79
10	50	0.80	885	912	938	±3.59
20	68	0.78	960	986	1012	±3.39
25	77	0.76	1000	1025	1050	±3.27
30	86	0.75	1037	1065	1092	±3.43
40	104	0.73	1115	1146	1178	±3.76
50	122	0.71	1196	1232	1267	±4.1
60	140	0.69	1280	1321	1361	±4.45
70	158	0.67	1368	1413	1459	±4.83
80	176	0.65	1458	1509	1560	±5.21
90	194	0.63	1552	1609	1666	±5.62
100	212	0.61	1648	1712	1775	±6.04
110	230	0.60	1748	1818	1889	±6.47
120	248	0.58	1851	1929	2006	±6.92
125	257	0.57	1904	1985	2066	±7.15
130	266	0.57	1957	2042	2128	±7.38
140	284	0.55	2066	2160	2253	±7.87
150	302	0.54	2178	2280	2383	±8.36
160	320	0.52	2293	2405	2517	±8.87
170	338	0.51	2411	2533	2655	±9.4
175	347	0.51	2471	2598	2725	±9.67

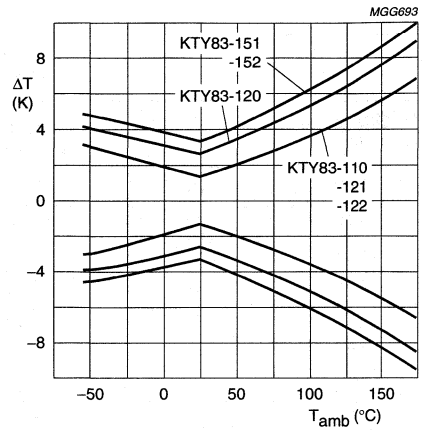

Fig.2 Maximum expected temperature error (ΔT).

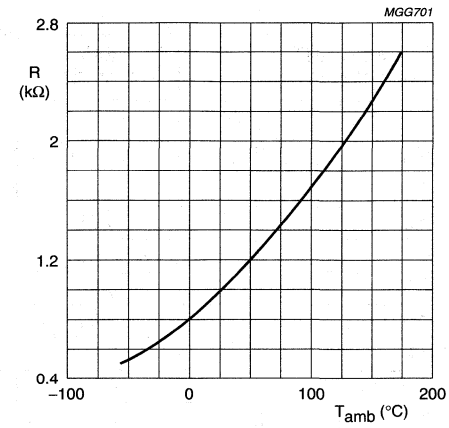

I_{cont} = 1 mA.

Fig.3 Sensor resistance as a function of ambient temperature; average values.

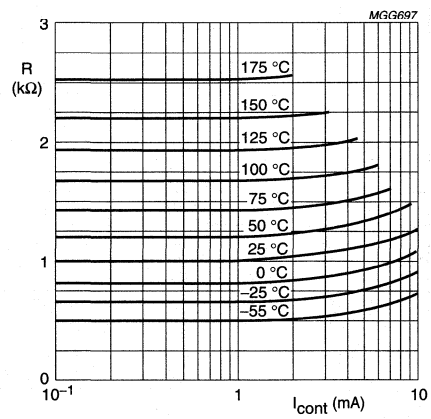

To keep the temperature error low, an operating current of I_{cont} = 1 mA is recommended for temperatures above 100 °C.

Fig.4 Sensor resistance as a function of operating current.

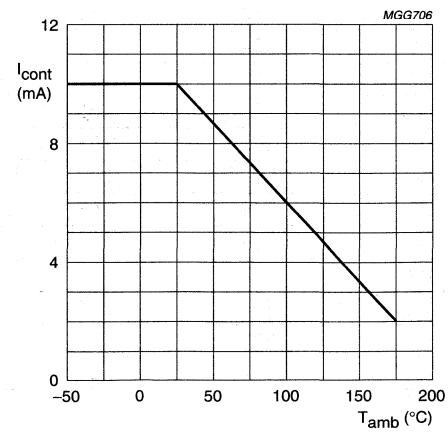

Fig.5 Maximum operating current for safe operation.

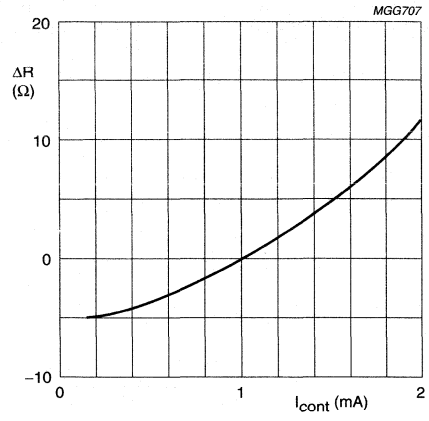

T_{amb} = 25 °C.

Fig.6 Deviation of sensor resistance as a function of operating current in still liquid.

APPLICATION INFORMATION

SYMBOL	PARAMETER	CONDITIONS	TYP.	UNIT
ΔR_{25}	drift of sensor resistance at 25 °C	10000 hours continuous operation; T_{amb} = 175 °C	1	Ω

PACKAGE OUTLINE

Hermetically sealed glass package; axial leaded; 2 leads **SOD68**

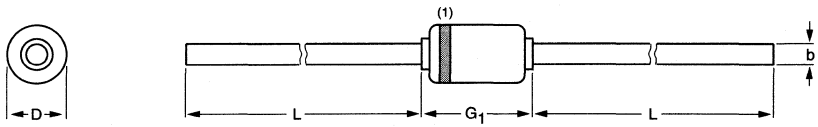

DIMENSIONS (mm are the original dimensions)

UNIT	b max.	D max.	G_1 max.	L min.
mm	0.55	1.6	3.04	25.4

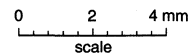

Note

1. The marking band indicates the cathode.

OUTLINE VERSION	REFERENCES				EUROPEAN PROJECTION	ISSUE DATE
	IEC	JEDEC	EIAJ			
SOD68		DO-34				97-06-09

Silicon temperature sensors KTY84-1 series

DESCRIPTION

The temperature sensors in the KTY84-1 series have a positive temperature coefficient of resistance and are suitable for use in measurement and control systems over a temperature range of −40 to +300 °C. The sensors are encapsulated in the SOD68 (DO-34) package. The leads are nickel plated.

Tolerances of 0.5% or other special selections are available on request.

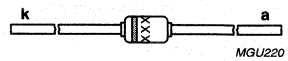

The black band indicates the negative connection.
The marking provides type identity.
The sensor must be operated with the lower potential at the marked connection.

Fig.1 Simplified outline (SOD68; DO-34).

MARKING

TYPE NUMBER	MARKING CODE
KTY84-130	KTY84L
KTY84-150	KTY84M
KTY84-151	KTY84O
KTY84-152	KTY84P

QUICK REFERENCE DATA

SYMBOL	PARAMETER	CONDITIONS	MIN.	MAX.	UNIT
R_{100}	sensor resistance	T_{amb} = 100 °C; I_{cont} = 2 mA			
	KTY84-130		970	1030	Ω
	KTY84-150		950	1050	Ω
	KTY84-151		950	1000	Ω
	KTY84-152		1000	1050	Ω
T_{amb}	ambient operating temperature		−40	+300	°C

LIMITING VALUES

In accordance with the Absolute Maximum Rating System (IEC 60134).

SYMBOL	PARAMETER	CONDITIONS	MIN.	MAX.	UNIT
I_{cont}	continuous sensor current	in free air; T_{amb} = 25 °C; note 1	–	10	mA
		in free air; T_{amb} = 300 °C	–	2	mA
T_{amb}	ambient operating temperature		−40	+300	°C
T_{stg}	storage temperature		−55	+300	°C

Note

1. For temperatures greater than 200 °C, a sensor current of I_{cont} = 2 mA must be used.

CHARACTERISTICS

T_{amb} = 100 °C, in liquid, unless otherwise specified.

SYMBOL	PARAMETER	CONDITIONS	MIN.	TYP.	MAX.	UNIT
R_{100}	sensor resistance	I_{cont} = 2 mA				
	KTY84-130		970	–	1030	Ω
	KTY84-150		950	–	1050	Ω
	KTY84-151		950	–	1000	Ω
	KTY84-152		1000	–	1050	Ω
TC	temperature coefficient		–	0.61	–	%/K
R_{250}/R_{100}	resistance ratio	T_{amb} = 250 °C and 100 °C	2.111	2.166	2.221	
R_{25}/R_{100}	resistance ratio	T_{amb} = 25 °C and 100 °C	0.595	0.603	0.611	
τ	thermal time constant; note 1	in still air	–	20	–	s
		in still liquid; note 2	–	1	–	s
		in flowing liquid; note 2	–	0.5	–	s
	rated temperature range		–40	–	+300	°C

Notes

1. The thermal time constant is the time taken for the sensor to reach 63.2% of the total temperature difference. For example, if a sensor with a temperature of 25 °C is moved to an environment with an ambient temperature of 100 °C, the time for the sensor to reach a temperature of 72.4 °C is the thermal time constant.
2. Inert liquid, e.g. FC43 manufactured by the 3M company.

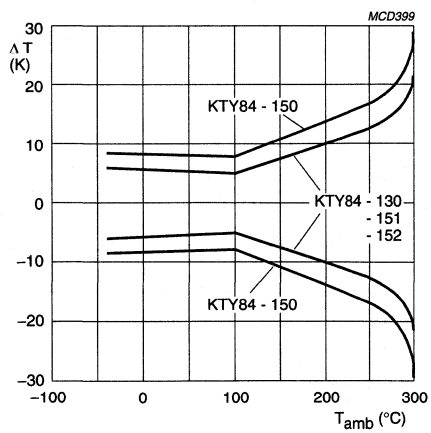

Fig.2 Maximum expected temperature error (ΔT).

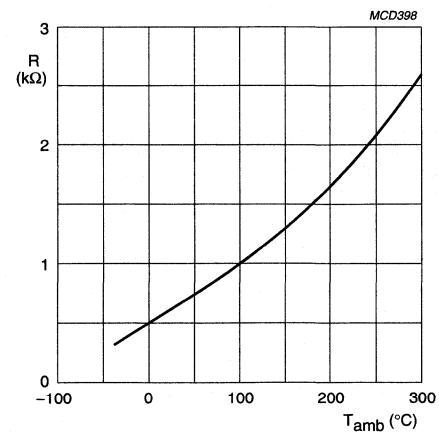

I_{cont} = 2 mA.

Fig.3 Sensor resistance as a function of ambient temperature; average values.

Table 1 Ambient temperature, corresponding resistance, temperature coefficient and maximum expected temperature error for KTY84-130 and KTY84-150

I_{cont} = 2 mA.

AMBIENT TEMPERATURE		TEMP. COEFF.	KTY84-130				KTY84-150			
(°C)	(°F)	(%/K)	RESISTANCE (Ω)			TEMP. ERROR (K)	RESISTANCE (Ω)			TEMP. ERROR (K)
			MIN.	TYP.	MAX.		MIN.	TYP.	MAX.	
–40	–40	0.84	340	359	379	±6.48	332	359	386	±8.85
–30	–22	0.83	370	391	411	±6.36	362	391	419	±8.76
–20	–4	0.82	403	424	446	±6.26	394	424	455	±8.7
–10	14	0.80	437	460	483	±6.16	428	460	492	±8.65
0	32	0.79	474	498	522	±6.07	464	498	532	±8.61
10	50	0.77	514	538	563	±5.98	503	538	574	±8.58
20	68	0.75	555	581	607	±5.89	544	581	618	±8.55
25	77	0.74	577	603	629	±5.84	565	603	641	±8.54
30	86	0.73	599	626	652	±5.79	587	626	665	±8.53
40	104	0.71	645	672	700	±5.69	632	672	713	±8.5
50	122	0.70	694	722	750	±5.59	679	722	764	±8.46
60	140	0.68	744	773	801	±5.47	729	773	817	±8.42
70	158	0.66	797	826	855	±5.34	781	826	872	±8.37
80	176	0.64	852	882	912	±5.21	835	882	929	±8.31
90	194	0.63	910	940	970	±5.06	891	940	989	±8.25
100	212	0.61	970	1000	1030	±4.9	950	1000	1050	±8.17
110	230	0.60	1029	1062	1096	±5.31	1007	1062	1117	±8.66
120	248	0.58	1089	1127	1164	±5.73	1067	1127	1187	±9.17
130	266	0.57	1152	1194	1235	±6.17	1128	1194	1259	±9.69
140	284	0.55	1216	1262	1309	±6.63	1191	1262	1334	±10.24
150	302	0.54	1282	1334	1385	±7.1	1256	1334	1412	±10.8
160	320	0.53	1350	1407	1463	±7.59	1322	1407	1492	±11.37
170	338	0.52	1420	1482	1544	±8.1	1391	1482	1574	±11.96
180	356	0.51	1492	1560	1628	±8.62	1461	1560	1659	±12.58
190	374	0.49	1566	1640	1714	±9.15	1533	1640	1747	±13.2
200	392	0.48	1641	1722	1803	±9.71	1607	1722	1837	±13.85
210	410	0.47	1719	1807	1894	±10.28	1683	1807	1931	±14.51
220	428	0.46	1798	1893	1988	±10.87	1760	1893	2026	±15.19
230	446	0.45	1879	1982	2085	±11.47	1839	1982	2125	±15.88
240	464	0.44	1962	2073	2184	±12.09	1920	2073	2226	±16.59
250	482	0.44	2046	2166	2286	±12.73	2003	2166	2329	±17.32
260	500	0.42	2132	2261	2390	±13.44	2087	2261	2436	±18.15
270	518	0.41	2219	2357	2496	±14.44	2172	2357	2543	±19.36
280	536	0.38	2304	2452	2600	±15.94	2255	2452	2650	±21.21
290	554	0.34	2384	2542	2700	±18.26	2333	2542	2751	±24.14
300	572	0.29	2456	2624	2791	±22.12	2404	2624	2844	±29.05

Table 2 Ambient temperature, corresponding resistance, temperature coefficient and maximum expected temperature error for KTY84-151 and KTY84-152

I_{cont} = 2 mA.

AMBIENT TEMPERATURE		TEMP. COEFF.	KTY84-151				KTY84-152			
(°C)	(°F)	(%/K)	RESISTANCE (Ω)			TEMP. ERROR (K)	RESISTANCE (Ω)			TEMP. ERROR (K)
			MIN.	TYP.	MAX.		MIN.	TYP.	MAX.	
−40	−40	0.84	332	350	368	±5.97	350	368	386	±5.82
−30	−22	0.83	362	381	399	±5.84	381	400	419	±5.69
−20	−4	0.82	394	414	433	±5.72	415	435	455	±5.57
−10	14	0.80	428	449	469	±5.62	451	472	492	±5.46
0	32	0.79	464	486	507	±5.51	489	511	532	±5.35
10	50	0.77	503	525	547	±5.41	530	552	574	±5.25
20	68	0.75	544	566	589	±5.31	573	595	618	±5.14
25	77	0.74	565	588	611	±5.25	595	618	641	±5.08
30	86	0.73	587	610	633	±5.2	618	641	665	±5.03
40	104	0.71	632	656	679	±5.08	665	689	713	±4.91
50	122	0.70	679	704	728	±4.96	715	740	764	±4.78
60	140	0.68	729	754	778	±4.83	767	792	817	±4.64
70	158	0.66	781	806	831	±4.68	822	847	872	±4.5
80	176	0.64	835	860	885	±4.53	879	904	929	±4.34
90	194	0.63	891	916	942	±4.37	938	963	989	±4.17
100	212	0.61	950	975	1000	±4.19	1000	1025	1050	±3.99
110	230	0.60	1007	1036	1064	±4.58	1060	1089	1117	±4.37
120	248	0.58	1067	1099	1131	±4.99	1123	1155	1187	±4.77
130	266	0.57	1128	1164	1199	±5.41	1187	1223	1259	±5.19
140	284	0.55	1191	1231	1271	±5.84	1254	1294	1334	±5.62
150	302	0.54	1256	1300	1345	±6.3	1322	1367	1412	±6.07
160	320	0.53	1322	1372	1421	±6.77	1392	1442	1492	±6.53
170	338	0.52	1391	1445	1500	±7.25	1464	1519	1574	±7.01
180	356	0.51	1461	1521	1581	±7.75	1538	1599	1659	±7.51
190	374	0.49	1533	1599	1664	±8.27	1614	1681	1747	±8.02
200	392	0.48	1607	1679	1751	±8.81	1692	1765	1837	±8.55
210	410	0.47	1683	1761	1839	±9.36	1772	1852	1931	±9.09
220	428	0.46	1760	1846	1931	±9.93	1854	1940	2026	±9.66
230	446	0.45	1839	1932	2024	±10.51	1937	2031	2125	±10.23
240	464	0.44	1920	2021	2121	±11.11	2022	2125	2226	±10.83
250	482	0.44	2003	2112	2220	±11.73	2110	2220	2329	±11.44
260	500	0.42	2087	2205	2321	±12.42	2198	2318	2436	±12.12
270	518	0.41	2172	2298	2424	±13.37	2288	2416	2543	±13.06
280	536	0.38	2257	2391	2525	±14.79	2376	2513	2650	±14.46
290	554	0.34	2335	2479	2622	±16.98	2459	2606	2751	±16.61
300	572	0.29	2406	2558	2710	±20.61	2533	2689	2844	±20.18

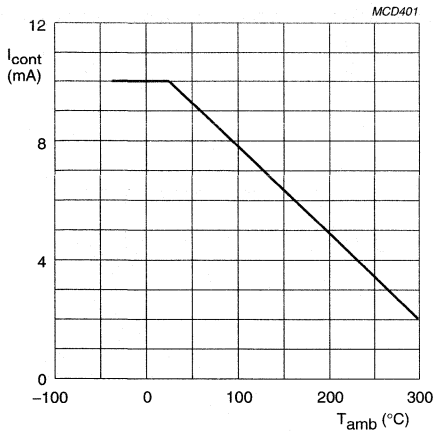

Fig.4 Maximum operating current for safe operation.

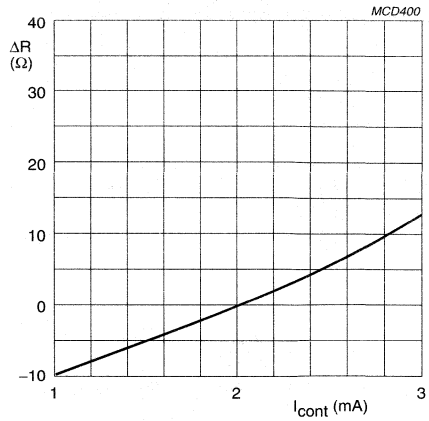

T_{amb} = 100 °C.

Fig.5 Deviation of sensor resistance as a function of operating current in still liquid.

PACKAGE OUTLINE

Hermetically sealed glass package; axial leaded; 2 leads **SOD68**

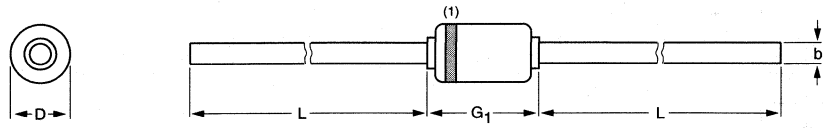

DIMENSIONS (mm are the original dimensions)

UNIT	b max.	D max.	G_1 max.	L min.
mm	0.55	1.6	3.04	25.4

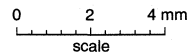

Note

1. The marking band indicates the cathode.

OUTLINE VERSION	REFERENCES				EUROPEAN PROJECTION	ISSUE DATE
	IEC	JEDEC	EIAJ			
SOD68		DO-34				97-06-09

DATA HANDBOOK SYSTEM

DATA HANDBOOK SYSTEM

Philips Semiconductors data handbooks contain all pertinent data available at the time of publication and each is revised and reissued regularly.

Loose data sheets are sent to subscribers to keep them up-to-date on additions or alterations made during the lifetime of a data handbook.

Catalogues are available for selected product ranges (some catalogues are also on floppy discs).

Our data handbook titles are listed here.

Integrated circuits

Book	*Title*
IC03	Semiconductors for Wired Telecom Systems
IC04	HE4000B Logic Family CMOS
IC05	Advanced Low-power Schottky (ALS) Logic
IC06	High-speed CMOS Logic Family
IC11	General-purpose/Linear ICs
IC12	I^2C Peripherals
IC14	8048-based 8-bit Microcontrollers
IC15	FAST TTL Logic Series
IC16	CMOS ICs for Clocks, Watches and Real Time Clocks
IC17	Semiconductors for Wireless Communications
IC19	ICs for Data Communications
IC23	BiCMOS Bus Interface Logic
IC24	Low Voltage CMOS & BiCMOS Logic
IC26	Integrated Circuit Packages
IC28	80C51 and XA Microcontrollers

Discrete semiconductors

Book	*Title*
SC03	Power Thyristors and Triacs
SC06	Power Bipolar Transistors
SC07	Small-signal Field-effect Transistors and Diodes
SC10	Small-signal Transistors and Diodes
SC11	Power Diodes
SC13	PowerMOS Transistors
SC14	RF Wideband Transistors
SC16	Wideband Hybrid Amplifier Modules for CATV
SC17	Semiconductor Sensors
SC18	Discrete Semiconductor Packages
SC19	RF & Microwave Power Transistors and RF Power Modules

MORE INFORMATION FROM PHILIPS SEMICONDUCTORS?

For more information about Philips Semiconductors data handbooks, catalogues and subscriptions contact your nearest Philips Semiconductors national organization, select from the **address list on the back cover of this handbook.** Product specialists are at your service and enquiries are answered promptly.

OVERVIEW OF PHILIPS COMPONENTS DATA HANDBOOKS

Our sister product division, Philips Components, also has a comprehensive data handbook system to support their products. Their data handbook titles are listed here.

Display Components

Book	*Title*
DC01	Colour Television and Multimedia Tubes
DC02	Monochrome Monitor Tubes and Deflection Units
DC03	Television Tuners, Coaxial Aerial Input Assemblies
DC04	Colour Monitor and Multimedia Tubes
DC05	Wire Wound Components

Advanced Ceramics & Modules

ACM1 (MA01)	Soft Ferrites
ACM2	Discrete Ceramics
ACM3 (MA03)	Piezoelectric Ceramics and Specialty Ferrites

BC Components

BC01	Electrolytic Capacitors
BC02	Varistors, Thermistors and Sensors
BC03	Potentiometers
PA04	Variable Capacitors
PA05	Film Capacitors
BC06	Leaded Ceramic Capacitors
PA06a	Surface Mounted Ceramic Multilayer Capacitors
PA06b	Leaded Ceramic Capacitors
PA08	Fixed Resistors
PA10	Quartz Crystals
PA11	Quartz Oscillators

MORE INFORMATION FROM PHILIPS COMPONENTS?

For more information contact your nearest Philips Components national organization shown in the following list.

Australia: Homebush, Tel. +61 2 9704 8141, Fax. +61 2 9704 8139
Austria: Wien, Tel. +43 1 60 101 12 41, Fax. +43 1 60 101 12 11
Belarus: Minsk, Tel. +375 172 200 924/733, Fax. +375 172 200 773
Benelux: Eindhoven, Tel. +31 40 25 90 772, Fax. +31 40 25 90 777
Brazil: São Paolo, Tel. +55 11 3841 2338, Fax. +55 11 829 1849
Canada: Scarborough, Tel. 1 416 292 5161, Fax. 1 416 754 6248
China: Shanghai, Tel. +86 21 6354 1088, Fax. +86 21 6354 1060
Denmark: Copenhagen, Tel. +45 3329 3333, Fax. +45 3329 3905
Finland: Espoo, Tel. 358 9 615 800, Fax. 358 9 615 80510
France: Suresnes, Tel. +33 1 4099 6161, Fax. +33 1 4099 6493
Germany: Hamburg, Tel. +49 40 2489-0, Fax. +49 40 2489 1400
Hong Kong: Kowloon, Tel. +852 2784 3000, Fax. +852 2784 3003
India: Mumbai, Tel. +91 22 4930 311, Fax. +91 22 4930 966/4950 304
Indonesia: Jakarta, Tel. +62 21 794 0040, Fax. +62 21 794 0080
Ireland: Dublin, Tel. +353 1 7640 203, Fax. +353 1 7640 210
Israel: Tel Aviv. Tel. +972 3 6450 444, Fax. +972 3 6491 007
Italy: Milano, Tel. +39 2 6752 2531, Fax. +39 2 6752 2557
Japan: Tokyo, Tel. +81 3 3740 5135, Fax. +81 3 3740 5035
Korea (Republic of): Seoul, Tel. +82 2 709 1472, Fax. +82 2 709 1480
Malaysia: Pulau Pinang, Tel. +60 3 750 5213, Fax. +60 3 757 4880
Mexico: El Paso, Tel. +52 915 772 4020, Fax. +52 915 772 4332
New Zealand: Auckland, Tel. +64 9 815 4000, Fax. +64 9 849 7811
Norway: Stockholm, Tel. +46 8 5985 2000, Fax. +46 8 5985 2745
Pakistan: Karachi, Tel. +92 21 587 4641-49,
Fax. +92 21 577 035/+92 21 587 4546
Philippines: Manila, Tel. +63 2 816 6345, Fax. +63 2 817 3474
Poland: Warszawa, Tel. +48 22 5710 000, Fax. +48 22 5710 001
Portugal: Linda-A-Velha, Tel. +351 1 416 3160/416 3333,
Fax. +351 1 416 3174/416 3366
Russia: Moscow, Tel. +7 95 755 6918, Fax. +7 95 755 6919
Singapore: Singapore, Tel. +65 350 2000, Fax. +65 355 1758
South Africa: Johannesburg, Tel. +27 11 470 5911, Fax. +27 11 470 5494
Spain: Barcelona, Tel. +34 93 301 63 12, Fax. +34 93 301 42 43
Sweden: Stockholm, Tel. +46 8 5985 2000, Fax. +46 8 5985 2745
Switzerland: Zürich, Tel. +41 1 488 22 11, Fax. +41 1 481 7730
Taiwan: Taipei, Tel. +886 2 2134 2900, Fax. +886 2 2134 2929
Turkey: Istanbul, Tel. +90 216 522 1800, Fax. +90 216 522 1814
United Kingdom: Dorking, Tel. +44 1306 512 000, Fax. +44 1306 512 345
United States:

- San Jose, Tel. +1 408 570 5600, Fax. +1 408 570 5700
- Ann Arbor, Tel. +1 734 996 9400, Fax. +1 734 761 2776
- El Paso, Tel. +1 877 250 5996 / +1 915 860 3267, Fax. +1 915 860 3270
- Roswell, Tel. +1 877 443 77483, Fax. +1 770 992 0725

Yugoslavia (Federal Republic of): Belgrade,
Tel. +381 11 3341 299, Fax. +381 11 3342 553

Internet:

- Discrete and Ferrite Ceramics: www.acm.components.philips.com
- Display Components: www.philipsdisplay.com

For all other countries apply to:
Philips Components, Marketing Communications, Building BAE-1,
P.O. Box 218, 5600 MD EINDHOVEN, The Netherlands,
Fax. +31-40-2722599

North American Sales Offices, Representatives and Distributors

PHILIPS SEMICONDUCTORS
811 East Arques Avenue
P.O. Box 3409
Sunnyvale, CA 94088-3409

ALABAMA
Huntsville
Philips Semiconductors
Phone: (256) 464-9101
(256) 464-0111

Elcom, Inc.
Phone: (256) 830-4001

ARIZONA
Tempe
Philips Semiconductors
Phone: (480) 752-6656

Centaur Corporation
Phone: (480) 839-2320

CALIFORNIA
Calabasas
Centaur Corporation
Phone: (818) 878-5800

El Dorado
Aspen Technologies, Inc.
Phone: (916) 939-9797

Irvine
Philips Semiconductors
Phone: (949) 453-0770

Centaur Corporation
Phone: (949) 261-2123

San Diego
Philips Semiconductors
Phone: (858) 509-0460

Centaur Corporation
Phone: (619) 278-4950

San Jose/Sunnyvale
B.A.E. Sales, Inc.
Phone: (408) 452-8133

Santa Clara
Aspen Technologies, Inc.
Phone: (408) 988-1300

Woodland Hills
Philips Semiconductors
Phone: (818) 710-1954

COLORADO
Englewood
Philips Semiconductors
Phone: (303) 792-9011

Thom Luke Sales, Inc.
Phone: (303) 649-9717

CONNECTICUT
(Burlington, Massachusetts)
New Tech Solutions, Inc.
Phone: (781) 229-8888

FLORIDA
Clearwater
Elcom, Inc.
Phone: (727) 524-1334

GEORGIA
Duluth
Elcom, Inc.
Phone: (770) 447-8200

IDAHO
(Englewood, Colorado)
Thom Luke Sales, Inc.
Phone: (303) 649-9717

ILLINOIS
Itasca
Philips Semiconductors
Phone: (630) 250-0050

INDIANA
Indianapolis
Mohrfield Marketing, Inc.
Phone: (317) 546-6969

Kokomo
Philips Semiconductors
Phone: (765) 459-5355

Leo
Mohrfield Marketing, Inc.
Phone: (219) 627-5355

KANSAS
(Bloomington, Minnesota)
High Technology Sales, Inc.
Phone: (612) 844-9933

KENTUCKY
(Indianapolis, Indiana)
Mohrfield Marketing, Inc.
Phone: (317) 546-6969

MARYLAND
(Falls Church, Virginia)
S-J Associates, Inc.
Phone: (703) 533-2233

MASSACHUSETTS
Burlington
New Tech Solutions, Inc.
Phone: (781) 229-8888

Chelmsford
Philips Semiconductors
Phone: (978) 367-9000

MICHIGAN
Farmington Hills
Philips Semiconductors
Phone: (248) 848-7600

Novi
Mohrfield Marketing, Inc.
Phone: (248) 380-8100

MINNESOTA
Bloomington
High Technology Sales, Inc.
Phone: (612) 844-9933

MISSOURI
(Bloomington, Minnesota)
High Technology Sales, Inc.
Phone: (612) 844-9933

NEBRASKA
(Bloomington, Minnesota)
High Technology Sales, Inc.
Phone: (612) 844-9933

NEVADA
(Tempe, Arizona)
Centaur Corporation
Phone: (480) 839-2320

NEW JERSEY
Mt. Laurel
S-J Associates, Inc
Phone: (856) 866-1234

Toms River
Philips Semiconductors
Phone: (732) 505-1200
(732) 240-1479

NEW MEXICO
(Tempe, Arizona)
Centaur Corporation
Phone: (480) 839-2320

NEW YORK
Rockville Centre
S-J Associates, Inc.
Phone: (516) 536-4242

NORTH CAROLINA
Cary
Philips Semiconductors
Phone: (919) 677-7900

Elcom, Inc.
Phone: (919) 678-9301

OHIO
Columbus
Mohrfield Marketing, Inc.
Phone: (614) 481-5451

Dayton
Mohrfield Marketing, Inc.
Phone: (937) 298-7322

Solon
Mohrfield Marketing, Inc.
Phone: (440) 349-2700

OKLAHOMA
(Richardson, Texas)
OM Associates, Inc.
Phone: (972) 690-6746

OREGON
Beaverton
Cascade-Tech
Phone: (503) 645-9660

PENNSYLVANIA
Ambridge
Mohrfield Marketing, Inc.
Phone: (724) 251-0576

(Mt. Laurel, New Jersey)
S-J Associates, Inc.
Phone: (856) 866-1234

TENNESSEE
Dandridge
Philips Semiconductors
Phone: (423) 397-5557

TEXAS
Austin
OM Associates, Inc.
Phone: (512) 794-9971

El Paso
OM Associates, Inc.
Phone: (915) 591-9123

Houston
Philips Semiconductors
Phone: (281) 251-8144

OM Associates, Inc.
Phone: (281) 376-6400

Richardson
Philips Semiconductors
Phone: (972) 705-2481

OM Associates, Inc.
Phone: (972) 690-6746

VIRGINIA
Falls Church
S-J Associates, Inc.
Phone: (703) 533-2233

WASHINGTON
Kirkland
Cascade-Tech
Phone: (425) 822-7299

WISCONSIN
Browndeer
High Technology Sales, Inc.
Phone: (414) 354-9029

CANADA
PHILIPS SEMICONDUCTORS CANADA, LTD.

Calgary, Alberta
Tech-Trek, Ltd.
Phone: (403) 291-6866

Kanata, Ontario
Tech-Trek, Ltd.
Phone: (613) 599-8787

Mississauga, Ontario
Tech-Trek, Ltd.
Phone: (905) 238-0366

Richmond, B.C.
Tech-Trek, Ltd.
Phone: (604) 276-8735

Ville St. Laurent, Quebec
Tech-Trek, Ltd.
Phone: (514) 337-7540

MEXICO
Guadalajara
OM Associates de Mexico, SA de CV
Phone: +52-3-647-7881

El Paso, TX
OM Associates, Inc.
Phone: +1 (915) 591-9123

Nogales
(Tempe, Arizona)
Centaur Corporation
Phone: (480) 839-2320

PUERTO RICO
(Clearwater, Florida)
Elcom, Inc.
Phone: (727) 524-1334

DISTRIBUTORS

Contact one of our local distributors:
Arrow Electronics, Inc.
Avnet EMG
Future Electronics
Pioneer Standard Electronics, Inc.

07/26/00

Philips Semiconductors – a worldwide company

Argentina: see South America

Australia: 3 Figtree Drive, HOMEBUSH, NSW 2140,
Tel. +61 2 9704 8141, Fax. +61 2 9704 8139

Austria: Computerstr. 6, A-1101 WIEN, P.O. Box 213, Tel. +43 1 60 101 1248,
Fax. +43 1 60 101 1210

Belarus: Hotel Minsk Business Center, Bld. 3, r. 1211, Volodarski Str. 6,
220050 MINSK, Tel. +375 172 20 0733, Fax. +375 172 20 0773

Belgium: see The Netherlands

Brazil: see South America

Bulgaria: Philips Bulgaria Ltd., Energoproject, 15th floor,
51 James Bourchier Blvd., 1407 SOFIA,
Tel. +359 2 68 9211, Fax. +359 2 68 9102

Canada: PHILIPS SEMICONDUCTORS/COMPONENTS,
Tel. +1 800 234 7381, Fax. +1 800 943 0087

China/Hong Kong: 501 Hong Kong Industrial Technology Centre,
72 Tat Chee Avenue, Kowloon Tong, HONG KONG,
Tel. +852 2319 7888, Fax. +852 2319 7700

Colombia: see South America

Czech Republic: see Austria

Denmark: Sydhavnsgade 23, 1780 COPENHAGEN V,
Tel. +45 33 29 3333, Fax. +45 33 29 3905

Finland: Sinikalliontie 3, FIN-02630 ESPOO,
Tel. +358 9 615 800, Fax. +358 9 6158 0920

France: 51 Rue Carnot, BP317, 92156 SURESNES Cedex,
Tel. +33 1 4099 6161, Fax. +33 1 4099 6427

Germany: Hammerbrookstraße 69, D-20097 HAMBURG,
Tel. +49 40 2353 60, Fax. +49 40 2353 6300

Hungary: see Austria

India: Philips INDIA Ltd, Band Box Building, 2nd floor,
254-D, Dr. Annie Besant Road, Worli, MUMBAI 400 025,
Tel. +91 22 493 8541, Fax. +91 22 493 0966

Indonesia: PT Philips Development Corporation, Semiconductors Division,
Gedung Philips, Jl. Buncit Raya Kav.99-100, JAKARTA 12510,
Tel. +62 21 794 0040 ext. 2501, Fax. +62 21 794 0080

Ireland: Newstead, Clonskeagh, DUBLIN 14,
Tel. +353 1 7640 000, Fax. +353 1 7640 200

Israel: RAPAC Electronics, 7 Kehilat Saloniki St, PO Box 18053,
TEL AVIV 61180, Tel. +972 3 645 0444, Fax. +972 3 649 1007

Italy: PHILIPS SEMICONDUCTORS, Via Casati, 23 - 20052 MONZA (MI), Tel.
+39 039 203 6838, Fax +39 039 203 6800

Japan: Philips Bldg 13-37, Kohnan 2-chome, Minato-ku, TOKYO 108-8507,
Tel. +81 3 3740 5130, Fax. +81 3 3740 5057

Korea: Philips House, 260-199 Itaewon-dong, Yongsan-ku, SEOUL,
Tel. +82 2 709 1412, Fax. +82 2 709 1415

Malaysia: No. 76 Jalan Universiti, 46200 PETALING JAYA, SELANGOR,
Tel. +60 3 750 5214, Fax. +60 3 757 4880

Mexico: 5900 Gateway East, Suite 200, EL PASO, TEXAS 79905,
Tel. +9-5 800 234 7381, Fax +9-5 800 943 0087

Middle East: see Italy

Netherlands: Postbus 90050, 5600 PB EINDHOVEN, Bldg. VB,
Tel. +31 40 27 82785, Fax. +31 40 27 88399

New Zealand: 2 Wagener Place, C.P.O. Box 1041, AUCKLAND,
Tel. +64 9 849 4160, Fax. +64 9 849 7811

Norway: Box 1, Manglerud 0612, OSLO,
Tel. +47 22 74 8000, Fax. +47 22 74 8341

Pakistan: see Singapore

Philippines: Philips Semiconductors Philippines Inc.,
106 Valero St. Salcedo Village, P.O. Box 2108 MCC, MAKATI, Metro MANILA,
Tel. +63 2 816 6380, Fax. +63 2 817 3474

Poland: Al.Jerozolimskie 195 B, 02-222 WARSAW,
Tel. +48 22 5710 000, Fax. +48 22 5710 001

Portugal: see Spain

Romania: see Italy

Russia: Philips Russia, Ul. Usatcheva 35A, 119048 MOSCOW,
Tel. +7 095 755 6918, Fax. +7 095 755 6919

Singapore: Lorong 1, Toa Payoh, SINGAPORE 319762,
Tel. +65 350 2538, Fax. +65 251 6500

Slovakia: see Austria

Slovenia: see Italy

South Africa: S.A. PHILIPS Pty Ltd., 195-215 Main Road Martindale,
2092 JOHANNESBURG, P.O. Box 58088 Newville 2114,
Tel. +27 11 471 5401, Fax. +27 11 471 5398

South America: Al. Vicente Pinzon, 173, 6th floor, 04547-130 SÃO PAULO, SP,
Brazil, Tel. +55 11 821 2333, Fax. +55 11 821 2382

Spain: Balmes 22, 08007 BARCELONA,
Tel. +34 93 301 6312, Fax. +34 93 301 4107

Sweden: Kottbygatan 7, Akalla, S-16485 STOCKHOLM,
Tel. +46 8 5985 2000, Fax. +46 8 5985 2745

Switzerland: Allmendstrasse 140, CH-8027 ZÜRICH,
Tel. +41 1 488 2741 Fax. +41 1 488 3263

Taiwan: Philips Semiconductors, 5F, No. 96, Chien Kuo N. Rd., Sec. 1, TAIPEI,
Taiwan Tel. +886 2 2134 2451, Fax. +886 2 2134 2874

Thailand: PHILIPS ELECTRONICS (THAILAND) Ltd.,
60/14 MOO 11, Bangna Trad Road KM. 3, Bagna, BANGKOK 10260,
Tel. +66 2 361 7910, Fax. +66 2 398 3447

Turkey: Yukari Dudullu, Org. San. Blg., 2.Cad. Nr. 28 81260 Umraniye,
ISTANBUL, Tel. +90 216 522 1500, Fax. +90 216 522 1813

Ukraine: PHILIPS UKRAINE, 4 Patrice Lumumba str., Building B, Floor 7,
252042 KIEV, Tel. +380 44 264 2776, Fax. +380 44 268 0461

United Kingdom: Philips Semiconductors Ltd., 276 Bath Road, Hayes,
MIDDLESEX UB3 5BX, Tel. +44 208 730 5000, Fax. +44 208 754 8421

United States: 811 East Arques Avenue, SUNNYVALE, CA 94088-3409,
Tel. +1 800 234 7381, Fax. +1 800 943 0087

Uruguay: see South America

Vietnam: see Singapore

Yugoslavia: PHILIPS, Trg N. Pasica 5/v, 11000 BEOGRAD,
Tel. +381 11 3341 299, Fax.+381 11 3342 553

For all other countries apply to: Philips Semiconductors, Marketing Communications, Building BE-p,
P.O. Box 218, 5600 MD EINDHOVEN, The Netherlands, Fax. +31 40 27 24825

Internet: http://www.semiconductors.philips.com

SCH70

Printed in USA 613519/20.900/05/480 Date of release: September 2000 Document order number: 9397 750 07532